JAAVSO

Volume 40
Number 1
2012

The Journal of the American Association of Variable Star Observers

Part B
of two parts
pages 267–608

100th Anniversary Edition

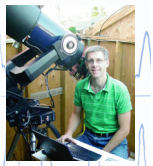

- History
- Associations
- Science
- Review Papers

THE AMERICAN ASSOCIATION OF VARIABLE STAR OBSERVERS
FOUNDED 1911

49 Bay State Road
Cambridge, MA 02138
U. S. A.

ISSN 0271-9053

JAAVSO

The Journal of
The American Association
of Variable Star Observers

Volume 40
Number 1
2012
Part B
of two parts:
pages 267–608

100th Anniversary Edition

History
Associations
Science
Review Papers

49 Bay State Road
Cambridge, MA 02138
U. S. A.

ISSN 0271-9053

The *Journal of the American Association of Variable Star Observers* is a refereed scientific journal published by the American Association of Variable Star Observers, 49 Bay State Road, Cambridge, Massachusetts 02138, USA. The *Journal* is made available to all AAVSO members and subscribers.

In order to speed the dissemination of scientific results, selected papers that have been refereed and accepted for publication in the *Journal* will be posted on the internet at the *eJAAVSO* website as soon as they have been typeset and edited. These electronic representations of the *JAAVSO* articles are automatically indexed and included in the NASA Astrophysics Data System (ADS). *eJAAVSO* papers may be referenced as *J. Amer. Assoc. Var. Star Obs., in press,* until they appear in the concatonated electronic issue of *JAAVSO*. The *Journal* cannot supply reprints of papers.

Page Charges

Unsolicited papers by non-Members will be assessed a charge of $15 per published page.

Instructions for Submissions

The *Journal* welcomes papers from all persons concerned with the study of variable stars and topics specifically related to variability. All manuscripts should be written in a style designed to provide clear expositions of the topic. Contributors are strongly encouraged to submit digitized text in MS WORD, LATEX+POSTSCRIPT, or plain-text format. Manuscripts may be mailed electronically to journal@aavso.org or submitted by postal mail to *JAAVSO*, 49 Bay State Road, Cambridge, MA 02138, USA.

Manuscripts must be submitted according to the following guidelines, or they will be returned to the author for correction:

Manuscripts must be:
1) original, unpublished material;
2) written in English;
3) accompanied by an abstract of no more than 100 words;
4) not more than 2,500–3,000 words in length (10–12 pages double-spaced).

Figures for publication must:
1) be camera-ready or in a high-contrast, high-resolution, standard digitized image format;
2) have all coordinates labeled with division marks on all four sides;
3) be accompanied by a caption that clearly explains all symbols and significance, so that the reader can understand the figure without reference to the text.

Maximum published figure space is 4.5" by 7". When submitting original figures, be sure to allow for reduction in size by making all symbols and letters sufficiently large.

Photographs and halftone images will be considered for publication if they directly illustrate the text.

Tables should be:
1) provided separate from the main body of the text;
2) numbered sequentially and referred to by Arabic number in the text, e.g., Table 1.

References:
1) References should relate directly to the text.
2) References should be keyed into the text with the author's last name and the year of publication, e.g., (Smith 1974; Jones 1974) or Smith (1974) and Jones (1974).
3) In the case of three or more joint authors, the text reference should be written as follows: (Smith *et al.* 1976).
4) All references must be listed at the end of the text in alphabetical order by the author's last name and the year of publication, according to the following format:
   Brown, J., and Green, E. B. 1974, *Astrophys. J.*, **200**, 765.
   Thomas, K. 1982, *Phys. Report*, **33**, 96.
5) Abbreviations used in references should be based on recent issues of the Journal or the listing provided at the beginning of *Astronomy and Astrophysics Abstracts* (Springer-Verlag).

Miscellaneous:
1) Equations should be written on a separate line and given a sequential Arabic number in parentheses near the right-hand margin. Equations should be referred to in the text as, e.g., equation (1).
2) Magnitude will be assumed to be visual unless otherwise specified.
3) Manuscripts may be submitted to referees for review without obligation of publication.

Journal of the American Association of Variable Star Observers
Volume 40, Number 1, 2012

100th Anniversary Edition

100th Spring Meeting of the AAVSO, in conjunction with the 218th Meeting of the American Astronomical Society, held in Boston, Massachusetts, May 21–25, 2011

100th Annual Meeting of the AAVSO, held in Cambridge and Woburn, Massachusetts, October 5–8, 2011

Table of Contents

Table of Contents continued on following pages

Table of Contents continued on following pages

History of Variable Star Organizations

History of AAVSO Observers, Programs, and Supporters

Table of Contents continued on following pages

Scientific session papers presented at the 100th Spring Meeting of the AAVSO, in conjunction with the 218th Meeting of the American Astronomical Society

Table of Contents continued on following pages

Papers and posters presented at the general and scientific paper sessions of the Spring and Annual Meetings

Table of Contents continued on following pages

Table of Contents continued on following pages

Table of Contents continued on next page

Invited review papers

Papers and posters presented at the general and scientific paper sessions of the Spring and Annual Meetings

Secular Variation of the Mode Amplitude-Ratio of the Double-Mode RR Lyrae Star NSVS 5222076, Part 2

David A. Hurdis
76 Harbour Island Road, Narragansett, RI 02882; hurdisd@cox.net

Tom Krajci
P.O. Box 1351, Cloudcroft, NM 88317; tom_krajci@tularosa.net

Presented at the 100th Spring Meeting of the AAVSO, May 21, 2011; received June 28, 2011; revised July 15, 2011; accepted July 15, 2011

Abstract We present results from our ongoing investigation of the double-mode RR Lyrae (RRd) star, NSVS 5222076, and specifically of the long-term temporal variation of the amplitude-ratio, A0/A1, of the star's fundamental and first-overtone pulsation modes. Our earlier paper on this subject (Hurdis and Krajci 2010) described a seemingly monotonic decrease of the amplitude-ratio in the *V* band, from 1.93 in 2005 to 1.76 in 2008 to 1.48 in 2009. After further observation of the star during the 2010 and 2011 observing seasons, we report that the *V*-band amplitude-ratio continued to decrease to 1.40 in 2010, but then increased to 1.82 in 2011. This suggests that, rather than decreasing monotonically toward a switch of dominant pulsation mode, A_0/A_1 may be varying in an oscillatory manner.

1. Introduction

The current paper is a continuation of our investigation of NSVS 5222076 (Hurdis and Krajci 2010), and in particular of the long-term temporal variation of the star's mode amplitude-ratio, A_0/A_1. Our equipment and methods remained the same as in the earlier study and the reader is referred to that paper for those details.

The earlier paper described a rapid, and seemingly monotonic, decrease of the amplitude-ratio in the *V* band, from 1.93 in 2005 to 1.76 in 2008 to 1.48 in 2009, and raised the possibility that NSVS 5222076 could be on the verge of switching its dominant pulsation mode from the fundamental to the first-overtone. It was noted that precedents for mode switching had been observed in the globular cluster M3, where four stars (V79, V166, V200, and V251) had been observed to switch their dominant pulsation modes (Corwin *et al.* 1999, Clementini *et al.* 2004, Clement and Thompson 2007). Among these, V79 has been the most changeable. Goranskij *et al.* (2010) have recently chronicled the history of its observed switches from fundamental mode pulsator to mixed-mode pulsator with dominant first-overtone, then returning to fundamental mode pulsation but with a Blazhko period of 65.4 days. V79 having revealed this menu of possible options for RR Lyrae behavior, it would seem important

for observers to continue to monitor the variation of the mode amplitude-ratio of NSVS 5222076, a field star located well out of the Galactic plane in Bootes, and unimpeded by the crowded star field of a globular cluster.

In 2010 and 2011, all observations were made with the Wright28 telescope, under the aegis of the AAVSO robotic telescope network (AAVSOnet). In 2010, 919 *V*-band images and 913 *I*-band images were taken on ten nights, between JD 2455272 and JD 2455367. In 2011, 892 *V*-band images and 886 *I*-band images were taken on twelve nights, between JD 2455600 and JD 2455666.

As in the earlier study, two software packages were used to perform period analysis of the photometric data extracted from the images. These were PERANSO version 2.20 (Vanmunster 2005), and PERIOD04 (Lenz and Breger 2005). The mode amplitudes were derived from PERIOD04 by least-squares fit of the computed Fourier frequencies to the measured light curves.

2. Results

Among the five individual data sets from the five years that the star has been observed, the computed pulsation periods for NSVS 5222076 vary slightly, but in a random manner, i.e., not in a manner clearly attributable to coherent period change. These random variations may be related to the Blazhko-like modulations reported in our earlier paper (Hurdis and Krajci 2010), which may overwhelm the detection of any long-term period changes. Moreover, we find no correlation between these small year-to-year variations in computed period and the corresponding variations in amplitude-ratio reported below. Our observations are all available in the AAVSO International Database for researchers to apply other statistical methods. The means of the five yearly values computed for the fundamental and first-overtone periods were P0 = 0.49405 ± 0.00005 day and P1 = 0.36684 ± 0.00011 day.

The 2010 and 2011 amplitude-ratio results were as follows. In the *V* band, A_0/A_1 decreased from 1.48 ± 0.01 in 2009 to 1.40 ± 0.02 in 2010, but then increased to 1.82 ± 0.02 in 2011. These results are graphically illustrated in Figure 1, where the upper half of the figure shows (for all five years that the star has been observed) the number and distribution of the time-series observations, while the lower half shows the time variation of A_0/A_1. We note that the 2005 observation time-series and amplitude-ratio results are those of Oaster *et al.* (2006). In the *I* band, A_0/A_1 decreased from 1.52 ± 0.03 in 2009 to 1.38 ± 0.03 in 2010, but then increased to 1.81 ± 0.03 in 2011. These results are illustrated in Figure 2.

In conclusion, two additional years of observation of NSVS 5222076 have revealed that the seemingly monotonic decrease of A_0/A_1 has ended in both wavelength bands, and that in 2011 it increased. This suggests the variation of A_0/A_1 with time may actually be oscillatory. We note that no observations of the star exist between those of 2005 (Oaster *et al.* 2006) and those in 2008

(Hurdis 2009), so it is unknown how A_0/A_1 may have varied during that interval. Continued observation of NSVS 5222076 will be needed to clarify the interesting behavior of its mode amplitude-ratio.

3. Acknowledgements

The authors acknowledge AAVSO Director, Arne Henden, for providing his Sonoita Research Observatory photometric calibration of the star field. They also gratefully acknowledge Director Henden and the AAVSO for authorizing our use of the AAVSO robotic telescope network (AAVSOnet). In addition, they acknowledge Prof. Christine Clement for her helpful comments and for calling to their attention the recent paper on the behavior of V79 in M3.

References

Clement, C. M., and Thompson, M. 2007, *J. Amer. Assoc. Var. Star Obs.*, **35**, 336.

Clementini, G., Corwin, T. M., Carney, B. W., and Sumerel, A. N. 2004, *Astron. J.*, **127**, 938.

Corwin, T. M., Carney, B. W., and Allen, D. M. 1999, *Astron. J.*, **117**, 1332.

Goranskij, V., Clement, C. M., and Thompson, M. 2010, in *Variable Stars, the Galactic Halo and Galaxy Formation*, eds. C. Sterken, N. Samus, and L. Szabados, Sternberg Astronomical Institute, Moscow, 115.

Hurdis, D. A. 2009, *J. Amer. Assoc. Var. Star Obs.*, **37**, 28.

Hurdis, D. A., and Krajci, T. 2010, *J. Amer. Assoc. Var. Star Obs.*, **38**, 1.

Lenz, P., and Breger, M. 2005, *Commun. Asteroseismology*, **146**, 53.

Oaster, L., Smith, H. A., and Kinemuchi, K. 2006, *Publ. Astron. Soc. Pacific*, **118**, 405.

Vanmunster, T. 2005, PERANSO period analysis software, www.peranso.com.

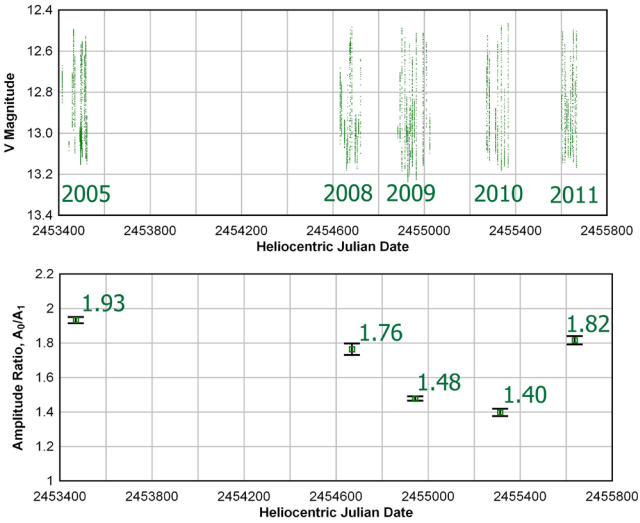

Figure 1. Secular variation of mode amplitude-ratio, A_0/A_1, for *V* band. Upper plot: combined data sets: Oaster *et al.* 2005, Hurdis 2008, Hurdis and Krajci 2009, 2010, and 2011, *V* filter. Lower plot: Time variation of amplitude ratio, A_0/A_1, *V* filter.

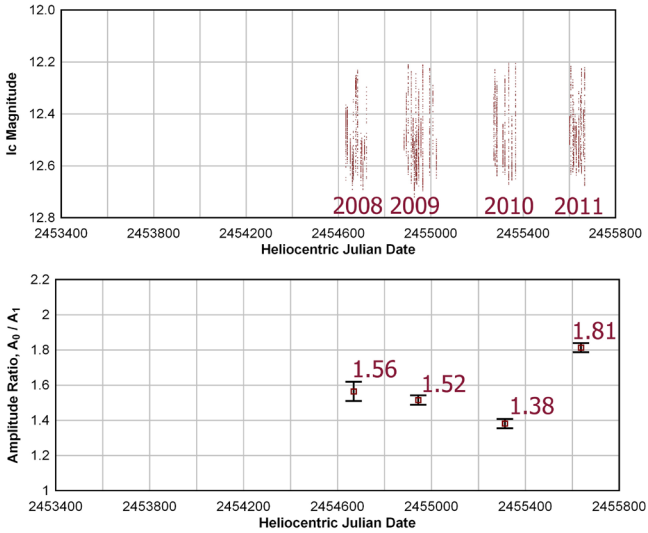

Figure 2. Secular variation of mode amplitude-ratio, A_0/A_1, for *I* band. Upper plot: combined data sets: Hurdis 2008, Hurdis and Krajci 2009, 2010, and 2011, *I* filter. Lower plot: Time variation of amplitude ratio, A_0/A_1, *I* filter.

The Pulsational Behavior of the High Amplitude δ Scuti Star RS Gruis

Jaime Rubén García
Instituto Copérnico, Gutiérrez 4500, 5603 Rama Caída, Mendoza, Argentina; jgarcia@institutocopernico.org

Presented at the 100th Spring Meeting of the AAVSO, May 21, 2011; received November 22, 2011; revised May 15, 2012; accepted May 15, 2012

Abstract RS Gruis is a high–amplitude δ Scuti–type variable star with a mean amplitude of almost half a magnitude in V and a period of almost 3.5 hours. The most recent study of this star by Derekas *et al.* (2009) suggests the presence of a low–mass dwarf star companion close to the variable star with a period of 11.5 days. Rodriguez *et al.* (1995) have also shown a decreasing rate of the period of $dP/Pdt = -10.6 \times 10^{-8}$ / y. Using an extended dataset comprising BVIc CCD observations acquired at the Astronomical Observatory of the Instituto Copérnico, data from ASAS and HIPPARCOS, and the existing CCD observations in the AAVSO International Database, we have performed an extensive periodgram and times of maximum analysis looking for long term variations. As a preliminary result, we confirmed that the period varies, but, since 1995, instead of decreasing, it has increased. We also found a small peak in the power spectrum in good agreement with the period suggested for the binary companion.

1. Introduction

RS Gru (HD 206379, HIP 107231) is a monoperiodic high–amplitude δ Scuti variable star, or HADS, for short, with a pulsation period of 0.147 d (3.5 h), corresponding to a frequency of 6.8027 d^{-1}, and a mean magnitude of 7.9 mag, and an amplitude of 0.6 magnitude in Johnson V filter.

Its light variation was first detected by Hoffmeister (1956) and studied later by Eggen (1956) and Oosterhoff and Walraven (1966).

Kinman (1961) made photometric and spectroscopic observations and measured a mean velocity of 81 km s^{-1} with a velocity amplitude of 45 km s^{-1}.

Further photometric studies from McNamara and Feltz (1976) and later by Rodriguez *et al.* (1995) led to determined period variations.

Extended radial velocity studies by McNamara and Feltz (1976), Balona and Martin (1978), and more recently by Derekas *et al.* (2009) show that RS Gru is a spectroscopic binary with a companion completing an orbit once approximately each 11.5 days.

2. Observations

We use the following datasets in V:

- AAVSO International Database (3,837 Johnson V measurements covering HJD 2454373–2455525) (Henden 2011)
- ASAS3 (479 V measurements covering HJD 2451873–2455129) (Pojmański 2002)
- HIPPARCOS (198 V measurements covering HJD 2447880–2449062) (Perryman *et al.* 1977)
- Our own observations (For this paper we used only the Johnson V dataset, 313 Johnson V, 343 Johnson B, 344 Cousins I_c measurements covering HJD 2455390–2455482)

Our observations were made using the remotely controlled equipment from the Instituto Copérnico Astronomical Observatory, located at Lat. 34° 42' 33" S, Long. 68° 21' 44" W, in Rama Caída, Mendoza, Argentina. The telescope is a Schmidt–Cassegrain Celestron 11–inch with a focal reducer operating at *f*/3.3. The telescope control software is THE SKY X+ASCOM without auto guiding system. The CCD camera is a ST402MXE with a KAF chip 765 × 510 pixels at 9 µm, with a field of view of 26' × 17'. The filters used were the standard set BVIc provided by the camera producer. The camera control and image calibration were performed using MAXIM DL software (Diffraction Limited 2004). For the photometry we used IRAF software.

All data were reduced with standard tools and procedures. The transformation coefficients for the Observatory were obtained using the M67 field photometry (Henden 2011). We performed the corrections for the model of the atmosphere for each night using Landolt (1992) standards and Cousins (1976) pairs.

The CCD observations were reduced in MAXIM DL, including bias and dark removal and flat–field correction using sky–flat images taken during the evening or morning twilight. Magnitudes were calculated with aperture photometry using two comparison stars of similar brightnesses; Table 1 gives information on these comparison stars. In Figure 1 we can see the field including the comparison stars.

To avoid a shift in magnitude, the V magnitudes of the HIPPARCOS dataset were corrected using the table published by Otero (2003).

3. Analysis

The aim of this work was an extensive study of period variations, since the most recent study covering this issue was seventeen years old (Rodriguez *et al.* 1995). Their study was carried out nineteen years after the previous one by McNamara and Feltz (1976). The very short period of the star means that in the seventeen years since the last study the star had completed more than 50,000 cycles.

This paper covers two analyses, first a Fourier analysis of the observed datapoints, and second a classical O–C analysis of maximum light epochs.

Using our data plus the three other datasests described above we performed a DCFT analysis by means of PERIOD04 software from Lenz and Breger (2005).

The result of the analysis gives the higher peak in frequency at 6.8021777 d^{-1} equivalent to a period of 0.14705874 d, clearly shown in Figure 2. The folded light curve for all four datasets over that frequency is shown in Figure 3.

After an extensive periodogram analysis (16 frequecies were pre–whitened), we found that the strongest peak in the region trough 0 to 2 d^{-1} was centered on ~0.087 d^{-1}, corresponding to a period of ~11.5 days (with a S/N ratio of 2.5). This result was in good agreement with the results for the binarity from radial velocity data obtained by Derekas *et al.* (2009). The portion of the power spectrum can be seen in Figure 4.

Regarding the O–C analysis, we picked times of maximum light available in the literature in order to improve the elements for the ephemeris and to try to verify the increase in period that we had already determined in the periodogram analysis. We also established times of maximum light in Heliocentric Julian Date for the sets of observations from the AAVSO International Database and for our own observations, for a total of 37 times of maximum light covering the long span from 1952 to 2010 (Table 2).

We computed the O–C diagram, adopting the ephemeris from Rodriguez *et al.* (1995):

$$\mathrm{HJDmax} = 2447464 + 0.147010864\ \mathrm{E}, \quad (1)$$

and we perceived that the tendency reflected in the periodogram analysis was also present in the O–C diagram.

We searched for a better linear fit, performing a least squares fit, and we found the new elements T_0 = 2447464.7228 (0.0008444) and P_0 = 0.147011323 (0.00000001773) d, reflecting the behavior in Figure 5 and with the computed O–C values in the fourth column of Table 2.

As the standard error of the fit was 0.005, we performed a further cubic regression. As a result we find the following ephemeris for the maximum light of RS Gru:

$$\begin{aligned} T_{max} = \mathrm{JD}\ & 2447464.71497 + 0.147011239\,\mathrm{E} + 4.230\times10^{-12}\,\mathrm{E}^2 + 4.188\times10^{-17}\,\mathrm{E}^3 \quad (2)\\ & \pm0.00101 \quad \pm0.000000026 \quad \pm0.511\times10^{-12} \quad \pm0.816\times10^{-17} \end{aligned}$$

The standard error of the fit was 0.0028, and the computed O–C values can be seen in the fifth column of Table 2.

4. Conclusions and future work

The increase in period seen in RS Gru is not usual behavior for a HADS, which normally present a decrease in period, such as seen in DY Per, VZ Cnc, or BS Aqr. We will continue the long term monitoring of RS Gru, and we will study other HADS in search for another specimen showing this unusual behavior.

5. Acknowledgements

I am grateful to AAVSO observers Roy Axelsen and Giorgio Di Scala for their valuable observations. I am in debt to the AAVSO and especially to Director Dr. Arne Henden for lending me the camera for use at the Instituto Copernico Astronomical Observatory. I also would like to acknowledge with thanks Dr. Matthew Templeton for facilitating the measurements of the comparison stars by the AAVSO Photometric All–Sky Survey (APASS) telescope.

References

Balona, L. A., and Martin, W. L. 1978, *Mon. Not. Roy. Astron. Soc.*, **184**, 1.

Cousins, A. W. J. 1976, *Mem. Roy. Astron. Soc.*, **81**, 25.

Dean, J. F., Cousins, A. W. J., Bywater, R. A., and Warren, P. R. 1977, *Mem. Roy. Astron. Soc.*, **83**, 69.

Derekas, A., *et al.* 2009, *Mon. Not. Roy. Astron. Soc.*, **394**, 995.

Diffraction Limited, 2004, MAXIM DL image processing software, http://www.cyanogen.com

Eggen, O. J., 1956, *Publ. Astron. Soc. Pacific*, **68**, 142.

Henden, A. A. 2011, Observations from the AAVSO International Database, private communication.

Hoffmeister, C. 1956, *Veröff. Sternw. Sonneberg*, **3**, 1.

Kinman, T. D. 1961, *Bull. Roy. Obs.*, **37**, 151.

Landolt, A. U. 1992, *Astron. J.*, **104**, 340.

Lenz, P., and Breger, M. 2005, *Commun. Asteroseismology*, **146**, 53 (http://www.univie.ac.at/tops/Period04/).

McNamara, D. H., and Feltz, Jr., K. A. 1976, *Publ. Astron. Soc. Pacific*, **88**, 510.

Oosterhoff, P. Th., and Walraven, Th. 1966, *Bull. Astron. Inst. Netherlands*, **18**, 387.

Otero, S. A. 2003, *Inf. Bull. Var. Stars*, No. 5482, 1.

Perryman, M. A. C., European Space Agency Space Science Department, and the Hipparcos Science Team 1997, *The Hipparcos and Tycho Catalogues*, ESA SP–1200, ESA Publications Division, Noordwijk, The Netherlands.

Pojmański, G. 2002, *Acta Astron.*, **52**, 397.

Rodríguez, E., Rolland, A., Costa, V., and Martín, S. 1995, *Mon. Not. Roy. Astron. Soc.*, **277**, 965.

Table 1. Comparison star information used to observe RS Gru.

Comparison Stars	*R. A. (J2000)* *h m s*	*Dec. (J2000)* ° ′ ″	*V*	*B*
C1 = HD 206480	02 43 41.37	–48 07 54.77	10.389	10.769
C2 = UCAC3 84–413359	21 43 53.04	–48 09 19.45	11.143	11.799

Table 2. Times of maximum light of RS Gru.

Max	*(HJD)*	*Epoch*	*(O–C)l*	*(O–C)c*	*Origin*
1	2434325.2940	–89377	0.00226859	–0.00133290	1
2	2434573.4510	–87689	0.00415386	0.00029731	1
3	2436756.5710	–72839	0.00599404	0.00142493	2
4	2436760.5380	–72812	0.00368829	–0.00087989	2
5	2436801.5540	–72533	0.00352893	–0.00102922	3
6	2436853.3030	–72181	0.00454292	–0.00000149	3
7	2441538.4027	–40312	0.00036174	0.00067392	4
8	2441538.5490	–40311	–0.00034958	–0.00003718	4
9	2441610.4379	–39822	0.00001304	0.00043395	4
10	2441611.3200	–39816	0.00004509	0.00046734	4
11	2441611.4677	–39815	0.00073377	0.00115624	4
12	2441612.3493	–39809	0.00026582	0.00068963	4
13	2441915.4856	–37747	–0.00078404	0.00010108	4
14	2442687.5892	–32495	–0.00065713	0.00141754	5
15	2443355.4610	–27952	–0.00130158	0.00179679	6
16	2443355.6092	–27951	–0.00011291	0.00298569	6
17	2443360.4584	–27918	–0.00228660	0.00081935	6
18	2443360.6050	–27917	–0.00269792	0.00040825	6
19	2447464.7095	0	–0.01332706	–0.00547332	7
20	2447468.5324	26	–0.01272149	–0.00486554	7
21	2447468.6793	27	–0.01283281	–0.00497678	7
22	2447472.6489	54	–0.01253856	–0.00468025	7
23	2452920.0196	37108	0.00056588	0.00359375	8
24	2452921.9311	37121	0.00091867	0.00394131	8
25	2452922.0772	37122	0.00000735	0.00302958	8
26	2452923.9905	37135	0.00216014	0.00517714	8
27	2452925.0188	37142	0.00138087	0.00439505	8
28	2454373.9612	46998	0.00017257	–0.00168922	9
29	2454374.9930	47005	0.00289331	0.00102738	9
30	2454387.9288	47093	0.00169680	–0.00022118	9
31	2454417.0373	47291	0.00195467	–0.00008102	10
32	2454417.9216	47297	0.00418673	0.00214745	10
33	2454423.9464	47338	0.00152245	–0.00054130	10
34	2455391.7254	53921	0.00497726	–0.00147251	11
35	2455394.6654	53941	0.00475078	–0.00171373	11
36	2455481.6920	54533	0.00064703	–0.00625784	11
37	2455482.5796	54539	0.00617909	–0.00073029	11

1 Hoffmeister (1956); 2 Oosterhoff and Walraven (1956); 3 Kinman (1961); 4 Dean et al. (1977); 5 McNamara and Fetz (1976); 6 Balona and Martin (1978); 7 Rodriguez et al. (1995); 8 Derekas et al. (2009); 9 AAVSO ID (ARX); 10 AAVSO ID (DSI); 11 present paper

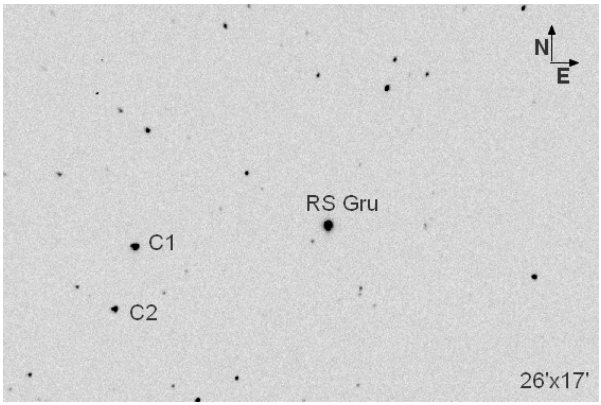

Figure 1. Finder chart for RS Gru. Information on comparison stars is in Table 1.

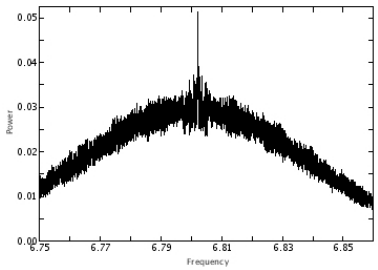

Figure 2. Fourier analysis results for RS Gru showing peak in frequency at 6.8021777 d^{-1} equivalent to a period of 0.14705874 d.

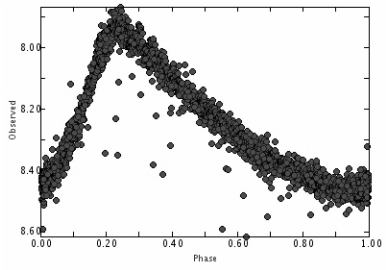

Figure 3. V–band light curve for RS Gru (AAVSO, ASAS, HIPPARCOS, and author's data) folded to frequency 6.8021777 d^{-1} = period 0.14705874 d.

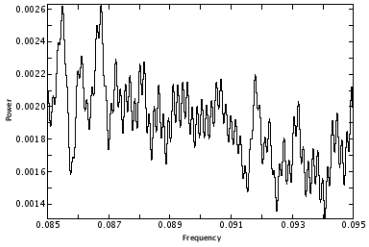

Figure 4. Power spectrum of RS Gru.

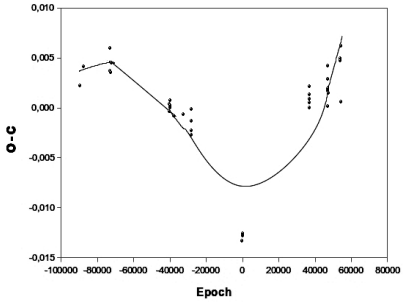

Figure 5. O–C diagram for RS Gru based on the new elements T_0 = 2447464.7228 (0.0008444) and P_0 = 0.147011323 (0.00000001773) d.

RS Sagittae: the Search for Eclipses

Jerry D. Horne
3055 Lynview Drive, San Jose, CA 95148; jdhorne@hotmail.com

Presented at the 100th Annual Meeting of the AAVSO, October 8, 2011; received November 9, 2011; revised January 3, 2012; accepted February 13, 2012

Abstract New V-, B-, I_c-, and R-band photometry of RS Sge has been obtained for 2010 and 2011. These new observations, when combined with previous observations, provide clear verification of RS Sge as an RVb-type variable. The observations also allowed development of B–V, V–I, and V–R color indexes for RS Sge and an examination of calculated vs. observed minima. The light curve shows evidence of both a primary and secondary eclipse with a period of 55.427 days, although the eclipse is difficult to detect because of the intrinsic short and long period variation of the star. The eclipse data have been analyzed following the principles of the Wilson-Devinney method resulting in development of a binary model for the RS Sge system.

1. Introduction

The designation for RS Sge in the *General Catalogue of Variable Stars* (GCVS; Samus *et al.* 2011) is RVB+EA. That is, this star is a RV Tauri, type b star (RVb). It is the only RV Tauri star in the GCVS which is also labeled as an eclipsing binary (EA) (GCVS 2011), since two "Algol-like" fades have been previously reported (Kardopolov and Filip'ev 1985). Since then, there have been no published reports of eclipses for this star.

As part of its *Eyepiece Views* notices, periodic observations of RS Sge were recommended by the AAVSO (Broens 2007). In part because of this recommendation, and other discussions at the AAVSO annual meeting in 2009, a detailed multi-year study of RS Sge was begun in 2010, utilizing both AAVSOnet and the author's telescopes in order to detect eclipses for RS Sge.

RV Tauri stars are giant or supergiant stars, having masses close to that the Sun, of spectral types of F or G at maximum light and G or early K at minimum light (Fokin 1994), and typically have periods between 30 and 150 days (Sterken and Jaschek 1996). Most have low metal abundances (Fokin 1994). RV Tauri stars are known to be strong infrared sources (Jura 1986) from substantial amounts of dust surrounding them (Fokin 1994). It has also been postulated that it is common for RV Tauri stars to be part of binary systems (Van Winckel *et al.* 1998). The majority of RV Tauri stars are in the RVa subclass, while a smaller percentage of these stars, the RVb subclass, also show a long term variation of hundreds to thousands of days (Pollard *et al.* 1996).

Because of the alternating shallow and deep minima of RV Tauri stars, the

usual method of determining the period from adjacent minima is not used. The established convention for these types stars places the primary or deepest minima at phase 0.0, and the secondary, or shallow minimum at phase 0.5. Additionally, the primary or fundamental period is defined to be the time between the deepest minima. The period between adjacent minima is then designated as the half-period (Fokin 1994).

2. Previous observations

RS Sge first appears as a variable in the German publication A*stronomiche Nachrichten* in 1905 (Wolf and Wolf 1905). It was also noted as a variable by Walter Baade, who provided more precise coordinates (Baade 1928).

The first detailed study of the star was published by Tsessevich in 1977. He reported both "fast" and "slow" fluctuations in the light curve over an approximately twenty-year period. Between JD 243600 and 2443000, Tssesevich noted the "fast" period, corresponding to the time between adjacent minima, as 41.1975 days. Tsessevich noted that "slow" fluctuations had a period of 1123 days. This first full light curve, generated for the long term variation in RS Sge, is shown in Figure 1.

Kardopolov and Filip'ev (1985) focused on the short term variability of RS Sge and observed two types of minima, one deep (11.1 to 12.0 V mag.), one more shallow (11.25 to 11.70 V mag.), and noted the fundamental period between deep minima was approximately 90 days. As was mentioned previously, they also noted two "Algol-like" fades on JD 2444837.22 and 2444865.17 of approximately 0.15 V magnitude. These fades appear as single data points on their light curve of RS Sge, and measurement of the eclipse width and depth is somewhat uncertain. It is solely from these two reported fades that the apparent eclipse period for RS Sge is given as 27.95 days. This short term variability and the apparent eclipses are shown in Figure 2.

A query of the current ASAS project database, (Pojmański 2000), shows that more than 350 observations of RS Sge were made between 2003 and 2008. The long and short term variation of RS Sge from these ASAS observations is shown in Figure 3.

Likewise, a query of the AAVSO database (AAVSO 2011) returns a number of observations were made by both CCD and visual observers over a longer period, approximately twenty years. A corresponding graph of those observations shows a long term variation of RS Sge that is very similar to the ASAS light curve in Figure 3 (bottom).

A period analysis was conducted using the software package PERANSO (Vanmuster 2007) for both the AAVSO and ASAS observations of RS Sge, and this analysis indicates that the long period variation is 1193.49 ± 0.9 days, the fundamental period as 80.90 ± 0.7 days, and the half period as 40.55 ± 0.3 days. It does not reveal any significant period of approximately 28 days corresponding to the eclipse period reported by Kardopolov and Filip'ev (1985).

Self-correlation analysis, (Percy and Mohammed, 2004) also illustrates the approximately 40- and 80-day half and full period respectively (Figure 4, top), and an approximately 1,200-day long term variation (Figure 4, bottom). Similar to the period analysis, a self-correlation analysis does not indicate the presence of a twenty-eight day eclipse period for RS Sge in the ASAS and AAVSO data.

3. Current observations

For 2010 and 2011, observations of RS Sge were carried out using a number of telescopes:

- W28—a 28-cm Celestron, part of the AAVSOnet, located at the Astrokolkhoz telescope facility near Cloudcroft, New Mexico;
- W30—a 30-cm Meade LX200, part of the AAVSOnet, also located at the Astrokolkhoz telescope facility;
- SRO50—a 0.5-m telescope, part of the AAVSOnet, located at the Sonoita Research Observatory in Arizona;
- a 0.25-m Meade LX200, located in San Jose, California.

Depending on the specific instrument and filter, exposures ranging from 60 to 300 seconds were made using Johnson B, V, R, and Cousins I filters. Each recorded image was processed using established procedures. Photometric measurements were made using the AAVSO VPHOT application, using the corresponding AAVSO photometric sequence for RS Sge. The air mass for observations ranged from 2.17, for those few observations made earlier in the year, to 1.02, when RS Sge was at higher elevations during the night. Uncertainties for the photometric measurements averaged 0.08 mag. for B band, 0.03 mag. for V and R band, and 0.05 mag. for I band.

3.1. Light curves and color indexes

BVRI light curves from 2011 are shown in Figure 5. The overall variation for the B band is approximately 1.1 magnitude, and 0.6 for the other color curves. While the minima are fairly well aligned among the color curves, the maxima occur at different time periods, with the B-band maxima being well in advance of the V- or I-band maxima. The color indexes from the 2011 observations are shown in Figure 6. Examination of the V–I and B–V color indexes shows that these color indices have a saw-tooth type pattern, with the index values rising to a sharp peak at the maxima, while the V–R color index shows a more rounded maxima. The largest range of differences occur in the B–V index, almost 0.6 magnitude, while the V–I and V–R indexes show range differences on the order of 0.4 magnitude.

3.2. Observed vs. calculated minima

Examination of the 2011 RS Sge light curves in Figure 5 shows the typical RV Tauri-type alternating deep and shallow minima in their light curves, (Pollard *et al.* 1996). For RS Sge, this effect is most pronounced in the V band, also shown in Figure 10, when one compares the minima at JD 2455763 (14.1 V mag.) , JD 2455820 (14.25 V mag.), and JD2455846 (14.08 V mag.).

Additionally, it is typical for RV Tauri stars to generally show random fluctuations in period from one cycle to the next, (Percy *et al.* 1997). RS Sge follows this tendency, as the difference between minima is not constant, and did vary by as much as twelve days during the 2010 and 2011 observations. It was noticed that RS Sge apparently also has short bursts of fairly regularly spaced minima. If the average magnitude of each minima cycle is calculated and subtracted from the magnitude of each data point, the long term variation can be extracted from the light curve and the minima of 2010 and 2011 can be directly compared. Additionally, using the half period, 40.55 days, obtained from the period analysis of the ASAS data for RS Sge, the observed vs. calculated minima from 2010 and 2011 can be graphed. As shown in Figure 7, RS Sge had a number of minima that closely match the calculated date for the minima in 2010 and 2011.

4. Evidence of eclipses

An important aspect of the RS Sge light curve is that the segments between maxima and minima are sections of time where the star's magnitude is changing very rapidly, at times more that 0.1 magnitude in a single day. While this change is small in comparison to other variable stars, such a change is sufficient to effectively mask an eclipse of 0.15 magnitude in depth over perhaps several days, as was reported for RS Sge (Kardopolov and Filip'ev 1985). One of the perhaps fortuitous aspects of the 1985 eclipses was that they happened during a relatively slow period of change in RS Sge's light curve, as seen in Figure 2.

The challenge then, in finding evidence of eclipses in the current set of data from 2010 and 2011, is to separate where possible, any effects from an eclipse from the overall long and short term variability of RS Sge.

4.1. Eclipse evidence from 2010

Although the ASAS data are generally too sparse to use for eclipse detection, certain segments are useful for light curve comparisons. If a comparison is made for RS Sge between a segment of ASAS data from 2007, Figure 8 (top), and the other 2010 data, in Figure 8 (bottom), it can be noted that almost every cycle is fairly smooth, with a rapid rise to maxima, then a more gradual decline to the minima. In the 2010 data, Figure 8 (bottom) a discrepancy is noted around JD 2455370, in that after reaching the maxima, the light curve immediately drops 0.15 magnitude, then has a short segment of minor variability before resuming the normal gradual decline at JD 2455380.

If it assumed that this maximum around JD 2455370 has been altered by an eclipse, it is possible to recalculate the star's light curve for this segment. By also assuming that the light curve should have been following a more constant slope between JD 2455370 and 2455410, a possible eclipse can be revealed by subtracting out the expected slope of the light curve for this segment. The result of modifying the observational data in such a manner is shown in Figure 9. This residual light curve shows good evidence of an eclipse centered on JD 2455376.81393, which is also 377 27.95-day cycles from the first 1985 eclipse. This eclipse is approximately 0.15 V mag., in depth, and occurs over multiple days. In examining both the residual and the observed light curve for 2010 in Figures 8 and 9, there is additional evidence of eclipses at JD 2455321 and 2455404, which are multiples of this same 27.95 day cycle, prior to, and after the JD 2455375 event, although these eclipses appear more shallow.

4.2 Eclipse evidence from 2011

The light curve from 2011, shown in Figure 10, also shows evidence of an eclipse around JD 2455763, which is fourteen 27.95-day cycles from the 2010 eclipse at JD2455375. In this case, the eclipse appears to last approximately five days and reaches a depth of at least 0.11 V mag. In examining the overall light curve for 2011 in Figure 10, there is additional evidence of an eclipse around JD 2455848, also separated by multiples of 27.95 days, from the other 2011 eclipse event. The apparent eclipse at JD 2455848 is definitely shallower, only about 0.04 V mag. in depth.

4.3 Eclipse discussion

This evidence, the case of the presence of more shallow eclipses, is slightly different than what was reported by Kardopolov and Filip'ev (1985). In examining their light curve in Figure 2, it can be noted that the second eclipse at JD 2444865.17 is only partially recorded. Plus, its overall depth is even more uncertain than the first eclipse at JD 2444837.22, so the interpretation that there were two similar "Algol-like" fades in 1985 may be incorrect.

Additionally, while there is evidence of eclipse activity happening in multiples of approximately twenty-eight days for RS Sge, this difference in depth raises the possibility that the actual eclipse period might actually be approximately 56 days. The difference in depth obviously could represent a primary and secondary eclipse. In fact, if a period analysis is performed on the RS Sge 2010 and 2011 data, there is a small, but apparently significant period found in the PERANSO (Vanmunster 2007) period diagram corresponding to 55.86 ± 0.54 days, which is very close to twice the 27.95 period from 1985. The theta value, or calculated Schwarzenberg-Czerny value from the ANOVA analysis method (Schwarzenberg-Czerny 1996) is 11.53 for this 55.86-day period. This compares to a theta value of 28.12 for an ANOVA analysis of the 40.55-day half period, and 37.4 for the 80.9-day full period of RS Sge from the ASAS data.

5. System modeling

There is some concern that despite some observational evidence, the fact that RV Tauri stars are supergiant stars (Jura 1986), the corresponding stellar radius of such a star might make the existence of such a stable eclipsing system with an orbital period of 27.95 or 55.86 days, with eclipses lasting multiple days, somewhat improbable.

5.1. Astrophysical considerations

A simple astrophysical calculation can be performed to test the orbital possibilities of such an RS Sge system. It can be assumed that RV Tauri stars have luminosities (L_{RV}) of 10^3 to 10^4 $L_\odot$ (Fokin 1994) and RV Tauri stars vary from F to G, or G to K (Samus *et al.* 2011). This corresponds to a T_{eff} range of 4800–6500 K, so it is possible to calculate a range of possible stellar radii (R_{RV}) for RV Tauri stars by using the formula for stellar luminosity:

$$L = 4\pi R^2 \sigma T^4 \quad (1)$$

Using the luminosity of an RV Tauri star, L_{RV}, then dividing by the luminosity of the sun, $L_\odot$, and cancelling the constants, this becomes:

$$L_{RV} / L_\odot = T^4_{RV} R^2_{RV} / T^4_\odot R^2_\odot \quad (2)$$

Utilizing the range of T_{eff} and luminosities for RV Tauri stars, the range of possible radii is then:

$$R_{RV} = 15 – 100\ R_\odot \quad (3)$$

In terms of Astronomical Units (A.U.), this range is: $R_{RV} = 0.07 – 0.46$ A.U.

For an eclipse period of 27.95 days, Kepler's Third Law gives us the semi-major axis of a possible secondary component of RS Sge as:

$$a = 0.18 \text{ A.U.} \quad (4)$$

A companion star is possible if the luminosity of RS Sge is constrained to the lower end of the assumed range. If the primary eclipse period is closer to 56 days, the size of the semi-major axis is of course correspondingly larger, as is the possible range of luminosities.

5.2. Binary stellar modeling

A more rigorous method of modeling the RS Sge system is possible through an examination of the RS Sge light curves via a binary star modeling program such as PHOEBE (Prsa and Zwitter 2005), which utilizes the methods of the Wilson-Devinney code (Wilson 1994).

A difficulty in using such a modeling program like PHOEBE for RS Sge is that the star exhibits complex light curve changes outside of any possible eclipse activity. The net effect is that different eclipse events, on approximately 28-day

centers, happen at very different magnitudes, ranging from approximately 11.5 to 14.0 V magnitude. While filtering for these eclipse data, some care must be taken to minimize any data selection bias, and these data, must, in turn, be converted to a common base magnitude so that the PHOEBE program can make sense of them. Nonetheless, as the JD 2455763 eclipse is the best defined, prior to input into PHOEBE, the magnitude of all eclipse V-band data from 2010 and 2011 was re-scaled to that JD 2455763 magnitude base of 14.02 V mag.

The best fit for the 2010 and 2011 RS Sge V-band data from PHOEBE is shown in Figure 11. This fit is for a detached binary system, based upon a 55.33-day orbital period with both primary and secondary eclipses, of 0.14 and 0.05 V magnitude, respectively. While the data are a good fit to the primary eclipse, there is some scatter about the secondary eclipse. The corresponding modeling of the RS Sge system is listed in Table 1.

The outputs from the binary model for RS Sge are consistent with the previous astrophysical calculations, in terms of stellar radius and effective temperature of RS Sge. The orbital period from the PHOEBE model is shorter than the one from the 2010 and 2011 period analysis, by about a half a day, but within the degree of uncertainty (0.54 day). It is also important to point out that because of limitations in the accuracy of the photometry, the small amount of eclipse data, and the inherent limitations of the binary models, the results offered here are from simply one solution, consistent with the available observational data, but it is not necessarily a mathematically unique solution.

6. Conclusions

This paper has reviewed previous and recent observations of RS Sge, including BVRI light curves, color indexes, period and self-correlation analyses, and an examination of observed versus calculated minima. There is good verification of the classification of RS Sge as a RVb-type variable star. The half-period of RS Sge was found to be 40.55 days, while the full period between the deep minima is 80.9 days. As is typical for RV Tauri stars, RS Sge shows some cycle-to-cycle variations in the timing of the minima. The long term variation of RS Sge was found to be 1193.5 days and spans more than 3.0 V magnitudes.

There is evidence of eclipse activity for RS Sge in the 2010 and 2011 data, seemingly confirming the eclipses first published in 1985. Because in some cases, the eclipse data are wrapped within the overall complex variation of this RV Tauri-type star, this confirmation is not totally unambiguous. Additional observations are needed to gather additional data and refine the nature of the RS Sge eclipses. Binary modeling of the current data does show a reasonable fit to a system with an orbital period of 55.33 days, with both primary and secondary eclipses being present.

7. Acknowledgements

This research has made use of the SIMBAD data base, operated at Centre de Données astronomiques de Strasbourg, the ASAS database, managed by Grzegorz Pojmański of the Warsaw University Observatory, and the GCVS databases, operated by the Sternberg Astronomical Institute, Moscow, Russia. Special acknowledgement is given for the data and resources of the American Association of Variable Star Observers (AAVSO), especially the telescopes and their operator at its Astrokolkhoz facility.

References

Baade, W. 1928, *Astron. Nachr.*, **232**, 65.

Broens, E. 2007, *Eyepiece Views*, No. 321 (July), 1 (http://www.aavso.org/sites/default/files/newsletter/EPViews/0707.pdf).

Fokin, A. B. *Astron. Astrophys.*, **292**, 133.

Henden, A. A. 2011, Observations from the AAVSO International Database (http://www.aavso.org/aavso-international-database), private communication.

Jura, M. 1986, *Astrophys. J.*, **309**, 732.

Kardopolov, V., and Filip'ev, G. 1988, *Sov. Astron.*, **32**, 424.

Percy, J., Bezuhly, M., Milanowski, M., and Zsoldos, E. 1997, *Publ. Astron. Soc. Pacific*, **109**, 264.

Percy, J., and Mohammed, F. 2004, *J. Amer. Assoc. Var. Star Obs.*, **32**, 9.

Pojmański, G. 2000, *Acta Astron.*, **50**, 177.

Pollard, K. R., Cottrell, P. I., Kilmartin, P. M., and Gilmore, A. C. 1996, *Mon. Not. Roy. Astron. Soc.*, **279**, 949.

Prša, A., and Zwitter, T. 2005, *Astrophys. J.*, **628**, 426.

Samus, N. N., *et al.* 2011, *General Catalogue of Variable Stars*, Sternberg Astronomical Institute, Moscow (http://www.sai.msu.su/groups/cluster/gcvs/gcvs/).

Sterken, C., and Jaschek, C. 1996, *Light Curves of Variable Stars, a Pictorial Atlas*, Cambridge Univ. Press, Cambridge, 96.

Schwarzenberg-Czerny, A. 1996, *Astrophys. J., Lett. Ed.*, **460**, L107.

Tsessevich, V. 1977, *Inf. Bull. Var. Stars*, No. 1371, 1.

Vanmunster, T. 2007, PERANSO period analysis software, http://www.peranso.com

Van Winckel, H., Waelkens, C., Fernie, J. D., and Waters, L. B. F. M. 1999, *Astron. Astrophys.*, **343**, 202.

Wilson, R. E. 1994, *Publ. Astron. Soc. Pacific*, **106**, 921.

Wolf, M., and Wolf, G. 1905, *Astron. Nachr.*, **170**, 361.

Table 1. Output from PHOEBE for the RS Sge data from AAVSOnet and the author's observations in 2010 and 2011.

Parameter	*Value*
Mass Ratio: q	0.95999
Primary Radius: R_p	13.02 $R_\odot$
Secondary Radius: R_s	5.92 $R_\odot$
Primary T_{eff}	6400 K
Secondary T_{eff}	5020 K
Semi-major axis: a	76.0 $R_\odot$
Inclination: i	81.1°
Eccentricity: e	0.05
Period: p	55.33 d
Epoch (HJD)	2455765.1008

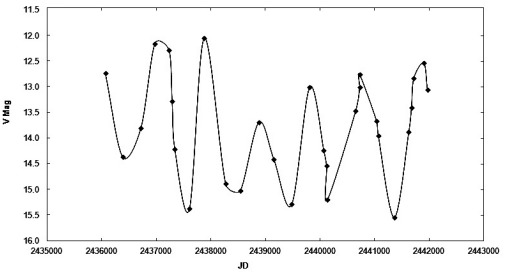

Figure 1. Long-term variability of RS Sge. From observations by Tsessevich (1977).

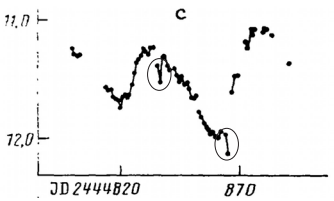

Figure 2: Short-term variability of RS Sge. The Algol-like fades are identified with a circle. From photoelectric observations by Kardopolov and Filip'ev (1985); light curve published in Kardopolov and Filip'ev (1988).

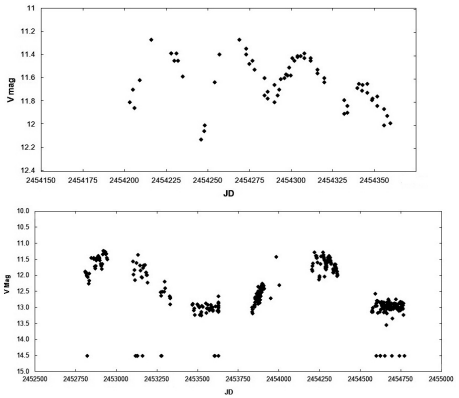

Figure 3. Short-term, April–September 2007 (top graph, black dots), and long-term (bottom graph, black dots) variability of RS Sge. From ASAS observations 2003–2008.

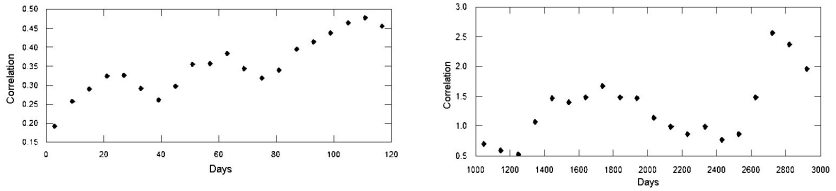

Figure 4: Short period (left graph, black dots) and long period (right graph, black dots), self-correlation analysis of the ASAS Data. From ASAS observations 2003–2008.

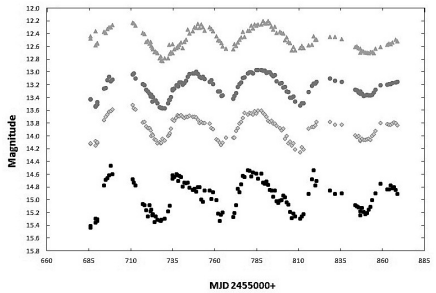

Figure 5: BVRI magnitudes of RS Sge (top to bottom: B, gray squares; V, gray diamonds; R, black dots; I, light gray triangles). From AAVSOnet and the author's observations in 2011.

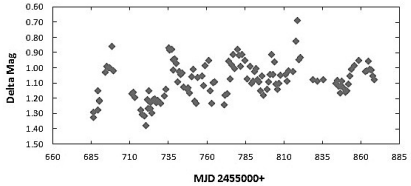

Figure 6: Color Indices of RS Sge: B–V, top left; V–I, bottom left; V–R, bottom right. From AAVSOnet and the author's observations in 2011.

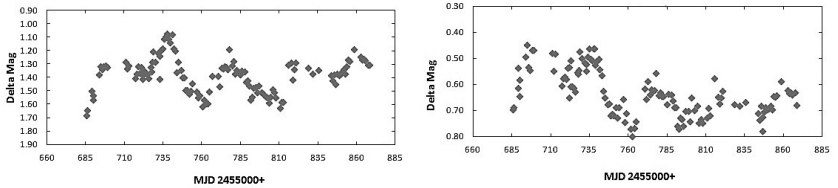

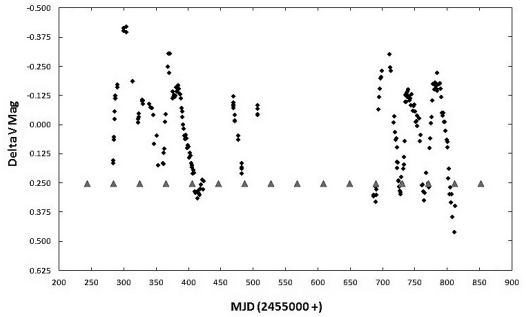

Figure 7: Calculated light curve (gray triangles) using a period of 40.55 days, and observed (black diamonds) minima for RS Sge. From AAVSOnet and the author's observations in 2010 and 2011.

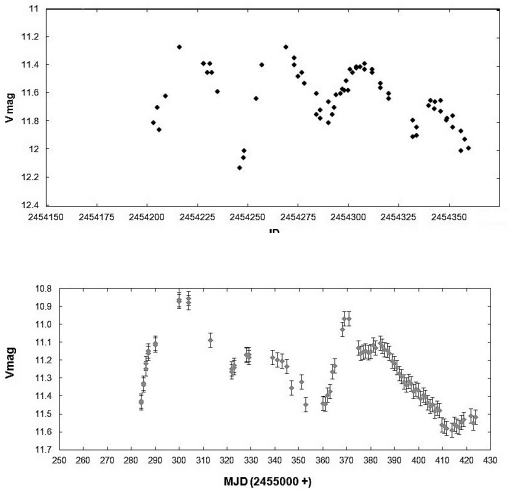

Figure 8: A comparison of RS Sge short term variability from ASAS data in 2007 (top graph) and from AAVSOnet and the authors observations in 2010 (bottom graph).

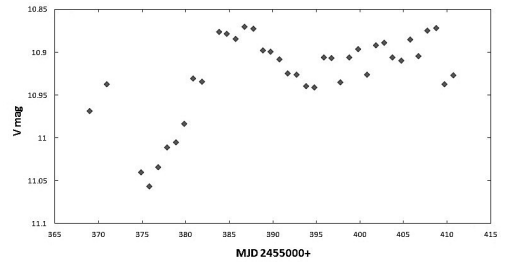

Figure 9: A residual light curve of RS Sge from AAVSOnet and the author's observations in 2010.

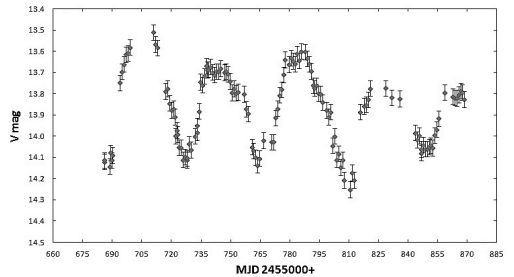

Figure 10: The V-band light curve of RS Sge from AAVSOnet and the author's observations in 2011.

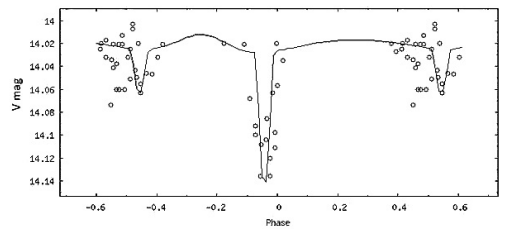

Figure 11: The calculated V-band light curve (line) from PHOEBE and the observed eclipse data of RS Sge from AAVSOnet and the author's observations in 2010 and 2011.

Intensive Observations of Cataclysmic, RR Lyrae, and High Amplitude δ Scuti (HADS) Variable Stars

Franz-Josef Hambsch
Oude Bleken 12, Mol 2400, Belgium; hambsch@telenet.be

Presented at the 100th Annual Meeting of the AAVSO, October 8, 2011; received February 15, 2012; revised March 13, 2012; accepted March 14, 2012

Abstract An intensive observing campaign is ongoing to study cataclysmic, RR Lyrae (with and without Blazhko effect), and High Amplitude δ Scuti (HADS) variable stars. These observations are based on requests and in collaboration with different organisations (CBA, VSNET, GEOS) and individuals. Observations are taken from my private observatories in Belgium, Chile, and through shared use of an observatory belonging to the AAVSOnet in New Mexico. Examples of individual stars intensively followed-up on are: CD Ind and BW Scl, two cataclysmic variables; NU Aur, an RR Lyr star with strong Blazhko effect; and GSC0762-0110, a HADS star. Many publications in different journals including *Astronomy and Astrophysics* have already emerged from this research.

1. Introduction

For the past couple of years I have been changing my interest in amateur astronomy, focussing towards variable star observations. Coming from "pretty picture" imaging and with my scientific background I have now fully dedicated my equipment and efforts towards following intensively short period variable stars like RR Lyr stars, Cataclysmic variables (CV), and High Amplitude Delta Scuti (HADS) stars. My roll-off observatory in my backyard has grown in recent years to house several telescopes dedicated to variable star observations. In Belgium, I observe mainly CV's in collaboration with the Center for Backyard Astrophysics (CBA) based on requests via the CBA e-mail alert list. Also, outburst observations of CV's are performed based on VSNET alerts and data are sent to Kyoto for further analysis. The telescopes used are nowadays a C14, a C11, and a Meade 14-inch, all equipped with SBIG CCD's and photometric filters. Parts of the data shown in Figures 1 and 5 have been taken with those telescopes. As the weather in Belgium is mostly cloudy, I have joined forces with AAVSO and share one of AAVSOnet telescopes (W30) with fellow AAVSOnet observers. With this telescope and the much better weather conditions in New Mexico most of the data from Figures 1 and 2 have been acquired. In addition, since mid-2011 I have found the ultimate observing site in the Atacama Desert in Chile. Since August 2011 a remote telescope (40 cm *f*/6.8 Optimized Dall Kirkham (ODK) from Orion Optics, UK) is operational utilizing an FLI ML16803 CCD with Astrodon photometric filters. The data

shown in Figures 3 and 4 have been acquired remotely. In the following some explanations about the variable type and some examples of observational results acquired at the different sites mentioned above are given.

2. RR Lyr stars

This type of variable star is named after the prototype, the variable star RR Lyrae in the constellation Lyra. RR Lyr stars are pulsating horizontal branch stars with a mass of around half of our Sun's. They are thought to have previously shed mass and, consequently, they were once stars with similar or slightly less mass than the Sun, around 0.8 solar mass. RR Lyr stars pulsate in a manner similar to Cepheid and δ Scuti variables, so the mechanism for the pulsation is thought to be similar, but the nature and histories of these stars is thought to be rather different. In contrast to Cepheids, RR Lyr stars are old, relatively low mass, metal-poor so-called "Population II" stars. They are much more common than Cepheids, but also much less luminous. Their period is shorter, typically less than one day.

The RR Lyr stars are conventionally divided into three main types based on the shape of the stars' brightness curves:

1) RRab, the majority type, which display steep rises in brightness;

2) RRc, a type with shorter periods and more sinusoidal variation; and

3) RRd, a rare type of double-mode pulsators.

RRab types are fundamental mode pulsators, RRc types are pulsating in the first overtone, and RRd are a combination of both modes.

My interest in observing RR Lyr stars is on one hand due to the short period of those stars: Within one night you can see already quite a change in brightness. On the other hand the stars also show brightness modulation which is known as the Blazhko effect. In 1907, S. Blazhko observed this effect for the first time on the star RW Dra (Smith 2004). The Blazhko effect is, to date, not really understood. Recently, thanks to the Kepler and CoRoT satellite missions, more insight into this phenomenon has been gained as the satellites can of course observe the stars continuously, which is impossible for Earth-bound observations (Kolenberg 2011). Nevertheless, observations from Earth are also very valuable as can be seen in many publications on this subject in the astronomical literature.

Examples of RR Lyr stars showing Blazhko effect are given in Figures 1 and 2. Both NU Aur and VY CrB are RRab types with a rather strong modulation of the light curve due to the Blahzko effect. Both the maximum brightness and the time of maximum are changed.

3. Cataclysmic variables

Cataclysmic variable (CV) stars undergo large brightness increases of several magnitudes which last for a few days and then they drop back to a quiescent state. The stars are novae, dwarf novae, or closely related objects which undergo these outburts in a regular or semiregular way. They are normally interacting binaries of which one star is a white dwarf and the second star is closer to the main sequence. The latter star loses matter in the direction of the white dwarf, usually forming an accretion disk. The repetitive outbursts are most probably due to material from the accretion disk accumulating on the white dwarf and causing, for example, a thermonuclear reaction. CVs are subdivided into several classes, for example, those which have strong magnetic fields are called polars, an example of which is CD Ind.

I came to this sort of object by subscribing to different variable star mailing lists and by my recent participation in the SAS meeting in Big Bear in 2009, where I joined the CBA (Center for Backyard Astronomy) group. There was a meeting adjacent to the SAS meeting in Big Bear, and I met Joe Patterson in person. Since then I have been contributing my observations to the CBA data repository as well as the AAVSO International Database. Also, through T. Kato's VSNET alerts, I get information about interesting CV's in outburst, which can be followed up on.

Some examples of Cataclysmic Variables are given in Figures 3 and 4 (CD Ind and BW Scl). The most recent outburst and the first ever detected was for BW Scl. Due to my remote observatory I could follow this star during the pre-outburst period nearly until the writing of this paper, over a period of more than two months. I just missed the rise to outburst. Figure 4 shows the observed light curve.

4. High Amplitude δ Scuti (HADS) stars

δ Scuti stars exhibit both radial and non-radial luminosity pulsations. Non-radial pulsations are when some parts of the surface move inwards and some outward at the same time. Radial pulsations are a special case, where the star expands and contracts around its equilibrium state by altering the radius to maintain its spherical shape. Throughout their lifetime δ Scuti stars exhibit pulsation when they are situated on the classical Cepheid instability strip. They then move across from the main sequence into the giant branch.

I have been observing this kind of star for a couple of years based on a collaboration with Patrick Wils and the Flemish Association of Variable Stars. This group has an intensive CCD campaign in following up on HADS stars. The list of stars is provided by P. Wils and can be accessed at the following URL:

http://www.vvs.be/werkgroepen/werkgroep-veranderlijke-sterren/over-werkgroep-veranderlijke-sterren/de-werkgroep/hads-0#overlay-context=werkgroepen/werkgroep-veranderlijke-sterren/hads-waarnemingen

Wils collects the data and analyzes them in terms of determining the epoch and period of the star over a longer time span of several years to look for variations in these parameters. Occasionally, multi-periodic stars are also found in the list. They are then more intensely observed by several observers distributed around the globe to get a continuous capture of the light curve and its variations due to multiple periods. Those stars are of course the more interesting ones, as the light curve changes from night to night. An example, the HADS star GSC0762-0110 (Wils *et al.* 2008), is given in Figure 5.

5. Acknowledgements

The Wikipedia online free encyclopaedia is used for the introductory explanations to RR Lyrae, Cataclysmic, and HADS variable stars. I would like to thank Patrick Wils for valuable comments on the manuscript.

References

Kolenberg, K. 2011, arXiv:1108.4987v1 [astro-ph.SR], (http://arxiv.org/abs/1108.4987) and references therein.

Smith, H. A. 2004, *RR Lyrae Stars*, Cambridge Univ. Press, Cambridge, 103.

Wils, P., Rozakis, I., Kleidis, S., Hambsch, F. -J., and Bernhard, K. 2008, *Astron. Astrophys.*, **478**, 865.

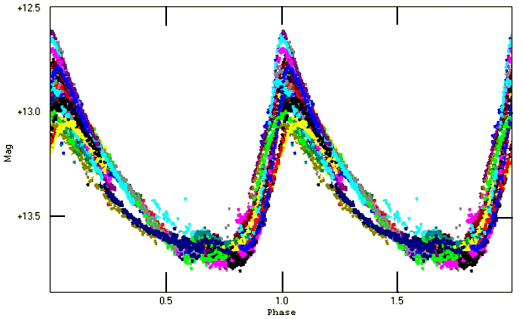

Figure 1. Phase diagram of NU Aur, a RR Lyr star with a strong Blazhko effect, which not only changes the maximum brightness but also the time of maximum. Data were taken from the author's backyard observatory and via the AAVSOnet scope W30 in New Mexico. The colors indicate different nightly runs.

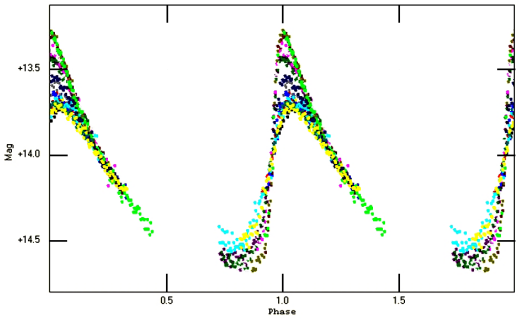

Figure 2. Phase diagram of VY CrB another example of a RR Lyr star showing the Blazhko effect. Data are via the AAVSOnet scope W30 in New Mexico. The colors indicate different nightly runs.

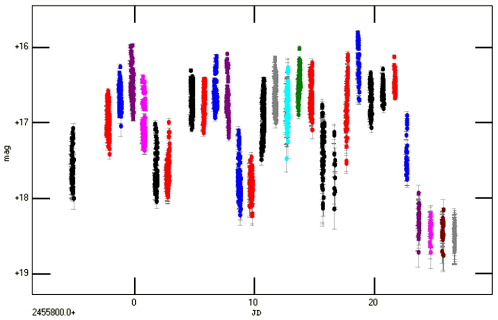

Figure 3. Example of an CV which showed several changes of about 1 mag in brightness during about three weeks of observations. Data were taken remotely from the author's observatory in Chile. The colors indicate different nightly runs.

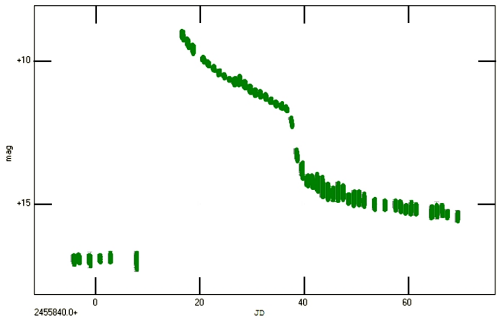

Figure 4. BW Scl showed its first ever detected outburst of more than 6 magnitudes and could be followed in its brightness decrease over more than two month. Also data before the outburst have been acquired. All data were taken remotely from the author's observatory in Chile.

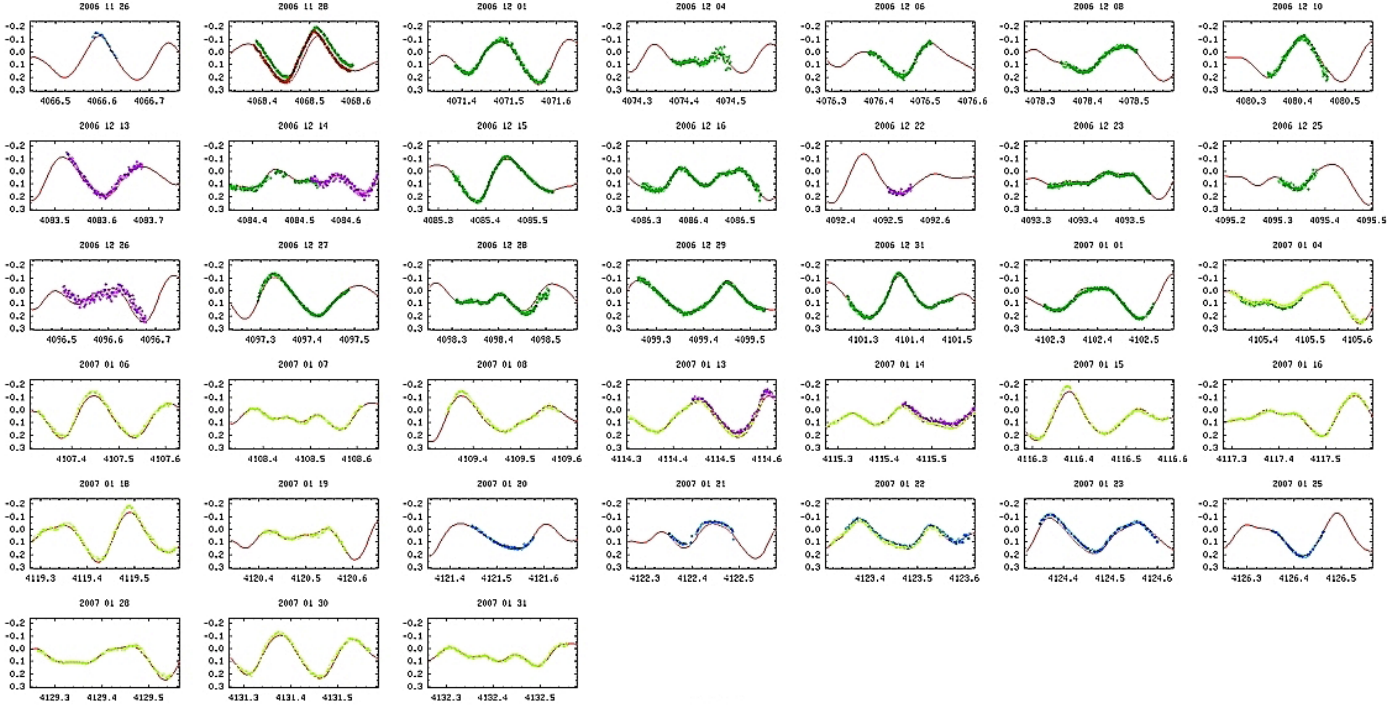

Figure 5. Example of a multi-periodic High Amplitude Delta Scuti (HADS) star, observed during several weeks by several observers. Data were taken from multiple sites by different observers including the author's backyard observatory in Belgium. (Wils *et al.* 2008).

A Study of the Orbital Periods of Deeply Eclipsing SW Sextantis Stars

David Boyd
5 Silver Lane, West Challow, Wantage, OX12 9TX, UK;
davidboyd@orion.me.uk

Presented at the 100th Spring Meeting of the AAVSO, May 21, 2011; received February 13, 2012; revised March 23, 2012; accepted March 25, 2012

Abstract Results are presented of a five-year project to study the orbital periods of eighteen deeply eclipsing novalike cataclysmic variables, collectively known as SW Sextantis stars, by combining new measurements of eclipse times with published measurements stretching back in some cases over fifty years. While the behavior of many of these binary systems is consistent with a constant orbital period, it is evident that in several cases this is not true. Although the time span of these observations is relatively short, evidence is emerging that the orbital periods of some of these stars show cyclical variation with periods in the range 10–40 years. The two stars with the longest orbital periods, V363 Aur and BT Mon, also show secular period reduction with rates of -6.6×10^{-8} days/year and -3.3×10^{-8} days/year. New ephemerides are provided for all eighteen stars to facilitate observation of future eclipses.

1. SW Sex stars

SW Sex stars are an unofficial sub-class of cataclysmic variables (CVs), not in the *General Catalogue of Variable Stars* (GCVS; Samus *et al.* 2012), which was first proposed by Thorstensen *et al.* (1991) with the comment "… these objects show *mysterious* behavior which is however highly *consistent* and *reproducible*." They are classified in the GCVS as novalike variables. The four prototype SW Sex stars were PX And, DW UMa, SW Sex, and V1315 Aql, which all appeared to share a common set of unusual properties (see below). Since then this class has expanded to include around fifty members of which about half are definite members and the others either probable or possible based on their observed characteristics. Don Hoard maintains an on-line list of SW Sex stars (Hoard *et al.* 2003).

These SW Sex stars have bright accretion disks, in some cases showing occasional VY Scl-type low states, but do not have the quasi-periodic outbursts seen in dwarf novae. They are often eclipsing systems with periods mostly in the range 3–4 hours. They may exhibit either positive or negative superhumps or both. Spectroscopically they show single-peaked Balmer and HeI emission lines, not double peaked lines as expected in high inclination CVs. Superimposed on the emission lines is a transient narrow absorption

feature around phase 0.5. Phase offsets are observed between the radial velocity and eclipse ephemerides. Some systems exhibit modulated circular polarization indicating magnetic accretion onto the white dwarf. There is much variation in detail between individual systems and current models of SW Sex stars have difficulty explaining all of their observed properties. The general consensus seems to be that SW Sex stars contain accretion discs which are maintained in a bright state by a high, sustained mass-transfer rate and that these discs are complex in structure and may be variously eccentric, precessing, warped, tilted, or flared at the edge. The inner edge of the disc may also be truncated if the white dwarf is magnetic. For more information, see for example Hellier (1999), Gänsicke (2005), Rodriguez-Gil (2005), Rodriguez-Gil *et al.* (2007a), and Rodriguez-Gil *et al.* (2007b). Recently it has been claimed that the majority of novalike variables in the 3–4 hour orbital period range exhibit SW Sex-like properties to some extent (see Schmidtobreick *et al.* 2011). If true, this suggests that the SW Sex phenomenon may be a normal stage of CV evolution.

However, the bottom line at the moment seems to be that we really don't have a full understanding of the mechanisms which operate in SW Sex stars, and how they relate to other CVs with similar periods. But, as they appear to constitute the majority of CVs with orbital periods in the range 3–4 hours, they are important and need further study.

2. Aims of the project

This project was suggested to me in early 2007 by Boris Gänsicke at Warwick University who was interested to find out if studying eclipses of SW Sex stars would reveal evidence of changes in their orbital periods. Several of these stars had not been observed systematically for many years and were in need of new observations. The idea was therefore to combine published data on eclipse times going back in some cases over fifty years with new eclipse measurements to investigate the stability of their orbital periods.

The aims of the project were, for each star:

- to research all previously published eclipse times;
- to measure new eclipse times;
- to look for evidence of a change in orbital period;
- if found, to investigate its nature;
- to update ephemerides to aid future observations.

The eighteen SW Sex stars in Hoard's list which are deeply eclipsing, observable from the UK, and bright enough to yield accurate eclipse times with amateur-sized telescopes are the subject of this project. They are listed in

Table 1 in order of increasing orbital period (P_{orb}) along with the numbers of eclipse times found in the literature and new measurements reported here.

3. Previously published eclipse times

Eclipse times of minimum of these stars were discovered in over twenty different publications. For each star a list of published eclipse times obtained photographically (PG), photoelectrically (PE), or using CCD cameras was assembled along with corresponding cycle (orbit) numbers. As far as possible all times were confirmed to be in Heliocentric Julian Date (HJD). A very small number of visual eclipse times were also found but after careful consideration it was decided not to use these in this analysis because of their significantly larger and generally unknown uncertainties. In total 740 published eclipse times were located for these eighteen stars. Limitation on space prevents listing previously published eclipse times here. These are available through the AAVSO ftp site at ftp://ftp.aavso.org/public/datasets/jboydd401.txt.

Many published eclipse times did not specify errors. By examining the scatter in eclipse times obtained photographically their error was estimated to be, on average, 0.005d and this value was assigned to all photographic times. For photoelectric and CCD measurements published without errors each published set of data was considered separately and the root-mean-square (rms) residual of all the times in that set calculated with respect to a locally fitted linear ephemeris. This value was then assigned as an error to all the times in that set. These errors were typically in the range 0.0004d to 0.001d. In cases where the errors quoted appeared to be unrealistically small, more realistic errors were estimated by the same method. Each published time of minimum was given a weight equal to the inverse square of its error.

4. New measurements of eclipse times

Eclipses were observed using either a 0.25-m or 0.35-m telescope, both equipped with Starlight Xpress SXV-H9 CCD cameras, located at West Challow Observatory near Oxford, UK. Image scales were 1.45 and 1.21 arcsec/pixel, respectively. All measurements were made unfiltered for maximum photon statistics. Images were dark subtracted and flat fielded and a magnitude for the variable in each image derived with respect to between three and five nearby comparison stars using differential aperture photometry.

The dominant light source in these systems is the bright accretion disk, and its progressive eclipse by the secondary star results in eclipse profiles which are generally V-shaped with a rounded minimum. A quadratic fit was applied to the lower part of each eclipse from which the eclipse time of minimum and an associated analytical error were obtained. The magnitude at minimum was also obtained from this fit, enabling eclipse depths to be estimated. Some of

these stars exhibit relatively large random fluctuations in light output which can persist during eclipses, indicating the source of these fluctuations has not been eclipsed. This can result in significant distortion of their eclipse profiles and consequently larger scatter in their measured times of minimum. In general it was found that the analytical errors from the quadratic fits underestimated the real scatter in eclipse times. By examining this scatter for each star over a short interval during which the eclipse times were varying linearly, a multiplying factor was found which was then applied to the analytical errors. For stars with the smoothest eclipses, a factor of 3 gave errors consistent with the scatter of eclipse times while for the most distorted eclipses a factor of 7 was required. Each measured time of minimum was given a weight equal to the inverse square of its associated error. All new times of minimum were converted to HJD. As shown in Table 1, 298 new eclipse times were measured, increasing the number of available eclipse times for these stars by 40%.

Initially a constant orbital period for each star was assumed and a linear ephemeris computed based only on published eclipse times. Predictions were then made of the expected times of future eclipses. Although in some cases these predictions were found to be inaccurate by up to an hour, in all cases it was possible to project the historical cycle count forward and unambiguously assign cycle numbers to new eclipses as they were observed.

For each star we now had the HJD of the time of minimum for every measured eclipse plus an error and a corresponding cycle number. New eclipse times measured for the eighteen stars in the project are listed in Table 2.

5. O–C analysis

For each star a constant orbital period was assumed and a weighted linear ephemeris was calculated based on all available eclipse times, both published and new. O–C (Observed minus Calculated) values for the time of each eclipse with respect to this linear ephemeris were calculated and an O–C diagram generated for each star. O–C values following the horizontal line at O–C = 0 would confirm that the orbital period was indeed constant. O–C values following an upwards curve would indicate that the period was increasing while a downwards curve would indicate that the period was decreasing. Sinusoidal behavior would indicate that the orbital period was varying in a cyclical way, alternately increasing and decreasing.

6. Eclipsing SW Sex stars with orbital periods less than 4 hours

Most of the thirteen eclipsing SW Sex stars with orbital periods less than 4 hours have O–C diagrams which appear to be consistent with having a constant orbital period over the time span covered by the available observations, in some cases more than thirty years. However, in a few cases there is an indication of

possible non-linear behavior. This was investigated by applying a weighted sine fit to their O–C values using PERIOD04 (Lenz and Breger 2005) and comparing the rms residuals of linear and sinusoidal ephemerides. The conclusion was that ten of the thirteen stars were consistent with having linear ephemerides and therefore a constant orbital period while three, SW Sex, LX Ser, and UU Aqr, gave at least 20% smaller rms residuals for sinusoidal ephemerides indicating possible cyclical variation of their orbital periods.

Linear ephemerides for these thirteen SW Sex stars are given in Table 3. These should provide an accurate basis for predicting the times of future eclipses. Table 4 lists the parameters of possible cyclical variation and rms residuals of sinusoidal and linear ephemerides for SW Sex, LX Ser, and UU Aqr.

Figure 1 shows O–C diagrams for the ten SW Sex stars with orbital periods less than 4 hours which are consistent with linear ephemerides. Previously published observations are marked as black dots and new eclipse times as light-colored squares in this and subsequent figures. The larger scatter for some stars is primarily due to the less regular shape of their eclipses as noted above. Figure 2 shows O–C diagrams for SW Sex, LX Ser, and UU Aqr with dashed lines representing their sinusoidal ephemerides.

Given the length of their cyclical periods relative to the observed coverage and their relatively small amplitudes, more data are required to substantiate these cyclical interpretations. We do, however, note that similar behavior has been recorded in several other eclipsing CVs, see for example Borges *et al.* (2008) and references therein.

7. Eclipsing SW Sex stars with orbital periods greater than 4 hours

Five of the SW Sex stars have orbital periods longer than 4 hours: RW Tri, 1RXS J064434.5+334451, AC Cnc, V363 Aur, and BT Mon. For all these stars the eclipse times appear, to varying degrees, to be inconsistent with the assumption of a constant orbital period. Each of these stars is now considered individually.

7.1. RW Tri

A total of 115 published and 21 new eclipse times are available for RW Tri starting in 1957. The O–C diagram for RW Tri representing the residuals to a linear ephemeris with long-term average orbital period 0.231883193(2) day is shown in Figure 3a. The scatter in the data is sufficiently large that a time calibration problem with some of the published times must be considered a possibility. We decided to exclude the eleven eclipse times around HJD 2449600 from subsequent analysis as their O–C values were more than 5 minutes larger than those before and after. Between approximately HJD 2442000 and HJD 2450000 the period slowly decreased. It then started to increase and is currently longer than the long-term average. Taken as a whole, the data suggest cyclical

variation of the orbital period. A weighted sine fit to the O–C data using PERIOD04 gives the results listed in Table 5 and shown as a dashed line in Figure 3a. Also listed in Table 5 are the rms residuals of sinusoidal and linear fits indicating that sinusoidal interpretation is statistically favored. However, given the large scatter in the data and the fact that just over one possible cycle has been observed, a convincing analysis will require data over a much longer time span. An earlier analysis by Africano *et al.* (1978) suggested sinusoidal variation with a period of either 7.6 or 13.6 years but with the addition of more recent data neither of these periods survives.

A linear ephemeris fitted to the data over the past seven years which should be useful for predicting eclipses in the near future is given in Table 3.

The out-of-eclipse magnitude of RW Tri, including early measurements reported by Walker (1963), observations from the AAVSO International Database and from ASAS (Pojmański *et al.* 2005), and new observations reported here, is plotted in Figure 3b. This shows a slight brightening around HJD 2450000 but otherwise little change. Eclipse depth has remained approximately constant over the observed time span (Figure 3c). Table 6 lists measurements of eclipse depth for the five stars with long orbital periods.

7.2. 1RXS J064434.5+334451

Twenty unpublished eclipse times for 1RXS J064434.5+334451 from 2005 to 2008 were kindly provided by David Sing and Betsy Green, who first identified this star as a CV (Sing *et al.* 2007). The first times reported here were in 2010 and these were consistent with those of Sing and Green, giving the orbital period 0.26937447(4) day and the linear eclipse ephemeris given in Table 3.

Surprisingly, eclipses in March 2011 were about three minutes late relative to this ephemeris. This behavior has since continued with most eclipses occurring between two and four minutes later than expected assuming a linear ephemeris based on observations up to and including 2010 (HJD < 2455500—see Figure 4a). Since March 2011 the mean orbital period has been slightly shorter at 0.2693741(2) day. The out-of-eclipse magnitude experienced a rise prior to, and a dip following, the O–C discontinuity (Figure 4b). Eclipses became, temporarily, about 10% deeper after the O–C discontinuity (Figure 4c and Table 6).

7.3. AC Cnc

For AC Cnc, forty-six published and eleven new eclipse times are available and fitting a linear ephemeris to these gives the O–C diagram shown in Figure 5a. Times measured before 1980 are photographic and have a large scatter. Using the more precise photoelectric and CCD measurements since 1980 (HJD > 2444000) gives an orbital period of 0.30047738(1) day and the linear eclipse ephemeris given in Table 3.

A recent paper by Qian *et al.* (2007) argues for a decreasing orbital period

and also proposes a third body in the system causing sinusoidal modulation in the O–C diagram. A quadratic ephemeris calculated using the more reliable photoelectric and CCD measurements following HJD 2444000 and including the new times reported here gives a rate of period change of $2.1(2.2) \times 10^{-9}$ days/year, considerably smaller than the rate of $12.4(4.4) \times 10^{-9}$ days/year found by Qian *et al.* and consistent with no secular period change. However, there is an indication of cyclical behavior in the O–C diagram in Figure 5a. A weighted sine fit to the O–C data after HJD 2444000 gives the results listed in Table 5 and shown as a dashed line in Figure 5a. This is a shorter period and smaller amplitude than proposed by Qian *et al.* Observations over a much longer period are required to establish the reality and true parameters of this modulation. With few measurements available, there is little indication of variation in either the out-of-eclipse magnitude of AC Cnc (Figure 5b) or the eclipse depth (Figure 5c and Table 6).

7.4. V363 Aur (also known as Lanning 10)

The data for V363 Aur comprise eighteen published and twenty-seven new eclipse times and show a significant curvature in the O–C diagram with respect to a linear ephemeris, indicating a reducing orbital period (Figure 6a). A quadratic ephemeris, shown as a dashed line in Figure 6a, gives a mean rate of period change of $dP/dt = -6.6(2) \times 10^{-8}$ days/year over the thirty-one years covered by the data. The O–C residuals to this quadratic ephemeris (Figure 6b) show an apparently cyclical variation. A weighted sine fit to the residuals of the quadratic ephemeris gives the results listed in Table 5 and shown as a dashed line in Figure 6b, but these results must be considered speculative as only one cycle has been observed.

Over the past six years the mean orbital period has been 0.32124073(3) day and the eclipse times are well fitted by the linear ephemeris given in Table 3.

Figure 6c shows the out-of-eclipse magnitude of V363 Aur obtained from the AAVSO database plus our new measurements. Although the scatter is large, there appears to have been a slight dip centred around HJD 2449000. Figure 6d and Table 6 show the depth of eclipses of V363 Aur over the same interval. Although there are little data in the early years, recently there has been a progressive reduction in eclipse depth.

7.5. BT Mon

BT Mon is the progenitor system of a classical nova outburst observed in 1939. There are eight published eclipse times plus fourteen new times covering a thirty-four year time span. An O–C diagram with respect to a linear ephemeris shows significant curvature indicating a reducing orbital period (Figure 7a). A quadratic ephemeris, shown as a dashed line in Figure 7a, gives a mean rate of period change of $dP/dt = -3.3(2) \times 10^{-8}$ days/year. The O–C residuals to this quadratic ephemeris are shown in Figure 7b along with a

dashed line indicating the results of a weighted sine fit whose parameters are listed in Table 5. This sinusoidal ephemeris is marginally favored over the quadratic ephemeris although, as before, this conclusion must remain tentative until more data are available.

Published eclipse times are scarce in the middle of this time span. Magnitude measurements of BT Mon obtained with the Roboscope system (Honeycutt 2003) between 1991 and 2005 were kindly provided by Kent Honeycutt. The Roboscope data were divided into two groups, before and after the start of 1999. By adopting mean orbital periods from the above quadratic ephemeris for each of these time intervals, two additional eclipse times have been synthesised using the Roboscope data. These have larger errors than directly measured eclipse times and are shown as triangles in Figures 7. They were not used in the above analysis but are consistent with its results and slightly favor the sinusoidal interpretation.

Over the last seventeen years the mean orbital period has been 0.33381322(2) day and eclipse times in the near future may be represented by the linear ephemeris given in Table 3.

Plotting out-of-eclipse magnitudes from Roboscope together with our new data (Figure 7c), we see a noticeable dip around HJD 2451000 followed by a gradual increase. Although there are little data, the eclipse depth shows a slowly decreasing trend over the same interval (Figure 7d and Table 6).

8. Conclusions

When this project started, most published analyses of SW Sex stars concluded that they had constant orbital periods. While the new data confirm that this is true for many of these stars, for some it is clearly not the case. There is a significant difference between the behavior of stars with orbital periods below and above 4 hours. Below 4 hours, ten of the thirteen stars appear to have constant orbital periods with three showing possible signs of low amplitude cyclical variation. The longer period stars all show more dynamic behavior with either a sudden change of orbital period or larger amplitude cyclical variation, either with or without a secular period change.

Eclipse times for all these stars will continue to be monitored to see if those with constant periods maintain this behavior and in the other more interesting cases with longer orbital periods to discover what light further data will shed on the tentative interpretations presented here.

9. Acknowledgements

I am grateful to Boris Gänsicke for suggesting this project and for his continuing support and encouragement. I am indebted to David Sing and Betsy Green for providing unpublished data on 1RXS J064434.5+334451

and to Kent Honeycutt for providing unpublished Roboscope data on BT Mon. I acknowledge with thanks that this research has made use of variable star observations from the AAVSO International Database contributed by researchers worldwide, data from the All Sky Automated Survey, and from NASA's Astrophysics Data System. Helpful comments from an anonymous referee have improved the paper.

References

Africano, J. L., Nather, R. E., Patterson, J., Robinson, E. L., and Warner, B. 1978, *Publ. Astron. Soc. Pacific*, **90**, 568.

Borges, B. W., Baptista, R., Papadimitriou, C., and Giannakis, O. 2008, *Astron. Astrophys.*, **480**, 481.

Gaensicke, B. 2005, in *The Astrophysics of Cataclysmic Variables and Related Objects*, ed. J. -M. Hameury and J. -P. Lasota. ASP Conf. Ser. 330, Astron. Soc. Pacific, San Francisco, 3.

Hellier, C. 1999, *New Astron. Rev.*, **44**, 131.

Hoard, D., Szkody, P., Froning, C. S., Long, K. S., and Knigge, C. 2003, *Astron. J.*, **126**, 2473 (see also http://www.dwhoard.com/home/biglist).

Honeycutt, R. K. 2003, *Bull. Amer. Astron. Soc.*, **35**, 752.

Lenz, P., and Breger M. 2005, *Commun. Asteroseismology*, **146**, 53.

Pojmański, G., Pilecki, B., and Szczygiel, D. 2005, *Acta Astron.*, **55**, 275.

Qian, S. -B., Dai, Z. -B., He, J. -J., Yuan, J. Z., Xiang, F. Y., and Zejda, M. 2007, *Astron. Astrophys.*, **466**, 589.

Rodriguez-Gil, P. 2005, in *The Astrophysics of Cataclysmic Variables and Related Objects*, ed. J. -M. Hameury and J. -P. Lasota. ASP Conf. Ser. 330, Astron. Soc. Pacific, San Francisco, 335.

Rodriguez-Gil, P., Schmidtobreick, L., and Gänsicke, B. T. 2007a, *Mon. Not. Roy. Astron. Soc.*, **374**, 1359.

Rodriguez-Gil, P., *et al.* 2007b, *Mon. Not. Roy. Astron. Soc.*, **377**, 1747.

Samus, N. N., *et al.* 2012, *General Catalogue of Variable Stars* (http://www.sai.msu.su/gcvs/gcvs/).

Schmidtobreick, L., Rodriguez-Gil, P., and Gänsicke, B. T. 2011, http://adsabs.harvard.edu/abs/2011arXiv1111.6678S

Sing, D. K., Green, E. M., Howell, S. B., Holberg, J. B., Lopez-Morales, M., Shaw, J. S., and Schmidt, G. D. 2007, *Astron. Astrophys.*, **474**, 951.

Thorstensen, J., Ringwald, F. A., Wade, R. A., Schmidt, G. D., and Norsworthy, J. E. 1991, *Astron. J.*, **102**, 272.

Walker, M. F. 1963, *Astrophys. J.*, **137**, 485.

Table 1. Eclipsing SW Sex stars studied in this project.

Name	P_{orb} *(hrs)*	*Previously published eclipse times*	*New eclipse times reported here*
HS 0728+6738	3.21	14	24
SW Sex	3.24	32	11
DW UMa	3.28	176	20
HS 0129+2933 = TT Tri	3.35	27	11
V1315 Aql	3.35	71	16
PX And	3.51	38	22
HS 0455+8315	3.57	5	15
HS 0220+0603	3.58	13	13
BP Lyn	3.67	16	13
BH Lyn	3.74	29	16
LX Ser	3.80	50	10
UU Aqr	3.93	50	15
V1776 Cyg	3.95	12	17
RW Tri	5.57	115	21
1RXS J064434.5+334451	6.47	20	22
AC Cnc	7.21	46	11
V363 Aur = Lanning 10	7.71	18	27
BT Mon	8.01	8	14
Total	—	740	298

Table 2. Eclipse times for stars measured in this project with errors and corresponding cycle numbers.

Star/Eclipse time of minimum (HJD)	*Error (d)*	*Cycle number*	*Star/Eclipse time of minimum (HJD)*	*Error (d)*	*Cycle number*
HS 0728+6738			2454895.39084	0.00009	21659
2453810.40077	0.00041	13539	2454907.41644	0.00022	21749
2453836.45653	0.00024	13734	2455188.41832	0.00021	23852
2453851.42254	0.00023	13846	2455191.35834	0.00014	23874
2453853.42648	0.00013	13861	2455200.31029	0.00019	23941
2454174.51418	0.00022	16264	2455515.38459	0.00024	26299
2454181.32859	0.00025	16315	2455520.32865	0.00038	26336
2454185.33706	0.00025	16345	2455533.42346	0.00028	26434
2454186.40643	0.00024	16353	2455889.38551	0.00036	29098
2454473.42029	0.00023	18501	2455891.39036	0.00024	29113
2454493.33001	0.00023	18650	2455893.39432	0.00019	29128
2454507.35967	0.00039	18755			
2454835.39541	0.00032	21210	SW Sex		
2454891.38182	0.00010	21629	2454185.43702	0.00044	72965

table continued on following pages

Table 2. Eclipse times for stars measured in this project with errors and corresponding cycle numbers.

Star/Eclipse time of minimum (HJD)	*Error (d)*	*Cycle number*	*Star/Eclipse time of minimum (HJD)*	*Error (d)*	*Cycle number*
2454186.38145	0.00029	72972	2455188.47729	0.00030	18963
2454553.41407	0.00048	75692	2455191.27007	0.00019	18983
2454564.34410	0.00020	75773	2455460.49099	0.00013	20911
2454906.41325	0.00019	78308	2455533.38206	0.00022	21433
2454907.49269	0.00019	78316	2455827.45860	0.00014	23539
2455260.35696	0.00018	80931	2455835.41776	0.00016	23596
2455278.43821	0.00012	81065	2455836.39518	0.00010	23603
2455630.35814	0.00026	83673			
2455660.44910	0.00014	83896	V1315 Aql		
2455662.33853	0.00028	83910	2454272.50437	0.00018	59916
			2454306.44865	0.00027	60159
DW UMa			2454313.43262	0.00072	60209
2454181.41978	0.00019	58214	2454651.48330	0.00048	62629
2454185.38111	0.00030	58243	2454670.48100	0.00046	62765
2454224.45051	0.00044	58529	2454810.31097	0.00082	63766
2454473.34780	0.00038	60351	2455004.47952	0.00029	65156
2454564.46466	0.00020	61018	2455006.43480	0.00049	65170
2454580.44785	0.00033	61135	2455038.42351	0.00055	65399
2454580.58433	0.00027	61136	2455052.39293	0.00070	65499
2454588.37104	0.00029	61193	2455463.36184	0.00047	68441
2454588.50711	0.00019	61194	2455464.33978	0.00036	68448
2454593.42488	0.00022	61230	2455490.32143	0.00026	68634
2454596.43092	0.00034	61252	2455777.38468	0.00040	70689
2454884.39723	0.00025	63360	2455783.39087	0.00040	70732
2454892.32009	0.00025	63418	2455903.24546	0.00047	71590
2455239.30026	0.00022	65958			
2455263.34322	0.00015	66134	PX And		
2455270.31000	0.00014	66185	2454318.44729	0.00051	34708
2455278.37037	0.00017	66244	2454319.47234	0.00046	34715
2455627.39978	0.00017	68799	2454325.47261	0.00036	34756
2455628.35604	0.00020	68806	2454448.40773	0.00061	35596
2455629.31205	0.00030	68813	2454473.28943	0.00051	35766
			2454503.29163	0.00022	35971
HS 0129+2933 = TT Tri			2454761.45718	0.00049	37735
2454061.46332	0.00014	10892	2454770.38547	0.00069	37796
2454081.29219	0.00016	11034	2455064.40680	0.00108	39805
2454086.45848	0.00008	11071	2455066.45577	0.00069	39819
2455106.37036	0.00038	18375	2455173.29503	0.00032	40549

table continued on following pages

Table 2. Eclipse times for stars measured in this project with errors and corresponding cycle numbers, cont.

Star/Eclipse time of minimum (HJD)	*Error (d)*	*Cycle number*	*Star/Eclipse time of minimum (HJD)*	*Error (d)*	*Cycle number*
2455186.32065	0.00020	40638	2455495.35697	0.00031	19649
2455188.36884	0.00125	40652	2455515.34977	0.00031	19783
2455191.29553	0.00055	40672	2455533.40410	0.00029	19904
2455201.24653	0.00014	40740	2455867.48013	0.00024	22143
2455460.43876	0.00028	42511	2455884.48964	0.00012	22257
2455495.26963	0.00061	42749			
2455515.46733	0.00025	42887	BP Lyn		
2455795.43984	0.00024	44800	2454186.44462	0.00069	41257
2455819.44115	0.00069	44964	2454891.36892	0.00095	45870
2455823.39248	0.00044	44991	2454906.49781	0.00084	45969
2455901.25250	0.00064	45523	2455239.32473	0.00058	48147
			2455260.41122	0.00042	48285
HS 0455+8315			2455263.31415	0.00049	48304
2454061.40139	0.00016	14807	2455571.38461	0.00074	50320
2454063.48351	0.00020	14821	2455594.30701	0.00042	50470
2454078.35643	0.00014	14921	2455619.52087	0.00059	50635
2454112.41335	0.00017	15150	2455914.44759	0.00041	52565
2454114.49593	0.00023	15164	2455930.34125	0.00063	52669
2454115.38831	0.00017	15170	2455932.32762	0.00066	52682
2454895.44552	0.00018	20415	2455942.41314	0.00039	52748
2454906.45070	0.00013	20489			
2454907.34318	0.00026	20495	BH Lyn		
2455065.43666	0.00029	21558	2454181.48914	0.00029	44915
2455495.39753	0.00032	24449	2454186.32132	0.00042	44946
2455519.49112	0.00017	24611	2454199.41436	0.00053	45030
2455526.48082	0.00018	24658	2454482.32954	0.00048	46845
2455835.38030	0.00021	26735	2454834.45234	0.00046	49104
2455850.40114	0.00018	26836	2454884.33284	0.00052	49424
			2455247.36666	0.00027	51753
HS 0220+0603			2455260.46000	0.00033	51837
2454061.32109	0.00048	10038	2455267.31793	0.00059	51881
2454081.31479	0.00032	10172	2455594.34608	0.00035	53979
2454081.46403	0.00018	10173	2455628.32676	0.00041	54197
2454086.38783	0.00026	10206	2455670.41251	0.00040	54467
2455156.35608	0.00028	17377	2455675.40111	0.00031	54499
2455188.43603	0.00027	17592	2455895.34197	0.00038	55910
2455200.37262	0.00034	17672	2455902.35570	0.00039	55955
2455490.43180	0.00028	19616	2455941.32605	0.00040	56205

table continued on following pages

Table 2. Eclipse times for stars measured in this project with errors and corresponding cycle numbers, cont.

Star/Eclipse time of minimum (HJD)	*Error (d)*	*Cycle number*	*Star/Eclipse time of minimum (HJD)*	*Error (d)*	*Cycle number*
LX Ser			2454994.46940	0.00068	50248
2454316.41420	0.00032	63266	2455037.46488	0.00052	50509
2454628.52570	0.00023	65236	2455057.39969	0.00051	50630
2454976.44297	0.00038	67432	2455176.34096	0.00062	51352
2454994.50414	0.00026	67546	2455460.34923	0.00100	53076
2455001.47525	0.00033	67590	2455494.45030	0.00101	53283
2455037.43960	0.00020	67817	2455778.46040	0.00052	55007
2455662.45627	0.00040	71762	2455849.46194	0.00052	55438
2455663.40637	0.00045	71768	2455893.28160	0.00088	55704
2455672.43730	0.00041	71825			
2455778.42860	0.00031	72494	RW Tri		
			2454392.38737	0.00024	57197
UU Aqr			2454419.51756	0.00027	57314
2454323.44995	0.00046	48760	2454447.34346	0.00020	57434
2454357.47405	0.00027	48968	2454789.37226	0.00041	58909
2454365.48955	0.00036	49017	2454810.47333	0.00064	59000
2454728.47437	0.00051	51236	2454835.28542	0.00050	59107
2454735.34486	0.00034	51278	2455063.45767	0.00047	60091
2454736.32601	0.00056	51284	2455106.35664	0.00047	60276
2454789.32574	0.00032	51608	2455172.44338	0.00026	60561
2455038.45994	0.00069	53131	2455487.34152	0.00042	61919
2455059.39716	0.00052	53259	2455490.35562	0.00017	61932
2455106.34585	0.00043	53546	2455533.48590	0.00023	62118
2455469.49424	0.00052	55766	2455822.41233	0.00026	63364
2455490.26865	0.00048	55893	2455828.44141	0.00023	63390
2455778.49715	0.00019	57655	2455867.39741	0.00048	63558
2455795.50952	0.00019	57759	2455881.31079	0.00014	63618
2455893.33048	0.00019	58357	2455889.42621	0.00028	63653
			2455914.23796	0.00028	63760
V1776 Cyg			2455950.41154	0.00024	63916
2454238.48406	0.00059	45659	2455953.42610	0.00051	63929
2454254.46252	0.00044	45756	2455957.36910	0.00018	63946
2454306.51977	0.00050	46072			
2454314.42730	0.00053	46120	1RXS J064434.5+334451		
2454646.54029	0.00092	48136	2455307.42924	0.00074	7067
2454668.44971	0.00092	48269	2455310.39210	0.00056	7078
2454670.42804	0.00080	48281	2455313.35557	0.00049	7089
2454770.42363	0.00115	48888	2455627.44814	0.00048	8255

table continued on next page

Table 2. Eclipse times for stars measured in this project with errors and corresponding cycle numbers, cont.

Star/Eclipse time of minimum (HJD)	*Error (d)*	*Cycle number*	*Star/Eclipse time of minimum (HJD)*	*Error (d)*	*Cycle number*
2455629.33392	0.00043	8262	2454810.38137	0.00031	31915
2455634.45149	0.00035	8281	2454827.40653	0.00042	31968
2455655.46296	0.00045	8359	2454835.43772	0.00044	31993
2455658.42635	0.00025	8370	2454891.33360	0.00054	32167
2455682.39947	0.00042	8459	2454892.29747	0.00021	32170
2455685.36351	0.00051	8470	2455188.48144	0.00054	33092
2455850.48993	0.00045	9083	2455191.37255	0.00040	33101
2455854.53082	0.00023	9098	2455200.36736	0.00026	33129
2455891.43482	0.00015	9235	2455515.50429	0.00013	34110
2455905.44214	0.00063	9287	2455516.46885	0.00021	34113
2455914.33106	0.00043	9320	2455524.49896	0.00034	34138
2455924.29847	0.00046	9357	2455526.42586	0.00026	34144
2455932.37955	0.00032	9387	2455627.29626	0.00020	34458
2455949.35041	0.00027	9450	2455634.36298	0.00020	34480
2455953.38926	0.00037	9465	2455649.46157	0.00047	34527
2455957.43085	0.00052	9480	2455854.41351	0.00026	35165
2455959.31737	0.00024	9487	2455888.46463	0.00016	35271
2455960.39430	0.00028	9491	2455891.35618	0.00021	35280
			2455905.49122	0.00039	35324
AC Cnc			2455914.48560	0.00015	35352
2454199.45197	0.00026	32978	2455950.46438	0.00013	35464
2454507.44198	0.00021	34003	2455954.31900	0.00028	35476
2454891.45161	0.00036	35281			
2454892.35306	0.00032	35284	BT Mon		
2455260.43835	0.00023	36509	2454447.47617	0.00043	32820
2455270.35440	0.00042	36542	2454891.44778	0.00052	34150
2455619.50814	0.00082	37704	2454892.44988	0.00045	34153
2455630.32565	0.00024	37740	2455238.27878	0.00050	35189
2455675.39674	0.00047	37890	2455239.28089	0.00082	35192
2455949.43118	0.00029	38802	2455257.30609	0.00035	35246
2455959.34723	0.00034	38835	2455260.31093	0.00041	35255
			2455277.33531	0.00068	35306
V363 Aur = Lanning 10			2455571.42510	0.00058	36187
2454181.39163	0.00043	29957	2455595.46030	0.00062	36259
2454392.44674	0.00017	30614	2455600.46698	0.00093	36274
2454447.37885	0.00024	30785	2455619.49354	0.00048	36331
2454471.47221	0.00031	30860	2455960.31808	0.00089	37352
2454473.39980	0.00037	30866	2455968.33013	0.00047	37376

Table 3. Linear ephemerides for the SW Sex stars in the project. For RW Tri, 1RXS J064434.5+334451, AC Cnc, V363 Aur, and BT Mon this linear ephemeris only represents behavior in the recent past. Over longer time intervals their behavior is more complex (see text).

Star	*Ephemerides*
HS 0728+6738	2452001.32739(8) + 0.133619437(4) E
SW Sex	2444339.64968(11) + 0.134938490(2) E
DW UMa	2446229.00601(8) + 0.136606547(2) E
HS 0129+2933 = TT Tri	2452540.53218(9) + 0.139637462(6) E
V1315 Aql	2445902.84037(10) + 0.139689961(2) E
PX And	2449238.83661(17) + 0.146352746(4) E
HS 0455+8315	2451859.24679(15) + 0.148723901(8) E
HS 0220+0603	2452563.57407(7) + 0.149207696(5) E
BP Lyn	2447881.85799(23) + 0.152812531(6) E
BH Lyn	2447180.33522(41) + 0.155875629(8) E
LX Ser	2444293.02345(18) + 0.158432492(3) E
UU Aqr	2446347.26651(6) + 0.163580450(2) E
V1776 Cyg	2446716.67956(27) + 0.164738679(6) E
RW Tri	2441129.35318(49) + 0.231883392(9) E
1RXS J064434.5+334451	2453403.75955(12) + 0.26937447(4) E
AC Cnc	2444290.30892(36) + 0.30047738(1) E
V363 Aur = Lanning 10	2444557.98318(89) + 0.32124073(3) E
BT Mon	2443491.72616(45) + 0.33381322(2) E

Table 4. Parameters of possible cyclical variation in orbital period for SW Sex, LX Ser, and UU Aqr.

Star	*Cyclical period (years)*	*Semi-amplitude (seconds)*	*Sinusoidal ephemeris rms residual*	*Linear ephemeris rms residual*
SW Sex	24.0(7)	69(5)	32.1	65.2
LX Ser	28(2)	48(6)	55.7	69.4
UU Aqr	20.3(6)	48(4)	34.9	43.6

Table 5. Parameters of possible cyclical variation in orbital period for RW Tri, AC Cnc, V363 Aur, and BT Mon.

Star	*Cyclical period (years)*	*Semi-amplitude (seconds)*	*Sinusoidal ephemeris rms residual*	*Linear ephemeris rms residual*	*Quadratic ephemeris rms residual*
RW Tri	36.7(4)	161(5)	80.8	128.0	—
AC Cnc*	13.5(3)	140(13)	106.8	141.3	139.5
V363 Aur	27.7(7)	119(6)	58.8	—	92.2
BT Mon	29(2)	113(15)	62.0	—	67.7

**Only including data after HJD 2444000.*

Table 6. Eclipse depth measured in this project for RW Tri, 1RXS J064434.5+334451, AC Cnc, V363 Aur, and BT Mon.

Eclipse time (HJD)	*Eclipse depth (magnitude)*	*Eclipse time (HJD)*	*Eclipse depth (magnitude)*
RW Tri		2455627.44814	1.26
2454392.38737	1.72	2455629.33392	1.27
2454419.51756	1.84	2455634.45149	0.90
2454447.34346	1.96	2455655.46296	1.22
2454810.47333	1.84	2455658.42635	1.29
2454835.28542	1.63	2455682.39947	1.31
2455063.45767	1.76	2455685.36351	1.23
2455106.35664	1.92	2455850.48993	1.17
2455172.44338	1.89	2455854.53082	1.11
2455487.34152	1.78	2455891.43482	1.12
2455490.35562	1.71	2455905.44214	1.13
2455533.48590	1.84	2455914.33106	1.08
2455822.41233	1.62	2455932.37955	1.14
2455828.44141	1.43	2455949.35041	1.02
2455867.39741	1.59	2455953.38926	1.07
2455881.31079	1.81	2455957.43085	0.94
2455889.42621	1.89	2455959.31737	0.97
2455914.23796	1.69	2455960.39430	1.14
2455950.41154	2.06		
2455953.42610	1.97	AC Cnc	
2455957.36910	1.56	2454199.45197	0.96
		2454507.44198	1.04
1RXSJ064434.5+334451		2454891.45161	0.94
2455307.42924	1.13	2454892.35306	0.92
2455310.39210	1.06	2455260.43835	1.00

table continued on next page

Table 6. Eclipse depth measured in this project for RW Tri, 1RXS J064434.5+334451, AC Cnc, V363 Aur, and BT Mon, cont.

Eclipse time (HJD)	*Eclipse depth (magnitude)*	*Eclipse time (HJD)*	*Eclipse depth (magnitude)*
2455630.32565	0.87	2455634.36298	0.68
2455949.43118	1.14	2455649.46157	0.69
		2455854.41351	0.58
V363 Aur = Lanning 10		2455888.46463	0.53
2454392.44674	0.80	2455891.35618	0.62
2454447.37885	0.71	2455905.49122	0.65
2454471.47221	0.90	2455950.46438	0.71
2454473.39980	0.83		
2454810.38137	0.62	BT Mon	
2454827.40653	0.66	2454891.44778	1.74
2454835.43772	0.77	2454892.44988	1.82
2454892.29747	0.64	2455257.30609	2.01
2455191.37255	0.76	2455260.31093	1.90
2455515.50429	0.56	2455277.33531	1.96
2455516.46885	0.68	2455571.42510	1.61
2455524.49896	0.60	2455960.31808	1.49
2455526.42586	0.48	2455968.33013	1.62
2455627.29626	0.62		

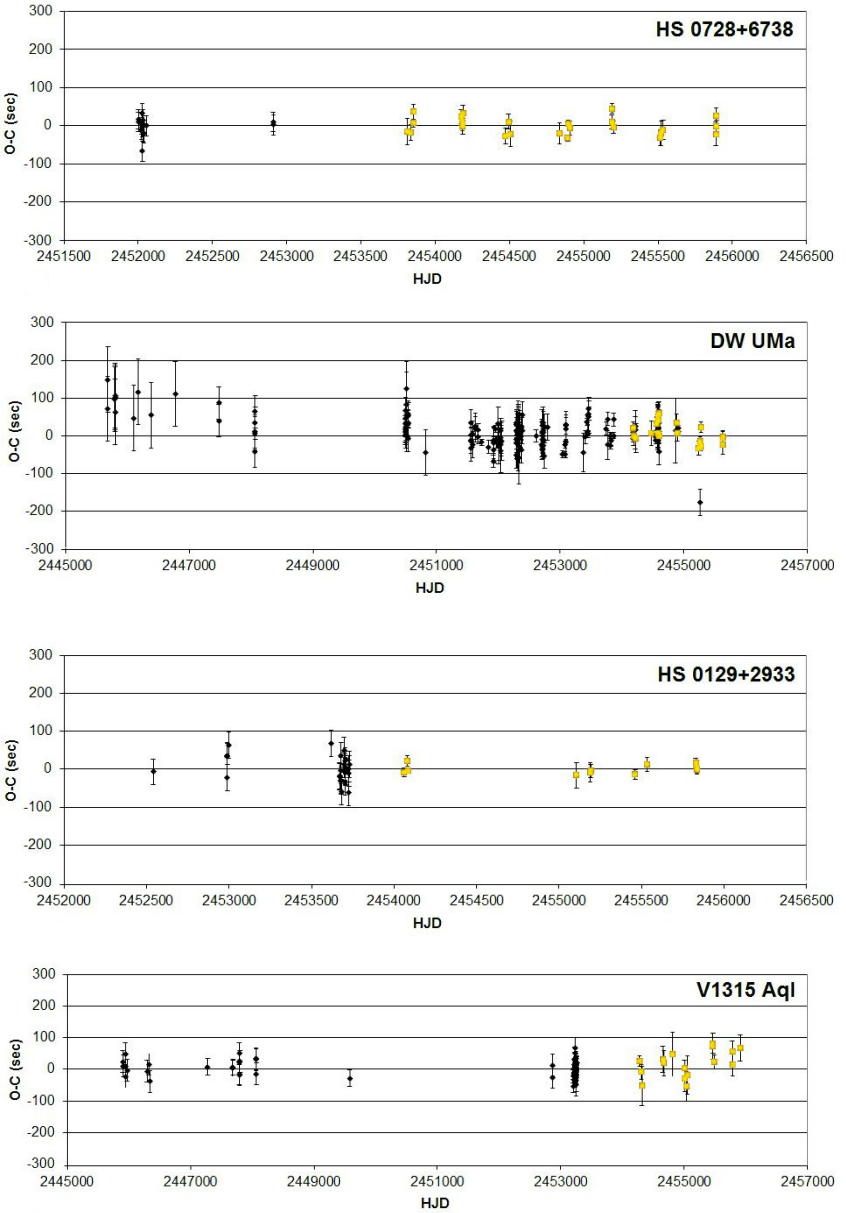

Figures 1a–j, O–C diagrams with respect to the linear ephemerides in Table 3 for those SW Sex stars with $P_{orb} < 4$ hours which are consistent with constant orbital periods. Previously published observations are marked as black dots and new eclipse times as light squares in this and subsequent figures (continued on next page).

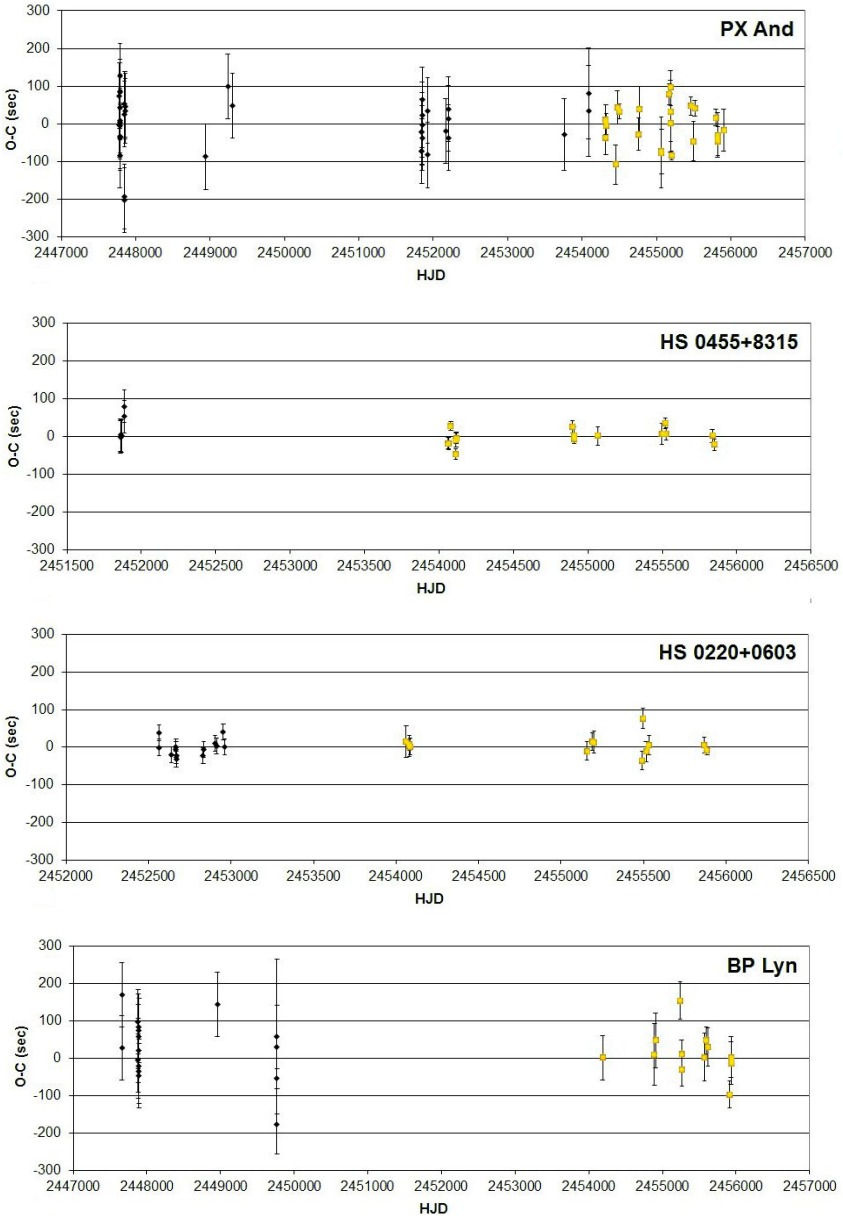

Figures 1a–j, cont. O–C diagrams with respect to the linear ephemerides in Table 3 for those SW Sex stars with $P_{orb} < 4$ hours which are consistent with constant orbital periods. Previously published observations are marked as black dots and new eclipse times as light squares in this and subsequent figures (continued on next page).

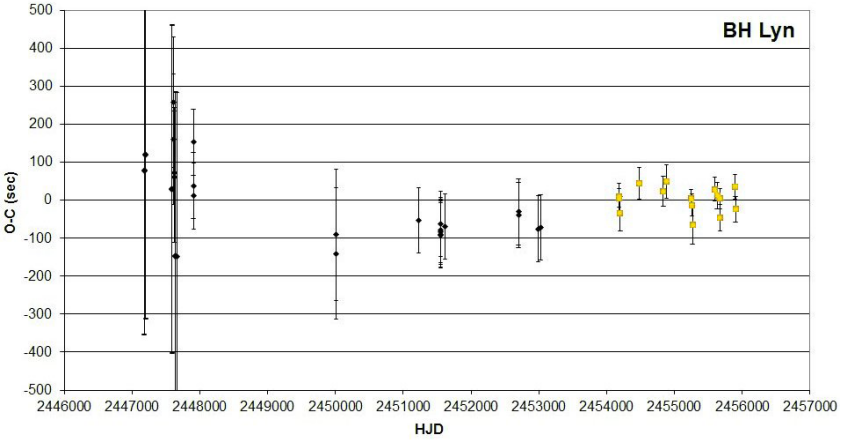

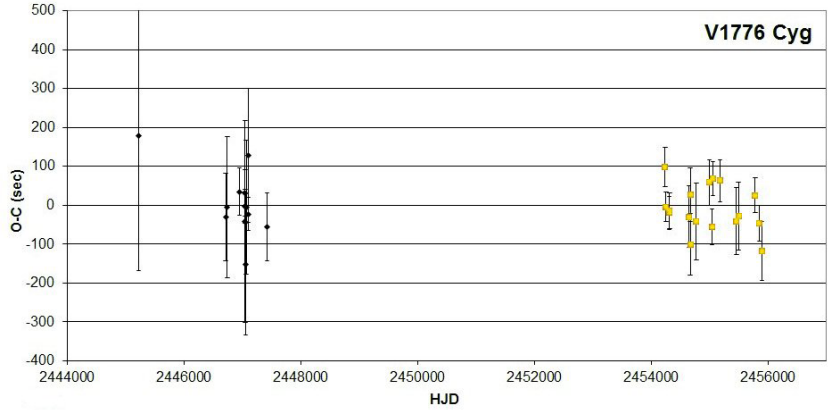

Figures 1a–j, cont. O–C diagrams with respect to the linear ephemerides in Table 3 for those SW Sex stars with $P_{orb} < 4$ hours which are consistent with constant orbital periods. Previously published observations are marked as black dots and new eclipse times as light squares in this and subsequent figures.

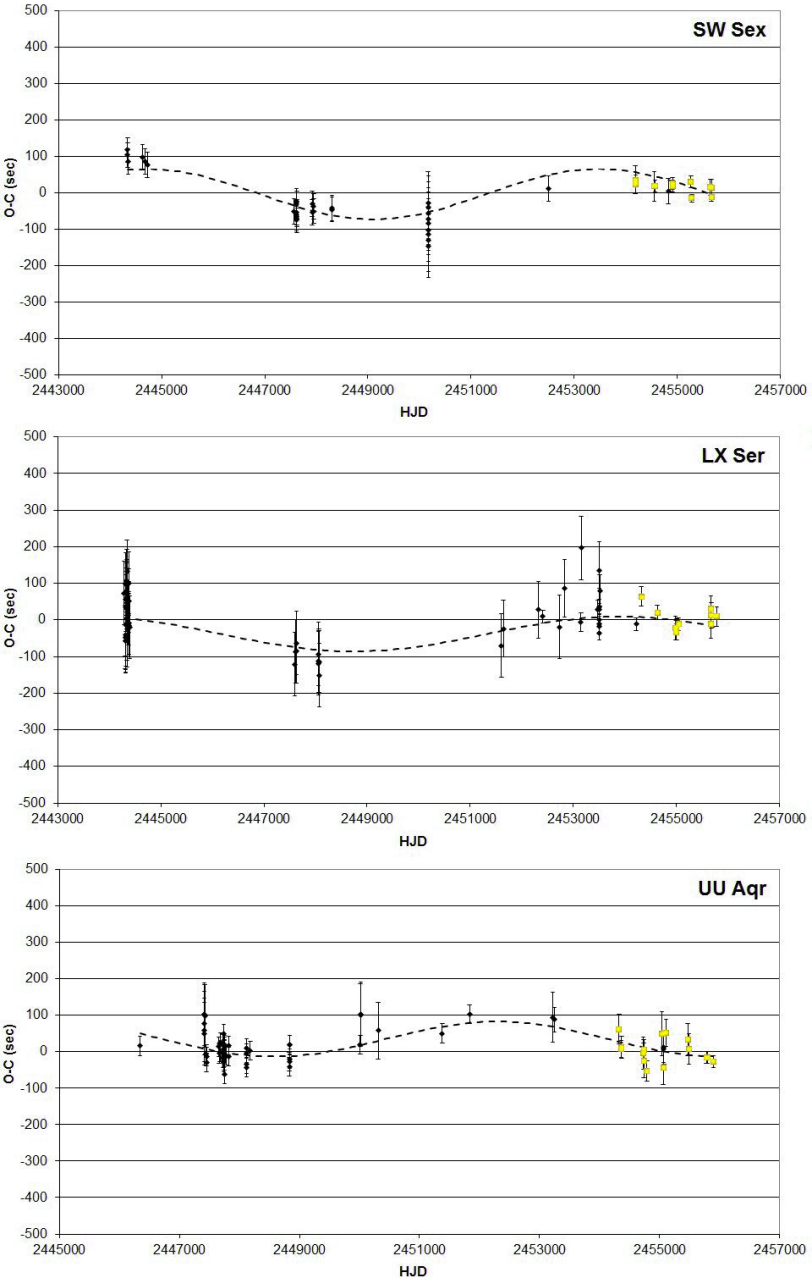

Figure 2. O–C diagrams with respect to the linear ephemerides in Table 3 for those SW Sex stars with $P_{orb} < 4$ hrs which show possible cyclical variation in orbital period (dashed lines).

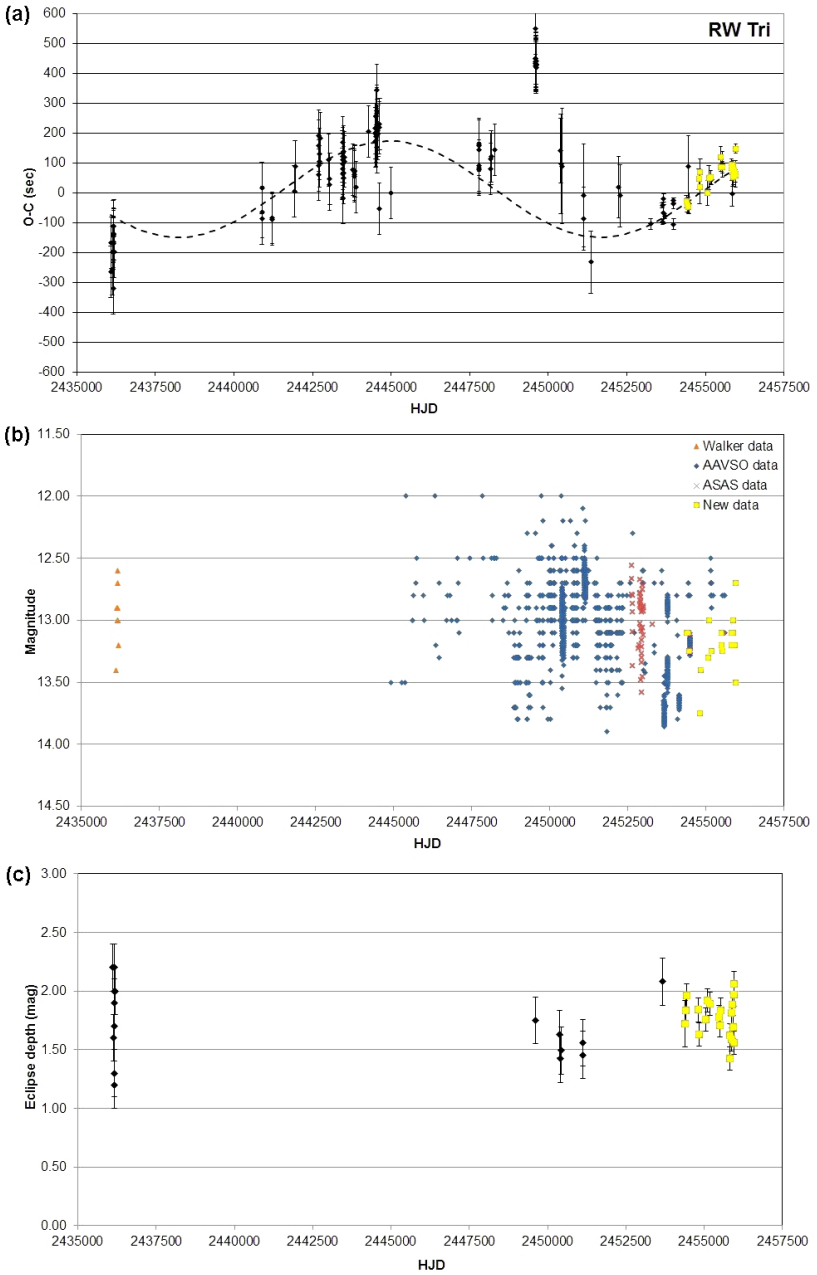

Figure 3. RW Tri: (a) O–C diagram with respect to a linear ephemeris showing a cyclical variation of orbital period (dashed line), (b) out-of-eclipse magnitude, and (c) eclipse depth.

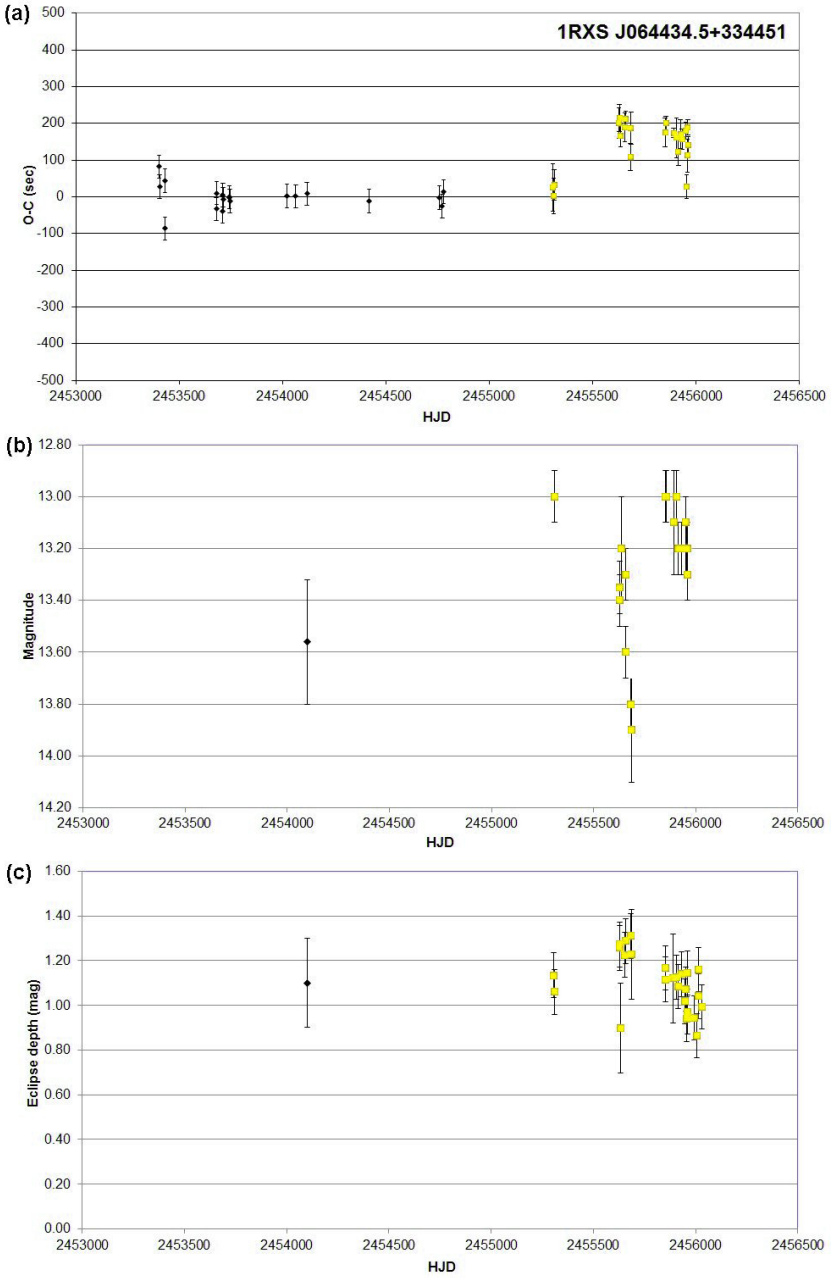

Figure 4. 1RXS J064434.5+334451: (a) O–C diagram with respect to a linear ephemeris for HJD < 2455500, (b) out-of-eclipse magnitude, and (c) eclipse depth.

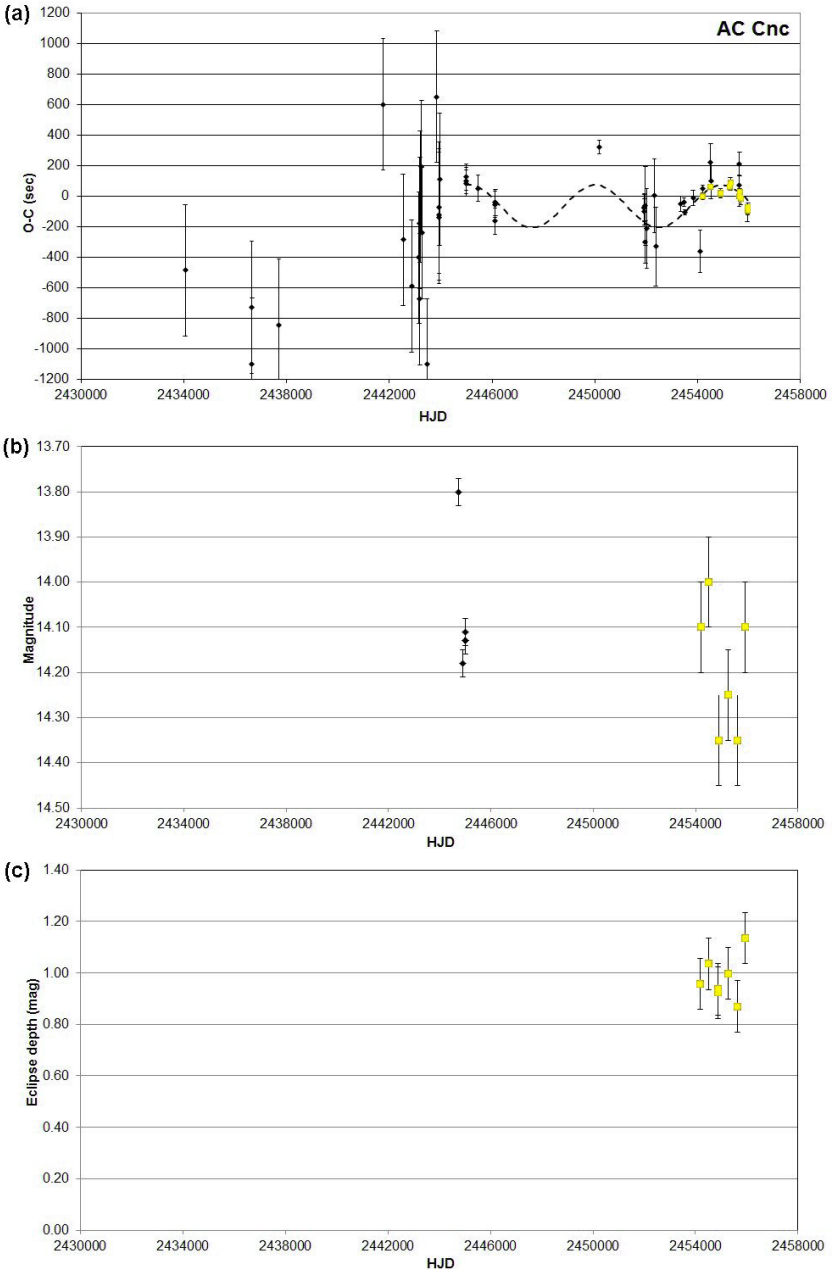

Figure 5. AC Cnc: (a) O–C diagram with respect to a linear ephemeris showing a cyclical variation of orbital period (dashed line), (b) out-of-eclipse magnitude, and (c) eclipse depth.

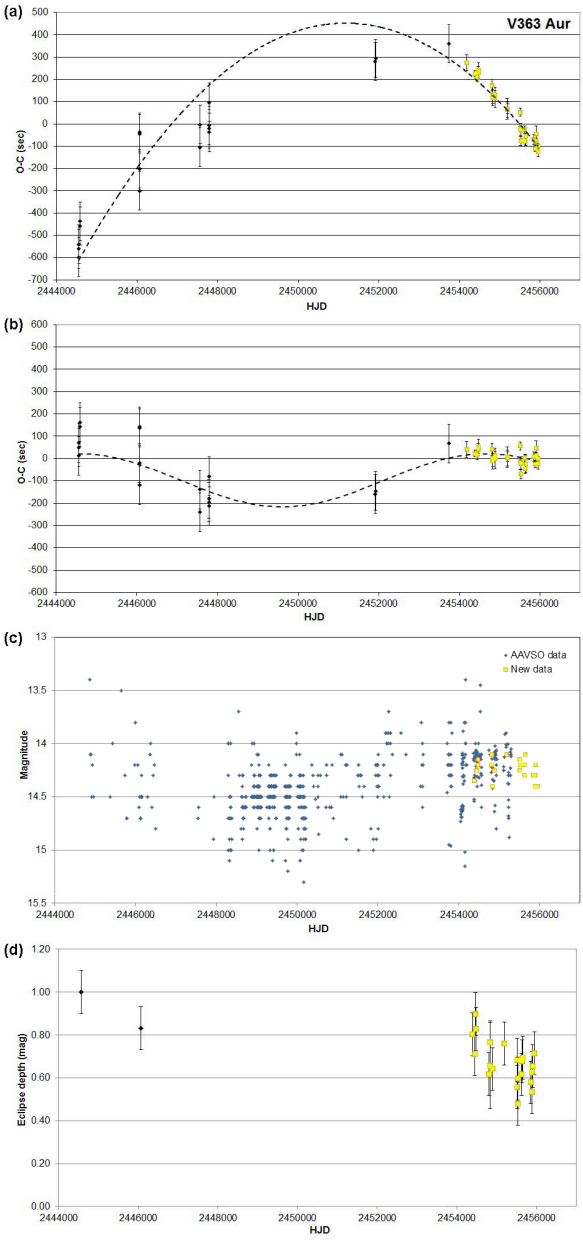

Figure 6. V363 Aur: (a) O–C diagram with respect to a linear ephemeris showing a quadratic ephemeris (dashed line), (b) O–C diagram with respect to a quadratic ephemeris showing a cyclical variation of orbital period (dashed line), (c) out-of-eclipse magnitude, and (d) eclipse depth.

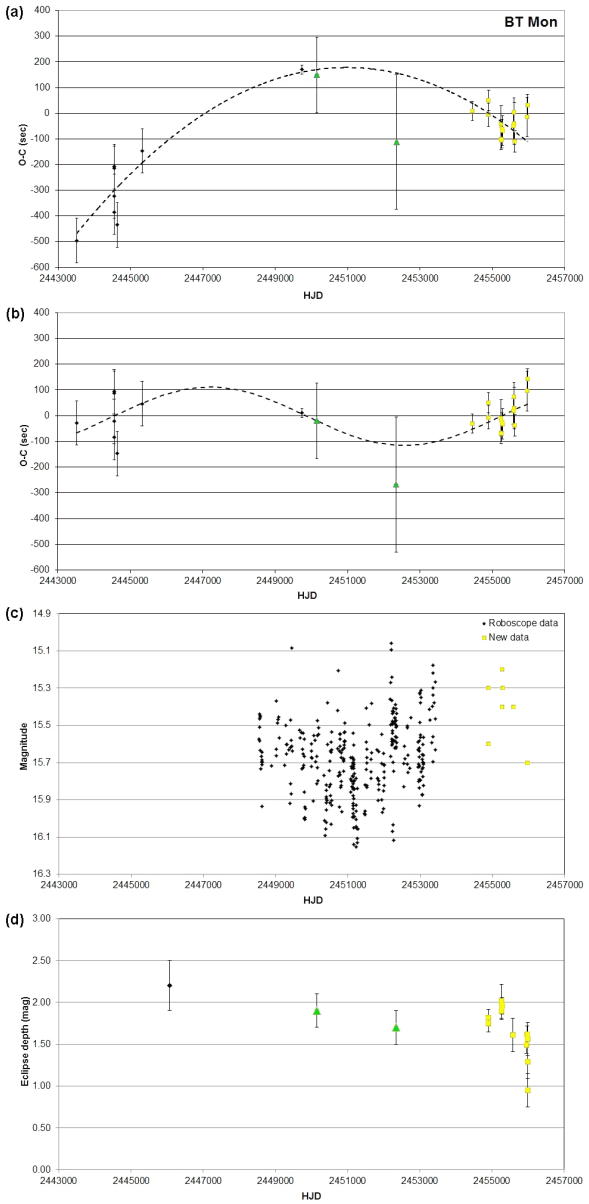

Figure 7. BT Mon: (a) O–C diagram with respect to a linear ephemeris showing a quadratic ephemeris (dashed line), (b) O–C diagram with respect to a quadratic ephemeris showing a cyclical variation of orbital period (dashed line), (c) out-of-eclipse magnitude, and (d) eclipse depth. Eclipses synthesised using Roboscope data are shown as triangles.

Hubble's Famous Plate of 1923: a Story of Pink Polyethylene

David R. Soderblom
Space Telescope Science Institute, 3700 San Martin Drive, Baltimore, MD 21218; soderblom@stsci.edu

Presented at the 100th Spring Meeting of the AAVSO, May 22, 2011; received March 26, 2012; accepted April 18, 2012

Abstract On October 6, 1923, Edwin Hubble used the Mount Wilson 100-inch telescope to take a 45-minute exposure of a field in the Andromeda galaxy. This is the now-famous plate marked with his "VAR!" notation. I will discuss this plate and that notation. I will also tell the story of flying copies of that plate on the deployment mission for HST in 1990 as a Hubble memento and then locating those copies afterwards, and how copies were flown on Servicing Mission 4 on 2009 as well. This has led to an effort in which AAVSO members joined to identify and re-observe that noted star, arguably the most important object in the history of cosmology, but largely ignored since Hubble's time.

1. Introduction—Hubble's discovery

On the night of October 6 (UT), 1923, Edwin Hubble took an astronomical photograph that is now famous (Figure 1). He used the 100-inch Hooker telescope on Mount Wilson to expose a 4 × 5-inch glass plate for 45 minutes under conditions of fair seeing. The object observed was the great nebula in Andromeda, M31. Standard practice with photographic plates was to use a dull pencil to write the plate number near the edge; the pressure activated the emulsion and caused the writing to show up when the plate was developed. Hubble wrote additional information on the emulsion side of the plate as well in ink (emulsion used, seeing conditions, and hour angle).

Hubble had been hired by the Director of Mount Wilson, George Ellery Hale, to do exactly what he was doing: to use the power of the world's largest telescope to study the size and structure of our Universe. Hale himself is best known for his pioneering work in solar physics at Mount Wilson, but he knew talent when he saw it, and Edwin Hubble was a very capable young astronomer. Hale was a gifted impressario of astronomy who pursued ground-breaking work of his own (particularly on solar magnetism) and who could enlist the assistance of people like Andrew Carnegie, a major supporter of Mount Wilson and the institutions that succeeded it under the aegis of the Carnegie Institution of Washington.

Hubble was hoping to find Cepheids in M31 because that would make it possible to determine its distance. To understand why that mattered, you need to take yourself back to the early 1920s. The big event for astronomy was the

Curtis-Shapley debate, held at the Smithsonian Museum of Natural History, in Washington, D.C., in April 1920. Virginia Trimble (1995) has written a particularly good account of the debate and its context that you should read in order to understand why Hubble made his observations. At the time, no one was sure how big our Galaxy is, where we are in it, or if there were other galaxies like ours.

Cepheids, of course, are variable stars of a particular type. They are intrinsically very bright, and so relatively easy to detect even in other galaxies. Also, the range of variation is a magnitude or more, also easily detectable even looking by eye at photographic plates. What makes them so valuable to cosmologists is that Cepheids are pulsating stars (as we know now) that have a definite relationship between the observed period and the star's intrinsic luminosity (the composition of the star also matters, but that wasn't known then). This period-luminosity relation for Cepheids had been measured by Henrietta Leavitt (Figure 2) at the Harvard College Observatory, using observations of the Magellanic Clouds. The distance to the Clouds wasn't known, but it was reasonable to assume all the stars were the same distance.

Leavitt's period-luminosity relation was published in 1912 (Leavitt and Pickering 1912) and was well known. A year later Ejnar Hertzsprung (1913) used observations of Cepheids in the Milky Way to calibrate the relationship so that absolute distances could be derived. If an object like M31 were indeed a separate, external galaxy and not part of the Milky Way (the crux of the debate), finding Cepheids was the way to do it, and only Hubble had the needed access to the telescope that could detect stars that faint.

Edwin Hubble's effort took years, being published in 1929. That was because he needed dozens of separate exposures well-spaced over time, followed by careful effort to determine magnitudes (Hubble 1929). But the critical first step was finding Cepheids to measure in the first instance, and that's why his excitement ("VAR!") showed.

2. The Hubble plate revisited

Why am I telling you this? The reason goes back more than twenty-five years for me. When I started working at the Space Telescope Science Institute, in May 1984, the launch of HST was scheduled for 1986, and I was especially thrilled because a friend from graduate school, Steve Hawley, had been named to the astronaut crew that would deploy the telescope on that flight of the space shuttle. It occurred to me that it would be a nice thing to carry something along on the deployment mission that would tie Hubble the man to Hubble the telescope: a memento. The first thing that came to mind in thinking about Hubble the man was his pipe (Figure 3), which seems to show up in almost every photo of him. I contacted Allan Sandage, himself an observational cosmologist and a protege of Edwin Hubble in the early 1950s at Mount Wilson. Sandage was

probably the one person most familiar with Edwin Hubble and his work, and he suggested the photographic plate shown in Figure 1. Indeed, it is pretty much the perfect Hubble memento: It was taken with Hubble's own hands and it embodies both the key science he pursued in his career and one of the primary goals for building the Space Telescope that was named after him, and it marked a key moment in modern science history.

I arranged to borrow the 4 × 5-inch original plate from the Mount Wilson archives (by then part of The Observatories, in Pasadena, California, and now known as the Carnegie Observatories), and a first question I asked myself was: Should we fly the original plate, or a copy of it? David De Vorkin at the Smithsonian's Air and Space Museum answered by noting that flying the original plate didn't really add to its historical value, and it's an important artifact in its own right, one worth preserving. Given that, and the likely reluctance of NASA to have something made of glass on the space shuttle, I opted to make film copies. Our staff photographer at STScI, John Bedke, had himself worked for years with Sandage in Pasadena and had helped to preserve many of Hubble's original plates by reprocessing them (Hubble was impatient and would pull plates from the fixer prematurely).

But why? Why do this at all? My idea at the time was that I would arrange to fly about ten copies of Hubble's plate, and, once they were returned, we'd have prints made from each, nicely matted and framed. Then we'd give these to the institutions that had played key roles in the development, construction, and launch of HST and send an astronomer to those places to say thanks for building us such a wonderful instrument, and here are some of the things we're doing with it. In other words, the idea was to reach back to the people who built HST.

But could you just ask NASA to fly something like that on the shuttle? Well, yes, actually you could. When a NASA facility like the Marshall Space Flight Center (MSFC), in Huntsville, Alabama, used the space shuttle to launch a mission that it had developed, they got to put on board something called the Official Flight Kit (OFK; you knew we were going to get into the three-letter abbreviations, right?). Also, the astronauts for a given flight got to take along personal items that could include just about anything, subject to size and weight limits. I could have given one of the film copies of Hubble's plate to Steve Hawley, but it didn't seem reasonable to ask him to take ten, and besides, I wanted to do this through official channels.

Once I had the copies of the plate I contacted the HST Project Manager at MSFC, Fred Wojtalik, and explained what I wanted to do. He agreed to include the film copies in the MSFC OFK, and so I sent them off to him. That gets us to the end of the beginning of this story.

Those of you of a certain age will recall vividly that after HST was launched it quickly became clear that Hubble's primary mirror was highly flawed and had significant spherical aberration. Instead of being an object of great pride,

Hubble turned into a huge embarrassment for NASA. Going to parties and seeing neighbors was an exercise in damage control, combined with a bit of spin ("It's not that bad." It really was that bad.). Nevertheless, I contacted Mr. Wojtalik at MSFC to get the flown negatives returned. He requested a description of how they would be used, given that they were now official NASA materials, and I provided that. But the negatives didn't come. Under the circumstances, my immediate enthusiasm for the project had diminished and I didn't ever get them (I should have tried harder). Over the subsequent years I would make inquiries of NASA people I would meet who might have information, all without success.

That gets us to the beginning of the end. In 2006, new NASA Administrator Mike Griffin reinstated Servicing Mission 4 (SM4) for HST. The history of servicing Hubble with the space shuttle involves lots of stories waiting to be told, but one particular aspect of SM4 was that NASA declared that it would be the last shuttle mission to the observatory, period. Obviously I had to find those missing negatives because if I could, and if I could refly them on SM4 then we would achieve a rare case of cosmic symmetry: artifacts flown on missions that bookended Hubble's connection to human spaceflight.

I called and e-mailed lots and lots of people, many involved in the HST project in the 1980s. I found lots of new friends—every single person I talked to was enthusiastic about what I was trying to do—but I never found the negatives. Over many months new leads would pop up, but all proved futile. At one point I ran into Steve Hawley while he was here at STScI attending a conference and we talked. He mentioned that there was a person at Johnson Space Center, in Houston, who was the OFK Coordinator, Ms. Abby Cassell. I called her in May, 2008, and explained why. I knew that the items flown in MSFC's OFK in 1990 had been returned to Marshall, and she confirmed that, noting that their OFK included a plaque, 7,000 American flags, and ten negatives. I at least had proof my negatives had flown! I asked her if something flown in an OFK would be recognizable if it were sitting on a shelf somewhere, and she said "Yes, we shrink-wrap everything in pink polyethylene before it's put on board the shuttle." But then a thought came to her and she asked me to wait while she looked in her vault. She came back in a few minutes to tell me that back in 1990, when the negatives were flown, they would have been shrink wrapped in lavender polyethylene. That is probably a completely useless piece of information, yet I treasure it.

By that time in 2008, the launch of SM4 was only months away and there was no longer time to go through the effort of including the negatives even if I found them. I had to give up. But I still had five copies left, and so this time I made sure that there was redundancy. I gave one to John Grunsfeld for him to carry personally as a member of the SM4 crew, and another to Dave Leckrone, the HST Project Scientist at Goddard Space Flight Center, for him to include in GSFC's OFK. I got both of them back, the first from John Grunsfeld (Figure 4); I was a happy guy.

3. The Hubble discovery reaffirmed

Once they were returned an obvious question came to mind: Had HST ever observed that Cepheid that Edwin Hubble discovered back in 1923? That star could be called the most significant object in the history of cosmology because of its key role in establishing the cosmic distance scale. But how could I tell? A blue-sensitive plate from 1923 can look a lot different from a modern digital sky image, and Hubble's published coordinates were rough. I could tell that Hubble's plate included M31's nucleus, but it was hard to say just what the scale or orientation was. Photographic plates do not come with World Coordinate System headers! Fortunately, here at STScI we have Tom Brown, an astronomer who has studied M31 extensively, particularly its outer regions. It was easy for him to pinpoint the coordinates and so we could then see that several recent HST/WFPC2 exposures were very close to Hubble's Variable no. 1, but not on it.

The Hubble Heritage Program here at STScI helped by using some of their HST time to observe the star and its field with the new WFC3 camera on HST. Hubble Heritage is well known for their extraordinary images that have captured the public's attention and delight. We wanted to catch the Cepheid both when it was near its brightest and faintest, but the star had not been observed in a very long time (since the 1960s) and so the phase was unknown. That's when the AAVSO stepped in to help by providing ground-based observations of the field to re-establish the light curve (Templeton *et al.* 2011; NASA 2011).

The result was released at the May 2011 joint meeting of the AAVSO and the American Astronomical Society (AAS) held in Boston. One poignant aspect to me is that in the 21st century, citizen-scientists have access to and can afford the means to put telescopes and instruments in their backyards that can do better than Edwin Hubble could with the world's largest telescope in 1923. We have come so very far.

So that's the story, pretty much to its end. Despite initial setbacks, HST has been an enormous success and continues to advance astronomy in ways that amaze. We now use it in ways its original proposers could not even conceive of, answering questions they could even yet ask. It deserves commemoration.

References

Hertzsprung, E. 1913, *Astron. Nachr.*, **196**, 201.
Hubble, E. 1929, *Astrophys. J.*, **69**, 103.
Leavitt, H. S., and Pickering, E. C. 1912, *Circ. Harvard Coll. Obs.*, No. 173, 1.
Natl. Aeronaut. Space Adm. (NASA). 2011, HubbleSite (http://hubblesite.org/newscenter/archive/releases/2011/15/image/a/).
Templeton, *et al.* 2011, *Publ. Astron. Soc. Pacific*, **123**, 1374.
Trimble, V. 1995, *Publ. Astron. Soc. Pacific*, **107**, 1133.

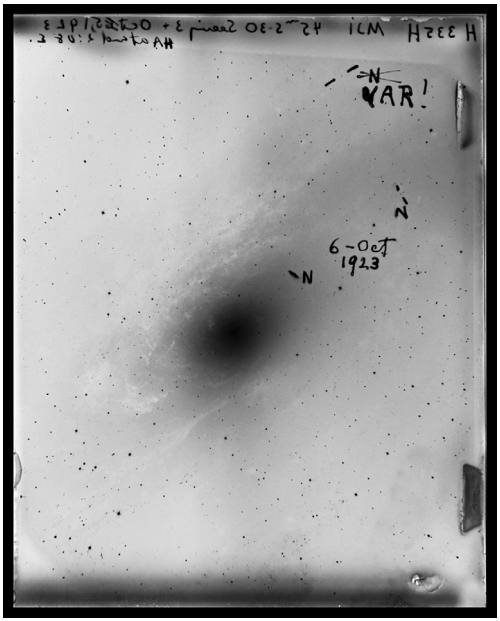

Figure 1. Hubble's plate of 1923.

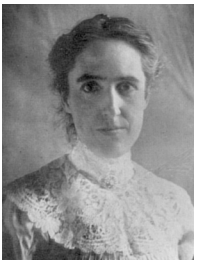

Figure 2. Henrietta S. Leavitt.

Figure 3. Edwin Hubble and his pipe.

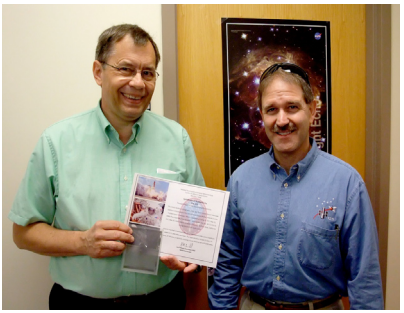

Figure 4. The author (left) and astronaut John Grunsfeld after one of the negatives was returned to me.

Things We Don't Understand About RR Lyrae Stars

Horace A. Smith
Michigan State University, Department of Physics and Astronomy, East Lansing, MI 48824; smith@pa.msu.edu

Presented at the 100th Annual Meeting of the AAVSO, October 8, 2011; received January 26, 2012; accepted January 26, 2012

Abstract RR Lyrae stars have been identified as a distinct class of variable star for slightly longer than the century the AAVSO has existed as an organization. Although considerable progress has been made in understanding RR Lyrae variables over the past century, several aspects of their pulsation remain puzzling. This paper reviews some of the more poorly understood properties of these pulsating variable stars, with emphasis on the contributions that might be made by observers associated with the AAVSO and similar organizations.

1. RR Lyrae stars

Although RR Lyrae itself, the brightest known member of its namesake type of variable star, was discovered by Williamina Fleming at the end of the 19th century (Pickering 1901), it was through observations of globular clusters that the properties of these short period variables were first defined. Solon Bailey and his associates identified numerous variable stars in their photographic studies of globular clusters during the 1890s and early 1900s. Most of these variables had short periods, between 0.2 and 0.9 day, and are what we should today call RR Lyrae stars. However, so closely were these short period variables associated with globular clusters that they were often called "cluster variables" until the 1950s (Smith 1995). Bailey (1902) divided RR Lyrae stars into subclasses based upon the periods and light curve shapes of variables in the globular cluster ω Centauri. Originally three in number, types a, b, and c, these Bailey types are now usually condensed to two varieties, type ab and type c. RRc variables have shorter periods than RRab stars, and usually have smaller amplitudes as well. Because of the smaller amplitudes, RRc stars are often more incompletely discovered than RRab stars in variable star surveys. It was later realized that RR Lyrae of type ab are pulsating in the fundamental radial mode, whereas those of type c are pulsating in the first overtone radial mode. Because of this, RRab stars are sometimes called RR0 stars, while RRc variables are RR1 stars. Double mode RR Lyrae stars (RRd or RR01 stars) have also been discovered, which pulsate simultaneously in the fundamental and first overtone modes. The existence of RR Lyrae variables pulsating in the second overtone mode, RRe stars, remains more controversial (Kovacs 1998).

Shapley (1918) realized that RR Lyrae stars were important standard

candles for measuring the distances to globular clusters, and they remain among the main objects for determining the distances to very old stellar populations. RR Lyrae stars are relatively low mass ($\approx 0.6-0.8 M_{\odot}$) stars that are undergoing core helium burning on the horizontal branch in the HR diagram. The very existence of RR Lyrae variables in a stellar system is indicative of a stellar population older than about 10 Gyr (Smith 1995; Percy 2007).

Despite the progress that has been made in understanding RR Lyrae stars, there are important questions that remain unanswered. The solutions to some of these questions probably will fall to professional astronomers. For example, accurate parallaxes for RR Lyrae stars are needed to calibrate their absolute magnitudes (Benedict *et al.* 2011), and space-based efforts such as the GAIA mission (de Bruijne 2012) may be needed fully to resolve that issue.

However, other open questions are more amenable to being tackled by amateur observers, or by amateurs and professionals working in tandem. These areas where ignorance continues are the focus of the remainder of this paper.

2. Long term period changes

Eddington (1918) posed an important observational question regarding the period changes of Cepheid variable stars that applies equally to RR Lyrae variables: "It would be of great interest to determine the change in period (if any) of these stars, some of which have been under observation for many years; because this would give a means of measuring a very slight change of density, and so determine the rate of stellar evolution and the length of life of a star." The connection of period changes to density changes comes via the basic pulsation equation: $P\sqrt{\rho} = Q$, where P is the pulsation period, ρ is the mean density of the star, and Q is the so-called pulsation constant.

Stellar evolution theory predicts that there ought to occur slow changes in the period of an RR Lyrae star as it gradually fuses its central helium into carbon and oxygen. These changes are predicted to occur at a small and nearly constant rate during the span of a century or two (Koopmann *et al.* 1994), though the rates of period change can become larger as the RR Lyrae star begins to exhaust its core helium. To test these predictions, photometry of RR Lyrae stars is needed extending over as long a time interval as possible. For some RR Lyrae variables, the observational record already spans more than a century.

While there are indeed some RR Lyrae variables for which the observed rates of period change are small and nearly constant, consistent with the predictions of stellar evolution theory, others present challenges to the theoretical framework. More RR Lyrae stars show large period changes than would be expected from their theoretical rates of period change. Moreover, some RR Lyrae stars have been observed to swing between period increases and period decreases on a timescale of a few years, something not predicted by stellar evolution theory. XZ Cygni, one example of such a misbehaving variable, is an RR Lyrae star

to which AAVSO observers have devoted particular attention. Discovered in 1905, XZ Cyg showed only a modest decrease in period during the first half century that it was observed (Klepikova 1958). However, beginning in 1965, the period of XZ Cyg declined steeply in several steps before sharply increasing again in 1979 (Baldwin and Samolyk 2003).

Thus, RR Lyrae stars appear to show some sort of period noise on top of any long term evolutionary period changes. Some have hypothesized the existence of short term instabilities that produce this period change noise but which, when observed long enough, would average out to the period change rate expected from stellar evolution theory (Sweigart and Renzini 1979).

Continued monitoring of the long term period behavior of field RR Lyrae stars is thus necessary to resolve several outstanding problems relating to period changes. Over the long term, will the period changes of all RR Lyrae stars fall into line with the predictions of stellar evolution theory? If so, how long do we have to watch an RR Lyrae star before the noisy observed period changes average out to the evolutionary rate? How often do episodes of large period change occur in a star like XZ Cygni?

In the 1960s Marvin Baldwin pioneered long term monitoring of the period changes of RR Lyrae stars by the AAVSO. Targeted RR Lyrae stars were at first observed visually but more recently almost entirely with CCD cameras (Baldwin 2011). The determination of the period changes of RR Lyrae variables has also been a major focus of the GEOS RR Lyrae survey (Le Borgne *et al.* 2011). All-sky surveys, such as ASAS (Pojmański 1998), are also useful for monitoring RR Lyrae period changes. It is important that these efforts continue long into the future if the questions associated with period changes are to find answers.

3. The Blazhko effect

Some RR Lyrae stars have light curves that repeat very precisely from one cycle to the next. That is not true of all RR Lyrae stars. Some exhibit periodic changes in light curve shape on a time scale typically of tens of days to hundreds of days—the Blazhko effect (Percy 2007; Smith 1995). Although the Blazhko effect was discovered a century ago, our understanding of what causes the phenomenon remains incomplete.

There has, nonetheless, been recent progress in several aspects of our understanding of the Blazhko effect. Smith (1995) stated that almost all of the Blazhko effect stars known at that time were RRab stars, and that perhaps 15–20% of all RRab variables showed the Blazhko effect. More recent researchers have upped that percentage nearer to 50% for RRab stars while more RRc variables have also been found to exhibit the Blazhko effect. This increase is attributable to high precision CCD photometry of RR Lyrae stars obtained from the ground (Jurcsik *et al.* 2009), and also to the monitoring of RR Lyrae

variables from space by the Kepler mission (Benkő *et al.* 2010). The Blazhko effect is thus something that occurs in many RR Lyrae variables, if they are watched carefully enough to detect it (Figure 1).

Recent observations with the Kepler mission (Szabó *et al.* 2010; Kolenberg *et al.* 2011) have shown that alternate peaks in the primary light cycle of at least some Blazhko effect stars can differ in brightness (Figure 2). The size of the difference is not the same for all Blazhko stars, and even changes over time for a single star. In studying this so-called period doubling, the Kepler mission has the advantage of being able to continuously observe its targets, without a dirunal gap in the observations. Successive peaks of a half-day period variable star are difficult to observe from a single ground-based location because of the interference of daylight unless the observer is so fortunate (if that is the right word) as to be observing during winter in the arctic or antarctic.

Although the primary light cycle of an RR Lyrae star may be only half a day, the Blazhko periods are many times longer. Determining the period of the Blazhko effect in RR Lyrae stars requires many observations over a time span considerably longer than the Blazhko period itself. Accomplishing that is not a project for one night or even a few nights of observing. Thus, there are RR Lyrae stars for which the primary pulsation period is known, and for which it is suspected that the Blazhko effect exists, but which do not have well determined Blazhko periods. Intensive CCD observations of such stars are needed to establish definitively whether or not the Blazhko effect exists and, if so, to determine the Blazhko period and the manner in which the primary light curve changes over the longer Blazhko cycle. This can be done by observers at a single longitude, but, as Doug Welch has noted (http://www.aavso.org/now-less-mysterious-blazhko-effect-rr-lyrae-variables), observers spread around the world at different longitudes potentially have the ability to detect the recently discovered differences in alternate maxima. The study of CX Lyr by de Ponthiere *et al.* (2009) illustrates the type of study that can be carried out to determine the Blazhko period of an RR Lyrae star, and also some of the complications that can make fixing that period difficult.

Much is unknown about the long term stability of the Blazhko effect and its relationship to changes in the primary pulsation period. Some well-known Blazhko variables, such as RR Lyrae itself, have been studied for several decades. The type of light curve changes that occur during the Blazhko cycle sometimes have been observed to themselves vary on a timescale of years, perhaps in some cases indicating a cycle even longer than that of the Blazhko effect itself (Szeidl and Kolláth 2000). Monitoring of Blazhko effect stars over a span not just of years but of decades is needed to keep track of these very poorly understood long term changes. XZ Cyg again affords an example of a study of this type (LaCluyzé *et al.* 2004). Not only have the amplitude and period of the Blazhko effect changed over time for this star, but at least some of the changes appear to be coincident with changes in the primary pulsation period.

4. Double-mode RR Lyrae stars

Double-mode RR Lyrae stars are rarer than those for which a single pulsation mode is dominant. Are these double-mode stars in the process of switching from one main pulsation mode to another, and, if so, on what timescale does the shift occur? By obtaining photometry of these stars over a timescale of years, one can determine whether the relative amplitudes of the fundamental mode and first overtone mode pulsations are changing. If they are observed to change, are the changes all in one direction (i.e. does the fundamental mode amplitude increase while the first overtone mode decreases, or vice versa) or does the direction of change itself switch over time? It is also perhaps noteworthy that, so far as I am aware, no one has yet detected the Blazhko effect in a double-mode RR Lyrae star. A good example of the type of work that can be done along these lines is the study of the double-mode RR Lyrae star NSVS 5222076 by Hurdis and Krajci (2010, 2011).

5. RR Lyrae stars in globular clusters

The AAVSO RR Lyrae program and the GEOS project have focused upon RR Lyrae stars in the field of the Galaxy, rather than those that are members of globular clusters. This is understandable. Many field RR Lyrae stars are brighter than their cluster counterparts. Moreover, magnitudes of field RR Lyrae stars can usually be obtained from CCD observations with aperture photometry, whereas observations of globular cluster RR Lyrae stars often require the more complicated methods of profile fitting photometry (Stetson 1987) or image differencing (Alard 2000). Nonetheless, RR Lyrae stars in a number of globular clusters are within the reach of modest telescopes equipped with CCD cameras, and observing clusters does have the advantage that many RR Lyrae stars can be recorded on a single image. The unknowns relating to RR Lyrae stars mentioned above apply to cluster as well as field stars (Jurcsik *et al.* 2012) and, in the future, more amateurs may decide to attempt observations of cluster variables.

6. The long haul

A theme that recurs in the discussions above is the need for observations of RR Lyrae stars that span years and decades. I don't know how much time will pass before all of these things we don't understand about RR Lyrae stars become things we do understand. I suspect that decades will go by before the answers to some of the questions posed are fully known. Who is going to provide those observations over such a timescale? An individual observer might be active for only a few years, or perhaps a few decades. However, the AAVSO is now into its second century, and it, and organizations like it, can be key to organizing and

encouraging observational programs that continue beyond the lifetimes of any individual observer.

7. Acknowledgements

The author thanks Marv Baldwin, Gerry Samolyk, and David Hurdis for their comments regarding outstanding problems in the study of RR Lyrae stars.

References

Alard, C. 2000, *Astron. Astrophys., Suppl. Ser.*, **144**, 36.
Bailey, S. I. 1902, *Ann. Harv. Coll. Obs.*, **38**, 1.
Baldwin, M. E. 2011, private communication.
Baldwin, M. E., and Samolyk, G. 2003, *Observed Maxima Timings of RR Lyrae Stars, No. 1*, AAVSO, Cambridge, MA.
Benedict, G. F., *et al.* 2011, *Astron. J.*, **142**, 187.
Benkő, J. M., *et al.* 2010, *Mon. Not. Roy. Astron. Soc.*, **409**, 1585.
de Bruijne, J. H. J. 2012, arXiv:1201.3238.
de Ponthiere, P., Le Borgne, J., and Hambsch, F. -J. 2009, *J. Amer. Assoc. Var. Star Obs.*, **37**, 117.
Eddington, A. S. 1918, *Mon. Not. Roy. Astron. Soc.*, **79**, 2.
Hurdis, D. A., and Krajci, T. 2010, *J. Amer. Assoc. Var. Star Obs.*, **38**, 1.
Hurdis, D. A., and Krajci, T. 2011, *J. Amer. Assoc. Var. Star Obs.*, **40**, 268.
Jurcsik, J., *et al.* 2009, *Mon. Not. Roy. Astron. Soc.*, **400**, 1006.
Jurcsik, J., *et al.* 2012, *Mon. Not. Roy. Astron. Soc.*, **419**, 2173.
Klepikova, L. A. 1958, *Perem. Zvezdy*, **12**, 164.
Kolenberg, K., *et al.* 2011, *Mon. Not. Roy. Astron. Soc.*, **411**, 878.
Koopmann, R. A., Lee, Y.-W., Demarque, P., and Howard, J. M. 1994, *Astrophys. J.*, **423**, 380.
Kovacs, G. 1998, in *A Half Century of Stellar Pulsation Interpretation*, eds. P. A. Bradley and J. A. Guzik, ASP Conf. Ser., 135, Astron. Soc. Pacific, San Francisco, 52.
LaCluyzé, *et al.* 2004, *Astron. J.*, **127**, 1653.
Le Borgne, J. F., Klotz, A., and Boer, M. 2011, *Inf. Bull. Var. Stars*, No. 5986, 1.
Percy, J. R. 2007, *Understanding Variable Stars*, Cambridge Univ. Press, Cambridge.
Pickering, E. C. 1901, *Astron. Nachr.*, **154**, 423.
Pojmański, G. 1998, *Acta Astron.*, **48**, 35.
Shapley, H. 1918, *Astrophys. J.*, **48**, 89.
Smith, H. A. 1995, *RR Lyrae Stars*, Cambridge Univ. Press, Cambridge.
Stetson, P. B. 1987, *Publ. Astron. Soc. Pacific*, **99**, 191.
Sweigart, A. V., and Renzini, A. 1979, *Astron. Astrophys.*, **71**, 66.

Szabó, R., *et al.* 2010, *Mon. Not. Roy. Astron. Soc.*, **409**, 1244.
Szeidl, B., and Kolláth, Z. 2000, in *The Impact of Large-Scale Surveys on Pulsating Star Research*, eds. L. Szabados and D. Kurtz, ASP Conf. Ser., 203 (IAU Colloq. 176), Astron. Soc. Pacific, San Francisco, 281.

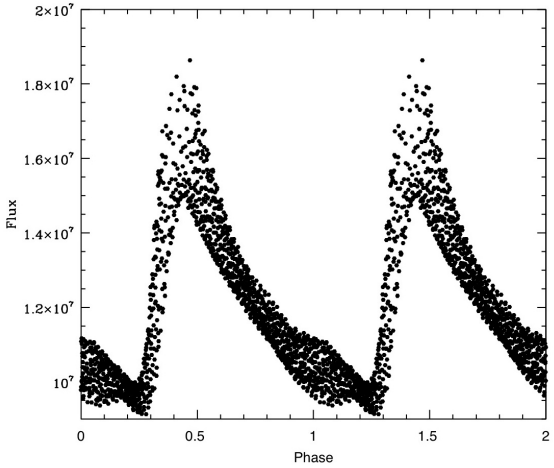

Figure 1. The Blazhko effect is shown in this light curve of RR Lyrae itself, based upon Kepler mission long cadence data. The data are folded with a primary period of 0.566868 day.

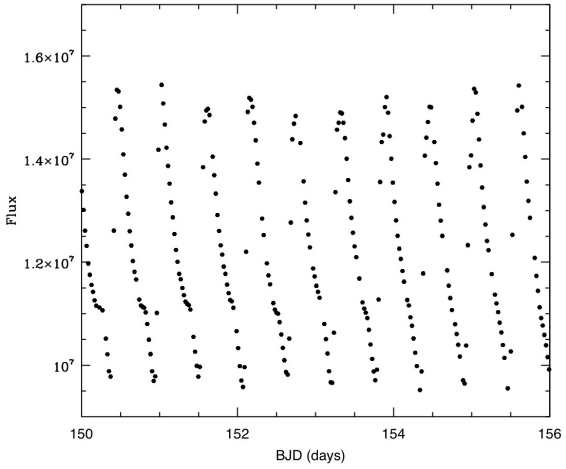

Figure 2. A portion of the Kepler data used to construct the light curve in Figure 1 is plotted against baryocentric Julian date.

The Usefulness of Type Ia Supernovae for Cosmology—a Personal Review

Kevin Krisciunas
George P. and Cynthia Woods Mitchell Institute for Fundamental Physics and Astronomy, Department of Physics and Astronomy, Texas A & M University, 4242 TAMU, College Station, TX 77843; krisciunas@physics.tamu.edu

Presented at the 100th Spring Meeting of the AAVSO, May 22, 2011; received February 6, 2012; revised March 8, 2012; accepted March 9, 2012

Abstract We review some results of the past twelve years derived from optical and infrared photometry of Type Ia supernovae. A combination of optical and infrared photometry allows us to determine accurately the extinction along the line of sight. The resulting distance measurements are much more accurate than can be obtained from optical data alone. Type Ia supernovae are very nearly standard candles in the near-infrared. Accurate supernova distances, coupled with other observational data available at present, allow us to determine the matter density in the universe and lead to evidence for the existence of Dark Energy. We can now address some questions on the grandest scale such as, "What is the ultimate Fate of the universe?"

1. Introduction

The basic supernova (SN) classification scheme stipulates that supernovae (SNe) with hydrogen emission in their spectra are called Type II SNe, and those without hydrogen are called Type I SNe (Minkowski 1941). For more than twenty years we have delineated subclasses. Type Ia SNe show absorption due to singly ionized silicon. The key line has a rest wavelength of 6355Å (Filippenko 1997). As it is observed at roughly 6150Å at the time of maximum light, this signifies that a typical outflow velocity at maximum light is about 10,000 km s^{-1}.

It is generally believed that a Type Ia SN is caused by the explosion of a carbon-oxygen white dwarf (WD) star (in a close binary system) which has approached the Chandrasekhar limit of $1.4\,M_{\odot}$. Two possible scenarios are envisioned. Either the WD gains mass from a nearby donor star (a main sequence star or a giant), or the explosion results from the merging of two white dwarfs.

In Figure 1 we show a schematic diagram of the light path from a SN to a telescope on the Earth. At maximum light (roughly 19 days after the explosion) the size of the expanding fireball is ~100 AU. Light is possibly scattered by circumstellar material near the SN (Wang 2005; Goobar 2008). The light may be dimmed by dust in the host galaxy. The light waves are shifted towards longer wavelengths owing to the expansion of the universe, given the redshift

of the host galaxy. The light is dimmed by dust in the Milky Way galaxy. Finally, the light passes through the Earth's atmosphere, is reflected and/or transmitted by the optical elements of the telescope, is spread out into a spectrum or passes through one of several broad band filters, and hits the light detector in our spectrograph or CCD camera, the quantum efficiency of which is a function of wavelength. Thus, the SN light is affected by many factors, and if we are to understand SNe well, we must standardize our spectra and broad band photometry.

Phillips (2012) has written an excellent review of the near-infrared (IR) properties of Type Ia SNe. We can hardly improve on his article. Here we shall emphasize our contributions over the past dozen or so years. One topic we shall not discuss here is the morphology of Type Ia SN lightcurves. We refer the reader to Hamuy *et al.* (1996), Riess *et al.* (1996), Kasen (2006), Jha *et al.* (2007), and the relationship between the *B*-band decline rate parameter and the strength of the *I*-band secondary maximum shown in Figure 17 of Krisciunas *et al.* (2001). Mandel *et al.* (2009) and Mandel *et al.* (2011) give sophisticated analysis of optical and near-IR light curves.

2. Standardizable candles and standard candles

In order to determine the distance to an astronomical object we make use of the standard relationship between absolute magnitude (M), apparent magnitude (m), and distance (d) in parsecs:

$$M = m + 5 - 5 \log (d), \quad (1)$$

where the apparent magnitude is corrected for any dust extinction along the line of sight. A century ago Henrietta Leavitt discovered that Cepheids with longer periods are brighter than those with shorter periods (Leavitt and Pickering 1912). This is the famous period-luminosity relation. In short, its significance is that while Cepheids do not all have the same intrinsic brightness, those of a given stellar population type show a specific linear relation between the logarithm of the period in days and the mean absolute magnitude. Thus, they are standardizable candles. The brightest Cepheids are more than 10,000 times more luminous than the Sun. By contrast, RR Lyrae stars of a particular metallicity pulsating in the fundamental radial mode have mean visual absolute magnitudes of about +0.7 (Layden *et al.* 1996). They are standard candles—all exhibit the same luminosity, like 100-watt light bulbs only much brighter. RR Lyr stars are roughly forty times more luminous than the Sun. Type Ia SNe are very useful for extragalactic astronomy because at maximum light they are four billion times more luminous than the Sun; they can be detected halfway across the observable universe with a 4-meter class telescope.

Baade (1938) first suggested that Type I SNe may be useful for measuring accurate cosmic distances. (The subclass of Type Ia SNe was first identified

by Elias *et al.* (1985).) Kowal (1968) made the first test of the usefulness of these objects as distance indicators. Phillips (1993) discovered the "decline rate relation" and established the usefulness of the parameter $\Delta m_{15}(B)$, which is the number of *B*-band magnitudes that a Type Ia SN declines in the first 15 days after *B*-band maximum; a typical value is 1.1 magnitudes, but the range is from 0.68 (Krisciunas *et al.* 2011) to 1.93 or so (Garnavich *et al.* 2004). As with Cepheids, the absolute magnitude is related to another observable. The most slowly declining Type Ia SNe are about 2.5 magnitudes more luminous in the *B*-band at maximum light than the fast decliners. The steepness of the decline rate relation becomes shallower as we proceed to longer wavelength bands (see Figure 2). Thus, at optical wavelengths, Type Ia SNe are standardizable candles.

Meikle (2000) presented a very useful compilation of IR photometry of Type Ia SNe published up to that time. Of particular note are the two papers of Elias *et al.* (1981, 1985); the latter paper presented the first IR Hubble diagram of Type Ia SNe, using the *H*-band magnitudes at 20 days after maximum light. Meikle (2000) also showed, on the basis of a small number of objects, that Type Ia SNe at ~14 days after maximum light may be standard candles. Krisciunas *et al.* (2003) also showed that Type Ia SNe might be standard candles in the near-IR. We based this on a sample of Type Ia SNe only slightly bigger than that of Peter Meikle, on the basis of their *H*-band (1.65 micron) magnitudes 10 days after *B*-band maximum.

One might ask why there are so many fewer near-IR data compared to optical photometry. Near-IR chips have fewer pixels than optical CCD cameras. A small field of view makes it more difficult to make mosaic images, as there would be fewer field stars of appropriate brightness near any SN. This is particularly important for images taken on non-photometric nights. Also, there are few telescopes systematically used for near-IR observations of SNe. Amongst them are the CTIO 1.3-meter telescope, the Las Campanas 1.0-meter and 2.5-meter telescopes, a 1.3-meter telescope at Mt. Hopkins, Arizona, and the Liverpool JMU 2-meter telescope at La Palma.

3. Uniformity of color curves for determining extinction

I began observing Type Ia SNe early in 1999 using the Apache Point Observatory 3.5-meter telescope. My collaborators were Gene Magnier, Chris Stubbs, and Alan Diercks of the University of Washington. (Stubbs and Diercks were members of the High-*Z* Supernova Team, whose highly cited paper (Riess *et al.* 1998) garnered a Nobel Prize in physics for Brian Schmidt and Adam Riess.) We published a paper (Krisciunas *et al.* 2000) which had two primary results, one dealing with color curves, the other dealing with unusual dust properties.

We found that Type Ia SNe whose decline rate parameter $\Delta m_{15}(B)$ was in the middle range delineated uniform optical vs. infrared color curves. This follows

up a suggestion by Elias *et al.* (1985) that *V–K* colors of Type Ia SNe may be quite uniform. An example of *V–K* color curves of Type Ia SNe is shown in Figure 3. Using our data of SN 1999cp and data of SNe 1972E, 1980N, 1983R, 1981B, and 1981D (see Elias *et al.* 1981, 1985, and data and references given by Meikle 2000) we constructed a "zero reddening" locus. Optical and IR data for SN 1998bu (Suntzeff *et al.* 1999, Jha *et al.* 1999, Hernandez *et al.* 2000) show the same basic color curve shape, but reddened in the *V–K* color index by nearly 1 magnitude. (The *UBVRIYJHK* bands are at 0.36, 0.44, 0.55, 0.65, 0.80, 1.03, 1.25, 1.65, and 2.2 microns, respectively.) Our observations of SN 1999cl (Krisciunas *et al.* 2000, 2006) show that this object was reddened even more.

We can parameterize dust reddening as follows. Say we somehow know the unreddened *B–V* color of a star or SN. The difference of the observed color and the unreddened color is the color excess E(*B–V*). The *V*-band extinction is related to this color excess as follows:

$$A_V = R_V E(B–V). \quad (2)$$

The standard value of $R_V = 3.1$ is for Milky Way dust (Cardelli *et al.* 1989), but this value can range from 1.5 to 5 depending on the line of sight in our Galaxy.

Extinction by interstellar dust is diminished at longer wavelengths. An analog of Equation 2, but using the *V*- and *K*-bands, is as follows:

$$A_V = \alpha E(V–K). \quad (3)$$

where parameter α is in the range 1.08 to 1.14.

Even for a wide range of dust grain size and composition the scaling parameter in Equation 3 has a very small range. Thus, if one can obtain a *V–K* color excess, increasing that by ten percent gives us the *V*-band extinction. How much extinction one expects for that SN in other bands can be obtained using the coefficients calculated by Jose Prieto and given in Table 8 of Krisciunas *et al.* (2006).

Krisciunas *et al.* (2004b) present coefficients to generate the *V–H* and *V–K* color curves of the mid-range decliners, and the *V–J*, *V–H*, and *V–K* color curves of the slowly declining Type Ia SNe. This paper also gives the coefficients to generate *JHK* light curve templates valid from 12 days before the time of *B*-band maximum until 10 days after $T(B_{max})$. While the fast-declining Type Ia SNe are considerably redder than more slowly declining objects of this type around maximum light, from 30 to 80 days after $T(B_{max})$ Type Ia SNe of all decline rates show a certain uniformity in the *V–H* and *V–K* color indices (Krisciunas *et al.* 2009b). (In optical bands researchers make use of the "Lira Law." It relates to the uniformity of the unreddened *B–V* colors of Type Ia SNe from 32 to 92 days after $T(B_{max})$ (Lira 1995, Phillips *et al.* 1999).) The uniformity of *V–H* and *V–K* colors of Type Ia SNe is backed up by modeling calculations by Peter Hoeflich and shown in Figure 12 of Krisciunas *et al.* (2003).

Our observations of SN 1999cl (Krisciunas *et al.* 2000, 2006) indicated that $R_V \approx 1.55 \pm 0.08$ for the host galaxy dust. Since then a small number of highly reddened Type Ia SNe have been observed, amongst them SN 2002cv (Elias-Rosa *et al.* 2008), 2003cg (Elias-Rosa *et al.* 2006), and SN 2006X (Wang *et al.* 2008). As Wang (2005) and Goobar (2008) point out, the light of a highly dimmed and reddened object can suffer from extinction and scattering. What the balance is of these processes is not understood at this time. With intrinsic color variations, which are expected for any group of cosmic objects, we thus have three sources of color effects.

Suffice it to say that adopting standard Galactic reddening of $R_V = 3.1$ for all Type Ia SNe is just wrong. The host of SN 1999cl, for example, is M88 in the Virgo cluster. Adopting $R_V = 3.1$ for the dust that affected SN 1999cl gives us a distance value that is halfway to the center of the Virgo cluster. Thus, either M88 is by chance in the same direction as the Virgo cluster, but not in it, or we need to adopt the value of R_V derived from a combination of optical and IR data.

4. Clones

Krisciunas *et al.* (2007) found that, for all intents and purposes, SN 2004S was a clone of the well studied object SN 2001el (Krisciunas *et al.* 2003). Since the former is essentially unreddened in its host, we can correct both objects for a small amount of Milky Way dust extinction and determine that the host galaxy dust of SN 2001el was characterized by $R_V = 2.15 \pm 0.24$ and that SN 2001el suffered 0.47 ± 0.03 magnitude more *V*-band extinction than SN 2004S (see Figure 4). This result exploits the advantage of using a combination of optical and infrared photometry of Type Ia SNe. Previously, if we were limited to using only *B*- and *V*-band photometry, the uncertainty in distance to a reddened SN might have been ±20 percent, but by using optical and IR data the uncertainty of the extinction corrections leads to uncertainties in distance that can be as small as the random errors of the photometry, a few percent. This is a considerable improvement!

Type Ia SNe are not the only exploding stars that show certain uniformities of their lightcurves and color curves. The Type II-P SNe 1999em and 2003hn were found to be near-clones of each other. This allowed us to use the optical and IR photometry to calculate that SN 2003hn was dimmed by 0.25 ± 0.03 magnitude more in the *V*-band than SN 1999em (Krisciunas *et al.* 2009a).

5. The first Hubble diagram of Type Ia SNe at maximum light in the near-IR

Our light curve templates for the near-IR *JHK* bands (Krisciunas *et al.* 2004b, Table 12) allowed us to derive the maximum magnitudes of Type Ia SNe as long as there were some observations between twelve days prior to $T(B_{max})$

and ten days afterward. We used our *V* minus near-IR color curves to correct these apparent magnitudes at maximum light for extinction along the line of sight. This led to the first Hubble Diagram of Type Ia SNe at maximum light in the IR (Krisciunas *et al.* 2004a) (see Figure 5). The fact that the data fit the three straight lines like beads on a string means two things. One is not a surprise, that light intensity decreases as the square of the distance. But the other will be significant for all future surveys of Type Ia SNe, namely that they are better than standardizable candles in the IR. This sample of objects shows that they are standard candles. Of course, one wants a sample bigger than sixteen objects, but this was a good start.

The scatter in the near-IR Hubble diagrams obtained so far is about ± 0.15 magnitude, comparable to what one finds for *BVRI* Hubble diagrams. However, as we push out into the Hubble flow (that is, redshift $z > 0.01$) we can expect the near-IR Hubble diagrams to have tighter fits because of the minimal systematic errors in the extinction corrections and the diminished effect of the peculiar velocities.

6. Deviations from uniform standard candle nature

In Figure 5 if there were any points above the lines, that would indicate SNe intrinsically fainter than the rest, and points below the lines would indicate SNe intrinsically brighter. More information on the standard candle nature of Type Ia SNe can be gleaned from a plot of the absolute magnitudes at maximum brightness vs. some other parameter. Figure 6 is a plot from Krisciunas *et al.* (2011), but we have added three regression lines to subsets of the data. Figure 6 shows that Type Ia SNe are (nearly) perfect standard candles in the near-IR. SN 2009dc may have been a "super-Chandra" event, rather than a more standard Type Ia SN that produces roughly 0.5 $M_{\odot}$ of ^{56}Ni. In our paper on SN 2003gs (Krisciunas *et al.* 2009b) we also used data of SN 1986G (Frogel *et al.* 1987) and four objects from the Carnegie Supernova Project (Contreras *et al.* 2010) to show that there is a bifurcation in the absolute magnitudes at peak brightness of the fast decliners. At the right hand side of Figure 6 the diamond shaped symbols correspond to objects that peaked in the near-IR after T(B_{max}). We have excluded these points and SN 2009dc from the regression lines shown in Figure 6. These lines have non-zero slopes only at the 1.3- to 2.2-σ levels of significance. (A 3-standard deviation result is usually the criterion for statistical significance. For a random sample of data this would occur only 0.5 percent of the time.) The data indicate that Type Ia SNe with $\Delta m_{15}(B) = 1.4$ are roughly 0.10–0.15 magnitude fainter in the near-IR than those with $\Delta m_{15}(B) = 0.8$. This is comparable to the uncertainties of the absolute magnitudes shown in Figure 6.

Folatelli *et al.* (2010, Figure 17) showed that there may be a non-zero slope to the *J*-band decline rate relation. More extensive data from the Carnegie

Supernova Project (Kattner *et al.* 2012) indicate non-zero slopes at the 2-σ level for the *YJH* bands.

Suffice it to say that Type Ia SNe at maximum brightness are excellent objects for determining extragalactic distances. They are nearly perfect standard candles in the near-IR. Excluding possible super-Chandra events and late-peaking subluminous objects, the slopes of the regression lines in Figure 6 are not statistically significantly different than zero.

7. Hubble Diagrams and evidence for Dark Energy

We do not have the space here to review the subject of high redshift SNe and the discovery of the acceleration of the universe. For a cosmology primer see the article "Fundamental cosmological parameters" (Krisciunas 1993, and references therein); also the discussion of "luminosity distances" in the Introduction to Krisciunas *et al.* (2005).

Two fundamental parameters used by observational cosmologists are the mean density of matter in the universe compared to the critical density, Ω_M, and the Dark Energy density parameter, Ω_Λ. If these two parameters sum to 1.00, then the geometry of the universe is flat. In Figure 7 we show the "distance modulus" (or $m-M$ from Equation 1) as a function of the logarithm of the redshift. Different models of the universe are shown. The "empty universe" has $\Omega_M = 0.0$, $\Omega_\Lambda = 0.0$. The "Einstein-de Sitter universe" (or critical density model) coasts to a stop after an infinite amount of time and has $\Omega_M = 1.0$. Prior to 1998 the expectation was that high redshift Type Ia SNe would show that $\Omega_M = 0.3$, $\Omega_\Lambda = 0.0$; this we call the "open model", as it would lead to the perpetual expansion of the universe even without a positive Cosmological Constant.

Figure 8 is a "differential Hubble diagram." We take the empty universe model from Figure 7 as a reference and plot the differences of the other loci with respect to the empty universe model. What Riess *et al.* (1998) and Perlmutter *et al.* (1999) found was that the high redshift SN data do not fall along the locus of the "open" model. Instead the SNe are "too faint" by about 0.19–0.25 magnitude from redshift 0.4–0.8. Possible explanations are: 1) that some kind of gray dust is dimming the light but not reddening it; 2) Type Ia SNe at this lookback time are inherently dimmer than nearby, more recent, Type Ia SNe; or 3) the SNe are further away than we would expect, given their redshifts, which is evidence for repulsive Dark Energy.

Riess *et al.* (2004) used the Hubble Space Telescope to find Type Ia SNe at even greater redshifts and found that the SNe at $z > 1.3$ were "too bright" compared to the empty universe model. This means that they looked far back enough in time to see the universe when it was small enough and dense enough that the gravitational attraction of matter on all other matter was stronger than any repulsive effect of a positive Cosmological Constant. At a redshift beyond 1.3 the universe is observed to be decelerating. The findings of Riess *et al.*

(2004) also proved that the faintness of Type Ia SNe at redshift ~0.5 was not due to some weird kind of gray dust.

We note that SN data alone do not give us enough leverage to determine the most accurate values of Ω_M and Ω_Λ. Wood-Vasey *et al.* (2007) and others used SN data combined with information from "baryon acoustic oscillations" (Eisenstein *et al.* 2005). The flatness of the geometry of the universe is best demonstrated from the characteristic angular size of the warmer and cooler spots of the Cosmic Microwave Background (CMB) radiation, such as shown by the analysis of seven years of data from the Wilkinson Microwave Anisotropy Probe (WMAP) by Komatsu *et al.* (2011).

Once we know the matter and Dark Energy content of the universe, we can determine the expansion history of the universe (Figure 9). The universe was dense enough for the first seven billion years that the gravitational attraction of all the matter caused the expansion to be decelerated. After that the effect of repulsive Dark Energy has caused an acceleration of the expansion.

8. Future analysis required

Hicken *et al.* (2009) presented data for 185 nearby Type Ia SNe observed by astronomers from the Harvard-Smithsonian Center for Astrophysics. Only thirty-one of them have values of $\Delta m_{15}(B)$, maximum *U*-band magnitudes, and are at a redshift greater than $z = 0.01$ (which is regarded to be the beginning of the smooth Hubble flow). The *U*-band data show a scatter of ± 0.25 magnitude for a decline rate relation graph or a Hubble diagram, which is almost twice the scatter one sees in other photometric bands. Some of this extra scatter may be due to a viewing angle effect (Maeda *et al.* 2010). It is known that some Type Ia SNe are polarized, implying that the explosions are not spherically symmetric. Since the *U*-band light is dimmed more than the longer wavelength bands, this could increase the scatter of the derived *U*-band absolute magnitudes.

The other factor affecting the *U*-band data is the perennial challenge to correct the photometry for differences in the effective bandpasses used for all the observations from all telescopes for a given SN. Using lab data obtained by us, or provided by manufacturers, and spectra of the SN themselves, the method of spectroscopically-derived corrections (the so-called "S-corrections") allows us to resolve this problem, in principle. The method was originated by Stritzinger *et al.* (2002), who applied it to SN 1999ee, and by Krisciunas *et al.* (2003), who applied it to SN 2001el. Other papers written by us show photometric corrections to optical and IR photometry of many objects (Candia *et al.* 2003, Krisciunas *et al.* 2004b, 2004c, 2007, 2009b, 2011).

Our paper on SN 2003gs (Krisciunas *et al.* 2009b), however, did not include *U*-band S-corrections, and we chose at that time not to publish *U*-band photometry from one telescope because it was systematically 0.4 magnitude brighter at one month after maximum light compared to data from two other

telescopes. We now have worked out corrections and can reconcile the otherwise discordant *U*-band data of SNe 2003gs and 2003hv obtained with three telescopes. This is a step in the right direction. Details will be published in a separate paper.

Why are the *U*-band data so important? Both the Sloan Digital Sky Survey supernova search (Kessler *et al.* 2009) and the CFHT Legacy Supernova Survey (Conley *et al.* 2011) discovered systematic errors in the distance moduli of high-redshift SNe when anchored with *U*-band photometry of nearby objects. Both projects decided to eliminate from the analysis data that originated in the restframe *U*-band. (For example, a SN at redshift 0.7 observed in the *R*-band gives us photons emitted in the *U*-band.) To utilize fully the SN surveys of the future such as the Dark Energy Survey and data from the Large Synoptic Survey Telescope we need to fix the old *U*-band photometry (which may be impractical or impossible), or we have to restrict ourselves to data obtained with a minimum number of telescopes and cameras, such as the Carnegie Supernova Project (Hamuy *et al.* 2006).

Until recently the effective filter profiles for S-corrections were obtained using laboratory data for the transmissions and reflectances of all the optics in a telescope and camera, then multiplying all these functions of wavelength together. This allowed us to reconcile previously discordant data obtained with cameras having significantly different filters. Stubbs *et al.* (2007) and Rheault *et al.* (2010) have shown the way to the future for SN calibration. They designed two systems to measure the effective filter profiles in situ. Stubbs *et al.* used a tunable laser and Rheault *et al.* use a "monochromator" to scan the transmission throughout the whole system from the ultraviolet through the near-IR.

9. Conclusions

Data obtained over the past decade have confirmed the suggestion of Elias *et al.* (1985) that optical minus infrared colors of Type Ia SNe are uniform within certain ranges of the *B*-band decline rate. A combination of optical and near-IR photometry allows us to determine the amount of extinction very well, and allows us to determine the reddening parameter R_V (Krisciunas *et al.* 2007). The suggestion of Meikle (2000) and Krisciunas *et al.* (2003) that Type Ia SNe are nearly standard candles in the near-IR has been borne out by subsequent analysis of the absolute magnitudes at maximum light (Krisciunas *et al.* 2004a, Wood-Vasey *et al.* 2008, Kattner *et al.* 2012). The goal of future photometry of Type Ia SNe will be to obtain well calibrated data at ultraviolet, optical, and IR wavelengths for nearby SNe and also for SNe out to redshift $z = 2$. Some of these observations must be made from space, such as with the satellites Euclid, WFIRST, or the James Webb Space Telescope. Infrared data in particular, whether in the observer's frame or the restframe, will be very important for observational cosmology.

10, Acknowledgements

The author thanks Max Stritzinger and Mark Phillips for reading a previous draft of this paper, and for useful comments.

References

Baade, W. 1938, *Astrophys. J.*, **88**, 285.
Candia, P., *et al.* 2003, *Publ. Astron. Soc. Pacific*, **115**, 277.
Cardelli, J. A., Clayton, G. C., and Mathis, J. S. 1989, *Astrophys. J.*, **345**, 245.
Conley, A., *et al.* 2011, *Astrophys. J., Suppl. Ser.*, **192**, 1.
Contreras, C., *et al.* 2010, *Astron. J.*, **139**, 519.
Eisenstein, D. J., *et al.* 2005, *Astrophys. J.*, **633**, 560.
Elias, J. H., Frogel, J. A., Hackwell, J. A., and Persson, S. E. 1981, *Astrophys. J.,* Lett. Ed., **251**, L13.
Elias, J. H., Matthews, K., Neugebauer, G., and Persson, S. E. 1985, *Astrophys. J.*, **296**, 379.
Elias-Rosa, N., *et al.* 2006, *Mon. Not. Roy. Astron. Soc.*, **369**, 1880.
Elias-Rosa, N., *et al.* 2008, *Mon. Not. Roy. Astron. Soc.*, **384**, 107.
Filippenko, A. V. 1997, *Ann. Rev. Astron. Astrophys.*, **35**, 309.
Folatelli, G., *et al.* 2010, *Astron. J.*, **139**, 120.
Freedman, W. L., *et al.* 2001, *Astrophys. J.*, **553**, 47.
Frogel, J. A., Gregory, B., Kawara, K., Laney, D., Phillips, M. M., Terndrup, D., Vrba, F., and Whitford, A. E. 1987, *Astrophys. J.*, **315**, 129.
Garnavich, P. M., *et al.* 2004, *Astrophys. J.*, **613**, 1120.
Goobar, A. 2008, *Astrophys. J.*, **686**, 103.
Hamuy, M., Phillips, M. M., Suntzeff, N. B., Schommer, R. A., Maza, J., Smith, R. C., Lira, P., and Aviles, R. 1996, *Astron. J.*, **112**, 2438.
Hamuy, M., *et al.* 2006, *Publ. Astron. Soc. Pacific*, **118**, 2.
Hernandez, M., *et al.* 2000, *Mon. Not. Roy. Astron. Soc.*, **319**, 223.
Hicken, M., *et al.* 2009, *Astrophys. J.*, **700**, 331.
Jha, S., Riess, A. G., and Kirshner, R. P. 2007, *Astrophys. J.*, **659**, 122.
Jha, S., *et al.* 1999, *Astrophys. J., Suppl. Ser.*, **125**, 73.
Kasen, D. 2006, *Astrophys J.*, **649**, 939.
Kattner, S., *et al.* 2012, *Publ. Astron. Soc. Pacific*, **124**, 114.
Kessler, R., *et al.* 2009, *Astrophys. J., Suppl. Ser.*, **185**, 32.
Komatsu, E., *et al.* 2011, *Astrophys. J., Suppl. Ser.*, **192**, 18.
Kowal, C. T. 1968, *Astron. J.*, **73**, 1021.
Krisciunas, K. 1993, in *Encyclopedia of Cosmology*, ed. N. S. Hetherington, Garland, New York and London, 218–244.
Krisciunas, K., Hastings, N. C., Loomis, K., McMillan, R., Rest, A., Riess, A. G., and Stubbs, C. 2000, *Astrophys. J.*, **539**, 658.
Krisciunas, K., Phillips, M. M., and Suntzeff, N. B. 2004a, *Astrophys. J., Lett. Ed.*, **602**, L81.

Krisciunas, K., Prieto, J. L., Garnavich, P. M., Riley, J.-L. G., Rest, A., Stubbs, C., and McMillan, R. 2006, *Astron. J.*, **131**, 1639.
Krisciunas, K., *et al.* 2001, *Astron. J.*, **122**, 1616.
Krisciunas, K., *et al.* 2003, *Astron. J.*, **125**, 166.
Krisciunas, K., *et al.* 2004b, *Astron. J.*, **127**, 1664.
Krisciunas, K., *et al.* 2004c, *Astron. J.*, **128**, 3034.
Krisciunas, K., *et al.* 2005, *Astron. J.*, **130**, 2453.
Krisciunas, K., *et al.* 2007, *Astron. J.*, **133**, 58.
Krisciunas, K., *et al.* 2009a, *Astron. J.*, **137**, 34.
Krisciunas, K., *et al.* 2009b, *Astron. J.*, **138**, 1584.
Krisciunas, K., *et al.* 2011, *Astron. J.*, **142**, 74.
Layden, A. C., Hanson, R. B., Hawley, S. L., Klemola, A. R., and Hanley, C. J. 1996, *Astron. J.*, **112**, 2110.
Leavitt, H. S., and Pickering, E. C. 1912, *Circ. Harvard Coll. Obs.*, No. **173**, 1.
Lira, P. 1995, Master's thesis, Univ. Chile.
Maeda, K., *et al.* 2010, *Nature*, **466**, 82.
Mandel, K., Narayan, G., and Kirshner, R. P. 2011, *Astrophys. J.*, **731**, 120.
Mandel, K., Wood-Vasey, W. M., Friedman, A. S., and Kirshner, R. P. 2009, *Astrophys. J.*, **704**, 629.
Meikle, W. P. S. 2000, *Mon. Not. Roy. Astron. Soc.*, **314**, 782.
Minkowski, R. 1941, *Publ. Astron. Soc. Pacific*, **53**, 224.
Perlmutter, S., *et al.* 1999, *Astrophys. J.*, **517**, 565.
Phillips, M. M. 1993, *Astrophys. J., Lett. Ed.*, **413**, L105.
Phillips, M. M. 2012, *Publ. Astron. Soc. Australia*, in press, arXiv:1111.4463.
Phillips, M. M., Lira, P., Suntzeff, N. B., Schommer, R. A., Hamuy, M., and Maza, J. 1999, *Astron. J.*, **118**, 1766.
Rheault, J.-P., Depoy, D. L., Behm, T. W., Kylberg, E. W., Cabral, K., Allen, R., and Marshall, J. L. 2010, in *Ground-based and Airborne Instrumentation for Astronomy III*, ed. I. S. McLean, S. K. Ramsay, H. Takami, SPIE 7735E, 201.
Riess, A. G., Press, W. H., and Kirshner, R. P. 1996, *Astrophys. J.*, **473**, 88.
Riess, A. G., *et al.* 1998, *Astron. J.*, **116**, 1009.
Riess, A. G., *et al.* 2004, *Astrophys. J.*, **607**, 665.
Stritzinger, M., *et al.* 2002, *Astron. J.*, **124**, 2100.
Stubbs, C. W., *et al.* 2007, in *The Future of Photometric, Spectrophotometric, and Polarimetric Standardization*, ed. C. Sterken, ASP Conf. Ser., 364, 373.
Suntzeff, N. B., *et al.* 1999, *Astron. J.*, **117**, 1175.
Wang, L. 2005, *Astrophys. J.*, **635**, 33.
Wang, X., *et al.* 2008, *Astrophys. J.*, **675**, 626.
Wood-Vasey, W. M., *et al.* 2007, *Astrophys. J.*, **666**, 694.
Wood-Vasey, W. M., *et al.* 2008, *Astrophys. J.*, **689**, 337.

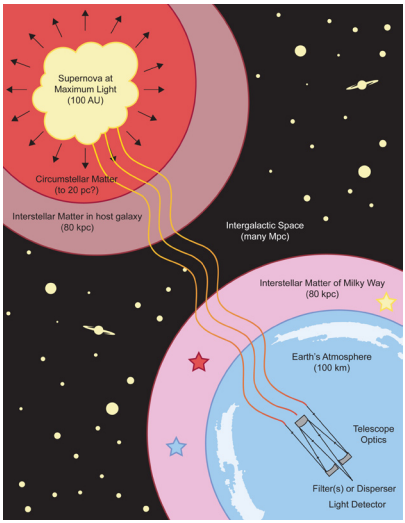

Figure 1. Schematic diagram of the light path of a Type Ia supernova to a telescope situated on the Earth. Figure by Elisabeth Button.

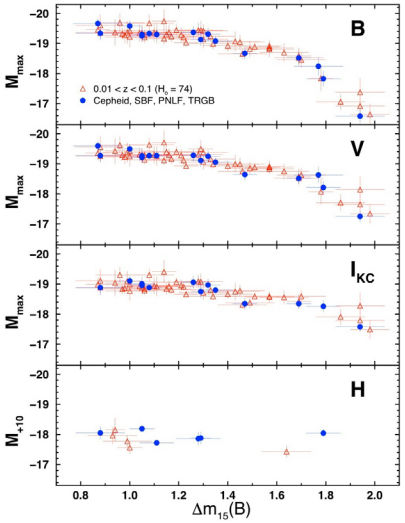

Figure 2. Decline rate relations of Type Ia SNe for the BVI and H-bands (Krisciunas et al. 2003). The x-axis parameter is the number of B-band magnitudes that a Type Ia SNe declines in the first 15 days after the time of B-band maximum. For BVI the absolute magnitudes are the maximum brightness values. For the near-IR H-band the absolute magnitudes are measured at 10 days after T(Bmax). Figure by Mark Phillips.

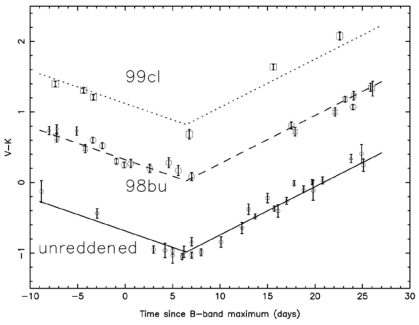

Figure 3. *V–K* colors of Type Ia SNe unreddened in their host galaxies (lowest locus) and for two reddened objects. Based on data discussed by Krisciunas *et al.* (2000).

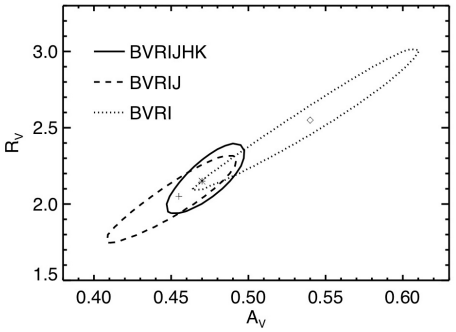

Figure 4. Reddening parameter R_V as a function of the difference of the amounts of *V*-band extinction suffered by SN 2001el and its clone SN 2004S (Krisciunas *et al.* 2007). Figure and analysis method by Peter Garnavich.

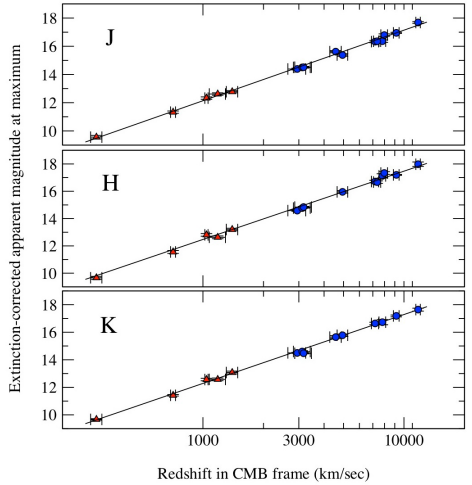

Figure 5. Infrared Hubble diagrams of Type Ia SNe at maximum brightness (Krisciunas *et al.* 2004a). If these objects are standard candles, then from Equation 1 it follows that the y-axis values are a simple function of the logarithm of the distance in parsecs. The slope of the line is fixed at 5.

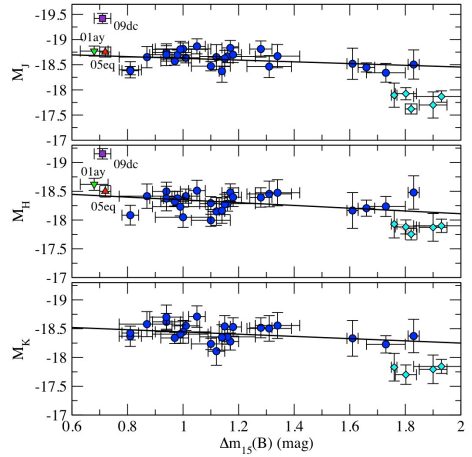

Figure 6. Near-IR absolute magnitudes of Type Ia SNe at maximum brightness, as a function of the *B*-band decline rate parameter (Krisciunas *et al.* 2011).

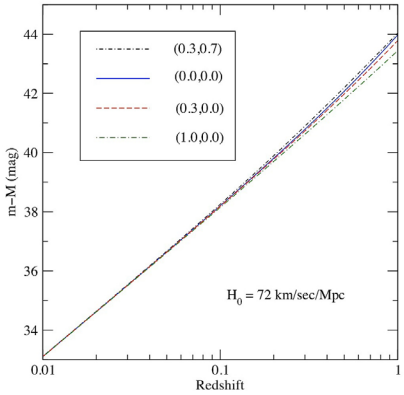

Figure 7. Theoretical Hubble diagram for various combinations of the mass density parameter Ω_M and the Dark Energy density Ω_Λ. The modern "concordance model" of the universe has $\Omega_M \approx 0.3$, $\Omega_\Lambda \approx 0.7$ and a Hubble constant ~ 72 km s^{-1} Mpc^{-1} (Freedman *et al.* 2001). Note that one only starts to detect evidence of Dark Energy from SN photometry at redshift greater than about $z \sim 0.2$.

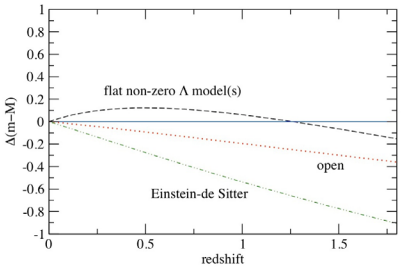

Figure 8. A differential Hubble diagram. We take the "empty universe model" as the reference from Figure 7. Prior to 1998 the expectation was that the data would lie along the "open" line: $\Omega_M = 0.3$, $\Omega_\Lambda = 0.0$. Data of Riess *et al.* (1998) and Perlmutter *et al.* (1999) showed that at redshift ~ 0.5 Type Ia SNe were "too faint" by about 0.2 mag compared to the open model.

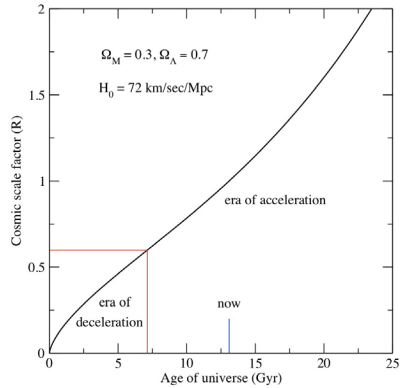

Figure 9. The expansion history of the universe. The y-axis is the cosmic scale factor, effectively the average distance between galaxies.

Amateur Observing Patterns and Their Potential Impact on Variable Star Science

Matthew R. Templeton
AAVSO, 49 Bay State Road, Cambridge, MA 02138; matthewt@aavso.org

Presented at the 100th Spring Meeting of the AAVSO, May 23, 2011; received February 13, 2012; accepted February 14, 2012

Abstract In this paper I highlight some trends seen in amateur observations submitted to the AAVSO over the past fifty years. Some systematic trends are noted in both the amount of data submitted and the frequency with which stars are observed. Two trends are evident: the decreasing number of days per year when individual stars are observed, and the overall decreasing number of visual observations submitted. The former is shown through an analysis of data submitted for a number of subclasses of cataclysmic variable, while the latter is generally evident across all variable star types through our overall annual totals. A decrease in nightly coverage may impact the kinds of science that can be done with AAVSO light curves. The decrease in visual observing may result in a loss of long-term coverage that impacts the usability of long-term light curves. I discuss possible impacts on the kinds of science that can be done with AAVSO data and long-term light curves, and suggest ways to address this issue.

1. Introduction

The AAVSO International Database (AID) contains over 20 million observations of thousands of individual stars. The data are a mix of both visual magnitude estimates and instrumental photometry, with visual data making up the vast majority of all data submitted prior to 1995. Instrumental observations now account for more than eighty percent of all data submitted to the AAVSO every year. Prior to 1995, most observations of variables were nightly or weekly visual observations, and the goal was to monitor these objects for phenomena that occurred on timescales from days to years. Now, a much larger fraction of data submitted consists of instrumental time-series of short-term phenomena (Figure 1). This shift in focus has drawn a number of observers away from long-term monitoring observations toward these more focused, short-term projects. It has also brought about a shift in observing method from visual to CCD; while the number of visual observers still numbers around 800 (Figure 2), the number of visual observations of all variable stars submitted per year is now about half the number submitted in the mid-1990s. When visual observers do observe, they do not do so in the numbers they once did.

The question of whether long-term visual observation of variable stars should be encouraged is an important one. Underlying this question is a more

fundamental one of whether the scientific questions that long-term monitoring of variable stars can answer are ones that are still of interest to the scientific community. Any observational program must be motivated by the pursuit of valid scientific questions in order to be relevant to astronomical research. This is as true of instrumental observations as visual ones. In order to motivate a discussion of this question, I present a simple study of the daily observational coverage of cataclysmic variable stars to quantify the shift in focus from long-term monitoring to more intensive short-term observations.

2. Selection of CV data sets for examination

To examine trends in long-term coverage, we searched the AID for observations of CVs of several important subclasses. We selected stars based upon the following criteria:

- star is classified as NL or UGx;
- at least 1000 observations/500 days covered since 1961;
- observations counted: visual, and (B,V, unfiltered) CCD;
- we are not counting the total number of observations, but *the number of days they were observed at least once.*

The last bullet is critical: this study aims to address not the raw number of observations made per year, but the daily coverage of individual stars. The number of days observed per year is a better indicator of how useful a light curve will be in performing studies of long-term behavior, potentially yielding information about mean light levels, outburst frequency, and outburst duration among other things.

3. Results

There are between two and three dozen stars among each of the NL, UGSS, UGSU, and UGZ types that meet these criteria. The results for each of these four subsets are as follows:

UGSS-type—See Figure 3. Many of these stars have been observed for many decades, with the longest-observed star being SS Cygni itself (SS Cyg is one of the best-observed stars in the AID, with nearly 365 days of coverage per year). Among the twenty best-observed stars, only SS Cyg has retained a near continuous level of daily coverage. The remainder of the twenty show declines in coverage of varying degree. Coverage slowly increased through the mid- to late-1990s, and then began to decline across the board. Some declines have been dramatic (a factor of two or more), but others show less of a decline. In most cases, the onset of declines appear to be in the late 1990s to early 2000s.

UGSU-type—Most of these stars show significant declines in coverage starting in 2000, with some well-known and observed stars (like SU UMa itself) losing nearly half of their daily coverage since 2000. Others have been even more precipitous, with southern stars in particular showing losses in daily coverage of greater than fifty percent (for example: TU Men, WX Hyi, Z Cha, and OY Car). For some stars, daily coverage has declined to levels not seen since 1970.

UGZ-type—Z Cam itself is well observed but as with the UGSS stars, the UGZs show generally declining coverage in the past five to ten years. Some of the small number of stars that first came under observation in the 1970s and 1980s (for example: EM Cyg, AT Cnc, BI Ori, VW Vul, and V344 Ori) have leveled off in coverage. EM Cyg is covered for around sixty percent of the nights per year, but the more equatorial sources have coverage only about one-third of the year, while the more southerly star TT Ind is hardly observed anymore—only around twenty percent of the nights per year have at least one observation.

Novalikes and UGWZ-types—It is difficult to make any blanket assessments of their long-term coverage. Few of these stars have been extensively observed for many decades, although UZ Boo (UGWZ) appears to receive consistent coverage for about seventy-five percent of the nights per year. Coverage of UGWZ stars with marginally predictable recurrence times may decline outside of expected outburst windows; WZ Sge itself is now only observed about 125 nights per year, about the same as in 1980. Among the novalikes only V Sge has good coverage throughout the fifty-year span of this study, and the vast majority of these objects were discovered within the past fifty years. Observations of these sources peaked in the 1990s, probably due to the interest generated from space-based X-ray observations in the 1970s–1990s. TT Ari has had consistent coverage of about 200 nights per year since the mid-1980s, around the time it returned from its previous deep fade (circa 1985).

4. Overall trends

Most of the objects under consideration here have shown some decline in coverage since the 1990s when interest in cataclysmic variables first peaked. While the trends show declines in the number of days covered, many of these stars also show declines in the number of observations made per year, despite the consistent increase in the total number of observations of all variable stars made per year. Figure 4 shows the number of observations submitted per year for six well-known dwarf novae. Although the totals for individual stars are occasionally punctuated by years with substantial time-series data, in general the number of observations per year per star is declining.

5. Time-Series versus long-term monitoring

The annual total of all observations submitted to the AAVSO includes several hundred thousand data points of time-series observations of a small number of stars. Often, these observations are of interest to that particular observer during a small window of time (for example: a study of an eclipsing binary or outbursting cataclysmic variable). In such cases, the total number of submitted data points is large, but the time-span of the data is very small—often days, weeks, or months—and the star may not be observed again. While the overall number of observations being submitted to the AAVSO is increasing, the coverage and quality of our long-term light curves is not keeping pace with this increase. For many important stars, coverage is in decline.

6. The roles of amateur monitoring and robotic surveys

There are several robotic surveys in existence whose purpose is to conduct nightly monitoring of the visible night sky. Surveys like the All-Sky Automated Survey (ASAS; Pojmański 2002), the Northern Sky Variability Survey (NSVS; Wozniak *et al.* 2004), and the Catalina Real-Time Transient Survey (CRTS; Drake *et al.* 2009) provide a possible means for overcoming the declining numbers of amateur observations of stars with long-term light curves. As of today there is no universally agreed-upon process by which survey data are guaranteed to remain publicly available beyond the lifetime of the individual project, and thus the long-term survivability of robotic survey data is unclear. It is not difficult to ensure that such data be preserved.

There is clearly room for both human and robotic observation of variable stars, and the benefits of both methods are numerous. They should be considered as complementary rather than conflicting. The variable star community needs to address both the declining long-term coverage by the amateur community, and the organized care and maintenance of large and valuable databases created by robotic surveys. Without such a discussion, there is a chance that the scientific value of long-term light curves such as those held by the AAVSO will no longer grow with time.

References

Drake, A. J., *et al.* 2009, *Astrophys J.*, **696**, 870.
Pojmański, G. 2002, *Acta Astron.*, **52**, 397.
Wozniak, P. R., *et al.* 2004, *Astron. J.*, **127**, 2436.

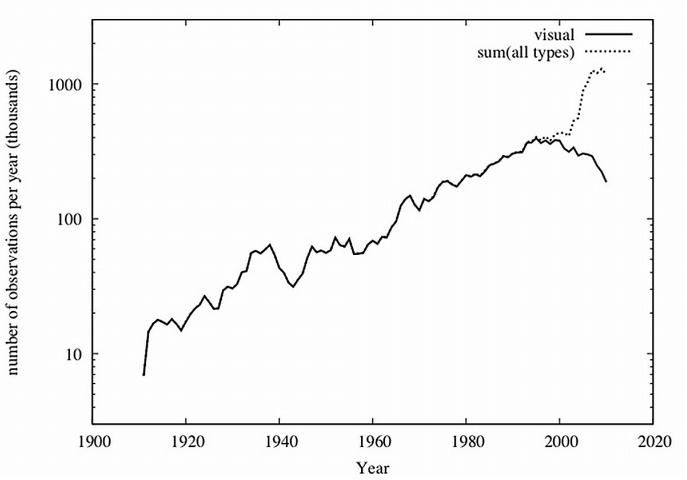

Figure 1. The number of observations per year found in the AAVSO International Database (AID): solid line, visual data; dotted line, all data. These numbers include data from the AFOEV and RASNZ. Beginning around the year 2000, CCD observations became the majority of observations submitted per year. The number of visual observations has been in decline since its historical maximum in 1995.

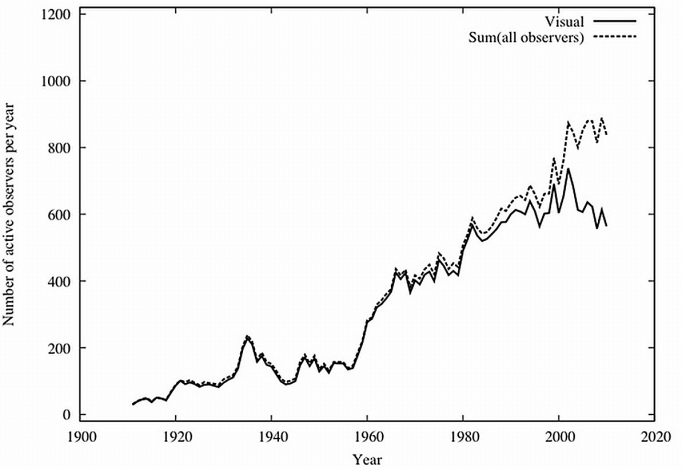

Figure 2. The number of observers whose data are submitted to the AID per year: solid line, visual data; dotted line, all data. Visual observers—including those who also observe with a CCD part of the time—still represent a majority of observers. Recent trends suggest the number of observers is holding steady or declining slightly.

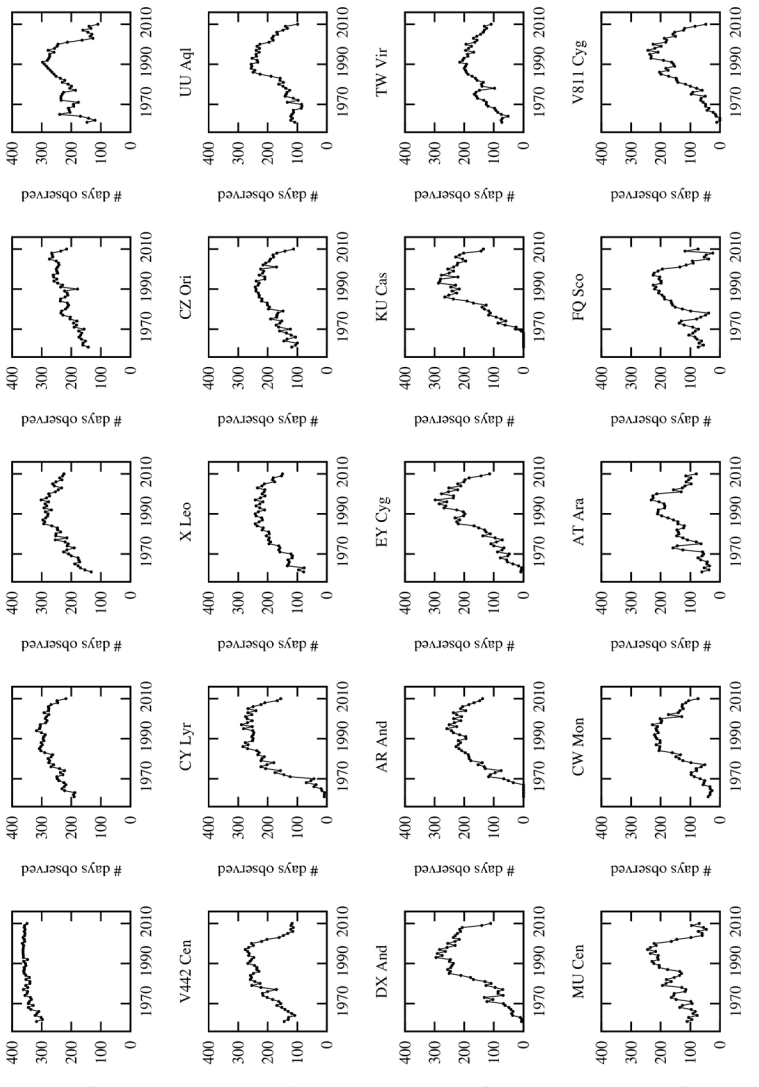

Figure 3. Daily coverage: The twenty best-observed dwarf novae of type UGSS (SS Cyg-type).

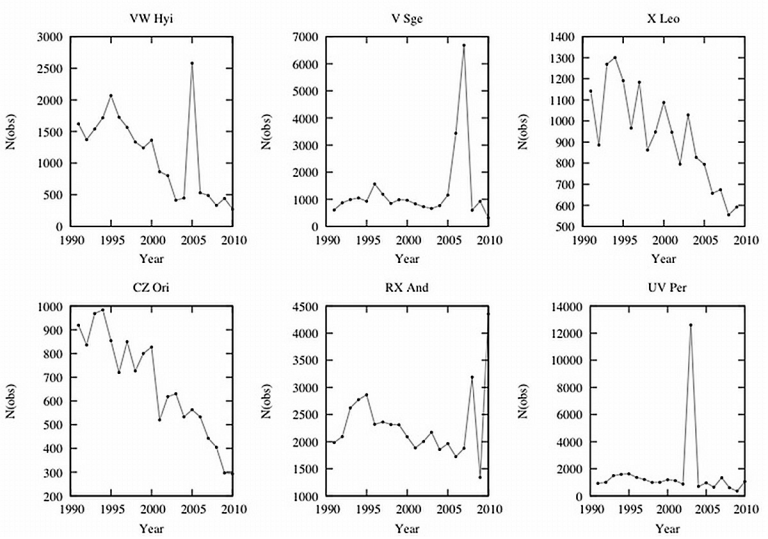

Figure 4. Yearly totals for six dwarf novae, 1991–2010. Coverage of these stars is declining, with some declines (especially CZ Ori, X Leo, and VW Hyi) being especially dramatic. With fewer observations and fewer days per year, it becomes increasingly difficult to study long-term changes in these stars.

The Acquisition of Photometric Data

Arlo U. Landolt
Department of Physics and Astronomy, Louisiana State University, Baton Rouge, LA 70803; landolt@phys.lsu.edu

Presented at the 100th Annual Meeting of the AAVSO, October 8, 2011; received January 6, 2012; accepted January 6, 2012

Abstract The planning and execution of a typical observing run will be outlined. Particular attention will be addressed to details which aid in the acquisition of quality photometry.

1. Introduction

The astronomical literature utilizes a number of terms which describe the kind of photometry undertaken for a given project. A description of the terminology is in order.

Relative photometry is the kind of photometry which most observers, and certainly virtually all AAVSO observers, do in their studies. It is photometry tied into sets of standard stars established around the sky, with zero points which can be traced back through photometric history. Such measurements are not tied into any laboratory system, but are related to nearby standard stars, in a variety of photometric standard systems. Examples of such photometric systems are the UBVRI system of Johnson, Kron and Cousins, the Stromgren four-color (uvby) system, and the Sloan u'g'r'i'z' photometric system.

Absolute photometry is based on spectrophotometry, or photometry tied to a laboratory source, such as a black body cavity, or something similar, all as an integral part of the data acquisition process. Absolute photometry is based on physical units. In spite of the terminology used on occasion in some of the recent literature, only a small number of astronomers (for example, Art Code, James Gunn, Bev Oke, and Don Hayes) ever have done absolute photometry.

Differential photometry is the direct comparison of two or more stellar images, historically done using a photographic plate, or a photomultiplier, but now best done with CCD imaging. Many stellar images are obtained on the same photograph, or CCD image (frame), and hence can be measured, intercompared, with high precision because the air masses essentially are identical. (This is not necessarily a true statement for some of the large CCD arrays.) One directly compares the intensities of two nearby images, determining the difference in intensity, and perhaps then plotting the result versus time to search for a light variation of the object under study. Most of the observing done by AAVSOers is this kind of photometry.

Be aware that all sky photometry does *not* lead to absolute photometry!

2. Interesting history and useful references

There appeared in the literature some decades ago an interesting series of papers by Weaver (1946a–f, 1962). He summarized therein a review of the history of astronomical photometry up to the beginning of the photoelectric photometry era. An excellent history of astronomical photometry was published by Hearnshaw (1996), covering the development of astronomical photometry from the times of the ancients to the beginning of the current epoch of charge-coupled devices (CCDs) as the detector of choice. A discussion of the most used photometric system over the past sixty years, the Johnson-Kron-Cousins UBVRI photometric system, appeared in Landolt (2007a, 2011).

Along with the history of actually completing photometric observations, it is of interest to review the accuracies achieved by the techniques available over the decades. Most photometry was accomplished in the first half of the twentith century either using the human eye, or photography. Early attempts to do what we now call photoelectric photometry included, for example, observations by Stebbins (1910). Also read chapter 9 in Hearnshaw (1996). Photometric accuracies which were achieved over time have been on the order of and have improved from 0.25 magnitude for the human eye (under controlled conditions, the accuracy is under 0.1 magnitude; see Williams and Saladyga (2011)), to 0.02 magnitude for photographic plates, to 0.005 magnitude for all sky photoelectric and CCD photometry, 0.0005 magnitude for CCD derived differential photometry. Space-based instrumentation, such as the Kepler spacecraft, can do an order of magnitude better in accuracy.

The AAVSO photometrists have at their disposal a number of books which describe procedures in data acquisition and analysis. Four such books, listed in order of publication date, are by Henden and Kaitchuck (1982), Sterken and Manfroid (1992), Howell (2006) with particularly useful references in his Appendix A, and Warner and Harris (2006). A new book on CCD photometry is in preparation (Henden 2012). The different viewpoints and approaches are a positive in understanding and in aiding observers in defining an approach with which they are comfortable.

3. Thoughts on observing

The two photometric filter systems of most interest to AAVSO members are the UBVRI Johnson-Kron-Cousins system, and the Sloan u'g'r'i'z' filter system. These two filter systems have the advantage that both are broad band filter systems. Both tie into a huge history of data (UBVRI) and as a tie into recent sky survey projects (Sloan Digitial Sky Survey = SDSS). The AAVSO has taken advantage of these facts in its APASS (AAVSO Photometric All Sky Survey) sky survey, using the Johnson B and V filters, plus the g'r'i' filters from the Sloan system.

It is *most* important to use a filter if at all possible! An observer will not be able to reach as faint magnitudes when using a filter, but the resulting measurement

will have more lasting scientific value. That is because an image through a standard filter, say Johnson V, is more easily compared to other observers' data. The transformation relations between the data sets have a better likelihood of being linear, of being a straight-line relation, of being better correlated.

Unfiltered images may be used to determine times of maxima or minima for variable celestial objects. However, one cannot as easily relate unfiltered data to other data sets. The relation between an unfiltered image formed from photoms from across the spectrum and an image resulting from a filtered image defined by a filter's band width, is not cleanly, linearly, defined.

While there is no one precisely correct way to observe, one that has proved fruitful has been described in some detail by Landolt (2007a). More specific situations are covered in several of his papers which provide standard stars for calibration of data taken using the UBVRI photometric system filters (Landolt 1983, 1992, 2007b, 2009; Landolt and Uomoto 2007). Much of what follows will be based upon this material, particularly from Landolt (2007a). No matter the observing program in which one uses CCDs as the detector, one has to obtain dark frames, bias frames, and dome flats or sky flats, for *each* night's observing in order to obtain the most accurate results. The dark and dome flat frames can be obtained during the afternoon. Suggestions may be obtained from AAVSO manuals and from books such as Howell (2006) and Henden (2012). Comparison stars should approximate the variable star as closely as possible, both in magnitude and color index.

A night's observing plan depends upon the program, of course. The most rewarding program is one which incorporates good science and is fun to pursue. So find a star, or a class of variable star, and observe and learn about them! If the need, or sky conditions, demand or allow differential photometry only, then one need know only the coordinates of the object or objects to be observed that night. The assumption is that the comparison stars exist in the field of the program object. They should approximate the brightness and color index of the variable star to provide the most consistent results. If non-photometric skies persist, one must ensure that the photometric measures, the CCD frames, will include the appropriate stars, in brightness and color index, which will permit good differential photometry to be done. The AAVSO chart and photometric sequence team in many instances will have provided an appropriate comparison star sequence. If the observer happens to be blessed with a proper astronomical environment, that is, a clear and photometric sky with some regularity, then the opportunity exists for the observer to establish a photometric sequence. For the majority of AAVSO observations, the observer will take a series of exposures of sufficient length to provide a good signal to noise ratio for the program object.

Since AAVSO members primarily are interested in variable stars, the observer must time observations as accurately as possible. The time at which each frame, each image, was exposed, must be recorded. The shorter the period of the variable star, the more accurate must be the timing measure. The time of the final magnitude determination should be taken as the central time of

the exposure. The central time of the exposure should be converted to the Heliocentric Julian Day (HJD). An AAVSO data submittal form can accept either the Julian Day (JD), that is the barycentric Julian Day, or the HJD. The HJD is the more accurate number, and especially is needed, is a must, for the short period variables. The JD is usable for the long period variable stars since their periods are long. Long term, though, even data for stars of long period benefit if the timings of observations are given in HJDs.

On the other hand, on photometric nights when the observational program involves standardization work, or all sky relative photometry, then the observer needs to plan more carefully. A sufficient number of appropriately placed, during the night, measures of extinction and transformation stars need to be observed (see Figures 4 and 5 in Landolt (2007a), together with the associated discussion). One must realize that extinction can and does vary throughout the night (see Landolt 2007a, Figure 8 and page 41). Although an observer can record images of fainter objects if a filter is not used, it is important to realize that photometric results have enhanced value if a filter is used in the light path. A Johnson V filter is preferred; its use will allow the best tie-ins to the AAVSO sequences and to most photometric systems, and hence enhances the value of the data.

When doing all sky relative photometry, an observer will want to intersperse standard star images with program star images with standard star images, and so on. This procedure is repeated throughout a night, the number of repetitions depending upon the length of the night. It is useful to observe in a pattern, like VBUUBV, so that one can average measures, images, frames, around a common air mass. This procedure works best for short exposures and when the CCD has a short read-out time.

In either situation an observer must keep good notes, an informative log book, so that during analysis one can recover and remember sky conditions, equipment behavior, and so on. State the size of the aperture used during data reductions. One must use the same size aperture for standard stars and for program stars in all sky photometry, and for the variable star and the comparison star(s) when doing differential photometry. Such information particularly is important during attempts to understand errant (outlying) data points. Such information is crucial for future users of the data, either the observer who by that time has forgotten just what happened at the telescope, or the person who downloaded the data, and now needs to understand how to meld the observer's measurements with data from other sources.

Given a "raw" CCD data frame, one immediately can difference the signal between a variable star and a comparison star, then add that difference to the comparison star's known magnitude, and get the magnitude of the variable at the moment of exposure. However, to get the best accuracy, the most accurate final magnitude for the variable object, whether or not the data were taken under a photometric sky or through cirrus, say, one first should subtract the bias frame and divide out the flat frame. One should apply extinction corrections, too. Here, on a non-photometric night, is the one time when it is useful to use "mean extinction coefficients." The observer is encouraged to reference the

detailed explanations in the *AAVSO CCD Observing Manual* (AAVSO 2011), as well as the reference books cited earlier.

Final results from all sky photometry will include magnitudes, color indices, and HJDs. Final results for differential photometry obtained under non-photometric skies, will include HJDs and associated differential magnitudes.

4. Acknowledgements

The author thanks James L. Clem and Arne A. Henden for their comments. The author's work in recent years has been funded by the National Science Foundation.

References

AAVSO 2011, *The AAVSO CCD Observing Manual*, AAVSO, Cambridge, MA.

Hearnshaw, J. B. 1996, *The Measurement of Starlight: Two Centuries of Astronomical Photometry*, Cambridge Univ. Press, Cambridge.

Henden, A. A., 2012, in preparation.

Henden, A. A., and Kaitchuck, R. H. 1982, *Astronomical Photometry*, Van Nostrand Reinhold, New York.

Howell, S. B. 2006, *Handbook of CCD Astronomy*, Cambridge Univ. Press, Cambridge.

Landolt, A. U. 1983, *Astron. J.*, **88**, 439.

Landolt, A. U. 1992, *Astron. J.*, **104**, 340.

Landolt, A. U. 2007a, in *The Future of Photometric, Spectrophotometric, and Polarimetric Standardization*, ed. C. Sterken, ASP Conf. Ser., 364, 27.

Landolt, A. U. 2007b, *Astron. J.*, **133**, 2502.

Landolt, A. U. 2009, *Astron. J.*, **137**, 4186.

Landolt, A. U. 2011, in *Astronomical Photometry: Past, Present and Future*, eds. E. F. Milone and C. Sterken, Astrophys. Space Sci. Libr., 373, 107.

Landolt, A. U., and Uomoto, A. K. 2007, *Astron. J.*, **133**, 2429.

Stebbins, J. 1910, *Astrophys. J.*, **32**, 185.

Sterken, C., and Manfroid, J. 1992, *Astronomical Photometry: A Guide*, Springer-Verlag, Berlin.

Warner, B. D., and Harris, A. W. 2006, *A Practical Guide to Lightcurve Photometry and Analysis*, Springer Science and Business Media, New York.

Weaver, H. F. 1946a, *Popular. Astron.*, **54**, 211.

Weaver, H. F. 1946b, *Popular Astron.*, **54**, 287.

Weaver, H. F. 1946c, *Popular Astron.*, **54**, 339.

Weaver, H. F. 1946d, *Popular Astron.*, **54**, 389.

Weaver, H. F. 1946e, *Popular Astron.*, **54**, 451.

Weaver, H. F. 1946f, *Popular Astron.*, **54**, 504.

Weaver, H. F. 1962, *Handb. Phys*, **54**, 130.

Williams, T. R., and Saladyga, M. 2011, *Advancing Variable Star Astronomy: The Centennial History of the American Association of Variable Star Observers*, Cambridge Univ. Press, Cambridge, 44.

Digital Archiving: Where the Past Lives Again

Kevin B. Paxson
20219 Eden Pines, Spring, TX 77379; kbpaxson@aol.com

Presented at the 100th Annual Meeting of the AAVSO, October 8, 2011; received October 21, 2011; revised February 2, 2012; accepted February 14, 2012

Abstract The process of digital archiving for variable star data by manual entry with an Excel spreadsheet is described. Excel-based tools including a Step Magnitude Calculator and a Julian Date Calculator for variable star observations where magnitudes and Julian dates have not been reduced are presented. Variable star data in the literature and the AAVSO International Database prior to 1911 are presented and reviewed, with recent archiving work being highlighted. Digitization using optical character recognition software conversion is also demonstrated, with editing and formatting suggestions for the OCR-converted text.

1. Introduction

When AAVSO Science Director Dr. Matthew Templeton initiated the Harvard Annals Digitization Project in August of 2010, archival digitizing activity at the AAVSO had been going on for some time. AAVSO Technical Assistant Dr. Michael Saladyga has, for example, digitized over 94,000 variable star observations of the late AAVSO member Wayne Lowder. Since October 2009, the Eggen Digitization Team (George Silvis and others) has begun to capture hundreds of thousands of photoelectric observations of Olin Eggen from the 1950s into the 1990s. Brian Skiff of the U.S. Naval Observatory in Flagstaff, Arizona, has digitized past visual and photoelectric data from the literature. Recently, Bob Stine, Christian Fröschlin, Hunter Johnson, Andrew Rupp, and this author have contributed numerous pre-1911 archival observations to the AAVSO International Database (AID). This paper was written to aid in the future research into and archiving of older variable star observations.

Digital archiving is the process of capturing and recording past variable star observations from the literature and from archival sources, culminating with the entry of data into the AID. Digital archiving either involves the manual entry of data into a spreadsheet or using optical character reading (OCR) software to convert image data into text. Digitization using OCR conversion requires additional editing and not all sources of archival variable star data are appropriate for this methodology. Manual data entry and OCR digitization are discussed in later sections.

The archiving of older variable star observations has many benefits. In addition to completing the record of historical observations, it also allows for

astrophysical studies to be performed on long timescales. It provides historical data sets for important variable stars (Figure 1), class prototypes, and novae, sometimes dating back to just after discovery (Figure 2). It also allows for the study of variable star evolution, helping to document phenomena such as changes in period, amplitude, or rates of mass transfer.

2. The archiving process

The digital archiving process consists of the following steps:

- Select your project.
- Check for existing data in the AID.
- Locate and download your data using NASA ADS (for papers) or Google Scholar (for books).
- Obtain AAVSO observer codes for observers in your data set.
- Create your spreadsheet template and then digitize your data.
- Proofread the spreadsheet and email it to the AAVSO.
- The spreadsheet will be converted into a version of the AAVSO Extended Visual ASCII format and entered into the AID by the AAVSO staff.

Variable star data in the literature usually exist in four different forms. In most references (including most of the *Harvard Annals* data), the Julian dates (JDs) are given and the magnitudes exist in reduced format (Figure 3). In older references, the magnitude estimates may exist as unreduced "step" or "step pair" data and calendar dates are given with no JD conversion (Figure 4). In very rare cases, magnitude estimates may exist as "decimal step" or "grade" data (Figure 5). Decimal step data divide the interval between two comparison stars into a number of steps and record just a single observation, i.e. "a6.5b." When working with grade data, magnitudes must then be derived by regression of magnitude versus grade (tables of magnitudes and grades of the comparison stars are usually given within the paper). Photoelectric data for variable stars also exist in the literature from the late 1940s to the 1990s (no example shown) and may provide additional archival material.

3. The spreadsheet template

The main spreadsheet template is shown in Figure 6. It consists of twelve columns (nine of which are kept) and may be up to several thousand rows deep. The key columns are labeled Observer (C), Type (D), Star (E), Julian Day (F), Fainter than (G), Magnitude (H), Comment Codes (I), Uncertain (J) and

Comments (K). Columns C through K are the portions of the spreadsheet which are kept and emailed to AAVSO Headquarters. Columns A and B are the partial JD columns which are summed in Column G. Splitting the JDs and using cell addition can save valuable keystrokes. The Observer Code goes in Column C. Visual observations are denoted with a "V" in Column D. Observations that are "fainter than" or "uncertain" are denoted with a "1" in Columns G and J, respectively. Column K is the Comments column, where the reference for each observation is noted in NASA ADS format with the year, journal, volume number, and page number indicated, along with the digitizer's observer code. Column L is an error check column, where for a given JD, the previous JD is subtracted. A progression of positive numbers downward indicates error-free JD entry. When the spreadsheet data entry is finished, be sure to "Highlight" all of the summed JDs in Column F and do a "Paste Special" and "Values" over the same highlighted contents to preserve the numerical JD values and hit "Save." After a final error check, delete Columns A, B, and L, "Save" the Spreadsheet Template, and email it to AAVSO Headquarters for uploading to the AID.

4. Excel-based archival tools

4.1. A step magnitude calculator

In many cases in the literature, the magnitude of an archival observation is not reduced but is commonly given as a "step" estimate using two comparison stars. In the example shown in Figure 7, an estimate for the Mira variable R Leonis is given as "n5R" and "R2l"—n5R2l—where R represents R Leonis. R Leonis is five steps fainter than comparison star "n" and is two steps brighter than comparison star "l". When the magnitudes of comparison stars "n" and "l" are known, the resultant magnitude is equal to the fractional ratio of the step range to the true magnitude range of the comparison stars. The magnitude for R Leonis can be calculated by the following equation:

$$mR = (\text{Steps (n to R)} / (\text{Steps (n to R)} + \text{Steps (R to l)}) \times (l - n)) + n, \quad (1)$$

where mR is the magnitude estimate for R Leonis, Steps (n to R) and Steps (R to l) are the step parts of the magnitude, and l and n are comparison star magnitudes for l and n, respectively.

The solution for the magnitude for R Leonis is:

$$mR = (5 / (5 + 2) \times (6.48 - 5.84)) + 5.84 = 6.30 \quad (2)$$

The construction of this step magnitude spreadsheet is straightforward. Enter the comparison star names (Columns A and I) and sequence magnitudes (Columns B and H). Follow the instructions and enter the equations given in Figure 7. When step numbers (dark green) are entered in Columns D and F, the

magnitudes of the comparison stars (light green) and step numbers are displayed in the Logic Columns C and G and in row 14. The final reduced magnitude (yellow) is displayed in Cell E16.

4.2. An Excel Julian date calculator

In other instances, archival variable star data may give the dates of the observation in calendar format, commonly with GMT times. In these cases, the Julian date (JD) will need to be calculated. A JD with no heliocentric correction is calculated by the equation:

JD (referenced from October 15, 1582) = 367 × Year – INT (7 × Year + INT ((Month + 9) / 12)) / 4) – INT (3 × (INT ((Year + (Month – 9) / 7) / 100 + 1) / 4 + INT (275 × Month / 9) + Day of the Month + 1721028.5 + UTC Hr. / 24 + UTC Min. / 1440 + UTC Secs. / 86400 (3)

As opposed to using another software package to compute the JD, it can be calculated in Excel by using the equation given above, where the year, month, day of the month, and GMT times in hours, minutes, and seconds become specific cell inputs in Columns A through F, respectively, as shown in Figure 8. In this screen shot of the Excel spreadsheet, Cell J2 is highlighted and the Excel version of the JD equation is shown in the function window and here as Equation 4; the JD (Excel equation to be entered for Cell J2, [all numbers and text between the parentheses]):

"=367*A2-INT(7*(A2+INT((B2+9)/12))/4)-INT(3*(INT((A2+(B2-9/7) /100+1)/4)+INT(275*B2/9)+C2+1721028.5+D2/24+E2/1400+F2/86400" (4)

Otherwise, this JD-calculating spreadsheet template in Figure 8 is similar to its counterpart shown in Figure 6.

When you are finished digitizing, be sure to "Highlight" all of the calculated JDs in Column J and do a "Paste Special" and "Values" over the same highlighted contents to preserve the numerical JD values and hit "Save." Columns A, B, C, D, E, F, and O can then be deleted, the spreadsheet template can then be edited, "Saved", and emailed to AAVSO Headquarters for uploading to the AID.

5. Digitizing suggestions and guidelines

Listed below are a list of suggestions and hints for digitization by spreadsheet entry:

- Research the AID and literature thoroughly.
- Correspond with AAVSO Headquarters (Dr. Matthew Templeton) before selecting of your project; digitize a complete paper, as opposed to doing partial digitization of a given reference.

- Obtain or request necessary AAVSO observer codes beforehand.
- Use a computer with a full-sized keyboard and keypad; use of an all-in-one generic laptop is not recommended.
- Use the "Copy" and "Paste" functions to create and fill the Spreadsheet Template.
- Review your archival article to understand the used of italics, observer abbreviations, and special symbols for "not seen" and "fainter than" observations.
- Record all data as presented in the journal or article.
- Omit "fainter than" and "not seen" observations if no comparison star data are given.
- Determine the photometric system of your paper, as the AAVSO uses the Harvard Photometric system; some papers or archival sources may use Schonfeld, Hagen ASV, or Potsdam photometric sequences; make a comment if the magnitude estimates are not on the Harvard system and enter the "Comment code" "K."
- Average multiple estimates made on the same JD (where no times are given) and make a note in the Comments column.
- Use the "additive columns" method to minimize JD keystrokes.
- Remember to "Copy," "Paste Special," and "Values" for saving JD's derived from mathematical cell operations.
- Check for errors in JD, magnitude, observer, star name, and page number.
- "Save" your work often and take breaks as needed to reduce fatigue.
- Enter Comments codes (Fainter than, Uncertain, etc.) as required.
- In the Comments column, enter the paper reference in ADS format with the page number (if the paper in listed by the ADS, otherwise use the standard AAVSO references format for books and other non-ADS references), your AAVSO observer code, and other comments.
- Run a JD-subtraction quality check to detect possible JD errors.

6. Review of variable star observation in the literature and archival sources

In 1890, Pickering presented and analyzed 125,720 variable star observations from the literature and those sent to Harvard College Observatory between 1837 and prior to 1888 from thirty-one worldwide observers and institutions (Pickering 1890). The observers and institutions identified in that paper

included: *Argelander, Backhouse, Baxendell (Sr. and Jr.), Chandler*, Duner, *Eadie*, Espin, *Harvard College Observatory*, Gore, Hartwig, *Hagen, Heis, Knott*, Lawrence, Markwick, National Observatory in Cordoba, Argentina, Oudemanns, Peck, Plassman, *Parkhurst, Schonfeld*, Sarafik, Shearman, *Sawyer, Schmidt*, Upton, Webb, Wilsing, *Zwack*, and *Zaiser* (observers in Table 1 are indicated here in italics). Until very recently, few observations prior to 1888 existed in the AID. Pickering (1890) is a key reference for variable star observations prior to 1888 and may be an important source for researching additional archival variable star observations.

Table 1 lists a number of variable star observation collections prior to 1911. A total of thirty-one individual sources from the literature and the AAVSO Archives are identified and summarized in the table. The individual columns going from left to right are: the paper, book or archival source; the observer(s); the number of observations (estimated observations are noted); the number of individual stars documented; the magnitude reduction status; the Julian Date conversion status, and the AAVSO digitization status as of this writing. All listed sources are detailed in the reference list. The variable star data sources that have been digitized and are currently in the AID are given in italics.

Table 1 represents over an estimated 222,000 variable star observations prior to 1911, of which over an estimated 39,000 have been digitized up to the present time. Of the 125,720 variable star observations known by Pickering to exist prior to 1888, over 100,000 remain to be digitized and an estimated 98,000 observations from 1888 to 1911 also remain to be digitized. Further research may yield tens of thousands of additional variable star observations.

Additional sources of variable star data include papers in journals of the past: *Astronomische Nachrichten, Astronomical Journal, Monthly Notices of the Royal Astronomical Society, The Observatory,* and others. While this paper mainly concerns itself with the pre-1911 observations, other sources of variable star data are equally important, including unpublished observations in Ph.D. dissertations, photoelectric observations in the literature from the late 1940s to the 1990s, and private collections of individual observatories and archives.

7. Digitization using optical character reading (OCR)

After the presentation of this paper at the AAVSO's Annual Meeting in 2011, the author began to investigate OCR digitization with the freeware program "FreeOCR Version 3.0", which is based on the Tesseract OCR engine. This Windows-based software shows promise with increased digitizing efficiency and accuracy relative to the previously described manual spreadsheet entry method. However, the resulting OCR converted text will have to be edited and formatted within Excel. Figure 9 shows a small highlighted selection of variable star data of RR Andromedae from Campbell and Pickering (1912; left) and the corresponding OCR output (right) using this software.

Several important points about OCR-converted text are noted:

- The thin vertical column lines of the source .pdf file do not affect the resulting OCR text output.
- Text conversion accuracy appears to be high, between 90 and 95%.
- The two-digit year data are offset from the remaining variable star data of the scanned output text; this is not a problem, since the text may be edited within Excel after "Copying and "Pasting."
- Some errors will result from the OCR-conversion process: the bold vertical column lines may introduce spurious text; some italicized and regular text may not be converted properly (C's may become G's, c's may become 0's, 3's or 6's may become 8's or 0's, etc.), decimal points may be skipped or converted to commas and blemishes on the original text file may result in spurious converted text.

The following steps are required to edit the OCR-converted text and to enter it into the standard spreadsheet template (Figure 6):

- Highlight and OCR-convert one column of variable star data at a time; trying to OCR convert an entire page of variable star data at once complicates the editing process.
- "Copy" data from the OCR text window and "Paste" the OCR text in column N or higher in the standard Excel spreadsheet template; the columns of the OCR-converted text should be automatically parsed into columns and rows of data in Excel.
- Edit the rows and columns of new OCR text in Excel as necessary, removing the spurious data, correcting errors, and maintaining the JDs, magnitudes, and observers in their respective columns.
- "Copy" and "Paste" your desired columns of data to their proper positions within the standard Spreadsheet Template as required.
- Use the cell-addition method to complete the JDs and replace any improvised observer abbreviations with their correct AAVSO Observer Code.
- Edit the "Fainter than" (usually expressed as italicized magnitude values) and "Uncertain" observations and cite the paper reference and submission details in the Comments column.
- Delete the originally "Pasted" OCR converted data within Excel and repeat the process.

The author has noted a potential 35% increase in efficiency in using OCR software for digital archiving when compared to manual spreadsheet entry, even with the additional editing steps. Corrections are readily made in Excel. The use of OCR digitization and the standard spreadsheet template following the suggestions and guidelines previously described are highly recommended on large data sets where JD's and magnitudes are already converted.

8. Conclusions

The archiving process, a spreadsheet template, suggestions, and Excel-based data tools have been reviewed and presented. Thirty-one sources of variable star data prior to 1911 have been identified and presented in tabular form. Of the 125,720 observations known to Pickering prior to 1888, over 100,000 observations still remain to be located and digitized. Over 98,000 archival observations from 1888 to 1911 have been identified and also remain to be digitized. Spreadsheet entry of data is not tedious by using the methods described. Digitization by optical character reading conversion is a very promising alternative to manual spreadsheet entry, but additional editing and formatting are required to get the variable star data into the standard spreadsheet template. However, manual spreadsheet entry of archival data needs to be used in cases when the conversion of calendar dates to JDs and/or step magnitudes are required. All archival variable star data have value, if we can locate and can capture them. This paper attempts to clarify the where and how of the digital archiving process.

9. Acknowledgements

The author would like to thank all of the past observers for their observations and past authors for their papers, publications, and books. Dr. Matthew Templeton of the AAVSO is acknowledged for his guidance and suggestions. Elizabeth O. Waagen of the AAVSO is recognized for her uploading of the archival observations to the AID and providing new observer codes. A special thanks goes to Michael Saladyga for his help in the preparation of this paper and providing AAVSO Archives information. The author also recognizes Robert Stine, Andrew Rupp, Christian Froschlin, and others for their efforts in digitization of variable star observations prior to 1911. The SAO/NASA Astrophysics Data System Abstract Service and Google Scholar were used for the online searching and retrieval of digitized papers, journals, and books which exist in the public domain.

References

Backhouse, T. W. 1905, *Publications of the West Hendon House Observatory, Sunderland, Observations of Variable Stars made in the Years 1866–1904*, Hills and Co., Sunderland, United Kingdom.

Blagg, M. A. 1924, *Mon. Not. Roy. Astron. Soc.*, **84**, 629.

Brook, C. L. 1908, *Mem. Roy. Astron. Soc.*, **58**, 50.

Campbell, L., and Pickering, E. C. 1907, *Ann. Harvard Coll. Obs.*, **57**, 1.

Campbell, L., and Pickering, E. C. 1912, *Ann. Harvard Coll. Obs.*, **63**, 1.

Chandler, S. C. 1883–1884, Variable star observations, AAVSO Archives, Cambridge, MA.

Daniel, Z., and Reid, S. 1903–1904, Variable star observations, AAVSO Archives, Cambridge, MA.

Eadie, J. H. 1884–1890, Variable star observations, AAVSO Archives, Cambridge, MA.

Eadie, J. H., Hagen, J. G., and Zaiser, A. 1884–1885, Variable star observations, AAVSO Archives, Cambridge, MA.

Fleming, W. P., and Pickering, E. C. 1912, *Ann. Harvard Coll. Obs.*, **47**, 119.

Furness, C. E. 1913, *Publ. Vassar Coll. Obs.*, No. 3, 1.

Guthnick, P., 1901, Neue Untersuchungen über den veränderlichten stern O (Mira) Ceti, Ehrhardt Karras, Halle, S.

Hagen, J. G. 1901, *Observations of Variable Stars made in the Years 1884 to 1890*, Georgetown Coll. Obs., Washington, D.C.

Hagen, J. G. 1903, *Beobachtungen Veranderlicher Sterner von Eduard Heis (1840–1877) und von Adalbert Krueger (1853–1892)*, Verlag von Felix L. Dames, Berlin.

Parkhurst, H. M., and Pickering, E. C. 1893, *Ann. Harvard Coll. Obs.*, **29**, 89.

Parkhurst, J. A. 1883–1885, Variable star observations, AAVSO Archives, Cambridge, MA.

Pickering, E. C. 1890, *Ann. Harvard Coll. Obs.*, **18**, 21.

Pickering, E. C. 1900a, *Ann. Harvard Coll. Obs.*, **33**, 1.

Pickering, E. C. 1900b, *Ann. Harvard Coll. Obs.*, **33**, 29.

Pickering, E. C. 1900c, *Ann. Harvard Coll. Obs.*, **33**, 75.

Pickering, E. C. 1900d, *Ann. Harvard Coll. Obs.*, **33**, 95.

Pickering, E. C. 1903, *Ann. Harvard Coll. Obs.*, **46**, 39.

Pickering, E. C. 1904, *Ann. Harvard Coll. Obs.*, **46**, 120.

Pickering, E. C. 1918, *Ann. Harvard Coll. Obs.*, **79**, 35.

Pickering, E. C., and Wendell, O. C. 1890, *Ann. Harvard Coll. Obs.*, **24** 1.

Sawyer, E. F. 1877–1892, variable star observations, AAVSO Archives, Cambridge, MA.

Townley, S. D. 1892, *Publ. Washburn Obs.*, **6** (Part 3), 1.

Turner, H. H. 1899, *Mem. Roy. Astron. Soc.*, **52**, 1.

Turner, H. H. 1905, *Mon. Not. Roy. Astron. Soc.*, **60**, 1.

Turner, H. H. 1912, *Mon. Not. Roy. Astron. Soc.*, **73**, 124.
Turner, H. H., and Blagg, M. A. 1914, *Mon. Not. Roy. Astron. Soc.*, **74**, 451.
Turner, H. H., and Blagg, M. A. 1915a, *Mon. Not. Roy. Astron. Soc.*, **75**, 398.
Turner, H. H., and Blagg, M. A. 1915b, *Mon. Not. Roy. Astron. Soc.*, **76**, 158.
Turner, H. H., and Blagg, M. A. 1916a, *Mon. Not. Roy. Astron. Soc.*, **77**, 125.
Turner, H. H., and Blagg, M. A. 1916b, *Mon. Not. Roy. Astron. Soc.*, **77**, 569.
Turner, H. H., and Blagg, M. A. 1917, *Mon. Not. Roy. Astron. Soc.*, **77**, 555.
Turner, H. H., and Blagg, M. A. 1918, *Mon. Not. Roy. Astron. Soc.*, **78**, 491.
Valentiner, W. 1900, *Veroffentlichungen der Grossherzoglichen Sternwarte zu Heidelberg (Astrometrisches Institut.),* **1**, Karlsruhe.
Wendell, O. C. 1909, *Ann. Harvard Coll. Obs.*, **69**, 1.
Wendell, O. C., and Pickering, E. C. 1902, *Ann. Harvard Coll. Obs.*, **37**, 145.
Yendell, P. S. 1888–1918, variable star observations, AAVSO Archives, Cambridge, MA.

Table 1. A selection of variable star observations in the AAVSO Archives and in literature prior to 1911. Data sources in italics have been digitized and are currently in the AID.

Source[1]	*Observer(s)*	*No. Observations*	*No. Stars*	*Magnitude Reduced*	*JD Converted*	*Status*
Sawyer (1877–1892)[2]	Sawyer	5000[3]	unknown	no	no	not digitized
Chandler (1883–1884)[2]	Chandler	700[3]	unknown	yes	no	not digitized
Parkhurst (1883–1885)[2]	Parkhurst, J.	2000[3]	unknown	no	no	not digitized
Eadie *et al.* (1884–1885)[2]	Eadie, Hagen, Zaiser	1000[3]	unknown	no	no	not digitized
Eadie (1884–1890)[2]	Eadie	2000[3]	unknown	no	no	not digitized
Yendell (1888–1918)[2]	Yendell	30000[3]	unknown	mixed	mixed	not digitized
Pickering and Wendell (1890)	Pickering and Wendell	1057	165	yes	no	digitized by Paxson
Townley (1892)	Townley	1085[2]	37	yes	no	digitized by Paxson
Parkhurst and Pickering (1893)	Eadie and Parkhurst, H.	4800[3]	135	yes	no	not digitized
Pickering (1900a)	various	6300[3]	17	yes	yes	not digitized
Turner (1899)	Knott	6683	23	yes	no	digitized by Paxson
Pickering (1900b)	Argelander	4290	16	yes	yes	digitized by Paxson
Pickering (1900c)	Schonfeld	1535	31	yes	yes	digitized by Paxson
Pickering (1900d)	Schmidt	7070	5	yes	yes	digitized by Paxson
Valentiner (1900)	Schonfeld	37000[3]	118	no	no	not digitized
Hagen (1901)	Hagen *et al.*	3000[3]	52	no	no	not digitized
Guthnick (1901)[4]	various	6200[3]	1	no	no	not digitized
Wendell and Pickering (1902)	various	4400	58	yes	yes	digitized by Rupp and Fröschlin

[1] *See reference list for more information.* [2] *In AAVSO Archives.* [3] *Estimated.* [4] *Observations of Mira only.*

Table continued on next page

Table 1. A selection of variable star observations in the AAVSO Archives and in literature prior to 1911. Data sources in italics have been digitized and are currently in the AID, cont.

Source[1]	*Observer(s)*	*No. Observations*	*No. Stars*	*Magnitude Reduced*	*JD Converted*	*Status*
Hagen (1903)	Heis and Krueger	8500[3]	61	no	yes	not digitized
Pickering (1903)	various	3346	1	yes	no	digitized by Stine
Daniel and Reid (1903–1904)[2]	Daniel and Reid	500[3]	unknown	yes	no	not digitized
Pickering (1904)	Wendell	5000[3]	150	yes	yes	not digitized
Turner (1905)	Peek and Grover	4133	22	yes	yes	not digitized
Backhouse (1905)	Backhouse	2300[3]	49	no	no	not digitized
Campbell and Pickering (1907)	various	8400[3]	75	yes	yes	not digitized
Brook (1908)	Pogson	4210	31	yes	yes	digitized by Paxson
Wendell (1909)	Wendell	6900[3]	44	yes	yes	not digitized
Campbell and Pickering (1912)	various	21,950[2]	328	yes	yes	digitized by Paxson
Blagg, Turner (1912–1924)[5]	Baxendell	6953	30	yes	yes	digitized by Paxson
Fleming and Pickering (1912)	Fleming	20000[3]	107	yes	yes	not digitized
Furness (1913)	various	4800[3]	101	yes	yes	not digitized

[1] See reference list for more information. [2] In AAVSO Archives. [3] Estimated. [4] Observations of Mira only. [5] Includes Turner (1912), Turner and Blagg (1914–1918), and Blagg (1924).

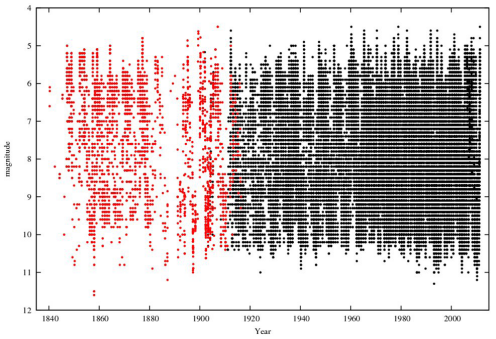

Figure 1. R Leonis observations in the AAVSO International Database. Black dots are data in AID prior to digitization project; red dots are observations digitized by the author to extend the light curve back to 1840.

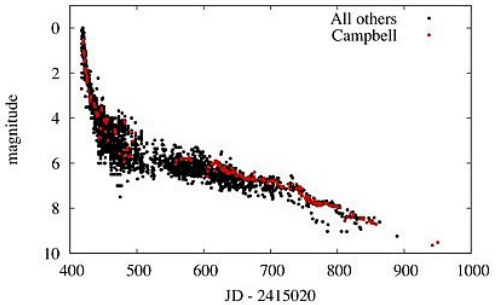

Figure 2. AAVSO light curve of Nova Persei 1901 No. 2 (GK Persei) digitized by Bob Stine from Pickering (1903). Black dots are pre-existing data; red dots are Stine-digitized data added to the AID.

Year.	J. D.	Magn.	Res.	Obs.	Year.	J. D.	Magn.	Res.	Obs.	Year.	J. D.	Magn.	Res.	Obs.	Year.	J. D.	Magn.	Res.	Obs.
	060547. SS Aurigae.					061647. V Aurigae.				*061702.* V Monocerotis.						063159. U Lyncis.			
10	9016.5	*13.8*	.	Hd.	08	7994.6	9.0	0	C.	05	6881.5	8.0	0	e.	10	8713.6	14.0	0	C.
	9018.5	*13.8*	.	Hd.		8025.6	9.4	4	C.		6902.5	9.0	3	Ca.		8738.6	*13.2*	.	*C.*
	9022.5	*12.4*	.	Hd.		8045.6	9.0	*1*	C.		6918.6	9.0	*4*	Ca.		8798.6	*12.5*	.	C.
	9023.4	*12.4*	.	Hd.		8053.5	9.0	*2*	C.		6936.6	10.5	4	Ca.		8846.6	13.9	0	C.
	9025.5	*12.4*	.	Hd.		8080.6	9.8	4	C.		6944.6	9.9	*4*	Ca.		8974.6	10.8	2	Hd.
	9028.6	N	.	Hd.		8215.6	*11.8*	.	e.		6958.5	10.5	*2*	e.		8993.7	11.1	0	Hd.
	9031.9	*12.4*	.	Hd.		8250.8	11.0	1	*C.*		7187.7	7.3	0	e.		9003.6	11.7	2	Hd.
	9036.7	10.8	0	T.		8277.6	9.8	*4*	*C.*	06	7227.6	8.2	0	e.		9008.5	12.4	7	Hd.
	9037.5	10.9	0	T.		8278.8	10.2	0	*C.*		7228.5	8.3	0	e.		9008.6	11.5	*2*	C.
					09	8328.6	9.6	*1*	Va.		7262.6	9.3	0	Ca.		9015.5	12.6	6	Hd.

Figure 3. Typical *Harvard Annals* format with JDs, reduced magnitudes, and observer identification (Campbell and Pickering 1912).

R Leonis.

Fernrohr: I = Refractor. II = Steinheil'scher Sucher. III = Operngl.

1865				1865				1866			
Jan. 3	10h7	R 1 e, f 2-5 R, Mond, II	April 24	9h2	R 3-5 g, h 1 R, II	März 22	9h0	R e–0.5 e, Mond, II
7	11.0	R 1-5 e, f 2 R, heller Mond, II	27	9.5	R 2 g, h 3 R, klar, II	April 7	9.4	R 3.5 e, f 1–1.5 R, I
28	9.5	R 4 f, R 2 g, h 1 R, II	29	10.2	R 1-5 g, h 3 R, schwacher Mond, II		9.8	R 2 d, e 2 R, im Sucher R unver-
29	8.6	R 2 g, h 1 R, noch etwas tief, II	Mai 1	10.2	R 1-5 g, h 3 R, Mond, II			kenbar –C e, d ist Schwerds f, II
31	12.7	R 0-5 h, k 4 R, II	7	9.7	R 2 g, h 3 R, heller Mond, II	10	12.4	R 1 d, e 3 R, II
Feb. 12	7.5	R 4 k, R 1 l, n 4–5 R, R sehr roth	14	11.0	R 2 f, g 3 R, Mond, II	13	11.7	R 0.5–1 e, f 4 R, I
		funkelnd, l = 19, n = 18 Leonis, II	17	9.8	R 1 f, g 3.5 R, II		12.0	R 2.5 d, e 2.5 R, II
15	8.8	R 4.5 l, R 3 k, n 4 R, (gestern k	20	9.7	R 1–1.5 f, g 4 R, II	15	9.6	R 1 e, f 4 R, I
		und l verwechselt ?), II	26	10.4	R 1–1.5 e, f 3.5 R, II		10.2	R 2.5 e, R 2 d, e 3 R, II
17	7.8	R 3.5 k, n 4.5 R, II	Dec. 13	11.4	R 1 f, g 3 R, II	18	9.8	R 1 e, f 4 R, Mond, I
März 1	9.7	R >5 k, n 1 R, II	15	11.6	R 4 f, g R, II	24	9.7	R 1 e, genau, heller Mond nahe,

Figure 4. Step magnitude data of Schonfeld with calendar dates and times, but with no JD conversion (Valentiner 1900).

62 6512 *T Herculis* *Series III.*

1800+	Gr. M. T.	Sky	Comparisons	I	II	Mean	2400000+	Remarks
			DECIMAL METHOD:					
83 July 25	15.2	II	a 6.5 b		15.6		09 017	
28	16.1	I	a 5.5 b		14.4		020	
30	15.2	II	a 7 b		16.2		022	
31	16.3	I	a 7 b		16.2		023	
Aug. 2	15.1	I	a 8 b		17.4		025	
3	14.7	I	a 8 b		17.4		026	
4	15.7	II	a 8 b		17.4		027	
5	15.2	γ	a 9 b		18.5		028	
9	15.9	II	a 8 b		17.4		032	
24	14.6	II	T = e		27.8		047	

Figure 5. An example of decimal step data (in the Comparisons column) and grade data (in Column II) with calendar dates and JDs being given (Hagen 1901).

	A	B	C	D	E	F	G	H	I	J	K	L
1	JD 7	JD 4	Observer	Type	Star	JD	Fainter than	Mag	Comment Codes	Uncertain	Comments	JD check
2	2390000	4970	SEX	V	OMI CET	2394970	0	4.30	na	0	1900AnHar-33-107. Submitted by PKV.	
3	2390000	4971	SEX	V	OMI CET	2394971	0	4.30	na	0	1900AnHar-33-107. Submitted by PKV.	1
4	2390000	4973	SEX	V	OMI CET	2394973	0	4.40	na	0	1900AnHar-33-107. Submitted by PKV.	2
5	2390000	4974	SEX	V	OMI CET	2394974	0	4.40	na	0	1900AnHar-33-107. Submitted by PKV.	1
6	2390000	4975	SEX	V	OMI CET	2394975	0	4.40	na	0	1900AnHar-33-107. Submitted by PKV.	1
7	2390000	4981	SEX	V	OMI CET	2394981	0	3.90	na	0	1900AnHar-33-107. Submitted by PKV.	6
8	2390000	4987	SEX	V	OMI CET	2394987	0	4.20	na	0	1900AnHar-33-107. Submitted by PKV.	6
9	2390000	4990	SEX	V	OMI CET	2394990	0	3.80	na	0	1900AnHar-33-107. Submitted by PKV.	3

Figure 6. The standard spreadsheet template for capturing archival variable star observations. Columns C–K are sent to the AAVSO. Data for observer Julius Schmidt (observer code SEX) are shown.

	A	B	C	D	E	F	G	H	I
1	Comp.	m.	Logic	>	Var.	<	Logic	m.	Comp.
2	v	5.18	0.00		R		0.00	5.18	v
3	n	5.84	5.84	5	R		0.00	5.84	n
4	l	6.48	0.00		R	2	6.48	6.48	l
5	k	6.73	0.00		R		0.00	6.73	k
6	h	6.70	0.00		R		0.00	6.70	h
7	g	7.30	0.00		R		0.00	7.30	g
8	f	7.84	0.00		R		0.00	7.84	f
9	e	8.29	0.00		R		0.00	8.29	e
10	d	8.82	0.00		R		0.00	8.82	d
11	Alp	9.14	0.00		R		0.00	9.14	Alp
12	Bet	9.65	0.00		R		0.00	9.65	Bet
13	Gam	9.54	0.00		R		0.00	9.54	Gam
14			5.84	5.00		2.00	6.48		
15									
16				Estimate	6.30				

Figure 7. A Step Magnitude Calculator. Reduction of the step values "n5R" and "R2l" gives an estimated magnitude of 6.30.

In cell C3 is the equation of =if(D3>0,B3,0). Copy and paste from cells C2 to C13.
In cell G4 is the equation of =if(F4>0, H4,0). Copy and paste from cells G2 to G13.
In cell C14 is the equation of =Sum(C2..C13).
In cell G14 is the equation of =Sum(G2..G13).
In cell E16 is the equation of =D14/(D14+F14)*(G14-C14)+C14.

	A	B	C	D	E	F	G	H	I	J	K	L	M	N	O	P
1	Year	Month	Day	GMT Hr.	Min.	Sec.	Observer	Type	Star	JD	Fainter than	Mag.	Comment Codes	Uncertain	Comments	JD Check
2	1880	10	23	9	5	0	KGB	V	U CEP	2408011.8785	0	8.10	na	0	MemRAS-52-7. Submitted by PKV.	
3	1880	10	23	10	25	0	KGB	V	U CEP	2408011.9340	0	9.00	na	0	MemRAS-52-7. Submitted by PKV.	0.0556
4	1880	10	23	10	47	0	KGB	V	U CEP	2408011.9493	0	9.05	na	0	MemRAS-52-7. Submitted by PKV.	0.0153
5	1880	10	23	11	7	0	KGB	V	U CEP	2408011.9632	0	9.10	na	0	MemRAS-52-7. Submitted by PKV.	0.0139
6	1880	10	23	11	39	0	KGB	V	U CEP	2408011.9854	0	9.00	na	0	MemRAS-52-7. Submitted by PKV.	0.0222
7	1880	10	23	12	30	0	KGB	V	U CEP	2408012.0208	0	8.95	na	0	MemRAS-52-7. Submitted by PKV.	0.0354
8	1880	10	23	12	44	0	KGB	V	U CEP	2408012.0306	0	8.80	na	0	MemRAS-52-7. Submitted by PKV.	0.0097
9	1880	10	23	13	7	0	KGB	V	U CEP	2408012.0465	0	8.60	na	0	MemRAS-52-7. Submitted by PKV.	0.0160

Figure 8. The spreadsheet template modified for Julian date calculation. See text for calculation equation.

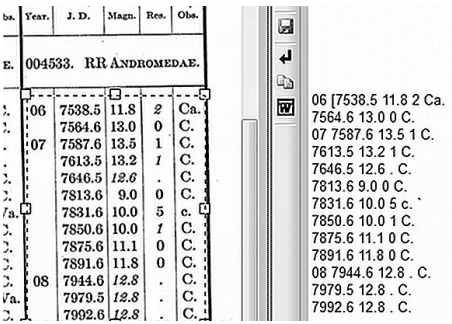

Figure 9. A comparison of RR Andromedae variable star data (Campbell and Pickering 1912) in an image file (left) versus its equivalent OCR converted output (right).

The Effect of Online Sunspot Data on Visual Solar Observers

Kristine Larsen
Physics and Earth Sciences, Central Connecticut State University, 1615 Stanley Street, New Britain, CT 06053; larsen@ccsu.edu

Presented at the 100th Spring Meeting of the AAVSO, May 22, 2011; Received June 29, 2011; revised September 13, 2011; accepted September 14, 2011

Abstract Solar observing affords opportunities for amateurs and students to contribute to the AAVSO. This study explores the use of online solar data and photographs in training solar observers, and the bias effects such data can have when not used judicially.

1. Estimating Sunspot Activity

As noted on the AAVSO's Solar Section web page (http://www.aavso.org/solar), solar observing is one way that amateur astronomers with relatively small telescopes can (with a proper white light filter) contribute useful data. The AAVSO's Solar Section aggregates and reduces the data contributed by its observers and publishes a monthly bulletin containing the Relative American Sunspot Number R_a for each day of that month (http://www.aavso.org/solar-bulletin). Since solar observing can be done during normal school hours and with modest equipment, it is an easy way to include telescopic observing in astronomy classes (both at the high school and college level) and introduce students to both the AAVSO and the collection and importance of individual astronomical observations.

There are a number of different organizations that collect and aggregate sunspot observations; each organization produces its own sunspot number or index. Each index is based on the Wolf index (developed by Rudolf Wolf in 1848), calculated as $R=10g + s$, where g is the number of sunspot groups (areas of sunspot activity) and s is the number of individual spots included in all the groups. Three commonly cited indices are the Boulder Index (computed at the NOAA Space Environment Center in Boulder, Colorado), International Index (computer by the Solar Influences Data Center in Belgium), and the aforementioned American Index (computed by the AAVSO Solar Section). Each uses data from a different set of observers/observatories, and each aggregates the data in a slightly different way. Because observers have a tendency to underreport the number of sunspots (due to differences in instrumentation, experience, and visual acuity), there will be a range of R values reported on any given day (Schaefer 1993, Foster 1997). In addition, observers will vary in the way they distinguish between different groups, and how well he or she can distinguish a pore from a sunspot (Schaefer 1993,

Schaefer 1997). In order to compensate for these differences, it has become customary to assign each observer a K-factor which is multiplied by his or her R value to correct for these differences. (For more information about the K-factor and how the AAVSO computes its values see Foster 1997, Schaefer 1997, and Feehrer 2000.) This "personal equation" is not uncommon in the aggregation and comparison of astronomical data. The term "personal equation" dates back to the nineteenth century, when astronomers discovered that their individual measurements of transit times for the same object/event differed (Schaffer 1988). Today each sunspot index uses a different technique to assign K-factors to contributing observers. The result is the values reported by each index will differ from one another.

One relatively simple way to introduce students to the concept of the sunspot cycle is through the Spaceweather website (www.spaceweather.com). This resource hosts on its main page a daily picture of the near-side of the sun from the Solar Dynamics Observatory and identifies some of the sunspot groups by number. The site also includes an overall Boulder sunspot number from the past twenty-four hours. While the Boulder index differs from R_a by a significant factor (Feehrer 2000), the beginning student solar observer does not need to delve into these subtleties from the onset. Also, since the AAVSO data are released after the fifteenth of the following month, students do not have real-time access to this data. Real-time photographs and sunspot indices can be helpful for visual sunspot observers who are just beginning to learn the techniques of careful visual sunspot counts (for example, how to identify complex groups and how to carefully examine the limb of the sun), but the "power of suggestion" these data might have on an observer cannot be ignored. An observer can check his or her observations against this "standard" and may be tempted to alter their data to conform to what he or she considers to be a more reliable standard. For example, while the AAVSO Solar Section includes the SOHO website real-time image (http://sohowww.nascom.nasa.gov/data/realtime/hmi_igr/512/) as one of its recommended resources for solar observers, and recommends an observer consult such a site when one has a break in observing (in order to follow the evolution of groups), an important caveat is included within the recommendation: "DO NOT use these resources to 'scale' your own observations. Most sources available via this medium use equipment and procedures that are different from the ones you use and can be expected to achieve different results" (Beck 2010). The study described in this paper first examined the effects of the Spaceweather site on a class of college students just beginning to learn white light solar observing, and then compared the results of a more experienced solar observer (the faculty course instructor) with the Spaceweather data. In no case was biased data submitted to any agency or organization.

2. Introducing Students to Sunspot Observing

In the middle of the Fall 2010 semester, twelve students in ESCI 278 (Observational Astronomy) at Central Connecticut State University were taught how to solar observe with a 6-inch *f*/1 1525 mm Schmidt-Cassegrain telescope, Thousand Oaks glass filter, and 35mm *f*/1 eyepiece. Students had been using other telescopes for night observing for six weeks beforehand and were therefore familiar with basic telescope usage and observing techniques. Solar activity was very low during this time; therefore, the instructor consulted the Spaceweather website before each sunny class period and observations were made only on days on which there were sunspots to observe. Each student individually observed the sun, drew a sketch, and estimated his or her observed sunspot number R=10g + s. Afterwards each student checked his or her sketch against the Spaceweather.com picture, observed a second time and drew a second sketch, noting if he or she could see all the areas of activity visible on the website. Students were aware of the fact that the posted R on the website was the previous day's data, and therefore concentrated on the actual photograph (which was on average several hours old).

There were 37 sets of before/after observations. In 19 cases the students could not see additional activity after viewing the photograph, while in 13 instances students were able to view additional activity afterwards. Sample comments from this latter group of observations include the following:

> "Without looking at the internet I observed two elliptical shaped sunspots making a group. After looking online I noticed that with the two sunspots I saw above are several more smaller spots but I couldn't divide them in the scope."

> "After I could see more spots in the lower group—about 2 more. Also, I could see one more spot in the higher group."

> "After looking at the computer I see a few more in the center."

> "For some reason after looking at the computer I was able to see two 'sets' of spots with a multitude of spots to be seen the second time. However, the spots seemed to be perforated."

> "When I observed I could not see anything. Image was fuzzy, could see a minimum of four spots (went back to look after seeing computer)."

Consulting the online photograph was therefore successful in prompting the students to both look more carefully at the groups they had seen in order to

count small spots and look at all areas of the sun more carefully to pick up small spots/groups. In the case of one student, it also reinforced an important lesson of observing in general: "One of the pieces of 'dirt' (on the eyepiece) turned out to be a group of sunspots."

Several student comments also raised important red flags, including the following (made by two different students):

> "After I think I might see one. But I'm not sure. It's hard for me to see anything. I could be making it up again."

> "I still can't see anything, including the one I made up before. The image seemed shakier than before."

The fact that students had (apparently) included spots in their logbooks that they had not seen speaks directly to the admonition of the AAVSO website and raises questions as to whether students felt they would either be graded lower or otherwise displease the instructor if they could not see spots (although they had been unequivocally advised otherwise). The honesty of the students is laudable, but reflects one of the dangers in utilizing such photographs or standardized data when instructing beginning observers—the tendency toward bias is powerful. Although students were often and firmly admonished never to change their original observation based on what their classmates saw, or what they saw on the website, this was clearly not followed. Even if the Spaceweather site was not used in this study, it is suggested that general peer pressure would have been sufficient to tempt some students to "make it up." While keeping one's observations secret from one's classmates may have stopped this, the need to improve one's technique (and attention to detail), and the ability to do this by sharing and consulting other sources, outweighs the downfalls *if* the students do not attempt to submit their data until they are confident enough in their own abilities to avoid such biases.

Even after viewing the Spaceweather picture, some of the students still could not see activity that his or her classmates could see, leading to some frustration (and possibly explaining the previously noted instances of "making spots up"). One student in particular—a science major—had difficulties on all four dates:

> "There were, supposedly, other sunspots found besides the ones I saw but I was unable to find them even after I saw their position online."

> "I was not able to make out any spots today even though there was at least one spot other people found. I was only able to see the yellow sun."

> "This whole semester I have had trouble with noting the sunspots. It was hard to see with my glasses and sun shining at me but it would also be difficult for me to focus clearly on the sun so I could see the spots. The spot on the top left is only a smudge on the eyepiece."

This particular student also had issues with some night observations as well, and began wearing her contact lenses to class near the end of the semester (after the solar observing had concluded) in order to help with her observations (with some success). It would be interesting to explore whether the use of glasses versus contact lenses affects the acuity of solar observers (although astigmatism should be compensated for by refocusing the telescope).

The general conclusions of this portion of the study are as follows:

1) Integrating Spaceweather.com's real-time sun pictures can aid students in taking care to look more carefully when solar observing.

2) Beginning observers can be tempted to "invent" sunspots if they know they are missing something that others can see. Students must be reminded on numerous occasions of the ethics involved in contributing individual data to collecting organizations.

3) By sharing their observations and noting the differences, students came to an understanding of the importance of the K-factor in solar data aggregation.

For a future extension of this study, it would be interesting to explore whether using the posted sunspot counts (posted on the next day) and the labeling of certain sunspot groups by number on the posted photo aid students in identifying individual groups in times of higher solar activity (as suggested by the AAVSO Guidelines for Solar Observers (http://www.aavso.org/solar-guidelines)).

3. Online Sunspot Counts as an Aid for Experienced Sunspot Observers

In the second portion of this study, the faculty instructor used the same equipment to observe the sun ten times (approximately once a week) from March 1 through May 1. The separation between observations was selected to avoid bias from previous observations. In each case, the Spaceweather.com photograph was consulted after the initial observation and a second observation was then commenced to note if additional activity could be seen. The observer's results were consistent with the AAVSO sunspot index R_a published in the following month (Howe 2011) and were (as expected) generally significantly lower than the Boulder index reported on the Spaceweather website. The most important outcome was the fact that in all cases, any additional activity visible

in the photograph but not seen in the initial observation was not seen in a second observation, confirming that the observer was consistently observing to the limits of her instrumentation, eyesight, and seeing (Schaefer 1993). The conclusion of this portion of the study is that Spaceweather.com and other similar websites are valuable to more seasoned observers as well as beginners in order to make sure one is taking care to view all spots visible to his or her limitations and not rushing through an observation or being sloppy. Again, the AAVSO's admonition to avoid bias is key. One can consult a website after concluding one's observation; if sunspots are found to be missing, one should never add to his or her data afterwards. If differences in the number of areas of sunspot activity had been found by the author in this study, those observations would not have been sent to the AAVSO, but instead used as practice. Similarly, the students in the first portion of this study did not submit their data to the AAVSO, and the consultations with the Spaceweather site were done to aid the students in improving his or her own ability, with the goal to become a competent solar observer.

4. Conclusion

In conclusion, both the AAVSO Solar Section's inclusion of such websites in its recommended resources for observers and the accompanying admonition are confirmed as appropriate (and necessary) for beginning observers and their more seasoned colleagues who wish to improve their solar observing technique. However, in order to prevent bias, these sources of information should be used for training purposes only, and in no case should an observer's report to the AAVSO (or any other organization) be anything other than his or her individual observations.

References

Beck, S. J. 2010, http://www.aavso.org/solar-guidelines

Feehrer, C. E. 2000 http://www.aavso.org/dances-wolfs-short-history-sunspot-indices

Foster, G. 1997, *J. Amer. Assoc. Var. Star Obs.,* **26**, 50.

Howe, R. 2011, *Solar Bulletin*, **67**, Nos. 3, 4, 5.

Schaefer, B. 1993, *Astrophys. J.,* **411**, 909.

Schaefer, B. 1997, *J. Amer. Assoc. Var. Star Obs.,* **26**, 40.

Schaffer, S. 1988, *Science in Context,* **2**, 115.

Spaceweather.com 2009, http://www.spaceweather.com/glossary/sunspotnumber.html

Adverse Health Effects of Nighttime Lighting

Mario Motta, M.D.
19 Skipper Way, Gloucester, MA 01930; mmotta@massmed.org

Presented at the 100th Annual Meeting of the AAVSO, October 7, 2011; received March 7, 2012; accepted March 29, 2012

Abstract The effects of poor lighting and glare on public safety are well-known, as are the harmful environmental effects on various species and the environment in general. What is less well-known is the potential harmful medical effects of excessive poor nighttime lighting. A significant body of research has been developed over the last few years regarding this problem. One of the most significant effects is the startling increased risk for breast cancer by excessive exposure to nighttime lighting. The mechanism is felt to be by disruption of the circadian rhythm and suppression of melatonin production from the pineal gland. Melatonin has an anticancer effect that is lost when its production is disrupted. I am in the process of developing a monograph that will summarize this important body of research, to be presented and endorsed by the American Medical Association, and its Council of Science and Public health. This paper is a brief overall summary of this little known potential harmful effect of poor and excessive nighttime lighting.

1. Introduction

The following is a brief summary of a longer monograph that will be presented by me to the American Medical Association (AMA) in June of 2012, written with contributions by Dr. Richard Stevens, Dr. David Blask, Dr. Steven Lockley, and Dr. George Brainard.

2. Human health issues

Since the introduction of electricity a little over a century ago, lighting the night has become a priority of modern societies due to many perceived advantages including for commerce and social activity. However, in the past two decades there has emerged a realization that with these benefits have come detriments, some of which may be substantial. The dialogue on electric light in the environment has focused on four topics: 1) esthetics, or loss of the starry night sky, 2) the energy cost of unnecessary electric light, especially at night, 3) the impact of the evolutionarily novel light at night on animal and plant life, and 4) impact of electric lighting on human health, primarily through disruption of circadian biological rhythms.

The Milky Way is no longer visible to the majority of people in the modern world. As societies have increasingly used electricity to light the night, it has

become difficult to see more than a few stars from Earth's surface. Though the major impact of electric light at night is in major metropolitan areas, even the once pristine nights of the U.S. National Parks are beginning to be degraded, more rapidly in the East but also in parks in the West as well.

Electric lighting accounts for about 19% of electricity consumption worldwide and costs about $360 billion annually (OECD/IEA 2006). Much of the light that is produced is wasted, for example by radiating up into space away from the task or environment intended to be illuminated. Estimates of how much is wasted vary; one estimate from the International Dark-Sky Association is 30% in the United States. Such a percentage worldwide would account for an annual cost of about $100 billion.

The 24-hour solar cycle of light and dark is ancient, and all life on the planet has evolved to accommodate it. Human imposition of light at night is a dramatic change in the environment but has only recently begun to attract the attention it deserves. Study of the effects of light at night on animal and plant life is in an early stage but already suggests major impacts on the entire spectrum of life including animal, plant, insect, and aquatic. Electric light at night disrupts the solar light cycle, and can be expected to have impact on any life form that is exposed to it.

About 30% of all vertebrate species and 60% of invertebrate species on Earth are nocturnal, and depend on dark for foraging and mating. Documented wildlife destruction by light at night has been evident on bird species and migrating amphibians. The most studied case is of sea turtle hatchlings on the coast of Florida which historically have scurried from their nest directly to the ocean; with increased development along the coast, and attendant increased electric lighting at night, these hatchlings become confused and often migrate away from shore to the lights. Hundreds of thousands of hatchlings are believed to have been lost as a result of this stray electric lighting at night in Florida.

The circadian biology of plants is as robust as animals, and the impact of light at night on plant life may also be considerable due to the role of light in photosynthesis and the fact that many plants are pollinated at night. In addition, light at night as a vector attractant for diseases such as malaria is beginning to be evaluated.

3. Disability glare and discomfort glare

Disability glare is unwanted and poorly directed light that blinds, causes poor vision by decreasing contrast, and creates an unsafe driving condition, especially at night. Disability glare is a particular problem on the older aging eye. Many older drivers have a difficult time driving at night, unaware of the etiology of their poor night vision, which is, in part, the result of badly engineered lights. A proper understanding of the human eye physiology would allow for engineering safer and better designed street lighting. There are natural causes of disability glare, such as solar glare at sunset on a dirty windshield. We have all

experienced such glare, and attempt to minimize its effects with sunglasses or a cleaning of the windshield. Unfortunately, glare at night while driving is not so easily remedied. Its cause is generally overly bright and unshielded or poorly directed light that enters the eye and then scatters off of eye structures resulting in diminished contrast and impeded vision. Such effects become dramatically worse as the human eye ages due to aging eye structures. As the human eye cannot be so easily fixed as cleaning a dirty windshield it thus behooves us to thus engineer our street lighting to minimize the effects of disability glare.

Disability and Discomfort in the nighttime driving environment have long been a topic of research. Disability glare has been fairly well defined based on the physiology of the human eye and behavior of light as it enters the ocular media. However, discomfort glare has been less defined. Discomfort glare is not based on a physical response but rather a psychological response. This means that the basis of the two responses is fundamentally different and the research into each of the effects is also fundamentally different.

Disability glare is, as the name implies, glare which limits the ability of the driver to see. Disability glare has a direct link to the physiology of the eye and has been researched for many years. The process which causes disability glare was originally discovered by Holladay (1927) and was determined to be light scatter from the ocular media in the eye. As light enters the eye, it collides with components of the ocular media such as the cornea, lens, and the vitreous humor. At each collision, photons scatter and cast a veil of light across the retina. According to Vos *et al.* (1964) and Boyton and Clark (1962) 25–30% of the stray light is from the cornea, approximately the same amount is from the lens, and the rest is scattered in the retina itself. Later measurements showed that much of the scattering also occurs in the vitreous humor. The veil of light has the effect of reducing the contrast of the object which the driver is trying to see which would have the same effect as raising the background luminance of the object.

This veiling light can be modeled and is represented by the term veiling luminance. Many equations have been developed over time, however, the same general form of the equation is used. Originally proposed by Holladay, the relationship is that veiling luminance is directly related to the illuminance of the light source and inversely related to the square of the angle of eccentricity of the light source with an age-dependant multiplier across the entire equation.

Discomfort glare is by far less defined than disability glare. Discomfort glare is defined as a glare source which causes the observer to feel uncomfortable. The definition of discomfort is not precise and some research has shown that a person's response to a glare source is based more on their emotional state than on the light source itself. Discomfort glare is based primarily on the observer's light adaptation level, the size, number, luminance, and location of the light sources in the scene. Models of Discomfort glare have been developed and rely on the illuminance of the light source on the eye. These models continue to need development and the overall impact of discomfort on fatigue and user safety remains an issue. Both discomfort and disability glare have specific impacts on

the user in the nighttime environment. Research has shown that both of these glare effects occur simultaneously. Research also shows that the effects of the glare are cumulative, meaning that the glare from two light sources is the sum of the glare from the individual light sources. As a result, every light source within the field of view has an impact on the comfort and visual capability of the driver.

For overhead roadway lighting, design standards include a methodology for controlling the disability glare through a ratio of the eye adaptation luminance to the veiling luminance caused by the light source. As the veiling luminance is related to the illuminance of the light source at the eye, a roadway luminaire which directs light horizontally has a much greater effect on the driver than a light source that cuts off the horizontal light. A trend towards flat glass luminaires which provide a cut-off of light at horizontal angles provides a lower level of both disability and discomfort glare.

Decorative luminaires such as those called acorn or drop lens luminaires have a high level of horizontal light, and the visible portion of the luminaire provides a different situation. Here, these luminaires are typically used for areas where pedestrians are the primary roadway users. The horizontal light in this situation is useful for facial recognition of a pedestrian but it limits the driver in their ability to perceive other objects in the roadway. As a result, many cities are designing and installing two lighting systems, one for the pedestrian and one for the roadway.

The final issue with glare from overhead lighting is the cyclic nature of the impact. Bennett found that as a driver passes through a roadway, they typically go from one luminaire to another. The glare experience will increase as they approach the luminaire and then fall off as they pass the luminaire. While typically not an issue for disability glare, this is a discomfort issue and can be quite fatiguing.

4. Importance of circadian biological rhythms

From the beginning, the solar cycle of light and dark has provided one of the essential bases for life on Earth. Adaptation to the solar cycle has resulted in fundamental molecular and genetic processes that are aligned to an approximately 24-hour period (the circadian biological rhythm) in virtually all life on the planet. The endogenous nature of this circadian rhythm was realized when researchers studied life forms, plant and animal, in laboratory environments devoid of any time cues. Previously it was assumed that plants and animals only responded to the sun rather than anticipated its cycle. It has now become clear that the circadian genetic clock mechanism is ubiquitous and intimately involved in many, if not most facets of cellular and organism function. It has also become clear that although capable of a self-maintaining rhythm, the master circadian clock in mammals (including humans) responds to light through a novel photoreceptive system in the retina. This tandem development

of an endogenous rhythm and a sensitivity of it to light were presumably designed by nature to allow for a precise 24-hour regulation of rest and activity, and for adapting to seasonal changes in day-length, while maintaining the advantages of a physiology that anticipates day and night. Understanding how these endogenous rhythms work at the molecular and physiological level and how light is communicated to this system have together become one of the hot topics in the life sciences today.

Biological adaptation to the Sun has evolved for a very long time. In the last hundred years, however, bright light increasingly invades the night as human societies gain industry, technology, and wealth; lighting of the night took a major turn for the brighter as the world began to use electricity. At the same time, ever greater numbers of people work inside buildings under electric lighting. This lighting is vastly dimmer than sunlight, and it provides a very different spectral irradiance; whereas daylight is strong at all visible wavelengths peaking in the blue region, electric lighting has extreme characteristic wavelength peaks (fluorescent) or monotonic increases in irradiance as wavelength lengthens (incandescent). Much of the modern world now lives in a murky cloud of dim light throughout the day and night in isolation from the sun; it is remarkable how little sun people get even in such sunny environments as San Diego.

It is imperative to determine if there are adverse health consequences of our electric lighting practices in the human environment, and if so, the mechanisms underlying these effects. Effective interventions could then be identified that would mitigate the downsides of suboptimal light exposure. Society will not go back to life before electricity, and light during the night is required for our way of life. However, there are undoubtedly ways of lighting the night that are less disruptive than others to our well-being. Considerations in this regard are light spectrum, intensity, duration, and timing during the day and night, all of which determine the effect of light on physiology.

As the research on the biology of circadian rhythms has advanced, the range of potential disease connections has expanded. The first focus was breast cancer, but many more are now being pursued as well such as other cancers (such as prostate cancer), obesity, and diabetes.

5. Light at night, cancer, and importance of melatonin

The first step in determining whether electric lighting affects human health is to understand the impact of light on human physiology. The endogenous human circadian rhythm is complex. Perhaps the most studied aspect of that rhythm is the hormone melatonin, both as a marker of the rhythm and also as an important modulator of the rhythm. There is scientific evidence in humans that support the following features of the impact on electric light exposure on melatonin production, and by extension to the circadian rhythm. The biology of phototransduction continues to be unraveled, and will undoubtedly yield further insights into potential health impacts of electric lighting.

Epidemiological studies are a critical component of the evidence base required to assess whether or not light-at-night (LAN) affects disease risk, including cancer. However, these studies are necessarily observational and can rarely provide mechanistic understanding of the associations observed. For this reason, a robust body of basic scientific studies is also needed before causal inference can be pursued. Only carefully designed and controlled basic laboratory studies in experimental animal models of cancer have the potential to provide the empirical support for a causal nexus between light at night and elevated cancer risk as well as for a plausible biological mechanism to explain such a connection.

The preponderance of experimental evidence supports the hypothesis that under the conditions of complete darkness, high circulating levels of melatonin during the night not only provide a potent circadian anticancer signal to established cancer cells but help protect normal cells from the initiation of the carcinogenic process in the first place. It has been postulated that disruption in the phasing/timing of the central circadian pacemaker in the brain's suprachiasmatic nucleus (SCN), in general, and the suppression of circadian nocturnal production of melatonin, in particular, by light at night (LAN), may be an important biological explanation for the observed epidemiological associations of cancer risk and surrogates for LAN (such as night shift work, blindness, reported hours of sleep, and so on).

The majority of earlier studies in experimental models of either spontaneous or chemically-induced mammary carcinogenesis in mice and rats, respectively, demonstrated an accelerated onset of mammary tumor development accompanied by increased tumor incidence and number in animals exposed to constant bright fluorescent LAN as compared with control animals maintained on a strict LD12:12 light/dark.

More recent work, however, has focused on the ability of light at night to promote the growth progression and metabolism in human breast cancer xenografts. Blask and co-workers (2005) assessed the dose-response effects of light exposure during darkness on the growth of tissue-isolated human breast cancer xenografts in nude female rats; these human tumors are estrogen receptor negative (ER–) and depend on the essential polyunsaturated fatty acid linoleic acid for their growth. Both ER– and ER+ human breast cancer xenografts are highly sensitive to the direct growth and linoleic acid metabolic inhibitory effects of nocturnal concentrations of melatonin. Five different groups of xenograft-bearing rats were each exposed to one of five increasing intensities of white, fluorescent polychromatic light, ranging from very dim to very bright, during the dark phase of each LD 12:12 cycle beginning two weeks before tumor implantation and continuing thereafter until the end of the tumor growth experiment; a sixth control group of tumor-bearing rats was exposed to complete darkness during the dark phase of each LD 12:12 cycle. Following several weeks of exposure of rats to increasingly brighter light during the dark phase there was a dose-dependent increase in the percent suppression of peak

nocturnal serum melatonin levels. There was also an accompanying marked, dose-related increase in tumor metabolism of linoleic acid and the rate of tumor growth as light intensity during the night increased and the nocturnal amplitude of blood melatonin levels decreased. A particularly important aspect of this study was that exposure to even the very dimmest intensity of LAN (0.2 lux), which induced approximately a 65% suppression of the nocturnal peak of circulating melatonin levels, resulted in a marked stimulation in the rates of tumor growth and linoleic acid metabolic activity that was nearly equivalent to that observed in constant bright light-exposed tumor-bearing rats in which there was complete melatonin suppression. Furthermore, as little as a 15% suppression of nocturnal melatonin levels, in response to an extremely low intensity of LAN, was required to elicit a small but significant increase in xenograft growth and linoleic acid metabolism. This finding suggested that even a seemingly marginal suppression of the nocturnal circadian melatonin signal induced by exposure to extremely dim LAN could translate into a significant stimulation of human breast cancer growth and metabolism.

Similar findings were also obtained by this group on the growth and linoleic metabolism of a highly melatonin-sensitive rat hepatoma in male rats exposed to the same increasing intensities of light at night. The stimulatory effects of dim LAN (0.2 lux) observed in rat hepatoma and human breast cancer xenograft growth were subsequently and independently corroborated with respect to the growth of DMBA-induced mammary carcinomas in female rats by Cos *et al.* (2006). They documented a significant decrease in nighttime urinary excretion of the main liver metabolite of melatonin, 6-sulfatoxymelatonin, in animals exposed to dim LAN as well as a marked increase in serum estradiol. More recently, Dauchy *et al.* (1997) reported high tumor growth and linoleic acid metabolic rates and completely suppressed nocturnal melatonin levels in rats bearing human breast cancer xenografts or rat hepatomas as a result of their initial exposure to LAN (24.5 lux). However, as the amount of LAN exposure was subsequently and sequentially reduced to zero, there was a gradual restoration of circulating melatonin concentrations to high nocturnal peak levels accompanied by a marked reduction in tumor growth and linoleic acid metabolic activity to baseline rates.

In the same investigation by Blask and colleagues cited above, important new relationships between circadian biology, the endogenous nocturnal melatonin signal, and its suppression by LAN, relative to human breast cancer risk were uncovered using a unique experimental strategy that combined blood collection from human subjects, exposed to either complete darkness or light at night, and the direct perfusion of human breast cancer xenografts with the resulting blood samples. The linoleic acid metabolic and growth activity of ER– (and ER+) human breast cancer xenografts (growing in nude rats) directly perfused in situ with whole blood collected during completely dark nights from young, healthy premenopausal female subjects (high melatonin), was markedly reduced as compared to when the xenografts were perfused with

blood collected during the daytime (low melatonin). Following dark exposure, the exposure of the same subjects to bright (such as 2800 lux), polychromatic, white fluorescent light during the night reduced their melatonin levels almost to daytime concentrations and extinguished the tumor and metabolic inhibitory activity of their blood.

That this effect was achieved via LAN-induced melatonin suppression was supported by the fact that addition of a physiological nocturnal concentration of melatonin to blood collected from light-treated subjects (low melatonin) restored the tumor inhibitory activity to a level comparable to that observed in the melatonin-rich blood collected at night during total darkness. Moreover, the addition of a melatonin receptor antagonist to the blood collected during darkness (high melatonin) completely eliminated the ability of the blood to inhibit the growth and metabolic activity of perfused tumors. Therefore, melatonin is the first soluble, nocturnal anticancer signal to be identified in humans that directly links the central circadian clock with some of the important mechanisms regulating breast carcinogenesis.

These findings provide the first definitive nexus between the exposure of healthy premenopausal female human subjects to bright, white LAN and the enhancement of human breast oncogenesis via circadian disruption (that is, suppression) of the nocturnal, anticancer melatonin signal.

6. Light-at-night and sleep disruption

As alluded to above, in addition to light-at-night suppression of the nocturnal melatonin signal, another type of circadian disruption can be caused by chronically advancing the phasing of light exposure (chronic jet lag). Filipski and co-workers (2004, 2005) maintained male mice in either an alternating LD12:12 light/dark cycle or exposed them to experimental chronic jet lag (through serial eight-hour advances of LD12:12 cycles every two days) in order to disrupt the rest-activity circadian rhythm. Ten days after the start of the light-dark cycle advances, animals in both groups were implanted with mouse osteosarcoma. In the mice undergoing "jet-lag" via repeated advances in circadian phase, tumor growth progression, during a narrow window of time between days 8 and 11 after tumor transplantation, was modestly but significantly faster as compared with that in mice kept in LD12:12. Although circulating melatonin levels were not assessed in the two groups, it is important to note that the specialized strain of mice used in this study exhibits an abnormal melatonin profile with highest levels of melatonin occurring during the light phase rather than during the dark phase. Nevertheless, this study indicated that in addition to light-at-night-induced melatonin suppression, circadian disruption induced by chronic phase advances in light exposure may represent another biological mechanism for increased cancer growth.

The human evidence, primarily from epidemiological studies, is indirect. The greatest amount of evidence so far is on cancer risk, particularly of breast.

Among the potential health effects of circadian disruption from electric lighting, the development of breast cancer has received the most attention. The idea that the increasing use of electricity to light the night might explain a portion of the high breast cancer risk in the industrialized world, and the increasing incidence and mortality in the developing world, was first articulated in 1987 by Stevens. The idea was originally based on suppression of the normal nocturnal rise in circulating melatonin, but has since expanded to include impact on circadian gene function. From this theory came a series of predictions, including that non-day shift work would raise risk, blind women would be at lower risk, reported sleep duration (as a surrogate for hours of dark) would be inversely associated with risk, and that population nighttime light level would co-distribute with breast cancer incidence worldwide. The most studied of these predictions is that non-day shift work would be associated with increased risk. Based on studies of non-day shift occupation and cancer (mostly breast cancer) published through 2007, the International Agency for Research on Cancer (IARC) concluded "shift-work that involves circadian disruption is probably carcinogenic to humans (Group 2A [level of confidence of carcinogenic potential])." The detailed review of the individual studies is also available (IARC 2010).

Since the IARC evaluation was conducted, several new studies of breast cancer have been published. Lie *et al.* (2011) conducted a large case-control study of nurses in Norway and found a significantly elevated risk in subjects with a history of regularly working five or more consecutive nights between days off. Hansen and Stevens (2011) evaluated the impact of type of shift (such as evening, night, rotating) and found a roughly increasing risk as the expected disruptiveness of the shift increased. Each of these studies has strengths and limitations common to epidemiology, particularly in exposure assessment and appropriate comparison groups; that is to say, no woman in the modern world is unexposed to light-at-night but quantifying that exposure is difficult. However, on balance the new evidence is consistent with the elevated risk from the previous studies evaluated by IARC.

Four case-control studies have now reported an association of some aspect of nighttime light level in the bedroom and breast cancer risk. The elevated risk estimate was statistically significant in two of them. As case-control designs, in addition to the limitation of recall error there is also the potentially severe limitation of recall bias. Despite the difficulty of gathering reliable information on bedroom light level at night, the possibility that even a very low luminance over a long period of time might have an impact on cancer risk is important. It is not yet clear what is the lower limit of light level that could, over a long time period, affect the circadian system.

Until 1980 when Lewy and colleagues (1980) published in *Science* magazine that bright light can suppress circulating melatonin concentration, it was thought that humans were insensitive to light. Since that time, the intensity believed to be adequate to inhibit melatonin production has steadily declined. In pioneering work, Brainard and colleagues (1988) have shown that very low

monochromatic photon flux density can have an effect which is wavelength dependent. And it has now been reported that the lighting typical in bedrooms in the evening after dusk (but before bedtime) can also suppress melatonin and delay its nocturnal surge.

After lights out for bedtime, it is not yet clear whether the ambient background light from weak sources in the bedroom or outside light coming through the window could influence the circadian system; a brief exposure at these levels may not have a detectable impact in a laboratory setting though long-term chronic exposure might. In the modern world few people sleep in total darkness. When eyelids are shut during sleep, only very bright light can penetrate to lower melatonin, and this in only some people. However, it is normal to awaken in the middle of the night as most people do, and there is often the need to use the facilities, which increases as people age. Therefore the potential for low level light in the bedroom to affect human health by disrupting the circadian system should be a research priority.

The modern world has an epidemic of obesity and diabetes that may in part be due to lack of sleep, lack of dark, and/or circadian disruption. The circadian rhythm and sleep are intimately related but not the same thing. It has long been known that non-day shift workers are at greater risk of diabetes and obesity. Epidemiological studies also show associations of reported sleep duration and risk of obesity and diabetes. Circadian disruption may be a common mechanism for these outcomes. This is based on the rapidly emerging understanding of the link between the circadian rhythm and metabolism.

Adequate daily sleep is required for maintenance of cognitive function, and for a vast array of other capabilities that are only partially understood. Sleep is not, however, required for maintenance of the endogenous circadian rhythm (such as melatonin cycling), whereas dark is required. The epidemiological and laboratory research on sleep and health cannot entirely separate effects of sleep duration from duration of exposure to dark, so that this work can be difficult to interpret. The distinction is quite important because a requirement for a daily and lengthy period of dark to maintain optimal circadian health has different implications than a requirement that one must be asleep during this entire period of dark; it may be normal to experience a wakeful period in the middle of a dark night.

Light during the night will disrupt circadian function as well as sleep, and the health consequences of short sleep and of chronic circadian disruption are both now the subject of intense research. There is a growing number of both observational and clinical studies of sleep and metabolism which suggest an alarming and important impact of short sleep on health; however it is not yet clear that sleep and dark have been entirely disentangled in these studies. An example of the difficulty of interpretation of the "sleep" studies is the carefully conducted study of Taheri *et al.* (2004), who reported that sleep duration, as verified by polysomnography, was associated with morning blood levels of leptin in a sample of 1,024 adults in Wisconsin. However, in the same analysis,

the duration of typical sleep reported by each subject was more strongly associated with leptin level. Mean verified sleep was 6.2 hours, whereas mean reported sleep was 7.2 hours, a full hour different. Reported "sleep" duration probably means the difference in time when a person turns out their light for bed, and when they get up in the morning; or actual hours of dark. An important question is: what portion of health effects of dark disruption is due to sleep disruption and what portion is due directly to circadian impact of electric light intrusion on the dark of night?

7. Conclusion

It is clear now that light-at-night has profound effects on human physiology, and many of these effects are just now becoming known. These effects have spawned a burgeoning field of research that shows how profoundly both humans and life on earth are affected by the loss of the dark at night. Light-at-night affects more than just our views of the night sky.

References

Blask, D. E., *et al.* 2005, *Cancer Res.*, **65**, 11174.
Boyton, R. M., and Clark, J. J. 1962, *J. Opt. Soc. Amer.*, **54**, 1326.
Brainard, G. C. *et al.* 1988, *Brain Res.*, **454**, 212.
Cos, S., *et al.* 2006, *Cancer Lett.*, **235**, 266.
Dauchy, R. T., *et al.* 1997, *Lab Animal Sci.*, **47**, 511.
Filipski, E., *et al.* 2004, *Cancer Res.*, **64**, 7879.
Filipski, E., *et al.* 2005, *J. Natl. Cancer Inst.*, **97**, 507.
Hansen, J., and Stevens, R. G. 2011, *Eur. J. Cancer*, in press.
Holladay L. L. 1927, *J. Opt. Soc. Amer.*, **14**, 1.
Int. Agency for Research on Cancer. 2010, IARC Monographs on the Evaluation of Carcinogenic Risks to Humans, **98** (http://monographs.iarc.fr/ENG/Monographs/vol98/index.php).
Lewy, A. J., Wehr, T. A., Goodwin, F. K., Newsome, D. A., and Markey, S. P. 1980, *Science*, **210**, 1267.
Lie, J. A. S., Kjuus, H., Haugen, A., Zienolddiny, S., Stevens, R. G., and Kjærheim, K. 2011, *Amer. J. Epidemiol*, in press.
Organization for Economic Co-operation and Development/International Energy Agency ((OECD)/IEA). 2006, *Light's Labour's Lost—Policies for Energy-efficient Lighting*, OECD/IEA, Paris.
Stevens, R. G. 1987, *Amer. J. Epidemiol.*, **125**, 556.
Taheri, S., Lin, L., Austin, D., Young, T., and Mignot, E. 2004, *PLoS Med.*, Dec. 1(3), e62.
Vos, J. J., and Bouman, M. A. 1964, *J. Opt. Soc. Amer.*, **54**, 95.

Star Watching Promoted by the Ministry of the Environment, Japan

Seiichi Sakuma
2-21-9, Kami-Aso, Asao-Ku, Kawasaki 215-0021, Japan; hgc02554@nifty.com

Presented at the 100th Annual Meeting of the AAVSO, October 7, 2011; received December 14, 2011; accepted December 14, 2011

Abstract In 1987 the author suggested to Japanese government authorities to promote star watching as a means of campaigning for the prevention of air pollution. The "Star Watching" program still continues today. Recently, it became a campaign not only for the prevention of air pollution, but also a campaign to educate about light pollution, energy-saving, and the reduction of greenhouse gas. This paper summarizes twenty years of activity in the "Star Watching" program.

1. Introduction

For variable star astronomers, the visibility of faint stars is an important concern. I made a study of the visibility of stars in the Tokyo city district, derived from observations of the members of the Japan Astronomical Study Association. Simply, it is an index of visibility based on the difference of magnitudes between the faintest comparison star and the calculated limit depending on the diameter of the telescope used. The results show that the visibility of stars in Tokyo since 1952 (Sakuma 1956) has been becoming rapidly poor. Because Japan's environment problem became serious, an "Environment Agency" (later, the Ministry of Environment) was established in 1971.

In the 1980s, traffic and diesel engines caused severe air pollution. Under these circumstances, the Environmental Agency carried out a campaign for pollution prevention, with regard to air pollution—visibility (in the meteorological sense) observation by elementary school children, and water pollution—making 100 selections of clear fountains and streams. I suggested to the government authority to promote "Star Watching" as their next campaign in 1986. Recently, the astronomical part became a campaign not only for the prevention of air pollution but also light pollution, energy-saving, and the reduction of greenhouse gas.

2. Star watching

The outline of a method had been introduced by Isobe and Kosai (1991), Kosai and Isobe (1991), Kosai, Isobe, and Nakayama (1992), and Crawford and O'Meara (1991), early enough to be of use. I also introduced my "Star

Watching" project in the *AAVSO Newsletter* (Sakuma 1987, 1989). The method is as follows: Visual observations are carried out on a moonless night about one hour after sunset during January and August. Observers try to find the Milky Way in the constellations of Perseus, Gemini, and Monoceros in winter, and Cassiopeia, Cygnus, and Sagittarius in summer. Use of 7×50 binoculars is recommended for star counting in an area encircled by six bright stars in the Pleiades cluster in winter, and in an area of the triangle formed by α Lyr (Vega), ε Lyr, and ζ Lyr. I consult the AAVSO's charts for these areas (BU Tau, AY Lyr, and LL Lyr) to obtain the magnitudes of stars in the target area. The positions of stars which one sees are then drawn in a notebook.

The Photographic method is carried out by a camera with a focal length of 50 to 55 mm, an *f*-ratio brighter than 2.0, and a reversal color film with a speed of ISO 400. The camera is fixed on a tripod and is set in the center of the α Tau field in winter, α Lyr in summer. Three exposures of 80, 150, and 300 seconds without guiding are carried out after setting the *f*-ratio at 3.5 or 4.0. Three exposed films are used to measure the density of the sky background relative to standard stars in that field using a densitometer. This method will be adapted to the use of a digital single lens reflex (DSLR) camera this summer.

3. Summary of results

The number of observer groups in the project has kept steady at more than 300 through most of its twenty-year history (Figure 1). In summer 2010, there were 6,786 observers in 418 groups; in winter 2011, 3,033 observers in 313 groups contributed.

Binocular observation results (Figures 2 and 3) in winter show limiting magnitudes slightly down (brighter). Judging from the results of twenty-three fixed points (Figures 4 and 5), the background brightness of the sky does not change over the past 20 years.

Japan's northeastern area was attacked by an earthquake and tsunami on March 11, 2011. Power plants were destroyed. To avoid a total shutdown of electricity, a projected, or programmed, power failure was carried out for four months, until, oil- and coal-burning power plants could restart. This summer, the Ministry restricted heavy users of power by 15%, and recommended that citizens save as much power as possible. Consequently, the visibility of stars during this summer became better than in the past. The results of "Star Watching" of this summer were not announced until now.

4. Future development

The Ministry of Environment enacts a positive policy for the prevention of light pollution. A "Guideline for prevention of light pollution" was established by the Ministry in 1998 and revised in 2006. A "lights down" campaign was carried

out when comet Hyakutake approached the earth on March 23–27, 1996, and when comet Hale-Bopp appeared on April 1–6, 1997. Such campaigns as star watching and lights down are becoming more and more important all over the world. For example, Dr. Kelly Beatty, of the International Dark Sky Association (IDA), at Kitt Peak proposed a "Great World Wide Star Count"; The British Astronomical Association's Centre for Dark Skies proposed a "Christmas and New Year Star Count"; and Dr. Mario Motta of the AAVSO gives talks on light pollution and adequate lighting. International cooperation can be expected the more that public awareness grows.

References

Crawford, D., and O'Meara, J. 1991, *Sky & Telescope,* **82**, 547.

Isobe, S., and Kosai, H. 1991, in *The Vanishing Universe*, ed. Derek, Cambridge Univ. Press, Cambridge, 1.

Kosai, H., and Isobe, S. 1991 in *Light Pollution, Radio Interference, and Space Debris*, ASP Conf. Ser., 17, ed. D. L. Crawford, Astron. Soc. Pacific, San Francisco, 35.

Kosai, H., Isobe, S., and Nakayama, H. 1992, *Sky & Telescope*, **84**, 564.

Sakuma, S. 1956, *Mem Japan Astron. Study Assoc.*, **1**, No. 3. (in Japanese).

Sakuma, S. 1987, *AAVSO Newsletter*, No. 2.

Sakuma, S. 1989, *AAVSO Newsletter*, No. 5.

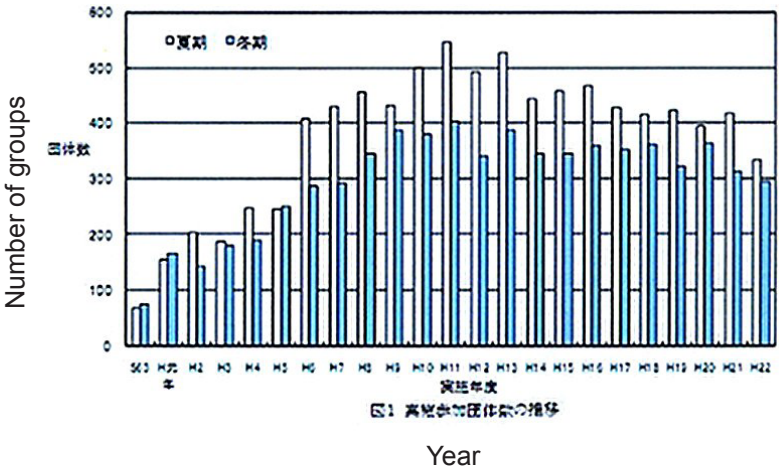

Figure 1. Growth in number of observer groups in the "Star Watching" project from 1988 to 2010. The number of groups has kept steady at more than 300 through most of its twenty-year history.

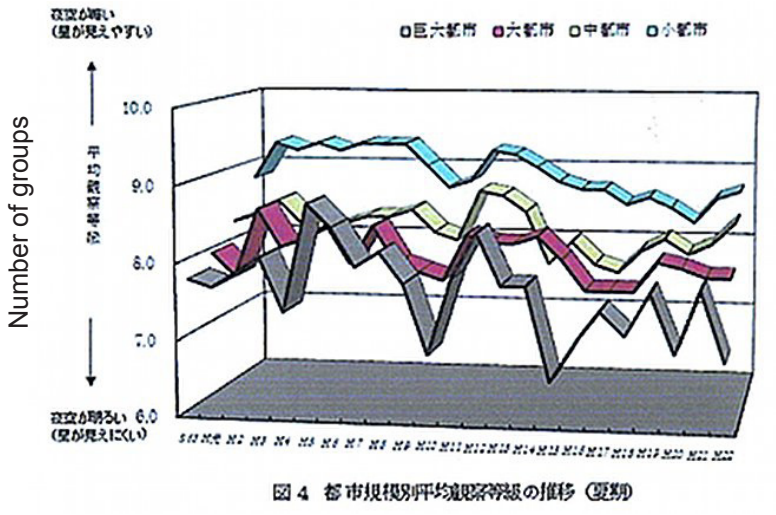

図 4 都市規模別平均観察等級の推移（夏期）

Figure 2. Binocular observation results 1988–2010, showing limiting magnitudes observed during winter seasons.

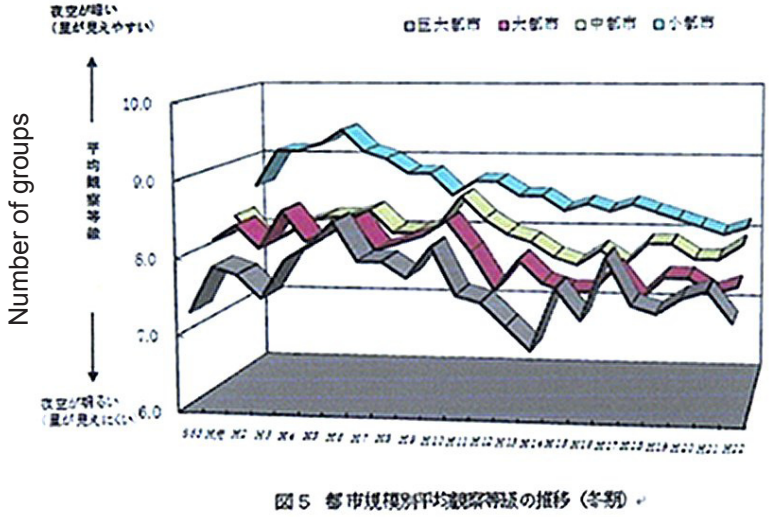

図 5 都市規模別平均観察等級の推移（冬期）

Figure 3. Binocular observation results 1988–2010, showing limiting magnitudes observed during summer seasons.

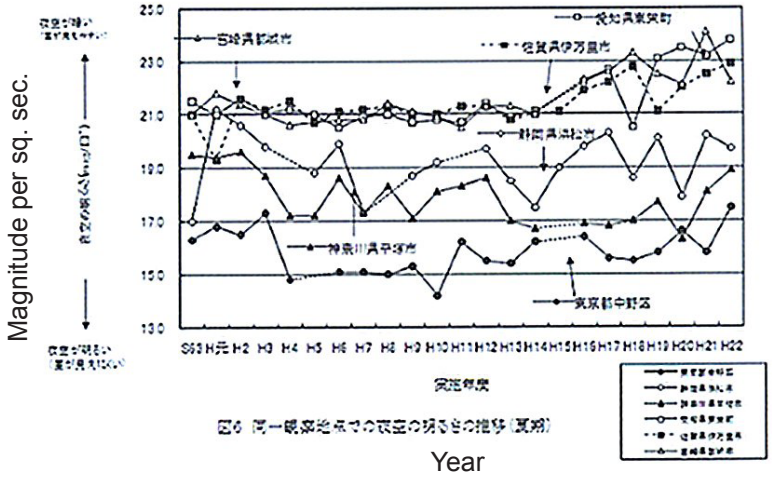

Figure 4. Results of photographic observations 1988–2010, summer seasons, showing magnitude per square second at several fixed points.

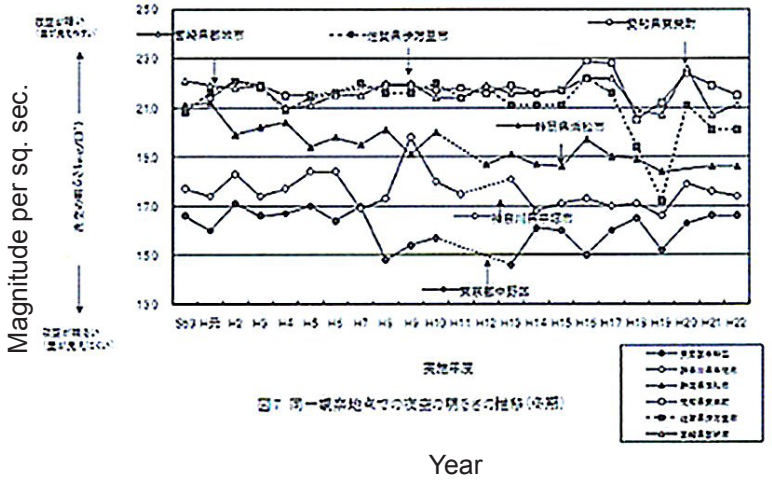

Figure 5. Results of photographic observations 1988–2010, winter seasons, showing magnitude per square second at several fixed points.

Progress Report for Adapting APASS Data Releases for the Calibration of Harvard Plates

Edward J. Los
Harvard College Observatory, 60 Garden Street, Cambridge, MA 02138

Presented at the 100th Annual Meeting of the AAVSO, October 8, 2011; received November 21, 2011; revised January 31, 2012; accepted January 31, 2012

Abstract The Digital Access to a Sky Century @ Harvard (DASCH) has scanned over 19,000 plates and developed a pipeline to calibrate these plates using existing photometric catalogues. This paper presents preliminary results from the use of the AAVSO Photometric All-Sky Survey (APASS) catalogue releases DR1, DR2, and DR3 for DASCH plate calibration. In the optimum magnitude 10–12 range of the DASCH patrol plates, the median light curve RMS with APASS calibration is 0.10–0.12 magnitude, an improvement from the 0.1–0.15 magnitude median light curve RMS with GSC 2.2.3 calibration.

1. Introduction

The Harvard College Observatory plate collection consists of approximately 525,000 photographs produced by over eighty telescopes spanning over 100 years from about 1885 to 1992. The goal of the Digital Access to a Sky Century @ Harvard project (DASCH; Grindlay 2009; see http://hea-www.harvard.edu/DASCH/) is to digitize this entire collection and provide photometry measurements for all objects. With the successful completion of a high speed plate digitizer (Simcoe *et al.* 2006) we have digitized over 18,000 plates and and used the SExtractor program (Bertin and Arnouts 1996) to extract an average of 90,000 objects per plate.

One of the primary goals of this project is to extract photometric data from these plates. The DASCH pipeline presented in Laycock *et al.* (2010) creates a calibration curve for each plate by using robust locally weighted scatterplot smoothing to match SExtractor isophotal magnitudes to magnitudes in a standard catalogue. The choice of a standard catalogue has been a continuing project issue because the catalogue must be all-sky and must match the magnitude 4–17 range of the plate collection. We are currently using the *Guide Star Catalog* version 2.3.2 (GSC 2.3.2; Lasker *et al.* 2008). The relatively poor photometric accuracy of the *Guide Star Catalog* is balanced by a good overlap in magnitude range with the Harvard plate collection and all-sky coverage. However, DASCH team member Sumin Tang reports that light curve searches using the *Kepler Input Catalog* (KIC; Brown 2011) for calibration showed less error contamination. This paper introduces a new metric, the normalized outlier count, in an attempt

to quantify the relative value of calibration catalogues with respect to such light curve searches.

Fortunately, the American Association of Variable Star Observers (AAVSO) has similar requirements for a bright star photometric catalogue and we welcome the initiative of AAVSO to produce the AAVSO Photometric All-Sky Survey (APASS; AAVSO 2009; see http://www.aavso.org/apass). We appreciate the willingness of the AAVSO to provide preliminary releases of their data and recognize that all results reported in this paper are preliminary until the final release of the APASS catalogue. Catalogue calibration of the APASS data for 18,308 plates takes 1.7 days on our current cluster configuration. Database entry is single threaded and takes an additional 3.3 days for the 16,640 plates that produce valid data with the APASS DR3 release. Because of these long processing times, the continued scanning of new plates, and the evolution of the pipeline algorithms, the design of strictly controlled experiments is not easily achieved.

The Harvard plate collection has full sky coverage, but we have been concentrating on the regions of the sky shown in Table 1. As a result, the current DASCH sky coverage from scanned plates is shown in Figure 1.

The first APASS data release (DR1) covered primarily regions North of +40 degrees declination and matched only the Northern part of our Kepler field for which we already had calibration magnitudes available from the *Kepler Input Catalog*. The second APASS data release (DR2) (Figure 2) provided a good match with our LMC field for which we had only GSC 2.3.2 calibration magnitudes. We began our tests with the APASS DR1 and DR2 releases and then migrated to the APASS Data Release 3 (DR3) as soon as it became available in August 2011. This paper discusses our experience with the DR1 and DR2 releases and the changes implemented with the DR3 release.

2. APASS DR1 and DR2 releases

For maximum performance, the calibration catalogues are reformatted into compact binary files sorted by "gsc_bin_index" which is a simple spatial hash index consisting of 1/64 degree declination bands beginning at the celestial South pole. Within each declination band, stars are sorted by right ascension into an integral number of bins approximately 1/64 degree wide. Although there is no closed form mathematical solution for the bin layout, a lookup table provides quick conversion of RA and Declination to one of the 168,966,386 gsc_bin_index values.

Figure 3 shows the steps for reformatting the calibration catalogue. Since APASS objects currently have no catalogue identification number, these objects are given a designation similar to the SDSS designations: "APASS Jhhmmss.s+ddmmss" where the J2000 Right Ascension is hh:mm:ss.ss and and the declination is +dd:mm:ss in sexagesimal format. The DASCH pipeline requires two magnitudes, a primary magnitude close to the blue spectral range where the

Harvard plates are most sensitive, and a secondary magnitude used to calculate plate-specific color corrections. With the GSC 2.3.2 catalogue, DASCH uses photographic blue and red (IIIaJ and IIIaF) magnitudes and for the KIC, SDSS g and r magnitudes. For DR1 and DR2 releases, the current study selected the APASS g and r magnitudes.

It is necessary to filter the entries for accuracy. Previous experience with KIC calibration of the DASCH plates show that the best accuracy produced by the DASCH photometric pipeline is about 0.1 magnitude RMS. Therefore, the combined APASS catalogue uses only observations for which more than one measurement is available for the SDSS g and r magnitudes and the magnitude error of each measurement is less than 0.1 magnitude. (Because of a software bug, the preferred filtering on color errors added in quadrature was not implemented in the DR1/DR2 phase of this study.) We also use a color check to filter out g-r colors which are not in the range of –1.0 and 2.5 mag. Of the 8,702,597 entries on the DR1 and DR2 releases, there are 7,173,325 entries between magnitudes 7 and 19 which meet the above criteria.

Because APASS DR1 and DR2 have overlapping fields on the celestial equator, the question arises as to whether the combined catalogue contains any duplicate objects. Matching the combined DR1 and DR2 catalogue against itself produced 79,173 matches, the majority of which were within the stated accuracy of 0.25 magnitude and 2.5 arcsec pixel size of the APASS telescopes. Before writing out the contents of a gsc_bin_index, a search for matches within a 1.0 arcsec radius accepts only the matching entry that has the lowest RMS of the magnitude accuracies added in quadrature. For the DR1 and DR2 combined catalogue, a total of 68,510 entries were rejected.

Because the earliest DASCH scanned plate to date was exposed on January 24, 1886, there is a need to correct all catalogue positions for proper motion. The final step is to match the combined APASS catalogue with the UCAC3 catalogue (Zacharias 2010) and add the UCAC3 proper motions to the APASS data. Using the same search algorithm described above, there were 6,231,923 UCAC3 matches for the 7,104,815 APASS entries.

3. APASS DR1 and DR2 results

Figure 4 shows that the coverage of the APASS-calibrated stars is most complete in the LMC region and the Northern half of the Kepler region. There was also some coverage near the equator for the M44 and 3c273 regions. Table 2 shows that 68% of the plates which yielded data for the GSC 2.3.2 catalogue also yielded data for the APASS catalogue, and about 25% of the stars that provided good data with GSC 2.3.2 also provided good data with APASS.

Three important metrics of DASCH photometry quality are derived from light curves which have at least ten points and pass all of the DASCH quality checks. Figure 5 shows the DASCH pipeline yield as a function of magnitude for all of the calibration catalogues. A major deficiency with the DR1 and DR2

combined release is its ninth magnitude limit for bright stars. Figure 6 shows the median RMS of DASCH light curves as a function of magnitude. By plotting the median RMS, this figure excludes variable stars. The best accuracy of DASCH light curves comes in two ranges, magnitude 9 to 12 and magnitude 15 to 17, because of the different types of telescopes used to generate the Harvard plate collection. Most of the plates that we scan are patrol plates with small aperture objectives which have a limiting magnitude of 13 to 14. Magnitudes dimmer than 15 are covered by a smaller collection of plates produced by telescopes with larger objectives. For objects dimmer than 11th magnitude, there is little differentiation among the various catalogues, suggesting that errors in the plates dominate. Brighter than 11th magnitude, the combined DR1 and DR2 catalogue is comparable to the KIC and noticeably better than GSC 2.3.2. The third metric shown in Figure 7 reflects the use of of the DASCH database to search for new variable stars. For this search, Sumin Tang (2012) defined a series of light curve parameters which show promise in identifying flares and other unusual variability. One such parameter is "nburst3" which is the number of points in a light curve that are at least 0.4 magnitude brighter than the median magnitude of the light curve. Figure 7 shows a "normalized nburst3" which is the sum of nburst3 for all light curves that have valid values of nburst3 divided by the number of light curves that have valid values of nburst3. For stars dimmer than magnitude 12 the three catalogues produce comparable results, although the APASS catalogue produces the highest outlier rate around magnitude 14. For stars brighter than magnitude 12, the APASS calibration is significantly better. These results should be taken with some caution: A problem with the "normalized nburst3" metric is that it does not reproduce Sumin Tang's qualitative assessment that the KIC produces fewer false outliers than the GSC 2.3.2 catalogue.

4. APASS DR3 release

Figure 8 shows that release of the APASS DR3 dataset in August 2011 provides expanded coverage in the Southern celestial hemisphere to include more of the DASCH M44, 3C273, and LMC fields. Since this release incorporates the DR1 and DR2 releases, there was no need to combine DR3 with the previous releases. This new release provided an opportunity to make four changes in the reformating of the APASS catalogue shown in Figure 9. First, the search radii for duplicates was expanded from 1 to 2 arcsec. Second, objects rejected for photometry use are now retained in the calibration catalogue to avoid confusion in searching for novae and other uncatalogued objects. These rejected objects are flagged as "variable" so that the pipeline code does not use them for plate calibration, but does assign a DASCH magnitude from the calibration data. Third, the DR3 release was merged with the *Tycho-2* catalogue (Høg 2000) as described below to improve coverage in the magnitude 4 to 9 range. Fourth, a bug was corrected in which not only individual magnitude uncertainties greater

than 0.1 magnitude were rejected, but the sum of these uncertainties added in quadrature were rejected. Correction of this bug, however, did not occur until the final processing run involving B and V Johnson magnitudes.

The *Tycho-2* catalogue was first filtered to reject B and V RMS values greater than 0.1 magnitude. While this step rejected nearly 60% of the stars, Figure 10 shows that most of the stars rejected were dimmer than 10th magnitude and would have been replaced by APASS stars.

The next step was to transform the *Tycho-2* magnitudes into the SDSS color system. Because the KIC also incorporates Tycho-2 stars, we used equations 6a and 6b in Brown *et al.* (2011) which are repeated below:

$$g = 0.54B + 0.46V - 0.07 \quad (1)$$

$$r = -0.44B + 1.44V + 0.12 \quad (2)$$

Since there was time for another photometry processing iteration, this iteration used the Johnson B and V data available with the APASS release. Høg (2000) says that the *Tycho-2* magnitudes are "close to Johnson B and V" and recommends that transformations not be used because these transformations are dependent on the luminosity class and reddening of each star. Since there are 55,718 direct matches between *Tycho-2* and APASS positions, these matches can be used to derive a transformation. However, the resulting transformation shows a standard deviation of 0.45 magnitude and is valid over only a 1- to 2-magnitude range. Consequently we followed the recommendation of Høg (2000) and used no transformation of the *Tycho-2* B–V data.

In combining *Tycho-2* with APASS DR3, there were 1,103,581 duplicates in 21,418,221 records. Preference was given to the object with the lowest magnitude error and to APASS stars as shown in Table 3.

The final step of matching the combined catalogue with the UCAC3 catalogue to obtain proper motions proceeded as described above. For the 20,434,140 objects in the combined SDSS g-r catalogue, we found UCAC3 proper motions for 16,671,675 stars. For the 20,314,720 objects in the combined Johnson B–V catalogue, we found UCAC3 proper motions for 16,580,857 stars.

Because refinements in object positions between DR2 and DR3 may cause the APASS designation to change, it is important to flush the photometry database of all references to the earlier APASS catalogue. This flushing is accomplished by a version ID which is incremented whenever new results for the same plate are inserted into the photometry database.

5. APASS DR3 results

When compared with Figure 4, Figure 11 shows expanded coverage of APASS-calibrated stars South of 30 degrees declination. Table 4 must be interpreted with caution because it reflects *Tycho-2* calibrated stars as well

as APASS calibrated stars. The new results are presented in the previously discussed Figures 5, 6, and 7. These figures contain data for both the APASS Johnson B and V calibration and the APASS SDSS g and r calibration.

Interpretation of these figures must recognize several underlying variables which may skew the results. First, there are the variations in coverage of the three catalogues which may produce systematic errors dependent on sky conditions. The GSC 2.3.2 catalogue may also have systematic variations between the different plate series used for the Northern and Southern hemispheres and for the Magellanic clouds. Experiments with subsets of Figure 6 show that there is indeed a large effect of sky position on the median RMS values between magnitudes 5 and 9. RMS values for Large Magellanic Cloud stars are higher than for Kepler satellite field stars. Second, there is the use of the *Tycho-2* catalogue to fill in the three calibration catalogues. Where APASS and *Tycho-2* overlap, most stars brighter than magnitude 9 have *Tycho-2* calibrations. Where there is no overlap, the *Tycho-2* calibrations can extend to magnitude 12. Our version of the GSC 2.3.2 catalogue uses independently derived transformations from *Tycho-2* to SDSS magnitudes. We learned that the KIC does not use a similar tranform. (According to Monet (2011), equations 6a and 6b in Brown *et al.* (2011) were used only for the calculation of the effective KIC magnitude.) Finally, there is the division of the DASCH data into patrol and deep-field telescopes. Each telescope is good for an optimum range of magnitudes, but this range is also a function of the exposure time for each individual plate and emulsion type.

Given the above uncertainties and the fact that both DASCH and APASS are continuing works in progress, the author can draw only limited conclusions at this stage. Except for the magnitude 13 to 15 range, the APASS calibration catalogue provides better results than the GSC 2.3.2 and KIC catalogues. The APASS B and V data produce comparable results to the APASS g and r data, though the former produce slightly fewer outliers over a large magnitude range. Finally, the attempt to merge in the *Tycho-2* catalogue should be abandoned in favor of a smaller but better-behaved dataset between magnitudes 8 and 11. Since we currently process every newly scanned plate with both the GSC 2.3.2 and the APASS catalogues, researchers seeking coverage for brighter stars should use the GSC 2.3.2 calibrated data. Subsequent to the processing of the APASS DR3 data, the DASCH team implemented a proposal by Sumin Tang to improve saturated star calibration, but the results from this change are not yet available. We are also interested in testing the new UCAC4 catalogue as a photometry calibration catalogue when it becomes available.

6. Acknowledgements

Thanks to the other members of the DASCH photometry team, principal investigator Prof. Jonathan Grindlay, Sumin Tang, and Dr. Mathieu Servillat for their advice and comments. Additional contributors to the DASCH project are

the Harvard College Plate Stacks Curator, Alison Doane; hardware engineer, Robert Simcoe; and our transcribers, plate cleaners, and scanners. Arne A. Henden of AAVSO provided us with early releases of the APASS data. Both Arne Henden and the anonymous reviewer provided valuable comments on the drafts of this paper. This work was supported in part by NSF grants AST0407380 and AST0909073 and now also the Cornel and Cynthia K. Sarosdy Fund for DASCH. The AAVSO APASS project was made possible with funding by the Robert Martin Ayers Sciences Fund.

References

Bertin, E., and Arnouts, S. 1996, *Astron. Astrophys., Suppl. Ser.*, **117**, 393.

Brown, T. M., Latham, D. W., Everett, M. E., and Esquerdo, G. A. 2011, *Astron. J.*, **142**, 112.

Grindlay, J., Tang, S., Simcoe, R., Laycock, S., Los, E., Mink, D., Doane, A., and Champine, G. 2009, in *Preserving Astronomy's Photographic Legacy: Current State and the Future of North American Astronomical Plates,* ed. W. Osborn and L. Robbins, ASP Conf, Ser., 410, Astron. Soc. Pacific, San Francisco, 101.

Henden, A. A., Welch, D. L., Terrell, D., and Levine, S. E. 2009, *Bull. Amer. Astron. Soc.*, **41**, 669.

Høg, E., *et al.* 2000, *The Tycho-2 Catalogue of the 2.5 Million Brighest Stars*, *Astron. Astrophys.*, **355**, L27.

Lasker, B., *et al.* 2008, *Astron. J.*, **136**, 735.

Laycock, S., Tang, S., Grindlay, J., Los, E., Simcoe, R., and Mink, D. 2010, *Astron. J.*, **140**, 1062.

Monet, D. 2011, private communication (September 10).

Simcoe, R. J., Grindlay, J. E., Los, E. J., Doane, A., Laycock, S. G., Mink, D. J., Champine, G., and Sliski, A. 2006, in *Applications of Digital Image Processing XXIX*, ed. A. G. Tescher, Proc. SPIE, 6312, 35.

Tang, S. 2012, in preparation.

Zacharias, N., *et al.* 2010, *Astron. J.*, **139**, 2184.

Table 1. DASCH Primary Coverage Regions.

Region	*R.A. (2000.0)* *h m*	*Dec. (2000.0)* ° ′
M44	08 40	+19 41
3C273	12 30	+02 03
Baade's Window	18 03	–29 00
Kepler Satellite	19 20	+45 00
Large Magellanic Cloud	05 23	–69 45

Table 2. Photometry Pipeline Output for APASS DR1 and DR2.

Catalogue	*Plates*	*Magnitudes*	*Stars Matched*	*Light curves**
GSC 2.3.2	15,942	1,566,000,000	72,411,000	4,307,000
KIC	3,673	322,733,487	3,978,000	533,000
APASS DR1 and DR2	10,853	812,740,385	2,834,509	1,115,651

**The light curve contains at least two points that match all of the DASCH acceptance criteria.*

Table 3. Truth Table for Star Selection Between *Tycho-2* and APASS Stars Within 2 Arcsec. There are sixteen possible combinations of catalogue source and RMS level. The note marks show the preferred entry.

Matches (g–r)	*Matches (B–V)*	*First Duplicate Source*		*Second Duplicate Source*	
3956	3137	Tycho-2	RMS < 0.1[b]	Tycho-2	RMS < 0.1[b]
1505	1706	Tycho-2	RMS < 0.1[a]	Tycho-2	RMS > 0.1
31	25	Tycho-2	RMS > 0.1	Tycho-2	RMS < 0.1[a]
484	956	Tycho-2	RMS > 0.1[b]	Tycho-2	RMS > 0.1[b]
74787	55740	Tycho-2	RMS < 0.1	APASS	RMS < 0.1[a]
53171	37827	Tycho-2	RMS < 0.1[a]	APASS	RMS > 0.1
222573	264450	Tycho-2	RMS > 0.1	APASS	RMS < 0.1[a]
38373	30812	Tycho-2	RMS > 0.1	APASS	RMS > 0.1[a]
105587	81575	APASS	RMS < 0.1[a]	Tycho-2	RMS < 0.1
293755	346859	APASS	RMS < 0.1[a]	Tycho-2	RMS > 0.1
85118	63032	APASS	RMS > 0.1	Tycho-2	RMS < 0.1[a]
51744	44900	APASS	RMS > 0.1[a]	Tycho-2	RMS > 0.1
25800	87652	APASS	RMS < 0.1[b]	APASS	RMS < 0.1[b]
29950	34671	APASS	RMS < 0.1[a]	APASS	RMS > 0.1
25337	26382	APASS	RMS > 0.1	APASS	RMS < 0.1[a]
91410	23777	APASS	RMS > 0.1[b]	APASS	RMS > 0.1[b]

Notes: a: Selected candidate. b: Selected candidate has the lowest RMS.

Table 4. Photometry Pipeline Output for APASS DR3.

Catalogue	*Plates*[a]	*Magnitudes*	*Stars Matched*	*Light curves*[b]
GSC 2.3.2	16989	1,666,000,000	76,209,000	4,325,000
APASS DR3 g–r	16642[c]	1,282,000,000	8,109,840[c]	3,052,942[c]
APASS DR3 B–V	16640	1,291,720,897	8,323,460	2,618,816

Notes: a: These totals reflect the additional 1,188 plates of the LMC scanned during August, 2011. b: The light curve contains at least two points that match all of the DASCH acceptance criteria. c: These numbers may include stale entries from previous processing iterations.

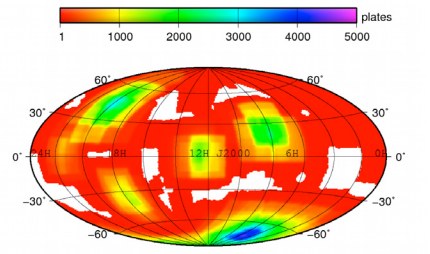

Figure 1. Current DASCH sky coverage from scanned plates.

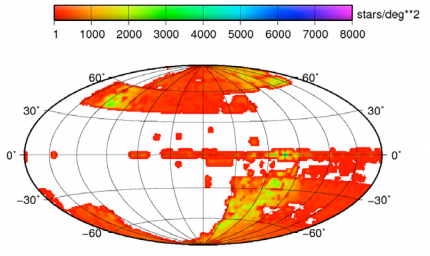

Figure 2. Coverage of APASS Data Releases 1 and 2.

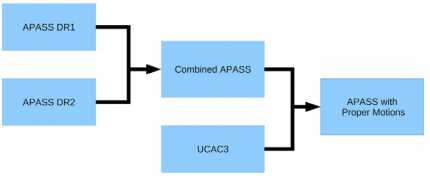

Figure 3. Preparation of DASCH/ APASS DR1 and DR2 calibration catalog.

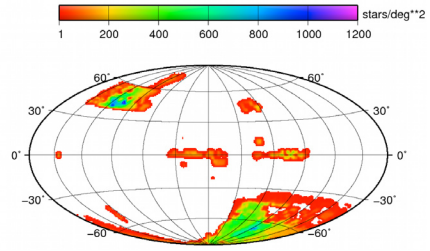

Figure 4. Coverage of APASS DR1 and DR2 calibrated plates.

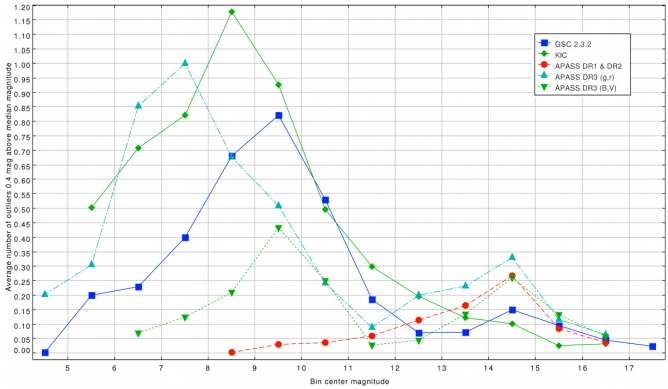

Figure 5. Number of DASCH light curves with at least ten good points after photometric processing.

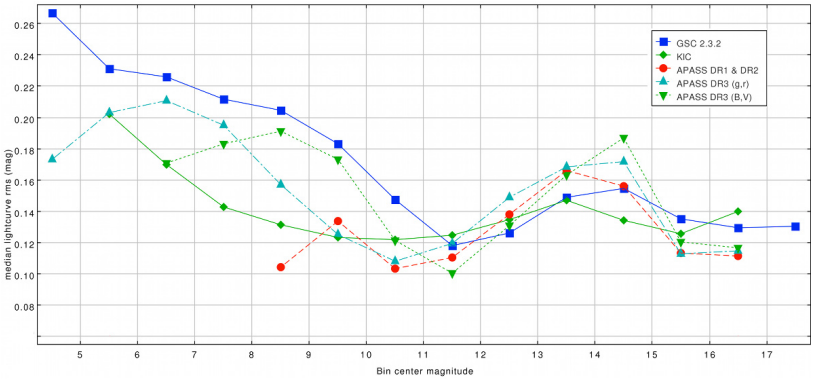

Figure 6. Median RMS of DASCH light curves with at least ten good points after photometric processing.

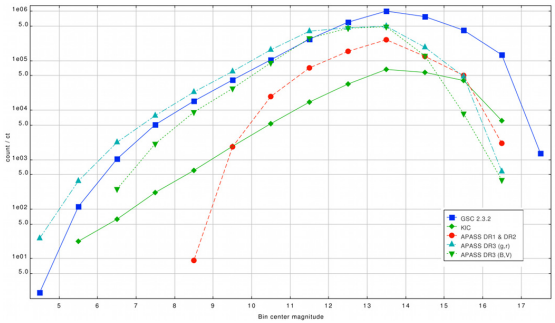

Figure 7. Average count light curve outliers: points 0.4 magnitude above the median light curve magntiude.

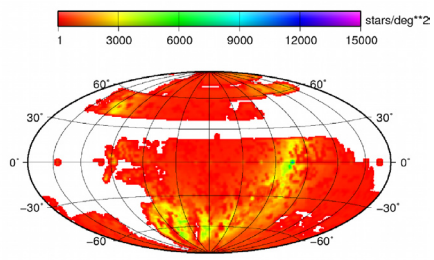

Figure 8. Coverage of APASS Data Release 3.

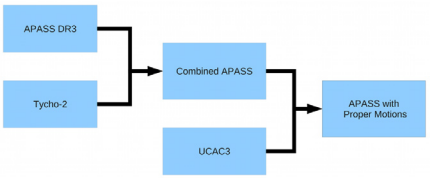

Figure 9. Preparation of DASCH/ APASS DR3 calibration catalog.

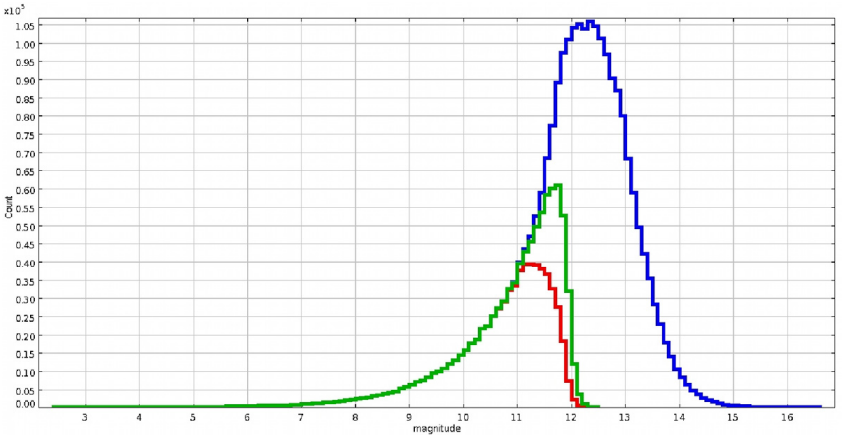

Figure 10. Magnitude Distribution of the Tycho2 Catalog. The full dataset (blue) contains all objects with valid magnitudes. The next most inclusive dataset (green) contains all objects with individual magnitude RMS values less than 0.1 mag. The most restricted dataset (red) contains objects with magnitude uncertainties added in quadrature less than 0.1 mag.

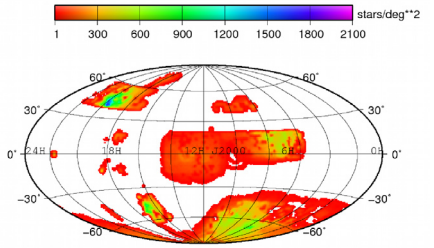

Figure 11. Coverage of APASS DR3 calibrated plates.

Flares, Fears, and Forecasts: Public Misconceptions About the Sunspot Cycle

Kristine Larsen
Physics and Earth Sciences, Central Connecticut State University, 1615 Stanley Street, New Britain, CT 06053; Larsen@ccsu.edu

Presented at the 100th Annual Meeting of the AAVSO, October 8, 2011; received December 28, 2011; revised February 22, 2012; accepted February 24, 2012

Abstract Among the disaster scenarios perpetrated by 2012 apocalypse aficionados is the destruction of humankind due to solar flares and coronal mass ejections (CMEs). These scenarios reflect common misconceptions regarding the solar cycle. This paper (based on an annual meeting poster) sheds light on those misconceptions and how the AAVSO Solar Section can address them.

1. Introduction

Despite the fact that the current 2012 end-of-the-world hysteria is usually (and correctly) disparaged for needlessly scaring members of the general public, the silver lining is that it offers a unique opportunity for educators and scientists to peer into the minds of the same science-phobic public. What is discovered is a plethora of misconceptions about science in general, and astronomy in particular. One of the most commonly touted apocalypse scenarios centers around the sunspot cycle; therefore a careful survey of the claims put forth by proponents of this "sun fries the earth" cataclysm affords solar observers and educators the opportunity to learn about what the public does and does not know about the sun and its cycles, and then attempt to turn those fears and misconceptions into a more healthy interest in and respect for our nearest star and its variability. This paper surveys some of the common misconceptions the public has concerning solar activity and offers suggestions as to how the AAVSO in general and the AAVSO Solar Section in particular could aid in the education of the general public in these matters.

2. Misconceptions, pseudoscience, and scientific illiteracy

Numerous studies have shown that the scientific literacy of the American public has stagnated at about 60% in recent decades—a grade of D-minus (National Science Board 2010). It is not merely a lack of knowledge that educators and scientific organizations have to worry about, however, but rather the prevalence of misconceptions about scientific concepts. These erroneous ideas are often deeply ingrained in a person's personal view of the world around them, and can be difficult to dislodge (Mestre 1991). Adding

to this is the general inability of many Americans to distinguish science from pseudoscience (explaining the tenacity of astrology in modern culture, for example) (Shermer 1997). Finally, the general public misinterprets the healthy professional debate that takes place between scientists (as they continue to investigate natural phenomena and the causal connections between them) as a sign of weakness: if science isn't absolutely certain, then any other suggested answer may be considered to be just as valid. The result is a general public that is easily swayed by purveyors of pseudoscience and conspiracies, especially in the age of the Internet. Without the ability or willingness to consider claims made by nonscientists with skepticism, the general public has fallen prey to a series of increasingly alarmist claims about the upcoming solar maximum, often perpetrated by adherents of the so-called 2012 apocalypse hoax—the claim that the end of the world (or at least the end of human civilization) will occur on December 21, 2012.

3. Misconceptions about the sunspot cycle

According to a lengthy list of astronomical misconceptions collected by University of Maine astronomy professor Neil Comins, the following are some of the misconceptions concerning the solar cycle:

- sunspots are regions of soot on the sun;
- sunspots occur on an Earth-based cycle;
- sunspots are places on the sun that have run out of fuel to burn;
- sunspots are hotter places on the sun;
- sunspots are permanent;
- sunspots are where meteors crashed (or are craters);
- sunspots are optical illusions due to staring at the sun;
- the sun does not rotate;
- the sun does not have a magnetic field;
- sunspots are volcanic in nature. (Comins, undated)

These misconceptions (and others) are addressed by Dooling and Kneale (1997), O'Neill (2008), International Solar Terrestrial Physics (ISTP) (Anon. 2012), and 2012Hoax (Anon. 2010). A related misconception that crops up in discussions of the 2012 apocalypse hoax is a belief that solar activity can affect volcanic activity on earth. For example, it appears in a thread of comments on the 2012Hoax webpage devoted to debunking a viral email/blog entitled "Seven Reasons Why the World Will End in 2012—Proven Scientifically." An example is an October 24, 2011, post by Cern: "What is this I hear about a

super-volcano forming in Bolivia? ...seems to coincide with the giant sun spots lately…. As the activity increases so will this volcanoes [sic]?" (Anon. 2009).

The existence of these misconceptions suggests that some among the general public lack basic knowledge concerning sunspots and their cycle. The result is that while members of the public may have heard of sunspots, they know little about them. Thus, when an item comes up in the press about sunspots, they may listen (after all, they know that sunspots must be somehow important because they have at least heard of them), but do they really hear what is being said? Unfortunately, the press capitalizes on the situation with sensational titles, such as:

- "Space Weather: Worse Than Hurricane Katrina" (New Scientist);
- "Huge Solar Flares Could Spell Catastrophe for Earth" (Forbes);
- "Sun unleashes huge solar flare towards Earth" (BBC).

The reader who ventures no further than the title will certainly be left with serious misconceptions. However, even those who read the entire article may leave with little more than a lingering impression from the title. Hence this author encourages science journalists and scientific agencies to think long and hard as they craft press releases and articles on the solar cycle that will be seen by the general public. The point is not that the information is being released, but rather how it is released. For example, Somerville and Hassol (2011) note that "Scientists typically fail to craft simple, clear messages and repeat them often…. We encourage them to speak in plain language and choose their words with care." They also offer that "By failing to anticipate common misunderstandings, scientists can inadvertently reinforce them." Their article also includes a useful chart that shows the differences between scientific terms and the way the public interprets them.

4. Misuse of scientific information: 2012

Like other scientific discoveries, those surrounding the sun have been used by groups and individuals to foster their own agendas. For example, earnest scientific studies as to the impact of solar activity on Earth's climate have routinely been used by global warming deniers to attempt to exonerate humanity from responsibility for changes in the environment. However, pseudoscience and conspiracy theory proponents have gone even further, using science in service to their desire to scare the general public into buying their survival guides or subscribing to their for-profit websites. The most important recent example is, of course, the 2012 apocalypse hoax.

For those few fortunate astronomers who have not yet come face to face with this rampant pseudoscience, in a nutshell (pun intended) the idea is that the Maya calendar (and/or Nostradamus, the Bible Code, etc.) predicts that the world will end on December 21, 2012, by asteroid impact, creation of an earth-

sucking black hole by the Large Hadron Collider, alignment with the black hole at the center of the Milky Way, flipping of Earth's poles (magnetic or otherwise), solar flares, or other catastrophe. The viral email/blog message "Seven Reasons Why the World Will End in 2012—Proven Scientifically" summarizes much of this hysteria, with the following in particular said about the sun:

> Solar experts from around the world monitoring the sun have made a startling discovery: our sun is in a bit of strife. The energy output of the sun is, like most things in nature, cyclic, and it's supposed to be in the middle of a period of relative stability. However, recent solar storms have been bombarding the Earth with so much radiation energy, it's been knocking out power grids and destroying satellites. This activity is predicted to get worse, and calculations suggest it'll reach its deadly peak sometime in 2012. (Anon. 2008)

A probable source of this exaggeration is a 2006 study by the National Center for Atmospheric Research (NCAR 2006) that suggested that the next solar maximum would be "30–50% stronger than the last one" and posited a peak in 2012.

A number of 2012 apocalypse proponents have twisted this prediction into a certain prophecy of doom, declaring that the largest solar flare on record will fry Earth (along with the electric grids and satellites). This is why NASA and other organizations should be mindful of the wording of their statements when releasing scientific data on the interactions between the sun's magnetic phenomena and terrestrial systems—the pseudoscientists are lurking in the shadows, ready to say "See! We told you!" As the Social Issues Research Centre/Amsterdam School of Communication Research (SIRC/ASCOR 2006) report on communicating science to the general public warns, "While there are numerous examples of how the media have 'hyped' science stories…there are equal examples of where scientists have communicated, say, data relating to risks in such a manner that public misunderstandings have been almost inevitable." As is commonly the case with pseudosciences, subsequent evidence provided by scientists attempting to clarify or update the situation is either ignored, or declared part of a conspiracy to withhold the truth from the general public. Thus subsequent announcements from various scientists about updated predictions for the peak of Cycle 24 (now to occur in 2013, after the world will have presumably ended) have largely gone ignored in the 2012 hoax community.

5. What the general public is reading and saying

One can rightly ask just how widespread these misconceptions and misrepresentations of the solar cycle are on the Internet. The answer is that they are far too prevalent. For example, Mitch Battros, an acupuncturist and trauma resolution therapist, asserts in the books *Solar Rain* and *Cosmic Rain* (and their

promotional websites) that the following original "equation" explains what we will expect to see in 2012:

> Sunspots → Solar Flares → Magnetic Field Shift → Shifting Ocean and Jet Stream Currents → Extreme Weather and Human Disruption (Battros, undated)

In his mind, since extreme weather is presumed to be caused by sunspots, the coming apocalypse will center around sunspots triggering weather catastrophes on Earth.

Michael E. Sallas, Ph.D. (who neglects to inform readers of his website that his degree is in Government Studies, not Astronomy) claims on his "Zero Sunspots, Global Consciousness, Solar Activity and 2012" website that not only is Battros's "theory" correct, but that he can use the model to explain the unusually low sunspot counts seen until recently as "due to changes in global consciousness brought about by the harmonizing of human interests and activities through the internet" (Sallas 2008). Thus, he reasons, Cycle 24 will be "unremarkable" as "changes in global consciousness produce greater planetary cooperation and harmony" over the next few years. If this is true, then why is self-described "student of consciousness and libertarian decentralist pacifist activist, writer, songwriter, and video producer" Carol Moore (2011) claiming on her website "Sunspot Cycles and Activist Strategy" that the upcoming cycle maximum will coincide with "mass demonstrations, riots, revolutions and wars"? The answer, of course, is that none of this is scientific. However, with all involved using the same sunspot cycle charts from NASA and NOAA, and "equations" to bolster their cases, does the general public understand the difference? Unfortunately not. The following are a handful of posts from the "Seven Reasons" website posted at buburuza.net (typos original):

> "the sun is dieing as we know it and by the tie there is the storm it wont be big enough."
>
> "yes the sun is becoming closer…."
>
> "No, the world will end after 1 billion years because the hydrogen at the sun will disappear."
>
> "volcanoes are going to happen because of the sun storms."

Clearly more needs to be done to educate the general public concerning the sunspot cycle, solar activity, and its influence on Earth. This certainly falls within the purview of the AAVSO's Mission Statement.

6. Conclusion

Various authors have sounded the call to action for a number of communities to come forward and aid in the debunking of the 2012 hoax, including AAS

members (Manning 2009), ASP members (Morrison 2009), amateur astronomers (Larsen 2010a, 2010b), geologists (Larsen 2010c), science teachers (Larsen 2010d), planetarium professionals (Larsen 2010e), and the AAVSO in general (Larsen 2009). Astrobiologist David Morrison has been an eloquent leader in the effort to debunk the 2012 apocalypse hoax, as have archaeoastronomer E. C. Krupp (2009), solar physicist Ian O'Neill (2008), and amateur astronomer Bill Hudson and his army of volunteers at the 2012Hoax website (Anon. 2009, 2010). In this spirit, this author makes the following claim: the AAVSO's Solar Section has a unique opportunity to join in the stamping out of misconceptions surrounding solar activity, and at the same time possibly generating interest in solar observing. Some of those who are interested in solar activity (and think that scientists are "hiding" information) may be motivated to take part in safe solar observing; thus effort should be taken to educate these individuals on solar activity and how they could gather more data for the AAVSO Solar Section. An encouraging development in this vein can be seen on the comments section to the 2012Hoax webpage on solar flares, where posters have discussed following the current solar cycle on the www.spaceweather.com website. For example, in a March 5, 2011, post, DieselHorseLAW admits, "I have become somewhat addicted to www.spaceweather.com and I notice the day to day sun spot number fluctuates a lot." Elsgeorge answers the following day: "So have I, I even downloaded their 3D Sun app" (2012Hoax, Anon. 2010).

On the down side, others may decide to take matters into their own hands and unsafely observe the sun. Well-meaning individuals can also convey erroneous information, opening up the possibility of unsafe observing. For example, a reply by obaeyens to DieselHorseLAW dated March 6, 2011, correctly advises that a pinhole projector could be safely used to see sunspots, as well as using binoculars to project an image. The author also correctly warns the readers to never look at the sun directly using a telescope or binoculars. However, the author incorrectly adds, "You can also look at the sunspots when the sun is about to go below the horizon for a short time." Therefore it is recommended that the AAVSO Solar Section capitalize on the current interest in the solar cycle and provide a valuable public service by both publicizing the need for new solar observers AND stressing the proper methods of solar observing. Having public demonstrations of the use of sunspotters and simple projection methods would serve dual purposes. It is also recommended that the AAVSO Solar Division be a model of best practices in terms of communicating with the general public, both through its website and bulletin, and as individual members discuss their solar observing (and its importance) with the general public. Campbell (2008) warns that "We may believe that data speaks for itself, but data is also subject to interpretations, including by laypersons, that are completely valid though not in line with the conclusions of scientists." Collecting sunspot data for the scientific community is an important function of the AAVSO Solar Division. Explaining to the general public how we collect these data, what value the data

have, and what is and is not predicable about the solar cycle despite the amount of data collected should also be central to the Solar Division's mission.

David Morrison (2009) has often noted that one of the "worst long-term consequences of the 2012 doomsday hoax" could be what he terms "cosmophobia," a fear of "astronomy and the universe." This can be seen in a January 4, 2001, post by Andrew Maxwell to the buburuza.net "Seven Reasons Why the World Will End in 2012—Proven Scientifically" webpage: "i'm terrified of the sun." Rather than merely trying to get rid of the lemons of misconceptions, solar observers can use the interest in solar activity spawned by purveyors of the 2012 apocalypse hoax to create lemonade, in the form of new solar observers (and interest in solar observing in general). As Manning (2009) notes, "This is a teachable moment. So let us teach." Let's change fear to awe, respect, and knowledge, one prospective solar observer at a time.

References

Anon. 2008, "Seven Reasons Why the World Will End in 2012—Proven Scientifically" (http://buburuza.net/2008/08/seven-reasons-the-world-will-end-in-2012-proven-scientifically/).

Anon. 2009, 2012Hoax: 7 Reasons (http://www.2012hoax.org/7-reasons).

Anon. 2010, 2012Hoax: Solar Flares (http://www.2012hoax.org/solar-flares).

Anon. 2012, International Solar Terrestrial Physics (ISTP): "Ten Things You Thought You Knew About Sun-Earth Science" (http://pwg.gsfc.nasa.gov/istp/outreach/sunearthmiscons.html).

Battros, M. (undated), "About Mitch Battros" (http://www.solarrainbook.com/about.php).

Campbell, H. 2008, "The Pitfalls and Perils of Communicating Science," *CAP Journal*, **2**, 22.

Comins, N. (undated), "Astronomical Misconceptions: Sun," http:www.physics.umaine.edu/sun.htm

Dooling, D., and Kneale, R. A. 1997, "The Sun-earth Connection" (http://eo.nso.edu/MrSunspot/answerbook/polarity.html).

Krupp, E. C. 2009, "The Great 2012 Scare," *Sky & Telescope*, **118** (No. 5), 22.

Larsen, K. 2009, "Scientists Look at 2012: Carrying on Margaret Mayall's Legacy of Debunking Pseudoscience," *J. Amer. Assoc. Var. Star Obs.,* **38**, 139.

Larsen, K. 2010a, "Astronomy EPO and the 2012 Hysteria: Your Personal Guide for Joining the Battle," *Mercury*, **39**, 22.

Larsen, K. 2010b, "The 2012 Apocalypse Hoax and How You Can Help Combat it," Stellafane Convention, Springfield, Vermont.

Larsen, K. 2010c, "The 2012 Apocalypse Hoax: A Geological Call to Arms." GSA Abstracts with Programs 42.1, 51 (http://gsa.confex.com/gsa/2010NE/finalprogram/abstract_168194.htm).

Larsen, K. 2010d, "12 Websites for Combating the 2012 Hysteria: Resources and Activities for Educators," *Classroom Astron.* **3**, 10.

Larsen, K. 2010e, "Planetariums and the 2012 Hysteria," *Planetarian: J. Int. Planetarium Soc.*, **39**, 13.

Manning, J. 2009, "Addressing the 'Science' of Doomsday," *AAS Newsletter*, **149**, 14.

Mestre, J. P. 1991, "Learning and Instruction in Pre-college Physical Science," *Physics Today*, **44** (No. 9), 56.

Moore, C. 2011, "Sunspot Cycles and Activist Strategy," (http://carolmoore.net/articles/susspot-cycle.html).

Morrison, D. 2009, "Doomsday 2012, the Planet Nibiru, and Cosmophobia," *Astronomy Beat 32* (http://www.astrosociety.org/2012/ab2009-32.pdf).

National Center for Atmospheric Research (NCAR) 2006, "Scientists Issue Unprecedented Forecast of Next Sunspot Cycle," NCAR News Release (http://www.ucar.edu/news/releases/2006/sunspot.shtml).

National Science Board 2010, *Science and Engineering Indicators*, National Science Foundation, Arlington, Virginia.

O'Neill, I. 2008, "2012: No Killer Solar Flare" (http://www.universetoday.com/14645/2012-no-killer-solar-flare/).

Sallas, M. 2008, "Zero Sunspots: Global Consciousness, Solar Activity and 2012," (http://exopolitics.blogs.com/exopolitics/2008/09/zero-sunspots-g.html).

Shermer, M. 1997, *Why People Believe Weird Things*, Holt, New York.

Social Issues Research Centre/Amsterdam School of Communication Research (SIRC/ASCOR) 2006, *MESSENGER: Final Report* (http://www.sirc.org/messenger/Final_Report_Draft_1.pdf).

Somerville, R. C. J., and Hassol, S. J. 2011, "Communicating the Science of Climate Change," *Physics Today*, **64** (No. 10), 48.

AAVSO Estimates and the Nature of Type C Semiregulars: Progenitors of Type II Supernovae *(Abstract)*

David G. Turner
K. Moncrieff
C. Short
Saint Mary's University, Department of Astronomy and Physics, 923 Robie Street, Halifax, NS B3H 3C3, Canada; turner@ap.smu.ca

Robert F. Wing
Ohio State University, Department of Astronomy, 140 W. 18th Avenue, Columbus, OH 43210; wing@astronomy.ohio-state.edu

Arne A. Henden
AAVSO Headquarters, 49 Bay State Road, Cambridge, MA 02138; arne@aavso.org

Presented at the 100th Spring Meeting of the AAVSO, May 21, 2011

Abstract The nature of the variability in the M supergiant type C semiregular (SRC) variables is examined using new and archival spectroscopic and spectrophotometric observations of the stars phased according to AAVSO magnitude estimates. SRC variables appear to be more regular than sometimes suggested, although the nature of their pulsation remains unclear in some cases. Some SRCs appear to undergo irregular fading episodes that may result from dust ejection. But recent light curves of the stars display large scatter that hinders reliable determination of their cycle lengths, a problem that needs to be addressed to improve the usefulness of AAVSO data for learning more about massive stars as they approach the terminal stage of their evolution as Type II supernovae.

Preliminary Analysis of MOST Observations of the Trapezium *(Abstract)*

Matthew R. Templeton
AAVSO Headquarters, 49 Bay State Road, Cambridge, MA 02138; matthewt@aavso.org

Joyce Ann Guzik
Los Alamos National Laboratory, XTD-2 MS T086, Los Alamos, NM 87545; joy@lanl.gov

Arne A. Henden
AAVSO Headquarters, 49 Bay State Road, Cambridge, MA 02138; arne@aavso.org

William Herbst
Wesleyan University, Department of Astronomy, Middletown, CT 06459; wherbst@wesleyan.edu

Presented at the 100th Spring Meeting of the AAVSO, May 21, 2011

Abstract We present our first assessment of light curves of the Trapezium stars obtained by the MOST satellite in early 2011. The data sets consist of four stars of the θ^1 Ori system (A, B, C, and D), along with 34 GSC stars in the field nominally used for guiding. The photometry of the brightest stars is sufficient to detect variability at a level well below one mmag, while photometry of the fainter guide stars has not yet been assessed. An early look at the data indicates intrinsic signals are clearly present; non-trivial systematics also related to the spacecraft and sampling are also present, and we discuss potential means for dealing with these issues. We will also discuss our plans for analyzing the data and deriving physical information on these stars.

High School Students Watching Stars Evolve *(Abstract)*

John R. Percy
Drew MacNeil
Leila Meema-Coleman
Karen Morenz
Department of Astronomy and Astrophysics, University of Toronto, Toronto, ON M5S 3H4, Canada; john.percy@utoronto.ca

Presented at the 100th Annual Meeting of the AAVSO, October 7, 2011

Abstract Some stars pulsate (vibrate). Their pulsation period depends primarily on their radius. The pulsation period changes if the radius changes, due to evolution, for instance. Even though the evolution is slow, the period change is measurable because it is cumulative. The observed time of maximum brightness (O) minus the calculated time (C), assuming that the period is constant, is plotted against time to produce an (O–C) diagram. If there is a uniform period change, this diagram will be a parabola, whose curvature—positive or negative—is proportional to the rate of period change. In this project, we study the period changes of RR Lyrae stars, old sun-like stars which are in the yellow giant phase, generating energy by thermonuclear fusion of helium into carbon.

We chose 59 well-studied stars in the GEOS database, which consists of times of maximum measured by AAVSO and other observers. We included about a dozen RRc (first overtone pulsator) stars, since these have not been as well studied as the RRab (fundamental mode) stars because the maxima in their light curves are not as sharp. We will describe our results: about 2/3 of

the stars showed parabolic (O–C) diagrams with period changes of up to 1.0 s/century, some with increasing periods and some with decreasing periods. The characteristic times for period changes (i.e. period divided by rate of change of period) were mostly 5–30 million years. These numbers are consistent with evolutionary models. Some stars showed too much scatter for analysis; we will discuss why. A few stars showed unusual (O–C) diagrams which cannot be explained simply by evolution.

This project was carried out by coauthors MacNeil, Meema-Coleman, and Morenz, who were participants in the prestigious University of Toronto Mentorship Program, which enables outstanding senior high school students to participate in research at the university. We thank the AAVSO and other observers who made the measurements which were used in our project.

Eclipsing Binaries That Don't Eclipse Anymore: the Strange Case of the Once (and Future?) Eclipsing Binary QX Cassiopeiae *(Abstract)*

Edward F. Guinan
Michael Bonaro
Scott G. Engle
Andrej Prsa
Villanova University, Department of Astronomy, Villanova, PA 19085; edward.guinan@villanova.edu

Presented at the 100th Annual Meeting of the AAVSO, October 8, 2011

Abstract We report on the cessation of eclipses of the former 6.005-day eclipsing binary QX Cas. This 10th-magnitude star is a member of the young open cluster NGC 7790; in 1954 QX Cas (B1 IV–V + B3 V) was discovered by Erleksova (1954: *Astr. Circ.* 155) to be an eclipsing binary. Subsequently Sandage (1958: *ApJ*,128,150) and Sandage and Tammann (1969: *ApJ*, 157, 683) obtained accurate photometry of QX Cas that confirmed its eclipsing nature and provided accurate measures of UBV magnitudes and colors. The early light curves display two narrow eclipses with depths of ~ 0.32 magnitude and ~0.28 magnitude, respectively. Moreover the Min II occurs at 0.37 P—indicating an moderately eccentric orbit. To secure modern light curves, we have carried out UBVRI photometry using the 0.8-m Four College Automatic Photoelectric Telescope (FCAPT). Photometry was conducted on >110 nights and the observations now cover all the orbital phasespace of the binary. However, this photometry (and overviews of all recent photometry) show no evidence of eclipses. Thus QX Cas is no longer an eclipsing binary! QX Cas joins another former eclipsing binary—SS Lac—that over twenty years ago also ceased eclipsing.

We present the analysis of previous light curves and the analysis of recent spectroscopy and HST observations of QX Cas to determine its orbital and physical properties. We discuss the reasons that could cause QX Cas to stop eclipsing. These include binary system disruption or an impulsive orbital change from a close encounter with another cluster star or (most likely) from orbital perturbations from a putative bound tertiary companion.

QX Cas and other related eclipsing binaries that stopped eclipsing or show changes in their eclipse depths could be interesting targets for AAVSO members to monitor using CCD or photoelectic photometry. In addition, the changing orbital inclination of QX Cas and other similar, previous eclipsing binaries can be studied with spectroscopic radial velocity observations which are dependent on the star's orbital inclination. This research is supported by NSF/RUI Grants AST05-07536 as well as NASA Grant HST-GO 10116 which we gratefully acknowledge.

High Speed UBV Photometry of ε Aurigae's 2009–2011 Eclipse *(Poster abstract)*

Aaron Price
AAVSO Headquarters, 49 Bay State Road, Cambridge, MA 02138; aaronp@aavso.org

Gary Billings
P.O. Box 263, Rockyford, AB T0J2R0, Canada; obs681@gmail.com

Bruce L. Gary
5320 E. Calle Manzana, Hereford, AZ 85615

Brian K. Kloppenborg
2499 S. Colorado Boulevard, Apt. 803, Denver, CO 80222; brian.kloppenborg@du.edu

Arne A. Henden
AAVSO Headquarters, 49 Bay State Road, Cambridge, MA 02138; arne@aavso.org

Presented at the 100th Spring Meeting of the AAVSO, May 23, 2011

Abstract We present rapid cadence U, B, and V photometry of ε Aurigae during its 2009–2011 eclipse. Data are analyzed to look for both periodic and random variation. Observations are presented from two observers. The first is from Rockyford, Alberta, Canada, and used a ST-7 and ST-8XME with 50mm and 135mm lenses, respectively. This observer recorded continuous filtered time series up to 11 hours long. The second is in Hereford, Arizona, and used a ST-10XME with a 0.36-m SCT.

δ Scorpii 2011 Periastron: Visual and Digital Photometric Campaign *(Poster abstract)*

Costantino Sigismondi Sapienza
University of Rome and CIRA, International Center for Relativistic Astrophysics, Rome, Italy; costantino.sigismondi@gmail.com

Presented at the 100th Annual Meeting of the AAVSO, October 8, 2011

Abstract Approximately a hundred observations of δ Scorpii, from April to September 2011, made for the AAVSO visually and digitally with a commercial CMOS camera, have been plotted. The three most luminous pixels either of the target star and the two reference stars are used to evaluate the magnitude through differential photometry. The main sources of errors are outlined. The system of δ Sco, a spectroscopic double star, experienced a close periastron in July 2011 within the outer atmospheres of the two giant components. The whole luminosity of δ Sco increased from about Mv = 1.8 to 1.65, peaking around 5 to 15 July 2011, but there are significant rapid fluctuations of 0.2–0.3 magnitude occuring over 20 days that seem to be real, rather than a consequence of systematic errors due to the changes of reference stars and observing conditions. This method is promising for being applied to other bright variable stars like Betelgeuse and Antares.

Bright New Type-Ia Supernova in the Pinwheel Galaxy (M101): Physical Properties of SN 2011fe From Photometry and Spectroscopy *(Poster abstract)*

Sai Gouravajhala
Edward F. Guinan
Villanova University, Department of Astronomy, Villanova, PA 19085; address correspondence to E. F. Guinan; edward.guinan@villanova.edu

Louis Strolger
Andrew Gott
Western Kentucky University, Physics and Astronomy, TCCW231, 1906 College Heights Boulevard, #11077, Bowling Green, KY 42101; address correspondence to L. Strolger; louis.strolger@wku.edu

Presented at the 100th Annual Meeting of the AAVSO, October 8, 2011

Abstract We report on the preliminary multi-wavelength photometry and spectroscopy of SN 2011fe, a bright, new Type-Ia supernova (SN Ia) that

occurred in the spiral galaxy M101 (Pinwheel Galaxy). One of the closest and brightest SN Ia in the last forty years, the supernova was discovered on August 24, 2011, by the Palomar Transient Factory during the star's initial rapid rise (Nugent *et al.* 2011). SN Iae occur in binary systems in which a degenerate white dwarf component accretes mass from its companion star (or undergoes a merger with another white dwarf), overcomes the Chandrasekhar limit, and deflagrates in a spectacular explosion. The peak brightnesses of most SN Iae are remarkably similar. This allows SN Iae to be used as accurate cosmic distance indicators and thus they are crucial to understanding cosmology, dark energy, and inflation. SN 2011fe is being extensively observed over a wide range of wavelengths by both amateur and professional astronomers (including several AAVSO members). The UBVRI photometric observations discussed here are being carried out with the 1.3-meter Robotically Controlled Telescope (RCT) located at Kitt Peak National Observatory. The RCT data show a peak apparent magnitude of mV (max) ~ +10.0 mag, in agreement with other measures. Using the M 101 distance modulus of (mV – MV)0 = 29.04 (~21 million LY) as determined by Shappee and Stanek (2011), and assuming interstellar reddening of AV = 0.03 (from E(B-V) = 0.008) toward the objects in SN 2011fe's neighborhood, we estimate the absolute magnitude in the V band of SN 2011fe to be MV = –19.07 mag, which appears to be slightly under-luminous than the SN Iae average of <MV> = –19.30 (Hillebrandt and Niemeyer 2000). Visual and IR spectroscopic data gathered from Buil and Theirry (2011) show strong absorption features, especially those of Co II ~ 3995 Å, Si II ~ 6150 Å, Fe II/Mg II blends ~ 4500 Å, and the Ca II near-IR triplet ~ 8250 Å. Crucially, the spectrum shows no hydrogen and helium lines, which, coupled with the strong Si lines, means that SN 2011fe is a Type-Ia SN. Constraints on the progenitor system (for a single degenerate model) by Li *et al.* (2011) rule out bright red-giant mass donors, but do not rule out faint secondaries. SN 2011fe is important because of its relatively high brightness and early detection in a nearby, well-studied, face-on galaxy with a good distance determination and little ISM extinction. The prodigious amount of data that continues to be gathered will lead to exciting opportunities in the future that include further study of the spectral time series evolution, Δm15(B) relation, and Hubble Constant calibration. In this poster, we discuss the up-to-date physical and photometric properties of this SN and compare them to those of other Type-Ia supernovae.

This research is supported, in part, by NSF/RUI grant AST1009903 and NSF/RUI grant AST0507542. We also gratefully thank both the RCT Consortium and AAVSO members for the photometric data.

References

Buil, C., and Thierry, P. 2011, ARAS (http://astrosurf.com/aras/surveys/supernovae/sn2011fe/obs.html)

Hillebrandt, W., and Niemeyer, J. C. 2000, *Ann. Rev. Astron. Astrophys.*, **38**, 191.
Li, W. *et al.* 2011, arXiv:1109.1593v1. (http://arxiv.org/abs/1109.1593v1)
Nugent, P. *et al.* 2011, *Astron. Telegrams*, No. 3581, 1.
Shappee, B. J., and Stanek, K. Z. 2011, *Astrophys. J.*, **733**, 124.

The World's Strangest Supernova May Not Be a Supernova At All *(Abstract)*

Caroline Moore
29 Deer Pond Drive, Warwick, NY 10990;
caroline.moore@deer-pond-observatory.com

Presented at the 100th Annual Meeting of the AAVSO, October 7, 2011

Abstract SN 2008ha is the least luminous supernova ever to be observed. It is unclear what caused this obscurity to occur. For the last three years I have been doing independent follow-up research on SN 2008ha.

SN 2008ha is believed to be 100 times brighter than a nova, but 1,000 times dimmer then a supernova. The spectrum to some degree was classic Type Ia supernova because of the lack of hydrogen and abundance of silicon, but there are many other factors to be considered. SN 2008ha had a short rise time of only 10 days (typical Type Ia is 19.5 days). It has low expansion velocities of only 2,000km compared to the typical Ia with very small kinetic energy per unit mass of ejecta. Although some elements of the spectrum are consistent with those of a Type Ia, narrow lines were observed. This is just one of several characteristics that SN 2008ha shares with the "SN 2002cx-like class" of supernovae. SN 2008ha is believed to be the most extreme of this sub-class of supernovae with the smallest amount of space between lines, 5 days shorter rise time, being significantly fainter, and having lower velocities. With all these things considered, it does make classification as a Type Ia questionable. In fact it is even questionable if this is a supernova at all, and not just an "imposter." This may have just been a "star burp" which means that the supernova may have failed, resulting in some parts of the star being left, maybe even enough remains to explode again as seen in the case of SN 2006jc. This may have occurred because the explosion was not deep enough in the core of the star, and only eliminating some or all of the hydrogen envelope and leaving behind the carbon and oxygen inner layers, instead resulting in a Type Ic supernova. It would be interesting to see what, if anything is left of the star; this could make it a possible Hubble candidate. The idea that it may "burp" again makes it especially important.

An Amateur-Professional International Observing Campaign for the EPOXI Mission: New Insights Into Comets *(Abstract)*

Karen J. Meech
46-035 Konohiki Street, #3865, Kaneohe, HI 96744; meech@ifa.hawaii.edu

Presented at the 100th Annual Meeting of the AAVSO, October 7, 2011

Abstract Comets are leftovers from the early solar system and may have played a role in delivering water and organics to the prebiotic Earth. Because comets may preserve a record of the early solar system conditions, they are the focus of small body missions. The EPOXI (Extrasolar Planet Observation and Characterization (EPOCh) + Deep Impact Extended Investigation (DIXI) = EPOXI) flyby of the nucleus of comet 103P/Hartley 2 provided us with physical properties of the nucleus and clear evidence of chemical heterogeneity with CO_2-driven jets as a dominant volatile loss mechanism at perihelion compared to subsurface water-ice sublimation. An international Earth-based observation campaign played a complementary role to the in-situ data, providing recovery images of the comet at large distances, physical information about the nucleus size, and from a coordinated multiwavelength program nearly continuous coverage from August 2010 through encounter on 4 November 2010. From the Earth-based campaign it was clear that comet Hartley 2 had a small nucleus (0.57 km radius), with a rotation period near 16.4 hours prior to the onset of activity. As the activity developed the periodicity was found to change significantly over a period of months. The highly active nucleus had long- and short-term gas production variability with peak activity shortly after perihelion. The comet's activity has been photometrically monitored (as scattered light from the dust coma) from the time of recovery to the present, and the nearly continuous coverage of the comet from August 2010 into 2011 would not have been possible without the amateur contributions. Using these brightness data, we have developed an ice sublimation model to estimate the amount of dust emitted from the comet (and hence the total scattered light) as a function of heliocentric distance as it is driven by a gas flow. The model includes nucleus ices: H_2O, CO_2, CO, and H_2O sublimating from the large chunks seen both from the EPOXI spacecraft and the Arecibo radar observations (Harmon *et al.* 2011). The model indicates that like other comets, water-ice sublimation began to create an observable dust coma/tail near 4–4.4 AU as the comet approached the sun, but that near perihelion, strong CO_2 outgassing in the form of jets (as seen by the spacecraft) was responsible for lifting large ice/dust grains from the surface. CO_2 is likely a strong contributor to activity on the outbound leg of the orbit. The models show that the fractional active nucleus area is small for water production (typical of other comets) and that at perihelion most of the water production is likely from the ice grain halo. Sublimation from deeper CO_2 reservoirs is

likely an important driver of activity for this comet, including out to and beyond aphelion, and this may be a characteristic of unusually active comets—relating to differences in chemistry from either formation or subsequent evolution. This paper will present mission highlights, and emphasize the important role that the amateur observations has in understanding the behavior of this comet.

Light Curve of Minor Planet 1026 Ingrid *(Poster abstract)*

Shelby Delos
Gary Ahrendts
Timothy Barker
Wheaton College, 26 E. Main Street, Norton, MA 02766; address correspondence to T. Barker; tbarker@wheatoncollege.edu

Presented at the 100th Annual Meeting of the AAVSO, October 8, 2011

Abstract We have imaged minor planet 1026 Ingrid over the time period of July 29, 2011, to late September 2011, using the Wheaton College 0.25m telescope at Grove Creek Observatory in Australia via internet access. This telescope is equipped with a Santa Barbara Instrument Group STL-1001E CCD Camera, used with a clear filter. Over 1,000 30-second images were obtained and imported into the MPO Canopus software package for light curve analysis. Our preliminary estimate of the rotation period of 1026 Ingrid is 5.390 ± 0.001 hours, which is consistent with the previous estimate of 5.3 ± 0.3 hours (Székely, P., *et al.* 2005, *Planet. Space Sci.*, **53**, 925).

Membership of the Planetary Nebula Abell 8 in the Open Cluster Bica 6 and Implications for the PN Distance Scale *(Poster abstract)*

David G. Turner
Saint Mary's University, Department of Astronomy and Physics, 923 Robie Street, Halifax, NS B3H 3C3, Canada; turner@ap.smu.ca

Joanne M. Rosvick
Thompson Rivers University, Department of Physics, 900 McGill Road, Kamloops, BC V2C 5N3, Canada; jrosvick@tru.ca

D. D. Balam
Dominion Astrophysical Observatory, 5071 West Saanich Road, Victoria, BC V9E 2E7, Canada

Arne A. Henden
AAVSO Headquarters, 49 Bay State Road, Cambridge, MA 02138; arne@aavso.org

Daniel J. Majaess
David J. Lane
Saint Mary's University, Department of Astronomy and Physics, 923 Robie Street, Halifax, NS B3H 3C3, Canada; dmajaess@ns.sympatico.ca; dlane@ap.smu.ca

Presented at the 100th Spring Meeting of the AAVSO, May 23, 2011

Abstract The potential link between the newly discovered open cluster Bica 6 and the planetary nebula (PN) Abell 8 (PN G167.0-00.9) proposed by Bonatto *et al.* (2008) is confirmed on the basis of new UBVRI CCD photometry for the cluster and spectroscopic observations of its brightest stars, in conjunction with an analysis of 2MASS data for the cluster. The reddening, estimated distance, and radial velocity (+58 ± 6 km/s) of Abell 8 are a close match to the parameters derived for Bica 6: E(B–V)(B0) ≈ 0.40, d = 1.6 kpc, Vr = +57 ±4 km/s (11 stars). The radial velocity match is particularly interesting given that the velocities are more than 50 km/s larger than expected for Galactic orbital motion at l = 167°. The cluster age of 1 billion years implies a mass of –2.5–3 $M_{\odot}$ for the planetary nebula progenitor star, although the picture is complicated by a few blue stragglers as likely cluster members. The central star of the PN is an optical double in the 2MASS survey, with the companion indicated to be a cluster M dwarf. Abell 8 is a highly evolved PN containing a low luminosity central star (Mv ≈ +8), with a distance implied by cluster membership favoring the short PN distance scale.

What Mass Loss Modeling Tells Us About Planetary Nebulae *(Abstract)*

Lee Anne Willson
Qian Wang
Iowa State University, Department of Physics and Astronomy, Ames, IA 50011; lwillson@iastate.edu

Presented at the 100th Annual Meeting of the AAVSO, October 8, 2011

Abstract Planetary nebulae are the result of mass loss from an AGB star (specifically, a Mira variable or post-Mira infrared source) that is swept up by a later fast wind and/or ionized when the central star becomes hot. The central stars of planetary nebulae are the naked cores of the former AGB star. Not all AGB stars form PNe, however, and the ones that do may be mostly binary

star systems. Using both a large grid of detailed mass loss models and some simple analytical mass loss formulae we can relate observations of PNe and their nuclei to the character of the late AGB (Mira stage) mass loss.

Stars, Planets, and the Weather: If You Don't Like It Wait Five Billion Years *(Abstract)*

Jeremy J. Drake
Harvard-Smithsonian Center for Astrophysics, 60 Garden Street, Cambridge, MA 02138; Jdrake@cfa.harvard.edu

Presented at the 100th Spring Meeting of the AAVSO, May 23, 2011

Abstract Over the last decade realization has grown that high-energy phenomena such as X-ray and EUV radiation, winds, and coronal mass ejections exhibited by stars like our own Sun have an importance far beyond local "stellar weather." From the stormy magnetic extremes of stellar youth to the gentle breeze of stellar middle age and beyond, I describe how stellar weather is now central to problems as diverse as the evolution of supernova Type Ia progenitor candidates, planet formation, and the development and survival of life in planetary systems.

The Hunt for the Quark-Nova: a Call for Observers *(Abstract)*

David J. Lane
Saint Mary's University, Department of Astronomy and Physics, 923 Robie Street, Halifax, NS B3H 3C3, Canada; dlane@ap.smu.ca

R. Ouyed
D. Leahy
University of Calgary, 2500 University Drive NW, Calgary, AB T2N 1N4, Canada; rouyed@uclagary.ca

Douglas L. Welch
McMaster University, Department of Physics and Astronomy, Hamilton, ON L8S 4M1, Canada; address correspondence to welch@physics.mcmaster.ca

Presented at the 100th Spring Meeting of the AAVSO, May 21, 2011

Abstract A Quark Nova is the explosive transition from a neutron star to a quark star that is theorized to take place days or weeks after a small fraction of "normal" Type II supernova events. The Quark Nova signature is the delayed brightening of the new object by about five magnitudes. The proposed close

long-term monitoring of Type II supernova events should reveal the presence or absence of the signature double-hump of a Quark Nova and allow us to estimate the frequency or upper limit to the rate of such events. Normal supernova search techniques and follow-up activities may miss the subsequent brightening that takes place during the Quark Nova event. We seek CCD-equipped observers with modest-sized telescopes to join a collaborative effort to search for these events. Your job would begin after Type II supernovae are discovered by others. You, with a team of other observers, would follow all new Type II discoveries for about one to two months looking for the signature "double-bump." As there are not many known Type II supernovae active at any given time, the observational commitment is not expected to exceed about one hour per night. We have set up an on-line database to manage the process and record the observations and a communications forum to provide support to the observers and structure to the project (see http://quarknova.ucalgary.ca). The confirmation that these objects exist will be a significant event in supernova research.

Collaborative Research Efforts for Citizen Scientists *(Poster abstract)*

Brian K. Kloppenborg
2499 S. Colorado Boulevard, Apt. 803, Denver, CO 80222; brian.kloppenborg@du.edu

Aaron Price
3238 N. Clark Street, Apt. 2F, Chicago, IL 60657; address email correspondence to R. Turner at rebecca@aavso.org

Rebecca Turner
Arne A. Henden
AAVSO Headquarters, 49 Bay State Road, Cambridge, MA 02138

Robert E. Stencel
University of Denver, Department of Physics and Astronomy, 2112 E. Wesley Avenue, Denver, CO 80208; rstencel@du.edu

Presented at the 100th Spring Meeting of the AAVSO, May 23, 2011

Abstract The AAVSO's Citizen Sky project encourages participants not just to collect and categorize data, but to critically analyze and publish research findings. Our participants form teams of different yet complementary skills that work together towards a common goal. Each team has a leader and a professional astronomer assigned to act as an advisor. In this work we explore the formation of teams, by what means they find research topics, and how they

manage their collaborations. We acknowledge support from the NSF Informal Science Education Division under grant DRL-0840188 to the AAVSO and the University of Denver.

Exploring the Breadth and Sources of Variable Star Astronomers' Astronomy Knowledge: First Steps *(Abstract)*

Stephanie J. Slater
2265 Broadleaf Loop, Castle Rock, CO 81019; sslaterwyo@gmail.com

Presented at the 100th Annual Meeting of the AAVSO, October 8, 2011

Abstract There is considerable interest related to the astronomy content knowledge of various groups, whether that group consists of 3rd graders who have just learned the phases of the moon, or astronomy graduate students who are working on original research. Similarly, the Center for Astronomy and Physics Education Research (CAPER) Team and the American Association of Variable Star Observers (AAVSO) are interested in the general astronomy content knowledge of the AAVSO members. To increase our understanding of the knowledge base of today's variable star astronomers, we asked a subset of members to respond to an online general astronomy content knowledge survey called the Test Of Astronomy Standards (TOAST). The TOAST is a twenty-nine-item, multiple-choice format assessment instrument which addresses the full range of topics commonly taught in an introductory astronomy survey course, and is criterion referenced aligned to the consensus learning goals stated by the AAS Chair's Conference on ASTRO 101, the AAAS Project 2061 Benchmarks, and the NRC National Science Education Standards. This paper presents preliminary results on this work to the AAVSO membership in the hope that the findings will begin a conversation about the kinds of experiences and education that are transformative for this important group of astronomy researchers.

Rasch Analysis of Scientific Literacy in an Astronomical Citizen Science Project *(Poster abstract)*

Aaron Price
3238 N. Clark Street, Apt. 2F, Chicago, IL 60657; email correspondence should be addressed to rebecca@aavso.org

Presented at the 100th Spring Meeting of the AAVSO, May 23, 2011

Abstract We investigate change in attitudes towards science and belief in the nature of science by participants in a citizen science project about astronomy.

A pre-test was given to 1,385 participants and a post-test was given six months later to 165 participants. Nine participants were interviewed. Responses were analyzed using the Rasch Rating Scale Model to place Likert data on an interval scale allowing for more sensitive parametric analysis. Results show that overall attitudes did not change, $p = .225$. However, there was significant change towards attitudes relating to science news (positive) and scientific self efficacy (negative), $p = .001$ and $p = .035$, respectively. This change was related to social activity in the project. Beliefs in the nature of science exhibited a small but significant increase, $p = .04$. Relative positioning of scores on the belief items suggests the increase is mostly due to reinforcement of current beliefs.

The Citizen Sky Planetarium Trailer *(Poster abstract)*

Rebecca Turner
Aaron Price
AAVSO Headquarters, 49 Bay State Road, Cambridge, MA 02138; rebecca@aavso.org

Ryan Wyatt
American Museum of Natural History, California Academy of Sciences, 875 Howard Street, San Francisco, CA 94103; rwyatt@calacademy.org

Presented at the 100th Spring Meeting of the AAVSO, May 23, 2011

Abstract Citizen Sky is a multi-year, citizen science project focusing on the bright variable star ε Aurigae. We have developed a six-minute video presentation describing eclipsing binary stars, light curves, and the Citizen Sky project. Designed like a short movie trailer, the video can be shown at planetariums before their regular, feature shows or integrated into a longer presentation. The trailer is available in a wide range of formats for viewing on laptops all the way up to state-of-the-art planetariums. The show is narrated by Timothy Ferris and was produced by the Morrison Planetarium and Visualization Studio at the California Academy of Sciences. This project has been made possible by the National Science Foundation.

The World Science Festival *(Abstract)*

John Pazmino
979 East 42nd Street, Brooklyn, NY 11210; john.pazmino@ferc.gov

Presented at the 100th Spring Meeting of the AAVSO, May 22, 2011

Abstract New York City in the late 20th century rose to be a planetary capital

for the sciences, not just astronomy. This growth was mainly in the academic sector but a parallel growth occurred in the public and home field. With the millennium crossing, scientists in New York agitated for a celebration of the City as a place for a thriving science culture. In 2008 they began World Science Festival. 2011 is the fourth running, on June 1–5, following the AAVSO/AAS meetings. World Science Festival was founded by Dr. Brian Greene, Columbia University, and is operated through the World Science Foundation. The Festival is "saturation science" all over Manhattan in a series of lectures, shows, exhibits, performances. It is staged in "science" venues like colleges and musea, but also in off-science spaces like theaters and galleries. It is a blend from hard science, with lectures like those by us astronomers, to science-themed works of art, dance, music. Events are fitted for the public, either for free or a modest fee. While almost all events are on Manhattan, effort has been made to geographically disperse them, even to the outer boroughs. The grand finale of World Science Festival is a street fair in Washington Square. Science centers in booths, tents, and pavilions highlight their work. In past years this fair drew 100,000 to 150,000 visitors. The entire Festival attracts about a quarter-million attendees. NYSkies is a proud participant at the Washington Square fair. It interprets the "Earth to the Universe" display, debuting during IYA-2009. Attendance at "Earth..." on just the day of the fair plausibly is half of all visitors in America. The presentation shows the scale and scope of World Science Festival, its relation to the City, and how our astronomers work with it.

New Life for Old Data: Digitization of Data Published in the *Harvard Annals (Abstract)*

Matthew R. Templeton
Michael Saladyga
AAVSO Headquarters, 49 Bay State Road, Cambridge, MA 02138; matthewt@aavso.org

Kevin B. Paxson
20219 Eden Pines, Spring, TX 77379; kbpaxson@aol.com

Robert J. Stine
C. Fröschlin
Andrew Rupp
address correspondence to R. J. Stine, 297 Eagle Ridge Street, Newbury Park, CA 91320; bobstine@verizon.net

Presented at the 100th Spring Meeting of the AAVSO, May 22, 2011

Abstract We describe the volunteer-driven project to digitize published

visual observations found in the *Annals of the Harvard College Observatory*, the publication of record for Harvard's variable star data archives prior to the founding of the AAVSO. The addition of published data from the 19th and early 20th centuries to the AAVSO International Database has the potential to enable significant new science by extending long term light curves farther back in time with high-quality visual and photographic data. AAVSO volunteers working on this project have together digitized over well over 10,000 observations from the *Harvard Annals*, adding decades to the light curves of some stars. We highlight the work done so far, and show the potential to expand the project by both AAVSO Headquarters and by the volunteers themselves.

Data Release 3 of the AAVSO All-Sky Photometric Survey (APASS) *(Poster abstract)*

Arne A. Henden
AAVSO Headquarters, 49 Bay State Road, Cambridge, MA 02138; arne@aavso.org

Stephen E. Levine
Lowell Observatory, 1400 West Mars Hill Road, Flagstaff, AZ 86001; sel@lowell.edu

Dirk Terrell
Southwest Research Institute, Space Studies, 1050 Walnut Street, #426, Boulder, CO 80301; terrell@boulder.swri.edu

T. C. Smith
Dark Ridge Observatory, 701 NM Highway 24, Weed, NM 88354; tcsmith@darkridgeobservatory.org

Douglas L. Welch
McMaster University, Department of Physics and Astronomy, Hamilton, ON L8S 4M1, Canada; welch@physics.mcmaster.ca

Presented at the 100th Spring Meeting of the AAVSO, May 23, 2011

Abstract APASS is an all-sky survey in five filters (B,V,g',r',i') covering the magnitude range 10–17. It is currently underway at two sites: Dark Ridge Observatory in New Mexico, and CTIO in Chile. The survey will take approximately two years to complete, and will provide a precision of 0.02 magnitude for well-sampled stars. This paper presents the current status of the project and provides the access methods to the catalog.

Data Evolution in VSX: Making a Good Thing Better *(Abstract)*

Sebastian Otero
Olazabal 3650-8 C, Buenos Aires 1430, Argentina; varsao@hotmail.com

Presented at the 100th Annual Meeting of the AAVSO, October 8, 2011

Abstract A review of the current status of the AAVSO International Variable Star Index (VSX) is presented. Starting with an heterogeneous set of catalogs automatically imported, the data included in VSX have been constantly evolving and the role of observers contributing their new discoveries or revising known variable stars is growing more important each day. Examples are given of the improvements made in several aspects of star data such as identification, classification, elimination of duplicate entries, and updates.

VSX: the Next Generation *(Abstract)*

Christopher L. Watson
12222 Mannix Road, San Diego, CA 92129; skygeex@gmail.com

Presented at the 100th Annual Meeting of the AAVSO, October 8, 2011

Abstract The AAVSO International Variable Star Index (VSX), the most comprehensive and up-to-date assemblage of publicly-maintained variable star data on the planet, will be undergoing a major overhaul in the coming year to greatly improve the database design, as well as the Web-based user interface. Five years after its official launch, VSX has evolved into an essential component of the AAVSO enterprise information architecture, tightly integrated with many of the technical organization's other mission-critical processes. However, its unique configuration and functionality are largely based on decades-old data formats and outmoded Web methodologies which will generally not scale well under the anticipated deluge of data from large-scale synoptic surveys. Here, we present the justifications and vision for VSX 2.0, the next generation of this indispensable research tool, including overviews of the creation of a brand new, fully-normalized, database schema, and the ground-up redesign of the front-end Web interface.

AAVSOnet: the Robotic Telescope Network *(Poster abstract)*

Mike Simonsen
AAVSO Headquarters, 49 Bay State Road, Cambridge, MA 02138; mikesimonsen@aavso.org

Presented at the 100th Spring Meeting of the AAVSO, May 23, 2011

Abstract AAVSOnet is the growing network of robotic telescopes owned and operated by the American Association of Variable Star Observers. With telescopes ranging from 60-mm to 0.61-m in aperture located around the globe, the network fulfills a multitude of science goals. The largest telescopes will be fitted with instruments capable of doing both spectroscopy and photometry. We have pairs of 20-cm telescopes in Chile and New Mexico conducting an all-sky photometric survey (APASS) from 10th to 17th magnitude. These pairs of telescopes monitor the sky in two filters simultaneously in Johnson B and V, as well as Sloan g, r, i, and z. There are telescopes in the 25–35-cm range available to conduct automated programs of stars selected by AAVSO members, and five small telescopes monitoring poorly studied stars brighter than 10th magnitude in both the southern and northern hemispheres. All the data for every star on every image are archived at AAVSO headquarters for future data-mining; images are uploaded to member accounts where they can be analyzed by a powerful suite of photometric tools and observations submitted to the AAVSO International Database.

Hα Emission Extraction Using Narrowband Photometric Filters *(Abstract)*

Gary Walker
Maria Mitchell Association Observatory, 4 Vestal Street, Nantucket, MA 02554; bailyhill14@gmail.com

Presented at the 100th Spring Meeting of the AAVSO, May 21, 2011

Abstract Maria Mitchell Observatory (MMO) has explored using Narrowband Photometric (<100Å) filters to substitute for spectroscopic observations. The method is thought to have significant signal-to-noise advantages over spectroscopic observations for small telescopes. These small telescopes offer advantages for projects requiring intensive monitoring where telescope time is limited on larger telescopes. RR Tau, a suspected UXOR, was intensively observed by the MMO 0.6-m Ritchey-Chrétien telescope in Nantucket, Massachusetts, and the 0.29-m W28 AAVSOnet telescope from Cloudcroft, New Mexico, during the 2010 Winter and Spring seasons. Observations were

made in Hα with 45Å and 100Å narrowband filters as well as the continuum at 6450Å with 50Å and 100Å filters. Hα emission was extracted with an error of 8% and compared to the change in the continuum. RR Tau exhibited a 30% change in emission while the continuum changed by over a factor of 5.

Automation of Eastern Kentucky University Observatory and Preliminary Data *(Poster abstract)*

Marco Ciocca
Ethan E. Kilgore
Westley W. Williams
Department of Physics and Astronomy, Eastern Kentucky University, 521 Lancaster Avenue, Moore 351, Richmond, KY 40475; address email correspondence to M. Ciocca at Marco.Ciocca@EKU.EDU

Presented at the 100th Annual Meeting of the AAVSO, October 8, 2011

Abstract Eastern Kentucky University is a regional comprehensive institution located in Richmond, Kentucky. Its service area includes much of the eastern part of Kentucky, commonly referred to as Appalachia. As such, Eastern has truly been a "school of opportunities" for the region. We offer three astronomy courses and one of them, AST 135, has an outdoor lab component, in which the students observe the moon and the brightest planets using 6-inch SCT. To expand our offerings by adding advanced classes in observational astronomy, and with support from the University and a small grant from the AAS (Small Research Grants), we constructed a small observatory for that purpose.

We have a 14-inch telescope (C14 from Celestron), with a research grade mount (Paramount ME), housed permanently in a two-room facility. The telescope room has a retractable roof and the control room is insulated against the elements. The telescope is conveniently located near campus, in a location away from city lights and vehicular traffic, with access via a secure gate. The observatory is on a concrete pad poured directly onto the ground, to minimize vibrations. The instrument package consists of a SBIG STL-6303E CCD camera with filter wheel and full complement of photographic, narrow-band, and photometric filters (Hα and UBVRI). Courtesy of the AAS grant, we also have a temperature-compensated focuser (TCF-S3i), off-axis guider, and SBIG AO-L adaptive optics accessory.

Our first step has been the measurement of our CCD transformation parameters, to assess the capabilities of our telescope-camera combination. We imaged a standard photometric field from Landolt (1992) (R.A. $09^h\ 21^m\ 32^s$, Dec. +02° 47' 00" (J2000, Plate 38 of Landolt). Data were obtained with a time integration of 90 seconds, binned 2 × 2 (~1 arcsec/pixel) at air mass X = 1.31. We determined the CCD transformation parameter as described by the AAVSO

document "Computing and Using CCD transformation coefficients" (Cohen 2003). We obtained the following:

$$T_{bv} = 1.329;\ T_{vr} = 1.000;\ T_{ri} = 0.912;\ T_{v} = -0.065;\ T_{r} = -0.042$$

We estimate a 5% uncertainty in our measurements. This past summer, with student support, we were able to perform our first measurements of light curves, particularly of the AAVSO Short Period Pulsator Program—suggested δ Scuti star DY Her and the RR Lyrae stars UU Boo and XX Cyg. Our light curves (we have two complete BVRI sets for DY her) were not corrected using our transformation parameters, but just compared with the reference stars provided by AAVSO. We will present the data obtained and our current efforts in automation of the observatory operations. We have the necessary hardware to monitor the environment via video and remotely operate the roof and the telescope.

References

Landolt, A. J. 1992, *Astron. J.*, **104**, 340.

Cohen, L. 2003, "Computing and using CCD Transformation Coefficients," AAVSO internal document (http://mira.aavso.org/sites/default/files/ccdcoeff.pdf).

Status of the USNO Infrared Astrometry Program *(Poster abstract)*

Frederick John Vrba
Jeffrey A. Munn
Christian B. Luginbuhl
T. M. Tilleman
U.S. Naval Observatory, Flagstaff Station, 10391 West Naval Observatory Road, Flagstaff, AZ 86001; address correspondence to J. Vrba at ffv@nofs.navy.mail

Arne A. Henden
AAVSO Headquarters, 49 Bay State Road, Cambridge, MA 02138; arne@aavso.org

Harry H. Guetter
U.S. Naval Observatory, Flagstaff Station, 10391 West Naval Observatory Road, Flagstaff, AZ 86001; guetter@commspeed.net

Presented at the 100th Spring Meeting of the AAVSO, May 23, 2011

Abstract The USNO Infrared astrometry program has been in a suspended state since a June 2006 cryogenic accident with our imaging camera. We describe the current status of bringing the program back to full operation. We expect to re-start an expanded astrometric program in the near future and present our initial list of targets. This will also provide an opportunity for the community to suggest potential cool, low-mass targets which are in need of high quality parallaxes and proper motions. We earlier published preliminary astrometric results for 40 L and T dwarf fields based on the first two years of observations (Vrba *et al.*, Astron. J., 127, 2948 (2004)). Those initial objects plus an additional nineteen fields added later comprise a total of one M dwarf, twenty-eight L dwarfs, and thirty-nine T dwarfs, including objects in binary systems. Final parallaxes and proper motions for these objects will be published later this year. The additional approximately four years of observations for the original forty objects improve the mean parallax errors orginially reported from 4.31 mas to 1.73 mas, with the best at 0.64 mas, and the mean proper motion errors from 6.56 mas/yr to 1.09 mas/yr.

Variable Star Observing With the Bradford Robotic Telescope *(Abstract)*

Richard C. S. Kinne
AAVSO Headquarters, 49 Bay State Road, Cambridge, MA 02138; rkinne@aavso.org

Presented at the 100th Spring Meeting of the AAVSO, May 22, 2011

Abstract The Bradford Robotic Telescope (BRT) is a collection of telescopes and other instruments located on Mount Teide, Tenerife, Canary Islands; this resource is available to all for use at no cost (http://www.telescope.org/info/BRT_information). With the recent addition of Johnson *BVRI* filters on the BRT's 24 square arc minute camera, this telescope has become a resource to be considered when monitoring certain stars such as LPVs. This presentation will examine the mechanics of observing with the BRT and show examples of work that has been done by the author and how those data have been reduced using VPhot.

Solar Cycle 24—Will It Be Unusually Quiet? *(Abstract)*

Rodney Howe
3343 Riva Ridge Drive, Fort Collins, CO 80526; ahowe@frii.com

Presented at the 100th Annual Meeting of the AAVSO, October 8, 2011

Abstract For the last forty years or so all the AAVSO (American Association of Variable Star Observers) Very Low Frequency (VLF) Sudden Ionospheric Disturbance (SID) data have been sent to NGDC (National Geophysical Data Center). In this paper these data are put into a database and graphed in hopes of understanding these VLF SID submissions. The graphics show the NGDC accumulated Importance Rating (an index of the duration of solar flares) for all the AAVSO VLF SID submissions over the past forty years. And, if we compare these VLF SID data with the last three solar cycles of sunspot number counts compiled by the Solen group (Jan Alvestad: http://www.solen.info/solar/cyclcomp.html), it seems that the AAVSO VLF SID submissions to NGDC show our accumulated Importance Rating signals lag by 18 to 24 months after the start of each of the last three solar cycles! That puts our VLF radio's SID IR index measure at a point where it takes at least 100 sunspot counts per month before the VLF SID accumulated IR index even shows a signal through the noise floor of our ionosphere. The VLF observer's importance rating index is just monitoring the tip of these solar cycles with our VLF radios when compared to the sunspot number count indexes. And if the Solen sunspot predictions are right for Cycle 24, the solar sunspot peak won't even reach the 70 mark for this next cycle. So, our VLF SID IR index signal submissions may not even be detectable in Cycle 24!

A Generalized Linear Mixed Model for Enumerated Sunspots *(Abstract)*

Jamie Riggs
Department of Applied Science and Research Methods, McKee 518, Campus Box 124, University of Northern Colorado, Greeley, CO 80639; Jamie.Riggs@unco.edu

Presented at the 100th Annual Meeting of the AAVSO, October 8, 2011

Abstract Monthly sunspot counts data from consistently submitting AAVSO observers were provided to determine monthly average sunspot numbers and the individual observer parameters that correct each observer's counts to the monthly average. The data span a fourteen-month period from May 2010 through June 2011. The parameters are determined from a mixed-effects, loglinear model constructed specifically from the fourteen months of Poisson-distributed sunspot numbers. This model differs in the treatment of the data distribution assumptions of the existing linear regression model developed by Shapley (1949). The loglinear model methodology exceeds the correction coefficient performance criteria set by Shapley, and provides a method for determining the relative sunspot number reported monthly by the American Association of Variable Star Observers Solar Section. Model improvements are discussed.

AAVSO 100th Annual Meeting After-Banquet Remarks

Centennial Highlights in Astronomy

Owen Gingerich
Harvard-Smithsonian Center for Astrophysics, 60 Garden Street, Cambridge, MA 02138; ginger@cfa.harvard.edu

After-banquet remarks presented at the 100th Annual Meeting of the AAVSO, October 8, 2011

For many years Harlow Shapley, director of the Harvard College Observatory, eminent observer of variable stars, and patron of the AAVSO, delivered an annual after-dinner talk at the AAVSO meetings where he summarized the highlights in astronomy in the past year. In 1961, at the AAVSO's 50th anniversary, he expanded his talk, giving nineteen highlights from the previous half century, beginning with the founding of the AAVSO itself.

In following in Dr. Shapley's footsteps (and "Doctor Shapley" was how we always referred to him), I decided to divide the century into its ten decades and to select a single highlight from each ten-year interval. Please note that in many cases the highlight is an important theme for the decade, even though the actual initial discovery may have been made earlier; this is particularly true for the discovery of dark matter, placed in the 1980s decade. In the event, choosing a single highlight proved in many cases rather more difficult than it might appear at first glance. Let me demonstrate with the problems of choosing a single highlight from the years 1911 to 1920.

The teens were the decade of Einstein's general relativity and the critical eclipse test of 1919, but also Shapley's own pioneering work on the structure of the Milky Way and the sun's place within our galaxy. Curiously, Shapley didn't mention his own Milky Way work in his 1961 list, nor did he mention Hubble's work on galaxy distances in the next decade. But, anonymously, he cited the pulsation theory of variable stars in connection with Henrietta Leavitt's period-luminosity relation. Now, around this time, in 1959 or '60, he showed me the preliminary list of selections he was proposing for his *Source Book in Astronomy, 1900–1950*. I noticed that he included his 1914 paper on δ Cephei, where he showed that if this famous variable star were an eclipsing binary star, as many astronomers thought at the time, then the secondary star had to revolve inside the primary! In other words, δ Cephei had instead to be an intrinsic variable, probably explained by physical pulsations. Nevertheless, I thought it was a little idiosyncratic to choose this paper for inclusion, and I told him so.

Recently I stumbled on his letter in reply. "Young man, you weren't there in 1915!" is essentially what he said. In effect, his paper provided the credentials for Henrietta Leavitt's period-luminosity relation to be used as a distance indicator, for if Cepheids were simply eclipsing binaries, Miss Leavitt's relation was simply accidental.

That's the first half of this story. The second half is that Shapley's English contemporary Arthur S. Eddington also made a list of highlights, but much earlier, in 1920 for the centennial of the Royal Astronomical Society. The only highlight he included from the 1911–1920 decade was the measurement of the diameter of Betelgeuse, made by Michelson and Pease with an interferometer attached to the Mt. Wilson 100-inch Hooker reflector. Why was this so significant? Because it credentialed the implications of the to-become-famous diagram drawn by Henry Norris Russell and independently by Einar Hertzsprung.

In fact, the sorting of stars made possible by the H-R diagram held the key for using highly luminous stars, such as supergiants and Cepheids, as distance indicators. The understanding it provided concerning the diverse luminosities of stars laid the foundation for Shapley's work on the structure of our galaxy, and for Hubble's work in the following decade on the distances of galaxies. Ultimately the diagram would enable astronomers to get a grip on the life history of stars themselves, and the clusters in which they live.

Therefore, my choice for **highlight number one, for the 1911–1920 decade, is establishing the H-R diagram**.

As the decade waned, in April of 1920, there was a famous debate between Harlow Shapley, then from Mt. Wilson Observatory, and Heber D. Curtis, from Lick Observatory, on the scale of the universe. Everyone knows what Shapley got wrong. At the time he didn't believe that the spirals were extragalactic nebulae. But few people realize what Curtis got wrong. He apparently didn't believe in the period-luminosity relation of the Cepheids, nor appreciate the significance of dwarf and giant stars!

For 1921–1930: In 1921, by finding Cepheid variables in the Andromeda nebula, Edwin Hubble demonstrated its great distance and opened up the universe of galaxies. Before the decade was out Georges Lemaître found the distance-red shift correlation, later established more firmly by Hubble. **Highlight number two is Hubble's opening the realm of the galaxies and the explosive flight as the universe expands.**

For 1931–1940: Although Cecilia Payne got some hint of the high hydrogen abundance in her 1925 thesis, her method was novel, unsubstantiated, and in any event it referred only to the atmospheres of the stars. Additional evidence marshaled by Russell helped credential the early hint, and in the next decade stellar interior calculations by Bengt Strömgren and Eddington showed that stars could be primarily hydrogen all the way through. Before the decade was out, C. F. Von Weizsäcker and Hans Bethe showed that a nuclear carbon cycle could power stars. **The hydrogen composition of the stars and the nuclear fusion that powers them is highlight number three.**

For 1941–1950: Taking advantage of the dark skies provided by the wartime blackout of Los Angeles, Walter Baade probed the starry composition of the Andromeda galaxy and developed his idea of **stellar populations**. Not until the following decade did he identify the populations with the ages of stars,

nor did he yet use the concept to double the accepted age of the universe.

For 1951–1960: The flowering of radio astronomy, and the discovery of the 21-cm line of hydrogen, led to the **delineation of the spiral structure of the Milky Way.**

For 1961–1970: New windows on the universe, epitomized by the discovery of quasars, pulsars, and X-ray sources, but above all for purposes of cosmology and the origin of the universe, the **discovery of the 3° background radiation.**

For 1971–1980: Recognition that our universe has an evolving history, brought about by studies of nucleosynthesis and by the cosmological distances of quasars.

For 1981–1990: The widespread appreciation that rather than hydrogen, mysterious **"dark matter" provided the overwhelming mass in the universe.** This had been suggested much earlier by Fritz Zwicky and in the 1970s advocated by Jan Oort, by Jerry Ostriker, James Peebles, and Amos Yahil, and observationally established by Vera Rubin and Kent Ford.

For 1991–2000: The Hubble Space Telescope decade, settling the much-debated age of the universe, but also **the discovery of the accelerating universe or dark energy.** A runner-up: the COBE mission and the Big Bang anisotropy, the "seeds" of galaxies.

And finally, for 2001–2011: The discovery of large numbers of exoplanets, and recognition of the long-term migration of planets. Another runner-up: WMAP, whose accurate measurements of the cosmic microwave background fluctuations not only demonstrated the cosmological flatness of our universe, but also showed within a few percent that non-baryonic "dark matter" is five times more abundant than the baryonic matter that makes up you, me, and the visible universe.

And now, through the looking glass: **A few predictions for 2012–2061!**

First, I predict the success of attempts to detect the gravitational waves, the ripples in space propagated from appropriate massive movements of material in the universe (sought by LIGO, the Laser Interferometer Gravitational-Wave Observatory and its successors). Second, the detection of non-equilibrium chemistry in the atmospheres of selected exoplanets (and I predict that the interpretation of the existence of life on distant planets will be highly controversial). I would also look forward to the clarification of two of the deepest mysteries now facing astrophysicists: the so-called dark energy and dark matter.

From the vantage point of 2011, with the world economy in confusion, it is difficult to predict the future of the giant James Webb space telescope. Let us hope it will be successfully launched, and that it will reap surprising, unpredicted new phenomena. Dare one predict unpredicted phenomena will be found? Such I predict! And I predict that the AAVSO, venerable by 2061, will still be collecting data, but in new and more efficient ways.

Invited review papers

Introduction: Variable Star Astronomy in the 21st Century

John R. Percy, Editor, *JAAVSO*
Department of Astronomy and Astrophysics, University of Toronto, Toronto ON M5S 3H4, Canada

The AAVSO has just celebrated an exciting and important milestone in its history—its centenary. At the age of 100, it is in excellent health (unlike most people), with a new(ish) home, an able and dedicated staff and council, a worldwide network of volunteer observers and friends, respect and support from professional astronomers, impressive technology, and a continuing mandate to engage in and facilitate research in variable star astronomy.

It therefore seems appropriate to review variable star astronomy in 2011–2012. Several years have gone by since my book (Percy 2007) attempted to review the field and, as in most areas of astronomy, much has happened in a short period of time. We therefore commissioned a set of short reviews of variable star types which are of special interest to AAVSOers by professional-astronomer friends of the AAVSO with special expertise on these topics. We thank them for taking the time, in their busy schedules, to provide these reviews.

We begin, appropriately, with a review of young stellar objects (YSOs) by Bill Herbst, Van Vleck Professor of Astronomy, Wesleyan University. Bill has been a leader in this field for many years, especially through international long-term photometric monitoring campaigns, and through mentoring undergraduate research students. Bill is the science advisor to the AAVSO's recently-formed YSO Section. He's also an award-winning teacher, active in public outreach, and a skilled tennis player!

Bryce Croll, NASA Sagan Fellow at the Massachusetts Institute of Technology (MIT), reviews exoplanet transits, one of the hottest fields in which amateurs can contribute. Exoplanets are planets around other stars. If they transit their star and dim its light, that variability can provide evidence for the exoplanet, and much information about its properties. Bryce recently completed a Ph.D. in the exoplanet group at the University of Toronto, studying the atmospheres and other properties of exoplanets. He also had several variable star publications, as an undergraduate, based on photometry with *MOST* (Microvariability and Oscillations of STars), Canada's "humble space telescope." At Toronto, he was a driving force behind our public outreach programs. And he's a triathlete.

Ed Guinan, Professor of Astronomy and Astrophysics, Villanova University, reviews eclipsing binaries. These provide fundamental and unique information about the properties and evolution of stars. Ed is an international leader in the study of stars and binaries, especially through the Variable Star Division of the International Astronomical Union (IAU). He is also a leader in international astronomy education and development; he chairs the IAU's Program Group on "Teaching for Astronomical Development," and works for astronomical

education and development in many countries around the world. His research interests include pulsating stars, binaries, black holes, sun-like stars, robotic telescopes, and exoplanets. He has served on the AAVSO Council since 2008.

RR Lyrae stars, which provide essential information about the properties of the oldest stars in galaxies, are reviewed by Katrien Kolenberg, Harvard-Smithsonian Center for Astrophysics, on leave from the University of Leuven, Belgium. I first met Katrien in Leuven when she was a graduate student, at an IAU Colloquium on pulsating stars. There, she stood out as a result of both her scientific and her artistic talents. Much of her research focuses on one of the oldest and most puzzling mysteries in variable star astronomy—the nature and cause of the *Blazhko effect*. She is currently at CFA on a Marie Curie Scholarship, using *Kepler* data to study RR Lyrae stars in ways not previously possible.

Doug Welch, Professor at McMaster University, Hamilton, Ontario, reviews Population II Cepheids. Doug began his interest in astronomy as a keen amateur in Ottawa, survived two summers as my undergraduate research assistant, doing photometry of variable stars, and went on to a very successful career as a researcher, professor, administrator, and promoter of astronomy outreach. He served on AAVSO Council in 1995–1999 and 2007–2008, and has assisted the Association in many other ways, including establishing the on-line discussion group. His research interests are in pulsating stars and, more recently, light echoes from supernovae and other transients.

Cepheids are reviewed by Dave Turner, Saint Mary's University, Halifax, Nova Scotia. Dave's research encompasses star clusters, especially those which contain Cepheids. He also carries out long-term studies of period changes in Cepheids, which provide important and unique information about Cepheid evolution. He is also a long-time supporter of pro-am collaboration, both through the Royal Astronomical Society of Canada (RASC) (he served for many years as Editor of *JRASC*), through the AAVSO, in which he is currently a Councillor, and through his collaboration with amateurs in the Halifax area.

Lee Anne Willson, University Professor, Iowa State University, reviews Miras. Lee Anne and the AAVSO are a perfect fit: she is an expert in constructing and interpreting theoretical models of Mira pulsation, which AAVSO observers have studied productively for over a century. She has been deeply involved in the AAVSO, as a Councillor for many years, and as President in 1999–2001. She has been publishing in *JAAVSO* for over thirty years. As Vice-President of the American Astronomical Society, she recently facilitated the May 2011 joint AAVSO-AAS meeting, part of the AAVSO centenary. Her extra-curricular interests include being the Founding President of the Creative Artists' Studio of Ames, Iowa.

Non-Mira pulsating red giants are reviewed by Laszlo Kiss and me. Laszlo graduated from the University of Szeged, Hungary, and spent several years at the University of Sydney, Australia, before returning to the Konkoly Observatory in Hungary. He already has 380 publications in the ADS data system, partly

because, in addition to his very productive professional career, he has been a very active participant and supporter of amateur astronomy, especially in Hungary. He is a member and good friend of the AAVSO. Professionally, he has a special interest in large-scale surveys of variable stars and, more recently, exoplanets (and exomoons), but he has made contributions to the understanding of many other types of variables as well.

Geoff Clayton, Ball Family Distinguished Professor of Physics at Louisiana State University, reviews R CrB stars, a field in which he has been a world leader for many years. He has written several comprehensive reviews of R CrB stars in the past, and we are honored that he has contributed his latest one to *JAAVSO*. He has served as an AAVSO Councillor and, like several of our reviewers, is a member of the Editorial Board of *JAAVSO*. For several years, he supervised summer undergraduate research students at the Maria Mitchell Observatory. His website is "The Centre for Fun Astrophysics; the home of 'Team Clayton'", expressing his enthusiasm for studying R CrB stars and interstellar matter.

The review of cataclysmic variables is contributed by Paula Szkody, Professor, University of Washington, and her colleague Boris Gaensicke. CVs have been a topic of great interest to AAVSO observers, especially since the dawn of the space age and high-energy astrophysics in the 1970s. Paula has been a user of AAVSO data for almost thirty years, a mentor to the Association and its observers and, more recently, a Councillor (2003–2009) and President (2007–2009). She has also served recently as Editor of *Publications of the Astronomical Society of the Pacific* (*PASP*). Boris Gaensicke is a professor in the Department of Physics, University of Warwick, UK, where he is engaged in a wide variety of projects on binaries containing white dwarf stars. He co-edits a *Newsletter on Interacting Binaries*.

Ulisse Munari, National Institute of Astrophysics INAF, Observatorio Astronomico di Padova, Italy, reviews the symbiotic stars, and also novae; we thank him especially for providing both these reviews. Symbiotic stars are among the most complex of all variables, since they vary on a wide range of time scales, for a wide range of reasons. And novae are the spectacular result of runaway thermonuclear reactions. Ulisse was the AAVSO's second Janet A. Mattei Research Fellow; he worked with Arne Henden to improve observer quality, to provide spectra of new transient objects to decipher their classification, and to provide calibrated photometric sequences for many variables. He will be returning to AAVSO Headquarters in fall 2012 to collaborate on the APASS photometric survey. He has over 500 publications listed on ADS!

Peter Garnavich, Professor of Astrophysics and Cosmology, Notre Dame University, reviews supernovae. Peter is a distinguished scientist. He shared the Gruber Prize in Cosmology in 2007, and was an integral part of the research that won the Nobel Prize in Physics in 2011 (and was invited to attend the Nobel Prize ceremony in Stockholm). Peter is keenly involved in communicating with the public and the media about the excitement of astronomy. He is also a great

friend of the AAVSO, and served as Councillor from 1996 to 2000. His first publication was an *Information Bulletin on Variable Stars* (*IBVS*) with Janet Mattei and Lee Anne Willson, and his second publication was a sole-author paper in *JAAVSO*!

Other types of variable stars

There are other types of variable stars which are not included in the reviews. generally because they are less suitable for study by amateurs. Most of these types have small amplitudes, and are most often found as variable comparison stars for visual, PEP, or CCD photometry. They are "fair game" for skilled amateurs who can achieve millimag precision. Since many of them have periods of hours to days, joining a multi-longitude network of observers is often a good strategy. Here are short notes on some of those variable star types. Another useful resource is the 2012 triennial report of the IAU Commission on Variable Stars (Handler 2012). Other excellent resources are the AAVSO "Variable Star of the Season" articles (www.aavso.org/vsots_archive), especially the more recent ones, and the "For Observers" page (www.aavso.org/observers#sections) which contains links to the observing sections, including data mining, solar, and high energy network, which are not discussed explicitly in these short science reviews.

δ *Scuti stars and* γ *Doradus stars* These are A5-F2 stars, near the main sequence, which pulsate in a complex mixture of modes, with periods of a few hours to a few days. They are analogues of the Cepheids, in that they are driven by the same helium opacity mechanism. Most δ Scuti stars have very small amplitudes, but there are a few HADS—high-amplitude δ Scuti stars—which are amenable to visual observation. The most active work on δ Scuti stars continues to be: (1) detecting and studying them, especially with high-precision photometry from space; (2) interpreting the complex spectrum of periods with models, a process called *asteroseismology*. δ Scuti stars are radial pulsators, though many have non-radial modes as well; γ Doradus stars are pure non-radial pulsators. Both, through asteroseismology, provide important information about the interiors and evolution of these stars.

Pulsating B stars These include β Cephei stars, which have been known for a century, and Slowly Pulsating B (SPB) stars, which are a more recent discovery. Their pulsation is driven by a similar opacity mechanism as the Cepheids, but involving iron-group elements, rather than helium, deep within the star. There are many dozens of these among the naked-eye stars. These are complex, multi-mode pulsators. The β Cephei stars are primarily radial p-mode pulsators, with periods of a few hours; the SPB stars are primarily g-mode pulsators, with periods of hours to a day or two. However, there are stars which show both types of modes. The most important recent development has been the availability of ultra-precise photometry from space missions, *MOST,*

CoRoT, and *Kepler*. But De Cat *et al.* (2011), in a recent review, end by saying that "there is still a clear need for ground-based follow-up observations." Another research frontier is the search for and study of magnetic fields in OB stars, which may explain some poorly-understood aspects of their behavior.

γ *Cas (Be) stars* These are non-supergiant B stars which have shown emission lines in their spectra on at least one occasion. They vary, photometrically and spectroscopically, on time scales from hours to years. They may brighten and fade unpredictably and, since there are about 200 among the naked-eye stars, they are well-suited for PEP and CCD monitoring. The emission lines and some of the photometric variability are due to an equatorial disc slowly moving away from the star. Now that spectroscopy of brighter stars is within the reach of suitably-equipped amateurs, Be stars can be monitored by amateurs using that technique as well. One of the most exciting new developments in Be star research is the ability, using optical interferometry, to image the discs of these stars.

A good place to learn about current research on Be stars is in the *Be Star Newsletter*, maintained by David McDavid at the University of Virginia: (http://www.astro.virginia.edu/$\sim$dam3ma/benews/ (click on "abstracts")).

Rotating variable stars and stellar activity Rotating variables are stars with non-uniform surfaces; their period of variability is their rotation period. Most have visual amplitudes less than 0.1 magnitude. They are of two types: (1) stars like the sun, or cooler, with starspots; and (2) peculiar A stars, with temperatures of typically 10,000K and strong global magnetic fields, inclined to the rotation axis ("oblique rotators"). Type (1) rotating variables are of current interest because they may host exoplanets. The rotational variability provides information on the rotation and activity of the star; it may also be confused with an exoplanet transit!

Related to the spotted rotating variables are the *flare stars* which, along with rotating variables, are the most numerous variable stars in our galaxy. That's because over ninety percent of stars are main sequence stars, like the sun or cooler, and virtually all of these rotate, have spots, and flare. Spots and flares result from magnetic fields, which are generated by rotation and convection. Papers on classical flare stars are still published, but stellar flares have become a standard, mainstream process in astrophysics—especially as similar processes occur on the sun.

Solar-type oscillations The sun vibrates in thousands of complex, non-radial modes, driven by convective motions in its outer layers, but these vibrations are so small that they require specialized observation techniques. On other stars, they are observable from the ground only with great difficulty, but they are most effectively observed with high-precision photometry from space, with *MOST, CoRoT*, and *Kepler*. As described in the Kiss and Percy review, they have been observed in many red giants, and are revolutionizing our understanding of the nature and structure of these stars.

RV Tauri and SRd stars These are mentioned briefly in Doug Welch's review, but I would like to highlight two continuing areas of interest in these stars: (1) the cause of the alternating deep and shallow minima in these stars—probably a combination of multiperiodicity, chaos, and convection effects—and (2) the nature of the long-period variability of the RVb stars—probably a result of binarity in a significant fraction of RV Tauri and other post-AGB stars.

Hypergiants The most luminous stars, of all temperatures, are unstable and variable in a variety of ways. Stars such as the hot P Cygni and the cooler ρ Cas are well-established targets for AAVSO observation, and there are current/recent AAVSO campaigns on the hot hypergiants S Dor (*AAVSO Alert Notice 453*) and on P Cygni (*AAVSO Alert Notice 440*). I was saddened, but also moved in a way to recently receive a copy of the last paper by Richard Stothers, who passed away in 2011, and who made important contributions to the theory and interpretation of stellar variability during his long career. His paper on "Yellow Hypergiants Show Long Secondary Periods?" (Stothers 2012) deals with the hypergiants ρ Cas and HR 8752—two of the first stars that I collaborated on with the AAVSO. It suggests that both show the mysterious "long secondary periods" found in pulsating red giants, red supergiants, and red hypergiants (see review by Kiss and Percy), and are regarded by some as being the most important unsolved problem in stellar pulsation theory. Stothers attributes these to the turnover of giant convection cells in the stars' convective envelopes.

References

De Cat, P., Uytterhoeven, K., Gutiérrez-Soto, J., Degroote, P., and Simón-Díaz, S. 2011, *Proc. IAU*, **272**, 433.

Handler, G. 2012, *Trans. IAU*, **28A**, in press (also at: http://arxiv.org/abs/1111.0846).

Percy, J. R. 2007, *Understanding Variable Stars*, Cambridge Univ. Press, Cambridge.

Stothers, R. 2012, *Astrophys. J.*, **751**, 151.

The Variability of Young Stellar Objects

William Herbst
Astronomy Department, Wesleyan University, Middletown, CT 06459; wherbst@wesleyan.edu

Invited review paper, received February 15, 2012

Abstract A brief review of the types and causes of the variability of young stellar objects (pre-main sequence stars) is given with an emphasis on what we do not yet understand and how amateur observers can continue to make important contributions to the field.

1. Introduction

Alfred H. Joy (1945) was the first to identify a class of eleven irregular variable stars with characteristics similar to his adopted proto-type T Tauri. The amplitude of the variability was large—typically several magnitudes—and irregular, with no evidence of periodicity and no discernible pattern. Some stars behaved erratically, changing brightness by a magnitude or more from night to night, while others were more quiescent. Individual stars went through active periods and quiescent periods, although some could be counted on to generally be more active than others. The close association of these stars with dark and bright nebulosity as well as their spectroscopic characteristics, including emission lines of CaII and HI, indicated that they might be very young stars, an hypothesis more or less proven by George Herbig (1960, 1962). There are now thousands of known T Tauri stars within reach of small telescopes. Many were discovered by their Hα emission and catalogued by Herbig and Bell (1988). Others were found in photometric studies, especially of young clusters such as the Orion Nebula Cluster (Herbst *et al.* 2002).

The range of spectral classes among the original eleven stars of Joy was rather narrow and did not extend later than G5. Today the typical T Tauri star is of K spectral class, while earlier-type counterparts are referred to as Herbig Ae/Be stars. T Tauri stars are the youthful versions of sun-like stars, with masses of a few tenths to a few times the mass of the Sun. Herbig Ae/Be stars are young stars of higher mass. T Tauri stars are further divided into two classes: classical T Tauri stars (CTTS) and weak-lined T Tauri stars (WTTS). The distinction is commonly, although not exclusively, made on the basis of the strength of the Hα emission line. If it exceeds about 10 Å in equivalent width the object is called a CTTS and if it is less than that amount, the object is called a WTTS. Since the strength of the Hα feature is now recognized as a proxy for the star's accretion rate, it is generally the case that CTTS are pre-main sequence stars that are still accreting from surrounding disks, while WTTS are only weakly

accreting from their disks, if at all. We have learned that the presence or absence of an accretion disk is in fact the most important determinant of the observed characteristics of a young star, including the type of variability it exhibits.

2. The evolutionary status and structure of young stellar objects

2.1. Pre-main sequence stars

Stars form from interstellar clouds of gas and dust when parts of them become dense enough and cold enough that gravity overcomes random thermal motions and initiates the inexorable collapse that leads to a star. During this time, the radius of the sphere of matter that will become a star decreases by about a million fold! At the center, there quickly accumulates a protostar that is transforming the infalling energy of the accreting gas into thermal energy as it crashes into the central sphere. Within a hundred thousand years (or less for more massive stars) the central object has reached stellar temperatures at its surface, but is not quite hot enough at its center to initiate nuclear burning of Hydrogen. Such stars are easily visible, nonetheless, and make up the general class of variable stars known as young stellar objects discussed here. They are also referred to as pre-main sequence stars because they have not yet fully contracted to their main sequence size, where they will stabilize as their cores become hot enough to initiate the H-burning needed to stop the collapse. Pre-main sequence stars shine primarily by slowly shrinking, thereby converting gravitational potential energy to thermal energy, some of which is radiated away. It takes about 30 My for a sun-like star to reach the main sequence and finally turn on its core nuclear burning, but its T Tauri phase is much shorter than that, only the 1–10 My it takes to dissipate its accretion disk and organized surface magnetic fields. Older pre-main sequence stars are sometimes called post T Tauri stars (PTTS) and show little variability at optical wavelengths although they may still be strong X-ray sources.

2.2. Accretion disks

Anything that collapses by a million-fold will also spin up by a huge factor due to the well known phenomenon of conservation of angular momentum. A skater who brings her arms in close to her body spins noticeably faster even though the contraction in distance is only a few times, not a million times! It is not hard to show that even the slightest amount of spin expected to be present in an initial cloud would produce a protostar spinning faster than the speed of light if angular momentum were conserved. Exactly how forming stars rid themselves of this excess spin energy is complicated and unknown in detail, but it is clear that two things often result. First, binary stars are a common outcome of the star formation process and they can store a good deal of angular momentum in the orbital motion of the stars. A second common outcome is a single star with planetary system—again a good sink for angular momentum. Note that it

is also possible and presumably common to have a binary system with planets, as recent observations with the Kepler satellite have demonstrated. Prior to forming individual planets, the systems collapse to a central pre-main sequence star (or binary) plus a disk. Spectacular Hubble Space Telescope images of the Orion Nebula Cluster, for example, have revealed these disks around many of the young stellar objects in that cosmic nursery.

Rapid rotation has a flattening effect on matter, as anyone who has watched pizza dough spun into a crust will recognize. Disks probably form around every young star although some may be disrupted by interactions with binary companions or neighboring stars within a cluster. The great success of the Kepler mission at finding planets shows that disks survive in most cases and planets form within them. Initially, however, the disks are primarily gaseous and have a viscosity that causes some matter to be driven inward towards the star. As the accreting matter reaches a distance of only a few stellar radii it encounters the star's magnetosphere, a region dominated by intense magnetic fields rooted at the stellar magnetic poles. Some of the incoming matter is caught in the rotating fields and ejected perpendicular to the disk, forming bipolar jets of outflowing material. The rest is funneled to the star's surface in the polar regions much like the solar wind is funneled into auroral rings on Earth (Hartmann 2001).

Figures 1 and 2 show the structure of a CTTS and a WTTS. In the CTTS the disk is more massive, composed of mostly gas and is still accreting onto the star, causing the irregular, large amplitude variability first noticed by Joy. In the WTTS there is still a disk, since planets have not yet formed, but the gas is largely gone and there is little or no accretion. Since the star still has a very strong surface magnetic field it still exhibits some variability due especially to its rotation and the presence of dark spots. A PTTS probably looks much like a WTTS except that the magnetic field has weakened or become more irregular so that the spots are more uniformly distributed around the star, resulting in less photometric variability.

3. Variability types among young stellar objects

While many different classification schemes have been used to characterize the sometimes bewildering observed phenomena, here we will follow the scheme proposed by Herbst *et al.* (1994) augmented by two types of eruptive variable described originally by George Herbig and a potential new form of variability signified by the unique behavior of KH 15D.

3.1. Periodic variables with cool spots (type I variables)

Most WTTS show regular, often nearly sinusoidal, variations of 0.1 to 0.3 magnitude in their optical light on time scales of 1 to 15 days. The largest amplitude example is V410 Tau (Herbst 1989). The shapes and amplitudes of these variations typically evolve on timescales of months or years but the

periods remain stable, supporting the view that the cause of the variation is the rotation of a cool spotted surface. For many beautiful examples of such light curves see Grankin *et al.* (2008). The scientific interest in these stars is that they provide a handy and reliable method to measure the rotation period of pre-main sequence stars. They are not an easy target for amateurs since they tend to be relatively faint stars with fairly small amplitude variations. For advanced amateurs with CCDs who wish to commit many months of rather continuous observing time (they require nightly or even hourly observation) and can deal with the analysis issues (normally the period is only revealed by a rather sophisticated mathematical analysis such as a Fourier transform) the payoff is a rotation period for a young star. We now have such periods for thousands of young stars so the incremental value of another one is not so great. But there may still be interesting objects out there and the possibility of changing periods, perhaps caused by differential rotation on the surface of the star, as occurs on the Sun, remains open.

3.2. Mostly irregular variables with hot spots (type II variables)

Most CTTS show this kind of variability due to the irregular nature of the accretion heating. Just as auroral displays wax and wane with the solar wind, the brightness of CTTSs wax and wane irregularly with accretion rate changes. While interesting, it is hard to get too much useful science out of these changes which can be like trying to understand the comings and goings of clouds! But there are some interesting projects for amateurs here and some new techniques for extracting useful information (Percy *et al.* 2010a, b). The prototype for these stars is T Tauri itself and it had a sufifciently stable variation during one epoch of observation that we were able to determine its rotation period of 2.8 days (Herbst *et al.* 1986, 1987). This work was done with the collaboration of many astronomers including amateurs because we needed data to be obtained at many different longitudes. There are undoubtedly more CTTS that will show periodicity when enough data are accumulated on them.

On the longer term, the modulation of the irregular behavior in these stars is very interesting and something that AAVSO observers have contributed to and can continue to contribute to. For example, T Tauri has a very extensive data base in the AAVSO archives that shows it has gone through periods of great activity and periods of relative quiescence. The cause of these modulations is unknown but could have to do with companions orbiting it (Beck *et al.* 2001), either stars or perhaps protoplanets. Continuing to keep an eye on this object and similar ones is a task well suited to the AAVSO and of potentially great scientific importance, especially should some unexpected behavior occur.

3.3. Irregular variables suffering occultations (type III variables): UXors

Many Herbig Ae/Be stars and earlier type CTTS such as RY Tau and CO Ori undergo this type of variability. While its cause is still debated, it seems clear

that these stars are irregularly occulted by circumstellar matter. The timescales are similar to, although perhaps a bit longer than, the Type II variables and there is probably a mixture of accretion-related heating and occultation going on in some sources. One characteristic of the class is that there can be rather sudden drops in the brightness of the star by one, two, or even three magnitudes followed by slower and often irregular recoveries. When very faint the stars are bluer and more polarized, indicating that scattered light by small grains is important (Voshchinnikov *et al.* 1988). A possible cause of the variations is obscuration of the photosphere by dusty accreting material. The interesting periodic star AA Tau may be of this type but apparently has the property that the occulting matter is confined to a warped disk rather than an accretion stream, leading to its periodicity (Bouvier *et al.* 1999, 2003). Alencar *et al.* (2010) have noted a number of AA Tau-like stars in young clusters that may be UXors. The prototype for the class is UX Orionis, hence the name.

The UXors probably represent the only major class of variable stars in which the exact mechanism of variability is still debated. As such they deserve all the observational attention they can get. The long records of the AAVSO are very important for understanding these variables and how they evolve. Since the occulting matter may, in some cases, be solids within protoplanetary disks there may be encoded in the variability information about the early stages of the formation of planets. As is often the case, data on these stars are of considerably more value if they are obtained at more than one wavelength. This allows astronomers to determine the optical properties of the occulting material, in particular whether it is the very small grains characteristic of the interstellar medium or larger solids expected to grow within disks during the first stages of planet formation. Many light curves of UXors can be seen in the paper by Herbst and Shevchenko (1999).

3.4. Large scale eruptive variables (FU Orionis stars): FUors

A few T Tauri stars are known to have gone through substantial eruptive events in which they brighten by several magnitudes and maintain their bright state for months or years. Their prototype is FU Orionis and the class was first proposed and discussed by Herbig (1977). While debate continues about the exact causes of this phenomenon it appears to be related to a rather abrupt increase in the accretion rate (Hartmann and Kenyon 1996). Such eruptive behavior in pre-main sequence stars, if common, could have substantial effects on forming planets, since the increased luminosity of the star would heat disk material well above what would be typical for a non-erupting T Tauri star.

The field of eruptive pre-main sequence stars is one which has benefitted from the participation of amateur astronomers and may continue to do so. Amateur astronomer J. McNeil discovered a new nebula that was produced as a result of a likely FUor outburst in 2004 (McNeil *et al.* 2004; Briceno *et al.* 2004). Regular patrolling observations of star forming regions may reveal

such eruptions well before they are noticed by professional astronomers. It is interesting that most, if not all, FUors are found in relatively isolated star forming locales, not within the denser regions of the populous clusters such as the Orion Nebula Cluster, IC 348, and NGC 2264 where many professional survey programs are concentrated. The statistics of the FUor phenomenon are quite uncertain owing to the small number of definitive cases. This makes it difficult to assess how important the phenomenon is to star and planet formation in general.

3.5. Small scale eruptive variables (EX Lupi stars): EXors

Herbig (2007) described the behavior of another rather large amplitude T Tauri variable, EX Lup, and suggested it may represent a class of eruptive variables with similarity to the FUors but on a smaller scale. Unfortunately the class remains rather heterogeneous and ill-defined (Herbig 2008). Presumably these are stars also suffering enhanced accretion events but not to the extent of the FUors. It is unclear at present whether these are just extreme examples of the Type II variability characteristic of most CTTS or represent something distinctly different and perhaps related to the FUor phenomenon. Again, improving the statistics of light curve behavior among these large amplitude CTTS, especially ones that are not concentrated into the massive clusters that professionals prefer to monitor, is a field in which amateur astronomers could make major contributions.

3.6. Periodic variables of KH 15D type

Kearns and Herbst (1998) described a large amplitude, strictly periodic variable now known as KH 15D, in NGC 2264. Its behavior is unique and now understood as arising from a binary T Tauri star with a warped, precessing circumbinary disk (Chiang and Murray-Clay 2004; Winn *et al.* 2004; Hamilton *et al.* 2005). Other large amplitude, strictly periodic variables have been found that may, like KH 15D, be caused by circumstellar matter within a disk periodically occulting a single star or one member of a binary. Possible members of this class include V718 Per (HMW 15) (Grinin *et al.* 2008) and CHS7797 (Ledesma *et al.* 2012). AA Tau (Bouvier *et al.* 1999, 2003) also may meet this definition, perhaps creating a bridge to the aperiodic UXors. In any event, the discovery of additional cases of large amplitude, periodic occultations would be very interesting. Since most of the stars in this class appear to exhibit the periodicity only episodically, this is another area in which careful, long-term monitoring programs such as amateurs can carry out under the auspices of the AAVSO may yield substantial scientific payoffs.

References

Alencar, S. H. P., *et al.* 2010, *Astron. Astrophys.*, **519**, 88.
Beck, T. L., Prato, L., and Simon, M. 2001, *Astrophys. J.*, **551**, 1031.
Bouvier, J., *et al.* 1999, *Astron. Astrophys.*, **349**, 619.
Bouvier, J., *et al.* 2003, *Astron. Astrophys.*, **409**, 169.
Briceno, C., *et al.* 2004, *Astrophys. J., Lett. Ed.*, **606**, L123.
Chiang, E. I., and Murray-Clay, R. 2004, *Astrophys. J.*, **607**, 913.
Grankin, K. N., Bouvier, J., Herbst, W., and Melnikov, S. Yu. 2008, *Astron. Astrophys.*, **479**, 827.
Grinin, V., Stempels, H. C., Gahm, G. F., Sergeev, S., Arkharov, A., Barsunova, O., and Tambovtseva, L. 2008, *Astron. Astrophys.*, **489**, 1233.
Hamilton, C. M., *et al.* 2005, *Astron. J.*, **130**, 1896.
Hartmann, L. 2001, *Accretion Processes in Star Formation*, Cambridge Univ. Press, Cambridge.
Hartmann, L., and Kenyon, S. 1996, *Ann. Rev. Astron. Astrophys.*, **34**, 207.
Herbig, G. H. 1960, *Astrophys. J., Suppl. Ser.*, **4**, 337.
Herbig, G. H. 1962, *Adv. Astron. Astrophys.*, **1**, 47.
Herbig, G. H. 1977, *Astrophys. J.*, **217**, 693.
Herbig, G. H. 2007, *Astron. J.*, **133**, 2679.
Herbig, G. H. 2008, *Astron. J.*, **135**, 637.
Herbig, G. H., and Bell, K. R. 1988, *Lick Obs. Bull.*, No. 1111, 1.
Herbst, W. 1989, *Astron. J.*, **98**, 2268.
Herbst, W., Bailer-Jones, C. A. L., Mundt, R., Meisenheimer, K., and Wackermann, R. 2002, *Astron. Astrophys.*, **396**, 513.
Herbst, W., Herbst, D. K., Grossman, E. J., and Weinstein, D. 1994, *Astron. J.*, **108**, 1906.
Herbst, W., and Shevchenko, V. S. 1999, *Astron. J.*, **118**, 1043.
Herbst, W., *et al.* 1986, *Astrophys. J., Lett. Ed.*, **310**, L71.
Herbst, W., *et al.* 1987, *Astron. J.*, **94**, 137.
Joy, A. H. 1945, *Astrophys. J.*, **102**, 168.
Kearns, K. E., and Herbst, W. 1998, *Astron. J.*, **116**, 261.
Ledesma, V. R., *et al.* 2012 *Astron. Astrophys.*, in press.
McNeil, J. W., Reipurth, B., and Meech, K. 2004, *IAU Circ.*, No. 8284, 1.
Percy, J. R., Esteves, S., Glasheen, J., Lin, A., Long, J., Mashintsova, M., Terziev, E., and Wu, S. 2010a, *J. Amer. Assoc. Var. Star Obs.*, **38**, 151.
Percy, J. R., Grynko, S., Seneviratne, R., and Herbst, W. 2010b, *Publ. Astron. Soc. Pacific*, **122**, 753.
Voshchinnikov, N. V., Grinin, V. P., Kiselev, N. N., and Minikulov, N. K. 1988, *Astrofizika*, **28**, 311.
Winn, J. N., Holman, M. J., Johnson, J. A., Stanek, K. Z., and Garnavich, P. M. 2004, *Astrophys. J., Lett. Ed.*, **603**, L45.

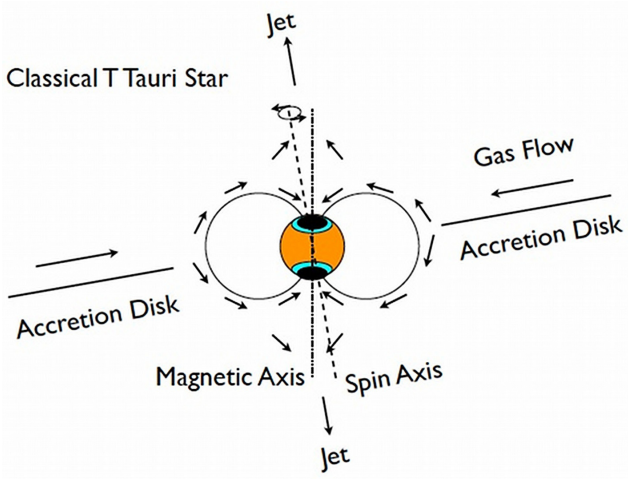

Figure 1. Schematic diagram of a CTTS showing the gas flows through the accretion disk and then into the jet or onto the star near the magnetic pole. The dark spots at the poles result from disruption of convective energy transport by the magnetic field, just like in sunspots. The bright rings around them represent parts of the photosphere heated by the accreting gas and are analogous to auroral rings on Earth. The small misalignment of the rotation and magnetic axes leads to periodic variability of the star as we view different parts of its inhomogeneous surface.

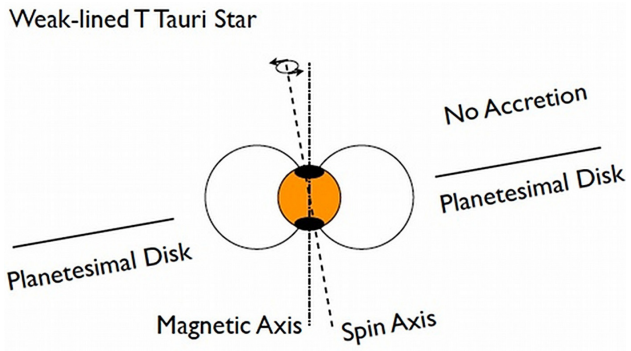

Figure 2. Schematic diagram of a WTTS showing that there is now little, if any, gas flow through the disk or accretion onto the star. Much of the irregular variability therefore disappears in these stars but they continue to show periodic variations of typically 0.1–0.3 mag. caused by the rotation of their spotted surfaces. For WTTS it is often possible to determine their rotation period since the surface spot distributions often remain stable for months or even years.

How Amateurs Can Contribute to the Field of Transiting Exoplanets

Bryce Croll
Kavli Institute for Astrophysics and Space Research, Massachusetts Institute of Technology, Cambridge, MA 02139; croll@space.mit.edu

and

NASA Sagan Fellow

Invited review paper, received June 4, 2012

Abstract In 1999 on two evenings in September, the first tell-tale dips of a transiting extrasolar planet passing in front of its star were detected with a 10-centimeter telescope that was set up in a parking lot beside a wooden shed. Although these observations were obtained by professional astronomers, their setup—a modest aperture telescope in an unassuming location—should sound familiar to many enterprising amateur astronomers. What should warm the heart of any amateur astronomer, while they man their telescope alone on a cold winter's eve, or as they gaze at the blinking glare of their computer monitor, is that there are still numerous avenues via which ambitious amateurs can significantly contribute to the evolving story of transiting extrasolar planets (exoplanets). In the brief review below, I'll summarize the current state of the field of transiting exoplanets, and then elucidate the ways that resourceful amateurs—those with and without access to telescopes—can contribute to the field, both in discovering new transiting exoplanets and in characterizing existing ones.

1. Transiting planets: the state of the field

The notion that we might be able to detect planets in other solar systems by the diminution of light when the planet passes in front of the star along our line-of-sight (a so-called transit) is not a new one. Struve (1952) presciently predicted that Jupiter-size planets should create transit dips on the order of a few percent more than half a century ago, and noted that the methods of the day even then were likely sufficient to achieve the precision necessary to detect these dips. The nearly half-century wait until the detection of a transiting exoplanet was not due to a lack of precision from observers, but mostly due to the fact that planetary theorists did not predict how odd the first exoplanets we detected around stars similar to our own would turn out to be. Although, Struve (1952) hypothesized that it might be possible for planets to exist a mere few stellar radii from their host stars, other planetary theorists were not so sanguine; they predicted that extrasolar systems would have orbital

configurations similar to our own solar system, with Jupiter-mass planets in orbits of several years or more (Isaacman and Sagan 1977). Thus any aspiring transit observer faced the daunting prospect of hoping to detect a single transit only once every few years. As a result Struve's prescient suggestion remained largely forgotten for decades.

Although the credit for the discovery of the first exoplanet rightly goes to Wolszczan and Frail (1992), for their discovery of what would turn out to be three planets (Wolszczan 1994) in what can only be described as an extreme environment orbiting a millisecond pulsar (a so-called "dead" star that has burned its nuclear fuel and already gone supernova), the true imagination of the scientific community was not excited until the discovery of a planet, 51Peg b, around a star similar to our own (Mayor and Queloz 1995). This first detection of an exoplanet around a sun-like star, made via the radial velocity (RV) technique, which indirectly reveals the presence of planets by the doppler shift in the stellar lines from the subtle tugging back and forth of the planet on the star, began the trickle that turned into a flood of exoplanet discoveries—at the time of writing the RV technique has confirmed the discovery of ~700 exoplanets in ~550 extrasolar systems (exoplanet.eu; accessed 23 March 2012).

For those of us who would eventually become enamoured with transiting planets, there was something else captivating about 51Peg b—something that would reinforce the impressive foresight of Struve's (1952) prediction that planets might be able to survive close to their host stars. This planet was not the true Jupiter analog that planetary theorists were expecting, with a few-year orbital period; instead, it was a so-called hot Jupiter—a Jupiter-mass planet orbiting with a period of a mere few days and thus roasting near its star with an equilibrium temperature in excess of ~1000 K. For the subset of planets that transit their host star, this meant that rather than having to wait several years between transits, they would occur every few days. Also, the chance that the planet would actually transit its star would greatly increase for these close-in planets (for a planet to transit, the cosine of the orbital inclination, $\cos i$, multiplied by the orbital distance during eclipse (the semi-major axis for a circular orbit), a, must be less than the radius of the star, R_*: $a \sin i < R_*$). The expected fraction of exoplanets that transit their stars is a healthy ~10% for hot Jupiters, and a much smaller fraction for planets of increasing orbital periods. It was this gift from nature—that these hot Jupiter planets exist and can survive, even briefly, roasting next to their host stars—that led to the explosion of interest in using transits to detect exoplanets, and as a result allowed the true potential of Struve's prescient prediction to be achieved.

The transition of this potential into reality started with the first detection of a transiting exoplanet in September 1999. From the unassuming location of a parking lot, using a size of telescope (10-centimeters) that even some amateurs might consider modest, Charbonneau *et al.* (2000) obtained photometry of a known RV-detected hot Jupiter, HD 209458, and observed the characteristic

loss of light resulting from the planet transiting across its star (Figure 1; Charbonneau 2001; Jayawardhana 2011. Henry *et al.* 2000 would discover that HD 209458 transits its host star independently). Since that seminal discovery, ~230 planets in ~200 systems have been confirmed to transit their stars, while the Kepler space satellite has identified an additional ~2,300 likely candidates (although many of these systems will remain candidates for the near-term future, because they are not amenable to RV follow-up and confirmation, most of these candidates stand a very good chance of being bona fide planets (Morton and Johnson 2011)) ranging in size from larger than Jupiter to smaller than Earth (Batalha *et al.* 2012). This impressive wealth and diversity in the current sample of known transiting exoplanets offers a compelling opportunity for both professionals and amateurs alike in both adding to the sample by detecting transiting exoplanets especially around bright host stars (section 2), as well as characterizing the atmospheres and orbits of known transiting exoplanets (section 3).

2. How amateurs can assist in detecting new transiting exoplanets

2.1. Searching for transits of known RV detected exoplanets

Excitingly, the very same method that was used to discover the first transiting exoplanet is one that amateurs can continue to use to discover planets. The first transiting exoplanet was discovered by looking at a relatively bright star that was already known from the RV technique to harbor an exoplanet. Not only does the RV technique reveal the period, eccentricity, and the minimum mass of the planet, it also reveals when the planet is expected to pass in front of its star along our line of sight (with an uncertainty of tens of minutes to a few hours in the best cases). Many of these radial velocity stars are relatively bright, and the expected transit depths for giant planets (~1% percent typically) are achievable with modest, CCD-equipped, amateur telescopes from pristine sites. Thus, all that is required is for interested amateur astronomers to be convinced to look at specific stars at specific times and obtain and share the hopefully-resulting high quality light curves. This was exactly the motivation behind one website that is soon to be retired, and another, which is being routinely updated with new RV exoplanet discoveries, that should adroitly take its place. The soon to be retired website is *Transitsearch.org*, which details the following details of known planets detected via the RV method: the Right Ascension, declination, expected transit depth, estimated percentage chance that the planet will actually transit in front of its parent star, and lastly, and most importantly, the ephemerides of the predicted transit window around which interested amateurs are encouraged to search for the tell-tale dip that would indicate that the known RV-detected planet in fact transits its star. Luckily the functionality of *Transitsearch.org* has been included in the NASA Exoplanet Archive (http://exoplanetarchive.ipac.caltech.edu/), which should allow interested amateurs to follow up on the latest RV discoveries.

A campaign organized by *Transitsearch.org* was exactly how one of the brightest transiting exoplanets that have been discovered to date was found; HD 17156b (Barbieri *et al.* 2007) was a known RV-detected exoplanet with a period of ~21.2 days and an eccentricity of e ~0.67. The orientation of its elliptical orbit compared to the Earth's line-of-sight was fortuitous such that, despite its longer period, it still had a relatively high chance (~13%) of transiting its parent star. Photometry obtained during the predicted transit window by a series of amateurs using telescopes that ranged in size from 0.18 m to 0.40 m revealed a ~1% dip, resulting in the confirmation of one of the brightest transiting planets discovered even to this day. This wasn't *Transitsearch.org*'s only success; another *Transitsearch.org* campaign assisted in the discovery that another bright RV-detected exoplanet (HD 80606b) transited its star (Fossey *et al.* 2009; Moutou *et al.* 2009; Garcia-Melendo and McCullough 2009).

With over ~230 confirmed transiting exoplanets, and Kepler's trove of an additional ~2,300 candidates, an additional transiting exoplanet, even if it is discovered by amateurs, may not seem especially significant. However, this is not the case. It may seem counterintuitive, but it is actually the brightest stars—the ones that amateurs can easily access—that have not been adequately searched by professional astronomers for transiting exoplanets. Many of the existing wide-field, ground-based efforts to detect transiting exoplanets examine fainter stars (V~8 and fainter) so as to not saturate their detectors, and to allow a great number of stars to be observed simultaneously in the field-of-view of the telescope. However, planets orbiting brighter hosts will always be more favorable for follow-up solely due to the increased number of photons. There are several professional endeavors that seek to fill in this parameter space, by both following up known RV-detected planets—an example is the Transit Ephemeris Refinement and Monitoring Survey (TERMS; Kane *et al.* 2009)—and by searching for transiting planets around relatively bright hosts—examples include the ground-based KELT-survey (Pepper 2007) and the proposed space-based Transiting Exoplanet Survey Satellite (TESS; Ricker *et al.* 2010).

At the current juncture, there still could be at least a handful of RV detected planets that could prove to be a needle of a transiting exoplanet in the haystack of all the RV candidates to date. Even for a dedicated amateur, robustly detecting a 1% transit dip on stars with visual magnitudes on stars as faint as V~8 is not for the faint of heart (Bruce Gary's (2012) *Exoplanet Observing for Amateurs: Second Edition*, which is freely available for download, is an excellent resource that explains the challenges associated with and how to actually achieve such precision; http://brucegary.net/book_EOA/x.htm). However, for the especially dedicated, ambitious amateur, observing from a pristine site with an equally impressive amateur telescope, observing the RV targets listed in the NASA Exoplanet Archive at the specified times may be just the opportunity to add to the short list of RV-detected exoplanets that have been found by amateurs to transit their host stars.

2.2. Planet Hunters

For those amateurs who don't necessarily have access to a telescope, but do have access to a computer, time, and enthusiasm, there is a way they may still discover transiting exoplanets—that way is Planethunters: a citizen science project (http://www.planethunters.org/; Fischer *et al.* 2012) that allows amateurs to seach for planets using data from the Kepler space telescope. NASA's Kepler spacecraft is a 0.95-m telescope in an Earth-trailing orbit (Borucki *et al.* 2011) that is designed to provide ultraprecise photometry of 150,000 stars in a 115-square degree patch of the sky near the constellation of Cygnus; the goal is to discover exoplanets of varying sizes and with periods out to a year, and therefore to determine the frequency of Earth-like planets in the habitable zones of other stars. The Kepler photometry is indeed extremely precise (Borucki *et al.* 2009), but nonetheless it has a variety of noise sources that are both intrinsic (photon-noise), and instrument-related hiccups (systematic errors in astronomy "lingo"); to detect the transits of "wee" planets despite this noise, the Kepler team has developed a variety of algorithms to pick out the tell-tale dips in the light curve. However, those of us who have developed such computer algorithms to accomplish simple tasks know that the human eye and brain are often better at pattern recognition than any algorithm. Thus instead of a single computer algorithm looking for periodic transits in each of the 150,000 light curves that Kepler observed, what if a series of amateurs could be convinced to look at these 150,000 light curves? Would they be able to detect planets that the algorithms had missed? Or possibly, something even more interesting?

Planet Hunters—an interface that allows users to scroll through a great many of the 150,000 Kepler light curves and identify possible transiting exoplanets—was developed to answer this very question. Perhaps, not surprisingly, the answer has turned out to be that indeed a dedicated group of citizen scientists (over 100,000 at last count) can discover transiting exoplanet candidates that Kepler's best algorithms missed on its first pass. At the time of writing, four planetary transiting exoplanetary candidates have been discovered by Planet Hunter collaborators (Lintott *et al.* 2012). It should be acknowledged that these objects are just "candidates" at this present time, which means they have yet to be confirmed as bona fide exoplanets with masses less than the deuterium-burning limit (< 13 Jupiter masses). The RV method is one of the most common ways for astronomers to confirm candidates as planets; the candidates discovered to date with Planet Hunters, however, are unsuitable for such follow-up with a signal too small to be realistically detected with our current best RV precision. There thus remains the possibility that these candidates are false positives (one of the most common false positives for transiting exoplanets is an eclipsing binary star blended or diluted by a tertiary or background star along the line of sight). Analytical research, however, has demonstrated that only a slim percentage of Kepler candidates (< 5–10%) can be expected to be false positives (Morton and Johnson 2011). For the amateur astronomers volunteering with the

Planet Hunter citizen project, I'm going to guess that having the opportunity to discover a candidate that has a 90 to 95% chance of being an exoplanet, just by sitting down at one's computer, has a pretty sweet ring to it. For those amateurs interested in searching for and possibly detecting an exoplanet, data on new Kepler targets and more data on existing targets are released every few months.

3. How amateurs can assist in the characterization of transiting exoplanets

For the talented and ambitious amateur, observing night after night of potentially flat light curves, and scrutinizing subtle dips that may or may not be due to clouds, seeing variations, and so on (see section 2.1), may not sound particularly appealing. What may sound considerably more attractive is to observe the transits of known transiting exoplanets. Known transiting exoplanets have transit depths up to a few percent of the stellar flux from stars as bright as V~6, with the majority of candidates with V~10 or fainter; thus detecting these transits will still only be accessible to experienced amateurs with modest or larger aperture telescopes with a sensitive camera. While it may be an intriguing challenge in its own right for an amateur to robustly detect the ~1% transit dips of most transiting exoplanets, amateurs may be even more intrigued that professional astronomers frequently use the light curves shared by amateurs to learn a great deal about exoplanets' orbits (section 3.1) and in the future, possibly even their atmospheres (section 3.2).

3.1. Characterization of the orbits of exoplanets

Observing a great number of transits of an exoplanet can be very helpful to professionals to characterize the orbit, and as a result the properties, of a transiting exoplanet. Transit-timing (Holman and Murray 2005; Agol *et al.* 2005) is one such obvious example where astronomers look for small differences in the timing of transits from a strictly periodic orbit that might be the telltale signs of other smaller planets in that system that are gravitationally tugging the known planet back and forth. Other small asymmetries in the light curves that may become apparent after frequent observations include transit-duration or inclination variations that may result from precession, or may be the tell-tale signs of exomoons or starspots. What usually happens in the cases that amateur observations prove to be useful is that after a professional astronomer analyzes their own data, they observe an intriguing hint of one of these aforementioned effects; confirming these effects often requires comparison to a robust archive of transit observations—an archive that is often provided by amateur observers. One such search for transit—more aptly eclipse—timing variations that benefited from access to a robust archive of amateur observations was from my own research.

In Croll *et al.* (2011) I used the mid-transit times from twenty light curves obtained by amateur astronomers to rule out that the hot Jupiter WASP-12b

was precessing at a detectable rate. The best-fit RV solution of WASP-12b indicated that, despite its very short orbital period (P~26 hours), its orbit was mildly eccentric (e~0.05)—that is, its orbit was not perfectly circular, but slightly elliptical in shape. Intriguingly, one of the secondary eclipse times (that is when the planet passes behind its star along our line-of-sight, and we experience a drop in flux due to the loss in light of the planet) for this planet was considerably offset from what one would expect for a circular orbit (Lopez-Morales *et al.* 2010), while another was not (Figure 2 top panel; Campo *et al.* 2011). If this discrepancy was not due to a systematic error or something more interesting, the best explanation for the offset of the times of secondary eclipse of this planet was that its orbit was precessing at a very rapid rate due to the stellar gravitational forces acting on the tidal bulge of the planet. The period of this precession is dependent on what is known as the tidal planetary Love number, k_2, of the orbit, which simply indicates how centrally condensed the planet is—that is, how massive the core of the planet is compared to its outer gaseous layers. For a planet like Jupiter, which has a ~10 Earth-mass core, k_2~0.5, while at the opposite extreme, a uniform density sphere will have a k_2 = 3/2 (Ragozzine and Wolf 2009). For the precession rate to be as rapid as these offset eclipse times indicated, the planet would, unexpectedly, have to have a very massive core. The best way to rule out this precession signal was to detect the secondary eclipse of this planet once again, and to determine whether the times were again offset from those of a circular orbit, or whether they fell exactly half an orbit after the transits. The problem was that professional astronomers had only observed a few more transits of this planet, and had not been routinely monitoring the transit, as was necessary to determine if the eclipses fell exactly half an orbit after the transits. Luckily, amateur observers had taken up the slack. By comparing my own observations of the secondary eclipse times of this planet with those published by both professional astronomers and a number of amateur astronomers shared on what is known as the Exoplanet Transit database (ETD; The Exoplanet Transit Database—http://var2.astro.cz/ETD/), I was able to show that the secondary eclipse times fell when we expected them, exactly half an orbit after the transits (Figure 2, bottom panel). This meant that the planet was not precessing at a detectable rate. The professionals and amateurs who shared their observations on the ETD likely had no idea at the time that their observations would eventually be used to elucidate whether we could answer how massive the core is of a gas giant planet ~1,400 light years (Chan *et al.* 2011) away from Earth.

3.2. Characterization of the atmospheres of exoplanets

Transiting exoplanets have been a significant boon to professional astronomers as it has allowed us to probe the atmospheric characteristics of these worlds many light-years from our own. One of the techniques for investigating the atmospheres of these alien planets is known as Transmission Spectroscopy,

where one looks for minute transit-depth differences in and out of predicted absorption features from molecules in the atmospheres of these planets. These transit-depth differences result from the fact that the opacity of the planet's atmosphere is greater at the wavelengths of the absorption feature, meaning that the planet actually appears larger, resulting in the planet blocking out a greater fraction of the stellar light and thus having a deeper transit depth. Although the first detection of the atmosphere of an exoplanet used a type of instrument, size of telescope, and observing location not readily accessible to amateurs (Charbonneau *et al.* (2002) used the space-based, 2.4-m aperture Hubble Space Telescope and a spectrograph to disperse light over a narrower spectral range to detect sodium in the atmosphere of HD 209458), more recent detections may fall within the realm that may be accessible to particularly ambitious and technically astute amateurs. The planet HD 189733b orbits a bright host star (V~6) and appears to display a transit depth that decreases monotonically with wavelength (Sing 2011), likely due to scattering from a haze/cloud layer in the upper atmosphere of that alien world. Although the differences between the transit depth of this planet in B-band (a wavelength of $\lambda \sim 0.44\,\mu m$) and in z-band (l~0.91 μm) is too small (only ~0.05% of the stellar signal) to be currently accessible to amateurs, it is certainly possible that new planets (especially ones with large-scale heights and deep transits) may display larger transit-depth differences across the optical wavelength range. For this reason, avid amateurs and semi-professionals should consider observing transits over a range of wavelengths and publishing these light curves on the ETD. Given the host of complicating factors (starspots, limb-darkening, telluric atmospheric effects, and so on) that may masquerade as a possible signal, amateur observations alone likely won't be sufficient to confirm such a signal. However, an existing trove of precise amateur observations of the transit depths of exoplanets across a wide wavelength range may be just the thing a professional astronomer needs to believe the tentative signal in their own data, and to request higher precision follow-up observations. If helping to answer what gases are in the atmosphere of an alien world, or whether a planet has prominent clouds and/or hazes is of interest, then professional astronomers would certainly appreciate amateurs uploading as many high quality light curves of transits at various wavelengths/filters as possible to the ETD.

4. Concluding thoughts

The field of transiting exoplanets is a relatively new one. From this field's early days, though, the synergy between amateurs and professionals has been particularly potent. Hopefully this review has elucidated the myriad ways that passionate amateurs, whether they own an advanced telescope that is the envy of all their friends at the star party, or they simply have a modest computer and an internet connection, can ensure that this synergy continues in this field for years to come.

5. Acknowledgements

BC's work was performed under contract with the California Institute of Technology funded by NASA through the Sagan Fellowship Program. The Natural Sciences and Engineering Research Council of Canada supports the research of BC.

References

Agol, E., Steffen, J., Sari, R., and Clarkson, W. 2005, *Mon. Not. Roy. Astron. Soc.*, **359**, 567.

Barbieri, M. *et al.* 2007, *Astron. Astrophys.*, **476**, L13.

Batalha, N.M. *et al.* 2012, submitted to *Astrophys. J., Suppl. Ser.*, arXiv:1202.5852.

Borucki, W. *et al.* 2009, *Science*, **325**, 709.

Borucki, W. *et al.* 2011, *Astrophys. J.*, **736**, 19.

Campo, C.J. *et al.* 2011, *Astrophys. J.*, **727**, 125.

Chan, T., Ingemyr, M., Winn, J. N., Holman, M. J., Sanchis-Ojeda, R., Esquerdo, G., and Everett, M. 2011, *Astron. J.*, **141**, 179.

Charbonneau, D. 2001, *Shadows and Reflections of Extrasolar Planets*, Ph.D. Thesis, Harvard Univ. (DAI-B 62/04).

Charbonneau, D., Brown, T. M., Latham, D. W., and Mayor, M. 2000, *Astrophys. J., Lett. Ed.*, **529**, L45.

Charbonneau, D., Brown, T. M., Noyes, R. W., and Gilliland, R. L. 2002, *Astrophys. J.*, **568**, 377.

Croll, B., Lafreniere, D., Albert, L., Jayawardhana, R., Fortney, J. J., and Murray, N. 2011, *Astron. J.*, **141**, 30.

Fischer, D. A. *et al.* 2012, *Mon. Not. Roy. Astron. Soc.*, **419**, 2900.

Fossey, S.J., Waldmann, I. P., and Kipping, D. M. 2009, *Mon. Not. Roy. Astron. Soc.*, **396**, L16.

Garcia-Melendo, E., and McCullough, P. R. 2009, *Astrophys. J.*, **698**, 558.

Gary, B. 2012, Exoplanet Observing for Amateurs: Second Edition (http://brucegary.net/book_EOA/x.htm).

Henry, G.W., Marcy, G. W., Butler, R. P., and Vogt, S. S. 2000, *Astrophys. J., Lett. Ed.*, **529**, L41.

Holman, M. J., and Murray, N. W. 2005, *Science*, **307**, 1288.

Isaacman, R., and Sagan, C. 1977, *Icarus*, **31**, 510.

Jayawardhana, R. 2011, *Strange New Worlds: The Search for Alien Planets and Life beyond Our Solar System,* Princeton Univ. Press, Princeton, NJ.

Kane, S. R., Mahadevan, S., von Braun, K., Laughlin, G., and Ciardi, D. R. 2009, *Publ. Astron. Soc. Pacific*, **121**, 1386.

Lintott, C. J., *et al.* 2012, arXiv:1202.6007.

Lopez-Morales, M., Coughlin, J. L., Sing, D. K., Burrows, A., Apai, D., Rogers, J. C., Spiegel, D. S., and Adams, E. R. 2010, *Astrophys. J., Lett. Ed.*, **716**, L36.
Mayor, M., and Queloz, D. 1995, *Nature*, **378**, 355.
Morton, T. D., and Johnson, J. A. 2011, *Astrophys. J.*, **738**, 170.
Moutou, C. *et al.* 2009, *Astron. Astrophys.,* **498**, L5.
Pepper, J. 2007, *Publ. Astron. Soc. Pacific*, **119**, 923.
Ragozzine, D., and Wolf, A. S. 2009, *Astrophys. J.*, **698**, 1778.
Ricker, G. R., *et al.* 2010, *Bull. Amer. Astron. Soc.*, **42**, 459.
Sing, D. K. 2011, *Mon. Not. Roy. Astron. Soc.*, **416**, 1443.
Struve, O. 1952, *Observatory*, **72**, 199.
Wolszczan, A. 1994, *Science*, **264**, 538.
Wolszczan, A., and Frail, D. A. 1992, *Nature*, **355**, 145.

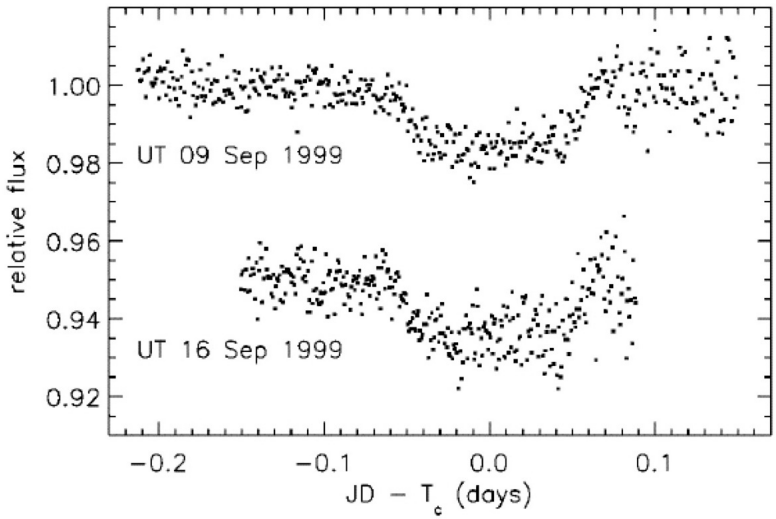

Figure 1. The dip in the light curve at JD – T_c = 0 day, signifies the first detection of the loss of light as a transiting exoplanet passes in front of its star. These observations were obtained with a 10-centimeter telescope set up in a parking lot. Figure obtained from Charbonneau *et al.* (2002).

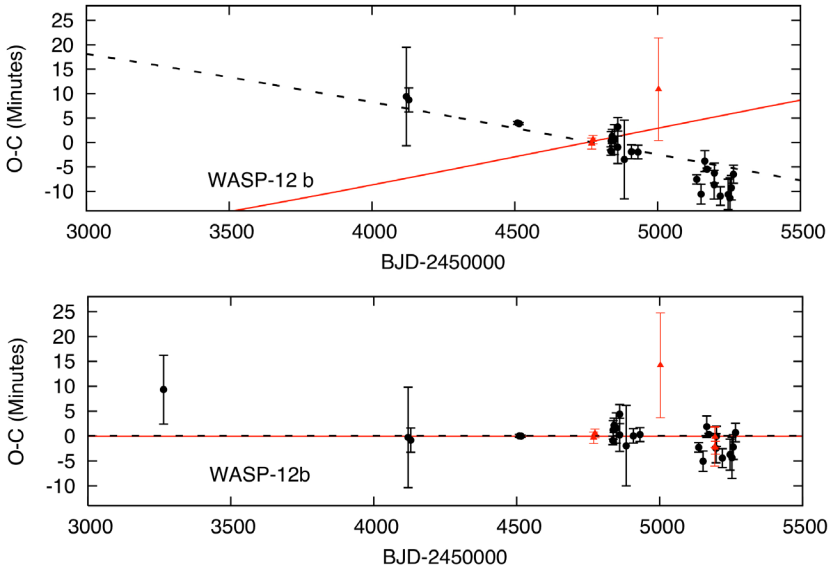

Figure 2. Transit (black points) and eclipse (red points) times of the hot Jupiter WASP-12b. The best-fit precessing model is shown with the dotted black line that indicates the expected transit times, while the solid red line indicates the expected eclipse times. The top panel indicates that a rapidly precessing model was favored before the addition of the Croll *et al.* (2011) eclipse times (bottom panel; red points); by comparing the Croll *et al.* (2011) eclipse times to the transit times of amateurs, it was shown that the planet was not precessing at a rate rapid enough to be currently detectable. Figure adapted from Croll *et al.* (2011).

Eclipsing Binaries in the 21st Century—Opportunities for Amateur Astronomers

Edward F. Guinan
Scott G. Engle
Edward J. Devinney
Department of Astronomy and Astrophysics, Villanova University, Villanova, PA 19085; edward.guinan@villanova.edu

Invited review paper, received June 5, 2012

Abstract Eclipsing binaries play major roles in modern astrophysical research. These stars provide fundamental data on the masses, radii, ages, atmospheres, and interiors of stars as well as serving as test beds for stellar structure and evolution models. The study of eclipsing binaries also returns vital information about the formation and evolution of close binaries themselves. Studying the changes in their periods from the observations of eclipse timings provides insights into evolution of close binaries, mass exchange and loss, apsidal motion for eccentric systems, as well as the discovery of the low mass (unseen) third bodies. Moreover eclipsing binaries in clusters and other galaxies can provide accurate distances to the star clusters and galaxies in which they reside. More recently observations of eclipsing exoplanet-star systems (that is, transiting exoplanets) when coupled with spectroscopy are yielding fundamental information about the frequency and the physical properties of planets orbiting other stars. For the reasons discussed above, observations of eclipsing binary systems have been popular for AAVSO observers and many papers have been published (see Williams *et al.* 2012, this volume). A recent example is the highly successful AAVSO's Citizen Sky Project focused on the enigmatic long-period eclipsing binary ε Aur. Building on the success of the AAVSO during the last century, this paper explores the present and future prospects for research in eclipsing binaries. We focus on what can be done by AAVSO members and other amateur astronomers in the study of eclipsing binaries. Several examples of observing strategies and interesting (and scientifically valuable) projects are discussed as well as future prospects. As discussed, there are many opportunities for AAVSO members to contribute to the study of eclipsing binary stars and an increasing variety of objects to observe.

1. Introduction to eclipsing binaries

We can date the beginning of the study of eclipsing binaries (EBs) with the discovery of Algol (β Per) as an eclipsing binary by young "amateur" astronomer John Goodricke in 1783. The importance of eclipsing binaries stems from the fact that photometry and spectroscopy of eclipsing binaries and the analysis of

their light and radial velocity curves returns essential information (which often cannot be found by any other means) about the physical characteristics of the stars—such as mass, radius, temperature, and luminosity (see Andersen 1991; Guinan and Engel 2006). Without eclipses most of these parameters could not be determined. These essential quantities are fundamental to the understanding of all stars, as well as to the star clusters and galaxies in which they reside, and to the basic physical laws that govern their behavior. Although the majority of stars in the solar neighborhood are members of binary or multiple star systems, only a tiny fraction (< 0.5%) of these have their orbital planes aligned closely enough to our line of sight that eclipses occur. To date about 15,000 eclipsing binaries have been discovered out of the possible ~100 million or more eclipsing binaries that are expected to be present in our Galaxy. Interestingly, most of these eclipsing binaries were discovered serendipitously in the Large and Small Magellanic Clouds and in the Galactic Bulge from photometric micro-lensing programs such as EROS, MACHO, and OGLE (see Guinan *et al.* 2004).

Nearly every type of star is represented as a member of an eclipsing binary system. These include main-sequence (as well as pre main-sequence) stars, subgiants, giants, and supergiants, with the entire range of spectral types and masses represented. Brown dwarfs, subdwarfs, white dwarfs, neutron stars, and black holes are also found as members of eclipsing binaries. And since 1999 with the discovery of HD 209458 as a short period eclipsing exoplanet system (Charbonneau *et al.* 2000), an increasing number of eclipsing planet-star systems (referred to as transiting exoplanet systems) have been discovered. Many of these systems have multiple planets. At the time of writing (May 2012) there are 2,321 exoplanet candidates, and 690 confirmed exoplanets—totaling about 3,012 possible exoplanets listed on the Kepler Mission web page. For a summary, see http://planetquest.jpl.nasa.gov. The vast majority of these exoplanets were discovered over the last three years from planetary transits in ultra-high precision photometry from the Kepler Mission (see Borucki *et al.* 2011) as well as many exoplanets found from the CoRoT Mission (see http://smsc.cnes.fr/COROT/).

2. Eclipsing binaries as astrophysical laboratories

The information provided by the study of eclipsing binaries quite often transcends the data obtained about stellar masses, radii, and luminosities (important as these quantities are to stellar physics and evolution). Certain types of eclipsing systems have properties that make them well-suited as astrophysical laboratories for the study of many diverse and important problems in modern physics and astronomy. A representative list of the major classes of binaries and the corresponding properties that make them astrophysically interesting is given in Table 1. Eclipsing binaries provide vital information on stellar atmospheres (limb darkening, gravity darkening, and atmospheric

eclipse studies), stellar interiors and structure (through apsidal motion studies of eccentric eclipsing binaries), stellar activity and magnetic dynamos (X-ray, *UV*, and radio eclipse mapping of stellar coronae and chromospheres), and plasma physics (binaries with accretion disks). Moreover, there are a small number of systems that are well-suited for testing general relativity through apsidal motion studies. Others can be used for independent determinations of cosmic fractional helium abundances (Y), and some eclipsing binaries can be used to check the importance of convective overshooting in the nuclear cores of stars. For more details see "The Brave New World of Binary Studies" (Guinan and Engle 2006).

3. The study of eclipsing binaries by amateur astronomers—past and future

With the availability of reasonably priced, high quantum-efficiency (>70%) charge-coupled devices (CCDs), it is now possible for amateur astronomers to produce high quality photometry and light curves of relatively faint (~10–18th magnitude) eclipsing binaries with small to moderate aperture (<0.5 m) telescopes. Moreover inexpensive (or free) software is available to reduce and analyze the CCD observations. With modest equipment and a good CCD photometer, the studies of many different kinds of interesting eclipsing binaries are within the reach of many amateur astronomers. These include astrophysically attractive eclipsing binaries (see Table 1) as well as those that are members of open clusters and globular clusters, and even those in some nearby galaxies have become possible (also see section 4 of this paper). Moreover, with CCDs, useful spectroscopy of many brighter eclipsing systems is now being acquired by an increasing number of amateur astronomers. This revolution in technology has led to some changes in the approach to the study of eclipsing binaries by amateur astronomers.

In 1965, an Eclipsing Binary Committee (EBC) was established within the AAVSO. There is an excellent summary paper about the accomplishments of the EBC by Williams *et al.* (2012, this volume) and the wealth of work done by the members of this group. From mostly visual observations, AAVSO observers determined and published ~17,000 eclipse timings, determined periods, and secured light curves of mostly neglected or newly discovered eclipsing systems. They also improved ephemerides and updated periods for many systems. However, in the amateur CCD photometry era (starting in the late 1990s), visual observations of eclipsing binaries have become less important. Because of this, in 2005 the EBC was reconstituted as the Eclipsing Binary Section of the AAVSO and now focuses on mostly CCD photometry. Eclipse timings determined from PEP or CCD measures are the order of ~10 to 100 times more accurate than can be realized from visual timings. Of course, as stated by Williams *et al.* (2012): "When visual eclipse timings were the only data available, they were invaluable." The unique value of visual timings of eclipsing

binaries is well illustrated in Figure 1 (from Kreiner *et al.* 2005), which shows the (O–C)-plot of eclipse timings of β Lyr going back to the time of Goodricke. The parabolic nature of the (O–C) values indicates that β Lyr's orbital period is increasing by (a huge) ~19 sec/yr. due to rapid mass exchange and loss.

However, even if visual observations of eclipsing binaries have become less valuable scientifically, watching a star fade by ~1 magnitude or more in a few hours (as in the case of Algol and many other similar systems) remains a thrill!

4. Some examples of observing and research programs of possible interest to amateur astronomers

In the following sections, we have selected several themes from this imposing list of binary studies for expanded development. The choices illustrate some new and exciting things we can learn about eclipsing binaries and that can be done by amateur astronomers.

• *The Pro-Am Cooperation and Collaboration:* Continue to partner with professional astronomers to carry out coordinated photometry and spectroscopy of astrophysically interesting eclipsing binary systems and selected transiting exoplanet systems that are being done (or planned) with space missions such as Kepler, Hubble Space Telescope (HST), Chandra X-ray Observatory, and XMM-Newton X-ray missions and others. Standardized *BVR* observations of X-ray binaries, chromospherically active binaries, and exoplanet systems are vital in correctly interpreting these stars. As in the case of CVs (some of which are eclipsing binaries), AAVSO members have played important roles in the past and will continue to do so. The cooperation between amateur and professional astronomers in the study of CVs is discussed by Szkody and Gaensicke (2012) in this volume. Participation in observing campaigns and Citizen Sky Programs on selected targets such as the recently completed program on the long-period eclipsing binary ε Aur is fun, engaging, and builds a sense of community as well as provides important contributions to Astronomy.

• *Photometry of bright Eclipsing Binaries undergoing rapid evolution:* For those who have photoelectric (PEP) or photodiode photometers, securing modern light curves of many eclipsing systems (brighter than ~5th mag.) is scientifically valuable. With sensitive CCD photometers photometry of bright (often neglected) eclipsing binaries is not practical or even feasible. Many of the brightest prototypical classical eclipsing binaries—such as Algol, β Lyr, U Cep, R Ara, VV Cep, μ Sgr, and many others are worth observing with photoelectric/diode photometers with standard *BVR* filters since in several cases their light curves and orbital periods change with time.

• *Eclipsing Binaries with Changing Eclipse Depths (orbital plane precession):* Photometry of eclipsing binaries that are undergoing rapid changes in their eclipse shapes and depths over time could be another interesting program. Most notable among these are several eclipsing binaries that have apparently stopped eclipsing, such as SS Lac (Torres 2001), QX Cas (Bonaro *et al.* 2009), and SV Gem (Guilbault *et al.* 2001). For QX Cas, Figure 2 shows the changes in the eclipse depths of QX Cas over the last fifty years and Figure 3 shows the derived model of the system depicted at secondary eclipse for these epochs. A recent list of such eclipsing binaries (or former eclipsing binaries) is given by Mayer (2005) and more recently by Zasche and Paschke (2012). Eclipsing binaries that have apparently stopped eclipsing include QX Cas, SV Cen, SV Gem, AY Mus, and SS Lac, while those whose eclipse depths are changing include IU Aur, V685 Cen, AH Cep,V699 Cyg, HS Hya, RW Per, V907 Sco, and possibly even Algol. The cause of these light curve variations, including the cessation of eclipses, is best explained from the precession of their orbital planes (that is, change of the inclination of their orbits) arising from the gravitational effects of a third star. The recent study of HS Hya by Zasche and Paschke (2012) indicates that its eclipses are becoming very shallow and that this would be an excellent star to observe as soon as possible. Also it would be worthwhile to secure photometry of the above systems to search for changes in their light curves (that is, eclipse depths). For example, the depth of the primary eclipse of Algol has not been checked for several years and this could also be a good project.

• *Coordinated* BVR *photometry of Eclipsing Binaries discovered by the Kepler Mission:* An interesting and important program would be to carry out coordinated CCD observations of interesting (and unusual) eclipsing binaries discovered recently by the Kepler Mission (see Prša *et al.* 2011; Slawson *et al.* 2011). Kepler returns exquisite ultra-high precision photometry and beautiful light curves but the photometry is essentially unfiltered, covering a very broad wavelength range. Standardized *BVR* photometry (even though much less precise than returned by Kepler) of selected ~10–14th magnitude Kepler eclipsing binaries would be very useful to help to better define the physical properties of the stars—especially the stars' temperatures. Systems with deep eclipses, or eccentric orbits, or with pulsating components, as well as those with changing light curves from the Kepler Mission sample of nearly 2,200 stars are the most compelling to observe. Carrying out photometry during the eclipses with multiband photometry is particularly valuable. It should be noted that the ultra-high precision photometry from Kepler on these stars (and ~150,000 others) is available for study from NASA's Mikulski Archive for Space Telescopes (MAST) website at http://archive.stsci.edu. The instructions for downloading, plotting, and analyzing

these exquisite data are also available at the MAST site or can be found at the Kepler Mission website. This is worth taking a look at on cloudy nights. Programs for analyzing light curves of eclipsing binaries are discussed later in the paper.

• *Supporting* BVR *photometry (and Spectroscopy) for the BRITE-Constellation Mission:* An interesting program suitable for amateurs would be to carry out standardized photoelectric (PEP) or photodiode *BVR* photometry of bright eclipsing binaries that will be monitored by the BRITE-Constellation Mission starting this year. The BRITE-Constellation Mission is a planned network of up to six Nano-satellites designed to carry out filtered time-series photometry of the brightest stars in the sky (down to ~4th mag.). Each will fly a small-aperture telescope (3 cm) with a CCD camera to perform high-precision filtered (one filter designated for each instrument) photometry of the brightest stars in the sky (< 4th mag.) continuously for up to several years. These Nano-satellites are 20-cm cubes and each "orbiting camera" has a field of view of ~24 degrees. The first two of these satellites are expected to be launched during 2012. The BRITE Mission research team would be interested in collaborations with amateurs to carry out coordinated photometry (or better yet spectroscopy) of BRITE targets when these stars are being observed by the mission. This could be an interesting project—see BRITE (http://www.brite-constellation.at/).

5. Data mining: "observing" without a telescope—exploiting archival eclipsing binaries

As discussed previously (in the case of the Kepler Mission), there are large photometric data sets on variable stars, including eclipsing binaries, that are available over the internet. These archival data can be used directly or to supplement photometry for the study of eclipsing binaries. For example, photometry from early micro-lensing programs such as EROS, MACHO, and OGLE are available over the internet. These programs operated during the 1990s and serendipitously discovered thousands of relatively faint (fainter than 14th magnitude) eclipsing binaries in the Large and Small Magellanic Clouds, and also in the direction of the center of our Galaxy in the Galactic Bulge region. Data from these programs are available over the internet but much of this photometry has been exploited and published. However, some astronomical nuggets could turn up with deeper data mining.

The All Sky Automated Survey (ASAS) is a Polish project started in 1997 as a follow-up to the successful OGLE program. But unlike the previous survey programs, the ASAS program is devoted to the study of variable stars. It is a wide field ($4 \times 4°$ per pointing) photometric monitoring program to observe ~18 million stars south of declination +28° and brighter than ~14th magnitude. This

highly successful variable star discovery and monitoring program uncovered over 50,000 variable stars including many eclipsing binaries (~80% of which are new variables). The photometry from ASAS is available over the internet (see: http://www.astrouw.edu.pl/asas/). Recently ASAS-North started operations so that photometry from that program may also soon be available.

In the near future, hundreds of thousands (possibly millions) of additional eclipsing system are expected to be discovered by Pan-STARRS, the Large Synoptic Survey Telescopes (LSST), and from space with the ESA Gaia Mission. Gaia has a billion-pixel CCD array that will measure positions and fluxes (magnitudes) for over one billion stars and galaxies (see http://gaia.esa.int/ for more information). Gaia is planned to be launched during 2013. Also, there are several transit planet search missions being carried out with networks of small telescopes. In addition to discovering exoplanet transit systems, they are also returning photometry for eclipsing binary stars. A partial list of some of these planet-search programs include: HATNet, MEarth, SuperWASP, and several others. And last but not least is AAVSOnet—a network of robotic photometric telescopes being developed by Arne Henden for use by AAVSO members and others to carry out photometry of variable stars (see http://www.aavso.org/aavsonet). AAVSOnet can be used free-of-charge by AAVSO members to carry out photometry of specific (~9–15th mag.) eclipsing binary systems (among other targets).

To help cope with the expected deluge of data (petabytes) in the near future from these programs, we are developing a Neural Network (NN) Artificial Intelligence (AI) based program to help to automatically analyze the light curves of tens of thousands of eclipsing binaries (see Prša *et al.* 2008; Guinan *et al.* 2009). More information can be found at the PHOEBE or EBAI websites.

6. Examples of useful programs and software for work on eclipsing binaries

Several examples of programs and software available for the study of eclipsing binaries are given below. These programs and websites are useful for modeling the light curves of eclipsing binaries and also to visualize most types of eclipsing binaries. Several additional programs (and software) are available over the internet.

PHOEBE (PHysics Of Eclipsing Binaries) is an excellent free downloadable astronomical software that permits the modeling of eclipsing binaries (EBs) based on real photometric and spectroscopic (radial velocity) data. It is based on the Wilson-Devinney code (Linux or Unix based). The software is highly recommended. The PHOEBE homepage is located at: http://phoebe.fiz.uni-lj.si. The contact person for PHOEBE is Dr. Andrej Prša.

BINARY MAKER 3 is commercial software (cost ~100 USD) that accurately calculates light and radial velocity curves for almost any type of binary, simultaneously displaying the theoretical and observed curves as well as a 3-D

model of the orbiting stars. Professional-quality PostScript output can be created of all the major displays. The program comes complete with an extensive User Manual on a CD as well as a very complete Help System which not only explains how to use the program but also gives details on how to analyze eclipsing binary light curves. Individual displays can be customized and saved to meet the user's needs. Star spot modeling, eccentric orbits, and asynchronously rotating stars can also be accurately modeled (www.binarymaker.com).

STARLIGHT PRO produces animations of eclipsing binary stars and generates synthetic light curves. The effects of limb darkening, temperature, inclination, stellar size, mass ratio, and star shape are included. There is a free download for Windows (see http://www.midnightkite.com/index.aspx?URL=Binary for more information) .

NIGHTFALL eclipsing binary star program is online software that can be used to produce animated views of eclipsing binary stars, calculate synthetic light curves and radial velocity curves, and eventually determine the best-fit model for a given set of observational data of an eclipsing binary star system (Linux or Unix based: www.hs.uni-hamburg.de/DE/Ins/Per/Wichmann/Nightfall.html).

ECLIPSING BINARY SIMULATOR (EBS) is a Window-based astronomy application to visualize the orbit and synthetic light curve of binary star systems. EBS was mainly developed for educational purposes and visualization of different types of eclipsing binary systems. This is an easy application to use to pass time on cloudy nights (see: http://astro.unl.edu/naap/ebs/anima).

7. Conclusions and future projections

Since the discovery of the first eclipsing binary system nearly 230 years ago by John Goodricke, these fascinating stars (and stars with transiting planets) have played important roles in the development of Astronomy. The availability of sensitive CCDs, photometric reduction and analysis programs, and reasonably priced telescopes has created a revolution, making it possible for motivated amateur astronomers to make significant contributions to this field. Moreover, CCDs, when coupled with commercially available spectrographs, also now make it possible to conduct useful spectroscopy of the brighter stars even with small telescopes.

Also past, present, and future wide-field photometry programs are providing (or will soon provide) the ever-expanding datasets on eclipsing binary stars in the Milky Way Galaxy and beyond. It is expected that over one million eclipsing binaries will be discovered within the next decade by these programs. It is hoped that important contributions will continue to be made by amateur astronomers in the exciting field of eclipsing binaries. It should be noted that many amateur astronomers today have more powerful equipment and telescopes (some completely robotic) than most professional astronomers had access to as recently as a few decades ago. So go for it and enjoy the ride! (and the eclipses!).

8. Acknowledgements

The authors acknowledge the hard work and efforts made over the last century (and up to the present) of the avid AAVSO, and other, amateur observers of eclipsing binary systems. Many have spent cold nights securing light curves or eclipse timings to improve orbital periods and study changes in periods. The authors wish to acknowledge support of grants from NASA and NSF for this study. We also thank the editors of this special AAVSO centennial volume for the work put in producing a fine compilation of papers. Also we wish to thank them for their patience and understanding for the late submission of this paper.

References

Andersen, J. 1991, *Astron. Astrophys. Rev.*, **3**, 91.

Bonaro, M., Guinan, E. F., Prša, A., and Zola, S. 2009, *Bull. Amer. Astron. Soc.*, **41**, 301.

Borucki, W. J., *et al.* 2011, *Astrophys. J.*, **728**, 117.

Charbonneau, D., Brown, T. M., Latham, D. W., and Mayor, M. 2000, *Astrophys. J., Lett. Ed.*, **529**, L45.

Guilbault, P. R., Lloyd, C., and Paschke, A. 2001, *Inf. Bull. Var. Stars*, No. 5090, 1.

Guinan, E. F., and Engle, S. G. 2006, *Astrophys. Space Sci.*, **304**, 5.

Guinan, E. F., Prša, A., Devinney, E. J., and Engle, S. G. 2009, in *The Eighth Pacific Rim Conference on Stellar Astrophysics*, ASP Conf. Ser. 404, Astron. Soc. Pacific, San Francisco, 361.

Guinan, E. F., Ribas, I., and Fitzpatrick, E. L. 2004, in *Variable Stars in the Local Group*, eds. D. W. Kurtz and K. R. Pollard, IAU Colloq. 193, ASP Conf. Ser. 310, Astron. Soc. Pacific, San Francisco, 363.

Kreiner, J. M., Kim, C. H., and Nha, Il-S. 2005, "An Atlas of O–C Diagrams of Eclipsing Binary Stars" (http://www.as.ap.krakow.pl/o-c/index.php3).

Mayer, P. 2005, *Astrophys. Space Sci.*, **296**, 113.

Moffett, T. J., and Barnes, T. G. 1983, *Inf. Bull. Var. Stars*, No. 2413, 1.

Prša, A., Guinan, E. F., Devinney, E. J., DeGeorge, M., Bradstreet, D. H., Giammarco, J. M., Alcock, C. R., and Engle, S. G. 2008, *Astrophys. J.,* **687**, 542.

Prša, A., *et al.* 2011, *Astron. J.*, **141**, 83.

Sandage, A., and Tammann, G. A. 1969, *Astrophys. J.*, **157**, 683.

Slawson, R. W., *et al.* 2011, *Astron. J.*, **142**, 160.

Szkody, P., and Gaensicke, B. T. 2012, *J. Amer. Assoc. Var. Star Obs.*, **40**, 563.

Torres, G. 2001, *Astron. J.*, **121**, 2227.

Williams, D. B., Baldwin, M. E., and Samolyk, G. 2012, *J. Amer. Assoc. Var. Star Obs.*, **40**, 180.

Zasche, P., and Paschke, A. 2012, *Astron. Astrophys.*, **542**, L23.

Table 1. Binary systems as astrophysical laboratories.

Type of system	*Properties*
Detached eclipsing systems: both components located within their Roche lobes; form the backbone for the Mass-Luminosity Law.	Masses, radii, luminosities, and densities of stars; checks on stellar evolution; fundamental properties and precise distances.
Eclisping binaries with pulsating components (such as δ Sct, β Cep, γ Dor variables, and Cepheids). Examples: δ Cap, RZ Cas, R CMa....	Permits the measurement of radii, masses, densities, age, and evolution of the pulsating components. Calibration of age-mass for astereoseismology studies.
Eclipsing binaries with eccentric orbits: apsidal motion studies—internal structure of stars / tests of General Relativity in a few cases. Also "Heart Beat" Stars—induced pulsations near orbital periastron observed from Kepler data. A possible bright "Heart-beat" binary is μ Sgr.	Apsidal motion—stellar structure and interiors; gravitationally induced pulsations; several systems provide tests of general relativity. "Heart beat" binaries can provide probes of the internal structure of stars.
Chromospherically active binaries: RS CVn, BY Dra, and related systems.	Magnetic activity; star spots, chromospheric and coronal emissions; "solar-stellar connection."
Semi-detached systems: Algol-type binaries; W Ser and β Lyr—mass exchanging / losing systems.	Stellar and binary star evolution; mass exchange and loss; accretion processes; enrichment of ISM from mass loss.
Contact Binaries: a) Cool: W UMa-type systems (W UMa, VW Cep….); b) W-type / A-type systems (AW UMa).	Stellar activity and magnetism; binary star evolution; angular momentum loss; binary star coalescence from studies of long-term changes in orbital periods.
Hot contact systems: AO Cas-type systems; Wolf-Rayet (WR) binaries (e.g. V444 Cyg).	Binary star evolution and dynamics; interacting winds; mass loss (chemical enrichment of ISM).

Table 1 continued on following pages

Table 1. Binary systems as astrophysical laboratories, cont.

Type of system	*Properties*
Near Contact Systems (NCBs): V1010 Oph-type and FO Vir-type systems.	Stellar evolution; mass transfer and loss; magnetic activity in systems with cool components; marginal contact systems. Light curves change with time.
ζ Aur and VV Cep Systems: Long period interacting supergiants systems and ε Aur; supergiant + large disk (see recent AAVSO Citizen Sky Project).	Properties of evolved supergiant stars: masses, radii and atmospheric structure (from atmospheric eclipses) of evolved stars; mass loss rates; accretion processes.
Cataclysmic variables (CV) and nova-like (NL) binaries: (see Szkody and Gaensicke 2012, this volume).	Masses of white dwarf stars; accretion/accretion disks; accretion and plasma physics; angular momentum loss from magnetic braking and relativistic effects.
X-ray binaries with neutron star and black hole components: Low mass X-ray binaries (LMXBs) with neutron stars and high mass X-ray binaries (HMXBs) with mostly black hole components and related systems.	Properties of neutron stars; accretion; physics of hot plasmas and magnetic fields; black holes (e.g. Cyg X-1, CAL 87, V404 Cyg, Cir X-1).
Planet-star systems (transiting exoplanets); HD 209458 / hot Jupiter transiting exoplanets; over 690 verified systems from radial velocity and transits studies.	Properties of exoplanets (mass, radii, and densities); frequency of exoplanets; discovery of Earth-size planets from transits from Kepler and CoRoT Missions (3,100+ verified and exoplanet candidates).
Symbiotic Binaries: (M III + wd); long period binaries (examples of eclipsing symbiotic variable include CH Cyg, AR Pav, and V1413 Aql).	Wind accretion and mass loss rates from red giants; plasma physics. Some with high mass white dwarfs could be SN Ia progenitors.

Table 1 continued on next page

Table 1. Binary systems as astrophysical laboratories, cont.

Type of system	*Properties*
Eclipsing binaries displaying rapid changes in their light curves: 1. Evolutionary changes/mass loss/ mass exchange (e.g. W Ser, β Lyr, R Ara…). 2. Changes in eclipse depths from variations in their orbital inclinations as viewed from Earth (examples: SS Lac, SV Gem, and QX Cas, have stopped eclipsing. 3. Varying star spot coverage and star spot cycles; RS CVn and related stars.	1. Test beds for stellar and binary star evolution. Studies of mass exchange and mass loss. 2. Dynamical test beds for effects of tertiary companions on the orbits of the close eclipsing binary. The third body causes the orbit to precess. 3. Study star spot properties and motions including differential rotation and also possible star spot cycles. Use eclipses to map star's surface.
Post common envelope binaries: main-sequence star + white dwarf systems: V471 Tau; Binary Nuclei of Planetary Nebulae; Pre-CV systems and double degenerate short period systems.	Common envelope evolution; mass loss / chemical enrichment of ISM / subdwarfs / white dwarf. Double-degenerate (D-D) systems are important to study but are faint and need high speed photometry. The more massive D-D systems are candidates for Type-Ia Supernovae.

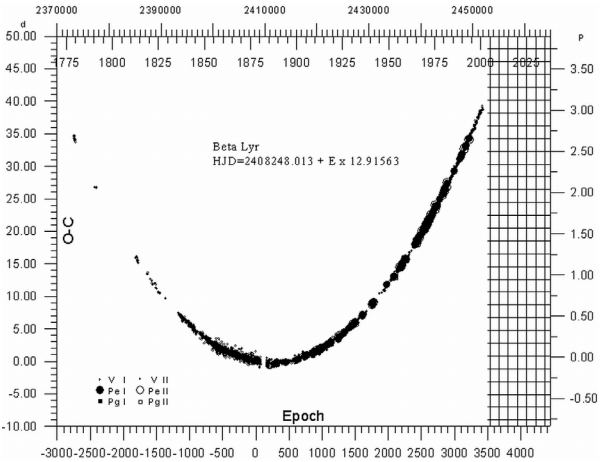

Figure 1. The O–C plot for β Lyr eclipse timings, including AAVSO data, from Kreiner *et al.* (2005). The orbital period is found to be increasing by ~19 sec/year due to rapid mass exchange and loss. The amount of mass being transferred between the two stars (or lost) is ~ 2×10^{-5} solar masses per year, or the equivalent of the Sun's mass every ~50,000 years.

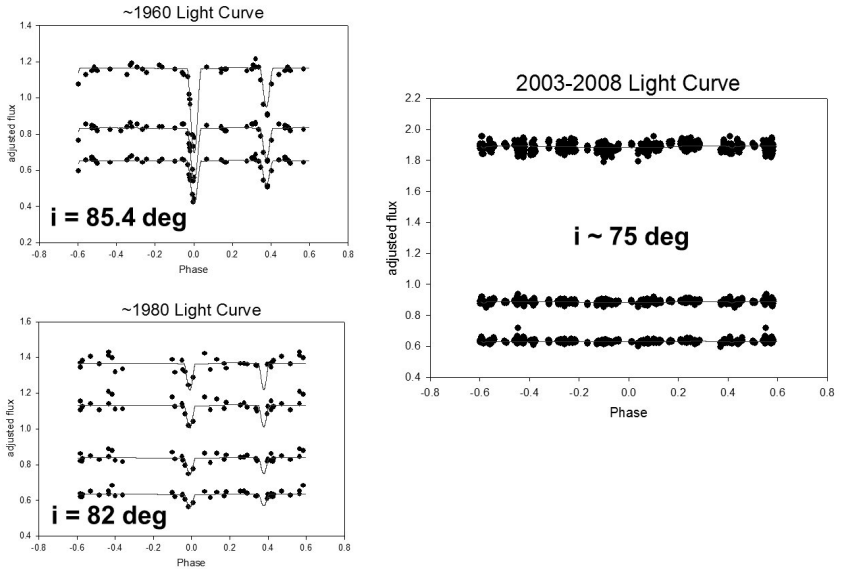

Figure 2. QX Cas light curves and PHOEBE model fits, showing changes in the orbital inclination. The epoch ~1960 UBV photometry is from Sandage and Tammann (1969) and the epoch ~1980 UBVR photometry is from Moffett and Barnes (1983); the 2003–2008 photometry was secured with the Four College Automatic Photoelectric Telescope by the authors. The photoelectric UBV and UBVR light curves of QX Cas (V ~ 10.5 mag; P = 6.007 days; e = 0.21) are shown for three observing epochs. Analyses of the light curves were carried out using the PHOEBE program and the best model fits are plotted among the data. No eclipses are evident from photometry secured after 2003 (even during the mid-1990s photometry of QX Cas from Arne Henden shows no evidence of eclipses). The resulting orbital inclinations are shown in the plots. The light curve analysis shows that QX Cas consists of B1.5V and B3IV stars with masses of M_1~ 5.5 $M_\odot$ and M_2 = 6.5 $M_\odot$, respectively and fractional radii (R/a) = 0.11 and 0.16. QX Cas is a member of the young open cluster NGC 7790 at an estimated distance of 3.3 kpc. Solutions adopted from Bonaro *et al.* 2009.

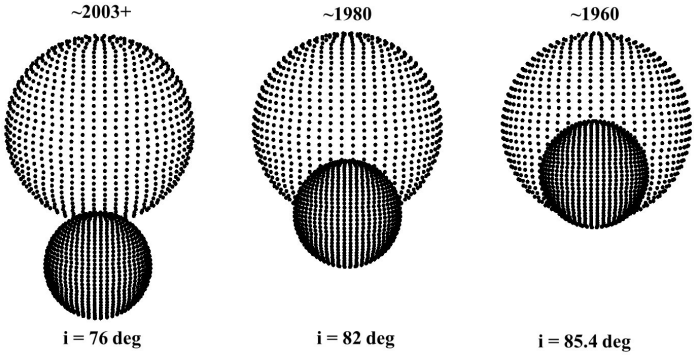

Figure 3. The models of the eclipsing binary QX Cas are shown at secondary eclipse. The relative sizes of the stars and orbital inclinations are derived from the analysis of the available photoelectric light curves using PHOEBE. As shown, the orbital inclination decreases from i ~85.4° during ~1960 to i ~76° from 2003 onward (from the analysis of the Villanova photometry).

RR Lyrae Stars: Cosmic Lighthouses With a Twist

Katrien Kolenberg
Harvard-Smithsonian Center for Astrophysics, 60 Garden Street, Cambridge, MA 02138; kkolenbe@cfa.harvard.edu

and

Instituut voor Sterrenkunde, University of Leuven, Celestijnenlaan 200D, B 3001 Heverlee, Belgium

Invited review paper, received May 7, 2012

Abstract Since their discovery over a century ago, RR Lyrae stars have proven to be valuable objects for the entire field of astrophysics. They are used as standard candles and witnesses of galactic evolution. Though the pulsations that cause their light variations are dominated by relatively "simple" radial modes, some aspects of RR Lyrae pulsation remain enigmatic. Besides the visual, photographic, and photometric observations of these stars that span several decades, spectroscopic data provide an in-depth view on the pulsations. In the past decade, particularly since the launch of the satellite missions with asteroseismology as part of their program (for example, MOST, CoRoT, and Kepler), several findings have helped us better understand the structure and pulsations of RR Lyrae stars. Nevertheless, ground-based observations and long-term monitoring of RR Lyrae stars, as done by the AAVSO members, remain of utmost importance.

1. A century of RR Lyrae studies

The story of the discovery of the RR Lyrae stars starts at the end of the 19th century with the globular cluster studies initiated by Harvard astronomer Solon I. Bailey, rendering many variable stars. Those variables that were seen in large numbers, with short periods of under a day and photographic amplitudes of about one magnitude, were called cluster variables. Soon thereafter, similar variables were found in the field. Initially, the "cluster variables" were put in the same basket as the Cepheids because of the similarities in their light curves. When it was recognized that there are notable differences between the two types of stars (period, location, population type, kinematical properties), RR Lyrae itself, the brightest field star of this type discovered by Williamina Fleming in 1899, became the eponym of the class.

Both Cepheids and RR Lyraes were first thought to be variable due to a binary nature. The foundations for stellar pulsation theory that explains the light variations in RR Lyrae stars were laid by Eddington (1926).

2. What are they and why do we care about them?

RR Lyrae stars are pulsating low-mass stars that have evolved away from the main sequence and are burning Helium in their core. In the Hertzsprung-Russell diagram (HRD) they are located on the horizontal branch and its intersection with the so-called instability strip (see Figure 1). In this strip, crossing the HR diagram nearly vertically, pulsations are driven by the kappa (κ) mechanism. Kappa stands for the opacity of a stellar layer, its capacity to block incoming radiation. In most of the inside of stars, the opacity of stellar gas decreases as its temperature increases. However, there are some regions where this tendency gets weak, or even reversed. For example, in the hydrogen and helium partial ionization zones, connected to specific temperatures, the opacity increases as the temperature increases, that is, with compression. These zones, especially the helium partial ionization zones, are considered to be the regions for pulsation excitation in classical Cepheids and RR Lyrae stars. At compression, ionized material increases the opacity and the layer is pushed upwards by radiation pressure. When the layer moves up and reaches lower temperatures, recombination happens, the opacity decreases, the layer falls back, and the cycle is repeated. In order to be efficient drivers of pulsation, these partial ionization zones should be located at a critical depth in the star. For this, a suitable combination of stellar properties is needed, which is why the κ mechanism driven pulsations are confined to specific regions in the HRD, such as the instability strip.

RR Lyrae stars have typical periods of ~0.2 to ~1 day, amplitudes in the optical of 0.3 up to 2 magnitudes, and spectral types of A2 to F6. Most of them pulsate in the radial fundamental mode (called Bailey type RRab stars), the radial first overtone (Bailey type RRc stars), and, in some cases, in both modes simultaneously (RRd stars), see Figure 2. Type RRab stars have the larger light curve amplitudes (around 1 magnitude) and longer periods (~0.35–1 day); type RRc stars generally have more sinusoidal light curves with lower amplitudes (around 0.5 magnitude) and shorter periods (~0.2–0.45 day), though the period ranges overlap. The RRd stars pulsate in both radial modes simultaneously and hence have more complex light curves.

Since the large scale surveys and the satellite missions, higher-order radial overtone modes have been detected in RR Lyrae stars (Olech and Moskalik 2009; Benkő *et al.* 2010).

As the RR Lyrae stars are indeed occupying a small range in V magnitude on the horizontal branch (see Smith 1995), they qualify as excellent distance indicators. When we know their luminosity or absolute magnitude, this can be of great help in estimating the distances (and hence the ages) of globular clusters, and to galactic and extragalactic (local group) locations. Moreover, as an old stellar population and found in large numbers, the RR Lyrae stars can be used as witnesses of chemical and dynamical galactic evolution.

They also serve as test objects for low-mass stellar evolution and radial pulsation theory.

A frequency spectrum of an RR Lyrae star will typically show the main pulsation frequency (corresponding to the radial fundamental mode or the first overtone) as well as its harmonics (double, triple, quadruple frequency, and so on). Especially for the RRab stars, pulsating with higher amplitudes reflected in their non-sinusoidal light curves, the harmonics will be very prominent.

3. So we know what they are all about?

Despite their numerous applications in various fields of astrophysics, several aspects of RR Lyrae pulsation remain not fully understood.

One not completely resolved issue concerns the *Oosterhoff dichotomy* (Oosterhoff 1939). RR Lyrae-rich globular clusters can be divided into two groups on the basis of the properties of their RR Lyrae stars. Oosterhoff type I clusters, such as M3 and M5, contain many more RRab stars than RRc stars. The mean periods of both types of pulsators are 0.55 day for RRab stars and 0.32 day for RRc stars, respectively. Oosterhoff type II clusters, such as ω Cen, M15, and M53 have more nearly equal numbers of RRab and RRc stars and longer mean periods of 0.64 day and 0.37 day, respectively. There is a correlation with metallicity: Oosterhoff type II are more metal-poor than their Oosterhoff type I counterparts.

The most popular theoretical explanation for this phenomenon relies on a so-called "hysteresis mechanism" (van Albada and Baker 1973). There is an "either-or" region in the middle of the RR Lyrae instability strip where the pulsation mode is determined by the star's previous evolutionary path. RR Lyrae stars in Oosterhoff type II clusters are evolved from a position on the blue horizontal branch, whereas those in Oosterhoff type I globulars contain a mix of evolved and unevolved stars.

The existence of the Oosterhoff gap at $< P_{ab} > = 0.60$ day, among the halo clusters, and its absence among the galaxy's satellite systems, indicates that the halo could not have been built through the merger of systems exactly like the early counterparts of the Milky Way's current satellite galaxies (Catelan 2006).

I will now focus on one of the most stubborn and long-standing mysteries in stellar pulsation theory, the so-called *Blazhko effect*, since it is a phenomenon that observers of RR Lyrae stars are likely to encounter.

In 1907, Sergei Nicolaevich Blazhko reported on the periodic variations in the timing of maximum light for the star RW Dra (Blazhko 1907). Soon after that, it was realized that other, similar stars showed modulations of their light curve shape over time scales of weeks or even months. In 1916 Harlow Shapley reported on the changes in the spectrum, period, and light curve of the prototype RR Lyr itself. The Blazhko effect, as this periodic amplitude and phase modulation is called nowadays, turned out to be rather common in

RR Lyrae stars. Previously reported galactic occurrence rates were 20–30% for Galactic RRab stars and a few percent for RRc stars (Szeidl 1988), and somewhat lower in the LMC: 12% RRab and 4% RRc (Alcock *et al.* 2000, 2003). The most recent surveys, however, both from the ground (Jurcsik *et al.* 2009b) and from space (Szabó *et al.* 2009; Benkő *et al.* 2010), seem to indicate that close to 50% of the fundamental mode RR Lyrae pulsators show the Blazhko effect (Figure 3).

In the frequency spectra of Blazhko stars we will see multiplets with equidistant spacing (equal to the Blazhko frequency) around the main frequency and its harmonics (some schematic examples are shown in Figure 4). These reflect the amplitude and phase modulation happening in the star (see also Benkő *et al.* 2011).

After several decades of dedicated studies of Blazhko stars, a variety of behavior is observed in these stars: changing Blazhko cycles, additional longer cycles, multiple modulation periods, complex multiplet structures in the frequency spectra, additional frequencies corresponding to higher overtone modes.

3.1. Multicolor data and spectroscopy

Early studies of RR Lyrae variables, including Blazhko variables, were based on photographic and photometric data of the stars, often focusing around maximum light for the purpose of O–C ("observed minus calculated," comparing expected with observed times of maximum light). From complete light curves of the stars we can get much more information on their pulsation properties.

For a real in-depth study of RR Lyrae stars, however, multicolor and spectroscopic data are the way forward.

Approaches to derive atmospheric parameters of RR Lyrae stars through multicolor photometry and/or spectroscopy, such as applied by De Boer and Maintz (2010), Sódor *et al.* (2009), Kolenberg *et al.* (2010a), and For *et al.* (2011), allow us to connect the complex atmospheric variations with the pulsation patterns, and even their modulations.

Sódor *et al.* (2009) devised an inverse photometric Baade-Wesselink method for determining physical parameters of RRab variables exclusively from multicolor light curves. Its application to the Blazhko star MW Lyr (Jurcsik *et al.* 2009a) shows how the mean global parameters, such as the radius, luminosity, and surface effective temperature of a modulated star vary over the Blazhko cycle. As a consequence, the instantaneous period varies over the Blazhko cycle. This modulation of the stellar parameters throughout the modulation is a very important result for the further development of Blazhko models.

RR Lyrae stars have rather tumultuous atmospheres due to high pulsation velocities in the outer layers of the star. This gives rise to shock waves in particular pulsation phases, reflected in spectral line broadening and doubling

(Gillet and Crowe 1988). Moreover, there is a gradient in velocity between different layers in the star, the so-called Van Hoof effect (Mathias *et al.* 1995).

In addition, new and exciting findings such as the occurrence of Helium emission (Preston 2009) and neutral line disappearance (Chadid *et al.* 2008) would be very interesting to study as a function of the Blazhko phase. These methods, and their extensions, in combination with high-precision and/or long-term photometric data, allow us to perform (literally) in-depth studies of the Blazhko phenomenon. As pointed out by Kovács (2009), accurate time-series spectral line analysis is needed to reveal any possible non-radial components.

3.2. Models for modulation

More than a century after the discovery of the Blazhko effect, we still are at a loss for a definitive explanation. But we are narrowing down the possibilities.

Until recently, the nonradial resonance model (Van Hoolst *et al.* 1998; Dziembowski and Mizerski 2004, and references therein) and the magnetic model (Shibahashi and Takata 1995; Shibahashi 2000, and references therein) were most commonly quoted. They both rely on the excitation of nonradial pulsation mode components in the modulated star, and state a connection between the modulation period and the rotation period. They provide predictions for the appearance of the Fourier spectra of modulated stars. The magnetic model for the Blazhko effect received some blows when spectropolarimetric observations indicated that a strong kiloGauss-order dipole field, a premise in the model (Shibahashi 2000), is not present in the prototype RR Lyr (Chadid *et al.* 2004) nor in a sample of seventeen selected modulated and non-modulated RR Lyrae stars (Kolenberg and Bagnulo 2009).

As neither of both models could explain the variety of observed behavior in Blazhko stars, an alternative idea was (re-)proposed by Stothers (2006, 2010). In this scenario, the amplitude and phase (period) modulation is caused by the cyclical weakening and strengthening of the convective turbulence in the star. The variations in convective turbulence can be caused by a transient magnetic field in the star. The presence of such a field, however, would be very hard to demonstrate. What makes the Stothers (2006) idea attractive is that it does not require the presence of nonradial modes, nor a clockwork regularity in the Blazhko cycles. Also, the variations of the mean parameters of the star, as mentioned above, are a consequence of the modulation of turbulent convection in this model. The Stothers model was recently challenged by the findings by Molnár and Kolláth (2010) and Smolec *et al.* (2011) that the modulation of the convective strength should be unphysically large to cause the observed modulation.

The latest development in the models for the Blazhko effect were triggered by uninterrupted, high-precision observations of Blazhko stars, as described in the next section.

4. Progress: expected and serendipitous

Several space telescopes have asteroseismology (or the study of pulsating stars) as an important part (or prime by-product) of their mission and have performed high-precision observations of RR Lyrae stars: the Canadian suitcase-sized MOST telescope (Gruberbauer *et al.* 2007), the French-led ESA space mission CoRoT (Chadid *et al.* 2010), and NASA's Kepler mission (Kolenberg *et al.* 2010b). These space missions deliver high-precision data and are not disturbed by daily and weather gaps, typical for Earth-based observations.

The new data on Blazhko stars reveal complex multiplet structures in the Fourier spectra and additional frequency peaks of which some can be explained in terms of radial overtones, and others not (Chadid *et al.* 2010, Benkő *et al.* 2010). The Kepler data allow us to find the smallest detectable amplitude and phase modulation values. However, still about half of the RR Lyrae stars do turn out to be unmodulated (see, for example, Nemec *et al.* 2011).

By a fortunate coincidence, the star RR Lyr itself, the prototype of the class and a Blazhko variable studied for over a century, is located in the Kepler field. Though initially thought to be too bright to be observed successfully with Kepler, the flux of the star can be recovered thanks to a custom aperture especially devised for the star (Kolenberg *et al.* 2011). In RR Lyr we detected a new phenomenon, reflected in alternatingly high and low maxima (Kolenberg *et al.* 2010b). This effect can be rather large, regularly 0.05 magnitude in RR Lyr. In the frequency spectrum, these variations with the double period result in the appearance of so-called half-integer frequencies. This phenomenon, called period doubling, was reported in models of Cepheids, stars that undergo radial pulsations just like RR Lyrae stars (Moskalik and Buchler 1990). It had, however, never been observed before in observational data of Cepheids or RR Lyrae stars. Szabó *et al.* (2010) find that a 9:2 resonance between the fundamental radial mode and the 9th overtone might be responsible for period doubling. The fact that period doubling was also found in a few other Blazhko stars, and not in non-modulated stars, revealed a possible connection between period doubling and modulation (Figure 5).

Period doubling does not occur at all phases in the Blazhko cycle. It can be very obvious in some phases, and invisible in others. And just like sometimes there is no strict repetition from one Blazhko cycle to the next, period doubling does not repeat in the same Blazhko phases for consecutive cycles.

Why was period doubling not detected earlier in ground-based data, particularly for a star as well-studied as RR Lyr? Besides the fact that period doubling does not always occur, the main reason is undoubtedly that RR Lyrae stars have periods of around half a day, and, when observing from one site on Earth, consecutive pulsation maxima are usually missed.

The observation of period doubling sparked new modelling efforts (Szabó *et al.* 2010; Kolláth *et al.* 2011), and recently a new model for the Blazhko

effect was proposed by Buchler and Kolláth (2011). Using the amplitude equation formalism to study the nonlinear, resonant interaction between the two modes, they showed that the (9:2) radial resonance can not only cause period doubling, but it may also lead to amplitude modulation. Moreover, in a broad range of parameters the modulations can be irregular, just like recent observations show.

Therefore, we are now left with a new hierarchy for the models for explaining the Blazhko effect (Figure 6).

5. Pro-Am observations and RR Lyrae stars

Their large pulsation amplitudes, their pulsation periods, and their characteristic light curve shapes make the RR Lyrae stars easily distinguishable from other variables and gratifying targets for amateur observations.

Several groups worldwide have carried out observations of RR Lyrae stars. GEOS (Groupe Européen d'Observations Stellaires) is a European group of variable star observers with nearly eighty active members (of which ten are professionals). The GEOS RR Lyrae database (http://dbrr.ast.obs-mip.fr/) is intended to help observations and studies on RR Lyrae stars. It contains the times of light maximum of RR Lyrae stars obtained either visually, with electronic devices, or photographically. The data are collected in the literature (dating back to the end of the 19th century) or are submitted by the observers themselves (since 2004 also through automated observations). This database is a useful resource for the study of period changes in RR Lyraes, as well as the Blazhko effect.

The AAVSO has an impressive database of observations dating back more than a century. This database is a treasure chest for variable star research (including RR Lyrae stars) and part of these observations remain unpublished to date. Observations of RR Lyrae stars are gathered in the framework of the AAVSO's Short Period Pulsation Section. From time to time there are organized efforts focusing on legacy stars that have a Blazhko effect (see, for example, the AAVSO's "Variable Star of the Season Archive," http://www.aavso.org./vsots_archive).

Although the satellite missions deliver data with unprecedented precision on RR Lyrae stars, long-term monitoring of RR Lyrae stars is most valuable. Only such data can reveal phenomena happening on time scales of years, decades, or even longer, such as period changes due to stellar evolution, long-term changes in the Blazhko effect, and additional cycles with periods of years or longer. Sometimes sudden changes and transient phenomena can be observed in stars that have been followed for decades. Satellite missions and dedicated campaigns are limited in time. Moreover, the number of RR Lyrae stars observed with the satellite missions is limited, and generally the brighter stars, those that also can be followed more easily through spectroscopy, are not observed by

the space missions. Nowadays, amateur observers play a very important role in contributing to the data that allow these discoveries. For these endeavors to be satisfying and optimally useful, interaction between professionals and amateurs is important, clarifying what kind of observations (of which targets) are needed.

6. Acknowledgements

I thank the "professional amateurs" with whom I have had the pleasure to interact and collaborate over the past years, for their enthusiasm and interest in variable stars and their valuable contributions to this field of research. I gratefully acknowledge the financial support of my Marie Curie project (Project PIOF-GA-2009-255267 - "SAS-RRL").

References

Alcock, C., *et al.* 2000, *Astrophys. J.,* **542**, 257.
Alcock, C., *et al.* 2003, *Astrophys. J.,* **598**, 597.
Benkő, J, Szabó, R., and Paparó, M. 2011, *Mon. Not. Roy. Astron. Soc.,* in press, 2011arXiv1106.4914B
Benkő, J. et al. 2010, *Mon. Not. Roy. Astron. Soc.,* **409**, 1585
Blazhko, S. N. 1907, *Astron. Nachr.*, **175**, 325.
Buchler, J. R., and Kolláth, Z. 2011, *Astrophys. J.,* **731**, 24.
Catelan, M. 2006, in *XI IAU Regional Latin American Meeting of Astronomy,* ed. L. Infante, M. Rubio, *Rev. Mex. Astron. Astrofis.* (Conf. Ser.), **26**, 93.
Chadid, M., Vernin, J., and Gillet, D. 2008, *Astron. Astrophys.,* **491**, 537.
Chadid, M., Wade, G. A., Shorlin, S. L. S., and Landstreet, J. D.2004, *Astron. Astrophys.,* **413**, 1087.
Chadid, M., *et al.* 2010, *Astron. Astrophys.,* **510**, 39.
Christensen-Dalsgaard, J. Corbard, T., Dikpati, M., Gilman, P. A., and Thompson, M. J. 2004, in *Helio- and Asteroseismology: Towards a Golden future* (ESA SP-559), ed. D. Danesy, ESA Publ. Division, Noordwijk, The Netherlands, 1.
De Boer, K. S., and Maintz, G. 2010, *Astron. Astrophys.,* **520**, 46.
Dziembowski, W. A., and Mizerski, T. 2004, *Acta Astron.,* **54**, 363.
Eddington, A. S. 1926, *The Internal Constitution of the Stars*, Cambridge Univ. Press, Cambridge.
For, B. -Q., Preston, G. W., and Sneden, C. 2011, *Astrophys. J., Suppl. Ser.,* **194**, 38.
Gillet, D., and Crowe, R. A. 1988, *Astron. Astrophys.,* **199**, 242.
Gruberbauer, M., *et al.* 2007, *Mon. Not. Roy. Astron. Soc.*, **379**, 1498.
Jurcsik, J., *et al.* 2009a, *Mon. Not. Roy. Astron. Soc.,* **393**, 1553.
Jurcsik, J., *et al.* 2009b, *Mon. Not. Roy. Astron. Soc.,* **400**, 1006.

Kolenberg, K., and Bagnulo, S. 2009, *Astron. Astrophys.,* **498**, 543.
Kolenberg, K., Fossati, L., Shulyak, D., Pikall, H., Barnes, T. G., Kochukhov, O., and Tsymbal, V. 2010a, *Astron. Astrophys.,* **519**, 64.
Kolenberg, K., *et al.* 2010b, *Astrophys. J., Lett. Ed.,* **713**, 198.
Kolenberg, K., *et al.* 2011, *Mon. Not. Roy. Astron. Soc.,* **411**, 878.
Kolláth, Z., Molnár, L., and Szabó, R. 2011, *Mon. Not. Roy. Astron. Soc.,* **414**, 1111.
Kovács, G. 2009, in *Stellar Pulsation: Challenges for Theory and Observation*, AIP Conf. Ser. 1170, Amer. Inst. Phys., Melville, NY, 261.
Mathias, P., Gillet, D., Fokin, A. B., and Chadid, M. 1995, *Astron. Astrophys.,* **298**, 843.
Molnár, L., and Kolláth, Z. 2010, *J. Phys.* Conf. Ser. 218, IOP Publishing, Bristol, UK, 2027.
Moskalik, P., and Buchler, J. R. 1990, *Astrophys. J.,* **355**, 590.
Nemec, J., *et al.* 2011, *Mon. Not. Roy. Astron. Soc.,*, in press, 2011arXiv1106.6120N
Olech, A., and Moskalik, P. 2009, *Astron. Astrophys.,* **494**, 17.
Oosterhoff, P. T. 1939, *Observatory*, **62**, 104.
Preston, G. W. 2009, *Astron. Astrophys.,* **507**, 1621.
Shibahashi, H. 2000, in *The Impact of Large-Scale Surveys on Pulsating Star Research*, eds. L. Szabados and D. Kurtz, ASP Conf. Ser. 203, Astron. Soc. Pacific, San Francisco, 299.
Shibahashi, H., and Takata, M. 1995, in *Astrophysical Applications of Stellar Pulsation*, eds. R. S. Stobie and P. A. Whitelock, ASP Conf. Ser. 83, Astron. Soc. Pacific, San Francisco, 42.
Smith, H. A. 1995, *RR Lyrae Stars*, Cambridge Astrophys. Ser. 27, Cambridge Univ. Press, Cambridge.
Smolec, R., Moskalik, P., Kolenberg, K., Bryson, S., Cote, M. T., and Morris, R. L. 2011, *Mon. Not. Roy. Astron. Soc.,* **414**, 2950.
Sódor, Á., Jurcsik, J., and Szeidl, B. 2009, *Mon. Not. Roy. Astron. Soc.,* **394**, 261.
Stothers, R. B. 2006, *Astrophys. J.,* **652**, 643.
Stothers, R. B. 2010, *Publ. Astron. Soc. Pacific,* **122**, 536.
Szabó, R., Paparó, M., Benkő, J. M., Chadid, M., Kolenberg, K., and Poretti, E. 2009, in *Stellar Pulsation: Challenges for Theory and Observation*, AIP Conf. Ser. 1170, Amer. Inst. Phys., Melville, NY, 291.
Szabó, R., *et al.* 2010, *Mon. Not. Roy. Astron. Soc.,*, **409**, 1244.
Szeidl, B. 1988, in *Multimode Stellar Pulsations*, eds. G. Kovacs, L. Szabados, B. Szeidl, Konkoly Observatory, Kultura, Budapest, 45.
van Albada, T. S., and Baker, N. 1973, *Astrophys. J.,* **185**, 477.
Van Hoolst, T., Dziembowski, W. A., and Kawaler, S. D. 1998, *Mon. Not. Roy. Astron. Soc.,* **297**, 536.

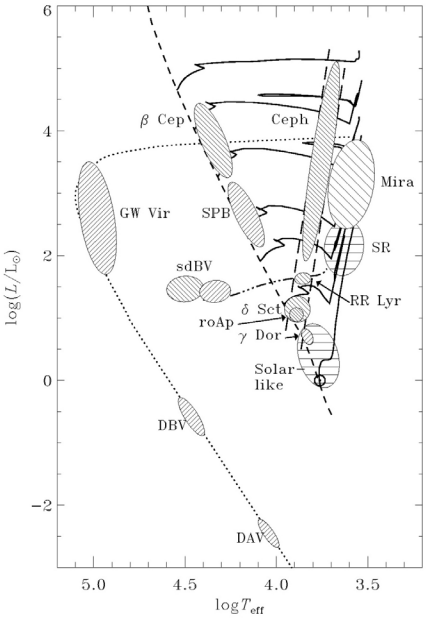

Figure 1. Stellar pulsations across the Hertzsprung-Russell diagram. Dashed line: zero-age main sequence; continuous lines: selected evolutionary tracks; triple-dot-dashed line: horizontal branch; dotted line: white dwarf cooling curve. The RR Lyrae stars are located on the horizontal branch in the instability strip. The hatching in the zones of pulsating stars represents the type of mode and the excitation mechanism: up-left for opacity-driven acoustic modes, up-right for opacity-driven internal gravity modes, and horizontal for stochastically excited modes. (From Christensen-Dalsgaard *et al.* 2004)

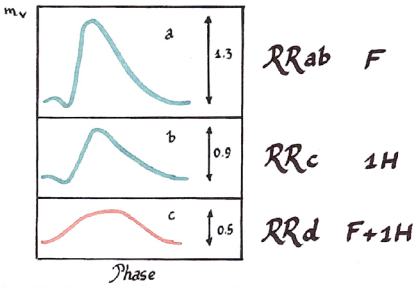

Figure 2. RR Lyrae Bailey subtypes. F: radial fundamental mode; 1H: radial first overtone.

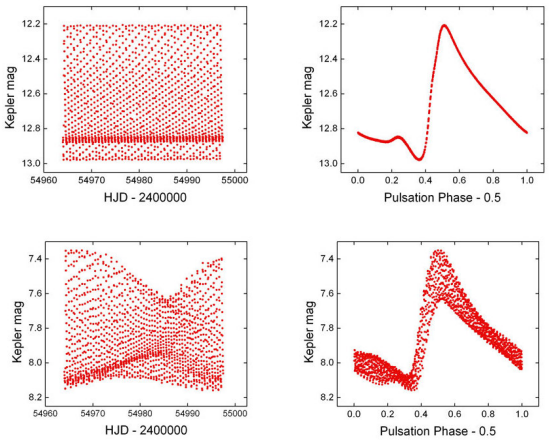

Figure 3. Kepler observations of a non-mdulated RR Lyrae star (top pair) and a Blazhko star (bottom pair). Left: 30-minute cadence data; right: folded light curve.

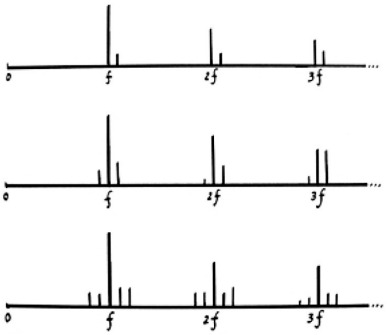

Figure 4. Typical frequency spectra for a Blazhko-modulated RR Lyrae star, showing multiplets. They can get even more complex than the schematic representations given here.

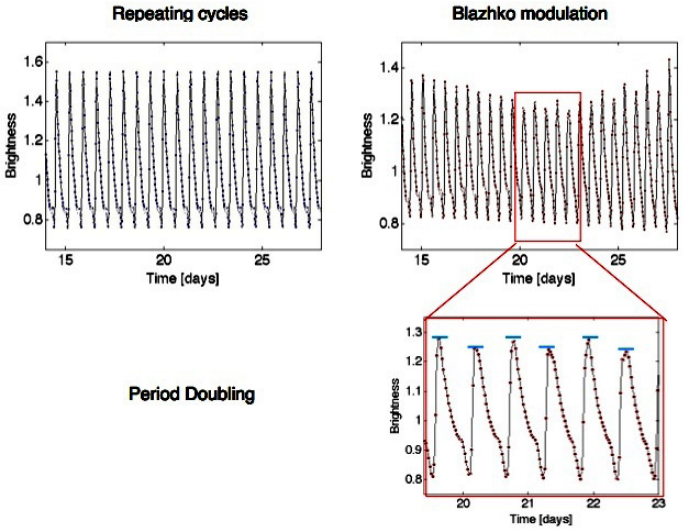

Figure 5. Period doubling manifesting in alternatingly higher and lower maxima, as seen in a star with Blazhko modulation (RR Lyr itself, top right panel). Period doubling is not seen in non-modulated stars (top left panel).

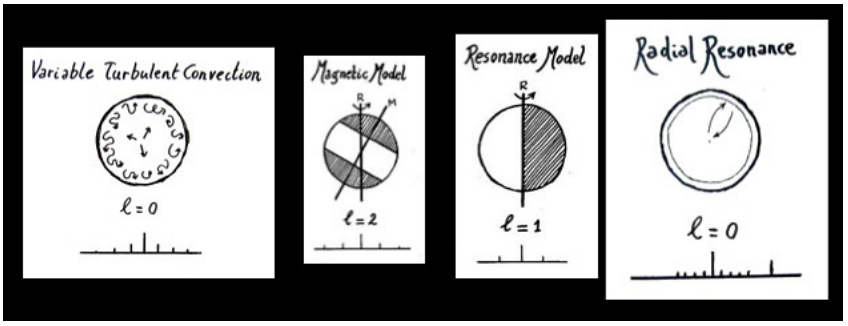

Figure 6. Models for the Blazhko effect: the present hierarchy.

Type 2 Cepheids in the Milky Way Galaxy and the Magellanic Clouds

Douglas L. Welch
Department of Physics and Astronomy, McMaster University, Hamilton, ON, L8S 4M1, Canada; welch@physics.mcmaster.ca

Invited review paper, received May 10, 2012

Abstract Type 2 Cepheids are radially pulsating variable stars that have been recognized as a distinct class for sixty years. As the lower-mass and hence lower-luminosity counterparts of the classical Cepheids, Type 2 Cepheids have attracted less observational and theoretical attention in the intervening decades. Fortunately, the recent availability of long, high-quality photometric time-series has renewed interest in these variables. The results from the OGLE-III surveys of the Large and Small Magellanic Clouds have been particularly exciting, especially with respect to the identification of "peculiar W Virginis" stars which appear to be components of binary systems. It has also become apparent that the sample of Milky Way field Type 2 Cepheids in catalogues is highly contaminated with other classes of variable stars. In this review, I describe important developments in the study of Type 2 Cepheids and suggest research opportunities—many of which do not require the acquisition on new data.

1. Introduction

In September 1952 the universe as we understood it became much larger. Ever since the first Type 2 Cepheids were discovered in globular clusters, it had been assumed that they shared the same luminosity at a given period as (classical) Cepheids in the disk of the Milky Way. In reality, there was a 1.5 magnitude difference between the two. The surprising announcement of this realization by Baade at the Rome IAU was quickly buttressed by followup remarks by Thackeray who had arrived at the same conclusion using observations of Large Magellanic Cloud variables. (See Baade (1956) for the complete firsthand account of how these events unfolded.) Reviews of Type 2 Cepheids and related stars have been published by Wallerstein and Cox (1984), Harris (1985b), and, most recently, by Wallerstein (2002). There have been a number of developments since the last work including the release of variable star catalogs from long-term, wide-area photometric surveys such as OGLE-III. In what follows, I will concentrate on work reported since Wallerstein (2002). I delve a little further back to review binary Type 2 Cepheids due to the recent realization that binarity is an importance influence on the production of certain Type 2 Cepheids.

2. Nomenclature

For the purposes of this review, Type 2 Cepheids are defined as those stars which are normally classified as BL Her variables (with periods between 1 and 4 days, also abbreviated CWB), W Vir stars (with periods greater than 4 days but most frequently greater than 8 days and less than 20 days, abbreviated CWA), and RV Tau stars (periods between maxima greater than 20 days). Somewhat confusingly, the RV Tau stars are subdivided into RVA and RVB types where RVB indicates an additional very long-period (500+ days) modulation of the light curve. Studies of Type 2 Cepheids in the Large Magellanic Cloud (LMC) and Small Magellanic Cloud (SMC)—discussed later in this review—have revealed a smooth progression of properties between W Vir and RV Tau stars and so the adoption of a discriminating period is not physically motivated. While the alternating minima of different depths of RV Tau stars seemed a distinctive classification characteristic of the time, it has since been seen in the prototype W Vir itself (Templeton and Henden 2007) and in BL Her stars (Smolec *et al.* 2012). Its usefulness as a discriminating factor between classifications may be diminished, but the fact that the phenomenon is more widespread is a positive finding in terms of testing theory against observation. In any case, Buchler and Moskalik (1990) claim that the period-doubling behavior for the more luminous Type 2 Cepheids (W Vir/RV Tau) is the result of a 5:2 period resonance between the fundamental and the second overtone radial modes.

Historically, Type 2 Cepheids have often been referred to as "Population II Cepheids" but our understanding of their range of metallicities and their kinematics has evolved to the point where continuing to make use of such a title would mislead the reader.

While RR Lyr variables are closely related, space constraints prevent the discussion of their very considerable literature. The anomalous Cepheids (intermediate in mass and luminosity between Type 2 and classical Cepheids) are often discussed in Type 2 Cepheid papers but also will not be reviewed here.

3. Evolutionary context

The early detection of Type 2 Cepheids in globular clusters provided an immediate degree of evolutionary context for these stars although our physical understanding of stellar structure and evolution emerged much later. However, the brightest Type 2 Cepheids in globular clusters are still much fainter than the brightest stars of the field population and consequently the determination of abundance patterns at high spectral resolution relies dominantly on field stars.

Our current understanding of the evolution of Type 2 Cepheids (and their subtypes) was outlined by Gingold (1985) and references therein. It is assumed that these variables have masses similar to 0.6 $M_{\odot}$ when they begin to evolve away from the horizontal branch.

Maas *et al.* (2007) studied 19 Type 2 Cepheids and found a number of abundance patterns. BL Her stars were found to have an overabundance of Na by up to a factor of 5 while the W Vir stars show no such anomaly. This careful and pivotal study also contains an excellent discussion of the evolutionary options available to core helium-burning blue horizontal branch stars heading towards the instability strip from the hot side. The Na anomaly suggests that BL Her stars do not normally end up becoming W Vir or RV Tau stars later in their evolution. Assuming single-star evolution, they suggest that the BL Her stars result from a phase of high-temperature CNO processing which both leave them with enhanced Na and "deposits" them at the red end of the blue horizontal branch, resulting in a single pass through the instability strip. W Vir stars are thought not to have experienced such high-temperature CNO processing and start their journey off the horizontal branch nearer the blue end of the blue horizontal branch. W Vir stars then may pass through the instability strip on their way to the asymptotic giant branch (AGB) but have an additional excursion back and forth across the instability strip at higher luminosity due to helium shell flashes and/or internal structure readjustments on the AGB.

The traditional interpretation of the "no man's land" in period, between about 4 and 10 days, where Type 2 Cepheids are rarely found therefore maps back to the horizontal branch and the way in which evolutionary tracks diverge from each other as the stars evolve to cooler temperatures and higher luminosities.

4. Type 2 Cepheids in binary systems

In the Milky Way field, there are presently five Type 2 Cepheids known to be members of binary systems.

AU Peg is a 2.4-day BL Her star with a rapidly changing period. Precision radial velocites obtained by Harris *et al.* (1979) led them to conclude that AU Peg was a component of a spectroscopic binary with a period of order 50 days. Harris *et al.* (1984) obtained additional photometry and spectrscopy and concluded that AU Peg was in a 53.32-day orbit, that it had an [*Fe/H*] = +0.1 and that it must be very close to filling its Roche lobe. AU Peg appeared to be redward of the instability strip and thus binarity was implicated as a possible source of excitation of pulsation as well as a driver of the rapid period change. Vinkó *et al.* (1993) published additional photometry and found the period change to be non-linear. Furthermore, they disputed the tidal excitation interpretion in the earlier work, suggesting instead that AU Peg was simply near the red edge of the Instabilty Strip. Vinkó *et al.* (1998) obtained R = 11,000 optical spectroscopy of a number of Type 2 Cepheids and found that AU Peg was unique among them in revealing a P Cygni profile in its Hα line—indicating outflow. More recently the entire Type 2 Cepheid interpretation of AU Peg has been challenged by Jurkovic *et al.* (2007), who instead conclude that AU Peg is a double-mode pulsator (fundamental/first overtone) and a classical Cepheid

despite its high galactic latitude and the enormous distance from the disk that such an interpretation would require. An interesting alternative explanation is that AU Peg is the first example of a double-mode Type 2 Cepheid.

Harris and Welch (1989) obtained new radial velocities and determined orbital characteristics for the single-lined spectroscopic binaries IX Cas and TX Del. They also pointed out that both stars had near-solar metallicities. The periods of IX Cas and TX Del, 9.2 and 6.2 days, respectively, are in a period range where few Type 2 Cepheids are known. Balog and Vinkó (1995) argue that the radius of TX Del is too large to be a Type 2 Cepheid and instead should be considered a classical Cepheid, despite the 1.2 kpc height above the disk that would require.

ST Pup is a 18.47-day W Vir star which was found by Gonzalez and Wallerstein (1996) to be in a spectroscopic binary with orbital period 410.4 days. Although it has a $[Fe/H] = -1.47$, it has a depletion pattern very similar to the longer-period stars in the sample of Maas *et al.* (2007) with the exception of an unexpectedly high Ca abundance.

Antipin *et al.* (2007) found the first galactic Type 2 Cepheid in an eclipsing binary: TYC 1031 01262 1. At present, there is no estimate of the Cepheid's metallicity, and no radial velocity observations suitable for determining other orbital characteristics are known to have been obtained.

Of the five systems discovered to date, it is noteworthy that three of the four that have had their composition estimated have near-solar or above-solar metallicities and have short orbital periods and distances. The most straightforward interpretation of this correlation is that there has been mass transfer from a more evolved companion prior to the current instability strip pass.

5. Type 2 Cepheids in Milky Way globular clusters

Clement *et al.* (2001) produced a catalog of all variable stars known in Milky Way globular clusters. Fifty-eight Type 2 Cepheids were identified at the time once two anomalous Cepheids are removed from their count. They note that all clusters containing Type 2 Cepheids have $[Fe/H] < -1.0$ and all except one have $[Fe/H] < -1.25$.

A recent census of Type 2 Cepheids in Milky Way globular clusters south of Declination −30° was provided by Matsunaga *et al.* (2006). Their new discoveries combined with previous work result in forty-six variables in twenty-six southern globular clusters. Their ten new discoveries bring the total number of Type 2 Cepheids in globular clusters to sixty-eight.

6. Type 2 Cepheids in the Milky Way field

The sample of Type 2 Cepheids associated with Milky Way globular clusters is likely to be complete or near-complete, since such stars are among

the very brightest cluster members and, along with the horizontal branch RR Lyrae pulsators, have large photometric amplitudes.

The identification of a clean sample of true Type 2 Cepheids among Milky Way field stars has been much more problematic. The list of Harris (1985a) contained 152 field Type 2 Cepheids but was compiled prior to the microlensing, wide-field, and all-sky surveys. The surveys have been a two-edged sword in terms of improving our sample. They have both increased the number of Type 2 Cepheids known and dramatically improved the duration over which high-quality photometry exists but they have also introduced a significant number of false positive Type 2 Cepheid classifications.

A search of the Variable Star Index (Watson 2006) on May 6, 2012, revealed the numbers of Type 2 Cepheid classifications shown in Table 1. The first two variable types (CEP and CEP:) almost certainly contain "underclassified" classical Cepheids as well as Type 2 Cepheids. It is also this pair of classes which likely has the largest contamination of non-pulsating variables—stars that have rotation or orbital periods similar to Cepheids of both kinds.

While the LMC and SMC samples are likely near-complete, the mix of selection biases for the discovery of Type 2 Cepheids in the Milky Way field does not yet lend itself easily to numerical comparisons of subtypes between our galaxy and those in our companion galaxies.

Ed Schmidt's group at the University of Nebraska has been one of the most active in the study of field Type 2 Cepheids, with a number of careful photometric studies (Schmidt 2002; Schmidt *et al.* 2005a; Schmidt *et al.* 2005b; Schmidt *et al.* 2007; Schmidt *et al.* 2009) and spectroscopic studies (Schmidt *et al.* 2003b; Schmidt *et al.* 2003a; Schmidt *et al.* 2011). Schmidt *et al.* (2011) is an important synthesis of early work with numerous significant findings. It reports a uniform set of low-resolution spectra of 288 stars from Schmidt *et al.* (2007) and Schmidt *et al.* (2009)—the first large-scale attempt to produce spectral confirmation of classifications made with light curves. Although the authors expected to find about 560 new Type 2 Cepheids based on the estimates of Wallerstein (2002), they found only nineteen (elsewhere in the paper, the number twenty-three is stated.) This class of variable is easily mistaken for others based on light curves alone. Schmidt *et al.* (2011) also found that Type 2 Cepheids frequently had small (0.1 to 0.4 mag) amplitudes, contrary to conventional wisdom. This amplitude finding has been confirmed by OGLE-III for the LMC and SMC samples (discussed below). Of the "Cepheid Strip Candidates," as the new Type 2 Cepheid candidates are called, most have $-1.0 < [F\ e/H\ ] < 0.0$, suggesting an evolutionary path distinct from their counterparts in globular clusters. Although the numbers are small (and therefore the statistics are uncertain), the period distribution of the "Cepheid Strip Candidates" is quite flat in the traditionally underpopulated 4- to 10-day period range. This finding, too, is consistent with the OGLE-III surveys of the LMC and SMC and suggests that there is not such an evolutionary avoidance for this period range—the gap

is at least partly due to photometric amplitude selection biases in discovery. The earlier correlation noted between Type 2 Cepheids in binaries and those with near-solar metallicities suggests that a significant fraction of the field population may be binary.

Another major study was that of Soszyński *et al.* (2011) who reported on the classical and Type 2 Cepheids of the OGLE-III microlensing survey fields in the galactic bulge. Of the 335 Type 2 Cepheids, there were 156 BL Her, 128 W Vir, and 51 RV Tau stars. This is the most uniformly observed and selected sample of galactic Type 2 Cepheids. Observations analyzed for this paper were acquired between 1997 and 2009.

7. Type 2 Cepheids in the Magellanic Clouds

Prior to the microlensing surveys of the 1990s few Type 2 Cepheids were recognized in the LMC and SMC.

The very first claim of a Type 2 Cepheid in either of the Magellanic Clouds was made by Tifft (1963) where 1.4300-day period was suggested for a star (6-31) in the field of the SMC which was possibly associated with the globular cluster NGC 121. Such a star would now be classified as a BL Her. Curiously, the star (now also cataloged as 2MASS J00262813-7136591) has not had further photometric follow-up. Payne-Gaposchkin and Gaposchkin (1966) reported only three "W Vir" stars in the SMC: HV 12901, HV 1828, and HV 206. The last of these had a period of 103.8 days which would fall into the period range of RV Tau stars by a more modern usage.

The first LMC Type 2 Cepheids, HV 5690 and HV 2351, were reported by Hodge and Wright (1969). Both were characterized by changing periods. Subsequently, Payne-Gaposchkin (1971) listed a total of seventeen "Population II Cepheids," including the two already discovered. The periods for the seventeen stars ranged from 11.439 to 50.87 days and ten of the stars have notes regarding observed period change. In the photographic surveys of the era, the shorter-period BL Her stars were below the detection threshold.

Welch (1987) obtained single-epoch, near-infrared (JHK) photometry of nine LMC and two SMC Type 2 Cepheids. Three of these with periods between 35.9 and 47.8 days showed K(2.2μm) excesses, indicating the presence of warm circumstellar dust.

The higher-quality, deeper CCD photometry acquired during the microlensing surveys dramatically improved our understanding of the Type 2 Cepheid populations of the LMC and SMC. The MACHO Project published its findings of Type 2 Cepheids (W Vir and RV Tau stars) in Alcock *et al.* (1998) which established the pattern of increased light curve variability with period and showed that there was no clear demarcation between the two classes. The existence of a common period-luminosity relation for the stars was also revealed.

The OGLE-III catalogs of LMC (Soszyński *et al.* 2008) and SMC (Soszyński *et al.* 2010) Type 2 Cepheids are the seminal observational works for these variables.

- In the LMC, 197 Type 2 Cepheids were found (64 BL Her, 96 W Vir, and 37 RV Tau—where the W Vir/RV Tau dividing period was taken to be 20 days).

- In the SMC, 43 Type 2 Cepheids were found (17 BL Her, 17 W Vir, and 9 RV Tau).

- "Exemplar" light curves for the LMC and SMC Type 2 Cepheids have been produced, providing definitive light curve shape classification. It is of interest to note that that light curve amplitude is the smallest in the period range 4–8 days where few Type 2 Cepheids were found in photographic surveys. The dearth of stars in that period range is thought to be due to evolutionary considerations, but amplitude-related discover selection biases may also have played a role.

- In both the LMC and SMC, a set of "Peculiar W Virginis" (hereafter, PCWA) stars were identified with distinctive light curve shapes (more symmetric) and bluer than their normal W Vir counterparts at the same period. The observed fraction of PCWA stars in eclipsing binaries or with ellipsoidal variation (4 of 16 in the LMC and 4 out of 7 in the SMC) is high enough to suggest that all such stars are in binary systems. A clear implication of this finding is that the production of PWCA stars is the result of binary interaction.

- In the LMC sample three of the seven Type 2 Cepheids in eclipsing systems have pulsation periods between 4 and 6 days where the frequency of Type 2 Cepheids is typically very low. Binary interaction may play an important role in populating this period range. If so, study of the few Type 2 Cepheids with similar periods in the Milky Way field may clarify whether such stars are always in binaries.

- The PCWA stars in the SMC all show multiperiodicity. Presumably the addition periods are the result of the Cepheid being non-spherical due to tidal effects.

While the Type 2 Cepheids in the LMC and SMC are too faint for detailed abundance work, they suggest additional avenues of exploration in the Milky Way field and bulge.

8. Opportunities

There is a surprising amount of discovery space available in the study of

Type 2 Cepheids. Here are some immediate suggestions for new observations and/or analysis:

- The great majority of photometry which exists for Type 2 Cepheids in globular clusters is photographic and imprecise. Since these stars are among the brightest in their clusters, they can be easily detected and measured with modern imagers in standard bandpasses. Profile-fitting photometry is needed in such crowded fields, but there are plenty of stars available to get the point spread function right.

- Suspected or uncertain Type 2 Cepheids in catalogs can be further assessed by examining the additional information now available in proper motion surveys, near-infrared colors, and cross-references with X-ray source catalogs. The rotation periods of spotted stars such as BY Dra and RS CVn variables frequently result in their misclassification as Type 2 Cepheids.

- There are few precise (± 2 km s^{-1}) radial velocities of field Type 2 Cepheids—a factor which limits our ability to understand both the frequency of binarity and the dynamical population from which they have been produced.

- No variable star catalog from a long-term photometric survey of the northen sky has yet been released. There are sure to be additional, relatively bright Type 2 Cepheids identified by such a survey and a program of routine photometry of newly-discovered stars will inevitably pay dividends.

- A re-classification of field W Vir stars into "normal" and "peculiar" is warranted as a result of the OGLE-III surveys of the LMC and SMC. It would be most interesting to investigate how metallicity and rates and directions of period change are correlated with these two classes of objects.

- The Type 2 Cepheids discovered in photometric surveys already have time-series available for period change analysis with hundreds to thousands of epochs. Patterns of non-pulsation modulation are waiting to be discovered and defined. The ellipsoidal modulation due to a tidally-distorted pulsator in orbit around a close companion can easily be teased out of available data - a purely photometric indication of binarity.

9. Acknowledgements

DW acknowledges support from the Natural Sciences and Engineering Research Council of Canada (NSERC). This paper has made use of the International Variable Star Index (VSX) operated at AAVSO, Cambridge, Massachusetts, U.S.A. [http://vsx.aavso.org/].

References

Alcock, C., *et al.* 1998, *Astron. J.*, **115**, 1921.
Antipin, S. V., Sokolovsky, K. V., and Ignatieva, T. I. 2007, *Mon. Not. Roy. Astron. Soc.*, **379**, L60.
Baade, W. 1956, *Publ. Astron. Soc. Pacific*, **68**, 5.
Balog, Z., and Vinkó, J. 1995, *Inf. Bull. Var. Stars*, No. 4150, 1.
Buchler, J. R., and Moskalik, P. 1990, in *Confrontation Between Stellar Pulsation and Evolution*, eds. C. Cacciari and G. Clementini, ASP Conf. Ser. 11, Astron. Soc. Pacific, San Francisco, 383.
Clement, C. M., *et al.* 2001, *Astron. J.*, **122**, 2587.
Gingold, R. A. 1985, *Mem. Soc. Astron. Ital.*, **56**, 169.
Gonzalez, G., and Wallerstein, G. 1996, *Mon. Not. Roy. Astron. Soc.*, **280**, 515.
Harris, H. C. 1985a, *Astron. J.*, **90**, 756.
Harris, H. C. 1985b, in *Cepheids: Theory and Observation*, IAU Colloq. 82, ed. B. F. Madore, Cambridge, Univ. Press, Cambridge, 232.
Harris, H. C., Olszewski, E. W., and Wallerstein, G. 1979, *Astron. J.*, **84**, 1598.
Harris, H. C., Olszewski, E. W., and Wallerstein, G. 1984, *Astron. J.*, **89**, 119.
Harris, H. C., and Welch, D. L. 1989, *Astron. J.*, **98**, 981.
Hodge, P. W., and Wright, F. W. 1969, *Astrophys. J., Suppl. Ser.*, **17**, 467.
Jurkovic, M., Szabados, L., Vinkó, J., and Csák, B. 2007, *Astron. Nachr.*, **328**, 837.
Maas, T., Giridhar, S., and Lambert, D. L. 2007, *Astrophys. J.*, **666**, 378.
Matsunaga, N., *et al.* 2006, *Mon. Not. Roy. Astron. Soc.*, **370**, 1979.
Payne-Gaposchkin, C. H. 1971, *Smithson. Contrib. Astrophys.*, **13**, 1.
Payne-Gaposchkin, C., and Gaposchkin, S. 1966, *Smithson. Contrib.Astrophys.*, **9**, 1.
Schmidt, E. G. 2002, *Astron. J.*, **123**, 965.
Schmidt, E. G., Hemen, B., Rogalla, D., and Thacker-Lynn, L. 2009, *Astron. J.*, **137**, 4598.
Schmidt, E. G., Johnston, D., Langan, S., and Lee, K. M. 2005a, *Astron. J.*, **129**, 2007.
Schmidt, E. G., Johnston, D., Langan, S., and Lee, K. M. 2005b, *Astron. J.*, **130**, 832.
Schmidt, E. G., Langan, S., Lee, K. M., Johnston, D., Newman, P. R., and Snedden, S. A. 2003a, *Astron. J.*, **126**, 2495.
Schmidt, E. G., Langan, S., Rogalla, D., and Thacker-Lynn, L. 2007, *Astron. J.*, **133**, 665.
Schmidt, E. G., Lee, K. M., Johnston, D., Newman, P. R., and Snedden, S. A. 2003b, *Astron. J.*, **126**, 906.
Schmidt, E. G., Rogalla, D., and Thacker-Lynn, L. 2011, *Astron. J.*, **141**, 53.
Smolec, R., *et al.* 2012, *Mon. Not. Roy. Astron. Soc.*, **419**, 2407.

Soszyński, I., Udalski, A., Szymański, M. K., Kubiak, M., Pietrzyński, G., Wyrzykowski, L., Ulaczyk, K., and Poleski, R. 2010, *Acta Astron.*, **60**, 91.
Soszyński, I., *et al.* 2008, *Acta Astron.*, **58**, 293.
Soszyński, I., *et al.* 2011, *Acta Astron.*, **61**, 285.
Templeton, M. R., and Henden, A. A. 2007, *Astron. J.*, **134**, 1999.
Tifft, W. G. 1963, *Mon. Not. Roy. Astron. Soc.*, **125**, 199.
Vinkó, J., Remage Evans, N., Kiss, L. L., and Szabados, L. 1998, *Mon. Not. Roy. Astron. Soc.*, **296**, 824.
Vinkó, J., Szabados, L., and Szatmary, K. 1993, *Astron. Astrophys.*, **279**, 410.
Wallerstein, G. 2002, *Publ. Astron. Soc. Pacific*, **114**, 689.
Wallerstein, G., and Cox, A. N. 1984, *Publ. Astron. Soc. Pacific*, **96**, 677.
Watson, C. L. 2006, *The Society for Astronomical Sciences 25th Annual Symposium on Telescope Science, Held May 23–25, 2006, at Big Bear, CA*, Soc. Astron. Sciences., Rancho Cucamonga, CA, 47.
Welch, D. L. 1987, *Astrophys. J.*, **317**, 672.

Table 1. Counts of Type 2 Cepheid types in VSX.

Variability type	*N*	*Variability type*	*N*	*Variability type*	*N*
CEP	491	CWA:	19	RVA	72
CEP:	141	CWB	237	RVA:	3
CW	11	CWB:	24	RVB	26
CW:	2	RV	81	RVB:	1
CWA	240	RV:	35		

Classical Cepheids After 228 Years of Study

David G. Turner
Saint Mary's University, Halifax, NS B3H 3C3, Canada;
turner@ap.smu.ca

Invited review paper, received October 19, 2011

Abstract A review is presented of much of our current observational knowledge of classical Cepheids. Outlined are the basic observational parameters of Galactic Cepheids derived over the past 228 years, with emphasis on current trends and ongoing problems. Although the calibration of the Cepheid period-luminosity (PL) relation has normally made use of variables in the Magellanic Clouds, presently that can be accomplished using only Galactic Cepheids. It is also possible to calibrate the PL relation without recourse to observations, given that their fundamental properties are well enough understood.

1. Introduction

Cepheids are yellow supergiant stars that can reveal to astronomers exactly how distant they are through regular measurement of their brightness variations in a few photometric bands. Much more is known about them today than fifty or one hundred years ago, yet, for every morsel of new information that is learned, further questions arise that make investigation of such stars a constantly challenging pursuit.

Cepheids are named for the bright example of the class, δ Cephei, whose regular variability over the course of 5.37 days was noticed by John Goodricke in October 1784, a month after his friend Edward Piggott noted light variations in η Aquilae, another bright Cepheid with a pulsation period of 8.36 days. The valuable characteristic of Cepheids as distance indicators was discovered more than a century later when Henrietta Leavitt noticed in 1908 that the mean brightness of Cepheids in the Small Magellanic Cloud correlated closely with the period of variability for the stars: the well-known Cepheid period-luminosity (PL) relation (Leavitt 1908; Leavitt and Pickering 1912). The relationship was calibrated using Galactic variables (Hertzsprung 1913), and Harlow Shapley was one of the first to make use of the feature for practical purposes in a study of the Sun's location within the Galaxy relative to globular clusters (Shapley 1918a, b), with distances to the latter inferred with respect to the short period "Cepheids" populating some of them. The distinction between classical Cepheids like δ Cep and η Aql and Type II Cepheids (BL Herculis objects, W Virginis variables, and RV Tauri stars) and RR Lyrae variables was not made until many years later. See Fernie (1969) for a detailed review.

The initial calibration of Cepheid luminosities and the application of the PL

relation to the measurement of distances to nearby galaxies came soon thereafter. In fact, it is probably true that much of what we understand about cosmology and the nature of the universe is tied to knowledge of the Hubble constant H_0, as derived from observations of Cepheids in relatively nearby galaxies (Freedman *et al.* 2001).

Cepheids are also a topic of interest for stellar interior modellers. The simple linear, non-rotating, adiabatic models of a few decades ago are currently being replaced by much more sophisticated calculations involving differential rotation, more physically realistic mixing, and proper consideration of changing element abundances on interior opacity sources. In the future, fully three-dimensional models may eventually become the norm, consuming extraordinary amounts of computer calculation time per model. The time may eventually arrive when it will take a complete suite of models to match individual Cepheids, which appear to differ from one to another in very distinct ways, particularly in atmospheric contamination by CNO elements (Turner and Berdnikov 2004).

2. Properties of classical Cepheids

Cepheids display very repeatable light curves, most being asymmetric with a rapid rise to maximum light followed by a slower decline, with light minimum occurring 0.6–0.7 cycle after light maximum. The radial velocity variations are almost a mirror image of the light variations in the variables, indicating that Cepheids are brightest roughly when their photospheres are most rapidly expanding, and faintest roughly when they are contracting the fastest. There is a small phase shift between the two relations, radial velocity minimum occurring a few percent of the cycle length after light maximum. Short period Cepheids (periods P < 10d) tend to be of spectral types F5-F8 at light maximum, and G or K at light minimum, with correspondingly cooler spectral types for longer period variables (Kraft 1963).

Cepheids also display a feature known as the Hertzsprung progression (Figure 1), a secondary bump in their light curves that appears near light minimum (~0.5 cycle after maximum) in Cepheids with periods of about 5 days, but gradually closer and closer to light maximum in Cepheids of longer period, being coincident with light maximum at pulsation periods of ~10 days, giving them the appearance of having a double maximum or a broad maximum. For Cepheids of longer period the bump appears on the rising light portion of the light curve, progressing towards light minimum and disappearing at periods of ~20 days.

The origin of the bump has been a matter of debate for decades, and has been attributed to either a light echo of the surface pulsation from the stellar core or surface excitation of the second overtone mode, for which the period is extremely close to one-half of the fundamental mode period (the periods of adjacent pulsation modes become shorter by a factor of ~0.7 as one goes to higher order modes, so the period of the second overtone mode relative to

the fundamental mode is 0.7 × 0.7 ≈ ½). A subset of short-period Cepheids displays light curves that are almost perfectly symmetric (Figure 2), matching sine waves so closely (see the sine wave light curve in the lower part of the figure) that they were referred to as s-Cepheids. The nature of such objects is controversial. Efremov (1968) argued that their symmetric light curves were the signature of Cepheids in the first crossing of the instability strip, although that may be a simple consequence of the small amplitudes for some stars. The two s-Cepheids SZ Tau and V1726 Cyg, whose light curves are plotted in Figure 2, are members of the clusters NGC 1647 (Turner 1992) and Platais 1 (Turner *et al.* 2006b), respectively, and appear to pulsate in the first overtone and fundamental mode, respectively, in high order strip crossings. Other s-Cepheids that are likely members of open clusters seem equally split between fundamental mode and overtone pulsation.

Thirty years ago Simon and Lee (1981) introduced Fourier diagnostics to the study of Cepheid light curves. It had been recognized previously that light curves could be matched to Fourier series quite well, the only question being how many terms to include when there were gaps in the light curve coverage. Simon took the matter further by noting that certain combinations of low-order Fourier series terms, sine term amplitudes and phase offsets, such as R_{21}, the ratio of amplitudes for the second order to first order terms, and ϕ_{21}, the normalized difference in phase offsets between the second and first order terms, correlated smoothly with pulsation period, except for a discontinuity at P = 10d where the secondary bump passes through light maximum (see, for example, the behavior of R_{21} shown by Zabolotskikh *et al.* 2005). For short-period Cepheids there is a heavily-populated primary sequence, considered to coincide with fundamental mode pulsators, and a less-populated secondary sequence, considered to represent overtone pulsators, subsequently confirmed by Fourier decomposition of the light curves of double mode Cepheids (e.g., Antonello and Mantegazza 1984; Pardo and Poretti 1997). The technique was also extended to s-Cepheids by Antonello and Poretti (1986) in order to demonstrate that they are likely overtone pulsators, although the definition of "s-Cepheid" was broadened somewhat in the process and it is unclear what parameters like R_{21} and ϕ_{21} mean when the data are noisy and the second order term in the Fourier series may actually be zero.

Another characteristic of Cepheids is that all undergo changes in pulsation period as a result of stellar evolution. Cepheids represent post-hydrogen burning stages of stars with main sequence masses in excess of about 4 $M_{\odot}$, progenitors that had spectral types hotter than B5 in a former life. They are currently yellow supergiants in a variety of short-lived evolutionary stages between that of B dwarfs and their later existence as red supergiants. Most are evolving through the instability strip for the second or third time as core helium burning objects, some may be passing through it for the fourth or fifth time as shell helium burning stars, and a rare few seem likely to be in the first crossing, the stage of

hydrogen shell burning that lasts an order of magnitude or more less time than other stages.

As yellow supergiants evolving through the instability strip in the Hertzsprung-Russell (H-R) diagram, Cepheids become unstable to pulsation because the regions of hydrogen (H) and helium (He, He^+) ionization lie deep enough to drive radial expansion and contraction through a piston-type mechanism. Evolution through the instability strip takes on the order of a half million years for some stars, so it is not a process normally detectable in the course of a human lifetime. But it does result in very small changes in average radius for the stars as they evolve, increases for stars evolving towards the cool side of the instability strip in the Hertzsprung-Russell (HR) diagram, and decreases for stars evolving towards the hot side. That produces small, cumulative changes in pulsation period that are readily detectable from O–C analyses of their light curves, as noted by Szabados (1983), Fernie (1984), Turner (1998), and Turner *et al.* (1999).

The study of Cepheid period changes through O–C analysis is an excellent way to test stellar evolutionary models (Turner *et al.* 2006a). But period changes can also arise from other effects: orbital motion about a companion, which produces cyclical variations in O–C data over the orbital period of the system, random changes in pulsation period, which for some Cepheids, for example, V1496 Aql (Berdnikov *et al.* 2004), can dominate evolutionary effects, and possibly mass loss (Neilson *et al.* 2012). The existence of such complications makes it imperative to establish Cepheid pulsation periods from existing photometric data as carefully as possible. Fourier techniques, for example, can sometimes generate erroneous results. By contrast, the Hertzsprung method takes full advantage of the repeatability of Cepheid light curves to best advantage, particularly when used in O–C analyses (Tsesevich 1971; Belserene 1988; Berdnikov 1992), and generates the most accurate results.

The light amplitudes for Cepheids vary in magnitude according to the filter used to observe them, being largest in the ultraviolet and smallest in the infrared. Maximum blue (ΔB) or visual (ΔV) light amplitude also increases progressively with pulsation period, with the exception of a small dip for $P \approx 10^d$ where the light curve bump is coincident with light maximum. The largest amplitude Cepheids are found just to the hot side of instability strip center, with variables of smaller amplitude towards the strip edges (Kraft 1963; Hofmeister 1967; Sandage and Tammann 1971; Payne-Gaposchkin 1974; Pel and Lub 1978; Turner 2001; Sandage *et al.* 2004). That characteristic was combined with rate of period change by Turner *et al.* (2006a) in order to produce a parameter capable of estimating the strip crossing mode for individual Cepheids (Turner *et al.* 2006b; Turner 2010).

For many years Polaris held the record as the smallest amplitude Cepheid, particularly in the decades around 1988, when its visual amplitude dropped to 0.025 magnitude (Turner 2009). But, at their current level near 0.055 magnitude,

the pulsations of Polaris are an order of magnitude larger than those of HDE 344787, a recently discovered double-mode Cepheid that is rapidly becoming a challenge to observe as its light amplitude decreases towards its eventual demise as a variable star (Turner *et al.* 2010b). Both stars display the largest rates of period increase for Cepheids with pulsation periods of 4 to 5 days, a signature of variables crossing the instability strip for the first time. The discovery of X-ray emission from Polaris and a few other bright Cepheids (Engle *et al.* 2009) is an additional complication that challenges our understanding of the stars.

3. Calibration of the PL relation

The calibration of the Cepheid PL relation was for many years accomplished by deriving the slope of the relationship using Cepheids in the Magellanic Clouds, where interstellar extinction and differential reddening is small, and fixing the zero-point using Milky Way Cepheids of known distance. The last step was not without challenges. The large masses and short-lived evolutionary state of Cepheids make them relatively rare objects. None are closer than ~100 parsecs, which was traditionally the limit for trigonometric parallax determinations with older refracting telescopes. Nearby Cepheids (e.g. Polaris) are also relatively bright, presenting problems for parallax measurements from photographic plates.

The launch of the Hipparcos satellite two decades ago changed the situation, since its on-board telescope/detector combinations had the capability of measuring absolute parallaxes of high precision for stars brighter than about tenth magnitude, including a sample of more than 200 Cepheids. Most Cepheids measured by Hipparcos have very accurate parallaxes, but there is a subset of objects of lower quality and precision that comprises a relatively large proportion (~1/2) of the sample (Turner 2010). A smaller group of ten classical Cepheids have also had their parallaxes measured using the Hubble Space Telescope (HST) by more traditional methods (Benedict *et al.* 2002, 2007), with improved precision and an accuracy generally better than the Hipparcos results. The zero-point for the PL relation is now considered to be firmly established (see Turner 2010; Turner *et al.* 2010a).

An alternate route to the calibration is by means of Cepheids belonging to open clusters, since zero-age main-sequence (ZAMS) fits for open clusters can provide distance estimates for cluster members with a precision reaching ~2% in the best cases, the accuracy depending upon the ZAMS calibration tied to the nearby Hyades and Pleiades clusters and the effects of metallicity on the main-sequence luminosity zero-point. In the 1960s the sample of Galactic clusters containing short period Cepheids as bona fide members was only a half dozen or so, which made it difficult to fix the slope of the relation with much confidence, but the sample now numbers twenty-four of all periods (Turner 2010), with a potential to reach forty to fifty stars, allowing both

the slope and zero-point to be established independent of Cepheids in the Magellanic Clouds.

Since Cepheids are so regular in their variability, their parameters can also be established by the Baade-Wesselink method, a technique proposed by Baade (1926) and developed for practical use by Wesselink (1946). The luminosity of a star is the product of its surface area and surface brightness. For a spherical object, a reasonable approximation for an evolved star like a Cepheid, the surface area is $4\pi R^2$, where R is the star's radius, and the surface brightness is the radiance, given by σT_{eff}^4, where σ is the Stefan-Boltzmann constant and T_{eff} is the star's effective temperature. The star's luminosity is therefore $L = 4\pi R^2 \sigma T_{\text{eff}}^4$. During a Cepheid's pulsation cycle it reaches the same effective temperature or surface brightness at different phases, yet there can be a difference in brightness at those phases of Δm, in magnitudes. The ratio of the star's radii at such times, R_2/R_1, is equal to $10^{0.2\Delta m}$, while the differences in the star's radius, $R_2 - R_1$, can be found independently using measures of its radial velocity, which track the cyclical motion of the surface layers, thereby allowing the average radius to be established. In particular, the radial motion of the star's surface is given by $v_R = p\,(V_R - V_0)$, where V_R is the measured radial velocity, V_0 is the systemic velocity of the star along the line of sight, and p is a factor, typically close to 4/3, to correct the measured velocity for the fact that it represents the combined light originating from photospheric radiation coming from the entire nearside hemisphere of the Cepheid.

Over the course of a complete light cycle, the surface of a Cepheid moves through a distance $4\Delta R$, where ΔR is the amount by which the mean radius of the star increases or decreases during the interval. That value can be obtained through numerical integration of the radial velocity curve, namely $4\Delta R = p \int (V_R - V_0)\, dt$ in calculus notation, where the integral is over the entire cycle. If the semi-amplitude of the radial velocity curve is denoted by ΔV_R (in km s^{-1}) and it is approximated by a sine wave, it follows that $\Delta R \approx 2.63 \times 10^{-2}\, P\, \Delta V_R\, R_\odot$, where P is the pulsation period in days and the projection factor has been approximated as 4/3. For the bright Cepheid δ Cep, P = 5.37 days and the radial velocity varies between +3 and –36 km s^{-1} (i.e., $\Delta V_R = \pm 19.5$ km s^{-1}). The estimated radius variations are therefore about $\pm 2.8\ R_\odot$, close to the actual value of $\pm 2.3\ R_\odot$ about a mean radius of 43 $R_\odot$ (Turner 1988), the difference being accounted for by a slightly smaller adopted value of p and the non-sinusoidal nature of the light and velocity curves for δ Cep. The radius variations for δ Cep therefore amount to ±5%, typical of most Cepheids, where the range is from less than 1% to ~10% in extreme cases.

The method of isolating phases of identical surface brightness during a Cepheid's cycle is all-important. When the technique is applied correctly, a plot of radius ratios versus radius differences should generate a tight loop traced out counterclockwise for phase pairs running from light maximum to light minimum (Evans 1976; Turner 1988), and the slope should be close to

the reciprocal of the minimum radius (Abt 1959). The use of a color index like *B–V* to isolate such phases, the situation for most early applications of the Baade-Wesselink method, generates results contrary to expectations (e.g., Turner 1988), primarily because the colors are affected by variable atmospheric line blanketing created by a combination of cyclical spectral line broadening arising geometrically from the general expansion and contraction of the stellar photosphere and a sudden, large increase in atmospheric microturbulence during the contraction phases (Benz and Mayor 1982; Turner *et al.* 1987). Most recent applications have used color indices less affected by such influences, such as *V–I* spanning visual to infrared wavelengths, or indices in the infrared itself, which are more closely linked to stellar surface brightness variations (e.g., Gieren *et al.* 1989). Narrow band spectrophotometric indices also work well (Turner 1988; Turner and Burke 2002). Current techniques mainly employ the former, typically using variants that employ sophisticated statistical methods to test the validity of the results.

An early estimate for the projection factor of $p = 1.412$ by Getting (1934) was later reduced to 1.31 from model atmosphere calculations (Parsons 1972; Karp 1975), then increased back to values near 1.4, with a period dependence, when Hindsley and Bell (1986) used more recent Kurucz model atmospheres. The values used in Baade-Wesselink analyses then varied from author to author over the next two decades, until more recent stellar atmosphere models were employed and Gray and Stephenson (2007) noted that a toy model for the pulsation of bright Cepheids implied values of p closer to 1.3 in some cases, depending upon the source of radial velocity measures. More recent work by Nardetto *et al.* (2009, and in press), Laney and Joner (2009), and Neilson and Lester (2011) continue to argue the case for different values near $4/3 \pm 0.1$, with a possible period dependence.

The method of measuring radial velocities is an extremely important consideration. Most lines visible in Cepheid spectra, the lines of neutral iron (Fe I) for example, are formed at higher layers of a Cepheid's atmosphere than the deeper regions generating the stellar continuum. Since pulsation results in a variable extension, or stretching, of the atmosphere rather than a simple up-down displacement, the lines used for radial velocity measurement should be higher ionization species like singly ionized iron (Fe II) to properly track the radial motion of the deeper layers where the light originates that is responsible for the brightness differences Δm. But many radial velocity observations in the literature were obtained using cross-correlation techniques, often dominated by low ionization species, which is why the value of p may continue to be debated.

The debate may be of only minor concern, however. Independent studies of the period-radius relation for Galactic Cepheids by Laney and Stobie (1995), Gieren *et al.* (1998), and Turner and Burke (2002) yield nearly identical values for the slope and zero-point of the relation, despite different methodologies, with

the average Cepheid radius being almost exactly proportional to $P^{3/4}$ (Turner *et al.* 2010a). The radius of any Cepheid can therefore be estimated reliably from its pulsation period, provided that it corresponds to fundamental mode pulsation in the star. A polynomial linking a star's effective temperature to its reddening-free *B–V* color index has been derived by Gray (1992), allowing one to derive a Cepheid's luminosity directly. The technique generates results that are a close match to Cepheid luminosities established from trigonometric and open cluster parallaxes (Turner and Burke 2002; Turner 2010; Turner *et al.* 2010a), where any such comparison also requires a knowledge of bolometric corrections for Cepheids in order to link absolute bolometric magnitudes M_{bol} (= –2.5 log *L*) to intensity-averaged absolute visual magnitudes $<M_V>$, where the bolometric correction BC = $M_{bol} - <M_V>$.

The importance of an accurate knowledge of the interstellar reddening affecting individual Cepheids now becomes clear. For the above technique to yield reliable results, it is essential to account properly for the reddening produced within our Milky Way Galaxy or, for extragalactic Cepheids, in other galaxies. For many years reddenings for Galactic Cepheids have been obtained from a variety of sources essentially linked to period-color relations, which do not account for the intrinsic temperature width of the instability strip and the distribution of individual Cepheids within it. Considerable use has been made, for example, of compilations by Fernie (1990a, b), which are of that type. More direct reddenings are available, for example those tied to reddening-free indices (e.g. Turner *et al.* 1987) or to space reddenings (Turner 2001; Benedict *et al.* 2002, 2007; Laney and Caldwell 2007; Turner *et al.* 2011), which entail use of reddenings derived for close neighbors of Cepheids to infer color excesses for the variables. Cepheids belonging to open clusters play an important role in the latter. Kovtyukh *et al.* (2008) have also used the relationship of Gray (1992) between stellar effective temperature and unreddened *B–V* color with model stellar atmosphere fits to Cepheid spectra over their pulsation cycles to deduce their reddenings from their observed color variations, a novel inversion of the normal procedure.

The period-luminosity relation that results from using the above relationships with Galactic Cepheids of well-established reddening and Cepheids with HST or cluster parallaxes is shown in Figure 3. The derived relationship is described by $\log L/L_{\odot} = 2.409 + 1.168 \log P$. The scatter is intrinsic, and results from the temperature width of the instability strip. Cepheids of a given period can be small amplitude variables on the hot or red edges of the strip, or large amplitude variables just blueward of strip center.

Cepheids that are members of binary systems or open clusters can also be used to establish a Cepheid period-mass relation. Cepheids in open clusters have identical ages to cluster members, which can be established from model isochrone fits to the unreddened color-magnitude diagrams for the clusters (e.g., Turner *et al.* 2008). The inferred ages for cluster Cepheids can then be

used with published models by Meynet *et al.* (1993) to establish masses for stars at the terminal stages of core hydrogen burning, designated as M_{RTO}, for stars at the red turnoff (RTO) for the clusters. Such masses should be close to, or perhaps slightly smaller than, the masses of the corresponding Cepheids. An analysis of that type was made by Turner (1996), subsequently updated by Turner *et al.* (2010a) to include more recent results for a few clusters (Turner *et al.* 2006b, 2008, 2009).

More recent results are now available for TW Nor in Lyngå 6 (Majaess *et al.* 2011) and SU Cas in Alessi 95 (Turner *et al.* 2012), and can be combined with masses derived for the binary Cepheids W Sgr (Evans *et al.* 2009), OGLE-LMC-CEP0227 (Pietrzyński *et al.* 2010), and V350 Sgr (Evans *et al.* 2011). The results, presented in Figure 4, confirm the consistency of binary masses and evolutionary masses for Cepheids, and suggest a simple relationship between the mass of a Cepheid and its pulsation period. Turner (1996) found that Cepheid masses scale as $P^{1/2}$, but the data of Figure 4 appear to vary as $P^{0.4}$. The implication is that the pulsation period varies as $M^{2½}$. The deviation of long-period Cepheids from a simple $P^{1/2}$ relationship could alternatively be evidence for the importance of mass loss for such stars (e.g., Marengo *et al.* 2010; Neilson *et al.* 2011).

The same data can be used to construct a period-age relation for Cepheids in open clusters, as displayed in Figure 5. The best-fitting linear relation to the data is given by $\log t = 8.48 - 0.724 \log P$. In this case, the slope of the relationship cannot be interpreted in terms of a simple power law, being tied as it is to the evolutionary models of Meynet *et al.* (1993).

4. The extragalactic setting

The use of the period-luminosity relation for extragalactic Cepheids usually involves a reddening-free formulation referred to as the Wesenheit function, after Madore (1976, 1982). An example for Johnson system *BV* magnitudes is $W_{BV} = \langle M_V \rangle - R_V (B-V)$, where R_V is the ratio of total-to-selective extinction for interstellar dust. For Cepheids a value of $R_V \cong 3.3$ seems valid, although there is no guarantee that it applies to dust in all directions of the Galaxy, or within other galaxies, for that matter. All reddening-free relations are at best an approximation; in the case of the Wesenheit function it reduces the intrinsic scatter in period-absolute magnitude relations, but overcorrects for intrinsic color spread of the instability strip. It works only if Cepheids in other galaxies are very similar in their intrinsic properties to Galactic Cepheids, and the dust extinction properties are more-or-less the same. Because of concerns about the latter, however, standard usage involves observations of Cepheids in the visible to near-infrared region, where the effects of interstellar extinction are reduced.

The extension of photometric imaging to increasingly fainter brightness

limits is also generating reliable photometry for Type II Cepheids and RR Lyrae variables in nearby galaxies. Type II Cepheids include BL Her variables (P = 1–8 days), W Vir stars (P = 8–20 days), and, in recent years, the RV Tau variables, which exhibit period doubling, a phenomenon that has attracted considerable attention in the last year from its ubiquitous nature. Together with the RR Lyrae variables, Type II Cepheids appear to describe a unique PL relation of their own that can be used to establish galaxy distances reliably (e.g., Majaess *et al.* 2009; Majaess 2010). Likewise, radially pulsating δ Sct variables follow a PL relation similar to that for classical Cepheids (Fernie 1992), and both relations, when combined, provide a powerful tool for establishing accurate distances to nearby galaxies.

5. Cepheids and the AAVSO

Despite the existence of over 200,000 visual observations of Cepheids in the AAVSO International Database, the variables have not received the same degree of attention from AAVSO observers as Miras and cataclysmic binaries, possibly because they represent a smaller sample of stars of perceived regular behavior. Nevertheless, the bright variable δ Cep has been a popular target for beginning observers and interested amateurs, and AAVSO visual and CCD observations have been extremely useful for studies of Cepheid period changes (Berdnikov *et al.* 2003; Turner 1998; Turner *et al.* 2001, 2007). Brightness estimates for Cepheids published in the *Journal of the AAVSO* by students at the Maria Mitchell Observatory (e.g., Starmer 1989) have also been useful for such studies (see references in Turner 1998), and there have also been relevant articles on period-finding and O–C analyses (Belserene 1988, 1989) that are useful for the analysis of Cepheid period changes. Visual observations of δ Cep by AAVSO observers appear to be accurate, despite large scatter, although the finder chart for visual observers needs to be updated to make it applicable for non-dark-adapted observers (Turner 1999, 2011). Reference magnitudes on AAVSO charts for the nearby variable μ Cep are more closely tied to the Johnson system, for example.

The future of Cepheid observations by the AAVSO is unclear, given the large survey instruments that are beginning to appear. Yet AAVSO observations of bright Cepheids should continue to fill a niche where data are needed. The recently developed project by Variable Stars South observers for precision monitoring of bright southern Cepheids (Walker 2011) is an excellent example. As evident from the recent AAVSO observing campaign on Hubble's variable V1 in the Andromeda galaxy M31, a Cepheid with a period of ~30 days (*AAVSO Alert Notice 422*), Cepheids continue to make interesting objects for observation.

References

AAVSO 2010, *AAVSO Alert Notice 422* (July 16), AAVSO, Cambridge, MA.
Abt, H. A. 1959, *Astrophys. J.*, **130**, 824.
Antonello, E., and Mantegazza, L. 1984, *Astron. Astrophys.*, **133**, 52.
Antonello, E., and Poretti, E. 1986, *Astron. Astrophys.*, **169**, 149.
Baade, W. 1926, *Astron. Nachr.*, **228**, 359.
Belserene, E. P. 1988, *J. Amer. Assoc. Var. Star Obs.*, **17**, 123.
Belserene, E. P. 1989, *J. Amer. Assoc. Var. Star Obs.*, **18**, 55.
Benedict, G. F., *et al.* 2002, *Astrophys. J.*, **124**, 1695.
Benedict, G. F., *et al.* 2007, *Astrophys. J.*, **133**, 1810.
Benz, W., and Mayor, M. 1982, *Astron. Astrophys.*, **111**, 224.
Berdnikov, L. N. 1992, *Sov. Astron. Lett.*, **18**, 207.
Berdnikov, L. N., Mattei, J. A., and Beck, S. J. 2003, *J. Amer. Assoc. Var. Star Obs.*, **31**, 146.
Berdnikov, L. N., Samus, N. N., Antipin, S. V., Ezhkova, O. V., Pastukhova, E. N., and Turner, D. G. 2004, *Publ. Astron. Soc. Pacific*, **116**, 536.
Efremov, Y. N. 1968, *Peremen. Zvezdy*, **16**, 365.
Engle, S. G., Guinan, E., Evans, N., and DePasquale, J. 2009, *Bull. Amer. Astron. Soc.*, **41**, 303.
Evans, N. R. 1976, *Astrophys. J.*, **209**, 135.
Evans, N. R., Berdnikov, L., Gorynya, N., Rastorguev, A., and Eaton, J. 2011, *Astron. J.*, **142**, 87.
Evans, N. R., Massa, D., and Proffitt, C. 2009, *Astron. J.*, **137**, 3700.
Fernie, J. D. 1969, *Publ. Astron. Soc. Pacific*, **81**, 707.
Fernie, J. D. 1984, in *Observational Tests of the Stellar Evolution Theory*, eds. A. Maeder and A. Renzini, IAU Symp. 105, D. Reidel, Dordrecht, The Netherlands, 441.
Fernie, J. D. 1990a, *Astrophys. J., Suppl. Ser.*, **72**, 153.
Fernie, J. D. 1990b, *Astrophys. J.*, **354**, 295.
Fernie, J. D. 1992, *Astron. J.*, **103**, 1647.
Freedman, W. L., *et al.* 2001, *Astrophys. J.*, **553**, 47.
Getting, I. A. 1934, *Mon. Not. Roy. Astron. Soc.*, **95**, 139.
Gieren, W. P., Barnes, T. G., III, and Moffett, T. J. 1989, *Astrophys. J.*, **342**, 467.
Gieren, W. P., Fouqué, P., and Gómez, M. 1998, *Astrophys. J.*, **496**, 17.
Gray, D. F. 1992, *The Observation and Analysis of Stellar Photospheres*, Cambridge Astrophys. Ser., 20, Cambridge Univ. Press, Cambridge.
Gray, D. F., and Stephenson, K. B. 2007, *Publ. Astron. Soc. Pacific*, **119**, 398.
Hertzsprung, E. 1913, *Astron. Nachr.*, **196**, 201.
Hindsley, R., and Bell, R. 1986, *Publ. Astron. Soc. Pacific*, **98**, 881.
Hofmeister, E. 1967, *Z. Astrophys.*, **65**, 194.
Karp, A. H. 1975, *Astrophys. J.*, **201**, 641.

Kovtyukh, V. V., Soubiran, C., Luck, R. E., Turner, D. G., Belik, S. I., Andrievsky, S. M., and Chekhonadskikh, F. A. 2008, *Mon. Not. Roy. Astron. Soc.*, **389**, 1336.

Kraft, R. P. 1963, in *Basic Astronomical Data*, ed. K. Aa. Strand, Univ. Chicago Press, Chicago, 421.

Laney, C. D., and Caldwell, J. A. R. 2007, *Mon. Not. Roy. Astron. Soc.*, **377**, 147.

Laney, C. D., and Joner, M. D. 2009, in *Stellar Pulsation: Challenges for Theory and Observation*, eds. J. Guzik and P. Bradley, AIP Conf. Ser., 1170, Amer. Inst. Physics, Melville, New York, 93.

Laney, C. D., and Stobie, R. S. 1995, *Mon. Not. Roy. Astron. Soc.*, **274**, 337.

Leavitt, H. S. 1908, *Ann. Harvard Coll. Obs.*, **60**, 87.

Leavitt, H. S., and Pickering, E. C. 1912, *Circ. Harvard Coll. Obs.*, **173**, 1.

Madore, B. F. 1976, *Roy. Greenwich Obs. Bull.*, **182**, 153.

Madore, B. F. 1982, *Astrophys. J.*, **253**, 575.

Majaess, D. J. 2010, *J. Amer. Assoc. Var. Star Obs.*, **38**, 100.

Majaess, D. J., Turner, D. G., and Lane, D. J. 2009, *Acta Astron.*, **59**, 403.

Majaess, D. J., *et al.* 2011, *Astrophys. J., Lett. Ed.*, **741**, L27.

Marengo, M., *et al.* 2010, *Astrophys. J.*, **725**, 2392.

Meynet, G., Mermilliod, J.-C., and Maeder, A. 1993, *Astron. Astrophys., Suppl. Ser.*, **98**, 477.

Milone, E. F. 1970, *Inf. Bull. Var. Stars*, No. 482, 1.

Moffett, T. J., and Barnes, T. G., III 1980, *Astrophys. J., Suppl. Ser.*, **44**, 427.

Moffett, T. J., and Barnes, T. G., III 1984, *Astrophys. J., Suppl. Ser.*, **55**, 389.

Nardetto, N., Gieren, W., Kervella, P., Fouqué, P., Storm, J., Pietrzyński, G., Mourard, D., and Queloz, D. 2009, *Astron. Astrophys.*, **502**, 951.

Nardetto, N., *et al.*, 2011, in press.

Neilson, H. R., Cantiello, M., and Langer, N. 2011, *Astron. Astrophys.*, **529**, 9.

Neilson, H. R., Engle, S. G., Guinan, E., Langer, N., Wasatonic, R. P., and Williams, D. B. 2012, *Astrophys. J., Lett. Ed.*, **745**, L32.

Neilson, H. R., and Lester, J. B. 2011, *Astron. Astrophys.*, **530**, 65.

Pardo, I., and Poretti, E. 1997, *Astron. Astrophys.*, **324**, 121.

Parsons, S. B. 1972, *Astrophys. J.*, **174**, 57.

Payne-Gaposchkin, C. H. 1974, *Smithson. Contrib. Astrophys.*, **16**, 1.

Pel, J. W., and Lub, J. 1978, in *The HR diagram—The 100th anniversary of Henry Norris Russell*, IAU Symp. 80, D. Reidel, Dordrecht, 229.

Pietrzyński, G., *et al.* 2010, *Nature*, **468**, 542.

Sandage, A., and Tammann, G. A. 1971, *Astrophys. J.*, **167**, 293.

Sandage, A., Tammann, G. A., and Reindl, B. 2004, *Astron. Astrophys.*, **424**, 43.

Shapley, H. R. 1918a, *Astrophys. J.*, **48**, 89.

Shapley, H. R. 1918b, *Astrophys. J.*, **48**, 154.

Simon, N. R., and Lee, A. S. 1981, *Astrophys. J.*, **248**, 291.

Starmer, K. B. 1989, *J. Amer. Assoc. Var. Star Obs.*, **18**, 129.

Szabados, L. 1983, *Astrophys. Space Sci.*, **96**, 185.
Tsesevich, V. P. 1971, in *Variable Star Research Methods*, ed. V. B. Nikonov, Nauka, Moscow, 49.
Turner, D. G. 1988, *Astron. J.*, **96**, 1565.
Turner, D. G. 1992, *Astron. J.*, **104**, 1865.
Turner, D. G. 1996, *J. Roy. Astron. Soc. Canada*, **90**, 82.
Turner, D. G. 1998, *J. Amer. Assoc. Var. Star Obs.*, **26**, 101.
Turner, D. G. 1999, *J. Roy. Astron. Soc. Canada*, **93**, 228.
Turner, D. G. 2001, *Odessa Astron. Publ.*, **14**, 166.
Turner, D. G. 2009, in *Stellar Pulsation: Challenges for Theory and Observation*, eds. J. Guzik and P. Bradley, AIP Conf. Ser., 1170, Amer. Inst. Physics, Melville, New York, 59.
Turner, D. G. 2010, *Astrophys. Space. Sci.*, **326**, 219.
Turner, D. G. 2011, *J. Amer. Assoc. Var. Star Obs.*, **39**, 148.
Turner, D. G., Abdel-Sabour Abdel-Latif, M., and Berdnikov, L. N. 2006a, *Publ. Astron. Soc. Pacific*, **118**, 410.
Turner, D. G., and Berdnikov, L. N. 2004, *Astron. Astrophys.*, **423**, 335.
Turner, D. G., Billings, G. W., and Berdnikov, L. N. 2001, *Publ. Astron. Soc. Pacific*, **113**, 715.
Turner, D. G., and Burke, J. F. 2002, *Astron. J.*, **124**, 2931.
Turner, D. G., Horsford, A. J., and MacMillan, J. D. 1999, *J. Amer. Assoc. Var. Star Obs.*, **27**, 5.
Turner, D. G., Kovtyukh, V. V., Majaess, D. J., Lane, D. J., and Moncrieff, K. E. 2009, *Astron. Nachr.*, **330**, 807.
Turner, D. G., Leonard, P. J. T., and English, D. A. 1987, *Astron J.*, **93**, 368.
Turner, D. G., MacLellan, R. F., Henden, A. A., and Berdnikov, L. N. 2011, *Rev. Mex. Astron. Astrofis.*, **47**, 345.
Turner, D. G., Majaess, D. J., Lane, D. J., Rosvick, J. M., Henden, A. A., and Balam, D. D. 2010a, *Odessa Astron. Publ.*, **23**, 119.
Turner, D. G., Majaess, D. J., Lane, D. J., Percy, J. R., English, D. A., and Huziak, R. 2010b, *Odessa Astron. Publ.*, **23**, 125.
Turner, D. G., Usenko, I. A., and Kovtyukh, V. V. 2006b, *Observatory*, **126**, 207.
Turner, D. G., *et al.* 2007, *Publ. Astron. Soc. Pacific*, **119**, 1247.
Turner, D. G., *et al.* 2008, *Mon. Not. Roy. Astron. Soc.*, **388**, 444.
Turner, D. G., *et al.* 2012, *Mon. Not. Roy. Astron. Soc.*, in press.
Walker, S. 2011, *Var. Stars South Newsletter*, 2011-3, 9.
Wesselink, A. J. 1946, *Bull. Astron. Inst. Netherlands*, **10**, 91.
Zabolotskikh, M. V., Sachkov, M. E., Berdnikov, L. N., Rastorguev, A. S., and Egorov, L. E., 2005, in *Proceedings of the Gaia Symposium: The Three-Dimensional Universe With Gaia*, ed. C. Turon, K. S. O'Flaherty, and M. A. C. Perryman, ESA Special Publ., 576 (http://www.rssd.esa.int/index.php?project=Gaia&page=Gaia_2004_Proceedings supercedes printed version), 723.

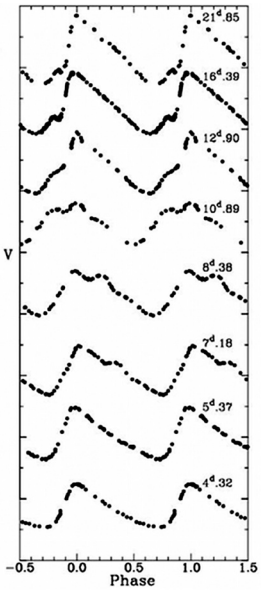

Figure 1. The Hertzsprung progression seen in the light curves of, from top to bottom, the Cepheids WZ Sgr, X Cyg, Z Sct, VX Per, S Sge, η Aql, δ Cep, and Y Lac. Visual magnitude steps are 1.0 magnitude between large divisions and the pulsation periods are indicated. The data are from Moffett and Barnes (1980, 1984), and have been offset in order to fit comfortably in the diagram.

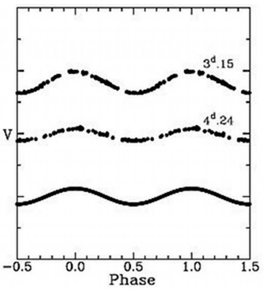

Figure 2. Light curves of, from top to bottom, the Cepheids SZ Tau, V1726 Cyg, and a simulated sine wave Cepheid with an amplitude of A_V = 0.25 magnitude. Terminology is the same as in Figure 1. The data are from Milone (1970) and Turner *et al.* (2001), offset to fit comfortably in the diagram.

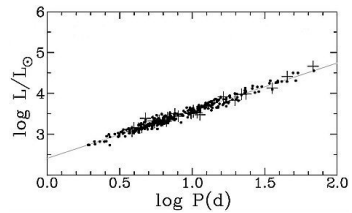

Figure 3. The period-luminosity relation for Galactic Cepheids of well-established reddening (points) and with HST or cluster parallaxes (plus signs).

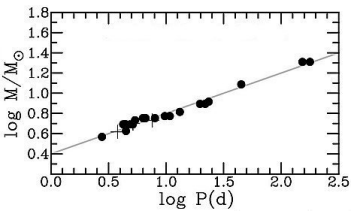

Figure 4. The Cepheid period-mass relation defined by members of open clusters (filled circles) and binaries (plus signs). The plotted relation is described by $M \sim P^{0.4}$.

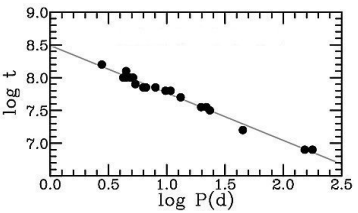

Figure 5. The Cepheid period-age relation defined by members of open clusters. The plotted relation is described by log t = 8.49 – 0.724 log P.

Miras

Lee Anne Willson
Massimo Marengo
Iowa State University, Department of Physics and Astronomy, Ames, IA 50011; address email correspondence to lwillson@iastate.edu

Invited review paper, received May 15, 2012

Abstract Mira variables share essential characteristics: High visual amplitude, periods of hundreds of days, red colors (spectral types M, S, and C), and the presence of emission lines at some phases. They are fundamental mode pulsators, with progenitor masses ranging from <1 to several solar masses. In this review, we summarize what is known from modeling and observational studies, including recent measurements from optical and IR interferometry, and studies involving large samples of stars particularly in the Magellanic Clouds. While we have a good idea of how these stars fit into the big picture of stellar evolution, many important details remain to be settled by a combination of more ambitious models and new observational techniques. Carrying on observations of bright Mira variables will be essential for interpreting observations of large numbers of fainter sources as well as for assessing the completeness and accuracy of the models.

1. Miras—fundamentals, mostly old news

Oxygen-rich Mira variables are red giants with visual amplitudes of 2.5 to > 7.5 magnitudes and relatively stable light curves; this corresponds to visual brightness changes from ×10 to ×1000. Their bolometric magnitude variation is about 1 magnitude, meaning the luminosity is varying only by a factor of 2–3. The reason that the visual brightness changes so much more over the cycle is that there are strong variations in the opacity of the atmosphere from minimum to maximum light, largely the result of variable amounts of TiO and other molecules.

There are fewer carbon-rich Miras, although plenty of variable carbon stars that are very similar to Miras in their bolometric variability. The difference in the atmospheric chemistry when C/O is > 1 vs. < 1 is part of the reason for this difference; the other is probably the sensitivity of the stellar radius to C/O, meaning the stars migrate across the zones of pulsational instability as C/O increases.

The pulsation of the Mira variables is driven by the same kind of process that drives the pulsation of Cepheids, and is a result of changes in the opacity and the dependence of pressure on temperature and density when hydrogen and helium are ionizing or recombining. In the Cepheids, the pulsation is rooted in

the He+ <–> He++ zone, and in the Miras, in the H <–> H+ and He <–> He+ zones. Early modeling that showed this was done by Wood (1974; also Fox and Wood 1982) and by Ostlie (Ostlie and Cox 1986; Cox and Ostlie 1993).

The mode of pulsation is usually derived by taking the observed period, mass, and radius and comparing this with the periods derived from models with the same M and R. Thus, for red giants with M and R appropriate for Mira variables Ostlie and Cox found:

Fundamental mode
$P = 0.012d\ R^{1.86}\ M^{-0.73}$ or $\log P = -1.92 - 0.73\ \log M + 1.86\ \log R$

First overtone
$P = 0.04d\ R^{1.5}\ M^{-0.5}$ or $\log P = -1.40 + 1.5\ \log R - 0.5\ \log M$

These are both radial modes—that is, all the motion is in and out—and differ in that for the fundamental mode, all parts of the star move out or in together while for the first overtone, part of the star moves out while another part moves in. Thus the overtone mode has a shorter effective wavelength and if we assume the pulsation is like a sound wave, with the same sound speed, shorter wavelength → shorter period.

For the Miras, there are two difficulties with this approach. One problem is that we don't have direct measurements of the masses of the stars, and the other is that the radius measurements can be ambiguous or misleading. These difficulties were the cause of a long debate over the correct mode assignment for the Mira variables. In recent years the radius measurements have been improved and disambiguated via interferometry, and we have some new constraints on the current masses—see section 3. However, the debate was mostly settled before these results came in, based on modeling of shock waves in the atmosphere and a better understanding of the dynamics of the stellar atmospheres and winds.

The gist of the dynamical argument for the pulsation mode is this: When material in the atmosphere goes through one of the pulsation-induced outward-propagating shocks, it is given a kick and begins to travel outward. This trajectory is close to ballistic, that is, like a ball tossed upward. The stellar gravity acts on the material, bringing it back to its original position, or close to it, in time for the next shock to hit—just as hitting a ping-pong ball with a paddle can keep it in the air indefinitely if you always hit it at the right moment at the same place. For a purely ballistic motion, the infall velocity when the next shock comes through is equal to the outward motion after the previous shock, so the change in velocity is from +v to –v or 2v. This is the shock velocity amplitude, and can be deduced observationally from the Doppler shifts in spectral lines. The observed shock amplitudes are sufficiently large that they dictate a large gravity, inconsistent with the radii that give the observed periods with reasonable guesses about the masses of these stars (Hill and Willson 1979 and Willson and Hill 1979).

There are other ways to get at least a clue about the mode of pulsation. Typically, for fundamental mode pulsation, the motions are large enough to produce an asymmetric light curve—this is seen in Cepheids, RR Lyrae stars, and Miras. Overtone pulsation, in contrast, tends to produce more symmetric or sinusoidal variation and also smaller amplitude variability—this is definitely true when M and R are fixed, and still likely if P is held constant while M and/or R are varied.

In section 3 we will discuss at somewhat greater length the results of interferometric studies deriving the stellar radii at various phases of the pulsation cycle and some of what this has taught us about these stars. In section 2 we briefly review recent evolutionary modeling of relevance for Miras; in section 4, light curves and their shapes and secular changes; in section 5, the relation of these stars to RV Tauri stars and to planetary nebulae (if any), and in section 6 we discuss the recent waves of observational data from surveys and what such data can tell us when carefully analyzed.

The mass of a Mira variable is less than or equal to the mass of the star when it was on the main sequence. If we had a reliable formula for the mass loss as a function of mass, radius, luminosity, and so on, then we could integrate over the evolution and get a current mass—but we do not have such a formula (Bowen and Willson 1991; Willson 2000, 2009). If we had very good constraints on their radii we could get estimates for the masses from their pulsation periods; however, as noted above, radii are uncertain.

We do have a handle on the progenitor masses based on the distribution of the Miras in the galaxy—in simplest terms, we assign Miras to an appropriate population (old, young) based on their galactic orbits and on their metallicity. In our galaxy there is a correlation of age (older = lower mass) and metallicity in the sense that the shortest-period Miras have the lowest masses and metallicities. This fits with the age-metallicity correlation in general for field stars, and suggests the progenitors of the 200- to 250-day Miras were main sequence stars with masses near 1 solar mass while the 400- to 600-day Miras come from stars with progenitor masses $\geq$ 2 solar masses.

The assignment of a progenitor mass to a particular star based on its period can be risky, however, as these stars experience period changes during the course of shell flash cycling (see section 2). A star that normally sits at 500 days will spend up to 10% of its time between 200 and 300 days, for example. So at least the shorter-P population is expected to be contaminated with some higher-progenitor-mass interlopers.

Some recent attempts to derive masses for particular Miras based on interferometric observations have yielded masses close to the expected progenitor masses—something that we expect from the period-luminosity relation but that is nice to have confirmed by a more direct measure. Thus, for example, Lacour *et al.* (2009) find a mass of about 2 solar masses for χ Cyg, consistent with its relatively long period and large amplitude.

2. Modeling Miras with an emphasis on recent progress

There are three categories of models that are relevant for the study of Miras. The first is evolutionary models—following a star as it progressively uses up its nuclear fuels. The second is pulsation modeling, including testing very small perturbations for whether they will grow or damp out, and nonlinear modeling that seeks to determine the full-amplitude behavior of the pulsating star. The third is modeling of the atmosphere and wind, for the dual purposes of reproducing observed light curves, colors, and spectra and of determining the mass loss rates and velocities of the outflow for stars with a range of properties.

Miras are stars at the tip of the asymptotic giant branch; this much was known by the time LAW began to work on these stars in the 1970s. From evolutionary models we know that a star that begins with about 1 solar mass—a typical Mira progenitor star—will convert H to He in its core on the main sequence, taking about 10 Gyr to achieve this very slow "burning" of H. Then, the now predominantly He core will collapse into a degenerate state about the size of Earth and the star will expand to become a red giant. As to why it makes this transition, and fairly quickly, see Renzini and Ritossa (1994) and Iben (1993) for some authoritative arguments; a classic review of the evolution of low to intermediate mass stars is Iben (1967).

The source of energy for the red giant is the conversion of H to He in a shell around its degenerate core; thus the core mass gradually increases as it collects the garbage of the H-burning process. When the core of degenerate He reaches about half a solar mass, conversion of He to C and O begins by the triple-alpha process, where a very temporary He+He pair in the form of unstable ^{8}Be is joined by a third He before it breaks up, and where the resulting C can add one more He to form O. Because the core is degenerate, it does not quickly readjust its structure when this new energy source turns on, and so, the process runs away—we call this the "Helium core flash." While one might expect this to explode the star, it does not, but after a brief disequilibrium the star settles into quiescent He burning as a horizontal branch star or clump giant, the extent to which it leaves the red giant track depending on the mass it has at this point.

When the He in the core has become C and O, the core again settles into a dense, degenerate state and the star once again evolves with increasing L up the "asymptotic giant branch" (AGB), so called because the track gradually converges to the earlier red giant track. Now, the conversion of H to He alternates with the conversion of He to C and O in a series of shell flashes or thermal pulses. (These pulses, which take perhaps 100,000 years to complete, are not to be confused with the pulsations that occur on a time scale of a few months or years.)

Some of the longer period Miras come from higher mass progenitors, 2 $M_{\odot}$ or more. Above about 2.8 solar masses the evolution is slightly different, with no He core flash. For a description of the evolution of these higher

masses, see for example Iben (1975) or recent papers by Herwig (e.g. 2008) or Marigo *et al.* (2011, 2008). Grids of models are available online at various sites, including http://stev.oapd.inaf.it/cgi-bin/cmd (see Nasi *et al.* 2008), and an evolution code is available via the MESA project, http://mesa.sourceforge.net/, in two forms—a version for education and exploration and a version for serious research projects.

Red giants and AGB stars have degenerate cores surrounded by very deep convection zones reaching nearly all the way from the core to the surface, or from about 0.01 to 100 times the present solar radius $R_{\odot}$. Convection is very hard to model, and the behavior of the gas near the edges of the convection zone turns out to be critical for, for example, the contamination of the outer envelope and atmosphere with the products of the nuclear burning. One consequence of such contamination is a gradual increase in the ratio of carbon to oxygen, C/O. Carbon stars have C/O > 1 and S stars have C/O ≈ 1 while most stars, including M-type Miras, have C/O < 1. As C/O changes, so does the internal opacity and thus the radius of the star for a given L and M (Marigo and Girardi 2007). Also, because C and O form a very stable molecule, CO, the chemistry of the surface layers, atmosphere, and wind changes dramatically as C/O passes 1, and the kinds of grains that form and assist in the mass loss process also change.

Evolutionary modeling in recent years has focused on the convection process, particularly on the effects of "convective overshoot" mixing material beyond the boundaries of what are otherwise the domains of convective instability. There have also been advances in modeling the variations that occur during He shell flashes. Very little has been done to study the pulsation in more detail—the linear analyses done in the late 1970s and 1980s give useful results, and models with full-up non-linear non-adiabatic pulsation in a fully convective envelope are just out of reach of existing codes and machines, although we expect advances in this area in the next decade.

3. Interferometry and other methods for probing the near-star environment

Interferometry is a means of seeing detail not possible with a single aperture or telescope. Long baseline interferometry, using two or more telescopes, provides the finest spatial resolution. Aperture masking and segment tilting interferometry, that involves dividing the mirror of a very large telescope into smaller sub-apertures (using a mask, for example), has also been used to study Miras (Haniff *et al.* 1992; Woodruff *et al.* 2008, 2009). Earlier papers also cite "speckle interferometry" which is not really interferometry at all but rather a method for getting around the effects of seeing by adding short exposure sub-images together (Labeyrie 1970; Bonneau and Labeyrie 1973).

To resolve the diameters of Miras requires milli-arcsec resolution even for the nearest stars (χ Cyg, R Leo, and Mira). Resolved diameters yield more than just a number; watching the variation of the diameter over the

cycle allows for determination of ΔR/R which, with observed velocities, can yield R and thus distance as well as a constraint on pulsation models. Another constraint on models comes from the variation of the apparent angular diameter with the wavelength of the observations, telling us how the atmospheric opacity varies with wavelength and revealing molecule-rich or dust-rich layers in the atmosphere.

Starting from the measurement of o Ceti's diameter by Pease in 1931 using an optical Michelson interferometer, the main goal of these studies was to resolve the controversy on Miras' pulsation modes by measuring their radius. While early results (Tuthill *et al.*1994) measured overly large radii, suggesting that Mira variables should be first overtone pulsators, subsequent analysis (Menesson *et al.* 2002; Perrin *et al.* 2004) found that these diameters were actually biased by the presence of molecular layers (mainly CO and H_2O) a few stellar radii above the photosphere. This breakthrough was enabled by the introduction of a new generation of instruments at world's largest interferometers (VLTI in the southern hemisphere and PTI/CHARA in the north), capable of simultaneously measuring the angular diameter at several broad and narrow bands. These observations can be directly compared with time-dependent hydrodynamic simulations (see, for example, Hillen *et al.* 2012), providing precious observational constraints to stellar models and pulsation theory (Le-Bouquin *et al.* 2009; Martí-Vidal *et al.* 2011) and allowing the exploration of non-equilibrium chemistry in the stellar atmosphere (Paladini *et al.* 2009).

Interferometry with more than two elements also yields information about departures from spherical symmetry in the system. Ragland *et al.* (2006) combined the light from the three apertures of the IOTA interferometer to study the asymmetry of M- and C-type giants with different pulsation properties. Non-zero closure phase (a signature of departure from spherical symmetry) was found in 30% of the targets, or essentially all that were reliably resolved. This asymmetry did not depend on the chemistry of the atmosphere, but was much more common among Miras than other types of long period variables. These asymmetries were located in close proximity of the stellar surface (1.5–2 stellar radii) suggesting an origin either related to the presence of large convective cells in the stellar photosphere, discrete dust clouds formation, or the interaction with a companion. Recent results using aperture synthesis techniques borrowed from radio-interferometry have allowed the reconstruction of true images for a few late-type pulsating variables (for example, χ Cyg in Lacour *et al.* 2009, or RR Aql in Karovicova *et al.* 2011). These images have provided direct evidence for the presence of hot cells in the stellar atmosphere and, combined with radial velocity measurements, have allowed the mapping of speed, density, and position of diverse molecular species in pulsation-driven atmospheres.

Asymmetric dust shells have also been detected around several targets, using either the thermal-infrared long baseline interferometry, or speckle,

aperture masking, or segment-tilting techniques on large-aperture telescopes. The recent detection of large, transparent grains as close as 1.5 stellar radii around a number of mass-losing cool giants (including the carbon Mira R Leo, Norris *et al.* 2012) shows the potential of these techniques for probing the dust formation processes that are key for understanding mass loss in Mira variables. While the current angular resolution is not sufficient to measure the motion of these dust layers during the pulsation cycle, the ultimate goal of these observations is to fully characterize the stratification, geometry, and kinematics of the extended Miras' atmosphere, in order to finally understand how mass loss processes are connected to the stellar pulsations, and the root causes for the asymmetries and inhomogeneity observed in their circumstellar environments (Wittkowski *et al.* 2012).

4. Light curves—shapes and secular changes

In addition to the dominant signature of pulsation, Mira variable light curves show an interesting variety of features. The ratio of rise time to cycle length, called *f* by Campbell (1955), varies over a range from about 0.5 down to 0.1 or 0.2 among some of the longest-period Miras. Some of the stars show bumps on their rising or falling branches, and these bumps may come and go over the course of a number of cycles—see, for example, the long-term light curve for χ Cyg. Some of the stars show long-term modulations of their periods or their amplitudes or their mean magnitudes, and these variations are not at all well understood. Some show steady decreases or increases in the periods, often with correlated amplitude changes. Some stars behave like regular Miras for some decades, then fairly abruptly switch to smaller amplitude and/or shorter period variation, causing them to be reclassified as SR stars; it is not clear whether, if we waited long enough, this would happen to a large or a small fraction of our Mira stars.

Templeton *et al.* (2005) looked at a century of AAVSO data for Miras and found that about 10% show significant long-term variability of their periods. The specific variations are, however, all over the map, from apparently sinusoidal (where we need another century to be sure) to apparently steady decrease or increase to abrupt changes from constant to steeply decreasing. While about 1% of the stars are expected to be in a rapidly varying phase of the shell flash cycle, and about 1% of the light-curves show period variations consistent with this explanation, the other 9% of Miras show period variations that are unexplained at present.

5. Relation of Miras to other classes of variables and to planetary nebulae (not)

SR variables differ from Miras in that they have smaller amplitudes, less stable light curves, or are not red giants. Classically, smaller amplitude ones are SRa, less stable ones are SRb, and supergiants are SRc. However, there

is substantial evidence that these distinctions are not the best for separating physically different objects, as some SRa appear to be very much like Miras apart from their visual amplitudes; some Miras start behaving erratically and are reclassified as SRb; and the sequence of pulsating AGB stars extends perhaps as high as seven or eight solar masses, making the distinction with SRc also a bit unclear. Some excellent discussions of these classes of objects may be found in the papers by Hron and Kerschbaum (Kerschbaum and Hron 1996; Kerschbaum *et al.* 1996; Hron *et al.* 1997; Lebzelter *et al.* 1995).

The RV Tauri stars are thought to be a post-Mira, possibly pre-planetary-nebula phase of evolution. The light curves have some characteristics in common with some Miras, including double maxima and long term modulations. Not all Miras become RV Tauri stars, only those from the low-mass, low-luminosity, low-metallicity end of the Mira distribution. For a discussion of RV Tauri stars and their relation to Mira variables see Willson and Templeton (2009).

While it is often stated that the same stars that go through a Mira stage later become central stars of planetary nebulae on their way to becoming white dwarf stars, recent work suggests that only a fraction of Miras can become the central stars of PNe and quite possibly none of the classical Miras will do so; it now appears likely some form of binarity is required for all but perhaps the highest mass progenitors of PNe. This conclusion is reached after recognizing that there are only about 15% as many PNe produced per year as there are stars leaving the AGB per year, so at most 15% of the Miras can become the central stars of PNe. Also, the time scale for evolution across the HR diagram after the AGB is too slow for most of the stars, being perhaps long enough for just the higher masses; finally, the fact that most PNe are not spherically symmetric hints at more than a single-star origin for the PNe. See, for example, papers presented at IAU Symposium 283, Planetary Nebulae, an Eye to the Future (held in 2011, proceedings soon to appear).

6. Using photometric surveys to characterize the Mira and carbon star components of populations

One of the most powerful tools to study variable stars populations in our and other galaxies is represented by unbiased multi-epochs photometric surveys at optical and infrared wavelengths. If the distance to the stars is known (for example, for stars in the same galaxy or cluster), it is then possible to plot the absolute magnitude of the stars as a function of log period. Pulsators with different mode and amplitude tend to be distributed on separate sequences, corresponding to different period-luminosity relations. This approach has been famously pioneered by Peter Wood, using the MACHO database for Large Magellanic Cloud (LMC) variables. Miras appear to be distributed at the bright end of a linear sequence (the "C" sequence as defined in Wood 2000) populated by fundamental mode pulsators, with semiregular (SR) variables at the lower,

fainter end of the sequence. Recent results from the OGLE-III survey (Soszyński *et al.* 2009, 2011) have confirmed these results and extended them to the Small Magellanic Cloud (SMC). This analysis is less successful for galactic Miras, due to the uncertainties in their distance stemming from the poor quality of their Hipparcos parallax. The Gaia mission, by collecting accurate parallaxes of Mira variables across the whole disk of our Galaxy, will be an invaluable resource towards the calibration of a precise period-luminosity relation, on par to what is currently available for Cepheids (Whitelock 2012). Given their higher intrinsic luminosity than other standard candles (Cepheids and RR Lyrae), Miras can be adopted as probes for galactic structure, and precise distance indicators for the farthest galaxies in the local group.

Optical and near-IR surveys offer only a limited capability in discriminating between M-type and carbon Miras. Thermal infrared photometry, on the other end, allows probing the wavelength range where dust features of mass-losing Miras are stronger, providing an excellent diagnostic for their extended atmosphere. Period-luminosity diagrams made for the LMC using Spitzer Space Telescope data show similar sequences as Wood (2000), but an increased level of separation between carbon- and oxygen-rich Miras (Riebel *et al.* 2010). Color-color and color-magnitude diagrams for both the LMC and the SMC in Spitzer bands (Blum 2006; Boyer 2011) provide an even better separation, and allow studying the statistics of carbon and M-type Miras at different metallicity. The main result of these surveys is the confirmation that a low metallicity environment favors the formation of carbon Miras, due to the smaller number of third dredge-up events that are required to push the C/O ratio above unity. These surveys have also highlighted a population of long period variables with very large infrared excess, usually referred to as "extreme AGB" stars. These objects, presumably associated with very large mass loss rates, in the LMC and SMC are generally characterized by a C-rich dust chemistry. While some of these sources lie at the top of the fundamental mode period luminosity sequence, most of them are overtone pulsators (Riebel *et al.* 2010). This result may, however, be the consequence of observational biases preventing the redder sources to be detected in optical and near-IR surveys like MACHO and OGLE-III.

7. Final comments

As Figure 1 shows, research on Miras has waxed and waned several times during the century of the AAVSO. Generally, new observing capabilities or much improved modeling codes lead to increased activity, followed by a decline in action until the next advance. Studies of individual stars and systems are fed by spectroscopy, interferometry, and detailed atmospheric modeling, while studies of the evolution of the stars and the consequences of mass loss associated with the Mira stage are being advanced by evolutionary modeling, infrared

observations, and the statistical analysis of large populations of variable stars.

The AAVSO has played and continues to play a central role in the study of Miras. Most of the papers in Figure 1 are observational; theory papers are a minority. Indeed, in 1972 when LAW's first refereed paper appeared, apparently one eminent astronomer commented "There's a theorist working on Miras. He must be out of his mind!" Nearly every observational study of galactic Miras includes reference to phases or light curves based on data collected by AAVSO or its sister organizations around the world. While the massive studies of Magellanic cloud Miras based on the dark-matter-search byproducts and the huge IR surveys turning up many more of these highly evolved stars described in section 6 mostly do not directly refer to AAVSO data, interpreting the resulting period-luminosity plots and understanding how the Miras and their SR cousins are related will again depend on long-term observations and studies of bright, relatively nearby stars. Future large surveys, including the LSST (Large Synoptic Survey Telescope), will focus on very faint stars and have a duration of observations ranging from a few years to a couple of decades; AAVSO already has a century of data. For stars with periods around a year, a decade is a very short window of observation.

At the present time the observational technologies are expanding our ability to probe the circumstellar environment, to study large samples of stars in a systematic way, and to model the essential physical processes in the interiors, atmospheres, and winds. However, in all of these areas much remains to be done as we are still limited by the capabilities of our computers, detectors, and telescopes.

References

Blum, R. D., *et al.* 2006, *Astron. J.,* **132**, 2034.

Bonneau, D., and Labeyrie, A. 1973, *Astrophys. J.,* **181**, L1.

Bowen, G. H., and Willson, L. A. 1991, *Astrophys. J.,* **375**, L53.

Boyer, M. L., *et al.* 2011, *Astron. J.,* **142**, 103.

Campbell, L. 1955, *Studies of Long Period Variables*, AAVSO, Cambridge, MA.

Cox, A. N., and Ostlie, D. A. 1993, *Astrophys. Space Sci.,* **210**, 311.

Fox, M. W., and Wood, P. R. 1982, *Astrophys. J.,* **259**, 198.

Haniff, C. A., Ghez, A. M., Gorham, P. W., Kulkarni, S. R., Matthews, K., and Neugebauer, G. 1992, *Astron. J.,* **103**, 1662.

Herwig, F. 2008, in *The Art of Modeling Stars in the 21st Century*, IAU Symp. 252, Cambridge Univ. Press, Cambridge, 205.

Hill, S. J., and Willson, L. A. 1979, *Astrophys. J.,* **229**, 1029.

Hillen, M., Verhoelst, T., Degroote, P., Acke, B., and van Winckel, H. 2012, *Astron. Astrophys.,* **538**, L6.

Hron, J., Aringer, B., and Kerschbaum, F. 1997, *Astron. Astrophys.,* **322**, 280.

Iben, I., Jr. 1967, *Ann. Rev. Astron. Astrophys.,* **5**, 571.

Iben, I., Jr. 1975, *Astrophys. J.,* **196**, 525.

Iben, I., Jr. 1993, *Astrophys. J.*, **415**, 767.
Karovicova, I., Wittkowski, M., Boboltz, D. A., Fossat, E., Ohnaka, K., and Scholz, M. 2011, *Astron. Astrophys.,* **532A**, 134.
Kerschbaum, F., and Hron, J. 1996, *Astron. Astrophys.,* **308**, 489.
Kerschbaum, F., Olofsson, H., and Hron, J. 1996, *Astron. Astrophys.,* **311**, 273.
Labeyrie, A. 1970, *Astron. Astrophys.,* **6**, 85.
Lacour, S., *et al.* 2009, *Astrophys. J.,* **707**, 632.
Le Bouquin, J.-B., Lacour, S., Renard, S., Thiébaut, E., Merand, A., and Verhoelst, T. 2009, *Astron. Astrophys.,* **496**, L1.
Lebzelter, T., Kerschbaum, F., and Hron, J. 1995, *Astron. Astrophys.,* **298**, 159.
Marigo, P., Bressan, A., Girardi, L., Aringer, B., Gullieuszik, M., and Groenewegen, M. A. T. 2011, in *Why Galaxies Care About AGB Stars II: Shining Examples and Common Inhabitants*, ASP Conf. Ser. 445, Astron. Soc. Pacific, San Francisco, 431.
Marigo, P., and Girardi, L. 2007, *Astron. Astrophys.,* **469**, 239.
Marigo, P., Girardi, L., Bressan, A., Groenewegen, M. A. T., Silva, L., and Granato, G. L. 2008, *Astron. Astrophys.,* **482**, 883.
Martí-Vidal, I., Marcaide, J. M., Quirrenbach, A., Ohnaka, K., Guirado, J. C., and Wittkowski, M. 2011, *Astron. Astrophys.,* **529A**, 115.
Mennesson, B., *et al.* 2002, *Astrophys. J.,* **579**, 446.
Nasi, E., Bertelli, G., Girardi, L., and Marigo, P. 2008, *Mem. Soc. Astron. Ital.*, **79**, 738.
Norris, B. R. M., *et al.* 2012, *Nature*, **484**, 220.
Ostlie, D. A., and Cox, A. N. 1986, *Astrophys. J.,* **311**, 864.
Paladini, C., Aringer, B., Hron, J., Nowotny, W., Sacuto, S., and Höfner, S. 2009, *Astron. Astrophys.,* **501**, 1073.
Pease, F. G. 1931, *Ergebn. Exacten, Naturwis*, **10**, 84.
Perrin, G., *et al.* 2004, *Astron. Astrophys.,* **426**, 279.
Ragland, S., *et al.* 2006, *Astrophys. J.,* **652**, 650.
Renzini, A., and Ritossa, C. 1994, *Astrophys. J.*, **433**, 293.
Riebel, D., Meixner, M., Fraser, O., Srinivasan, S., Cook, K., and Vijh, U. 2010, *Astrophys. J.,* **723**, 1195.
Soszyński, I., *et al.* 2009, *Acta Astron.,* **59**, 239.
Soszyński, I., *et al.* 2011, *Acta Astron.,* **61**, 217.
Templeton, M. R., Mattei, J. A., and Willson, L. A. 2005, *Astron. J.,* **130**, 776.
Tuthill, P. G., Haniff, C. A., Baldwin, J. E., and Feast, M. W. 1994, *Mon. Not. Roy. Astron. Soc.,* **266**, 745.
Whitelock, P. A. 2012, *Astrophys. Space Sci.,* **45**, in press.
Willson, L. A. 2000, *Ann. Rev. Astron. Astrophys.*, **38**, 573.
Willson, L. A. 2009, in *The Biggest, Baddest, Coolest Stars*, eds. D. G. Luttermoser, B. J. Smith, and R. E. Stencel, ASP Conf. Ser. 412, Astron. Soc. Pacific, San Francisco, 137.
Willson, L. A., and Hill, S. J. 1979, *Astrophys. J.,* **228**, 854.

Willson, L. A., and Templeton, M. 2009, in *Stellar Pulsation: Challenges for Theory and Observation*, AIP Conf. Proc. 1170, Amer. Inst. Physics, Melville, NY, 113.

Wittkowski, M., Boboltz, D. A., Gray, M. D., Humphreys, E. M. L., Karovicova, I., and Scholz, M. 2012, arXiv:1204.3546.

Wood, P. R. 1974, *Astrophys. J.,* **190**, 609.

Wood, P. R. 2000, *Publ, Astron. Soc. Australia*, **17**, 18.

Woodruff, H. C., Tuthill, P. G., Monnier, J. D., Ireland, M. J., Bedding, T. R., Lacour, S., Danchi, W. C., and Scholz, M. 2008, *Astrophys. J.,* **673**, 418.

Woodruff, H. C., *et al.* 2009, *Astrophys. J.,* **691** 1328.

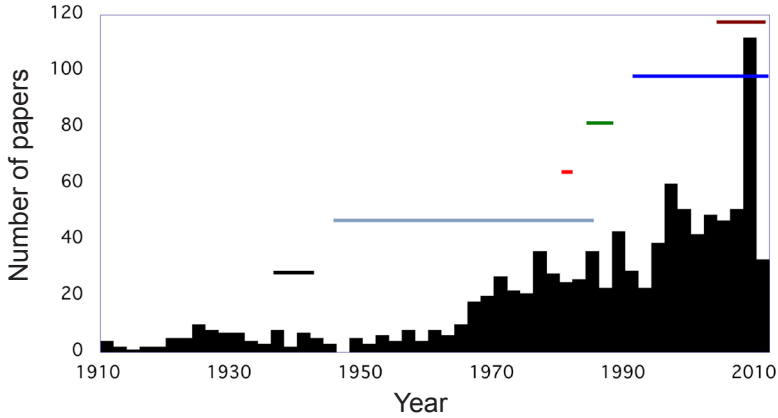

Figure 1. 1,000 refereed papers pulled up by ADS on a search for the words "Mira," "Long period variable," or "AGB star" in the title, from 1910 to 2010, plotted as a function of time. Some events that may have influenced the graph include (horizontal bars) WW II 1939–1945, the Palomar era 1949–1992, IRAS 1983, Hipparcos 1989–1993, the dark-matter searches MACHO, OGLE, and so on (starting 1993), and Spitzer (from 2003). IRAS and Spitzer, being infrared missions, definitely boosted interest in these stars. A big surge also came about three years after the beginning of the MACHO, OGLE, and similar projects.

Non-Mira Pulsating Red Giants and Supergiants

László L. Kiss
Konkoly Observatory, Research Centre for Astronomy and Earth Sciences, Hungarian Academy of Sciences, H-1121 Budapest, Konkoly Th. M. 15-17, Hungary; kiss@konkoly.hu

and

Sydney Institute for Astronomy, School of Physics A28, University of Sydney, Australia

John R. Percy
Department of Astronomy and Astrophysics, University of Toronto, Toronto, ON M5S 3H4, Canada; john.percy@utoronto.ca

Invited review paper, received February 27, 2012

Abstract We review the present understanding of (i) non-Mira pulsating red giants, that is, those with visual amplitudes less than 2.5 magnitudes, and (ii) pulsating red supergiants. We also identify some unsolved problems with these stars. We highlight the contributions by skilled amateur astronomers in the AAVSO and other organizations, using visual, photoelectric, and CCD photometry.

1. Definition

This paper reviews the development of our present understanding of pulsating red giants (PRGs) with V amplitudes less than 2.5. For convenience, we shall call them smaller-amplitude pulsating red giants or SAPRGs. Those with larger amplitudes are classified in the *General Catalogue of Variable Stars* (GCVS; Kholopov *et al.* 1985) as Mira stars, and are reviewed by Willson (2012) elsewhere in this volume. The choice of Δmag = 2.5 as a cutoff is somewhat arbitrary. First of all, the amplitude is highly wavelength dependent; a Mira star can have a visual amplitude of almost ten magnitudes, and a bolometric amplitude of less than two magnitudes. This phenomenon is due to the behavior of molecular bands in the spectrum, such as TiO; it is therefore dependent on the chemical composition of the atmosphere. Furthermore: there are stars with amplitudes equal to 2.5, and stars whose amplitude varies from above to below 2.5.

Red stars of luminosity class II and I (bright giants, and supergiants) show variability properties similar to those of red giants. We shall discuss pulsating red supergiants in section 9.

Henry *et al.* (2000) carried out a photometric survey of 187 G and K giants, and concluded that giants cooler than K5 are all variable, due to radial pulsation.

Some warmer giants are also pulsating variables, but the pulsation is more similar to that of the sun than to the K5-M-type pulsators. Here we exclude the discussion of G-K giants, for which asteroseismology with the Kepler space telescope has completely revolutionarized the field (see, for example, Bedding *et al.* 2010, 2011).

There are a dozen excellent essays on Mira and semiregular/SAPRG variables in the "Variable Star of the Season" archives on the AAVSO website. There are also many relevant papers in the proceedings of the *Biggest, Baddest, Coolest Stars* workshop (Luttermoser *et al.* 2009).

2. Discovery and observation

Variable star observing was initially done visually. Variables with amplitudes of 2.5 are easy to detect and study visually, those with smaller amplitudes less so. Many bright red giants (and other stars) were initially suspected of variability—incorrectly.

Photographic monitoring programs, such as that at the Harvard College Observatory, led to the discovery and study of large numbers of Miras and semiregulars, leading to the determination of periods of hundreds and thousands of days. Many of these stars have been in the AAVSO visual observing program for a century. Only with such systematic, long-term monitoring is it possible to study the variability of these stars on all relevant time scales.

By 1930, photoelectric photometry of PRGs was well underway; Stebbins and Huffer (1930) published a photoelectric study of the variability of such stars, carried out at Washburn Observatory. During the 1970s, Olin Eggen (1977 and references therein) published several photoelectric studies of SAPRGs of various kinds, with a view to determining their kinematical, physical, and pulsational properties.

In the 1980s, long-term photoelectric photometry of SAPRGs was carried out both by the AAVSO PEP Program (Percy *et al.* 1996) and by robotic telescopes (for example, Percy *et al.* 2001). By the 1990s, massive CCD surveys of SAPRGs in galactic fields and in the Magellanic Clouds were being carried out; some of these are described in section 10. See Figure 1 for examples of PEP V light curves of a selection of SAPRGs.

3. Incidence

All M-type giants (and supergiants) are variable, as are mid- to late-K giants—but with very small amplitude. Pulsating red giants are the most numerous variables among the bright stars. Of the 9,096 stars in the *Bright Star Catalogue* (Hoffleit and Jaschek 1982), 545 are M type or equivalent, and all these are giants or supergiants. There are an additional 2,233 K stars, almost all giants or supergiants. About ten percent of the stars in the catalogue are K5-M9

giants, almost all of them SAPRGs, so they are the most numerous variables among the bright stars (followed closely by pulsating B/Be stars).

In the *General Catalogue of Variable Stars* (on-line version, Samus *et al.* 2012), there are 7,587 Mira or Mira: stars, 6,063 SR stars, and 3,746 Lb or Lc or L: stars.

4. Classification

Pulsating red giants, other than Mira (M) stars, are classified in the GCVS (Kholopov *et al.* 1985) as semiregular (SR) or irregular (L); SR are subdivided into SRa and SRb (giants), where SRb have less obvious periodicity than SRa, and SRc (supergiants). There are also SRs variables which are SR variables with "short" periods (generally 30 days or less); about 100 stars are placed in this (arbitrary) class. L are divided into Lb (cool giants) and Lc (cool supergiants).

These types are defined thus: SR: "...giants or supergiants of intermediate and late spectral types showing noticeable periodicity in their light changes, accompanied or sometimes interrupted by various irregularities...." L: "Slow irregular variables. The light variations of these stars show no evidence of periodicity, or any periodicity present is very poorly defined, and appears only occasionally...." Clearly these definitions are qualitative at best, but they were reasonable in the early days of variable star astronomy, especially if they were based on dense, long-term visual or photographic light curves.

Eggen (1977 and references therein) obtained extensive photoelectric photometry of pulsating red giants, and classified them as large-amplitude (LARV), medium-amplitude (MARV), small-amplitude (SARV), and σ Lib stars with very small amplitude. Again: there is actually a continuous spectrum of amplitudes from 2.5 mags to very small; the subclasses are arbitrary.

It is also useful to classify red giants according to their atmospheric composition: M (normal oxygen-rich), C (carbon rich), or S (intermediate).

An important classification is by pulsation mode. This can be done if the star is pulsating in two or more modes, or if its luminosity and temperature are both known, as described below.

5. Physical properties

SAPRGs are solar-type stars which, towards the ends of their lives, are exhausting the hydrogen fuel in their cores, and expanding and cooling to become red giants. They occupy the red giant branch in the Hertzsprung-Russell Diagram. Subsequently, they ignite helium fusion in their cores; as they exhaust the helium, they again expand and cool to become "asymptotic red giants" because they occupy the asymptotic giant branch in the HRD. In the sun, energy is transported by convection in a "convection zone" in the outer layers. In a red giant, the convection zone extends deep in the star. Convection

is a poorly-understood process in astrophysics, so theoretical models of PRGs are uncertain.

One consequence of the convection is that, in some red giants, material which has been processed by nuclear reactions is transported to the surface, and the spectrum of the star shows strong lines of carbon. The star is a carbon star, as compared with normal red giants whose composition is similar to that of the sun. Indeed, the spectra of red giants can be very complex because, at their low temperatures, molecules such as TiO are very abundant in their atmospheres.

The best-understood SAPRGs are those near enough to have accurate *Hipparcos* parallaxes. They also have negligible reddening, especially at near-infrared wavelengths. The excellent study by Tabur *et al.* (2010) shows the power of studying nearby SAPRGs.

6. Pulsation properties

The stars that we are reviewing have periods between a few days and a few hundred days. For stars with known physical properties (especially distance), these periods can be shown to be low-order radial pulsation periods (Percy and Parkes 1998; Percy and Bakos 2003). This can also be shown by stars with two or more pulsation modes (Kiss *et al.* 1999: larger-amplitude SAPRGs, Percy *et al.* 2003: smaller-amplitude SAPRGs), since period ratios can be determined observationally, and compared with theoretical pulsation models of the stars. The radial pulsation can be confirmed by spectroscopic radial velocity measurements (Cummings 1999).

Massive surveys of stars in the Magellanic Clouds, or of nearby stars with known physical properties (discussed below) show that the stars obey sequences of period-luminosity relations, corresponding to different low-order radial modes.

The amplitudes of these stars range downward from 2.5 magnitudes (by definition) to the limits of detectability; the majority of red giants have pulsation amplitudes of only a few hundredths of a magnitude.

Kiss *et al.* (1999) have carried out a comprehensive time-series analysis of AAVSO visual observations of a large sample of SR variables; most have one period; some have two periods; and a few have three periods. Their sample included five L-type variables: AA Cas, DM Cep, TZ Cyg, V930 Cyg, and CT Del. They found a period of 367 days for DM Cep (possibly an artifact), 247 days for V930 Cyg, and 138 and 79 days for TZ Cyg, and apparently no periods for the other two stars. Some of the stars in this study showed significant changes in amplitude (Kiss *et al.* 2000). Percy *et al.* (2003) also found significant changes in amplitude in their multi-mode pulsators, on time scales of 2,000–3,500 days.

Percy and his students are currently analyzing several dozen SRa/SRb stars not analyzed by Kiss *et al.* (1999), using visual observations in the AAVSO

International Database (AID). These stars exhibit a very wide range of behavior, from highly periodic, to irregular, to non-variable.

As for the irregular (L-type) variables, Percy and Terziev (2011) analyzed visual observations of 125 such stars in the AID. They found 20 to be periodic, 18 to be possibly periodic, but with small amplitude, 55 to be truly irregular, some with amplitudes less than 0.1, and 32 to be probably non-variable.

7. Long secondary periods

Astronomers have known for decades that large numbers of PRGs have long secondary periods (LSPs), an order of magnitude longer than the primary pulsation periods (Payne-Gaposchkin 1954; Houk 1963). When period-luminosity relations can be formed, it is clear that the LSPs are correlated with the primary periods, or both are correlated with some property of the star such as its radius. The nature and cause of the LSPs is not known. Peter Wood and his collaborators have investigated a multitude of possible causes; most recently, Nicholls *et al.* (2009) have examined both physical and geometrical mechanisms for producing such periods, and conclude "We are unable to find a suitable model for the LSPs...."

8. Importance of SAPRGs

Mira variability plays an important role in mass loss and evolution of stars with masses of approximately 1 to 8 solar masses, and therefore in the general recycling of matter in galaxies. SAPRGs do not undergo significant mass loss. However, because of their shorter periods and smaller amplitudes, SAPRGs are easier to analyze in detail, and their physical properties are easier to determine—especially for nearby stars. It may therefore be possible to use them to refine evolution and pulsation models of these stars. Since they obey period-luminosity relations, it may also be possible to use them for distance determination.

9. Pulsating red supergiants

All red supergiants are pulsating variables; Antares, Betelgeuse, and μ Cephei are well-known examples. These are of special interest to the public because of their brightness and color, and their "imminent" demise as supernovae. They are also of astrophysical interest because of their crucial role in stellar evolution and mass loss, and therefore in galactic ecology. Also: because these stars are very luminous, there have been many studies of possible period-luminosity relations in these stars (Stothers 1969; Pierce *et al.* 2000).

The most comprehensive study of light variations in pulsating red supergiants was published by Kiss *et al.* (2006), who analyzed AAVSO data

for forty-eight supergiants, collected over the last century. They were able to measure two significant and distinctly different periods for more than a third of the studied stars (Figure 2). Theoretical models imply low-order radial pulsations for the shorter periods, while periods greater than 1,000 days form a period-luminosity relation that is similar to that of the long secondary periods of the asymptotic giant branch stars. Despite the well-defined periodicities, red supergiant variability is far from being predictable: there is strong evidence that oscillations are constantly affected by stochastic processes, adding a certain level of irregularity that is very similar to the pulsation characteristics seen in the sun.

Systematic, sustained spectroscopic observations have also provided useful insight into both the regular and the chaotic motions in red supergiants such as Betelgeuse (Gray 2008).

10. Massive surveys of pulsating red giants in selected starfields

Time-domain surveys have become one of the hottest topics in observational astronomy with the advent of the largely autonomous or fully remote-controlled telescopes with digital detectors. The flagship surveys included the MACHO, OGLE, and EROS projects, each observing millions of stars towards the Magellanic Clouds and the Galactic Bulge, hunting for unpredictable brightenings and fadings of background stars caused by the gravitational microlensing effect of a massive object passing in front of the stars. Of these, the OGLE (Optical Gravitational Lensing Experiment) project, so far with three distinct phases of operations and the fourth in progress, has been the most successful in making a full census of pulsating red giants in the Magellanic Clouds. The importance of these objects lies in the fact that all stars are located at a known distance and the luminosities are thus well known. Recently, Soszyński *et al.* (2009) and Soszyński *et al.* (2011) presented the most extensive catalogues for the Large Magellanic Cloud (LMC) and the Small Magellanic Cloud (SMC), with almost 92,000 long period variables in the LMC and 20,000 in the SMC, drawing an exquisite picture of red giant variability in whole galaxies. These samples are dominated by short-period (less than 100 days) and small-amplitude (less than 0.5 magnitude in the *I* band) semiregular variables, identified by Kiss and Bedding (2003) as stars still evolving on the first red giant branch, when their energy production is located in hydrogen-burning shells around the yet-to-be-ignited helium cores.

The most fruitful approach so far has been the study of period-luminosity (PL) relations in the Magellanic Clouds. The rich structure in the period-absolute magnitude plane has been studied by many authors, see Soszyński *et al.* (2007) and references therein. OGLE data analyzed by Soszyński *et al.* (2007) revealed fourteen different period-luminosity sequences, some of them consisting of three closely spaced ridges. The multitude of the PL relations

comes partly from the presence of many different modes of pulsations, partly from the full sample being a mixture of red giants with different chemical composition and evolutionary state.

The latest and still ongoing survey producing M giant light curves never seen before is that of the Kepler space telescope, which has been observing several thousand red giants since mid-2009 in its fixed field of view in the constellations Cygnus and Lyra. The unprecedented light curves—in most cases well into the sub-millimagnitude range in precision—are becoming more and more useful for the semiregular variables as their time-span becomes longer by each day of operations. Kepler targets include such well-known bright variable stars as the semiregular variable AF Cyg and the symbiotic semiregular star CH Cyg, with promising results to come soon.

11. Surveys of nearby pulsating red giants with known physical properties

Tabur *et al.* (2010) presented the results of a unique five and a half-year photometric campaign that monitored 247 southern bright semiregular variables with useful Hipparcos parallaxes. Using the periods from the light curves and geometric distances, they constructed the period-luminosity sequences of the sample, revealing a negligible difference between the red giant PL-relations in the two Magellanic Clouds and in the Milky Way. A comparison of other pulsation properties, including period-amplitude and luminosity-amplitude relations, has shown that pulsation properties of stars on the first red giant branch are consistent and universal, indicating that their PL-sequences are suitable as high-precision distance indicators. Also, M-type giants with the shortest periods (less than 10 days) bridge the gap between G and K giant solar-like oscillations and M-giant pulsation, revealing a smooth continuity as we ascend the giant branch.

12. Current problems and directions in SAPRG research

- Studies of multiperiodicity, mode switching, amplitude and period variations in these stars. Can these be linked with evolution?
- What is the source of the semiregularity or irregularity?
- Specifically: what is the relative role of kappa-mechanism pulsation, and convection, and how does this vary with the physical properties of the star?
- What determines which mode(s) will be excited in a given star?
- What is the nature and cause of the long secondary periods?
- How can we use pulsating red giants as distance indicators and tracers of Galactic structure?

All the surveys mentioned above have nicely demonstrated that studying ensemble properties is a powerful new way of scientific research, one that has only become available in the recent years of enormous technical development. We can expect that answers to most of these questions will be found by further studies of large samples or extremely sophisticated analyses of individual stars.

13. The roles of amateur observations

The time-scale of M giant variability is so long that meaningful analyses require many years, often decades of observations. The longest, homogeneous surveys with modern instrumentation are barely longer than ten years in time-span. Consequently, the role the amateurs play will remain very important in the studies of long period variables. Even though the visual observations have very limited accuracy, their real strength comes from being homogeneous for many cycles of the pulsations. For example, for a semiregular star with a dominant pulsation period of 200 days (think of Z UMa and alikes), detecting the effects of convection on the oscillations requires several decades of data, something that is only possible with the coordinated work of amateur astronomers. On the other hand, an increasing number of amateurs are getting involved in photometric measurements, either with CCDs or DSLR cameras. These enable the observers to improve accuracy by one or two orders of magnitude compared to the visual data, hence detecting variability at much lower amplitudes (and usually with much shorter periods) than ever seemed to be possible for non-professionals.

In conclusion, pulsating red giants have always been prime targets for amateurs and they will remain so. While large surveys have been extremely successful in finding tens of thousands of (faint) pulsating red giants, the bright end is still problematic, with stars that saturate in almost every survey data. We think this field will keep being an important meeting point of amateurs and professionals, where the shared interest in these beautiful stars will bring us together in the forthcoming years.

14. Acknowledgements

We thank the AAVSO observers for a century of measurements, and the AAVSO staff for making them available. JRP thanks his students for their hard work and inspiration, and the Natural Sciences and Engineering Research Council of Canada for support of his research. LLK has been supported by the "Lendület" Young Researchers' Program of the Hungarian Academy of Sciences and the Hungarian OTKA Grants K76816, MB08C 81013, and K83790.

References

Bedding, T. R., *et al.* 2010, *Astrophys. J., Lett. Ed.*, **713**, L176.
Bedding, T. R., *et al.* 2011, *Nature*, **471**, 608.
Cummings, I. N. 1999, *J. Astron. Data*, **5**, 2.
Eggen, O. J. 1977, *Astrophys. J.*, **213**, 767.
Gray, D. F. 2008, *Astron. J.*, **135**, 1450.
Henry, G. W., Fekel, F. C., Henry, S. M., and Hall, D. S. 2000, *Astrophys. J. Suppl. Ser.*, **130**, 201.
Hoffleit, D., and Jaschek, C. 1982, *The Bright Star Catalogue*, Yale Univ. Obs., New Haven.
Houk, N. 1963, *Astron. J.*, **68**, 253.
Kholopov, P. N., *et al.* 1985, *General Catalogue of Variable Stars*, 4th ed., Moscow.
Kiss, L. L., and Bedding, T. R. 2003, *Mon. Not. Royal Astron. Soc.*, **343**, L79.
Kiss, L. L., Szabó, Gy. M., and Bedding, T. R., 2006, *Mon. Not. Roy. Astron. Soc.*, **372**, 1721.
Kiss, L. L., Szatmáry, K., Cadmus, R. R., Jr., and Mattei, J. A. 1999, *Astron. Astrophys.*, **346**, 542.
Kiss, L. L., Szatmáry, K., Szabó, Gy. M., and Mattei, J. A. 2000, *Astron. Astrophys., Suppl. Ser.*, **145**, 283.
Luttermoser, D. G., Smith, B. J., and Stencel, R. E., eds. 2009, *The Biggest, Baddest, Coolest Stars*, ASP Conf. Ser., 412, Astron. Soc. Pacific, San Francisco.
Nicholls, C. P., Wood, P. R., Cioni, M. -R. L., and Soszyński, I. 2009, *Mon. Not. Royal Astron. Soc.*, **399**, 2063.
Payne-Gaposchkin, C. 1954, *Ann. Harvard Coll. Obs.*, **113**, 189.
Percy, J. R., and Bakos, A. G. 2003, in *The Garrison Festschrift*, eds. R. O. Gray, C. J. Corbally, and A. G. D. Philip, L. Davis Press, Schenectady, New York, 49.
Percy, J. R., Besla, G., Velocci, V., and Henry, G. W. 2003, *Publ. Astron. Soc. Pacific*, **115**, 479.
Percy, J. R., Desjardins, A., Yu, L., and Landis, H. J. 1996, *Publ. Astron. Soc. Pacific*, **108**, 139.
Percy, J. R., and Parkes, M. 1998, *Publ. Astron. Soc. Pacific*, **110**, 1431.
Percy, J. R., and Terziev, E. 2011, *J. Amer. Assoc. Var. Star Obs.*, **39**, 1.
Percy, J. R., Wilson, J. B., and Henry, G. W. 2001, *Publ. Astron. Soc. Pacific*, **113**, 983.
Pierce, M. J., Jurcevic, J. S., and Crabtree, D. 2000, *Mon. Not. Roy. Astron. Soc.*, **313**, 271.
Samus, N. N., *et al.* 2012, *General Catalogue of Variable Stars*, Sternberg Astronomical Institute, Moscow (http://www.sai.msu.su/groups/cluster/gcvs/gcvs/).
Soszyński, I., *et al.* 2007, *Acta Astron.*, **57**, 201.

Soszyński, I., *et al.* 2009, *Acta Astron.*, **59**, 239.
Soszyński, I., *et al.* 2011, *Acta Astron.*, **61**, 217.
Stebbins, J., and Huffer, C. M. 1930, *Publ. Washburn Obs.*, **15**, 140.
Stothers, R. 1969, *Astrophys. J.*, **156**, 541.
Tabur, V., Bedding, T. R., Kiss, L. L., Giles, T., Derekas, A., and Moon, T. T. 2010, *Mon. Not. Royal Astron. Soc.*, **409**, 777.
Willson, L. A. 2012, *J. Amer. Assoc. Var. Star Obs.*, **40**, 516.

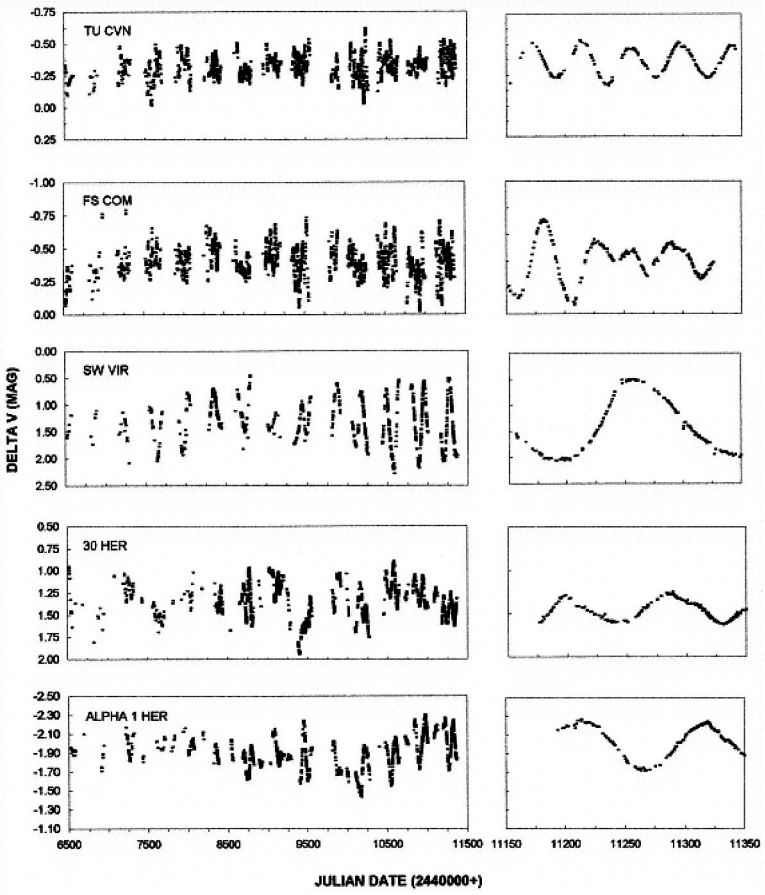

Figure 1. A selection of PEP V light curves of SAPRGs; left: 5,000 days, right: 200 days. TU CVn has a single short period; FS Com is multiperiodic; SW Vir has a longer period and larger amplitude; all of the stars show variability on both shorter and longer periods. From Percy *et al.* (2001).

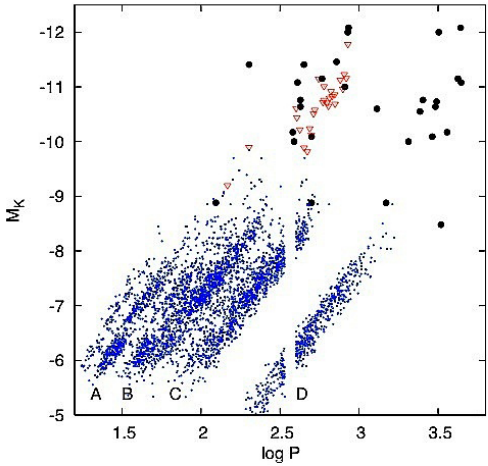

Figure 2. Period-luminosity (absolute K magnitude) relations for red supergiants in our galaxy (black circles) and the Large Magellanic Cloud (red triangles) and for red giants in the LMC (blue dots), the latter taken from the MACHO database. See Kiss *et al.* (2006) for further details. Note the separate PRG period-luminosity relations, corresponding to different pulsation modes; the supergiant sequences are extensions of these. Sequence D corresponds to long secondary periods.

What Are the R Coronae Borealis Stars?

Geoffrey C. Clayton
Department of Physics and Astronomy, Louisiana State University, Baton Rouge, LA 70803; gclayton@fenway.phys.lsu.edu

Invited review paper, received May 7, 2012

Abstract The R Coronae Borealis (RCB) stars are rare hydrogen-deficient, carbon-rich, supergiants, best known for their spectacular declines in brightness at irregular intervals. Efforts to discover more RCB stars have more than doubled the number known in the last few years and they appear to be members of an old, bulge population. Two evolutionary scenarios have been suggested for producing an RCB star, a double degenerate merger of two white dwarfs, or a final helium shell flash in a planetary nebula central star. The evidence pointing toward one or the other is somewhat contradictory, but the discovery that RCB stars have large amounts of ^{18}O has tilted the scales towards the merger scenario. If the RCB stars are the product of white dwarf mergers, this would be a very exciting result since RCB stars would then be low-mass analogs of type Ia supernovae. The predicted number of RCB stars in the Galaxy is consistent with the predicted number of He/CO WD mergers. But, so far, only about sixty-five of the predicted 5,000 RCB stars in the Galaxy have been discovered. The mystery has yet to be solved.

1. Introduction

R Coronae Borealis (R CrB) was one of the first variable stars identified and studied. It received the "R" which designates it as the first variable star discovered in the constellation Corona Borealis. Its brightness variations have been monitored since its discovery over 200 years ago (Pigott and Englefield 1797). Early spectra showed variations in the strengths of the Swan bands of C_2 (Espin 1890) and evidence of the absence of hydrogen was soon detected (Ludendorff 1906; Cannon and Pickering 1912), although not confirmed until later (Berman 1935; Bidelman 1953). In addition, the explanation behind the large declines in brightness, the production of thick clouds of carbon dust, was deduced very early on (Loreta 1935; O'Keefe 1939). But the stellar evolution that produced R CrB remains mysterious.

The R Coronae Borealis (RCB) stars are a small group of carbon-rich supergiants. About sixty-five RCB stars are known in the Galaxy and over twenty in the Magellanic Clouds. Their defining characteristics are hydrogen deficiency and unusual variability. RCB stars undergo massive declines of up to 8 magnitudes due to the formation of carbon dust at irregular intervals. The RCB stars can be roughly divided into a majority group which share similar

abundances, and a small minority of stars, which show extreme abundance ratios, particularly Si/Fe and S/Fe (Asplund *et al.* 2000). There are also six hydrogen-deficient carbon (HdC) stars that are RCB stars spectroscopically, but do not show declines in brightness or IR excesses (Warner 1967; Goswami *et al.* 2010; Tisserand 2012).

Two scenarios have been proposed for the origin of an RCB star: the double degenerate (DD) and the final helium-shell flash (FF) models (Iben *et al.* 1996; Saio and Jeffery 2002). The former involves the merger of a CO- and a He-white dwarf (WD) (Webbink 1984). In the latter case, thought to occur in 20% of all AGB stars, a star evolving into a planetary nebula (PN) central star undergoes a helium flash and expands to supergiant size (Fujimoto 1977). Three stars (Sakurai's Object, V605 Aql, and FG Sge) have been observed to undergo FF outbursts that transformed them from hot evolved PN central stars into cool giants with spectroscopic properties similar to RCB stars (Clayton and De Marco 1997; Gonzalez *et al.* 1998; Asplund *et al.* 1998, 1999, 2000; Clayton *et al.* 2006).

Recent observations and population synthesis models imply that there are a significant number of close DD binaries in the Galaxy. A majority of binaries, close enough to interact sometime during their evolution, will end up as DD systems where both stars are WDs (Nelemans *et al.* 2005; Badenes and Maoz 2012). If the resulting DD system has a short enough period ($\lesssim$ 0.2 hr) it will enter a phase of mass-transfer and may merge in less than a Hubble time due to the loss of energy due to gravitational radiation. This may result in a SN Ia explosion if the total mass of the DD system is greater than the Chandrasekhar limit, or in RCB and HdC stars if the mass is lower than this limit (Webbink 1984; Yungelson *et al.* 1994).

Recently, the surprising discovery was made that RCB stars have $^{16}O/^{18}O$ ratios that are orders of magnitude lower than for any other known stars (Clayton *et al.* 2005, 2007; García-Hernández *et al.* 2010). Greatly enhanced ^{18}O is evident in every HdC and RCB that has been measured and is cool enough to have detectable CO bands. IR spectra of Sakurai's Object, obtained when it had strong CO overtone bands, showed no evidence for ^{18}O (Geballe *et al.* 2002). Therefore, Sakurai's Object and the other FF stars on the one hand, and most of the RCB and HdC stars on the other hand, are likely to be stars with different origins. No overproduction of ^{18}O is expected in the FF scenario but in a DD merger, partial helium burning may take place leading to enhanced ^{18}O (Clayton *et al.* 2007). This strongly suggests that the RCB stars are the results of mergers of close WD binary systems. These discoveries are important clues which will help to distinguish between the proposed DD and FF evolutionary pathways of HdC and RCB stars.

There have been three conferences devoted to hydrogen-deficient stars held in 1985, 1995, and 2007. The proceedings of these conferences contain many papers concerning the RCB stars and related objects (Hunger *et al.* 1986; Jeffery and Heber 1996; Werner and Rauch 2008). The last general review

of the RCB stars appeared sixteen years ago (Clayton 1996). Since then, the number of RCB stars known has more than doubled and about 250 papers have been written. This review will concentrate on the advances in our knowledge of RCB stars that have been made since 1996.

2. How to identify an RCB star

2.1. The light curve

As seen in Figure 1, the RCB light curve is unique. No other type of star displays such wild, irregular, large amplitude variations (see, for example, Payne-Gaposchkin and Gaposchkin 1938; Clayton 1996).

- An RCB star will stay at uniform brightness at maximum for months or years. Then, there will be a sudden drop in brightness of more than three magnitudes taking a few days or weeks, followed by a recovery to maximum light, which is typically slower, taking months or years. Notice the latest decline of R CrB, itself, shown in Figure 1. After over 1,000 days at maximum, it plunged seven magnitudes in less than 100 days and has stayed in a deep decline for almost 2,000 days.

- The characteristic time between declines in RCB stars is typically about 1,000 days, but there is a wide range in activity among the RCB stars (Feast 1986; Jurcsik 1996).

- The stars also show regular or semiregular pulsations with a small amplitude ($\Delta V \lesssim 0.1$ magnitude) and periods of 40–100 days (see, for example, Lawson *et al.* 1990; Percy *et al.* 2004).

2.2. The spectrum

Figure 2 shows the maximum light spectra of the RCB stars, S Aps ($T_{eff} \sim 5000$ K) and RY Sgr ($T_{eff} \sim 7000$ K), and the carbon star, RV Sct.

- The RCB spectra are characterized by weak or absent hydrogen Balmer lines, and weak or absent CH λ4300 band. But, there is a wide range of hydrogen abundance in the RCB stars. For example, V854 Cen shows significant hydrogen in its spectrum (Kilkenny and Marang 1989; Lawson and Cottrell 1989). There is an anti-correlation between hydrogen and metallicity in the RCB stars (Asplund et al. 2000).

- The RCB star spectrum contains many lines of neutral atomic carbon. The cooler stars ($T_{eff} < 6000$ K) show strong absorption bands of C_2 and CN, as seen in S Aps, but in the warmer stars, such as RY Sgr, these bands are weak or absent. A warm RCB star can appear almost featureless in the visible, having no Balmer lines, helium lines, or molecular bands.

• In most, but not all, RCB stars, the abundance of ^{13}C is very small. This can be seen in the two wavelength sections shown in Figure 2. The isotopic Swan bands of C_2 are separated in wavelength, so the spectra can be inspected to see the relative strengths of $^{12}C^{12}C$ λ4737.0 and $^{12}C^{13}C$ λ4744.0 in the blue, and $^{12}C^{12}C$ λλ6059, 6122, 6191, and $^{12}C^{13}C$ λλ6100, 6168 in the red (Lloyd Evans *et al.* 1991; Kilkenny *et al.* 1992; Alcock *et al.* 2001).

• The strength of the CN λ6206 band compared to the $^{12}C^{12}C$ λ6191 band is relatively weak in the RCB stars compared to the carbon stars (Lloyd Evans *et al.* 1991; Morgan *et al.* 2003).

The description above applies to RCB spectra at or near maximum light. In deep declines, a rich narrow-line emission spectrum appears consisting of lines of neutral and singly ionized metals, and a few broad lines including Ca II H and K, and the Na I D lines (Payne-Gaposchkin 1963; Alexander *et al.* 1972; Feast 1975). The decline spectrum is described in detail in Clayton (1996). More recent papers detailing the decline spectra of RCB stars include Rao and Lambert (1997), Rao *et al.* (1999), Clayton *et al.* (1999a), Skuljan and Cottrell (1999), Lawson *et al.* (1999), Rao and Lambert (2000), Clayton and Ayres (2001), Kipper (2001), Skuljan and Cottrell (2002a, 2002b), Rao *et al.* (2004), Kipper and Klochkova (2006b), and Rao *et al.* (2006). A small subclass of RCB stars is much hotter with effective temperatures of about 20,000 K. See De Marco *et al.* (2002, and references therein) for a description of their spectra.

2.3. Infrared emission

• Every RCB star has an IR excess, from the K-band to far-IR wavelengths due to warm circumstellar dust ($T_{eff} \sim 400–1000$ K) (Feast *et al.* 1997). Most Galactic RCB stars have been detected by 2MASS, IRAS, AKARI, and WISE (see, for example, Walker 1985; Tisserand 2012). Recently, two RCB stars, R CrB and HV 2671, were detected out to 500 μm by the Herschel Space Observatory (Clayton *et al.* 2011a, 2011b).

• The mid-IR spectra of RCB stars are mostly featureless since there are usually no silicate, SiC, or polycyclic aromatic hydrocarbon (PAH) features present (Lambert *et al.* 2001; Kraemer *et al.* 2005; García-Hernández *et al.* 2011a). However, V854 Cen and DY Cen do show emission features attributed to PAHs and C_{60} (Lambert *et al.* 2001; García-Hernández *et al.* 2011b).

3. The population of RCB stars

Clayton (1996) listed thirty-four Galactic and three LMC RCB stars. Since then, the number of confirmed RCB stars has almost doubled in the Galaxy, and greatly increased to over twenty in the Magellanic Clouds. Tables 1 and 2

list all the RCB and HdC stars known in the Galaxy and the Magellanic Clouds which have been confirmed by spectral classification, light curve behavior, and IR excesses. V2331 Sgr is a strong new candidate from its light curve and IR excess, but does not have a spectrum (Tisserand *et al.* 2012). EROS2-LMC-RCB-6, and OGLE-GC-RCB-2 are also good candidates that do not have spectra (Tisserand *et al.* 2009, 2011; Tisserand 2012). V391 Sct was originally classified as a dwarf nova that brightened from V = 17 to 13 magnitudes. But Brian Skiff (2010) suggested that this star might be an RCB star based on brightness variations seen on a few plates. This is supported by the ASAS-RCB-3 light curve which, while it does not show any declines, reveals that the star is normally V = 13, not V = 17. Its spectrum shows it to be a warm RCB star, very similar to RY Sgr and it has an IR excess (Tisserand *et al.* 2012). A strong spectroscopic candidate, KDM 6546, has no light curve (Morgan *et al.* 2003). It was previously classified as a CH star (Hartwick and Cowley 1988). Three stars included in the RCB list of Clayton (1996), GM Ser, V1773 Oph, and V1405 Cyg, had not been spectroscopically confirmed (Kilkenny 1997). GM Ser is not an RCB star (Tisserand *et al.* 2012). The other two stars are still unconfirmed and so are not included in Table 1. Another star, MACHO 118.18666.100, previously identified as an RCB star (Zaniewski *et al.* 2005), has been shown to be misidentified (Tisserand *et al.* 2008).

There are also four hot (15,000–20,000 K) RCB stars known. One, HV 2671, was recently discovered in the LMC (Alcock *et al.* 1996). The three Galactic stars are, V348 Sgr, MV Sgr, and DY Cen. These stars are all hydrogen-deficient, carbon-rich stars, and have RCB-type light curves (Clayton 1996; De Marco *et al.* 2002; Clayton *et al.* 2011b). DY Cen and MV Sgr have the typical RCB-star large helium abundances, but V348 Sgr and HV 2671 are in general agreement with a born-again post-AGB evolution, and are similar to Wolf-Rayet central stars of PNe with carbon and helium being close to equal in abundance (De Marco *et al.* 2002). So DY Cen and MV Sgr seem to be related to the cooler RCB stars, but V348 Sgr and HV 2671 may be [WC] central stars. The six known HdC stars are also listed in Table 1. One of these stars, HD 175893, may be an RCB star since it has an IR excess (Tisserand 2012). However, no declines have been observed for this star.

There is a small group of stars, of which DY Per is the prototype, that resemble the RCB stars (Alksnis 1994). These stars have very deep declines at irregular intervals, but the rate of fading is very slow and the shape of the declines is much more symmetrical than the typical RCB decline (Alcock *et al.* 2001). DY Per is significantly cooler ($T_{eff} \sim 3500$ K) than the coolest RCB stars (Keenan and Barnbaum 1997).

Both of the evolutionary theories, the DD and the FF scenarios, suggest that the RCB stars are an old population (Clayton 1996). The distribution on the sky and radial velocities of the RCB stars tend toward those of the bulge population (Drilling 1986; Cottrell and Lawson 1998; Zaniewski *et al.* 2005). Tisserand

et al. (2008) determined that the RCB stars follow a disk-like distribution inside the Bulge with a scale-height < 250 pc. The distribution of the RCB stars on the sky, including the new expanded sample from Table 1, is plotted in Figure 3. There is no direct measurement of the distance to any Galactic RCB star (Alcock *et al.* 1996). But, now that significant numbers of RCB stars have been identified in the LMC, whose distance is well known, the absolute brightness of the RCB stars has been determined to range from $M_V = -3$ for stars with $T_{eff} \sim 5000$ K to –5 for stars with $T_{eff} \sim 7000$ K (Feast 1979; Alcock *et al.* 2001). HV 2671, the hot RCB star in the LMC, has $M_V \sim -3$ (Alcock *et al.* 2001; Tisserand *et al.* 2009).

Webbink (1984) suggested that the DD scenario would result in a population of about 1,000 Galactic RCB stars. Iben *et al.* (1996) put the Galactic RCB population resulting from the same scenario at about 300 stars, and calculated that the FF scenario would imply anywhere from 30 to 2,000 RCB stars at any given time. All of the evidence thus far suggests that there are many more than the ~65 known RCB stars in the Galaxy (see, for example, Zaniewski *et al.* 2005). The number of RCB stars expected in the Galaxy can be extrapolated from the LMC RCB population, using the method described by Alcock *et al.* (2001), and including all the new LMC stars. This implies a population of RCB stars in the Galaxy of almost 5,700. RCB stars are thought to be ~0.8–0.9 $M_\odot$ from pulsation modeling (Saio 2008), and this mass agrees well with the predicted mass of the merger products of a CO- and a He-WD (Han 1998). On the other hand, FF stars, since they are single WDs, should typically have masses of 0.55–0.6 $M_\odot$ (Bergeron *et al.* 2007).

The merger rate of He+CO DDs is predicted to be ~0.018 yr^{-1} in the Galaxy (Han 1998). As of 1988, only one such DD system was actually known to exist (Saffer *et al.* 1988). The SPY project and other surveys have studied many WDs for evidence of binarity and the number of known DD systems is now ~100 (see, for example, Nelemans *et al.* 2005; Kilic *et al.* 2010, 2011; Parsons *et al.* 2011; Brown *et al.* 2011; Badenes and Maoz 2012). To see how well this number matches the predicted number of RCB stars in the Galaxy, we need to estimate how long an RCB star formed from a DD merger will live. This lifetime can be calculated as, $t = \Delta M \times X \times Q/L$, where L is the luminosity of RCB stars, ΔM is the accreted mass of He, X is the mass fraction of He in the accreted material, and Q is the energy generated when one gram of He is burned to ^{12}C. Assuming that $Q \sim 7 \times 10^{18}$ erg, $\Delta M = 0.1 M_\odot$, $X = 0.3$, and $L = 10{,}000\, L_\odot$, $t \sim 3 \times 10^5$ yr. Using the estimate of Han (1998) for the production of RCB stars from DD mergers, then the predicted population of RCB stars in the Galaxy at any given time would be ~5,400 which agrees well with the number extrapolated from the LMC above.

4. Evolutionary history

Table 3 summarizes the observational data that must be addressed by evolutionary models of RCB stars (Asplund *et al.* 2000, Jeffery *et al.* 2011). They are discussed below with respect to the FF and DD models. Two entries, the high abundance of silicon and sulphur, and the anti-correlation of hydrogen with iron, cannot be well explained by either scenario. The condensation of certain elements into dust has been suggested for the Si/S problem, although it is unclear that this would work (Asplund *et al.* 2000). The H/Fe anti-correlation is unexplained but Sakurai's Object follows the same trend.

4.1. Do RCB stars evolve from final flash stars?

The light curve behavior and spectroscopic appearance of V605 Aql in 1921 and more recently of Sakurai's Object are reminiscent of the RCB class. There are, however, several reasons why FF stars are unlikely to be the evolutionary precursors of the majority of RCB stars. The FF objects have deeper light declines (>10 magnitudes) than do RCB stars (~8 magnitudes). This may be due to the fact that RCB stars have more dust lying near the star which scatters light around the intervening dust cloud. This may account for the flat-bottom appearance of deep RCB declines. See Figure 1. The abundances of FF objects, shortly after the outburst, do appear similar to those of RCB stars, except for some interesting differences. First there are significant amounts of ^{13}C present in Sakurai's Object, but not in most RCB stars. In the two years after it appeared, Sakurai's Object had $^{12}C/^{13}C \sim 4$ (Pollard *et al.* 1994; Asplund *et al.* 1999; Pavlenko *et al.* 2004). In general, RCB stars have $^{12}C/^{13}C \geq 100$. However, a few RCB stars do have detectable ^{13}C including both majority and minority stars. V CrA, V854 Cen, VZ Sgr, and UX Ant have measured $^{12}C/^{13}C < 25$ (Rao and Lambert 2008; Hema *et al.* 2012). Second, there is no sign of ^{18}O in the IR CO bands of Sakurai's Object (Eyres *et al.* 1998). Finally, several Galactic and LMC RCB stars, including R CrB, itself, show significant Lithium in their atmospheres (Rao and Lambert 1996; Asplund *et al.* 2000; Kipper and Klochkova 2006a). Renzini (1990) suggested that in a FF the ingestion of the H-rich envelope leads to Li-production through the Cameron-Fowler mechanism (Cameron and Fowler 1971). The abundance of Li in the atmosphere of the FF star, Sakurai's object, was actually observed to increase with time (Asplund *et al.* 1999).

In general, Sakurai's abundances resemble V854 Cen and the other minority-class RCB stars with 98% He and 1% C (Asplund *et al.* 1998). Although only low resolution spectra are available for V605 Aql from 1921, it likely had similar abundances (Clayton and De Marco 1997). New spectra obtained of V605 Aql in 2000 indicate that it has evolved from $T_{eff} \sim 5000$ K in 1921 to ~95,000 K today (Clayton *et al.* 2006). The new spectra also show that V605 Aql now has stellar abundances similar to those seen in [WC] central

stars of PNe with ~55% He, and ~40% C. In the present state of evolution of V605 Aql, we may be seeing the not too distant future of Sakurai's Object. There are indications that Sakurai's Object is evolving along a similar path (Kerber *et al.* 2002; Hajduk *et al.* 2005). Some doubt has recently been thrown on the FF nature of V605 Aql on the grounds of high neon abundances found in its ejecta (Wesson *et al.* 2008; Lau *et al.* 2011).

For a very short time, perhaps as short as two years, both V605 Aql and Sakurai's Object were almost indistinguishable from the RCB stars. Unfortunately, this extremely short RCB phase of the FF stars means that they cannot account for even the small number of RCB stars known in the Galaxy.

4.2. Do RCB stars evolve from white dwarf mergers?

RCB and HdC stars have $^{16}O/^{18}O$ ratios close to and in some cases less than unity, values that are orders of magnitude lower than measured in any other stars (the Solar value is 500) (Clayton *et al.* 2005, 2007; García-Hernández *et al.* 2010). The three HdC stars, that have been measured, have $^{16}O/^{18}O < 1$, lower values than any of the RCB stars. These discoveries are important clues in determining the evolutionary pathways of HdC and RCB stars, whether the DD or the FF. No overproduction of ^{18}O is expected in the FF scenario. New hydrodynamic simulations indicate that WD mergers may very well be the progenitors of O^{18}-rich RCB and HdC stars (Longland *et al.* 2011; Staff *et al.* 2012).

Webink (1984) proposed that an RCB star evolves from the merger of a He-WD and a CO-WD which has passed through a common envelope phase. He suggested that as the binary begins to coalesce because of the loss of angular momentum by gravitational wave radiation, the (lower mass) He-WD is disrupted. A fraction of the helium is accreted onto the CO-WD and starts to burn, while the remainder forms an extended envelope around the CO-WD. This structure, a star with a helium-burning shell surrounded by a ~100 $R_\odot$ hydrogen-deficient envelope, closely resembles an RCB star (Clayton 1996; Clayton *et al.* 2007). The merging times (~10^9 yr) might not be as long as previously thought, which makes the DD scenario an appealing alternative to the FF scenario for the formation of RCB stars (Iben *et al.* 1996, 1997). In addition, Sai"EHo and Jeffery (2002) suggested that a WD-WD merger could also account for the elemental abundances seen in RCB stars. Pandey *et al.* (2006) have suggested a similar origin for the EHe stars.

The isotope, ^{18}O, can be overproduced in an environment of partial He-burning in which the temperature and the duration of nucleosynthesis are such that the $^{14}N(\alpha,\gamma)^{18}F(\beta^+)^{18}O$ reaction chain can produce ^{18}O, if the ^{18}O is not further processed by $^{18}O(\alpha,\gamma)^{22}Ne$ (Warner 1967; Lambert 1986; Clayton *et al.* 2007). The surface compositions of HdC and RCB stars are extremely He-rich (mass fraction 0.98), indicating that the surface material has been processed through H-burning. After H-burning via the CNO cycle, ^{14}N is by far the most

abundant of the CNO elements, because ^{14}N has the smallest nuclear p-capture cross-section of any stable CNO isotope involved. However, the majority of RCB stars have log *C/N* = 0.3 and log *N/O* = 0.4 by number, equivalent to mass ratios of *C/N* = 1.7 and *N/O* = 2.2 (Asplund *et al.* 2000). The N/O ratio represents the average for the majority RCB stars although the individual stars show a large scatter. Thus C is the most abundant and O the least abundant CNO element. These abundances are consistent if the material at the surfaces of HdC and RCB stars experienced a small amount of He-burning, as, for example, at the onset of a He-burning event that is quickly terminated. This partial He-burning would not significantly deplete He, but could be sufficient for some of the ^{14}N to be processed into ^{18}O. At the onset of He-burning, ^{13}C is the first α-capture reaction to be activated because of the large cross-section of ^{13}C(α, n) ^{16}O. Thus, a large ^{12}C/^{13}C ratio and enhanced s-process elements are both consistent with partial He-burning.

As mentioned above, some RCB stars show enhanced Li abundances, as does the FF star Sakurai's Object (Lambert 1986; Asplund *et al.* 1998). As shown by Herwig and Langer (2001), Li enhancements are consistent with the FF scenario. However, the production of ^{18}O requires temperatures large enough to at least marginally activate the ^{14}N(α,γ) reaction. The α capture on Li is eight orders of magnitude more effective than on ^{14}N. For that reason, the simultaneous enrichment of Li and ^{18}O is not expected in the WD merger scenario. This is an important argument against the FF evolution scenario as a progenitor of RCB and HdC stars with excess of ^{18}O. The abundance of ^{18}O cannot be directly measured in R CrB because it is too hot to have CO, but it is overabundant in ^{19}F, which does imply a high ^{18}O abundance (Pandey *et al.* 2008). Since ^{18}O strongly supports the DD merger/accretion scenario, the obvious solution is that there could be (at least) two evolutionary channels leading to RCB, HdC and EHe stars, perhaps with the DD being the dominant mechanism. Unfortunately the division between majority- and minority-class RCB stars does not lend itself naturally to this explanation, since Li has only been detected in the majority group (Asplund *et al.* 2000).

4.3. Mass-Loss and dust formation

It has long been accepted that the characteristic RCB declines in brightness are caused by the formation of optically thick clouds of carbon dust (Loreta 1935; O'Keefe 1939; Clayton 1996). But the formation mechanism is not well understood. Empirical analysis of the spectroscopic and light curve evolution during declines implies that the dust forms close to the stellar atmosphere and then is accelerated to hundreds of km s^{-1} by radiation pressure (Clayton *et al.* 1992; Whitney *et al.* 1993). There is strong evidence for variable, high-velocity winds in RCB stars associated with dust formation (Clayton *et al.* 2003, 2012). The HdC stars, which produce no dust, also have no evidence for winds (Geballe *et al.* 2009). Other observational evidence indicates that there is also

gas moving much more slowly away from the star (see, for example, García-Hernández *et al.* 2011a and references therein).

The observed timescales for RCB dust formation fit in well with those calculated by carbon chemistry models which show that the dust forms near the surface of the RCB star due to density and temperature perturbations caused by stellar pulsations (Feast 1986; Woitke *et al.* 1996). There is a strong correlation between the onset of dust formation and the pulsation phase in several RCB stars (Crause *et al.* 2007). All RCB stars show regular or semiregular pulsation periods in the 40- to 100-day range (Lawson *et al.* 1990). The dust forming around an RCB star does not form in a complete shell, but rather in small "puffs" (Clayton 1996). Only when a puff forms along the line of sight to the star will there be a decline in brightness. Studies of UV extinction and IR re-emission of stellar radiation indicate that the covering factor of the clouds around RCB stars during declines is $f<0.5$ (Feast *et al.* 1997; Clayton *et al.* 1999b; Hecht *et al.* 1984, 1998). The typical dust mass of a puff is $\sim 10^{-8} M_{\odot}$ (Feast 1986; Clayton *et al.* 1992).

In the recent deep decline of R CrB, shown in Figure 1, the puff dust mass is $\sim 10^{-8} M_{\odot}$, assuming the dust forms at $2 R_*$ ($R_* = 85 R_{\odot}$), and that a puff subtends a fractional solid angle of 0.05 (Clayton *et al.* 2011a). Since the dust would accelerate and dissipate quickly due to radiation pressure, dust must be formed continually by R CrB to maintain itself in a deep decline for four years or more. If a puff forms during each pulsation period (~40 days), R CrB would be producing $\sim 10^{-7} M_{\odot}$ of dust per year. Assuming a gas-to-dust ratio of 100 (Whittet 2003), the total mass loss rate is $10^{-5} M_{\odot}\,yr^{-1}$.

Little is known about the lifetime of an RCB star. We have a lower limit from the fact that R CrB itself has been an RCB star for 200 yr (Pigott and Englefield 1797). The large diffuse dust shell around R CrB, seen in the far-IR, could possibly be a fossil PN shell (Clayton *et al.* 2011a). Assuming an expansion velocity of a PN shell (~20 km s^{-1}), then the shell would take 10^5 yr to form. If the mass-loss was more like the high-velocity winds seen in RCB stars today (~200 km s^{-1}), then the shell would be about an order of magnitude younger (Clayton *et al.* 2003). If R CrB is the result of a FF rather than a DD, then the size and timescales would be consistent with the nebulosity, now seen in far-IR emission, being a fossil PN shell. The nebulosity, including cometary knots, seen around R CrB and UW Cen looks very much like a PN shell (Clayton *et al.* 1999b, 2011a). The mass of the shell is estimated to be $\sim 2 M_{\odot}$, which is consistent with it being a PN (Clayton *et al.* 2011a). Adaptive optics and interferometry have been used to study dust very close to RCB stars (de Laverny and Mékarnia 2004; Bright *et al.* 2011, and references therein).

Any gas lost during a DD event would have far less mass. If the shell is an old PN shell then this would suggest that R CrB is the product of an FF event rather than a DD merger. R CrB is one of the stars with lithium on its surface, also a possible indicator of an FF. About 10% of single stars will undergo a

final-flash event (Iben *et al.* 1996). About this percentage of RCB stars (R CrB, RY Sgr, V CrA, and UW Cen) show evidence of resolved fossil dust shells (Walker 1994).

Understanding the RCB and HdC stars is a key test for any theory that aims to explain hydrogen deficiency in post-AGB stars. Solving the mystery of how the RCB stars evolve is an exciting possibility, but it will also be a watershed event in the study of stellar evolution that could lead to a better understanding of other types of stellar merger events such as type Ia supernovae.

The observations in the AAVSO database have been invaluable to my research on RCB stars throughout my career. For R CrB alone, there are a staggering 238,136 brightness estimates in the AAVSO International Database, stretching back to 1843. The usefulness of the AAVSO data is only increasing with the addition of digital data which allow the low-amplitude RCB star pulsations to be studied in detail. The AAVSO International Database is a model for the many other photometric databases coming on line. The need for longterm monitoring combined with reliable photometry is essential for the identification and characterization of the many transient objects that are being discovered.

5. Acknowledgements

I acknowledge with thanks the variable star observations from the AAVSO International Database contributed by observers worldwide and used in this research. I would especially like to thank Albert Jones for his many visual estimates of the RCB stars. This work has been supported, in part, by grant NNX10AC72G from NASA's Astrophysics Theory Program.

References

Alcock, C., *et al.* 1996*, Astrophys. J.,* **470**, 583.

Alcock, C., *et al.* 2001*, Astrophys. J.,* **554**, 298.

Alexander, J. B., Andrews, P. J., Catchpole, R. M., Feast, M. W., Lloyd Evans, T., Menzies, J. W., Wisse, P. N. J., and Wisse, M. 1972, *Mon. Not. Roy. Astron. Soc.,* **158**, 305.

Alksnis, A. 1994, *Baltic Astron.,* **3**, 410.

Asplund, M., Gustafsson, B., Kameswara Rao, N., and Lambert, D. L. 1998, *Astron. Astrophys.,* **332**, 651.

Asplund, M., Gustafsson, B., Lambert, D. L., and Rao, N. K. 2000, *Astron. Astrophys.,* **353**, 287.

Asplund, M., Lambert, D. L., Kipper, T., Pollacco, D., and Shetrone, M. D. 1999, *Astron. Astrophys.,* **343**, 507.

Badenes, C., and Maoz, D. 2012, *Astrophys. J.*, **749**, 11.

Bergeron, P., Gianninas, A., and Boudreault, S. 2007, in 15th European Workshop on White Dwarfs, eds. R. Napiwotzki and M. R. Burleigh, ASP Conf. Ser. 372, 29.

Berman, L. 1935, *Astrophys. J.,* **81**, 369.

Bidelman, W. P. 1953, *Astrophys. J.,* **117**, 25.

Bright, S. N., Chesneau, O., Clayton, G. C., de Marco, O., Leao, I. C., Nordhaus, J., and Gallagher, J. S. 2011, *Mon. Not. Roy. Astron. Soc.,* **414**, 1195.

Brown, W. R., Kilic, M., Hermes, J. J., Allende Prieto, C., Kenyon, S. J., and Winget, D. E. 2011, *Astrophys. J., Lett. Ed.,* **737**, L23.

Cameron, A. G. W., and Fowler, W. A. 1971, *Astrophys. J.,* **164**, 111.

Cannon, A. J., and Pickering, E. C. 1912, *Ann. Harvard Coll. Obs.*, **56**, 65.

Clayton, G. C. 1996, *Publ. Astron. Soc. Pacific,* **108**, 225.

Clayton, G. C., and Ayres, T. R. 2001, *Astrophys. J.,* **560**, 986.

Clayton, G. C., Ayres, T. R., Lawson, W. A., Drilling, J. S., Woitke, P., and Asplund, M. 1999a, *Astrophys. J.,* **515**, 351.

Clayton, G. C., and De Marco, O. 1997, *Astron. J.,* **114**, 2679.

Clayton, G. C., Geballe, T. R., and Bianchi, L. 2003, *Astrophys. J.,* **595**, 412.

Clayton, G. C., Geballe, T. R., Herwig, F., Fryer, C., and Asplund, M. 2007, *Astrophys. J.,* **662**, 1220.

Clayton, G. C., Geballe, T. R., Zhang, W., and Brozek, C. 2012, *Astron. J.,* submitted.

Clayton, G. C., Hammond, D., Lawless, J., Kilkenny, D., Evans, T. L., Mattei, J., and Landolt, A. U. 2002, *Publ. Astron. Soc. Pacific,* **114**, 846.

Clayton, G. C., Herwig, F., Geballe, T. R., Asplund, M., Tenenbaum, E. D., Engelbracht, C. W., and Gordon, K. D. 2005, *Astrophys. J., Lett. Ed.,* **623**, L141.

Clayton, G. C., Kerber, F., Gordon, K. D., Lawson, W. A., Wol, M. J., Pollacco, D. L., and Furlan, E. 1999b, *Astrophys. J., Lett. Ed.,* **517**, L143.

Clayton, G. C., Kerber, F., Pirzkal, N., De Marco, O., Crowther, P. A., and Fedrow, J. M. 2006, *Astrophys. J., Lett. Ed.,* **646**, L69.

Clayton, G. C., Kilkenny, D., Wils, P., and Welch, D. L. 2009, *Publ. Astron. Soc. Pacific,* **121**, 461.

Clayton, G. C., Whitney, B. A., Stanford, S. A., and Drilling, J. S. 1992, *Astrophys. J.,* **397**, 652.

Clayton, G. C., *et al.* 2011a, *Astrophys. J.,* **743**, 44.

Clayton, G. C., *et al.* 2011b, *Astron. J.,* **142**, 54.

Cottrell, P. L., and Lawson, W. A. 1998, *Publ. Astron. Soc. Australia*, **15**, 179.

Crause, L. A., Lawson, W. A., and Henden, A. A. 2007, *Mon. Not. Roy. Astron. Soc.,* **375**, 301.

de Laverny, P., and Mekarnia, D. 2004, *Astron. Astrophys.,* **428**, L13.

De Marco, O., Clayton, G. C., Herwig, F., Pollacco, D. L., Clark, J. S., and Kilkenny, D. 2002, *Astron. J.,* **123**, 3387.

Drilling, J. S. 1986, in *Hydrogen Deficient Stars and Related Objects*, eds. K. Hunger, D. Schoenberner, and N. Kameswara Rao, IAU Colloq. 87, Astrophys. Space Sci. Libr. 128, D. Reidel Publ. Co., Dordrecht, 9.

Espin, T. E. 1890, *Mon. Not. Roy. Astron. Soc.,* **51**, 11.

Eyres, S. P. S., Evans, A., Geballe, T. R., Salama, A., and Smalley, B. 1998, *Mon. Not. Roy. Astron. Soc.,* **298**, L37.

Feast, M. W. 1975, in *Variable Stars and Stellar Evolution*, eds. V. E. Sherwood and L. Plaut, IAU Symp., 67, D. Reidel Publ. Co., Dordrecht, 129.

Feast, M. W. 1979, in *Changing Trends in Variable Star Research*, eds. F. M. Bateson, J. Smak, and I. H. Urch, IAU Colloq. 46, Univ. Waikato, Hamilton, New Zealand, 246.

Feast, M. W. 1986, in *Hydrogen Deficient Stars and Related Objects*, eds. K. Hunger, D. Schoenberner, and N. Kameswara Rao, IAU Colloq. 87, Astrophys. Space Sci. Libr. 128, D. Reidel Publ. Co., Dordrecht, 151.

Feast, M. W., Carter, B. S., Roberts, G., Marang, F., and Catchpole, R. M. 1997, *Mon. Not. Roy. Astron. Soc.,* **285**, 317.

Fujimoto, M. Y. 1977, *Publ. Astron. Soc. Japan*, **29**, 331.

García-Hernández, D., Kameswara Rao, N., and Lambert, D. L. 2011a*, Astrophys. J.,* **739**, 37.

García-Hernández, D. A., Kameswara Rao, N., and Lambert, D. L. 2011b*, Astrophys. J.,* **729**, 126.

García-Hernández, D. A., Lambert, D. L., Kameswara Rao, N., Hinkle, K. H., and Eriksson, K. 2010*, Astrophys. J.,* **714**, 144.

Geballe, T. R., Evans, A., Smalley, B., Tyne, V. H., and Eyres, S. P. S. 2002, *Astrophys. Space Sci.,* **279**, 39.

Geballe, T. R., Rao, N. K., and Clayton, G. C. 2009*, Astrophys. J.,* **698**, 735.

Gonzalez, G., Lambert, D. L., Wallerstein, G., Rao, N. K., Smith, V. V., and McCarthy, J. K. 1998, *Astrophys. J., Suppl. Ser.,* **114**, 133.

Goswami, A., Karinkuzhi, D., and Shantikumar, N. S. 2010*, Astrophys. J., Lett. Ed.,* **723**, L238.

Greaves, J. 2007, *Perem. Zvezdy,* **27**, 7.

Hajduk *et al.*, M. 2005, *Science*, **308**, 231.

Han, Z. 1998, *Mon. Not. Roy. Astron. Soc.,* **296**, 1019.

Hartwick, F. D. A., and Cowley, A. P. 1988*, Astrophys. J.,* **334**, 135.

Hecht, J. H., Clayton, G. C., Drilling, J. S., and Jeery, C. S. 1998*, Astrophys. J.,* **501**, 813.

Hecht, J. H., Holm, A. V., Donn, B., and Wu, C.-C. 1984*, Astrophys. J.,* **280**, 228.

Hema, B. P., Pandey, G., and Lambert, D. L. 2012*, Astrophys. J.,* **747**, 102.

Herwig, F., and Langer, N. 2001, *Nucl. Phys. A*, **688**, 221.

Hesselbach, E., Clayton, G. C., and Smith, P. S. 2003, *Publ. Astron. Soc. Pacific,* **115**, 1301.

Hunger, K., Schoenberner, D., and Kameswara Rao, N., eds. 1986, *Hydrogen Deficient Stars and Related Objects*, IAU Colloq. 87, Astrophys. Space Sci. Libr. 128, D. Reidel Publ. Co., Dordrecht.

Iben, Jr., I., Tutukov, A. V., and Yungelson, L. R. 1996, *Astrophys. J.,* **456**, 750.

Iben, Jr., I., Tutukov, A. V., and Yungelson, L. R. 1997, *Astrophys. J.,* **475**, 291.

Jeffery, C. S., and Heber, U., eds. 1996, *Hydrogen Deficient Stars*, ASP Conf. Ser. 96, Astron. Soc. Pacific, San Francisco.

Jeffery, C. S., Karakas, A. I., and Saio, H. 2011, *Mon. Not. Roy. Astron. Soc.,* **414**, 3599.

Jurcsik, J. 1996, *Acta Astron.,* **46**, 325.

Keenan, P. C., and Barnbaum, C. 1997, *Publ. Astron. Soc. Pacific,* **109**, 969.

Kerber, F., Pirzkal, N., De Marco, O., Asplund, M., Clayton, G. C., and Rosa, M. R. 2002, *Astrophys. J., Lett. Ed.,* **581**, L39.

Kijbunchoo, N., *et al.* 2011, *Publ. Astron. Soc. Pacific,* **123**, 1149.

Kilic, M., Brown, W. R., Allende Prieto, C., Kenyon, S. J., and Panei, J. A. 2010, *Astrophys. J.,* **716**, 122.

Kilic, M., *et al.* 2011, *Mon. Not. Roy. Astron. Soc.,* **413**, L101.

Kilkenny, D. 1997, *Observatory*, **117**, 205.

Kilkenny, D., Lloyd Evans, T., Bateson, F. M., Jones, A. F., and Lawson, W. A. 1992, *Observatory*, **112**, 158.

Kilkenny, D., and Marang, F. 1989, *Mon. Not. Roy. Astron. Soc.,* **238**, 1P.

Kipper, T. 2001, *Inf. Bull. Var. Stars,* No. 5063, 1.

Kipper, T., and Klochkova, V. G. 2006a, *Baltic Astron.,* **15**, 531.

Kipper, T., and Klochkova, V. G. 2006b, *Baltic Astron.,* **15**, 521.

Kraemer, K. E., Sloan, G. C., Wood, P. R., Price, S. D., and Egan, M. P. 2005, *Astrophys. J., Lett. Ed.,* **631**, L147.

Lambert, D. L. 1986, in *Hydrogen Deficient Stars and Related Objects*, eds. K. Hunger, D. Schoenberner, and N. Kameswara Rao, IAU Colloq. 87, Astrophys. Space Sci. Libr. 128, D. Reidel Publ. Co., Dordrecht, 127.

Lambert, D. L., Rao, N. K., Pandey, G., and Ivans, I. I. 2001, *Astrophys. J.,* **555**, 925.

Lau, H. H. B., de Marco, O., and Liu, X. 2011, *Mon. Not. Roy. Astron. Soc.,* **410**, 1870.

Lawson, W. A., and Cottrell, P. L. 1989, *Mon. Not. Roy. Astron. Soc.,* **240**, 689.

Lawson, W. A., Cottrell, P. L., Kilmartin, P. M., and Gilmore, A. C. 1990, *Mon. Not. Roy. Astron. Soc.,* **247**, 91.

Lawson, W. A., *et al.* 1999, *Astron. J.,* **117**, 3007.

Lloyd Evans, T., Kilkenny, D., and van Wyk, F. 1991, *Observatory*, **111**, 244.

Longland, R., Loren-Aguilar, P., Jose, J., Garca-Berro, E., Althaus, L. G., and Isern, J. 2011, *Astrophys. J., Lett. Ed.,* **737**, L34.

Loreta, E. 1935, *Astron. Nachr.,* **254**, 151.

Ludendorff, H. 1906, *Astron. Nachr.,* **173**, 1.

Miller, A. A., Richards, J. W., Bloom, J. S., Cenko, S. B., Silverman, J. M., Starr, D. L., and Stassun, K. G. 2012, ArXiv e-prints, 2012arXiv1204.4181M.

Morgan, D. H., Hatzidimitriou, D., Cannon, R. D., and Croke, B. F. W. 2003, *Mon. Not. Roy. Astron. Soc.,* **344**, 325.

Nelemans, G. *et al.* 2005, *Astron. Astrophys.,* **440**, 1087.

O'Keefe, J. A. 1939*, Astrophys. J.,* **90**, 294.

Pandey, G., Lambert, D. L., Jeery, C. S., and Rao, N. K. 2006*, Astrophys. J.,* **638**, 454.

Pandey, G., Lambert, D. L., and Rao, N. K. 2008*, Astrophys. J.,* **674**, 1068.

Parsons, S. G., Marsh, T. R., Gaensicke, B. T., Drake, A. J., and Koester, D. 2011*, Astrophys. J., Lett. Ed.,* **735**, L30.

Pavlenko, Y. V., Geballe, T. R., Evans, A., Smalley, B., Eyres, S. P. S., Tyne, V. H., and Yakovina, L. A. 2004, *Astron. Astrophys.,* **417**, L39.

Payne-Gaposchkin, C. 1963*, Astrophys. J.,* **138**, 320.

Payne-Gaposchkin, C., and Gaposchkin, S. 1938, *Variable Stars*, Harvard Obs. Monogr. 5, Harvard Coll. Obs., Cambridge, MA.

Percy, J. R., Bandara, K., Fernie, J. D., Cottrell, P. L., and Skuljan, L. 2004, *J. Amer. Assoc. Var. Star Obs.*, **33**, 27.

Pigott, E., and Englefield, H. C. 1797, *Philos.Trans. Roy. Soc. London*, Ser. I, **87**, 133.

Pollard, K. R., Cottrell, P. L., and Lawson, W. A. 1994, *Mon. Not. Roy. Astron. Soc.,* **268**, 544.

Rao, N. K., and Lambert, D. L. 1996, in *Hydrogen Deficient Stars*, eds. C. S. Jeffery and U. Heber, ASP Conf. Ser. 96, Astron. Soc. Pacific, San Francisco, 43.

Rao, N. K., and Lambert, D. L. 1997, *Mon. Not. Roy. Astron. Soc.,* **284**, 489.

Rao, N. K., and Lambert, D. L. 2000, *Mon. Not. Roy. Astron. Soc.,* **313**, L33.

Rao, N. K., and Lambert, D. L. 2003, *Publ. Astron. Soc. Pacific,* **115**, 1304.

Rao, N. K., and Lambert, D. L. 2008, *Mon. Not. Roy. Astron. Soc.,* **384**, 477.

Rao, N. K., Lambert, D. L., and Shetrone, M. D. 2006, *Mon. Not. Roy. Astron. Soc.,* **370**, 941.

Rao, N. K., Reddy, B. E., and Lambert, D. L. 2004, *Mon. Not. Roy. Astron. Soc.,* **355**, 855.

Rao, N. K., *et al.* 1999, *Mon. Not. Roy. Astron. Soc.,* **310**, 717.

Renzini, A. 1990, in *Confrontation Between Stellar Pulsation and Evolution*, eds. C. Cacciari and G. Clementini, ASP Conf. Ser. 11, Astron. Soc. Pacific, San Francisco, 549.

Saffer, R. A., Liebert, J., and Olszewski, E. W. 1988*, Astrophys. J.,* **334**, 947.

Saio, H. 2008, in in *Hydrogen-Deficient Stars*, eds. A. Werner and T. Rauch, ASP Conf. Ser. 391, Astron. Soc. Pacific, San Francisco, 69.

Saio, H., and Jeffery, C. S. 2002, *Mon. Not. Roy. Astron. Soc.,* **333**, 121.

Skiff, B. 2010, private communication.

Skuljan, L., and Cottrell, P. L. 1999, *Mon. Not. Roy. Astron. Soc.,* **302**, 341.
Skuljan, L., and Cottrell, P. L. 2002a, *Observatory*, **122**, 322.
Skuljan, L., and Cottrell, P. L. 2002b, *Mon. Not. Roy. Astron. Soc.,* **335**, 1133.
Staff, J. E. *et al.*, 2012*, Astrophys. J.,* submitted.
Tisserand, P. 2012, *Astron. Astrophys.,* **539**, A51.
Tisserand, P., *et al.* 2004, *Astron. Astrophys.,* **424**, 245.
Tisserand, P., *et al.* 2008, *Astron. Astrophys.,* **481**, 673.
Tisserand, P., *et al.* 2009, *Astron. Astrophys.,* **501**, 985.
Tisserand, P., *et al.* 2011, *Astron. Astrophys.,* **529**, A118.
Tisserand, P., *et al.* 2012, in preparation.
Walker, H. J. 1985, *Astron. Astrophys.,* **152**, 58.
Walker, H. J. 1994, *CCP7 Newsl.*, **21**, 40.
Warner, B. 1967, *Mon. Not. Roy. Astron. Soc.,* **137**, 119.
Webbink, R. F. 1984*, Astrophys. J.,* **277**, 355.
Werner, A., and Rauch, T., eds. 2008, *Hydrogen-Deficient Stars*, ASP Conf. Ser. 391, Astron. Soc. Pacific, San Francisco.
Wesson, R., Barlow, M. J., Liu, X., Storey, P. J., Ercolano, B., and de Marco, O. 2008, *Mon. Not. Roy. Astron. Soc.,* **383**, 1639.
Whitney, B. A., Balm, S. P., and Clayton, G. C. 1993, in *Luminous High-Latitude Stars*, ed. D. D. Sasselov, ASP Conf. Ser. 45, 115.
Whittet, D. C. B. 2003, *Dust in the Galactic Environment*, 2nd ed., Institute of Physics (IOP) Publ., Bristol, UK.
Woitke, P., Goeres, A., and Sedlmayr, E. 1996, *Astron. Astrophys.,* **313**, 217.
Yungelson, L. R., Livio, M., Tutukov, A. V., and Saer, R. A. 1994*, Astrophys. J.,* **420**, 336.
Zaniewski, A., Clayton, G. C., Welch, D. L., Gordon, K. D., Minniti, D., and Cook, K. H. 2005, *Astron. J.,* **130**, 2293.

Table 1. Spectroscopically confirmed Milky Way RCB stars.

Name	*R.A. (2000)*			*Dec. (2000)*			*Max*	*Spec. Ref.*[1]	*^{18}O*	*F*	*Li*	*Notes*[2]
	h	*m*	*s*	°	′	″						
XX Cam	04	08	38.75	+53	21	39.5	8.7	1		x	x	—
SU Tau	05	49	03.73	+19	04	22.0	9.5	1		✓	✓	—
UX Ant	10	57	09.06	–37	23	55.0	12.2	1		x	x	^{13}C
UW Cen	12	43	17.18	–54	31	40.7	9.6	1	x	✓	✓	—
Y Mus	13	05	48.19	–65	30	46.7	10.5	1	x		x	—
DY Cen	13	25	34.08	–54	14	43.1	12.0	1				hot RCB
V854 Cen	14	34	49.41	–39	33	19.2	7.0	1	x	x	x	Minority, ^{13}C
Z UMi	15	02	01.33	+83	03	48.6	11.0	1	x		✓	Minority
S Aps	15	09	24.53	–72	03	45.1	9.6	1	✓			—
ASAS-RCB-1	15	44	25.08	–50	45	01.2	11.9	2				V409 Nor
R CrB	15	48	34.41	+28	09	24.3	5.8	1		✓	✓	—
ASAS-RCB-9	16	22	28.83	–48	35	55.8	11.3	2, 3				IO Nor
RT Nor	16	24	18.68	–59	20	38.6	11.3	1			x	—
RZ Nor	16	32	41.66	–53	15	33.2	11.1	1			✓	
ASAS-RCB-2	16	41	24.75	–51	47	43.4	12.0	2				—
ASAS-RCB-3	16	54	43.60	–49	25	45.0	11.8	2, 3				—
ASAS-RCB-12	17	01	01.41	–50	15	34.8	11.8	2				—
ASAS-RCB-4	17	05	41.25	–26	50	03.4	13.3	2, 3				GV Oph
V517 Oph	17	15	19.74	–29	05	37.6	12.6	1				—
ASAS-RCB-10	17	17	10.21	–20	43	15.7	11.5	2				—
EROS2-CG-RCB-12	17	19	58.50	–30	04	21.3	14.1	4				—

Table continued on following pages

Table 1. Spectroscopically confirmed Milky Way RCB stars, cont.

Name	*R.A. (2000)*			*Dec. (2000)*			*Max*	*Spec. Ref.*[1]	*^{18}O*	*F*	*Li*	*Notes*[2]
	h	*m*	*s*	°	′	″						
V2552 Oph	17	23	14.55	–22	52	06.3	10.8	5, 6		✓	x	—
EROS2-CG-RCB-7	17	29	37.09	–30	39	36.7	14.1	4				—
EROS2-CG-RCB-6	17	30	23.83	–30	08	28.3	12.8	4				V1135 Sco
V532 Oph	17	32	42.61	–21	51	40.8	11.7	7				—
OGLE–GC–RCB–1	17	35	18.12	–26	53	49.2	14.6	8				—
EROS2-CG-RCB-8	17	39	20.72	–27	57	22.4	13.0	4				—
EROS2-CG-RCB-10	17	45	31.41	–23	32	24.4	12.5	4				—
EROS2-CG-RCB-5	17	46	00.32	–33	47	56.6	13.5	4				—
EROS2-CG-RCB-4	17	46	16.20	–32	57	40.9	12.5	4				—
EROS2-CG-RCB-9	17	48	30.87	–24	22	56.5	15.2	4				—
EROS2-CG-RCB-11	17	48	41.53	–23	00	26.5	12.3	4				—
ASAS-RCB-7	17	49	15.70	–39	13	16.0	12.7	2				V653 Sco
EROS2-CG-RCB-1	17	52	19.96	–29	03	30.8	12.4	4				—
ASAS-RCB-5	17	52	25.30	–34	11	28.0	12.3	2				—
EROS2-CG-RCB-2	17	52	48.70	–28	45	18.9	14.5	4				—
MACHO 401.48170.2237	17	57	59.02	–28	18	13.1	14.5	9				—
EROS2-CG-RCB-3	17	58	28.27	–30	51	16.4	11.1	4				—
EROS2-CG-RCB-13	18	01	58.22	–27	36	48.3	11.4	4				—
V1783 Sgr	18	04	49.74	–32	43	13.4	12.5	2				—
WX CrA	18	08	50.48	–37	19	43.2	11.0	1	✓			—
ASAS-RCB-11	18	12	03.30	–28	08	33.0	12.0	2				—

Table continued on following pages

Table 1. Spectroscopically confirmed Milky Way RCB stars, cont.

Name	*R.A. (2000)*			*Dec. (2000)*			*Max*	*Spec. Ref.*[1]	*^{18}O*	*F*	*Li*	*Notes*[2]
	h	*m*	*s*	°	′	″						
V739 Sgr	18	13	10.54	–30	16	14.7	14.0	1				—
EROS2-CG-RCB-14	18	13	14.86	–27	49	40.9	12.5	4				—
V3795 Sgr	18	13	23.58	–25	46	40.8	11.5	1		✓		Minority
VZ Sgr	18	15	08.58	–29	42	29.4	11.8	1		✓	x	Minority, *^{13}C*
IRAS 18135–2419	18	16	39.20	–24	18	33.4	12.8	2, 10				—
RS Tel	18	18	51.22	–46	32	53.4	9.3	1			x	—
MACHO 308.38099.66	18	19	27.36	–21	24	08.2	16.3	9				—
MACHO 135.27132.51	18	19	33.87	–28	35	57.8	14.3	9				—
GU Sgr	18	24	15.58	–24	15	26.5	11.3	1		✓?	x	—
V581 CrA	18	24	43.46	–45	24	43.8	10.0	2				—
V391 Sct	18	28	06.57	–15	54	44.7	13.3	2				—
MACHO 301.45783.9	18	32	18.60	–13	10	48.9	17.3	9				—
NSV 11154	18	37	51.26	+47	23	23.5	12.0	11				—
V348 Sgr	18	40	19.93	–22	54	29.3	10.6	1				hot RCB
MV Sgr	18	44	31.97	–20	57	12.8	12.0	1				hot RCB
FH Sct	18	45	14.84	–09	25	36.1	13.4	1		✓?	x	—
V CrA	18	47	32.30	–38	09	32.3	9.4	1		✓?	x	*^{13}C*
ASAS-RCB-8	19	06	39.87	–16	23	59.2	10.9	2				—
SV Sge	19	08	11.76	+17	37	41.2	11.5	1	✓			—
V1157 Sgr	19	10	11.83	–20	29	42.1	12.5	1				—
RY Sgr	19	16	32.76	–33	31	20.4	6.5	1		✓	x	—

Table continued on next page

Table 1. Spectroscopically confirmed Milky Way RCB stars, cont.

Name	*R.A. (2000)* *h*	*m*	*s*	*Dec. (2000)* °	′	″	*Max*	*Spec. Ref.*[1]	^{18}O	*F*	*Li*	*Notes*[2]
ES Aql	19	32	21.61	–00	11	31.0	11.6	12	✓			—
V482 Cyg	19	59	42.57	+33	59	27.9	12.1	1		✓?	x	—
ASAS-RCB-6	20	30	04.96	–62	07	59.2	13.1	2, 3				AN 141.1932
U Aqr	22	03	19.70	–16	37	35.2	10.5	1	✓		✓?	—
UV Cas	23	02	14.62	+59	36	36.6	11.8	1		✓	x	—
HdC Stars												
HE 1015–2050	10	17	34.232	–21	05	13.87	16.0	13				—
HD 137613	15	27	48.316	–25	10	10.15	7.5	14	✓			—
HD 148839	16	35	45.788	–67	07	36.69	8.3	14	x		✓	—
HD 173409	18	46	26.627	–31	20	32.07	9.5	14	x			—
HD 175893	18	58	47.29	–29	30	18.08	9.4	14	✓			IR Excess
HD 182040	19	23	10.08	–10	42	11.54	7.0	14	✓			—

[1]*Spectroscopic references: 1) Clayton (1996, and references therein), 2) Tisserand et al. (2012, in preparation), 3) Miller et al. (2012), 4) Tisserand et al. (2008), 5) Hesselbach et al. (2003), 6) Rao and Lambert (2003), 7) Clayton et al. (2009), 8) Tisserand et al. (2011), 9) Zaniewski et al. (2005), 10) Greaves (2007), 11) Kijbunchoo et al. (2011), 12) Clayton et al. (2002), 13) Goswami et al. (2010), 14) Warner (1967), .*

[2]*Note: RZ Nor has a faint blue star nearby. This may explain why the RZ Nor declines are not very deep and it appears bluer during declines.*

Table 2. Spectroscopically confirmed LMC and SMC RCB stars.

Name	*R.A. (2000)* *h*	*m*	*s*	*Dec. (2000)* °	′	″	*Max*	*Spec. Ref.*[1]	^{18}O	*F*	*Li*	*Notes*
LMC Stars												
EROS2-LMC-RCB-3	04	59	35.78	–68	24	44.68	14.3	1				—
HV 12524	05	01	00.36	–69	03	43.2	14.5	2				MACHO 18.3325.148
KDM 2373	05	10	28.50	–69	47	04.3	13.8	1, 3				MACHO 5.4887.14, EROS2-LMC-RCB-2
HV 5637	05	11	31.37	–67	55	50.6	15.8	4				MACHO 20.5036.12
EROS2-LMC-RCB-1	05	14	40.17	–69	58	40.1	15.2	1				MACHO 5.5489.623
HV 2379	05	14	46.20	–67	55	47.4	14.9	2				MACHO 16.5641.22
MACHO 79.5743.15	05	15	51.79	–69	10	08.6	15.2	2				—
MACHO 6.6575.13	05	20	48.21	–70	12	12.5	15.3	2				—
HV 942	05	21	48.00	–70	09	57.4	15.0	2				MACHO 6.6696.60
MACHO 80.6956.207	05	22	57.37	–68	58	18.9	16.0	2				—
W Men	05	26	24.52	–71	11	11.8	13.8	4			✓	MACHO 21.7407.7
MACHO 80.7559.28	05	26	33.91	–69	07	33.4	15.8	2				—
MACHO 81.8394.1358	05	32	13.36	–69	55	57.8	16.3	5				—
HV 2671	05	33	48.94	–70	13	23.4	16.1	5				MACHO 11.8632.2507, Hot RCB
EROS2-LMC-RCB-4	05	39	36.97	–71	55	46.4	15.1	1				MACHO 27.9574.93
KDM 5651	05	41	23.49	–70	58	01.8	14.4	3				MACHO 15.9830.5
HV 12842	05	45	02.88	–64	24	22.7	13.7	4			✓	—

Table continued on next page

Table 2. Spectroscopically confirmed LMC and SMC RCB stars, cont.

Name	*R.A. (2000)* *h*	*m*	*s*	*Dec. (2000)* °	′	″	*Max*	*Spec. Ref.*[1]	^{18}O	*F*	*Li*	*Notes*
MACHO 12.10803.56	05	46	47.74	–70	38	13.5	15.1	2				—
KDM 7101	06	04	05.53	–72	51	23.1	14.2	1, 3				EROS2-LMC-RCB-5
SMC Stars												
RAW 21	00	37	47.40	–73	39	02.0	15.6	1, 3, 6				EROS2-SMC-RCB-1
RAW 476	00	48	22.87	–73	41	04.7	15.5	1, 6				EROS2-SMC-RCB-2
EROS2-SMC-RCB-3	00	57	18.12	–72	42	35.3	16.0	1, 6				MACHO 207.16426.1662

[1]*Spectroscopic references: 1) Tisserand et al. (2009), 2) Alcock et al. (2001), 3) Morgan et al. (2003), 4) Clayton (1996, and references therein), 5) Alcock et al. (1996), 6) Tisserand et al. (2004).*

Table 3. DD vs FF[1]

Property	*DD*	*FF*
Extreme H deficiency but some H present	yes?	yes
H abundance anti-correlated with Fe	?	?
Li abundance high in 5 stars (all majority)	no	yes
C/He ~ 1%	yes	no
$^{12}C/^{13}C > 500$	yes	no
High N, O	yes	yes
High Na, Al	yes?	yes
High Si, S	?	?
Enrichment of s-process elements	yes?	yes
Abundance uniformity/non-uniformity for majority/minority	no?/yes	yes/no?
Similar to Sakurai's object	no	yes
Nebulosity present in a few stars	yes?	yes
RCB Lifetime	yes	no
Lack of binarity	yes	no?
^{18}O and ^{19}F greatly enhanced in (all?) stars	yes	no
$M_V = -3$ to -5 mag	yes	yes
Mass = 0.8–0.9 $M_\odot$	yes	no?

[1]*Adapted and updated from Table 7 of Asplund et al. (2000).*

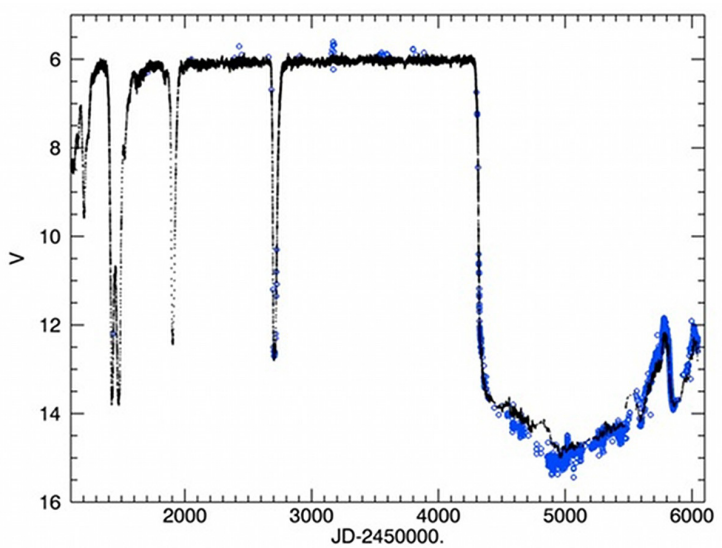

Figure 1. Light curve of R CrB from 1998 to 2012 using AAVSO data. Visual magnitudes are plotted as black dots. Johnson V data are plotted as open circles.

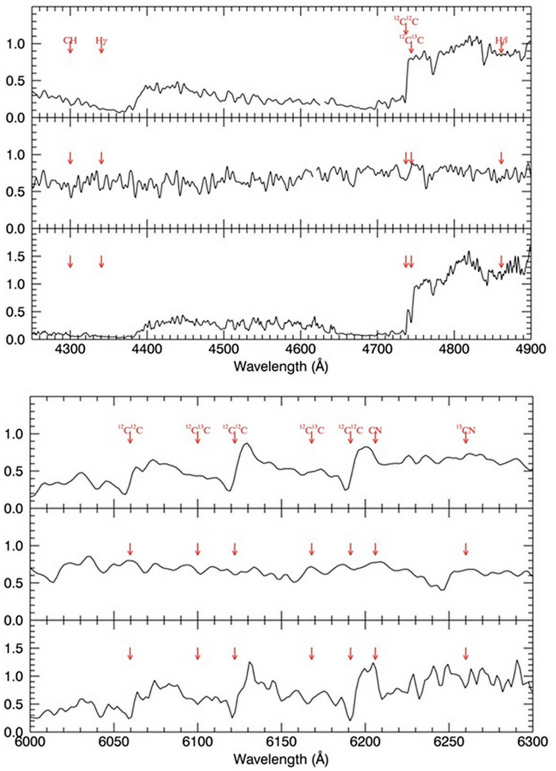

Figure 2. Blue (upper figure) and red (lower figure) sections of the spectra of a cool RCB star, S Aps (top plots), and a warm RCB star, RY Sgr (middle plots), as well as the carbon star, RV Sct (bottom plots), showing some of the spectroscopic features that define RCB stars.

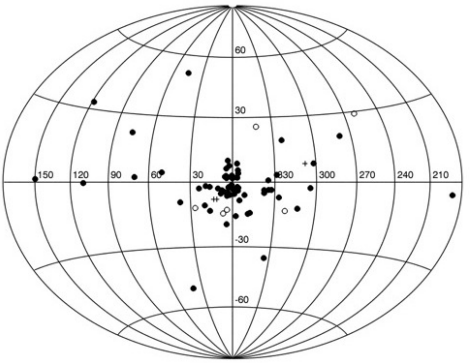

Figure 3. Distribution of RCB stars on the sky in the Galaxy showing that they are consistent with an old, bulge popularion. Cool RCB stars (filled circles), hot RCB stars (crosses), HdC stars (open circles).

Cataclysmic Variables

Paula Szkody
Department of Astronomy, University of Washington, Seattle, WA 98195; szkody@astro.washington.edu

Boris T. Gaensicke
Department of Physics, University of Warwick, Coventry CV4 7AL, UK; Boris.Gaensicke@warwick.ac.uk

Invited review paper, received April 3, 2012

Abstract This paper presents a concise summary of our current knowledge of cataclysmic variables, including definitions of types and the observational basis for classification, what we have been able to piece together about evolution, and discoveries from recent surveys. We provide a list of unanswered problems and questions and references for seeking additional information. The importance of AAVSO observations in the past and for the future is highlighted.

1. What we know about CVs

The basic definition of a cataclysmic variable (CV) is a mass-transferring close binary containing a white dwarf primary and a secondary that is usually a late-type main sequence star (although a few cases with giant or brown-dwarf secondaries exist). A good starting point for understanding the general properties of CVs is the book by Warner (1995) or by Hellier (2001). Various catalogs of CVs have been compiled over the years by Downes *et al.* (1997; on-line version frozen in 2006 at http://archive.stsci.edu/prepds/cvcat/), Ritter and Kolb (2003; current on-line version at http://www.MPA-Garching.MPG.DE/RKcat/), Drake *et al.* (2009; online at http://nesssi.cacr.caltech.edu/catalina/AllCV.html) and Szkody *et al.* (2011; online catalog at http://www.astro.washington.edu/users/szkody/cvs).

CVs are thought to form from wider binaries composed of two main sequence stars when the more massive star becomes a giant and forms a common envelope around the system. As the two stars orbit within this common envelope, their separation decreases and the orbital period shrinks from days to hours. Once the common envelope dissipates, the resulting white dwarf-main sequence binary system evolves without mass transfer, continually losing momentum through a braking wind from the secondary and decreasing its orbital period until the secondary fills its Roche lobe and begins to transfer mass to the white dwarf. At this point, it becomes a bona-fide CV. As the period continues to shrink to 3 hours, the secondary star structure changes, becoming completely convective, and at a period near 2 hours, gravity waves become the source of

momentum loss (resulting in low mass transfer rates) until a period minimum near 80 minutes is reached. After this point, the structure of the secondary again changes (becoming degenerate) and the orbital period increases.

A cataclysmic variable is usually identified by its variability on timescales of minutes (from flickering) to hours (from orbital variations) to weeks-years (from mass accretion variations), by its peculiar spectrum showing broad, usually doubled, Balmer emission lines, or by the detection of X-ray emission, which is generated by the material that accretes onto the white dwarf. The observational appearance of a CV depends primarily on two parameters: the amount of mass transfer, and the magnetic field strength of the white dwarf.

In a non-magnetic CV, where the white dwarf has no detectable field (typically much less than 1MG), the mass flow from the companion star builds up an accretion disk around the white dwarf. In these accretion disks, the material slowly spirals inwards towards the white dwarf. The rate at which the mass migrates through the disk depends on the viscosity of the material, as it is this "stickiness" that allows the exchange of angular momentum. There are two regimes in which accretion disks can be found, one of low viscosity, where the mass flow through the disk is slow, and one of high viscosity, where the mass flow is correspondingly much faster. In which of these states a CV is found depends on the rate at which the companion star supplies fresh material to the outer edge of the disk. For high mass transfer rates, the disk is in a stable state of high viscosity, hot, and the dominant source of light. These systems typically have orbital periods longer than 3 hours and are called nova-likes. They have no large-amplitude outbursts, and their spectra are often lacking the emission lines that are typical of most CVs, that is, they are rather inconspicuous. Thus, some of the brightest known CVs were found only very recently, and rather serendipitously, such as LSIV-08°3 with V=11.5 (Stark *et al.* 2008).

For low mass transfer systems, the material in the accretion disk has a low viscosity and is cool. The rate at which material flows through the disk is actually lower than that provided by the companion star. Thus, the disk gradually grows in mass and heats up, until its temperature becomes sufficiently high to switch into the hot, high-viscosity state, where the accumulated mass is rapidly flushed onto the white dwarf. Systems that undergo these quasi-regular outbursts are called dwarf novae, and are the most common sub-class of CVs. The underlying physical mechanism of the accretion disk instability is important in a wide range of other astronomical objects; for example, it is thought that the protostellar accretion disks in T Tauri stars and the disks around supermassive black holes in the centers of galaxies also undergo outburst cycles.

Because of their short timescales, CVs are the best "laboratory" to study accretion disk physics. A particularly interesting sub-class among the non-magnetic CVs is the Z Cam type of system: here, the accretion rate is close to the borderline between hot, stable, and cool, unstable disks, and these systems can switch back and forth between being a dwarf nova and a novalike.

Mike Simonsen (2011) has initiated a dedicated project to obtain high-quality light curves for a large number of Z Cam stars. For orbital periods between 3 and 4 hours, a peculiar class of CVs exist called SW Sex stars (Thorstensen *et al.* 1991). These systems show single Balmer emission lines as well as a prominent HeII 4686 emission line, show transient absorption at some phases, and are often discovered as eclipsing systems. A list of SW Sex objects is provided by Hoard *et al.* (2003; an online updated list is at http://www.dwhoard.com/home/biglist). A few of these SW Sex stars show low circular polarization, indicating a relatively high magnetic field for the white dwarf (for example, Rodriguez-Gil *et al.* 2001). Some novalikes, including the SW Sex stars, occasionally fade by several magnitudes, for weeks to years. During these low states, the mass transfer from the secondary star is interrupted, and the accretion disk becomes very faint, or vanishes altogether. Consequently, the white dwarf and the secondary star can be observed directly. It appears that the white dwarfs in these systems are extremely hot, which suggests that the high accretion rates observed during the high states probably prevail for thousands of years.

A completely different picture is found among the magnetic CVs. If the white dwarf has a very high magnetic field (> 10 MG), the mass transfer stream impacts directly onto the white dwarf magnetic poles without forming a disk (King and Lasota 1993). In these systems (called Polars), the field locks the secondary and the white dwarf spin to the orbit so all variations are on the orbital timescale. The high field is identified from the presence of strong circular polarization or from Zeeman splitting. At very low accretion rates, broad cyclotron humps are prominent in the spectrum. Polars, just like the novalikes mentioned above, can cycle aperiodically between low and high states. This suggests that variations in the mass transfer rate from the companion star are inherent to all CVs, but that in dwarf novae, these variations are smoothed out by the accretion disk. For white dwarf fields of about 1–10 MG, an outer accretion disk forms but the inner disk is disrupted by the field so the material rains onto the white dwarf in broad accretion curtains. In these Intermediate Polars (IPs), the white dwarf spin is usually evident as a strong pulse visible in optical or X-ray at about one-tenth of the orbital period, even though the last years have seen the discovery of IPs with both much smaller and larger spin-to-orbital period ratios.

As CVs accrete from their companion stars, a layer of hydrogen-rich material builds up on the white dwarf, which will eventually ignite in a violent thermonuclear reaction, called a classical nova. All CVs should undergo many classical nova eruptions, with typical recurrence times of thousands of years. However, for high mass white dwarfs, this recurrence time can be as short as a few decades. A spectacular example is T Pyx, which showed regular nova eruptions every ~20 years until 1966, but then went unexpectedly quiet—until 2011, when it surprised astronomers who had already started to develop theories why it would not erupt any time soon. These recurrent novae may eventually explode as type Ia supernovae, if the white dwarf reaches the Chandrasekhar limit.

The realm of satellite observations in the last few decades enabled ultraviolet, X-ray, and IR observations of CVs that vastly contributed to our knowledge of the components within these binaries. In disk CVs, the accretion disk was shown to be a dominant source of UV light, especially during an outburst. The delay between the start of the outburst in optical vs UV light led to increased understanding of the way the outburst proceeds through the disk. In the systems where the white dwarf could be seen as well as the disk, studies throughout the outburst interval showed how the white dwarf was heated by the outburst and subsequently cooled over months to years. Determination of the temperatures of the white dwarfs at quiescence revealed the difference in heating efficiency between magnetic accretion onto a pole vs disk accretion onto a boundary layer, as the white dwarfs in Polars had lower temperatures than disk CVs (Sion 1991; Araujo-Betancor *et al.* 2005). X-ray observations also showed differences between disk and magnetic CVs. The IPs revealed the hardest, most absorbed X-ray spectra, leading to models of accretion curtains, while the Polars typically showed both soft and hard X-rays (the hard from the accretion column and the soft from the heating of the white dwarf surface by the x-rays from the column). Spitzer observations of disk CVs produced surprising results on dust rings within and around several CVs (Brinkworth *et al.* 2007; Hoard *et al.* 2009). Ground-based near-IR spectroscopy also revealed some surprises. When the secondary stars could be observed, the majority of those in disk CVs showed a depletion of CO and metals compared to normal main-sequence stars, whereas the secondaries in Polars do not show this effect (Howell *et al.* 2010). In some short period systems, no evidence of a secondary is seen, implying a very low mass, brown-dwarf type object (Patterson 2011).

In the last decade, the Hamburg Quasar Survey (HQS) and the Sloan Digital Sky Survey (SDSS) produced many new CV candidates. Followup photometry and spectroscopy confirmed several new IPs and SW Sex stars from the brighter objects found by HQS (Rodriguez-Gil *et al.* 2007), and more than 200 CVs from the SDSS which could reach to fainter magnitudes (Szkody *et al.* 2011). Determination of the orbital periods of over 100 of the CVs from the SDSS revealed a period distribution that was much closer to that predicted by population models, with the majority of objects having periods less than 2 hours (Gaensicke *et al.* 2009). However, the minimum period where most of the CVs appear occurs at a slightly larger value (80 minutes) than the 70 minutes predicted by population models (Kolb and Baraffe 1999). These results confirm the basic picture of angular momentum losses via magnetic braking at periods longer than 3 hours and via gravitational radiation at periods under 2 hours, but will require some tweaking of these parameters along with the structure of the stars to obtain a perfect match (Knigge *et al.* 2011). Many new eclipsing CVs are found among the SDSS systems, in which accurate masses and radii can be measured (Littlefair *et al.* 2006). These studies led to the puzzling fact that the white dwarfs in CVs are on average much more massive compared to both

single white dwarfs and those in pre-CVs (Zorotovic *et al.* 2011). The only two answers to this discrepancy are that either the white dwarfs in CVs grow in mass, or that the current-day CV population descends from progenitors that are different from the pre-CVs we have found so far.

Other results from SDSS included the discoveries that there are significant populations of Polars with mass transfer rates three orders of magnitude lower than typical Polars (Low Accretion Rate Polars or LARPs; Schwope *et al.* 2002; Schmidt *et al.* 2005), and there are many CVs containing accreting, pulsating white dwarfs (Szkody *et al.* 2010).The LARPS provide a means to study wind loss from a low mass star, as the low accretion rates preclude the existence of an accretion shock above the white dwarf surface and the visible cyclotron radiation likely stems from the concentration of the wind from the secondary by the interaction of the fields of the two stars. This magnetic interaction has been explored by Kafka *et al.* (2010) for a variety of systems, demonstrating that magnetic prominences occur in many systems other than solar-type stars.

The pulsating white dwarfs have also led to probes of the instability region of white dwarfs. Asteroseismology of white dwarfs has shown their importance for the determination of stellar parameters of mass, age, spin, core composition, magnetic field strength, and distance (Winget and Kepler 2008), The white dwarf pulsators in CVs have the added advantage of undergoing accretion, which heats the white dwarf and changes the composition and rotation, allowing the study of how these parameters affect the instability strip. In addition, the presence of outbursts allows the unique advantage of observing a white dwarf move out of the instability strip (when its heated by the outburst) and then moving back in (as it cools to its quiescent temperature), changes which take millions of years for single white dwarf but only a few years for CVs.

2, Open questions

While the general evolutionary picture and the characteristics of the types of CVs are known at some level, there are major unsolved questions which remain. These include:

1) What is the actual number density and distribution of CVs in the Galaxy? As future surveys push to fainter limits and sample the disk as well as the halo, we can finally determine the real population of CVs in the Milky Way.

2) What happens to CVs once they reach the period minimum? Theory predicts that they evolve back to longer periods, and that ~70% of all CVs should have evolved to that state. Yet, among more than a thousand CVs, at best a handful of those "period bouncers" are known. Does this imply that these highly evolved CVs look very different from the CVs we know now, and we have so far simply not been able to identify them? Or are the models fundamentally flawed?

3) What are the detailed physics occurring in the common envelope? So far, many of the theoretical models of cataclysmic variable evolution rely on rather crude parametrization of the complex processes in the common envelope, but with the large samples found by Sloan, it will become possible to provide some observational constraints for these parameters.

4) What is the correct physics to describe viscosity in accretion disks? Magnetic turbulence is generally accepted to be the most important effect, yet, no model of this magneto-rotational instability can so far reproduce the observed characteristics of dwarf nova outbursts. Will we finally be able to determine the spectral energy distribution (SED) of a low mass accretion rate disk?

5) What is the correct angular momentum prescription below the gap (besides gravitational radiation) that can account for the observed period minimum spike and the exact period distribution? Is it related to some residual magnetic braking?

6) What causes the period gap? The classic idea is that magnetic braking becomes inefficient, however, recent studies of single M-dwarfs suggest that the reality may be more complex.

7) How do Polars form and why are no magnetic white dwarfs in wide binaries observed? Are LARPS the progenitors of polars? Is there a difference in the emergence of systems containing magnetic white dwarfs versus non-magnetic?

8) What causes Polars, as well as the novalike disk systems with orbital periods between 3 and 4 hours, to cease mass transfer and enter low states? Are the associated mass transfer variations of the companion stars a general phenomenon among all CVs?

9) Can the white dwarfs in CVs grow in mass? Current classical nova models seem to categorically rule out this possibility, yet, observations show that the average mass in CVs is much higher than among pre-CVs.

10) What are the secondaries like in period-bouncers?

11) Do CVs contain exoplanets? Long-term studies of the ephemeris of eclipsing CVs reveal variations of the mid-eclipse times, which can be explained by a third, unseen body tugging on the CV binary. However, many other effects can result in the observed variations, and a much longer baseline of eclipse time monitoring will be necessary to unambiguously confirm or refute the presence of circumbinary planets.

3. The importance of the AAVSO for CVs

Since the very early days of CV research, the AAVSO has played a vital part in obtaining the data on which discoveries and resulting breakthroughs in understanding are based. The long term light curves of the dwarf novae SS Cyg and U Gem, spanning more than a century, provided the impetus for the modeling of dwarf novae outbursts (Cannizzo and Mattei 1998). Observations of the onset of outbursts that triggered UV and satellite observations revealed a delay between the optical and UV light that led to further understanding of the outburst scenario (Cannizzo 2001). The simultaneous monitoring of SS Cyg by the AAVSO observers and the EUVE and RXTE satellites revealed a strong anti-correlation between the soft and hard X-rays during an outburst, providing new insight into the processes at the boundary between the white dwarf and the accretion disk (Wheatley *et al.* 2003). After Polars were found, the long term records of the AAVSO showed the various high and low states of accretion and helped reveal that Polars spend most of their time in low states. Combined with multi-epoch X-ray observations, Hessman *et al.* (2000) used twenty years' worth of AAVSO observations to accurately measure the accretion rate in AM Her, the prototypical polar, and to estimate the fraction of the companion that is covered by star spots. Most recently, HST observations on CVs have required a ground based optical measurement within twenty-four hours of the scheduled HST time to confirm the objects at quiescence. Due to vagaries of weather at any one site, this requirement has led to a vital need for AAVSO monitoring prior to and during observation. The AAVSO CV Section page handled by Mike Simonsen provides campaigns and highlights requests to promote the best interaction between observers and scientists. The Z CamPaign is one productive example of an ongoing campaign that is unique to AAVSO. No single individual or professional could accomplish the concentrated observations that recently produced new scientific results on the number of Z Cam systems and some unique members (Simonsen 2011). The installation of AAVSOnet, providing robotic telescope access at a variety of sites, has been used in these campaigns and other programs, enabling productive observations at both hemispheres and at good weather sites. The archive provided by all of these observations is used by scientists around the world.

The future is moving toward large surveys and large satellites. If funding is realized, PanSTARRS and LSST will provide constant monitoring of the southern and northern skies by the next decade. These surveys will change the landscape for some AAVSO programs, eliminating the need for monitoring of some stars, but enhancing the need in many other areas. The proposed surveys saturate at fairly bright limits of 16–18 magnitudes. This means that there will continue to be a need to continue the long term archive of brighter CVs that is the fodder for theorists. While the surveys will sample some timescales, the coverage is not ideal for CVs with orbital periods of hours, not days, and outbursts that can

rise within one night. The survey filters are mostly concentrated toward the red, while CVs have more activity levels in the blue than the red. The survey telescopes are pre-programmed to move around the sky for a certain pattern so observations that are simultaneous with satellites will still be in demand. Another major mission to be launched next year is GAIA, which will observe the entire sky for at least five years, measuring distances to about a billion stars. Given its location above the Earth's atmosphere, GAIAs scanning pattern is not affected by bad weather, and the mission's first data to become available will be alerts of variable objects identified during the repeated observations. Ground-based confirmation and time-series follow-up will be a key area where AAVSO observers can play a very important role. The surveys will expose a huge number of variables at all magnitudes. The bright end will be a bonanza for AAVSO to scavenge and determine types of objects and behavior at times when the survey is not looking. The era of new opportunities in the field of CVs is just beginning.

References

Araujo-Betancor, S., Gaensicke, B. T., Long, K. S., Beuermann, K., de Martino, D., Sion, E. M., and Szkody, P. 2005, *Astrophys. J.*, **622**, 589.

Brinkworth, C. S., *et al.* 2007, *Astrophys. J.*, **659**, 1541.

Cannizzo, J. K. 2001, *Astrophys. J.*, **556**, 847.

Cannizzo, J. K., and Mattei, J. A. 1998, *Astrophys. J.*, **505**, 344.

Downes, R., Webbink, R. F., and Shara, M. M. 1997, *Publ. Astron. Soc. Pacific*, **109**, 345.

Drake, A. J., *et al.* 2009, *Astrophys. J.*, **696**, 870.

Gaensicke, B. T., *et al.* 2009, *Mon. Not. Roy. Astron. Soc.*, **397**, 2170.

Hellier, C. 2001, *Cataclysmic Variable Stars*, Springer, New York.

Hessman, F. V., Gaensicke, B. T., and Mattei, J. A. 2000, *Astron. Astrophys.*, **361**, 952.

Hoard, D. W., Kafka, S., Wachter, S., Howell, S., Brinkworth, C., Ciardi, D., and Szkody, P. 2009, in T*he Eighth Pacific Rim Conference on Stellar Astrophysics: A Tribute to Kam-Ching Leung*, eds. B. Soonthornthum, S. Komonjinda, K.S. Cheng, and K.C. Leung, ASP Conf. Ser. 404, Astron. Soc. Pacific, San Francisco, 234.

Hoard, D. W., Szkody, P., Froning, C. S., Long, K. S., and Knigge, C. 2003, *Astron. J.*, **126**, 2473.

Howell, S. B., Harrison, T. E., Szkody, P., and Silvestri, N. M. 2010, *Astron. J.*, **139**, 1771.

Kafka, S., Tappert, C., Ribeiro, T., Honeycutt, R. K., Hoard, D. W., and Saar, S. 2010, *Astrophys. J.*, **721**, 1714.

King, A. R., and Lasota, J. P. 1993, in *The Realm of Interacting Binary Stars*, Astron. Space Sci. Libr. 177, 169.

Knigge, C., Baraffe, I., and Patterson, J. 2011, *Astrophys. J., Suppl. Ser.*, **194**, 28.

Kolb, U., and Baraffe, I. 1999, in *Annapolis Workshop on Magnetic Cataclysmic Variables*, eds. C. Hellier, and K. Mukai, ASP Conf. Ser. 157, Astron. Soc. Pacific, San Francisco, 273.

Littlefair, S. P., Dhillon, V. S., Marsh, T. R., Gaensicke, B. T., Southworth, J., and Watson, C. A. 2006, *Science*, **314**, 1578.

Patterson, J. 2011, *Mon. Not. Roy. Astron. Soc.*, **411**, 2695.

Ritter, H., and Kolb, U. 2003, *Astron. Astrophys.*, **404**, 301.

Rodríguez-Gil, P., Casares, J., Martínez-Pais, I. G., Hakala, P., and Steeghs, D. 2001, *Astrophys. J, Lett. Ed.*, **548**, 49.

Rodriguez-Gil, P., *et al.* 2007, *Mon. Not. Roy. Astron. Soc.*, **377**, 1747.

Schmidt, G. D., *et al.* 2005, *Astrophys. J.*, **630**, 1037.

Schwope, A. D., Brunner, H., Hambaryan, V., and Schwarz, R. 2002, in *The Physics of Cataclysmic Variables and Related Objects*, eds. B. T. Gaensicke, K. Beuermann, and K. Reinsch, ASP Conf. Ser. 261, Astron. Soc. Pacific, San Francisco, 102.

Simonsen, M. 2011, *J. Amer. Assoc. Var. Star Obs.*, **39**, 66.

Sion, E. M. 1991, *Astron. J.*, **102**, 295.

Stark, M. A., Wade, R. A., Thorstensen, J. R., Peters, C. S., Smith, H. A., Miller, R. D., and Green, E. M. 2008, *Astron. J.* **135**, 991.

Szkody, P., *et al.* 2010, *Astrophys. J.*, **710**, 64.

Szkody, P., *et al.* 2011, *Astron. J.*, **142**, 181.

Thorstensen, J. R., Ringwald, F. A., Wade, R. A., Schmidt, G. D., and Norsworthy, J. E. 1991, *Astron. J.* **102**, 272.

Warner, B. 1995, *Cataclysmic Variable Stars*, Cambridge Univ. Press, Cambridge.

Wheatley, P. J., Mauche, C. W., and Mattei, J. A. 2003, *Mon. Not. Roy. Astron. Soc.* **345**, 49.

Winget, D. E., and Kepler, S. O. 2008, *Ann. Rev. Astron. Astrophys.*, **46**, 157.

Zorotovic, M., Schreiber, M. R., and Gaensicke, B. T. 2011, *Astron. Astrophys.* **536**, 42.

Symbiotic Stars

Ulisse Munari
National Institute of Astrophysics (INAF), Astronomical Observatory of Padova, 36012 Asiago (VI), Italy; ulisse.munari@oapd.inaf.it

Invited review paper, received May 3, 2012

Abstract Symbiotic stars are interacting binary systems composed of a white dwarf (WD) accreting at high rate from a cool giant companion, which frequently fills its Roche lobe. The WD usually is extremely hot and luminous, and able to ionize a sizeable fraction of the cool giant wind, because it is believed the WD undergoes stable hydrogen nuclear burning on its surface of the material accreted from the companion. This leads to consider symbiotic stars as good candidates for the yet-to-be-identified progenitors of type Ia supernovae. Symbiotic stars display the simultaneous presence of many different types of variability, induced by the cool giant, the accreting WD, the circumstellar dust and ionized gas, with time scales ranging from seconds to decades. The long orbital periods (typically a couple of years) and complex outburst patterns, lasting from a few years to a century, make observations from professionals almost impossible to carry out, and open great opportunities to amateur astronomers to contribute fundamental data to science.

1. Introduction

Observing symbiotic stars (hereafter SySts) is real fun and a great opportunity for the amateur astronomer (hereafter AA) to contribute fundamental, better to say "unique" data. In fact, the long orbital periods and outburst phases (measured in years) make observations by professionals almost impossible to carry out, especially for those that have to access, on highly competitive grounds, to telescopes at large observatories. SySts show variability over a wide range of time scales: seconds/minutes (accretion flickering), minutes/hours (rotation of the white dwarf), days/months (rotation, pulsations of the cool giant, recombination in the ionized circumstellar gas, shock fronts, bipolar jets), months/years (orbital periods, eclipses, reflection effects, ellipsoidal distortions, Mira pulsations), months/centuries (outbursts). Some of these types of variability are best seen and display larger amplitude in the red, others at blue wavelengths, as we will see later on in detail.

To enhance their value, to provide firmer grounds for physical modeling, and to allow astronomers to safely combine data collected by various AAs (sometimes different *generations* of AA), the photometric observations should be carried out in standard photometric bands, well-calibrated into accurate local photometric sequences by application of suitable color equations. Henden

and Munari (2000, 2001, 2006) have calibrated photometric sequences around eighty-one well-known SySts and are working to extend them to all other catalogued SySts. By adopting these photometric sequences, the AAs can bring their observations closer to (and easier to integrate with) data collected by professionals who frequently use the same photometric sequences for their observations or when reconstructing past photometric histories from measurement of old photographic plates preserved in plate stacks around the world (like those at Harvard, Sonneberg, Pulkovo, and Asiago).

Even though this review focuses on photometry, it's a pleasure to note how spectroscopy is now becoming wide-spread among AA. Useful low resolution spectra of about twenty known SySt in quiescence are within the grasp of AAs using 0.5m telescopes, and a similar number of additional SySts can be reached during their outburst phases. The Hα is so bright that high resolution profiles of this emission line can be obtained for numerous SySts even with 0.5m telescopes. The profile and intensity of Hα is deeply modulated by the orbital motion, and it strongly responds also to the ionization of the circumstellar gas, eclipses, outbursts, winds, bipolar jets, and so on: monitoring the Hα of SySts is really fun! As a guideline, low resolution spectra should cover from 4000 to 7000Å at 2–5 Å/pixel, while high resolution observations of Hα should cover an interval of 100–200Å at 0.1–0.35 Å/pixel.

2. A typical symbiotic star

Let's begin with outlining what type of binary system a typical SySt is, and to this aim Figure 1 presents the optical spectrum of Z Andromedae, a prototype of this class of objects (see also Skopal 2011). A SySt is composed of: (1) a late type giant (LTG), most frequently of M2-M5III spectral types, not pulsating (in only ~20% of the cases it pulsates like a long period Mira), with its strong TiO absorption molecular bands modulating the spectrum at red wavelengths. The LTG dominates spectra and photometry at R_C-, I_C-band wavelengths.; and (2) an extremely hot (≥80,000 K) and luminous (of the order of a thousand solar luminosities) white dwarf (WD). It orbits the LTG and accretes from it, both via wind capture or Roche lobe overlow. The WD is so hot that its emission is concentrated in the far ultraviolet and X-rays, and it becomes directly observable at *U*, *B*, and *V* bands usually only during outbursts when its outer layers expand and cool.

The large temperature and luminosity of the WD (much larger than accountable by release of potential energy of accreting material, or by plain thermal irradiance along the cooling track) are explained by assuming that the WD undergoes stable hydrogen nuclear burning on its surface of the material accreted from the LTG (Munari and Buson 1994; Sokoloski 2003). The presence of many Super-Soft X-ray Sources (SSSx) among SySts is a direct confirmation of this scenario (many other SySts are not detected as

SSSx simply because there is so much circumstellar material around them that the X-rays are all locally absorbed). To keep the nuclear burning stable, the WD has to accrete at a high rate (a rate much larger than in the other types of interacting binaries, like the cataclysimc variables). This rate is fine tuned by the mass of the WD: below the critical value, the nuclear burning switches off; above it the material accreted in excess expands under the effect of the huge radiation pressure, and the overall structure would thus resemble a red giant star (in such a case our binary system would appear as if composed of two red giants in mutual orbit, no emission line would be seen, and the object would not be classified as a SySt).

The stable nuclear burning at the surface of the WD has one very important implication for SySts. Contrary to novae, where the nuclear burning is a highly explosive process that ejects into space essentially all the accreted material, the non-explosive burning occurring in SySts (both during quiescence and outbursts) allows the WD to retain the accreted matter, and stably grow in mass. If the companion LTG has enough material to transer, the WD can grow in mass until the Chandrasekhar limit of 1.4 $M_{\odot}$ is reached, at which point the WD could explode as a type Ia supernova (Munari and Renzini 1992). The exact nature of the precursors of SN Ia is still a matter of debate, but there is wide consensus that SySts are promising candidates.

There are two additional very important components in a typical SySt: circumstellar gas and dust. A SySt is embedded in a great amount of circumstellar gas (hereafter CG), created mostly by the wind blowing off the LTG, and which is ionized by hard radiation from the WD. The ionized fraction of the CG extends up to 100 astronomical units from the central binary, and it gives rise to two spectacular phenomena (compare the spectrum of the prototype SySt Z And in Figure 1): (i) very bright emission lines (in particular Hα) adorning the spectrum at all wavelengths and tracing conditions of high ionization (Allen 1984 classification criterion dictates the presence of emission lines from HeII or higher ionization species like [Fe VII] or [NeV]), and (ii) a bright blue continuum that, over *U* and *B* bands, is much brighter than the LTG, frequently pushing the *U–B* colors of SySts to largely negative values. If the number of energetic photons emitted by the WD goes up, also the amount and the brightness of the ionized circumstellar gas increases, and the reverse holds true. Thus the CG acts like a calorimeter, reverberating for us at optical wavelengths what the embedded WD does in far ultraviolet and X rays. Photo-ionization modeling of the observed flux of emission lines (corrected for reddening) can accurately fix the luminosity and temperature of the WD without the need for observations by orbiting satellites in the far ultraviolet and X-rays.

Circumstellar dust is almost always present when the LTG is a Mira variable. The dust is concentrated around the LTG and can be so thick as to cause spectacular extinction: in He 1-36 Allen (1983) estimates that the circumstellar dust dims the LTG by 20 magnitudes in the *V* band while the external ionized

gas is left unaffected. Sometimes the SySts harbouring a Mira variable undergo periods of what seems to be protracted dust extinction. It is believed that this is caused by the dust being concentrated in a shadow cone produced by the LTG itself, where the dust is shielded from the disruptive ionizing radiation of the WD. Periodically, along the orbital motion, the SySt is seen through such dust cone and an attenuation results.

SySts belong mostly to the Old Bulge/Thick Disk stellar population of the Galaxy and as such they appear concentrated toward the plane of the Galaxy and in particular its central regions. We know about 300 SySts, and the total population in the Galaxy is estimated to range from 30,000 (Kenyon *et al.* 1993) to 300,000 (Munari and Renzini 1992). Symbiotic stars have been discovered also in external galaxies, including the Magellanic Clouds, M31, M33, IC 10, NGC6822, and the Draco dwarf galaxy. Most of the known SySts have been discovered as emission-line objects during objective prism surveys of the Milky Way, and many were originally classified as compact planetary nebulae (PNe); the true nature of some transition objects is still hotly debated (for example, V471 Per = VV-8). Additional SySts lie probably still unrecognized among poorly studied PNe. There is a natural and smooth overlap between PNe with binary nuclei and SySts, the main difference being: in PNe the ionized gas has been ejected by the progenitor of the current WD nucleus, while in SySts the gas is blown off the LTG companion and that ejected by the WD progenitor has already long gone.

3. Various types of variability seen in symbiotic stars

In describing the major types of variability displayed by SySts we will refer to observations carried out in the Johnson *UBV*-Cousins R_C I_C bands. Similar considerations hold true for the corresponding bands of the Sloan u'g'r'i'z' system. The main types of variability seen in SySts are:

- *ellipsoidal*, when the cool giant fills its Roche lobe. Due to orbital motion, the area of the Roche lobe projected onto the sky varies continuously, with two maxima (when the binary system is seen at quadrature) and two minima (when the cool giant passes at superior or inferior conjunctions) per orbital cycle. Popular examples of SySts showing ellipsoidal distortion of their light-curve are T CrB (orbital period 227 days, amplitude $\Delta m = 0.3$ magnitude) and BD–21.3873 (orbital period 285 days, amplitude $\Delta m = 0.2$ magnitude). The ellipsoidally modulated I_C-band light curve of LT Del is illustrated in Figure 2;

- *heating-reflection effect*, caused by the hard radiation field of the hot and luminous WD (radiating mainly in the X-ray and far ultraviolet domains) that illuminates and heats up the facing side of the LTG (which thus reprocesses to the optical domain the energy received in the X-ray and far ultraviolet

from the WD). The heated side of the LTG is therefore brighter and hotter (bluer) than the opposite side (which is not illuminated by the WD radiation field). During an orbital period, the heated side comes and goes from view, causing a sinusoid-like light-curve characterized by a single sharp minimum and a broader, single maximum (compare the *B*-band light-curve of LT Del in Figure 2). The effect is strongly wavelength-dependent, being maximum in the *U* band and declining in amplitude toward the I_C band where it is usually undetectable. It is also stronger in systems seen equator-on, and vanishes for those seen pole-on. The amplitude may be fairly large, as in LT Del where its accounts for $\Delta B = 0.7$ (compare Figure 2) and $\Delta U = 1.6$, $\Delta V = 0.2$ (Arkhipova and Noskova 1988). The heating-reflection effect is the principal tool to derive orbital periods of SySts (Mikolajewska 2003);

• *pulsation*, like that of a Mira variable (about 20% of the known SySts harbor a Mira). Popular examples are R Aqr (pulsation period of 386 days, minima as faint as $V = 12$, maxima as bright as $V = 5$ magnitudes) or UV Aur (pulsation period of 395 days, minima as faint as $V = 11$, maxima as bright as $V = 7.5$ magnitude);

• *rotational*, of both the LTG and the WD. The rotation period of the LTG is of the same order as of the orbital one, thus measured in years. The rotation period of the WD is instead measured in hours, and its photometric amplitude is always pretty small;

• *eclipses of the WD* (and/or the ionized gas around it) by the LTG. Sometimes the eclipses escape detection by optical photometry during quiescence because the WD is small in radius and radiates mostly in the X-rays and far ultraviolet. During the outbursts the white dwarf emission shifts to longer wavelengths and becomes conspicuous in the optical, thus allowing the eclipses to be detected if the orbital inclination is sufficiently large. Classical examples of SySts for which the eclipses passed undetected in quiescence and instead became outstanding features of the outburst light-curve are FG Ser and V1413 Aql. Because the eclipsing body is cool and the eclipsed one is hot, the visibility of eclipses increases toward shorter wavelengths (for example for FG Ser in outburst it was $\Delta V = 1.4$, $\Delta B = 1.9$, and $\Delta U = 2.3$ magnitudes);

• *re-processing* by the CG of the energy radiated by the WD. The amount of ionized CG (and therefore its luminosity) is directly related to the amount of energy radiated by the WD and its *quality*, that is, the fraction of radiated photons which are energetic enough to ionize hydrogen and thus make it shine. A change in the WD radiation output would reflect in a different amount of ionized CG, and therefore in a variation of its brightness, especially in *U* and *B* bands;

• *outbursts*. There are three basic types of outburst displayed by SySts: (1) Type A—the one most frequently seen in SySts, presents amplitudes of ΔB = 2–5 magnitudes (invariably declining toward red wavelengths) and durations of a few years, usually with many different maxima and minima during a single outburst episode. After such a train of multiple maxima, the SySt returns to flat quiescence conditions where it stays for a period of time usually much longer than spent in outburst. Light curves typical of such type of outburst are shown in Figure 3. Their cause is probably an increase in the mass transfer from the LTG to the WD. While the nuclear burning at the surface of the WD continues, the extra transferred material causes the WD to react by expanding its outer envelope. This expansion occurs at roughly constant luminosity and therefore causes a drop in the surface temperature (following the black body law $L = 4\pi R^2 \sigma T^4$), from ≥80,000 K to ~12,000–7,000 K. The peak of the WD radiation field shifts from the X-rays to the optical, where the SySt appears much brighter, in "outburst." The much cooler radiation field from the WD is thus lacking energetic photons, and the high ionization emission lines quickly disappear from SySts undergoing this type of outburst; (2) Type B—outbursts lasting for about a century, like the example of BF Cyg shown in Figure 4 or other well known cases, like V1016 Cyg, HM Sge, and AG Peg. All of them are characterized by a rapid rise to maximum (a couple of years at most), and then a slow, century-long decline with superimposed a lot of other smaller amplitude activity; (3) Type C—we could call them "a nova within a symbiotic binary." Outstanding examples are RS Oph, T CrB, and V407 Cyg, all being celebrated recurrent novae, characterized by very rapid evolutions (from a few weeks to a few months). The WDs of these systems are quite massive, close to the Chandrasekhar limit, and undergo eruptions like those of normal novae every few decades. The light curve of the 2010 such eruption of V407 Cyg is shown in Figure 5, and the spectacular evolution of Hα is presented in Figure 6 (which is within the observational possibilities of 0.7-m AA telescopes equipped with high resolution spectrographs). In quiescence, the slowly expanding LTG wind is ionized only in the immediate vicinity of the WD (sharp and weak Hα). When the WD undergoes a true nova eruption, the initial intense flash of hard radiation ionizes a vast fraction of the LTG wind still slowly expanding (sharp component in the March 15, 2010, Hα profile). The suddenly ionized LTG wind soon starts to recombine to neutral conditions, which it completes in less than a week, while the fast nova ejecta began to expand around the WD (broad component in the March 15, 2010, Hα profile). As the fast nova ejecta attempt to continue their expansion within the pre-existing dense and slow wind blown off the LTG, they are progressively slowed down (resulting in the narrowing of the Hα profile for April 7, 2010, spectrum in Figure 6). After some months, the nova ejecta have been almost entirely stopped by the pre-existing slow

wind. The low electronic density characterizing the cavity the nova ejecta have swept within the LTG wind allows feeble emission from forbidden lines to appear (see the [NII] emission lines at 6548 and 6584 Å flanking Hα in the profile for September 22, 2010, in Figure 6).

References

Allen, D. A. 1983, *Mon. Not. Roy. Astron. Soc.,* **204**, 113.
Allen, D. A. 1984, *Proc. Astron. Soc. Australia,* **5**, 369.
Arkhipova, V. P., and Noskova, R. I. 1988, *Sov. Astron. Lett.,* **14**, 188.
Henden, A., and Munari, U. 2000, *Astron. Astrophys., Suppl. Ser.,* **143**, 343.
Henden, A., and Munari, U. 2001, *Astron. Astrophys.,* **372**, 145.
Henden, A., and Munari, U. 2006, *Astron. Astrophys.,* **458**, 339.
Kenyon, S. J., Livio, M., Mikolajewska, J., and Tout, C. A. 1993, *Astrophys. J., Lett. Ed.,* **407**, L81.
Leibowitz, E. M., and Formiggini, L. 2006, *Mon. Not. Roy. Astron. Soc.,* **366**, 675.
Mikolajewska, J. 2003, in *Symbiotic Stars Probing Stellar Evolution*, ed. R. L. M. Corradi, R. Mikolajewska, T. J. Mahoney, ASP Conf. Ser., 303, Astron. Soc. Pacific, San Francisco, 9.
Munari, U., and Buson, L. M. 1994, *Astron. Astrophys.,* **287**, 87.
Munari, U., and Renzini, A. 1992, *Astrophys. J., Lett. Ed.,* **397**, L87.
Munari, U., *et al.* 2011, *Mon. Not. Roy. Astron. Soc.,* **410**, L52.
Skopal, A. 2011, in *Evolution of Compact Binaries*, ASP Conf. Ser., 447, Astron. Soc. Pacific, San Francisco, 233.
Sokoloski, J. L. 2003, in *Symbiotic Stars Probing Stellar Evolution*, ed. R. L. M. Corradi, R. Mikolajewska, T. J. Mahoney, ASP Conf. Ser., 303, Astron. Soc. Pacific, San Francisco, 202.

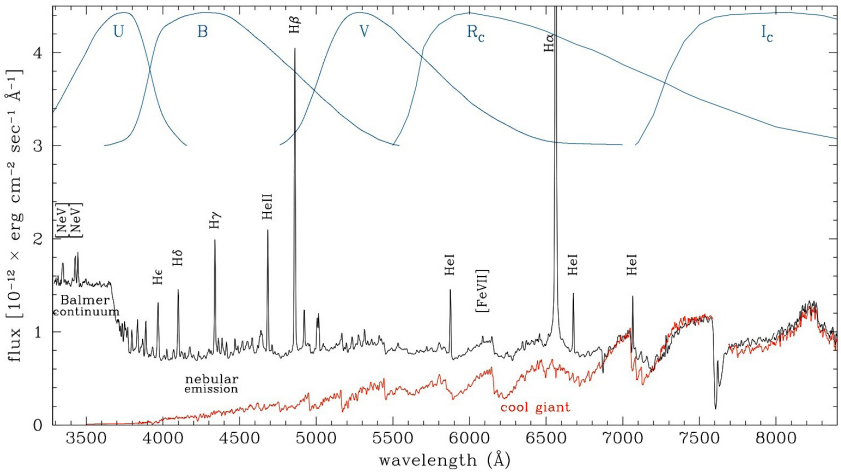

Figure 1. Optical spectrum of Z And in quiescence (Dec. 22, 2011, Asiago 1.22m telescope), with major emission lines identified. The contribution by the cool giant is highlighted, and the transmission profiles of Johnson UBV and Cousins R_C I_C bands are overplotted. The Hα line is truncated to enhance visibility of the rest.

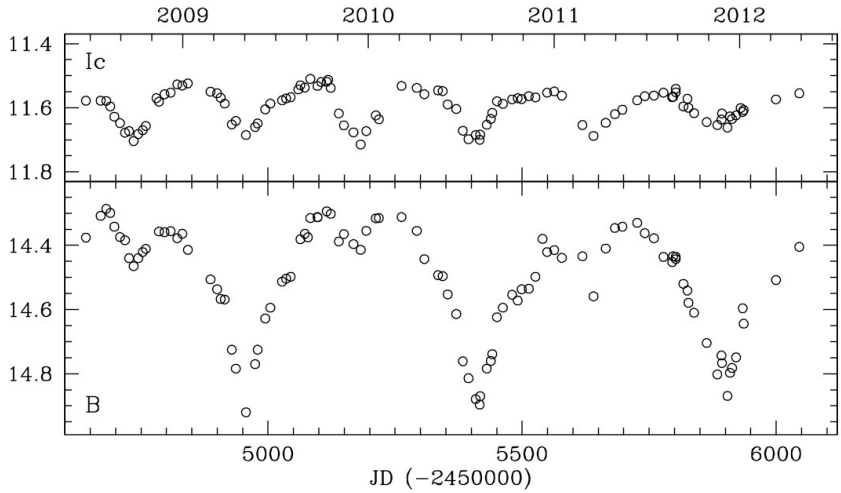

Figure 2. Recent light curve of the symbiotic star LT Del in quiescence (ANS Collaboration observations). The B-band lightcurve at the bottom is dominated by the heating-reflection effect, with one deep minimum per orbital period (when cool giant passes at inferior conjunction). The I_C-band light curve at the top is modulated by the ellipsoidal distortion of the cool giant filling its Roche lobe (two equal maxima and two equal minima per orbital period).

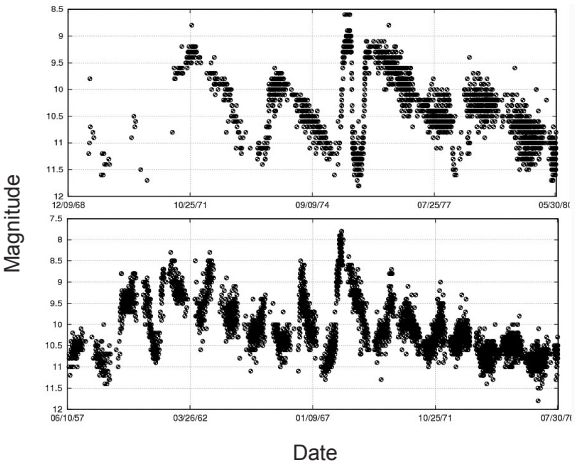

Figure 3. AAVSO light curves for the 1970–1978 outburst of CI Cyg (top) and 1957–1973 outburst of Z And (bottom). They are classical examples of type A outbursts of SySts, characterized by a train of multiple maxima before the system returns to quiescence and where it will remain for a period of time usually much longer than spent in outburst.

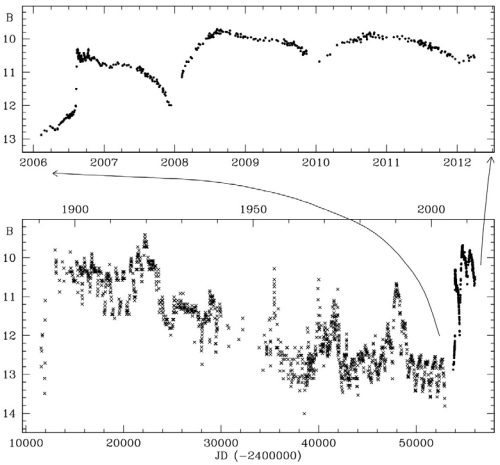

Figure 4. The historical B-band light curve of the symbiotic star BF Cyg. The object entered a major outburst around 1894, and took the whole of the 20th century to decline back to quiescence conditions, while displaying a lot of superimposed activity (including eclipses of the outbursting WD by the cool giant). In 2006, BF Cyg entered a new major outburst; whether it will last long as the previous one is a matter of speculation (crosses from Leibowitz and Formiggini 2006; dots from ANS Collaboration observations).

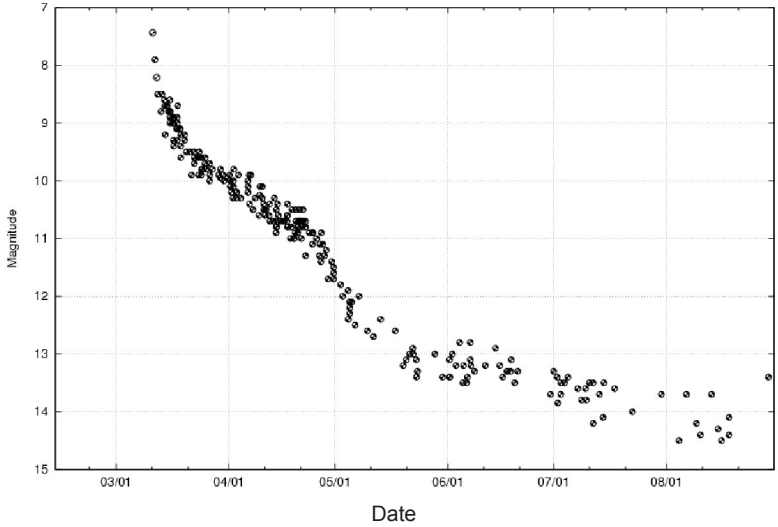

Figure 5. AAVSO light curve of the outburst of V407 Cyg during the spring-summer of 2010.

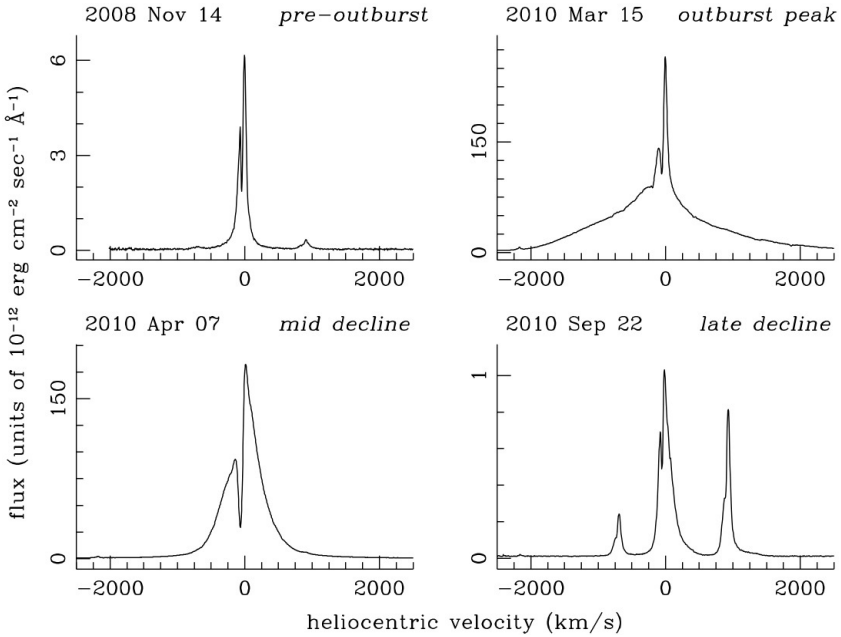

Figure 6. Evolution of the Hα emission line profile of V407 Cyg during the 2010 outburst. Note the ordinate scale which is different in each panel (adapted from Munari *et al.* 2011).

Classical and Recurrent Novae

Ulisse Munari
National Institute of Astrophysics (INAF), Astronomical Observatory of Padova, 36012 Asiago (VI), Italy; ulisse.munari@oapd.inaf.it

Invited review paper, received June 12, 2012

Abstract The physical nature and principal observational properties of novae are reviewed. Suggested improvments to optical photometry and discovery strategies are discussed. Nova eruptions occur in close binary systems, in which a white dwarf (WD) steadily accretes material on its surface from a lower mass cool companion. The accreted envelope is in electron degenerate conditions and grows steadily in mass with time, until a critical amount is accreted (which is inversely related to the WD mass). At that point, a fast evolving thermo-nuclear runaway starts burning hydrogen, in a short flash lasting about a hundred seconds, which is terminated by the violent ejection into the surrounding space (at a speed in excess of the escape velocity) of the whole accreted envelope (or a sizeable fraction of it). The nova is discovered only when, several hours or a few days later, the expansion and cooling of the fireball ejecta make them emit profusely at optical wavelengths; the later decline in brightness is regulated by interplay between dilution of the ejecta into surrounding space, gas and dust opacities, and temperature/luminosity of the central WD when the ejecta eventually become optically thin. The time interval between consecutive outbursts from the same nova is usually (far) longer than recorded history, but for a small number of objects (named recurrent novae) it is short enough that more than one outburst has been observed for them.

1. Introduction

For centuries, the term *nova* simply meant the unexpected appearance of a *new star* in the sky, fixed with respect to the other stars (to distinguish it from planets and comets), that after some time usually vanished from view. Now we know that quite different types of object can emerge from obscurity, sometimes briefly, as the result of completely different physical processes, like supernovae of various types, pre-main-sequence young objects of the FU Ori variety, very evolved objects undergoing late thermal pulses as displayed by V4334 Sgr (Sakurai's Object), cataclysmic variables in outburst, enigmatic events like V838 Mon (widely celebrated for its light-echo), and obviously the classical novae.

From an observational point of view, a *classical nova* (hereafter *nova* for short) is a stellar outburst characterized by a rapid rise toward maximum brightness (a matter of hours or days), a large amplitude in the optical ($8 \leq \Delta \text{mag} \leq 16$), mass

ejected at high velocity (from a few hundreds to a few thousands km sec^{-1}, as indicated by the very wide emission lines and/or largely blue-shifted absorption components in P Cyg profiles), post-maximum optical spectra evolving toward increasing excitation and ionization, and nebular conditions usually prevailing during advanced decline (that is, forbidden emission lines dominating the spectra). For the vast majority of novae, only one outburst has been observed in historical times. However, a few novae (like the celebrated U Sco, RS Oph, or T CrB) have undergone more than one outburst. They are called *recurrent novae*. It is believed that, should the monitoring time extend for hundreds or thousands of years, all novae would be seen to erupt again (and again). About 500 galactic novae are known. Duerbeck (1987) presented an accurately researched catalog and atlas of essentially all novae that erupted before 1986, which also included finding charts especially useful for old objects, long returned to quiescence conditions. Accurate coordinates, basic information, and finding charts for more recent novae were provided by Downes and Shara (1993) and Downes *et al.* (1997, 2001, 2005).

2. A model nova

Cataclysmic variables (CVs) and novae are believed to be the same binary systems, in which a low mass cool companion transfers material via Roche lobe overflow to a more massive white dwarf (WD). The orbital periods are a few hours long, and the orbital separations are on the order of the Sun's radius. During the hundreds or thousands of years spent away from nova outbursts, the material lost by the companion goes to form an accretion disk before terminating its journey by piling up on the surface of the WD (if the WD is strongly magnetized, the formation of an accretion disk is prevented and the material flows onto the WD via the magnetic poles). The accretion disk is prone to instabilities that cause regular, low amplitude bright phases termed CV-type outbursts (unfortunately, they are also called *dwarf* nova outbursts, a confusing terminology and another example of the irresistible attraction of astronomers for inapt terminology when better alternatives would be at hand). SS Cyg is a famous CV, whose accretion disk every two months goes through a CV-type outburst that brightens the system from $V=12$ to $V=8$. This cycle has continued uninterrupted since when SS Cyg was discovered in the late nineteenth century; (a wonderful AAVSO historical light curve covering about 110 years of observations and every outburst since discovery has been presented by Cannizzo and Mattei 1998).

The envelope accreted on the surface of the WD is in *electron degenerate* conditions, an unusual state of matter characterized by the fact that the pressure is not related to the temperature. In normal experience, you heat up something and it reacts by expanding: to lift a balloon, you raise the temperature of the air it contains and the resulting increase in pressure swells the balloon, which

begins to ascend following Archimedes's principle (the density of the hot air in the balloon is lower than that of the cooler outside air). We write this by saying that its *equation of state* is $P \propto \rho T$, that is, the pressure is proportional to density times temperature. For electron degenerate material the equation of state modifies to $P \propto \rho^{\alpha}$, that is, there is no more dependence on temperature. Let's turn back to our nova in the making. With passing time, the envelope of material accreted on the surface of the WD steadly grows in mass until a critical value is reached (which is inversely related to the WD mass). When this occurs, the hydrogen present in the envelope starts to be burned via the CNO cycle, whose energy production rate (ε_N) is extremely sensitive to temperature: $\varepsilon_N \propto T^{18}$. The energy released by the nuclear burning heats up the envelope which however cannot react by expanding (its pressure is independent of temperature), and in turn the rise in temperature increases the nuclear energy production rate, that is, a circular argument. The temperature in the envelope rises exponentially out of control; (the envelope is experiencing a *thermo-nuclear runaway* or TNR). In a matter of few tens of seconds, it reaches the *Fermi temperature* (of the order of 350 million Kelvin) at which point the electron degeneracy is suddenly removed and the equation of state instantaneously reverts to that of ordinary gas ($P \propto \rho T$): the envelope can now react to its extremely high temperature by expanding. The expansion is so violent that the envelope is actually ejected into the surrounding space at a speed exceeding the escape velocity, and it will never return. The resulting drop in temperature first slows down and then effectively stops the TNR. A few minutes were enough to ignite the TNR, let it develop, and stop it. At this stage the nova has not been discovered yet: it will become visible only hours/days later when the fireball of the expanding ejecta has grown in size enough and its surface temperature as declined to about 10,000 K to shift the peak of radiated energy from the initial γ- and X-rays to the optical range.

When SS Cyg undergoes such a TNR and the consequent resulting nova outburst (maybe tomorrow, maybe a thousand years from now), it will rise in brightness so much that it will probably become, for days/weeks, the brightest star of the whole sky, rivalling or surpassing Vega and Sirius. But do not worry: a few months later SS Cyg will be back to quiescence and in a few decades more, it will resume its CV-type, ~60-day cycle outbursts, for the fun of future enthusiastic observers!

3. Some statistics on novae

3.1. Where they appear

Novae do not appear randomly on the sky, but they concentrate along the Milky Way and in particular in its central regions. There are eighty-eight constellations on the sky, but no nova has ever been observed in over twenty-two of them, most notably Hydra, Ursa Major, Pegasus, and Draco that together cover an area of 4,800 square degrees, or about 12% of the whole

sky (the statistics in this review are based exclusively on official International Astronomical Union (IAU) data, in particular *IAU Circulars* and *CBET*s). A list of the constellations arranged according to the number of novae they produced is given in Table 1. Sagittarius, with its 114 novae, leads the group.

Sagittarius is however favored by being a large constellation (867 square degrees). To assess the productivity of the various constellations, it is better to refer to the number of novae which appeared there, per unit area, essentially dividing the data in Table 1 by the constellation area. The results are given in Table 2, expressed as the number of novae appearing in the given constellation over an area of 100 square degrees. The small Scutum (covering just 109 square degrees on the sky; only Circinus, Sagitta, Equuleus, and Crux being smaller) now stands out as where the concentration of novae is the highest (therefore, Scutum would be a good target to image if your are considering starting to look for novae yourself !).

3.2. How bright they are

The distribution of novae in terms of magnitude at maximum and of outburst amplitude (that is, the difference in magnitude between quiescence and outburst maximum) is presented in Figure 1 (panels a and d). The data are rather heterogeneous (coming from old blue-sensitive photographic plates, visual estimates, unfiltered CCDs, properly calibrated BVRI observations, and so on; when the information is available, they refer to the actual maximum brightness, but sometimes only the brightness at the time of discovery is known).

The distibution of magnitude at maximum looks like a Gaussian distribution peaking around magnitude = 8.7. Such a distribution suggests that most of the novae peaking to magnitude 8 or brighter have indeed been discovered. Conversely, the majority of those reaching only magnitude 11 or 12 pass unnoticed. However, the number of Galactic novae does not increase indefinitely toward fainter magnitudes (contrary to the case of supernovae, where fainter magnitudes means larger volumes of space and greater numbers of host galaxies): the size of our Galaxy is limited and the novae are intrinsically very bright objects. Let's take for example Figure 2, which summarizes the distribution in magnitude of the ninety-five novae discovered in the Andromeda galaxy (M31) over the five-year interval 2007–2011 (an average of ~20 novae per year): the distribution peaks between 17.0 and 17.5 in R_C, corresponding to a peak $M(R_c)=-7.3$ magnitude in the absolute magnitude distribution. The discovery of real faint novae in the central bulge region of M31 is no doubt adversely biased; nonetheless the peak of the distribution in Figure 2 seems well established observationally. A $M(R_c)=-7.3$ magnitude Galactic nova would appear to us shining at

$$R_c = M(R_c) + 5 \log d - 5 + A_R = -12.3 + 5 \log d + A_R \qquad (1)$$

where d is the distance expressed in parcsecs and A_R is the amount of interstellar extinction in the R_C band (which relates to E_{B-V} reddening as $A_R = 2.6 \times E_{B-V}$). At a distance of 3 kpc and an extinction $A_R = 1.6$ magnitude, our $M(R_c) = -7.3$ nova would shine at a comfortably $R_c = 6.7$ magnitude. Even pushing it to the center or our Galaxy ($d = 8.5$ kpc, $A_R \approx 5$ mag.), it would still score $R_c \approx 12.3$, well within the observing capability of amateur telescopes (provided their focal length is long enough to discern the nova among the myriads of similarly bright stars crowding the views of telescopes aimed at the center of the Galaxy).

The average magnitude of discovered novae has not significantly changed over the last eighty years, since photographic emulsions substituted for the eye as detector in patrol searches (Figure 1c). What has been continously improving is instead the frequency of nova discoveries, as illustrated in Figure 1b. From about 2.5 novae per year on average at the beginning of the twentieth century, it rose to about 4 during 1980–1990. The surge to about 8 novae per year over the last 5 to 10 years is undoubtedly connected to the widespreading use of sensitive CCDs as detectors and electronic blinking of images. Figure 1b suggests we are currently on a steep rise, and the number of novae discovered per year should appreciably increase during the next 5 to 10 years.

3.3. Who discovers them

Table 3 lists the most prolific nova discoverers, nearly all of them amateur astronomers, a group of highly motivated and dedicated people led by William Liller, who works from Viña del Mar, in Chile. He has for a long time recorded sky images with a 35-mm camera, an 85-mm lens, Kodak Technical Pan 2415 film, and an orange filter, and then made use of a homemade, 25-power stereo viewer. One eye looks at the new sky photograph, while the other at an archival image. If a candidate nova appears in one image but not the other, that prompts further investigation and confirming observations. Such an eye inspection is equivalent to blinking on a computer monitor electronic images taken with CCDs. Their dropping costs, the ever-increasing area of their detectors, and the real-time inspection of their images allowed by electronic blinking (either via automated software or eye inspection on a computer monitor), are making DSLR cameras the primary tool for current nova hunters. The discovery of novae will presumably remain, for a long time, a business reserved for amateurs: professional telescopes are too inefficient to cover large areas of the sky at bright limiting magnitudes night after night.

4. The light curve

A schematic light curve for a nova is shown and described in Figure 3. With the increasing number and quality of photometric observations, the great diversity among the observed light curves is increasingly evident, to the point that speaking of a *typical* light curve for novae is losing its meaning. Many

examples of light curves of novae have been presented, among others, by Payne-Gaposchkin (1957), Kiyota *et al.* (2004), and Strope *et al.* (2010), the latter offering also a new morphological classification scheme.

After the initial rapid rise (a matter of just a few hours in very fast novae like U Sco), the nova goes through a maximum optical brightness phase that can be anything from an immediate rebound toward decline, to a smooth and well-behaved round phase, or a series of erratic ups-and-downs on top of a flat plateau, or a second and equally well-behaved maximum, and so on. A non-exhaustive compilation of observed behaviors at maximum brightness is shown in Figure 4. Then, past maximum phase, the decline toward quiescence sets in, and it is usually characterized by two phases: a faster one, when the ejecta are still optically thick (the central source cannot be seen from outside) and that lasts until the nova has declined by 3–4 magnitudes from maximum, and then a slower one, when the ejecta become optically thin (the whole body of them becomes directly exposed to the hard ionizing radiation emanating from the central star, and the latter is visible from outside the ejecta).

The time when the transition from optically thick to optically thin conditions occur in the ejecta also marks in some novae the onset of transient events perturbating an otherwise smooth decline, either dust formation or (semi-periodic) oscillations. Dust grains can form in the ejecta, and the resulting dust obscuration can dim by several magnitudes the brightness of the nova. After a maximum is reached, the obscuration by dust progressively reduces and, after a while, the nova resumes the decline path it would have followed in the absence of dust formation. The dilution of the dust grains caused by the ongoing expansion of the ejecta is the main reason for the end of the obscuration phase. The radiation absorbed in the optical heats up the dust grains which re-emit it at longer wavelengths, and the nova appears several magnitudes brighter at infrared wavelengths (thus, during the dust phase, the infrared light curve is a mirror image of the optical light curve). With the transition from optically thick to optically thin conditions in the ejecta, oscillations of various types may be seen in several novae. They can be either of the type making the nova look temporarily fainter (like for instance V2467 Cyg / N Cyg 2007) or brighter (as in V2468 Cyg / N Cyg 2008 No. 1). These oscillations can either appear irregular in both phase and amplitude, or follow a regular, sinusoidal-like pattern. One of the novae showing the most spectacular set of oscillations was GK Per (N Per 1901). They started when the nova was 3.5 magnitude down from maximum brightness, and lasted several months; at least 20 oscillation cycles were counted, with peak-to-valley amplitudes ranging from 1.0 to 1.5 magnitudes. A generally agreed physical explanation for the oscillations does not yet exist, though various models have been suggested.

5. The spectrum

The spectra of novae, right at maximum brightness, are dominated by an

underlying hot continuum with only relatively weak emission lines, sometimes only Hα being visible in emission. All absorption lines show large negative radial velocities, indicating that they are forming in a rapidly expanding medium. As soon as the nova begins to decline, the emission lines rapidly get progressively stronger than the continuum. This is the combined effect of the underlying continuum declining in intensity while, for some time, the emission lines increase in their absolute flux. After the transition from optically thick to optically thin ejecta has been completed, the underlying continuum essentially vanishes, and nearly all the flux recorded from the nova comes from emission lines only.

The spectrum of a nova around maximum and early decline can be either of the *FeII* or the *He/N* type, and an example of them is shown in Figure 5 (note that the ordinate scales are in logarithm of the flux to enhance visibility of the weak features). A FeII-type nova displays, in addition to hydrogen Balmer emission lines, many permitted emission lines from FeII, especially from multiplets 27, 28, 37, 38, 42, 48, 49, 73, 74. Conversely, a He/N-type nova, in addition to Balmer lines, will display emission lines from helium and nitrogen but not from FeII.

The early classification of a nova spectrum is important because it will set the stage for what to expect next in its evolution. In comparison with FeII-type, He/N novae usually decline faster, show larger expansion velocities (that is, broader emission lines), and eject a lower amount of mass. While FeII novae appear to belong to an older stellar population, heavily concentrated toward the bulge of the Galaxy, He/N novae show a lower concentration toward the center of the Galaxy and are instead more concentrated along the disk of the Galaxy, suggesting a younger parental stellar population and more massive WDs. All FeII novae display a nebular spectrum during their advanced decline, while a few He/N novae sometimes do not. An example of a nebular spectrum is shown in Figure 6 (note how the flux of the continuum in between the emission lines is almost null). Conversely, only He/N may display coronal emission lines (lines of extremely high ionization such as [FeX] 6375, [FeXI] 3987, 7892, [FeXIV] 5303, [NiXIII] 5114, [NiXV] 6702, [ArX] 5532, [ArXI] 6915, all seen during the 2006 outburst of RS Oph).

Amateur spectroscopic observations can provide both a confirmation and a classification (FeII or He/N types) of candidate novae, and then follow their early post-maximum evolution. A 60-cm telescope equipped with a spectrograph working at dispersions from 2 to 4 Ångstroms/pixel can do that for novae brighter than V = 11. The exceptional intensity of the Hα emission line in nearly all novae allows one to follow the evolution of its profile (frequently multi-peaked and with P Cyg absorption components varying with time) for a long time into the decline. A spectrograph working at 1 Ångstrom/pixel on a 60-cm telescope can easily observe and resolve the Hα profile for novae down to $V = 12$ magnitude.

6. Hints about observing novae

Amateur astronomers are already providing fundamental photometric data on novae. However, significant improvements, easy to implement, are still possible, and some of them are suggested in this concluding section.

6.1. Discovery

Most amateurs carry out their patrols for novae and discover them on unfiltered CCD images. It would be advisable to carry out the search with well-known photometric filters instead. The on-line AAVSO Photometric All-Sky Survey (APASS) provides suitable Jonhson *BV* and Sloan *g′r′i′* comparison stars down to 16th magnitude anywhere on the sky. Cousins' R_c, I_c magnitudes can be easily obtained from the following relations calibrated on APASS data:

$$\begin{aligned} R_c &= r' - 0.095 \times (g' - i') - 0.141 \\ I_c &= i' - 0.055 \times (g' - i') - 0.364 \\ (R-I)_C &= 0.894 \times (r' - i') + 0.212 \end{aligned} \quad (2)$$

for APASS fields south of the equator, while for APASS fields north of the equator they are:

$$\begin{aligned} R_c &= r' - 0.065 \times (g' - i') - 0.174 \\ I_c &= i' - 0.044 \times (g' - i') - 0.365 \\ (R-I)_C &= 0.918 \times (r' - i') + 0.198 \end{aligned} \quad (3)$$

There is very little to lose if the observations are carried out, for example, in the standard R_c Cousins or Sloan *r′* bands: the sensitivity of most CCDs peaks there; they include the emission of the strong Hα line; and the background sky brightness is lower there than at bluer wavelengths. The discovery images will be the only ones covering that part of the light curve, that is, the critical phases preceding or around optical maximum, but if they were not obtained in a proper photometric system it will be very difficult to extract solid physical information from them. Frequently, the un-filtered photometry is unavoidably ignored in subsequent analysis and modeling.

6.2. Maximum brightness

It happens too frequently that a nova is rapidly forgotten after the initial discovery. While the discovery is surely personally rewarding and an important contribution to the field, accurate photometric monitoring (especially in the *B* and *V* bands) of the nova while it is passing through maximum brightness, is vital to fix fundamental quantities like the exact time of maximum, its brightness and its color. From the *B–V* color the reddening and extinction will easily follow. The *B* and *V* magnitudes exactly 15 days past maximum constrain

the distance to the nova. Knowing the exact *B* and *V* magnitudes at maximum brightness will allow one to define the fundamental quantities t_2 and t_3 in both bands (that is, the time required for the nova to decline by 2 and 3 magnitudes, respectively). From t_2 and t_3 the distance to the nova can be derived, and many other parameters (like the mass of the ejecta, the mass of the WD, or when the optically thin phase will begin) can be constrained. In most cases, by the time professionals can access a telescope and turn it to a recently discovered nova, it will be already past maximum, and a fundamental piece of information would be lost if not provided by amateurs.

In addition, the time of maximum brightness is a period of unexpected behavior by many novae. Some examples are illustrated in Figure 4. So far, very few novae have been accurately and multi-band monitored through their maxima. Consequently, this phase is still so poorly documented that many theoretical models do not treat it in a way able to account for the observed peculiarities. Providing accurate multi-band monitoring of maximum brightness for a greater number of novae could allow one to search for correlations between behavior at maximum and other parameters of the nova light curve or spectral properties. This in turn would both motivate and constrain theoretical efforts attempting to model peculiar maxima.

6.3. Novae in the center of the Galaxy

Compared to the novae normally discovered by amateurs, those erupting close to the center of the Galaxy will appear fainter (because of the greater distance and larger intervening extinction) and will be harder to spot against their higher stellar density backgrounds. The extremely high stellar densities at the core of the Galaxy suggests that many novae that erupt there go undiscovered every year.

The reason they escape detection lies probably in the use of DSLR cameras for nova patrol. While entirely appropriate to search for novae elsewhere on the sky, their limiting magnitude is too bright and their focal length too short to be able to detect most of the novae erupting in the central regions of our Galaxy.

To discover them, a longer local length and a larger lens than in DSLR cameras seems appropriate. The area to patrol is limited (of the order of 12×12 degrees) and a longer focal length could cover it with a limited number of overlapping images, providing a sufficient spatial resolution to isolate a $V = 12$ magnitude nova from the dense surrounding stellar background. The dividends paid by such a program focused just on novae at the heart of our Galaxy could be high.

6.4. The interesting case of V2672 Oph (Nova Oph 2009)

Nova Oph 2009 (V2672 Oph) reached maximum brightness at $V = 11.35$ on 2009 August 16.5 UT. With observed $t_2(V) = 2.3$- and $t_3(V) = 4.2$-day decline

times, it is one of the *fastest* known novae, being rivalled only by V1500 Cyg (Nova Cyg 1975) and V838 Her (Nova Her 1991) among classical novae, and U Sco among the recurrent ones. The line of sight to the nova passes within a few degrees of the Galactic Center, crosses the whole bulge, and ends at a galacto-centric distance larger than that of the Sun. This is probably a record distance and position among known Galactic novae. It is not incidental that, to discover it, K. Itagaki used an *f*/3 21-cm reflector, providing light gathering power and spatial resolution far in excess than a DSLR camera. On the basis of its many remarkable similarities to U Sco, it is highly probable that this nova is a recurrent one, possibly with a recurrence time as short as that of U Sco (Munari *et al.* 2011), and it should be inserted among the areas to be monitored regularly in the future.

The central region of the Galaxy has been imaged (on films and with CCDs) countless times, especially by amateurs looking for impressive pictures. It is quite possible that other outbursts of V2672 Oph lie unnoticed on such archival images, especially those imaging at red wavelengths. A devoted search is highly encouraged and I would be pleased to be informed (at the e-mail address given above) about the results. A list of negative results (reporting about date, UT, band, focal length, limiting magnitude of the image) would also be relevant to put constraints on the recurrence time scale. Figure 7 identifies the nova on a R_C image obtained close to maximum brightness, and provides magnitudes for reference stars.

6.5. Photometric monitoring

If observers provide only a few photometric points each, to cover the entire light curve of a nova it is necessary to combine data from many different observers. The dispersion of points in such a combined light curve is however so large (up to 1 magnitude) that all details are smeared out. The main reason is that during decline the flux from a nova is mainly concentrated in a few emission lines. Two nearly identical filters can produce drastically different data, if one includes in the transmission profile a strong emission line and the other not. This is what usually happen with the *V* filter, whose steep rising blue transmission edge coincides with the [OIII] 4959, 5007 doublet, usually the strongest emission line during the nebular phase. Figure 6 illustrates the situation.

It is advisable that once an observer begins to observe a nova (the earlier in its evolution the better), they should try to keep focused on it for the longest possible period of time. Their photometric equipment will remain the same through the observing campaign, and the collected data will be self-consistent: all the finer details of the light curve will be visible because it will not be necessary to combine with other external data.

To avoid the strongest emission lines and collect an important measurement of the true continuum underlying them, Stromgren *b* and *y* filters could be used in addition to standard Johnson *B* and *V* throughout the whole light curve. It

is true that being narrower they will collect less light and the exposure times will consequently be longer, but this will be counter-balanced by the increasing physical value of the measurements. The following relations

$$\begin{aligned} y &= V - 0.062 \times (B-V) + 0.027 \\ b &= B - 0.469 \times (B-V) + 0.060 \\ (b-y) &= 0.593 \times (B-V) + 0.033 \end{aligned} \quad (4)$$

provide an useful mean to estimate Stromgren *b* and *y* magnitudes of comparison stars from their APASS *B* and *V* values.

References

Cannizzo, J. K., and Mattei, J. A. 1998, *Astrophys. J.*, **505**, 344.

Downes, R. A., and Shara, M. M. 1993, *Publ. Astron. Soc. Pacific,* **105**, 127.

Downes, R. A., Webbink, R. F., and Shara, M. M. 1997, *Publ. Astron. Soc. Pacific,* **109**, 345.

Downes, R. A., Webbink, R. F., Shara, M. M., Ritter, H., Kolb, U., and Duerbeck, H. W. 2001, *Publ. Astron. Soc. Pacific,* **113**, 764.

Downes, R. A., Webbink, R. F., Shara, M. M., Ritter, H., Kolb, U., and Duerbeck, H. W. 2005, *J. Astron. Data*, **11**, 2.

Duerbeck, H. W. 1987, *A Reference Catalogue and Atlas of Galactic Novae*, Kluwer, Dordrecht.

Kiyota, S., Kato, T., and Yamaoka, H. 2004, *Publ. Astron. Soc. Japan*, **56**, S193.

Munari, U., Siviero, A., Navasardyan, H., and Dallaporta, S. 2006a, *Astron. Astrophys.*, **452**, 567.

Munari, U., Henden, A., Pojmański, G., Dallaporta, S., Siviero, A., and Navasardyan, H. 2006b, *Mon. Not. Roy. Astron. Soc.,* **369**, 1755.

Munari, U., Henden, A., Valentini, M., Siviero, A., Dallaporta, S., Ochner, P., and Tomasoni, S. 2008, *Mon. Not. Roy. Astron. Soc.,* **387**, 344.

Munari, U., Ribeiro, V. A. R. M., Bode, M. F., and Saguner, T. 2011, *Mon. Not. Roy. Astron. Soc.,* **410**, 525.

Munari, U., Henden, A., Valisa, P., Dallaporta, S., and Righetti, G. L. 2010, *Publ. Astron. Soc. Pacific,* **122**, 898.

Munari, U., and Moretti, S. 2012, *Baltic Astron.*, **21**, 22.

Payne-Gaposchkin, C. 1957, *The Galactic Novae*, North-Holland Publ. Co., Amsterdam.

Strope, R. J., Schaefer, B. E., and Henden, A. A. 2010, *Astron. J.*, **140**, 34.

Warner, B. 2008, in *Classical Novae*, 2nd ed., eds. M. F. Bode and A. Evans, Cambridge Astrophys. Ser. 43, Cambridge Univ. Press, Cambridge, 16.

Table 1. Number of novae that appeared in the listed constellations, updated to 2012. The constellations that never displayed a nova (such as Ursa Major) are not listed.

Sgr	114	Vul	10	Mus	5	Leo	3	Lup	2	Tau	1	Crv	1
Oph	45	Car	10	Vel	4	CrA	3	Lib	2	Pyx	1	CrB	1
Sco	43	Ser	8	TrA	4	Boo	3	Eri	2	Psc	1	Com	1
Aql	33	Nor	8	Sge	4	Aur	3	Cru	2	Pic	1	CMa	1
Cyg	22	Her	8	Mon	4	Ari	3	Ara	2	Lyr	1	Cha	1
Sct	18	Cir	7	Lac	4	And	3	Vir	1	LMi	1	Cet	1
Cen	14	Per	6	Cas	4	Tri	2	UMi	1	For	1	Cep	1
Pup	11	Gem	6	Ori	3	Pav	2	Tel	1	Del	1	Aqr	1

Table 2. Ranking of the constellations in Table 1 in terms of nova productivity per unit area on the sky (here expressed as the number of novae that appeared over an area of 100 square degrees).

Sct	16.50	Mus	3.61	Gem	1.17	CrB	0.56	Tel	0.40	Cep	0.17		
Sgr	13.14	Cru	2.92	Per	0.98	Crv	0.54	UMi	0.39	Tau	0.13		
Sco	8.66	Cyg	2.74	Ara	0.84	Pav	0.53	Lib	0.37	Psc	0.11		
Cir	7.50	CrA	2.35	Mon	0.83	Del	0.53	Lyr	0.35	Aqr	0.10		
Aql	5.06	Car	2.02	Vel	0.80	Ori	0.50	Boo	0.33	Vir	0.08		
Sge	5.00	Lac	1.99	Cha	0.76	Aur	0.46	Leo	0.32	Cet	0.08		
Nor	4.84	Pup	1.63	Ari	0.68	Pyx	0.45	Com	0.26				
Oph	4.75	Tri	1.52	Cas	0.67	LMi	0.43	CMa	0.26				
Vul	3.73	Cen	1.32	Her	0.65	And	0.42	For	0.25				
TrA	3.64	Ser	1.26	Lup	0.60	Pic	0.41	Eri	0.18				

Table 3. List of the most prolific nova discoverers and the number of novae credited to them (from official International Astronomical Union discovery documentation).

40	W. Liller	9	M. Mayall	7	Y. Nakamura
14	K. Nishiyama	9	P. Camilleri	6	M. Wolf
14	H. Nishimura	8	G. Pojmański	6	D. MacConnell
14	F. Kabashima	8	L. Plaut	6	Y. Kuwano
14	H. Honda	8	A. Cannon	6	C. Hoffmeister
12	G. Haro	7	M. Yamamoto	6	K. Haseda
11	I. Woods	7	J. Seach	6	C. Burwell
11	W. Fleming	7	Y. Sakurai		

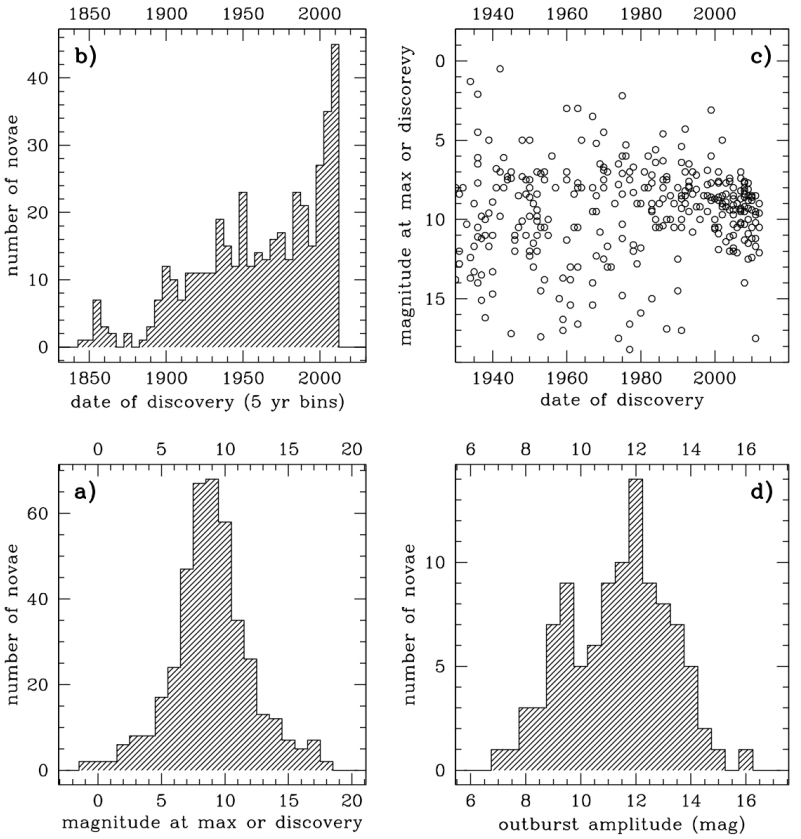

Figure 1. Statistics about Galactic novae updated to 2012: a. distribution in magnitude at maximum (or, when not available, at the time of discovery); b. number of novae discovered, counted in five-year-wide bins; c. brightness of discovered novae as function of time; d. distribution of the amplitude of nova outburst (this panel adapted from Figure 2.3 of Warner 2008).

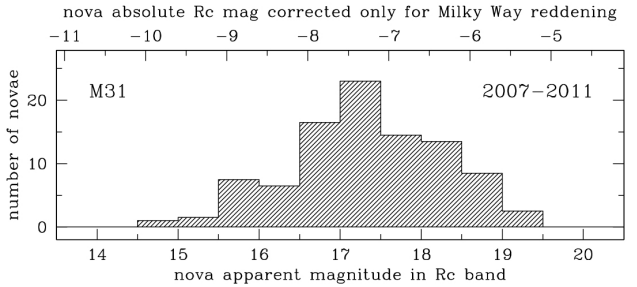

Figure 2. Distribution in R_C magnitude of the 95 novae discovered in M31 over the five-year period between 2007 and 2011.

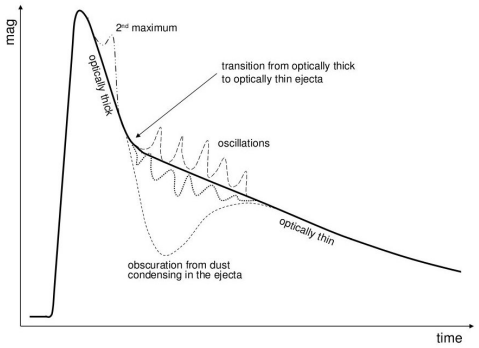

Figure 3. Schematic representation of the optical light curve of a nova. The thicker solid line provides the reference background behavior, the thinner and dashed/dotted lines represent alternative behaviors displayed by some novae.

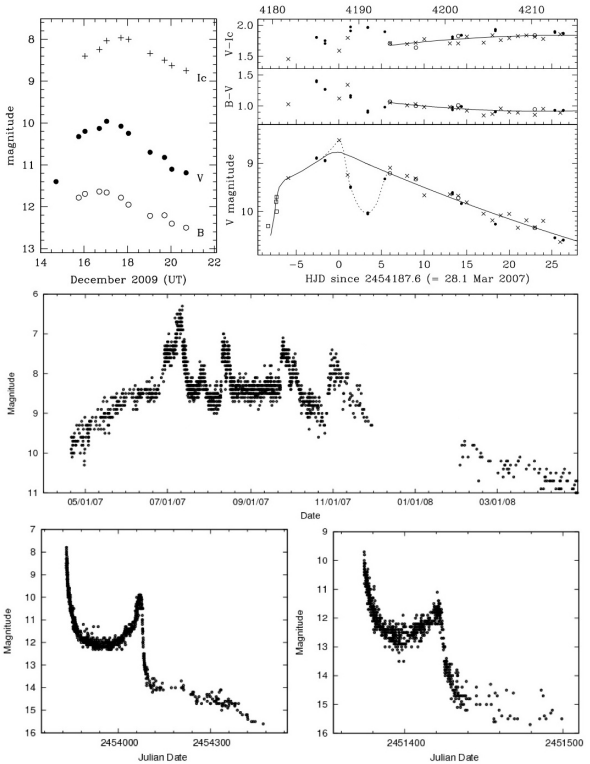

Figure 4. Some examples of the many different behaviors shown by novae around maximum brightness: the textbook smoothness exhibited by V1722 Aql/N Aql 2009 (upper left; Munari *et al*. 2010); the single pulsation-like cycle displayed by V2615 Oph/N Oph 2007 (upper right; Munari *et al.* 2008); the chaotic train of several maxima presented, over a flat plateau, by V5558 Sgr/N Sgr 2007 (center; AAVSO); the second maximum shown by V2362 Cyg/N Cyg 2006 (bottom left; AAVSO); and V1493 Aql/N Aql 1999 No.1 (bottom right; AAVSO).

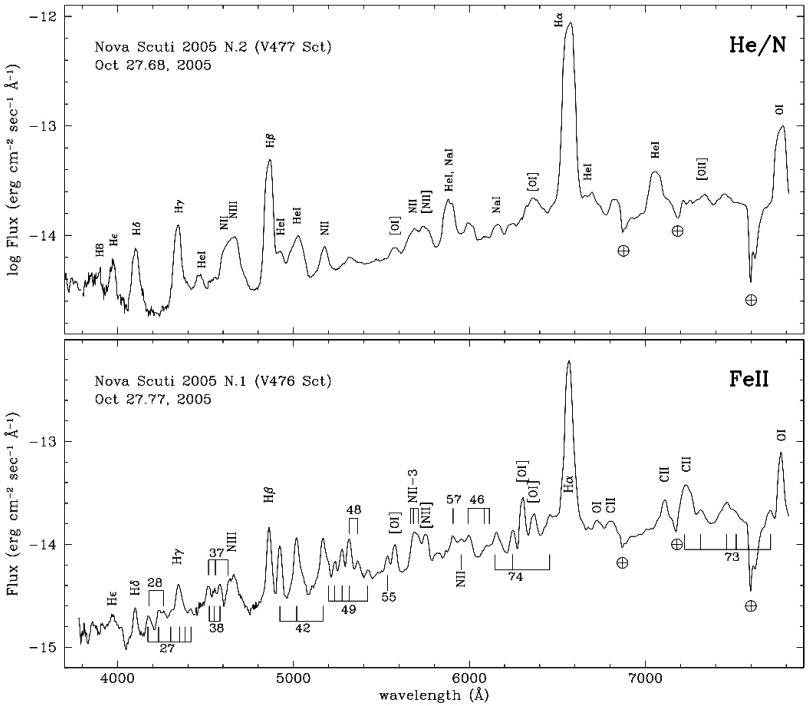

Figure 5. Examples of spectra of FeII and He/N types of novae (around maximum and along the optically thick part of the decline light-curve; Munari *et al.* 2006a, 2006b). To enhance visibility of the weak features, the absolute fluxes on the ordinate scale are plotted in logarithmic units. Major emission lines are identified. Comb-like markings identify FeII lines and the associated number the respective multiplet. Strong telluric absorption bands at 6850, 7160, and 7580 are also marked. Note the larger width of the lines in V477 Sct, tracing a large ejection velocity than in V476 Sct.

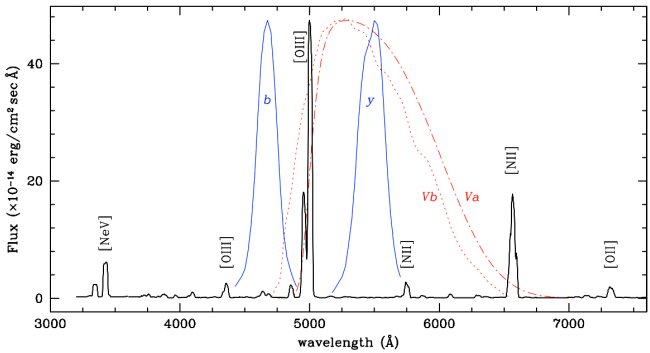

Figure 6. The nebular spectrum of Nova Cir 1995, as observed in 1996. The major forbidden emission lines are identified ([OIII] 4363, 4959, 5007 Å, [NII] 5755, 6458, 6584 Å, [NeV] 3346, 3426 Å, [OII] 7325). The transmission profiles of two commercially available *V*-band filters (labelled *Va* and *Vb*) are overplotted to show their difference in trasmitting the [OIII] 4959, 5007 Å and the [NII] 6458, 6584 + Hα 6563 Å blends (from Munari and Moretti 2012). The transmission profiles of Stromgren *b* and *y* filters are also overplotted. By avoiding the strongest emission lines, they provide a direct measurement of the true continuum emission of the nova.

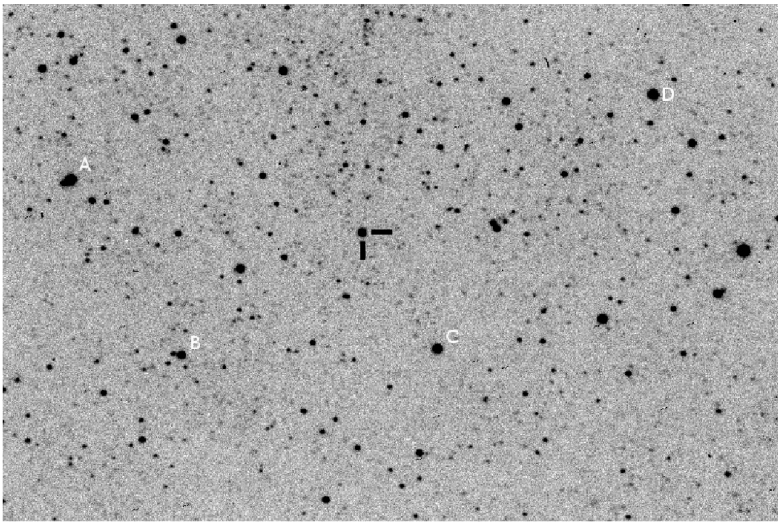

Figure 7. Finding chart for V2672 Oph/N Oph 2009 (J2000: R.A. $17^h\ 38^m\ 19.72^s$, Dec. –26° 44' 13.7") when it was shining at $R_C = 11.64$ a couple of days past maximum. The *V*, *B*–*V*, *V*–R_C, *V*–I_C values for the four comparison stars are: 11.250, +2.032, +0.990, +1.991 for A; 12.039, +0.689, +0.300, +0.746 for B; 11.620, +1.518, +0.763, +1.560 for C; and 11.290, +1.814, +0.916, +1.797 for D. 18 × 13 arcmin image courtesy S. Dallaporta (Meade 10-inch + SBIG-ST8).

A Century of Supernovae

Peter Garnavich
Physics Departement, University of Notre Dame, Notre Dame, IN 46556; pgarnavi@nd.edu

Invited review paper, received June 28, 2012

Abstract The concept of "supernova," a class of exploding stars more than 100 times the luminosity of an ordinary nova, was introduced almost eighty years ago. Over that time the physics of supernovae has matured into a rich field of study with the identification of several types of explosions and models to explain many of the observations. While there has not been a supernova visible in our Galaxy in over 300 years, only twenty-five years ago a naked-eye supernova, SN 1987A, was intensively studied in a companion galaxy to the Milky Way. Type Ia supernovae have proven to be a reliable way to estimate cosmological distances and these standardizable "candles" have greatly improved the estimate of the local expansion rate of the universe. Pushed to great distances these supernovae have demonstrated that the universe is accelerating, a discovery recognized with the 2011 Nobel Prize in physics.

1. Introduction

The founding of the AAVSO predates the concept of "supernova" by twenty years. New stars, or novae, had been seen through the centuries and introduced to western science by Tycho's and Kepler's observations, but the differentiation between the luminosities of ordinary novae and supernovae required the development of a extragalactic distance scale in the late 1920s and early 1930s (Baade and Zwicky 1934). Hubble had recognized a class of particularly luminous events he referred to as "exceptional novae" (Hubble 1929), but for a new age of "supermarkets" and comic books featuring "Superman," it was Baade and Zwicky's "super-nova" that caught the imagination of the public (Koenig 2005).

Supernovae are stellar explosions that completely disrupt their progenitor star while classical novae result from the thermonuclear fusion on the surface of a compact stellar remnant such as a white dwarf. Novae leave their binary star system intact to nova again another day, decades or millennia down the road. Supernovae yield high velocity gas, luminous energy, and sometimes a neutron star or a black hole. The creation of a neutron star was one of Zwicky's early explanations for the power of these explosions (Baade and Zwicky 1934) although the neutron had been discovered less than two years earlier.

Supernovae were clearly more energetic than novae, based on the new extragalactic distance scale of the 1930s. The absolute magnitude (the apparent

magnitude of a star if it were placed 10 parsecs (32.6 light-years) from the Earth) of supernovae range from –16 to –19 while the brightest novae reached –10 magnitude. Searches for intermediate luminosity events have been recently made possible with new, wide-field instrumentation (Kasliwal 2011). Gamma-ray astrophysics and wide-field optical searches have also identified classes of explosions more luminous than supernovae—"hypernovae" (Iwamoto *et al.* 2000; Garnavich *et al.* 2010). Hypernovae have absolute magnitudes of –20 to –21 but their explosion mechanisms are uncertain and their origins appear diverse.

Supernovae and their cousins are important to the ecology of galaxies and the universe. These stellar explosions inject energy into the interstellar gas that triggers star formation. The heavy elements synthesized in supernovae have polluted the pristine hydrogen and helium from the Big Bang, allowing the formation of planets (and people). Supernovae have also become valuable tools for the study of cosmology and have led to the discovery of the accelerating universe and "dark energy" (Reiss *et al.* 1998; Perlmutter *et al.* 1999).

2. Searching for supernovae

In the late 1930s Baade and Zwicky teamed up with Johnson and Minkowski to begin the world's first systematic search for supernovae (Baade and Zwicky 1938) using a Schmidt telescope on Palomar Mountain. They soon discovered one of the three brightest supernovae of the last century, SN 1937C (supernovae are named by the year of their discovery followed by a letter matching the order of discovery within that year), which reached an apparent magnitude of 8. By the start of the Second World War they had found fifty supernovae and made critical spectroscopic observations that led to the standard classification scheme for supernovae that is still used today. If a supernova has no hydrogen in its spectrum, it is called a "Type I," while if hydrogen is present it is a "Type II." Future supernova discoveries would lead to division of these broad classes into sub-types and the physics of the explosions are not well described by this binary scheme, but taxonomy comes before understanding.

Some form of supernova search using photographic plates continued at Palomar for the next forty years. Other observatories began to contribute as well, leading to an average of about fifteen supernova discoveries per year by the start of the 1980s. It is also possible (but difficult) to discover supernovae visually. Robert O. Evans has discovered over forty supernovae mostly through directly visual observation with a small telescope. But a transformation in the way supernovae are discovered and studied arrived with the availability of Charged-Coupled Device (CCD) detectors in the late 1980s. CCDs are nearly ten times more sensitive than photographic plates or the eye, meaning that a 12-inch telescope plus a CCD goes as deep as a 1-meter scope using photography.

CCDs opened up a much larger volume of space for the amateur astronomer to search for supernovae. Arbour, Aoki, Armstrong, Boles, Puckett, Schwartz,

and others made important contributions to supernova studies by discovering hundreds of events over the past twenty years.

Professional astronomers also put the new technology to use. Electronic detectors plus computer image manipulation led to automated searches that minimize human interaction (Li *et al.* 2000). The increasing size of CCD chips and the ability to mosaic detectors in a single instrument revolutionized supernova searching. Instead of shooting an image of a single galaxy with the hope that a supernova will appear, hundreds or even thousands of galaxies could be imaged simultaneously with a single exposure. This led to mass production of supernova discoveries at intermediate and high redshift (Frieman *et al.* 2008; Schmidt *et al.* 1998).

3. The core-collapse supernovae

Zwicky's speculation that supernovae result from the formation of a neutron star was right on, at least for a significant fraction of supernovae. Stars that begin their lives with masses more than about eight times the mass of the Sun eventually run out of energy production in their cores. Once this happens they are unable to resist gravity and the core collapses into a neutron star or black hole. The gravitational energy is turned into kinetic as the outer envelope is ejected at high velocity. In fact, the process we call a core-collapse supernova is more complicated. It probably requires neutrino deposition, asymmetric shocks, and additional exotic physics to launch the envelope into space.

The model of supernova production, gravitational energy released in core collapse, did not fully explain the variety of spectra seen in the 1930s through the 1960s. The broad features in the spectra caused by the high velocity of the ejected gas made it difficult to identify the lines. The presence of hydrogen was clear in Type II events but the identification of other elements in Type II and those found in Type I supernovae remained controversial (Branch 1990).

In fact, nature was playing a trick on astronomers. Type I supernovae actually came from two completely different progenitors and energy sources. It was not until the early 1980s that the peculiar spectra seen in a number of Type I supernovae led to the division of that class into subtypes Ia and Ib. Wheeler and Levreault (1985) asserted that the origin of the Type Ib supernovae was similar to Type II despite significant differences in their spectra. Soon, another subclass, Type Ic, was added that, like Type II and Type Ib, was from massive star core-collapse. We now know that Type Ia supernovae are not generated by the collapse of the center of a massive star, but are caused by the nuclear fusion of a compact, low mass star.

The spectral classification scheme was well established by the early 1990s. Hydrogen-rich spectra are from Type II events just as Zwicky had set out. Type Ib supernovae are core-collapse events rich in helium and Type Ic explosions are core-collapse supernovae with little hydrogen or helium. Type Ib and

Ic progenitors have lost their hydrogen and/or helium through a wind or by transferring it to a companion star.

The success of the scheme was short-lived, as a supernova was discovered in the nearby galaxy M81 at the end of March 1993 that did not stick to a single category. SN 1993J showed hydrogen in its early spectrum (Garnavich and Ann 1994) but later displayed strong lines of helium. Apparently SN 1993J had only a thin layer of hydrogen atop a helium atmosphere so that as the supernova aged and we viewed deeper layers, the classification shifted from II to Ib. Other, less bright supernovae have since shown this transformation and this intermediate class has been called "Type-IIb."

4. The supernova of the century: SN 1987A

There has not been a supernova discovered in our Galaxy for over 300 years, but in 1987 we got the next best thing. The first supernova of 1987 was found in the nearest galaxy to the Milky Way, the Large Magellanic Cloud (LMC) at a distance of only 150,000 light-years. This sounds like a huge distance, but SN 1987A became the first naked-eye supernova since Kepler's in 1604 and reached 2nd magnitude (see Figure 1). It explosion was so bright major observatories with their large telescopes had difficulty observing it near maximum light. Its proximity and location in a well-studied galaxy meant that the progenitor of a supernova could finally be identified from archival studies.

SN 1987A was a Type II event and was clearly caused by the core collapse of a massive star. The prevailing theory for core-collapse supernovae was that they happened during the red supergiant phase of stellar evolution when the outer layers are puffed out and reach cool temperatures at the surface. But careful astrometry of archival plates showed that the star at the position of the explosion was a blue, more compact star (Lasker 1987). Confusion dominated the early days of this historic event, but eventually it was confirmed that the first supernova progenitor identified was not what had been expected. Further stellar modeling showed that the low heavy element content in the LMC means that evolving massive stars spend some of their time as blue compact supergiants and can explode during that phase.

SN 1987A had more surprises in store. Several months after discovery the ultraviolet spectrum of the supernova began to change. Emission lines from highly ionized atoms grew in strength over a year and then began to fade. When the Hubble Space Telescope finally reached orbit and its bad optics were fixed, images of SN 1987A revealed one of the most spectacular sights in the sky: a triple ring system tilted to our line-of-sight and centered on the supernova debris. The gas in the rings had been released during the red supergiant phase of the star and left drifting slowly away from the star as it shrank to a blue supergiant. This circumstellar gas was then ionized and set glowing by the X-rays and ultraviolet light from the explosion (Figure 2).

SN 1987A has been intensively studied by HST for nearly a decade. From the observations it is clear that SN 1987A is beginning to make a comeback. The fast-moving supernova ejecta is beginning to sweep up the inner circumstellar ring and the collision is creating hard radiation as well as heating the gas. The entire remnant is getting brighter (Larsson *et al.* 2011). How bright the rejuvenated supernova will become is hard to predict, but it is possible that SN 1987A will again be visible in small telescopes in the southern hemisphere.

5. The GRB/supernova connection

Gamma-ray bursts (GRB) are short bursts of high energy photons that appear to come from all directions on the sky. They were first detected by Defense Department satellites in the 1960s, but were a national security secret so they were known to very few people. Throughout the 1990s, NASA's Compton Gamma-ray Observatory discovered thousands of GRB, but with little improvement in understanding their origin. From this study it became clear that there were two classes of GRB, short bursts that last less than 2 seconds and long bursts than can last a couple of minutes. The range of models published to explain the GRB phenomenon was vast. Some theorists speculated that GRB came from within our Solar System, others from the halo of the Milky Way, and still others that believed GRB were at cosmological distances.

But there was no way to estimate the distance and, therefore the energetics, of GRB from gamma-rays alone. Gamma-rays are difficult to focus, so the positional errors on any burst covered large tracts of sky. In 1997 the small Italian satellite BeppoSAX began detecting GRB. It was designed to also look for X-rays from the bursts which could be localized to a small patch of sky. This led to the discovery of optical afterglows from GRB and a revolution in GRB science (Groot *et al.* 1997). Optical afterglows were clearly connected with very distant galaxies, meaning the bursts were at cosmological distances and extremely energetic events.

The optical afterglows from GRB fade very quickly, on timescales of hours to days. The light curves of long GRB often show breaks in the rate of fading and these are signs of beaming of the energy output (Stanek *et al.* 1999). That the burst comes out as a narrow beam greatly reduces the energy budget of GRB and places them near the total energy derived from core-collapse supernovae.

Late-time bumps in the optical light curves of GRB afterglows and the association between GRB and young stars produced speculation that the long GRB phenomenon has its origin in supernova explosions. This was finally proven by the nearby GRB 030329, which reached 13th magnitude and was widely studied. Days after the burst spectroscopy revealed a Type Ic supernova getting brighter while the GRB afterglow light faded (Stanek *et al.* 2003). Since then several more Type Ic supernovae have been directly associated with long GRB. The prevailing model is that very massive star cores collapse directly to

black holes and that accretion into the black hole can power an "engine" for seconds or minutes. Narrow jets shoot out from the star, producing gamma-rays and later X-rays, optical, and radio emission. If the jets are pointed in our direction we get to see a GRB.

Short GRB are even more difficult to study than long bursts and less is known about their origin.

6. Thermonuclear supernovae

Type Ia supernovae (SNIa) derive their energy from thermonuclear fusion. A low mass star like the Sun will eventually evolve into a white dwarf star. This is a remnant core after the outer layers of hydrogen and helium have been ejected. The white dwarf is rich in the elements synthesized in the late stages of its stellar life: carbon and oxygen. It is also very small and extremely dense. A white dwarf has the mass of the Sun but the diameter is close to that of the Earth. These white dwarf stars sound exotic, but they are the most common way stars end their lives.

Normal stars resist collapse by fusing elements in their cores and the resulting energy creates a pressure that pushes against gravity. Failure to generate energy is what makes massive star cores collapse. What prevents white dwarf stars from losing to gravity? Quantum mechanics. The density of white dwarfs is so high that electrons nearly occupy the same position, so in the quantum world they must have different momentum. In fact, electrons must have very high momenta to avoid occupying the same quantum states and the pressure created by these "degenerate" electrons supports the white dwarf from collapse. A young Chandrasekhar (1931) predicted that electrons could only support stars with masses less than about 1.4 $M_{\odot}$, so we expect no white dwarfs more massive than this.

An isolated white dwarf will stay unchanged for as long as atoms last. But a white dwarf in a binary star system has a chance of becoming an energy producer once again. That is, if some of the matter of the companion can be transferred to the white dwarf, then the mass of a white dwarf could be pushed toward Chandrasekhar's limit. Exactly how mass is transferred remains uncertain. A normal star may leak mass on to the white dwarf through the gravitationally neutral point between the two. Or, the white dwarf can capture mass from the wind of a stellar giant. It may even be that a companion white dwarf merges with the heavier white dwarf and that sets the fusion reaction starting. Whichever way mass is transferred, as the white dwarf approaches 140% of the mass of the Sun, carbon is predicted to begin to fuse near its center. Once fusion begins the energy generated is enough to continue the burning and a runaway fusion explosion occurs.

Despite the small mass of a white dwarf, SNIa tend to generally be more energetic than core-collapse events. Some of the brightest supernovae of the

past century, such as SN 1937C, SN 1972E, and SN 2011fe, have been Type Ia thermonuclear supernovae. The reason SNIa are bright is that they synthesize a sizable amount of radioactive nickel during the carbon fusion. The mass of nickel produced ranges from 0.1 to 0.9 $M_{\odot}$ and this is the main source of luminosity and light curve shape diversity in SNIa.

The radioactive nickel decays to radioactive cobalt (week time scale) that then decays to stable iron (three month time scale), emitting energetic gamma-rays and positrons that are thermalized in the thick ejecta and drive the optical light curve. Arnett (1982) showed that maximum light occurs when the radioactive energy deposition equals energy loss through light emission. This "Arnett rule" allows us to directly estimate the nickel yield in supernovae just by measuring the peak luminosity.

The light curves and spectra of SNIa tend to be very uniform. Theory says they explode near the Chandrasekhar limit, so they come from a fairly narrow range of mass and conditions. This is not to say that all SNIa are identical. Some of the most interesting supernova research in the past 20 years has been attempts to understand the extreme SNIa events. Still, the majority of SNIa are very predictable, almost boring in their consistency.

7. The distance scale and the accelerating universe

Progress in astrophysics over the last century has only been possible by the ever-improving methods of distance estimation. Accurate distances are critical for the physical modeling of new phenomena and the development of cosmological models. Variable stars such as Cepheid and RR Lyrae pulsators have played critical roles in mapping the size of the Milky Way and the distances to nearby galaxies. The current expansion rate of the universe, the Hubble parameter, has been tightly constrained by the distance indicators pioneered over many decades. But supernovae, in particular Type Ia supernovae, appear to be the best distance indictors of the century.

While SNIa are very uniform, their peak luminosities vary by more than a factor of two, making them poor "standard candles." But Phillips (1993) calibrated a relation between the peak luminosity and the decline rate of the SNIa light curve. The absolute magnitude of a SNIa could be determined by observing the optical light curve near maximum light. The technique was expanded by Riess *et al.* (1996) to use the color of the supernovae as an estimate of the amount of dust scattering light coming from the explosion. Using the color and light curve information, SNIa distances were accurate to 7%, an unheard-of precision for astronomical distances.

With this new and powerful tool, cosmologists set off to sharpen estimates of the local expansion rate of the universe. This still required using Cepheid variables to calibrate the zeropoint of the SNIa distance scale using the handful of galaxies where both stars could be studied (Jha *et al.* 1999). Hubble (1929)

estimated the Hubble parameter was 500 km/s/Mpc early in the century, but with the help of SNIa, we now know H_o = 72 km/s/Mpc with an precision of 5%.

SNIa are bright at maximum light and can be seen to very large distances. Their refinement as standardizable candles in the 1990s set two groups off on a quest for the next big cosmological parameter: the matter density of the universe. The "Supernova Cosmology Project" and the "High-Z Supernova Search" began discovering SNIa five to seven billion light-years away with the goal of measuring the expansion rate in the past (see Figure 3). The idea was that matter in the universe slows the universal expansion over time due to gravity, so by measuring the change in the expansion rate one can infer the mass density (Garnavich *et al.* 1998).

To their surprise, both research groups discovered that the expansion rate of the universe has not been slowing down, but has been speeding up. That is, the universal expansion is accelerating (Reiss *et al.* 1998; Perlmutter *et al.* 1999)! This was shocking news since it requires something other than matter to be a major player in the mass/energy budget of the universe. The unknown energy that drives the accelerating universe has been dubbed "dark energy" and remains one of the biggest mysteries to be solved in the next century of the AAVSO.

References

Arnett, W. 1982, *Astrophys. J.*, **253**, 785.

Baade, W., and Zwicky, F. 1934, *Proc. Natl. Acad. Sci.*, **20**, 254.

Baade, W., and Zwicky, F. 1938, *Astrophys. J.*, **88**, 411.

Branch, D. 1990, in *Supernovae*, Astron. Rechen-Institut (ARI), Heidelberg, 30.

Chandrasekhar, S. 1931, *Astrophys. J.*, **74**, 81.

Frieman, J. A., *et al.* 2008, *Astron. J.*, **135**, 338.

Garnavich, P. M., and Ann, H. B. 1994, *Astron. J.*, **108**, 1002.

Garnavich, P. M., *et al.* 1998, *Astrophys. J.*, **493**, 53.

Garnavich, P. M., *et al.* 2010, *Bull. Amer. Astron. Soc.*, **42**, 358.

Groot, P. J., *et al.* 1997, *IAU Circ.*, No. 6584, 1.

Hubble, E. 1929, *Proc. Natl. Acad. Sci.*, **15**, 168.

Iwamoto, K., *et al.* 2000, *Astrophys. J.*, **534**, 660.

Jha, S., *et al.* 1999, *Astrophys. J., Suppl. Ser.*, **125**, 73.

Kasliwal, M. M. 2011, Ph.D. thesis, California Inst. Technol.

Koenig, T. 2005, in *1604–2004: Supernovae As Cosmological Lighthouses*, eds. M. Turatto, S. Benetti, L. Zampieri, W. Shea, ASP Conf. Ser. 342, Astron. Soc. Pacific, San Francisco, 53.

Larsson, J., *et al.* 2011, *Nature*, **474**, 484.

Lasker, B. 1987, *IAU Circ.*, No. 4318, 1.

Li, W. D., *et al.* 2000, in *Cosmic Explosions*, AIP Conf. Ser, 522, Amer. Inst. Physics, Melville, NY, 103.

Perlmutter, S., *et al.* 1999, *Astrophys. J.*, **517**, 565.

Phillips, M. M. 1993, *Astrophys. J., Lett. Ed.*, **413**, L105.
Riess, A. G., Press, W. H., and Kirshner, R. P. 1996, *Astrophys. J.*, **473**, 88.
Riess, A. G., *et al.* 1998, *Astron. J.*, **116**, 1009.
Schmidt, B. P., *et al.* 1998, *Astrophys. J.*, **507**, 46.
Stanek, K. Z., Garnavich, P. M., Kaluzny, J., Pych, W., and Thompson, I. 1999, *Astrophys. J., Lett. Ed.*, **522**, L39.
Stanek, K. Z., *et al.* 2003, *Astrophys. J., Lett. Ed.*, **591**, L17.
Wheeler, J. C., and Levreault, R. 1985, *Astrophys. J., Lett. Ed.*, **294**, L17.

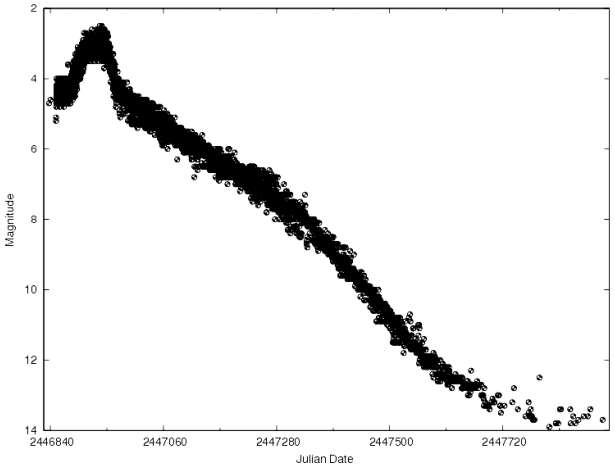

Figure 1. The AAVSO light curve of SN 1987A. The light curve begins a faster decline 400 days after peak brightness because dust begins to form in the inner ejecta.

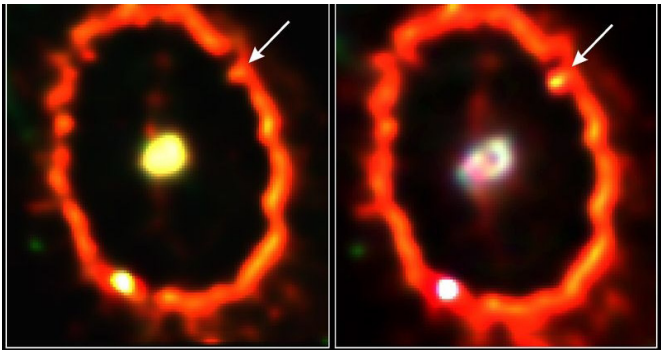

Figure 2. HST images of SN 1987A and the inner ring in 1994 (left) and 1997 (right). The arrow points to the first "hotspot" on the ring where the fast-moving supernova ejecta is running into the slower circumstellar gas. The ring is now filled with these hotspots as the ejecta begins to sweep up the circumstellar gas.

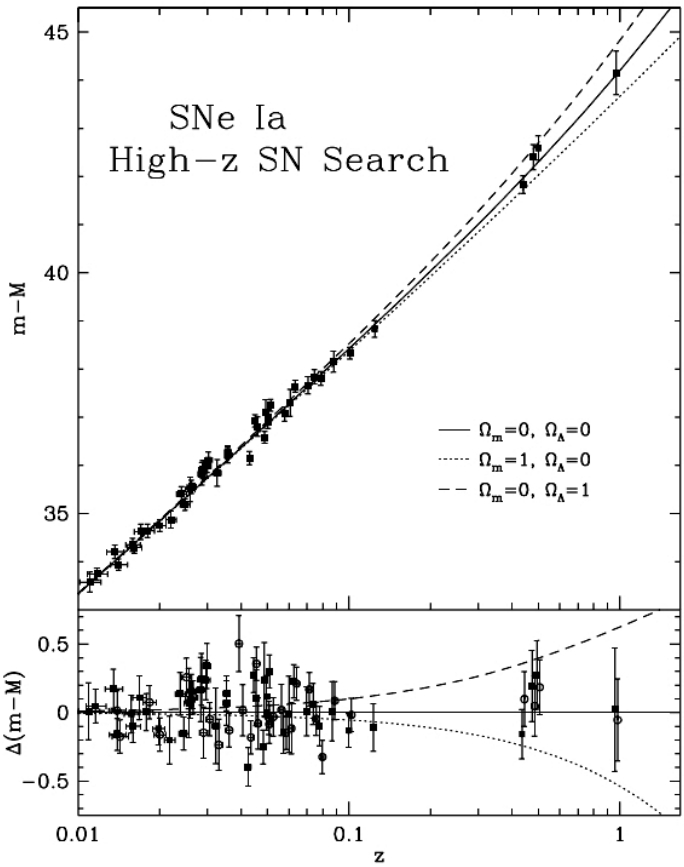

Figure 3. The Hubble diagram (distance versus velocity) for nearby supernovae and four high-redshift supernovae discovered by the High-Z Supernova Search Team (Garnavich *et al.* 1998). The lower panel displays the distance residuals about a universe with no matter (Ω_m) and no dark energy (represented by a vacuum energy Ω_Λ). The squares and circles indicate the supernova distances calculated by two different techniques. The high-redshift supernovae in the diagram tend to fall on the empty universe model meaning that the matter density in the universe is low. A few months after publication of these results more supernovae were added to the analysis that demonstrated the expansion is accelerating and a dark energy is required.

NOTES